

DEVELOPMENT OF CATALYTIC, ENANTIOSELECTIVE HALOFUNCTIONALIZATION  
REACTIONS OF OLEFINS AND THE INVESTIGATION OF CYCLIC ORTHOESTERS AS  
SYNTHETIC BUILDING BLOCKS FOR CHIRAL MOLECULES.

By

Arvind Jaganathan

A DISSERTATION

Submitted to  
Michigan State University  
in partial fulfillment of the requirements  
for the degree of

Chemistry – Doctor of Philosophy

2014

## ABSTRACT

### DEVELOPMENT OF CATALYTIC, ENANTIOSELECTIVE HALOFUNCTIONALIZATION REACTIONS OF OLEFINS AND THE INVESTIGATION OF CYCLIC ORTHOESTERS AS SYNTHETIC BUILDING BLOCKS FOR CHIRAL MOLECULES

By

Arvind Jaganathan

This thesis details the efforts to discover and develop novel asymmetric halofunctionalization reaction of olefins. Chapter 1 describes the numerous challenges associated with this transformation and the current state of the art in enantioselective alkene halogenation reactions. Chapter 2 describes the development of the first asymmetric halocyclization reaction of unsaturated amides. This reaction has uncovered an unprecedented route to chiral heterocyclic compounds such as oxazolines and dihydro-oxazines. The optimized reaction conditions that employed 1 – 2 mol% of the commercially available (DHQD)<sub>2</sub>PHAL catalyst and chlorohydantoins as terminal chlorenium sources gave the cyclized products in >95% *ee* for a wide variety of substrates. A more practical and scalable second-generation protocol that affords comparable or better enantioselectivities was also developed. Chapter 2 also discloses preliminary results for the enantioselective chlorocyclization of unsaturated carbamates; this related transformation was eventually optimized to afford either enantiomer of the oxazolidinone product by a judicious choice of the reaction solvent while employing the same catalyst.

Chapter 3 details the development of the first kinetic resolution in a chlorocyclization reaction. The different hydrogen-bonding affinity of the two enantiomers of racemic unsaturated amides for protonated (DHQD)<sub>2</sub>PHAL catalyst was exploited for enabling this transformation.

The same catalyst was shown to mediate two highly enantioselective events in a synergistic fashion– the stereodiscrimination of the two enantiomers and a highly face selective alkene chlorination. Excellent diastereoselectivity (up to 99:1) and enantioselectivities (typically greater than 95% *ee*) was obtained for the products with 0.5 mol% catalyst loading with selectivity factors of >50 for many substrates. Slight modifications to the optimized conditions could be used for the desymmetrization of *meso*-dienes and kinetic resolution of racemic propargyl amides via chlorocyclization. Preliminary optimizations for these related transformations are also provided in Chapter 3.

Efforts to expand this chemistry to enantioselective C-C bond forming reactions are presented in Chapter 4. A Friedel-Crafts reaction initiated by a chiral chloronium ion was used as a test-bed for developing such a reaction. Extensive optimizations studies that have focused on reaction variables, catalyst structures and substrate structures have led to up to 83% *ee* for this reaction. A preliminary substrate scope evaluation and kinetic studies are provided for this transformation.

Chapter 5 discloses efforts to expand the utility of cyclic orthoesters as synthetic building blocks for the construction of chiral molecules. Although these efforts were met with limited success, reactivity that was hitherto unknown for cyclic orthoesters was discovered. An unprecedented semi-pinacol rearrangement of cyclic acetoxonium ions was discovered.

To my parents

## ACKNOWLEDGEMENTS

There are numerous people that I am grateful to have met and worked with during the course of my graduate studies, without whose constant support, help and encouragement, my journey through this process would have been enormously difficult, if not impossible. Few people have been as influential in my life as my graduate advisor Prof. Babak Borhan, from both a professional and a personal perspective. I have met few people who are capable of teaching and sharing their knowledge as effectively as Babak. He gave me the freedom and the responsibility of pursuing many projects and giving them a sense of direction. I cannot recall an occasion where he was unavailable to talk about chemistry, mechanisms or an insane idea that I would have scribbled on his office whiteboard! Above all, I am grateful to him for having molded me into an independent researcher by teaching me to identify a significant transformation when I see it and seeing the 'bigger picture' in the scheme of things as well as for letting me write my own papers, research grants and train undergraduates and junior graduate students in the lab.

I am grateful to Prof. Wulff, for serving as the second reader on my committee and also for teaching me what it is to love wine and read scientific literature! I would also like to thank Profs. Maleczka and Smith for serving on my committee and Prof. Jackson, for his insightful discussions regarding the mechanistic aspects of the chemistry described in my thesis. Drs. Dan Holmes and Kermit Johnson have helped me on numerous occasions with NMR studies. Dr. Richard Staples – our champion crystallographer has met few crystals whose structures he hasn't been able to solve.

I am thankful to Chrysoula for all the advice and for the numerous other conversations regarding research, or life in general and for hosting many of the wonderful group parties at her place.

I have been fortunate enough to be surrounded by some incredibly intelligent and talented chemists as my peers over the years. Dan and Aman have been wonderful seniors and have taught me an enormous amount over the 2 – 3 years of overlap in our graduate careers. I am grateful to Carmin and Camille – my batch mates and dear friends over the years – for being my partners in crime and for all the help with my seminar, papers, thesis writing endeavors and classes. I thank Kumar, Hadi, Yi and Roozbeh for being wonderful lab mates. I am also thankful to the people who have worked with me on collaborative projects – Atefeh, Nastaran and Bardia. Thanks are also due to my friends Alok, Shipra and Abhishek.

Lastly, and most crucially, I express my gratitude to my parents, Neha and my family for their unwavering and unconditional support, patience and love through thick and thin. Their unquestioning and unbounded encouragement and support in all my endeavors has allowed me to be the best that I can be – professionally and personally.

## TABLE OF CONTENTS

|                                       |       |
|---------------------------------------|-------|
| LIST OF TABLES.....                   | xi    |
| LIST OF FIGURES .....                 | xv    |
| LIST OF SCHEMES.....                  | xviii |
| KEY TO SYMBOLS AND ABBREVIATIONS..... | xxiii |

### CHAPTER I

|   |    |
|---|----|
| <i>Reagent controlled asymmetric halogenation of alkenes: A brief overview.</i> .....   | 1  |
| <b>I.1. Introduction.</b> .....   | 1  |
| <b>I.2. Nomenclature of species encountered in alkene halogenation reactions.</b> .....   | 2  |
| <b>I.3. Mechanistic considerations for the asymmetric halogenation of alkenes.</b> .....  | 3  |
| <b>I.3.1. Erosion of stereochemistry of halonium ions by olefin-to-olefin halonium transfer.</b> .....                                      | 5  |
| <b>I.3.2. Isomerization of halonium ions to halocarbenium ions.</b> .....   | 9  |
| <b>I.4. Development of enantioselective halocyclization reactions.</b> .....  | 13 |
| <b>I.4.1. Asymmetric halocyclizations that employ stoichiometric quantities of chiral promoters.</b> .....                                  | 14 |
| <b>I.4.1.1. Metal mediated enantioselective halocyclization.</b> .....  | 14 |
| <b>I.4.1.2. Chiral Lewis base mediated halocyclizations.</b> .....  | 14 |
| <b>I.4.2. Catalytic asymmetric halocyclization reactions.</b> .....   | 18 |
| <b>I.4.2.1. Transition metal catalyzed enantioselective halocyclizations.</b> .....   | 18 |
| <b>I.4.2.2. Organocatalytic enantioselective halocyclizations.</b> .....  | 21 |
| <b>I.4.2.2.1. Chiral Bronsted acid catalyzed enantioselective halocyclizations.</b> .....   | 21 |
| <b>I.4.2.2.2. Chiral Lewis bases and polyfunctional catalysts for enantioselective halocyclizations.</b> .....                              | 25 |
| <b>I.4.2.2.3. Chiral phase transfer catalyzed enantioselective halocyclizations.</b> .....  | 31 |
| <b>I.4.3. Intermolecular nucleophilic capture of chiral halonium ions.</b> .....  | 32 |
| <b>I.4.3.1. Stereoselective interception of chiral halonium ions by alcohols, carboxylic acids and amine derivatives.</b> .....             | 33 |
| <b>I.4.3.2. Stereoselective interception of chiral halonium ions by halide anions – asymmetric vicinal dihalogenation of alkenes.</b> ..... | 36 |
| <b>I.5 Challenges and future directions</b> .....   | 40 |
| REFERENCES .....  | 43 |

### Chapter II

|  |    |
|--|----|
| <i>Organocatalytic asymmetric chlorocyclization of unsaturated amides.</i> ..... | 47 |
| <b>II.1. Introduction.</b> .....   | 47 |

|  |     |
|--|-----|
| II.1.1. Literature precedence for chemoselectivity in the halocyclization of amides.   | 51  |
| II.2. Results and discussions.   | 52  |
| II.2.1. Preliminary results.   | 52  |
| II.2.2. Optimization of reaction variables.  | 58  |
| II.2.2.1. Retracing the optimization of the asymmetric chlorolactonization reaction.   | 58  |
| II.2.2.2. Catalyst and chlorine source loading studies.  | 60  |
| II.2.2.3. ee as a function of solvent polarity.  | 66  |
| II.2.2.4. Serendipitous discovery of CF <sub>3</sub> CH <sub>2</sub> OH as the optimal solvent.  | 69  |
| II.2.2.5. Catalyst loading reaction concentration studies.   | 70  |
| II.2.3. Steric and electronic fine-tuning of the chlorocyclization substrates.   | 72  |
| II.2.4. Substrate scope evaluation for the synthesis of chiral oxazolines by asymmetric chlorocyclization of 1,1-disubstituted allyl amides. | 75  |
| II.2.5. Determination of absolute stereochemistry of cyclized products.  | 78  |
| II.2.6. Evaluation of trans-disubstituted alkenes as viable substrates for asymmetric chlorocyclization of allyl amides.                     | 79  |
| II.2.7. Rendering substrates with aliphatic alkene substituents compatible with the asymmetric chlorocyclization chemistry.                  | 83  |
| II.2.8. Synthetic utility of the amide chlorocyclization reaction and the cyclized products.   | 87  |
| II.2.9. Development of more cost-effective and ambient temperature conditions for the highly enantioselective chlorocyclization of amides.   | 89  |
| II.2.9.1. Chloramine salts as superior electrophilic chlorine precursors.  | 89  |
| II.2.9.2. Oxone®/KCl as the chlorenium source.   | 95  |
| II.2.10. Attempted asymmetric bromo- and selenocyclization of unsaturated amides.  | 97  |
| II.2.10.1. (DHQD) <sub>2</sub> PHAL catalyzed enantioselective bromocyclization of unsaturated amides.                                       | 97  |
| II.2.10.2. Attempted enantioselective selenocyclization of unsaturated amides.   | 99  |
| II.2.11. Asymmetric chlorocyclization of unsaturated carbamates.   | 100 |
| II.3. Summary and future work.   | 107 |
| II.4. Acknowledgements.  | 109 |
| II.5. Experimental section.  | 110 |
| II.5.1. General information.   | 110 |
| II.5.2. General procedure for the catalytic asymmetric chlorocyclization of unsaturated amides.  | 111 |
| II.5.3. Characterization of cyclized products.   | 111 |
| II.5.4. General procedure for the synthesis of substrates II-18 and II-21-A – II-31A.  | 133 |
| II.5.5. General procedure for the synthesis of substrates for substrate scope evaluation.  | 138 |
| II.5.6. Wittig olefination of II: General procedure.   | 141 |
| II.5.7. General procedure for the synthesis of substrates II-32-A to II-36-A.  | 144 |
| II.5.8. General procedure for the synthesis of substrates II-41-A and II-45-A - II-51-A.   | 148 |
| II.5.9. Determination of absolute stereochemistry of oxazolines.   | 156 |
| REFERENCES   | 158 |

|   |     |
|---|-----|
| <b>Chapter III</b>  |     |
| <b><i>Kinetic Resolution of Unsaturated Amides in a Chlorocyclization Reaction: Concomitant Enantiomer Differentiation and Face Selective Alkene Chlorination by a Single Catalyst.</i></b> | 161 |
| <b>III.1. Introduction.</b>   | 161 |
| <b>III.2. Literature precedence for kinetic resolution of halofunctionalization reactions.</b>  | 168 |
| <b>III.3. Results and discussion.</b>   | 169 |
| <b>III.3.1. Investigation of substrate control: Non-catalyzed halocyclization of unsaturated amides.</b>  | 169 |
| <b>III.3.2. Reagent controlled chlorocyclization of racemic unsaturated amides</b>  | 171 |
| <b>III.3.3. Optimization of reaction variables.</b>   | 175 |
| <b>III.3.3.1. Effect of the chlorenium source and temperature on the stereoselectivity of the reaction.</b>   | 175 |
| <b>III.3.3.2. Catalyst loading studies</b>  | 180 |
| <b>III.3.4. Matched and mismatched substrates for kinetic resolution</b>  | 181 |
| <b>III.3.5. Determination of absolute stereochemistry of cyclized products</b>  | 182 |
| <b>III.3.6. Substrate scope.</b>  | 183 |
| <b>III.3.7. Mechanistic studies.</b>  | 187 |
| <b>III.3.7.1. NMR analysis of stoichiometric substrate-catalyst mixtures.</b>   | 187 |
| <b>III.3.7.2. Effect of protic additives.</b>   | 190 |
| <b>III.3.8. Features and utility of the resolution.</b>   | 192 |
| <b>III.3.8.1. Determination of selectivity factors</b>  | 192 |
| <b>III.3.9. Chemical transformation of products and recovered substrates</b>  | 196 |
| <b>III.3.10. Development of a tandem kinetic resolution/diastereoselective iodocyclization cascade.</b>   | 197 |
| <b>III.3.11. Catalyst recycling studies.</b>  | 199 |
| <b>III.3.12. Attempted kinetic resolution in the bromo- and iodocyclization reactions.</b>  | 200 |
| <b>III.3.13. Limitations of the kinetic resolution protocol.</b>  | 203 |
| <b>III.3.14. Kinetic resolution of propargyl amides in a chlorocyclization reaction</b>   | 203 |
| <b>III.3.15. Desymmetrization of meso dienes via chlorocyclization</b>  | 208 |
| <b>III.4. Conclusion and future directions.</b>   | 212 |
| <b>III.5. Acknowledgements.</b>   | 213 |
| <b>III.6. Experimental section.</b>   | 215 |
| <b>III.6.1. General information.</b>  | 215 |
| <b>III.6.2. General procedure for screening and optimization of kinetic resolution.</b>   | 216 |
| <b>III.6.3. General procedure for kinetic resolution of unsaturated amides for substrate scope evaluation.</b>  | 216 |
| <b>III.6.4. Characterization of cyclized products.</b>  | 217 |
| <b>III.6.5. General method for the preparation of substrates for kinetic resolution.</b>  | 231 |
| <b>III.6.6. Analytical data for kinetic resolution substrates.</b>  | 233 |
| <b>III.6.7. Chemical transformations.</b>   | 245 |
| <b>III.6.8. Stoichiometric NMR experiments.</b>   | 249 |
| <b>REFERENCES</b>   | 258 |

## Chapter IV

|  |     |
|--|-----|
| <b><i>Organocatalytic arylation of chiral chloronium ions: Paralyzing the stereochemistry of an enantioselective C-Cl bond formation to a C-C bond forming reaction.</i></b> ..... | 262 |
| <b>IV.1. Introduction.</b> .....   | 262 |
| <b>IV.2. Prior work in stereoselective C-C bond formation initiated by halonium ions.</b> .....  | 263 |
| <b>IV.3. Challenges associated with rendering C-nucleophiles compatible with halonium chemistry.</b> .....   | 266 |
| <b>IV.4. Results and discussion.</b> .....   | 268 |
| <b>IV.4.1. Preliminary studies: Determination of test reaction and scale.</b> .....  | 268 |
| <b>IV.4.2. Serendipitous discovery of a halonium ion initiated benzoate transposition of tertiary allylic amides.</b> .....  | 269 |
| <b>IV.4.3. Development of a halocyclization route to racemic benzopiperidines.</b> .....   | 272 |
| <b>IV.4.4. Catalyst screen for asymmetric arylation of chloronium ions.</b> .....  | 274 |
| <b>IV.4.5. Reaction variables' optimization.</b> .....   | 280 |
| <b>IV.4.5.1. Determination of optimal co-solvent.</b> .....  | 280 |
| <b>IV.4.5.2. Identification of the optimal chloronium source.</b> .....  | 283 |
| <b>IV.4.5.3. Optimization of the catalyst loading.</b> .....   | 285 |
| <b>IV.4.5.4. Optimization of the reaction temperature.</b> .....   | 286 |
| <b>IV.4.6. Variation of <i>N</i>-protecting group.</b> .....   | 288 |
| <b>IV.4.6.1. Screening other protecting groups.</b> .....  | 288 |
| <b>IV.4.6.2. Temperature dependence of enantioselectivity as a function of protecting groups.</b> .....  | 291 |
| <b>IV.4.7. Eyring plot analyses to map the enthalpic and entropic drivers of enantioselectivity with different protecting groups.</b> .....  | 292 |
| <b>IV.4.7.1. Rational design of protecting groups based on Eyring plot analyses.</b> .....   | 297 |
| <b>IV.4.8. Sampling lower reaction temperatures with the aid of additional co-solvents.</b> .....  | 298 |
| <b>IV.4.9. Enantioselectivity as a function of electron density of nucleophile.</b> .....  | 300 |
| <b>IV.4.9.1. Correlation of enantioselectivity and the Hammett constants of substituents on nucleophilic arene ring.</b> .....   | 302 |
| <b>IV.4.10. Design and evaluation of second-generation cinchona alkaloid derived catalysts.</b> .....  | 305 |
| <b>IV.4.11. Limitations of the methodology.</b> .....  | 310 |
| <b>IV.4.12. Synthesis of substrates.</b> .....   | 312 |
| <b>IV.5. Summary and future work.</b> .....  | 315 |
| <b>IV.6. Acknowledgements.</b> .....   | 317 |
| <b>IV.7. Experimental section.</b> .....   | 318 |
| <b>IV.7.1. General procedure for synthesis of substrates for carbocyclization (Variation of protecting group on N).</b> .....  | 318 |
| <b>IV.7.2. Characterization of cyclized products.</b> .....  | 337 |
| <b>REFERENCES</b> .....  | 347 |

## Chapter V

|  |     |
|--|-----|
| <b><i>Cyclic orthoesters as synthetic building blocks for the synthesis of chiral molecules.</i></b> ..... | 351 |
| <b>V.1. Introduction.</b> .....  | 351 |
| <b>V.1.1. Reactivity of orthoesters.</b> .....   | 351 |
| <b>V.1.2. Prior reports of nucleophilic functionalization of cyclic orthoesters.</b> .....                 | 353 |

|   |     |
|---|-----|
| <b>V.2. Results and discussions.</b> .....  | 358 |
| <b>V.2.1. Discovery of a 1,2-aryl migration in cyclic orthoesters.</b> .....  | 358 |
| <b>V.2.2. Attmpted arylation of orthoesters: Discovery of a new route to<br/>        cyclotriveratrylenes (CTVs).</b> ..... | 365 |
| <b>V.2.3. Other attempts of C-Heteroatom bond formation reactions on<br/>        orthoester scaffolds.</b> .....            | 372 |
| <b>V.3. Summary and Future work.</b> .....  | 375 |
| <b>V.4. Experimental section.</b> .....   | 377 |
| <b>V.4.1. General information.</b> .....  | 377 |
| <b>V.4.2. Generation of standard curve used for determination of yield of V-54.</b> .....                                   | 377 |
| <b>V.4.3. General protocol for the synthesis of V-54.</b> .....   | 379 |
| <b>V.4.4. Characterization of compounds.</b> .....  | 380 |
| <b>REFERENCES</b> .....   | 395 |

## LIST OF TABLES

|   |    |
|---|----|
| <b>Table II-1.</b> Preliminary studies of the non-catalyzed chlorocyclization of <b>II-11</b> .....   | 53 |
| <b>Table II-2.</b> Enantioselective chloro- and bromocyclization of <b>II-11</b> by <b>II-16</b> .....  | 56 |
| <b>Table II-3.</b> Preliminary studies of the asymmetric chlorocyclization of <b>II-18</b> to <b>II-19</b> .....                                | 58 |
| <b>Table II-4.</b> Preliminary optimizations guided by the results of the asymmetric chlorolactonization reaction .....                         | 59 |
| <b>Table II-5.</b> Catalyst loading studies .....   | 60 |
| <b>Table II-6.</b> Effect of DCDPH stoichiometry on the enantioselectivity of asymmetric chlorocyclization of <b>II-18</b> .....                | 61 |
| <b>Table II-7.</b> Solvent screen for the asymmetric chlorocyclization of <b>II-18</b> to <b>II-19</b> .....                                    | 62 |
| <b>Table II-8.</b> Evaluation of mixed solvent systems for the asymmetric chlorocyclization of <b>II-18</b> .....                               | 64 |
| <b>Table II-9.</b> CCl <sub>4</sub> -MeCN co-solvent study .....  | 65 |
| <b>Table II-10.</b> MeNO <sub>2</sub> -MeCN co-solvent study .....  | 66 |
| <b>Table II-11.</b> Enantioselectivity as a function of the dielectric constant of the reaction medium .....                                    | 67 |
| <b>Table II-12.</b> Temperature dependence of enantioselectivity in <i>i</i> -PrNO <sub>2</sub> .....   | 69 |
| <b>Table II-13.</b> Enantioselectivity of chlorocyclization of <b>II-18</b> in alcohol solvents .....   | 70 |
| <b>Table II-14.</b> Catalyst loading studies for chlorocyclization of <b>II-18</b> in CF <sub>3</sub> CH <sub>2</sub> OH .....                  | 71 |
| <b>Table II-15.</b> Effect of initial substrate concentration on the enantioselectivity of the chlorocyclization reaction of <b>II-18</b> ..... | 71 |
| <b>Table II-16.</b> Enantioselectivity as a function of solvent for the chlorocyclization of <b>II-39</b> .....                                 | 80 |
| <b>Table II-17.</b> Influence of temperature on the asymmetric chlorocyclization of <b>II-42-A</b> .....  | 81 |
| <b>Table II-18.</b> Identification of optimal reaction conditions for the asymmetric chlorocyclization of <b>II-52-A</b> .....                  | 85 |

|  |     |
|--|-----|
| <b>Table II-19.</b> Evaluation of chloramine salts as the terminal chlorenium source for the asymmetric chlorocyclization of <b>II-18</b> .....    | 91  |
| <b>Table II-20.</b> Substrate scope evaluation with (DHQD) <sub>2</sub> PHAL/TsNNaCl•3H <sub>2</sub> O system .....                                | 94  |
| <b>Table II-21.</b> Chlorocyclization of trans-disubstituted and trisubstituted alkene substrates by (DHQD) <sub>2</sub> PHAL/TsNNaCl .....        | 95  |
| <b>Table II-22.</b> Evaluation of Oxone®/KCl as a chlorenium precursor in asymmetric chlorocyclization of <b>II-41-A</b> .....                     | 96  |
| <b>Table II-23.</b> Asymmetric bromocyclization of <b>II-18</b> .....  | 98  |
| <b>Table II-24.</b> Catalyst loading studies for the asymmetric bromocyclization of <b>II-18</b> .....   | 98  |
| <b>Table II-25.</b> Evaluation of different solvents for the asymmetric chlorocyclization of <b>II-69</b> .....                                    | 103 |
| <b>Table II-26.</b> Substrate scope evaluation for the asymmetric chlorocyclization of unsaturated carbamates .....                                | 106 |
| <b>Table III-1.</b> Diastereoselectivity of the non-catalyzed chlorocyclization of <b>III-11</b> .....   | 170 |
| <b>Table III-2.</b> Comparison of chloro-, bromo- and iodocyclization reactions <b>III-11</b> .....  | 171 |
| <b>Table III-3.</b> Catalyst screen for the enantioselective chlorocyclization of <b>III-11</b> .....  | 173 |
| <b>Table III-4.</b> Influence of chlorenium precursor and reaction variables on the stereoselectivity of kinetic resolution of <b>III-11</b> ..... | 178 |
| <b>Table III-5.</b> Catalyst loading studies .....   | 181 |
| <b>Table III-6.</b> Substrate scope evaluation.....  | 185 |
| <b>Table III-7.</b> Inhibitory effects of protic additives .....   | 191 |
| <b>Table III-8.</b> Catalyst recycle studies .....   | 199 |
| <b>Table III-9.</b> Attempted kinetic resolution in the bromo- and iodocyclization reactions of <b>III-11</b> .....                                | 201 |
| <b>Table III-10.</b> Regioselectivity in the non-catalyzed halocyclization of <b>III-51</b> .....  | 205 |
| <b>Table III-11.</b> Kinetic resolution of <b>III-51</b> <i>via</i> halocyclization.....   | 206 |
| <b>Table III-12.</b> Preliminary optimization for the desymmetrization of <b>III-57</b> .....  | 211 |
| <b>Table IV-1.</b> Preliminary attempts to synthesize <b>IV-28</b> <i>via</i> chlorocyclization of <b>IV-27</b> .....                              | 270 |

|   |     |
|---|-----|
| <b>Table IV-2.</b> Preliminary results for the non-asymmetric chlorocyclization of <b>IV-37</b> .....       | 273 |
| <b>Table IV-3.</b> Catalyst evaluation for the test reaction.....   | 279 |
| <b>Table IV-4.</b> Evaluation of HFIP-co-solvent mixtures as a reaction medium .....                        | 281 |
| <b>Table IV-5.</b> Optimization of reaction concentration and co-solvent composition .....                  | 283 |
| <b>Table IV-6.</b> Evaluation of chlorenium sources .....   | 284 |
| <b>Table IV-7.</b> Catalyst loading studies.....  | 285 |
| <b>Table IV-8.</b> Enantioselectivity as a function of temperature .....                                    | 287 |
| <b>Table IV-9.</b> Segregation of enthalpic and entropic contirbutions to $\Delta\Delta G^\ddagger$ .....   | 295 |
| <b>Table IV-10.</b> Evaluation of co-solvent anti-freezes.....  | 299 |
| <b>Table IV-11.</b> <i>ee</i> as a function of nucleophile electron density .....                           | 301 |
| <b>Table IV-12.</b> Bromocarbocyclization reaction using $\text{Br}^+$ / <b>IV-55</b> reagent system.....   | 311 |
| <b>Table V-1.</b> Exploration of diols and alcohols as nucleophilic traps for rearrangement products .....  | 360 |
| <b>Table V-2.</b> Identification of optimal solvent for the semi-pinacol rearrangement of <b>V-38</b> ..... | 361 |
| <b>Table V-1.</b> Data for standard curve analysis of <b>V-54</b> .....                                     | 378 |

## LIST OF FIGURES

|   |     |
|---|-----|
| <b>Figure I-1.</b> Representative examples of catalytic asymmetric alkene functionalization reactions .....   | 2   |
| <b>Figure I-2.</b> Nomenclature of halogen ions .....   | 3   |
| <b>Figure I-3.</b> The fate of chloronium and bromonium ions as predicted by experiment and theory respectively .....   | 10  |
| <b>Figure I-4.</b> Dissecting the stereochemical elements of the asymmetric chlorolactonization reaction by employing D-labeled substrate .....                                     | 12  |
| <b>Figure I-5.</b> Ternary complex of alkenoic acid substrate, <b>I-74</b> and <b>I-75</b> leads to rate acceleration and highly face-selective chloronium delivery to alkene ..... | 26  |
| <b>Figure II-1.</b> Some natural products with stereodefined C-halogen bonds .....  | 47  |
| <b>Figure II-2.</b> Proposed asymmetric chlorocyclization of unsaturated amides to oxazoline heterocycles .....   | 51  |
| <b>Figure II-3.</b> Modulation of enantioselectivity by the sacrificial benzamide motif .....   | 74  |
| <b>Figure II-4.</b> 1,1-disubstituted allylic amide substrates for asymmetric chlorocyclization reaction .....  | 76  |
| <b>Figure II-5.</b> Substrate scope for the asymmetric chlorocyclization of <i>N</i> -2-aryl-2-propenylbenzamides .....   | 77  |
| <b>Figure II-6.</b> Influence of benzamide motif on the enantioselectivity for the chlorocyclization reaction of <i>N</i> -(3-aryl-propenyl)-benzamides .....                       | 80  |
| <b>Figure II-7.</b> Substrate scope evaluation for the asymmetric chlorocyclization of trans-disubstituted allyl amide substrates .....   | 82  |
| <b>Figure II-8.</b> Substrate scope evaluation of trisubstituted and alkyl substituted allyl amides .....   | 87  |
| <b>Figure II-9.</b> Proposed asymmetric chlorocyclization of unsaturated carbamates .....   | 101 |
| <b>Figure II-10.</b> Crystal structure of <b>II-41-B</b> .....  | 123 |
| <b>Figure II-11.</b> Crystal structure of <b>II-38</b> .....  | 157 |
| <b>Figure III-1.</b> Mechanistic possibilities for the enantioselective chlorocyclization of racemic unsaturated amides .....   | 166 |
| <b>Figure III-2.</b> Synergistic effects of the individual stereodetermining steps .....  | 167 |

|   |     |
|---|-----|
| <b>Figure III-3.</b> Catalysts evaluated for kinetic resolution of test substrate.....  | 172 |
| <b>Figure III-4.</b> NMR analysis of stoichiometric substrate-catalyst mixtures.....  | 188 |
| <b>Figure III-5.</b> NMR of free and protonated (DHQD) <sub>2</sub> PHAL in CDCl <sub>3</sub> and CF <sub>3</sub> CH <sub>2</sub> OH.....                                 | 189 |
| <b>Figure III-6.</b> Plausible protonated forms of (DHQD) <sub>2</sub> PHAL in the presence of protic additives.....  | 191 |
| <b>Figure III-7.</b> Conversion-enantioselectivity- <i>K<sub>Rel</sub></i> value correlations for substrates and products for a typical kinetic resolution reaction ..... | 194 |
| <b>Figure III-8.</b> Determination of <i>K<sub>Rel</sub></i> values for selected transformations.....   | 196 |
| <b>Figure III-9.</b> Proposed kinetic resolution of proargyl amides <i>via</i> halocyclization .....  | 204 |
| <b>Figure III-20.</b> Crystal structure of <b>III-56</b> .....  | 209 |
| <b>Figure III-11.</b> Crystal structure of <b>III-12</b> .....  | 217 |
| <b>Figure III-13.</b> Crystal structure of <b>III-13</b> .....  | 218 |
| <b>Figure III-14.</b> Crystal structure of drawing of <b>III-44</b> .....   | 247 |
| <b>Figure III-14.</b> <sup>1</sup> H NMR of 1:1 <b>III-11</b> : DHQD <sub>2</sub> PHAL in CDCl <sub>3</sub> .....   | 250 |
| <b>Figure III-15.</b> <sup>1</sup> H NMR of 1:1 <b>III-11</b> : DHQD <sub>2</sub> PHAL in CD <sub>3</sub> CN.....   | 251 |
| <b>Figure III-16.</b> <sup>1</sup> H NMR of 1:1 <b>III-11</b> : DHQD <sub>2</sub> PHAL in Acetone-d <sub>6</sub> .....  | 252 |
| <b>Figure III-17.</b> <sup>1</sup> H NMR of 1:1 <b>III-11</b> : DHQD <sub>2</sub> PHAL in C <sub>6</sub> D <sub>6</sub> .....   | 253 |
| <b>Figure III-18.</b> <sup>1</sup> H NMR of 1:1 <b>III-11</b> : DHQD <sub>2</sub> PHAL in CF <sub>3</sub> CH <sub>2</sub> OH.....   | 254 |
| <b>Figure III-19.</b> <sup>1</sup> H NMR of 1:1 <b>III-38</b> : DHQD <sub>2</sub> PHAL in CF <sub>3</sub> CH <sub>2</sub> OH.....   | 255 |
| <b>Figure III-20.</b> <sup>1</sup> H NMR of 1:1 <b>III-39</b> : DHQD <sub>2</sub> PHAL in CF <sub>3</sub> CH <sub>2</sub> OH.....   | 256 |
| <b>Figure IV-1.</b> Nucleophiles explored thus far (2013) in catalytic asymmetric halocyclization reactions .....   | 262 |
| <b>Figure IV-2.</b> Taguchi's asymmetric iodocarbocyclization of malonate esters .....  | 264 |
| <b>Figure IV-3.</b> Ishihara's chiral iodonium ion initiated polyene cascade .....  | 264 |
| <b>Figure IV-4.</b> Tu's enantioselective alkene bromination/semi-pinacol rearrangement cascade .....   | 265 |

|  |     |
|--|-----|
| <b>Figure IV-5.</b> Gouverneur's <b>IV-17</b> mediated asymmetric fluorocarbocyclization reaction.....                                       | 265 |
| <b>Figure IV-6.</b> Braddock's demonstration of negligible racemization rates for chiral bromonium ions in a carbocyclization reaction ..... | 267 |
| <b>Figure IV-7.</b> Mechanistic hypothesis for an asymmetric Friedel-Crafts reaction initiated by a chiral chloronium ion .....              | 269 |
| <b>Figure IV-8.</b> Plausible mechanism for chloronium ion initiated 1,4-benzoate transposition of tertiary allylic amides .....             | 271 |
| <b>Figure IV-9.</b> Catalysts evaluated for the asymmetric carbocyclization reaction .....   | 277 |
| <b>Figure IV-10.</b> Conversion as a function of time and catalyst loading .....   | 286 |
| <b>Figure IV-11.</b> Influence of the protecting group structure on enantioselectivity .....   | 289 |
| <b>Figure IV-12.</b> Temperature dependence of enantioselectivity as a function of protecting group .....                                    | 292 |
| <b>Figure IV-13.</b> Eyring plots for different <i>N</i> -protecting groups.....   | 294 |
| <b>Figure IV-14.</b> Steric and electronic fine-tuning of protecting groups .....  | 298 |
| <b>Figure IV-15.</b> Correlation of <i>ee</i> and Hammett substituent constants ( $\sigma_p/\sigma_m$ ) .....                                | 303 |
| <b>Figure IV-16.</b> Evaluation of second generation of cinchona alkaloid dimer catalysts .....  | 307 |
| <b>Figure IV-17.</b> Evaluation of catalysts with triazine linker .....  | 309 |
| <b>Figure IV-18.</b> Substrate scope limitations of the current carbocyclization protocol.....   | 312 |
| <b>Figure IV-19.</b> The non-asymmetric chlorocyclization of other substrates .....  | 314 |
| <b>Figure V-1.</b> Mechanistic considerations for translation of stereochemistry of vicinal diols to $\alpha,\alpha$ -diaryl aldehydes ..... | 363 |
| <b>Figure V-2.</b> Standard curve for determining GC yields of <b>V-54</b> .....   | 378 |

## LIST OF SCHEMES

|  |    |
|--|----|
| <b>Scheme I-1.</b> A stereotypical enantioselective halocyclization reaction .....   | 4  |
| <b>Scheme I-2.</b> The generation and NMR characterization of halonium ions .....  | 6  |
| <b>Scheme I-3.</b> Synthesis and isolation of stable bromonium and iodonium salts .....  | 7  |
| <b>Scheme I-4.</b> Demonstration of rapid olefin-to-olefin halenium transfer .....   | 8  |
| <b>Scheme I-5.</b> Partial racemization of chiral bromonium ions via olefin-to-olefin halenium transfer .....                                | 9  |
| <b>Scheme I-6.</b> First examples of reagent controlled asymmetric halocyclization reactions .....   | 14 |
| <b>Scheme I-7.</b> An asymmetric iodocarbocyclization cascade mediated by a stoichiometric chiral Lewis base .....                           | 15 |
| <b>Scheme I-8.</b> Chiral Selectflor <sup>®</sup> analogs for asymmetric fluorocarbocyclization reactions .....                              | 16 |
| <b>Scheme I-9.</b> Early examples of stoichiometric chiral Lewis base promoted asymmetric halocyclization reactions .....                    | 17 |
| <b>Scheme I-10.</b> 5- <i>endo</i> -iodolactonization promoted by <b>I-51</b> .....  | 18 |
| <b>Scheme I-11.</b> Co-salen ( <b>I-55</b> ) catalyzed asymmetric iodoetherification and iodolactonization reactions .....                   | 19 |
| <b>Scheme I-12.</b> Catalytic asymmetric bromolactonization of alkenoic acid mediated by TBCO/ <b>I-60</b> .....                             | 20 |
| <b>Scheme I-13.</b> Structure of ( <i>S</i> )-TRIP ( <b>I-63</b> ) and <b>I-63</b> /NBS mediated asymmetric bromocyclization reactions ..... | 22 |
| <b>Scheme I-14.</b> Cooperative asymmetric catalysis of <b>I-63</b> /PPh <sub>3</sub> =Se in the bromoetherification of alkenols .....       | 23 |
| <b>Scheme I-15.</b> Chiral Bis-amidine base/achiral Bronsted-acid co-catalyzed enantioselective iodolactonization .....                      | 24 |
| <b>Scheme I-16.</b> An asymmetric chlorolactonization reaction mediated by <b>I-74</b> /(DHQD) <sub>2</sub> PHAL .....                       | 25 |
| <b>Scheme I-17.</b> (DHQD) <sub>2</sub> PHAL catalyzed asymmetric chlorocyclization of allylic amides amides and carbamates .....            | 27 |

|   |    |
|---|----|
| <b>Scheme I-18.</b> The <b>I-83/I-84</b> mediated asymmetric iodolactonization of 5-aryl-5-hexenoic acids                             | 28 |
| <b>Scheme I-19.</b> Enantioselective bromolactonization of <i>Z</i> -1,3-enynes catalyzed by <b>I-88</b>                              | 30 |
| <b>Scheme I-20.</b> <b>I-93</b> catalyzed enantioselective bromolactonization   | 31 |
| <b>Scheme I-21.</b> Chiral anionic phase transfer catalyzed fluorocyclization of unsaturated amides                                   | 32 |
| <b>Scheme I-22.</b> SnCl <sub>4</sub> /DIPT catalyzed chiral halohydrin synthesis from cycloalkenes in the presence of TMSCl and BTSP | 34 |
| <b>Scheme I-23.</b> Sc(OTf) <sub>3</sub> / <b>I-104</b> catalyzed intermolecular asymmetric bromoamination of chalcones               | 35 |
| <b>Scheme I-24.</b> The first catalytic enantioselective intermolecular bromoesterification reaction                                  | 36 |
| <b>Scheme I-25.</b> (DHQD) <sub>2</sub> PHAL catalyzed intermolecular bromoesterification of allylic sulfonamides                     | 36 |
| <b>Scheme I-26.</b> Asymmetric dichlorination of <b>I-112</b> mediated by <b>I-113</b>  | 37 |
| <b>Scheme I-27.</b> Enantioselective vicinal dichlorination of <b>I-115</b> mediated by <b>I-116</b> /BH <sub>3</sub> complex         | 38 |
| <b>Scheme I-28.</b> (DHQD) <sub>2</sub> PHAL/ <b>I-120</b> mediated enantioselective dichlorination of cinnamyl alcohols              | 39 |
| <b>Scheme I-29.</b> Enantioselective dibromination of allylic alcohols mediated by <b>I-124/I-125</b> complex                         | 40 |
| <b>Scheme II-1.</b> Komatsu's synthesis of chiral oxazolines <i>via</i> interrupted asymmetric nitrene transfer to olefins            | 49 |
| <b>Scheme II-2.</b> An organocatalytic asymmetric chlorolactonization reaction reported by Whitehead <i>et.al.</i>                    | 50 |
| <b>Scheme II-3.</b> Goodman and Winstein's demonstration of bromocyclization of <i>N</i> -allylbenzamide to oxazoline heterocycles    | 52 |
| <b>Scheme II-4.</b> Taguchi's iodocyclization of <b>II-11</b> to <b>II-14</b>   | 52 |
| <b>Scheme II-5.</b> Ruling out <b>II-16</b> as a precursor to <b>II-15</b>  | 54 |
| <b>Scheme II-6.</b> Asymmetric chlorocyclization of <b>II-18</b> under optimized reaction conditions                                  | 72 |

|  |     |
|--|-----|
| <b>Scheme II-7.</b> Establishment of the absolute stereochemistry of <b>II-30-B</b> after hydrolysis .....                     | 78  |
| <b>Scheme II-8.</b> Non-catalyzed chlorocyclization of <b>II-52-A</b> .....  | 83  |
| <b>Scheme II-9.</b> Asymmetric chlorocyclization of <b>II-52</b> and <b>II-55-A</b> under ‘optimized’ reaction conditions..... | 84  |
| <b>Scheme II-10.</b> Gram-scale asymmetric chlorocyclization reactions.....  | 88  |
| <b>Scheme II-11.</b> Acid hydrolysis of oxazoline and dihydrooxazine heterocycles .....  | 89  |
| <b>Scheme II-12.</b> Selenocyclization reaction of <b>II-18</b> .....  | 100 |
| <b>Scheme II-13.</b> Preliminary studies of the chlorocyclization of carbamates <b>II-69</b> and <b>II-71</b> .....            | 102 |
| <b>Scheme II-14.</b> Solvent dependent enantiodivergence in the chlorocyclization of <b>II-69</b> .....                        | 102 |
| <b>Scheme II-15.</b> Chemical transformation of oxazolidinone product <b>II-70</b> .....                                       | 107 |
| <b>Scheme II-16.</b> Proposed synthesis of Mycestericin A from dihydrooxazine <b>II-84</b> .....                               | 109 |
| <b>Scheme III-1.</b> Enantioselective chlorocyclization of unsaturated amides.....   | 164 |
| <b>Scheme III-2.</b> Kinetic resolution in an iodolactonization reaction .....   | 168 |
| <b>Scheme III-3.</b> Kinetic resolution in a 4- <i>exo</i> -bromolactonization reaction .....                                  | 169 |
| <b>Scheme III-4.</b> Matched and mismatched substrates for kinetic resolution with (DHQD) <sub>2</sub> PHAL.....               | 182 |
| <b>Scheme III-5.</b> Determination of absolute stereochemistry of cyclized products.....                                       | 183 |
| <b>Scheme III-6.</b> Chemical transformations of products and recovered substrates.....  | 197 |
| <b>Scheme III-7.</b> Development of a tandem one-pot kinetic resolution/diastereoselective iodocyclization cascade .....       | 198 |
| <b>Scheme III-8.</b> Preliminary result of desymmetrization of <b>III-55</b> via chlorocyclization.....                        | 209 |
| <b>Scheme III-9.</b> Fate of <b>III-58</b> under reaction conditions .....   | 212 |
| <b>Scheme IV-1.</b> Results of the test reaction with best conditions thus far .....   | 288 |
| <b>Scheme IV-2.</b> Evaluation of electronically tuned nucleophiles in the carbocyclization reaction .....                     | 304 |
| <b>Scheme IV-3.</b> Synthetic approaches to the substrates for the carbocyclization chemistry .....                            | 313 |

|   |     |
|---|-----|
| <b>Scheme IV-4.</b> Proposed routes for varying C6 substituents of the dimeric catalyst.....                        | 316 |
| <b>Scheme V-1.</b> Reactivity of orthoesters.....   | 351 |
| <b>Scheme V-2.</b> Conversion of chiral diols to epoxides through the intermediacy of cyclic orthoester.....        | 352 |
| <b>Scheme V-3.</b> Interception of acetoxonium ions by phenol nucleophiles.....                                     | 353 |
| <b>Scheme V-4.</b> Anionic cobalt complexes as viable nucleophiles for intercepting acetoxonium.....                | 354 |
| <b>Scheme V-5.</b> Intramolecular capture of acetoxonium ions by pendant alcohols.....                              | 355 |
| <b>Scheme V-6.</b> Nucleophilic addition of enol-equivalents into acetoxonium ions.....                             | 356 |
| <b>Scheme V-7.</b> Intramolecular capture of acetoxonium ions by pendant silyl-enol ethers.....                     | 357 |
| <b>Scheme V-8.</b> Exploration of dithiols as nucleophiles in orthoester chemistry.....                             | 358 |
| <b>Scheme V-9.</b> Mechanism of 1,2-aryl ring migration in cyclic acetoxonium ions.....                             | 359 |
| <b>Scheme V-10.</b> Characterization of the primary products of the semi-pinacol rearrangement of <b>V-39</b> ..... | 360 |
| <b>Scheme V-11.</b> Synthesis of enantioenriched vicinal diols.....   | 364 |
| <b>Scheme V-12.</b> Semi-pinacol rearrangements of enantioenriched cyclic acetoxonium ions.....                     | 365 |
| <b>Scheme V-13.</b> Proposed arylation of cyclic acetoxonium ions.....  | 366 |
| <b>Scheme V-14.</b> Synthesis of precursor <b>V-79</b> for arylation of acetoxonium ions.....                       | 366 |
| <b>Scheme V-15.</b> The unexpected trimerization of <b>V-79</b> to <b>V-81</b> .....                                | 367 |
| <b>Scheme V-16.</b> Attempted nucleophilic interception of putative <i>p</i> -quinone methide intermediate.....     | 368 |
| <b>Scheme V-17.</b> BF <sub>3</sub> •OEt <sub>2</sub> mediated dehydrative trimerization of <b>V-77</b> .....       | 369 |
| <b>Scheme V-18.</b> Synthesis and dehydrative trimerization of <b>V-88</b> and <b>V-89</b> .....                    | 370 |
| <b>Scheme V-19.</b> Synthesis and attempted arylation of orthoester derived from <b>V-94</b> .....                  | 371 |
| <b>Scheme V-20.</b> A Ritter-type reaction of orthoester <b>V-101</b> .....   | 372 |
| <b>Scheme V-21.</b> Sulfonamide as an intermolecular nucleophilic trap for acetoxonium ions.....                    | 373 |

|   |     |
|---|-----|
| <b>Scheme V-22.</b> Attempted synthesis of oxazoline and imidazolinone heterocycles<br>from orthoesters.....                | 374 |
| <b>Scheme V-23.</b> Investigation of amides, carbamates and sulfonamides as nucleophilic<br>traps for acetoxonium ions..... | 375 |

## KEY TO SYMBOLS AND ABBREVIATIONS

|                                  |   |
|----------------------------------|---|
| $\alpha$                         | Angle of rotation                       |
| $[\alpha]$                       | Specific rotation                       |
| $[\alpha]_D$                     | Specific rotation at 589 nm             |
| Å                                | Angstrom                                |
| Ac                               | Acetyl                                  |
| AcCl                             | Acetylchloride                          |
| AcOH                             | Acetic acid                             |
| $[(\text{allyl})\text{PdCl}]_2$  | Allylpalladium (II) chloride dimer      |
| Alk                              | Alkyl                                   |
| aq                               | Aqueous                                 |
| Ar                               | Aryl, Argon                             |
| $\text{ArSO}_2\text{Cl}$         | Arylsulfonylchloride                    |
| $\text{BBr}_3$                   | Boron tribromide                        |
| $\text{BH}_3 \cdot \text{SMe}_2$ | Borane dimethylsulfide                  |
| $\text{BF}_4^-$                  | Tetrafluoroborate                       |
| $\text{BF}_3 \cdot \text{OEt}_2$ | Boron trifluoride diethyl etherate      |
| Bn                               | Benzyl                                  |
| BnBr                             | Benzylbromide                           |
| Boc                              | <i>tert</i> -butyloxycarbonyl           |
| $(\text{Boc})_2\text{O}$         | <i>tert</i> -butyloxycarbonyl anhydride |
| brsm                             | Based on recovered starting material    |
| <i>t</i> -Bu                     | <i>tert</i> -butyl                      |

|                                     |  |
|-------------------------------------|--|
| $n\text{-BuLi}$                     | $n$ -butyllithium                                    |
| $t\text{-BuOH}$                     | <i>tert</i> -butanol                                 |
| $t\text{-BuOCl}$                    | <i>tert</i> -butylhypochlorite                       |
| Bz                                  | Benzoyl  |
| C                                   | Celsius  |
| $\text{CCl}_4$                      | Carbon tetrachloride                                 |
| $\text{CaH}_2$                      | Calcium hydride                                      |
| $(\text{CD})_3\text{Tz}$            | Cinchonidine triazine-1,3,5-triyl ether              |
| $(\text{CD})_2\text{-OMe-Tz}$       | Cinchonidine triazine-1-methoxy-3,5-diyl ether       |
| $(\text{CD})_2\text{PHAL}$          | Cinchonidine 1,4-phthalazinediyl ether               |
| $(\text{CN})_2\text{PYDZ}$          | Bis-(cinchonine)-3,6-pyridazine                      |
| Cl                                  | chloro-  |
| $\text{ClCH}_2\text{CH}_2\text{Cl}$ | 1,2-dichloroethane                                   |
| $\text{CH}_3\text{CCl}_3$           | 1,1,1-trichloroethane                                |
| $\text{CH}_2\text{Cl}_2$            | Dichloromethane                                      |
| $\text{CHCl}_3$                     | Chloroform   |
| CO                                  | Carbon monoxide, carbonyl                            |
| $\text{Co}_2(\text{CO})_8$          | Dicobalt octacarbonyl                                |
| CuI                                 | Copper Iodide  |
| $\Delta$                            | Change   |
| $\Delta G$                          | Change of Gibbs free energy                          |
| $\Delta G^\ddagger$                 | Change of Gibbs free energy for the transition state |

|  |   |
|--|---|
| $\Delta H^\ddagger$                      | Change of enthalpy free energy for the transition state |
| $\Delta S^\ddagger$                      | Change of entropy free energy for the transition state  |
| d  | Doublet   |
| dd                                       | Doublet of doublets                                     |
| ddd                                      | Doublet of doublet of doublets                          |
| DABCO                                    | 1,4-Diazabicyclo[2.2.2]octane                           |
| DBU                                      | 1,8-diazabicyclo[5.4.0]undec-7-ene                      |
| DCDMH                                    | 1,3-Dichloro-5,5-dimethylhydantoin                      |
| DCDPH                                    | 1,3-dichloro-5,5-diphenylhydantoin                      |
| DCE                                      | 1,2-dichloroethane                                      |
| DCH                                      | 1,3-dichlorohydantoin                                   |
| DDQ                                      | 2,3-dichloro-5,6-dicyano-1,4-benzoquinone               |
| DIAD                                     | Diisopropyl azodicarboxylate                            |
| (DHQ) <sub>2</sub> AQN                   | Hydroquinine anthraquinone-1,4-diyl ether               |
| (DHQD) <sub>2</sub> (benzo-PHAL)         | Hydroquinidine 7,8-benzophthalazine-1,4-diyl ether      |
| (DHQD) <sub>2</sub> Cl <sub>2</sub> PHAL | Hydroquinidine 7,8-dichlorophthalazine-1,4-diyl ether   |
| (DHQD) <sub>2</sub> PHAL                 | Hydroquinidine 1,4-phthalazinediyl ether                |
| (DHQD) <sub>2</sub> PYDZ                 | Bis-(dihydroxyquinidine)-3,6-pyridazine                 |
| ( <i>i</i> Pr-DHQD) <sub>2</sub> PYDZ    | Bis-(6-isopropoxydihydroxyquinidine)-3,6-pyridazine     |
| DMAP                                     | <i>N,N</i> -4-(dimethylamino)pyridine                   |
| DMA                                      | <i>N,N</i> -dimethylacetamide                           |
| DME                                      | 1,2-dimethoxyethane                                     |
| DMF                                      | <i>N,N</i> -dimethylformamide                           |

|                               |                       |
|-------------------------------|-----------------------|
| DMSO                          | Dimethylsulfoxide     |
| dt                            | Doublet of triplets   |
| E                             | Energy                |
| ee                            | Enantiomeric excess   |
| e.g.                          | exempli gratia        |
| EI                            | Electron impact       |
| equiv                         | Equivalents           |
| etc                           | Et cetera             |
| Et <sub>3</sub> N             | Triethylamine         |
| Et <sub>2</sub> O             | Diethyl ether         |
| EtOAc                         | Ethyl acetate         |
| EtOH                          | Ethanol               |
| eV                            | Electron volts        |
| g                             | Gram                  |
| h                             | Hour                  |
| H                             | Proton                |
| H <sub>2</sub>                | Hydrogen              |
| HCO <sub>2</sub> H            | Formic acid           |
| H <sub>2</sub> O              | Water                 |
| H <sub>2</sub> O <sub>2</sub> | Hydrogen peroxide     |
| HCl                           | Hydrochloric acid     |
| HClO <sub>4</sub>             | Perchloric acid       |
| HFIP                          | Hexafluoroisopropanol |

|   |   |
|---|---|
| H <sub>2</sub> SO <sub>4</sub>                                  | Sulfuric acid   |
| Hz  | Hertz   |
| HMPA  | Hexamethylphosphoramide                                     |
| HPLC  | High pressure liquid chromatography                         |
| HRMS  | High-resolution mass spectrometry                           |
| HSiMe <sub>3</sub>  | Hydrotrimethylsilane  |
| I   | iodo-   |
| I <sub>2</sub>  | Iodine  |
| i.e   | id est  |
| <i>i</i> -PrCN  | Iso-butyronitrile   |
| IR  | Infrared spectroscopy                                       |
| Ir  | Iridium   |
| <i>J</i>  | Coupling constant   |
| K <sub>a</sub>  | Constant of association, binding affinity, binding constant |
| K <sub>2</sub> CO <sub>3</sub>                                  | Potassium carbonate   |
| KHMDS   | Potassium hexamethyldisilazide                              |
| K <sub>2</sub> O <sub>5</sub> O <sub>2</sub> ·2H <sub>2</sub> O | Potassium osmate(IV) dihydrate                              |
| KOAc  | Potassium acetate   |
| KOH   | Potassium hydroxide   |
| K <sub>3</sub> PO <sub>4</sub>                                  | Potassium phosphate   |
| L   | Liter   |
| LAH   | Lithium aluminum hydride                                    |
| m   | Multiplet   |
| M   | Molar   |

|                                   |  |
|-----------------------------------|--|
| M <sup>+</sup>                    | Mass with positive charge              |
| [M+H] <sup>+</sup>                | Mass + hydrogen with a positive charge |
| m/z                               | Mass per charge                        |
| Me                                | Methyl                                 |
| MeC(OMe) <sub>3</sub>             | Trimethyl orthoacetate                 |
| MeCN                              | Acetonitrile                           |
| MeOH                              | Methanol                               |
| MeNO <sub>2</sub>                 | Nitromethane                           |
| MeSO <sub>2</sub> NH <sub>2</sub> | Methansulfonamide                      |
| mg                                | Milligram                              |
| MgSO <sub>4</sub>                 | Magnesium sulfate                      |
| MHz                               | Megahertz                              |
| min                               | Minute                                 |
| mL                                | Milliliter                             |
| mmol                              | Millimole                              |
| MnO <sub>2</sub>                  | Magnesium dioxide                      |
| mol                               | Mole                                   |
| MsCl                              | Mesitylchloride                        |
| MTBE                              | Methyl <i>t</i> -butyl ether           |
| N <sub>2</sub>                    | Nitrogen                               |
| NBS                               | <i>N</i> -bromosuccinimide             |
| NCS                               | <i>N</i> -chlorosuccinimide            |
| NaH                               | Sodium hydride                         |

|                                    |   |
|------------------------------------|---|
| NaHCO <sub>3</sub>                 | Sodium bicarbonate                        |
| NCSach                             | <i>N</i> -chlorosaccharin                 |
| NIS                                | <i>N</i> -iodosuccinimide                 |
| NaOH                               | Sodium Hydroxide                          |
| Na <sub>2</sub> SO <sub>4</sub>    | Sodium sulfate                            |
| NCP                                | <i>N</i> -chlorophthalimide               |
| nd                                 | not determined                            |
| NH <sub>4</sub> Cl                 | Ammonium chloride                         |
| NMO                                | 4-methylmorpholine <i>N</i> -oxide        |
| NMR                                | Nuclear magnetic resonance                |
| NSO <sub>2</sub> Bph               | <i>N</i> -biphenylsulfonyl                |
| NSO <sub>2</sub> Nap               | <i>N</i> -naphthylsulfonyl                |
| NTs                                | <i>N</i> -toluenesulfonyl                 |
| Nu                                 | Nucleophile                               |
| O <sub>2</sub>                     | Oxygen                                    |
| OMe                                | Methoxy                                   |
| OsO <sub>4</sub>                   | Osmium tetroxide                          |
| <i>p</i>                           | Para-                                     |
| Pd                                 | Palladium                                 |
| Pd/C                               | Palladium on Charcoal                     |
| Pd(OH) <sub>2</sub> /C             | Palladium hydroxide on Charcoal           |
| Pd(PPh <sub>3</sub> ) <sub>4</sub> | Palladium(0) tetrakis(triphenyl)phosphine |
| PG                                 | Protecting group                          |

|                               |  |
|-------------------------------|--|
| Ph                            | Phenyl                                   |
| PhCF <sub>3</sub>             | Trifluorotoluene                         |
| PhCH <sub>3</sub>             | Toluene                                  |
| PhCl                          | Chlorobenzene                            |
| PhNCO                         | Phenylisocyanate                         |
| POCl <sub>3</sub>             | Phosphorous oxychloride                  |
| P <sub>2</sub> O <sub>5</sub> | Diphosphorus pentoxide                   |
| PPh <sub>3</sub>              | Triphenylphosphine                       |
| PPTS                          | Pyridinium <i>para</i> -toluenesulfonate |
| ppm                           | Parts per million                        |
| <i>n</i> -PrNO <sub>2</sub>   | Nitropropane                             |
| quant                         | Quantitative                             |
| qt                            | Quartet of triplets                      |
| R                             | Gas constant                             |
| rt                            | Room temperature                         |
| s                             | Singlet                                  |
| sat                           | Saturated                                |
| SES                           | Trimethylsilylethanesulfonyl             |
| t                             | Triplet                                  |
| TBAI                          | Tetrabutylammonium iodide                |
| TBS                           | <i>tert</i> -butyldimethylsilyl          |
| TCCA                          | Trichloroisocyanuric acid                |
| TES                           | Triethylsilyl                            |

|   |  |
|---|--|
| TFA                                       | Trifluoroacetic acid   |
| TFE                                       | 1,1,1-trifluoroethane, $\text{CF}_3\text{CH}_2\text{OH}$                 |
| THF                                       | Tetrahydrofuran  |
| THP                                       | Tetrahydropyran  |
| $\text{TiCl}_4$                           | Titanium(IV) chloride  |
| $\text{Ti}(\text{O}i\text{Pr})_4$         | Titanium(IV) isopropoxide  |
| TLC                                       | Thin-layer chromatography  |
| TMEDA                                     | Tetramethylethylenediamine   |
| TMS                                       | Trimethylsilyl   |
| TMSBr                                     | Trimethylsilyl bromide   |
| TMSCl                                     | Trimethylsilyl chloride  |
| TMSOMe                                    | Trimethylsilyl methoxide   |
| $\text{TsNNaCl}\cdot 3\text{H}_2\text{O}$ | Chloramine-T, <i>N</i> -Chloro- <i>p</i> -toluenesulfonamide sodium salt |
| $\text{TsNCl}_2$                          | Dichloramine-T, <i>N,N</i> -Dichloro- <i>p</i> -toluenesulfonamide       |
| Trityl                                    | Triphenylmethyl  |
| Ts  | Tosyl, toluenesulfonyl   |
| TsCl                                      | Tosylchloride  |
| $\text{TsNH}_2$                           | <i>para</i> -toluenesulfonamide  |
| $\mu\text{L}$                             | Microliter   |
| UV-Vis                                    | Ultraviolet-Visible Spectroscopy   |
| XRD                                       | X-Ray Dispersion   |
| xs  | Times  |

## Chapter I

### ***Reagent controlled asymmetric halogenation of alkenes: A brief overview***

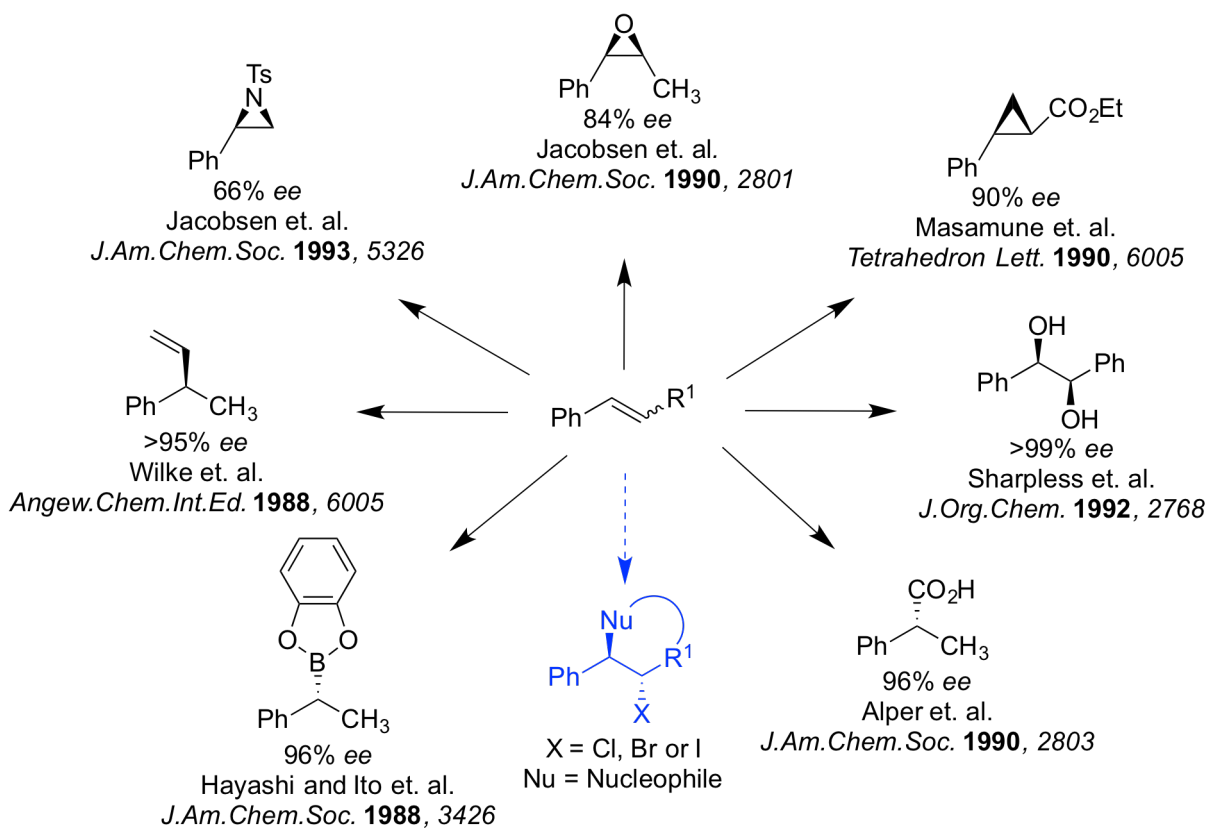
#### **I.1. Introduction.**

Alkenes are amongst the most versatile synthetic building blocks in organic chemistry. Nucleophilic, electrophilic and radical functionalization of alkenes are well-established transformations.<sup>1</sup>

Over the last 4 decades, catalytic, enantioselective alkene functionalization reactions have gained in prominence. Many landmark discoveries in organic chemistry have dealt with the asymmetric functionalization of alkenes; these include asymmetric alkene dihydroxylation, epoxidation, aziridination, reduction, hydroformylations, cyclopropanations, metathesis reactions and many others. Some of the seminal examples of asymmetric variants of the aforementioned reactions are schematically represented in Figure I-1.

All this progress notwithstanding, a stereotypical difunctionalization of alkenes namely the halocyclization reaction has witnessed limited success in terms of developing enantioselective variants (see the transformation highlighted in blue in Figure I-1). Catalytic asymmetric halofunctionalization of alkenes has remained an elusive and long sought after transformation in organic chemistry. Despite being one of the most frequently encountered electrophiles in organic chemistry, rendering a halonium ion 'chiral' is evidently a non-trivial challenge.

**Figure I-1** Representative examples of catalytic asymmetric alkene functionalization reactions



## I.2. Nomenclature of species encountered in alkene halogenation reactions.

Prior to a detailed account of the historical and current developments in this research area, a brief digression is in order to clarify the nomenclature that will be used for the numerous species encountered in alkene halogenation reactions.

Per convention, *hypocoordinate* ions retain the '-enium' suffix and are referred to as '*halenium ions*'; for example naked I<sup>+</sup>, Br<sup>+</sup> and Cl<sup>+</sup> ions will be referred to as iodenium, bromenium and chlorenium ions respectively. All *hypercoordinate* ions are indistinguishably referred to as '*halonium ions*' in accordance with the '-onium' nomenclature for such species. In order to further distinguish amongst the numerous hypercoordinate species, classical prefixes are used. A few representative examples are shown in Figure I-2. It must be emphasized that

most references to hypercoordinate halogen ions encountered in this chapter and in the rest of this thesis will be the ‘haliranium ions’ derived from the halogenation of alkenes. These species will be referred to ‘halonium ions’ unless a distinction is needed for clarity.

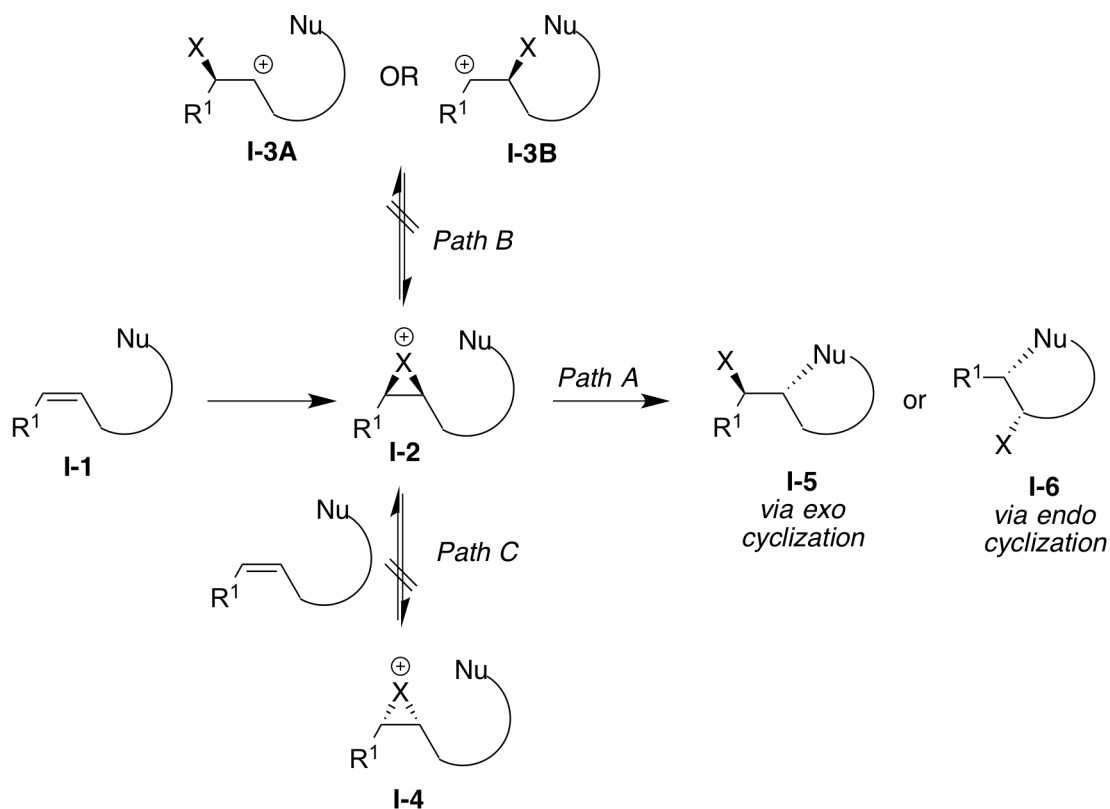
**Figure I-2** Nomenclature of halogen ions

| Species  | Nomenclature      | Example  |   |   |
|--|-------------------|--|---|---|
| $\overset{\oplus}{\text{X}}$   | <i>halenium</i>   | $\overset{\oplus}{\text{Cl}}$<br><i>chlorenium</i>   | $\overset{\oplus}{\text{I}}$<br><i>iodenium</i> | $\overset{\oplus}{\text{Br}}$<br><i>bromenium</i> |
| $\text{R}-\overset{\oplus}{\text{X}}-\text{R}$   | <i>halonium</i>   | $\overset{\oplus}{\text{I}}$<br><br><i>iodonium</i>       |   |   |
| $\overset{\oplus}{\text{X}}$<br>  | <i>haliranium</i> | $\overset{\oplus}{\text{Br}}$<br><br><i>bromiranium</i>   |   |   |
| $\overset{\oplus}{\text{X}}$<br> | <i>halirenium</i> | $\overset{\oplus}{\text{Cl}}$<br><br><i>chlorirenium</i> |   |   |

### I.3. Mechanistic considerations for the asymmetric halogenation of alkenes.

If successful, asymmetric halogenation reaction of alkenes will have tremendous implications due to the synthetic utility of the products. Nonetheless, this transformation is yet to witness the generality or the success of many other oxidative and reductive asymmetric alkene functionalization reactions. This is certainly not attributable to a lack of interest in enantioselective olefin halogenation. Numerous approaches to achieve this goal have been made over the years; these efforts will be summarized in subsequent sections. This state of affairs is more likely due to the challenges associated with this reaction on a mechanistic level; the factors that dictate the kinetic and stereochemical stability of chiral halonium ions are only now being understood.

**Scheme I-1.** A stereotypical enantioselective halocyclization reaction



A stereotypical enantioselective halocyclization reaction of **I-1** to **I-5** or **I-6** is shown in Scheme I-1. A classical text-book mechanism for such a transformation would require a face-selective delivery of the halonium ion ( $X^+$ ) on the olefin functionality followed by an intramolecular opening of the resulting halonium ion intermediate **I-2** to give the cyclized products (Path A in Scheme I-1). Many assumptions are implicit in such a mechanistic scenario. First, the face-selectivity in the alkene halogenation event dictates the enantioselectivity of the final product i.e., once the stereochemistry of **I-2** is established, processes leading to stereorandomization of **I-2** (such as racemization via degenerate olefin-to-olefin halonium transfer; see Path C in Scheme I-1) are either unavailable or negligibly slow. Second, isomerization of **I-2** to  $\beta$ -halocarbenium ions (**I-3A** or **I-3B**) is not a competing process

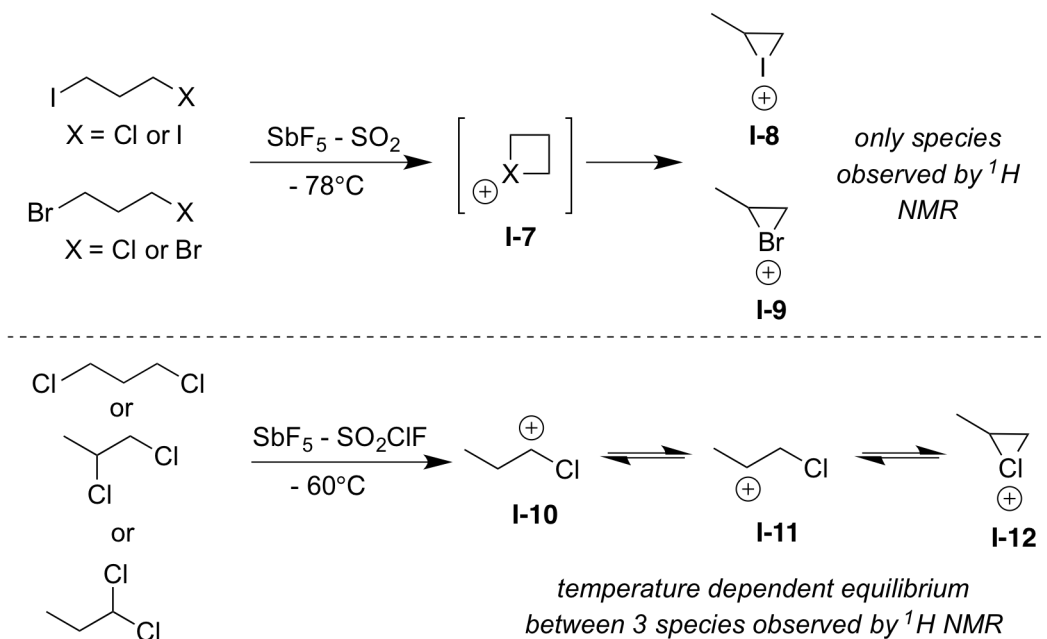
thereby precluding the possibility of formation of a constitutional isomer of the product (see Path B in Scheme I-1). Third, the opening of the halonium ion by the pendant nucleophile proceeds with an inversion at the center that undergoes the nucleophilic attack i.e. the net addition of the halogen atom and the nucleophile will always be *anti* with respect to each other.

If all these criteria are met, asymmetric halocyclization reactions ought to work efficiently. Seemingly, the biggest challenge in these reactions is to enable a face-selective alkene halogenation (i.e. a problem confined to catalyst design and asymmetric catalysis). Nonetheless, studies by numerous research groups, including ours, seem to suggest that a highly face-selective alkene halogenation is *not* a sufficient condition to render these reactions enantioselective. The putative chiral halonium ions are both chemically and stereochemically labile. Studies that have uncovered these phenomena are presented in the following sections. These results should convince the reader that the simplistic mechanistic paradigm for an asymmetric halocyclization as shown in Scheme I-1 is seldom realized and may very well be misleading if represented as such in certain instances.

### **I.3.1. Erosion of stereochemistry of halonium ions by olefin-to-olefin halonium transfer.**

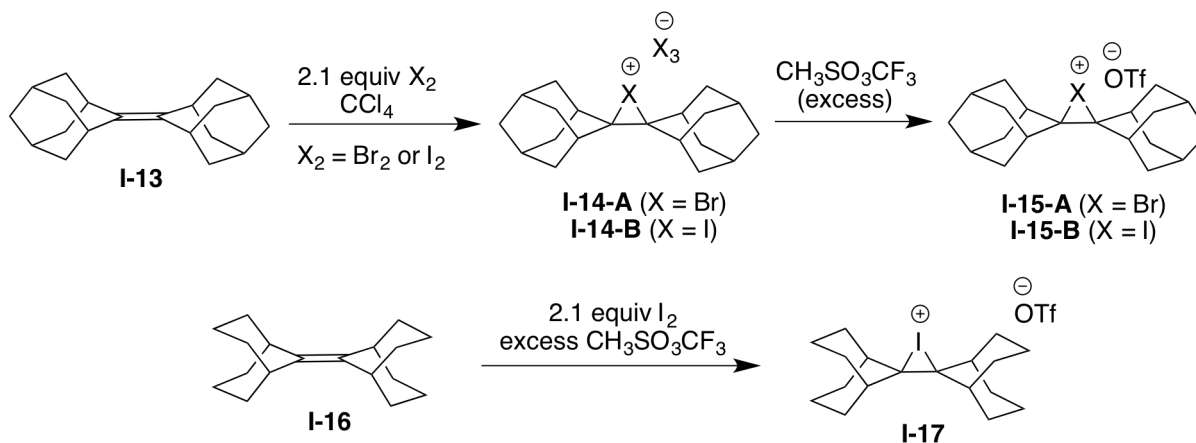
Roberts and Kimball were the first to propose the intermediacy of cyclic halonium ions in alkene halogenation reactions in 1937.<sup>2</sup> It was not until 1967 that the first experimental evidence for the existence of cyclic halonium ions emerged.

**Scheme I-2.** The generation and NMR characterization of halonium ions



Olah and co-workers were able to synthesize and characterize numerous halonium ions at cryogenic temperatures using  $^1\text{H}$  NMR studies.<sup>3-5</sup> One of the key observations of these seminal studies was the evidence that cyclic bromonium and iodonium ions (see **I-8** and **I-9** in Scheme I-2) were stable under the experimental conditions, but the analogous chloronium ions **I-12** exhibited a temperature dependent equilibrium between three different species. Furthermore, all three dichloride precursor isomers gave identical product distributions. The three species were assigned as the cyclic chloronium ion **I-12** and the two isomeric  $\beta$ -chlorocarbenium ions **I-10** and **I-11**. (Ohta and co-workers have recently revisited this work and shown that the observed NMR chemical shifts are not consistent with Olah's proposal for isomerization of **I-12** ions into **I-10** and **I-11**; an alternate hypothesis was put forward to explain the temperature dependent equilibrium, *vide infra*)

**Scheme I-3.** Synthesis and isolation of stable bromonium and iodonium salts

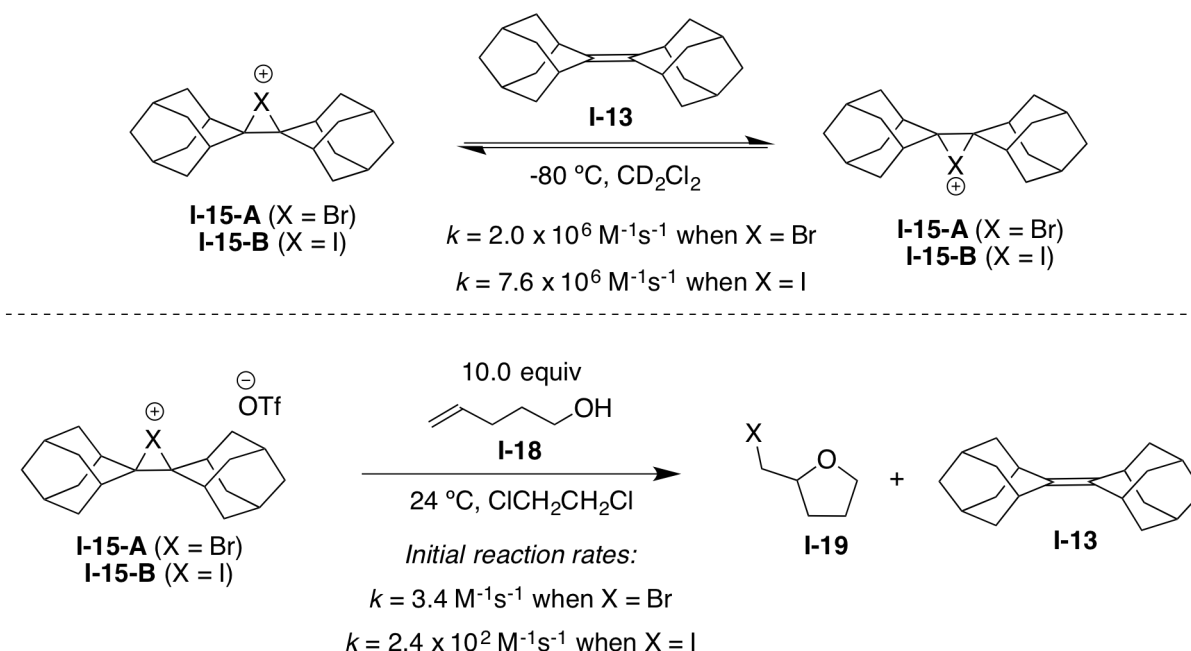


Yet another landmark discovery in this research area was the isolation and characterization of stable bromonium and iodonium ion salts of hindered alkenes by Brown and co-workers.<sup>6</sup> When adamantylene adamantane (**I-13** in Scheme I-3) is treated with molecular  $\text{Br}_2$  or  $\text{I}_2$  in non-polar solvents, the corresponding halonium salts (**I-14**) are formed in excellent yields. Similar reactions are also seen with the alkene **I-16**. It merits mention that Wynberg and co-workers had first synthesized and proposed the structure for **I-14-A** based on elemental analysis and mass spectrometry information in 1969.<sup>7</sup> Brown and co-workers were able to obtain conclusive evidence for the structure of **I-14-A**, **I-14-B** and the related salts **I-15** and **I-17** by NMR analysis and crystallographic means. In a series of studies, they were also able to demonstrate that alkene halogenation leading to the formation of the cyclic halonium ion is reversible for bromination and iodination reactions.

Furthermore, transfer of a halonium ion from the hindered species **I-15** to the parent alkene **I-13** was found to be diffusion controlled (these transfer rates were calculated to be in the order of  $10^6 \text{ M}^{-1} \text{ s}^{-1}$  based on line shape analysis of the NMR signals that characterize this rapid equilibrium; see Scheme I-4). Transfer of the halonium ion from **I-15** to a typical halocyclization

substrate such as **I-18** was also determined to be a facile process.<sup>8</sup> This transfer process was 30 – 100 fold faster for iodonium transfer as compared to analogous bromonium transfers depending on the substrate used for the halocyclization reaction. This single result underscores the enormity of the challenge for developing enantioselective variants of alkene halogenation reactions. Suppressing this practically barrierless olefin-to-olefin halonium transfer process is non-trivial and could lead to rapid racemization the chiral halonium ion even if it was initially formed in highly enantioenriched form.

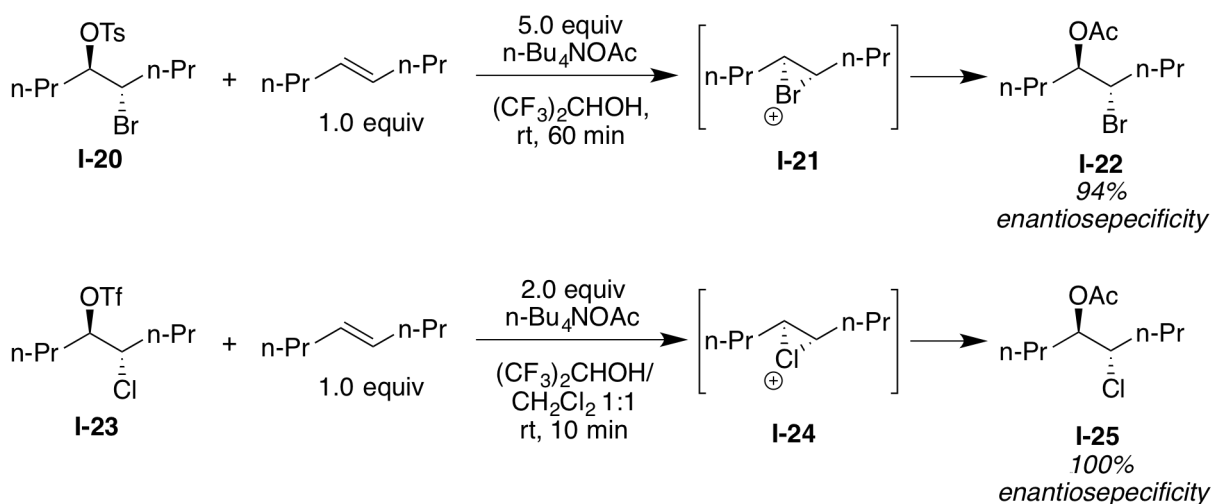
**Scheme I-4.** Demonstration of rapid olefin-to-olefin halonium transfer



Recently, Denmark and co-workers were able to demonstrate that olefin-to-olefin halonium transfer was indeed a challenge to be reckoned with for enantioselective bromination of alkenes. When the *in-situ* generated chiral bromonium ion **I-21** was intercepted by acetate nucleophiles (see Scheme I-5), noticeable erosion of stereospecificity was seen in the presence of 1.0 equivalent of added *trans*-4-octene. In contrast, the same reaction with enantioenriched

chloronium ion **I-24** was not susceptible to such a racemization process. The conjecture is that bromonium transfer from **I-21** to the added *trans*-4-octene is facile leading to the erosion of stereochemistry of **I-21**. A similar chloronium ion transfer from **I-24** to the *trans*-4-octene is likely not occurring at rates that outcompete the rate of the reaction.

**Scheme I-5.** Partial racemization of chiral halonium ions via olefin-to-olefin halonium transfer



At first blush, these results seem encouraging for the development of asymmetric chlorocyclization reactions. Unfortunately, the more reactive chloronium ions tend to rapidly isomerize to the corresponding  $\beta$ -chlorocarbenium ions that often lead to the formation of a mixture of products. Studies that have uncovered this phenomenon will be presented in the next section.

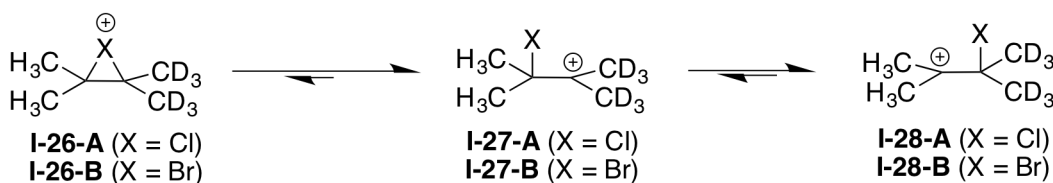
### I.3.2. Isomerization of halonium ions to halocarbenium ions.

Olah's group reported the first direct evidence for the isomerization of cyclic chloronium ions to the corresponding  $\beta$ -chlorocarbenium ions (see Scheme I-2). The same studies had ruled out such isomerization processes for bromonium and iodonium ions. When Ohta and co-workers revisited this study, their preliminary experimental results seemed to confirm the observations of Olah's group.<sup>9</sup> When the halonium ions **I-26-A** and **I-26-B** were generated

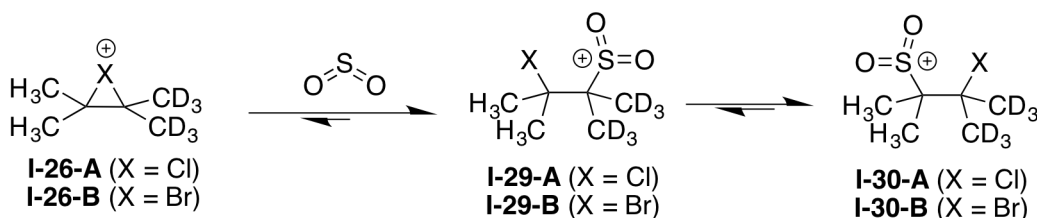
under the superacid conditions reported by Olah's group and characterized using cryogenic NMR studies, it seemed plausible that the species obtained after alkene chlorination and bromination is a rapidly equilibrating mixture of the open carbocation forms and not the bridged halonium ion intermediates (see structures **I-27** and **I-28** in Figure I-3).<sup>9</sup> The 'isotopic perturbation of degenerate equilibrium' phenomenon was used to verify this. The NMR spectra of asymmetrically labeled ions exhibited <sup>13</sup>C NMR shifts that were consistent with a perturbation of a rapid equilibrium rather than a singular structure such as a cyclic halonium ion.

**Figure I-3.** The fate of chloronium and bromonium ions as predicted by experiment and theory respectively

*Ohta's initial proposal of the fate of halonium ions in solution (see text for description)*



*Theoretically predicted revised proposal of the fate of halonium ions in liquid SO<sub>2</sub>*



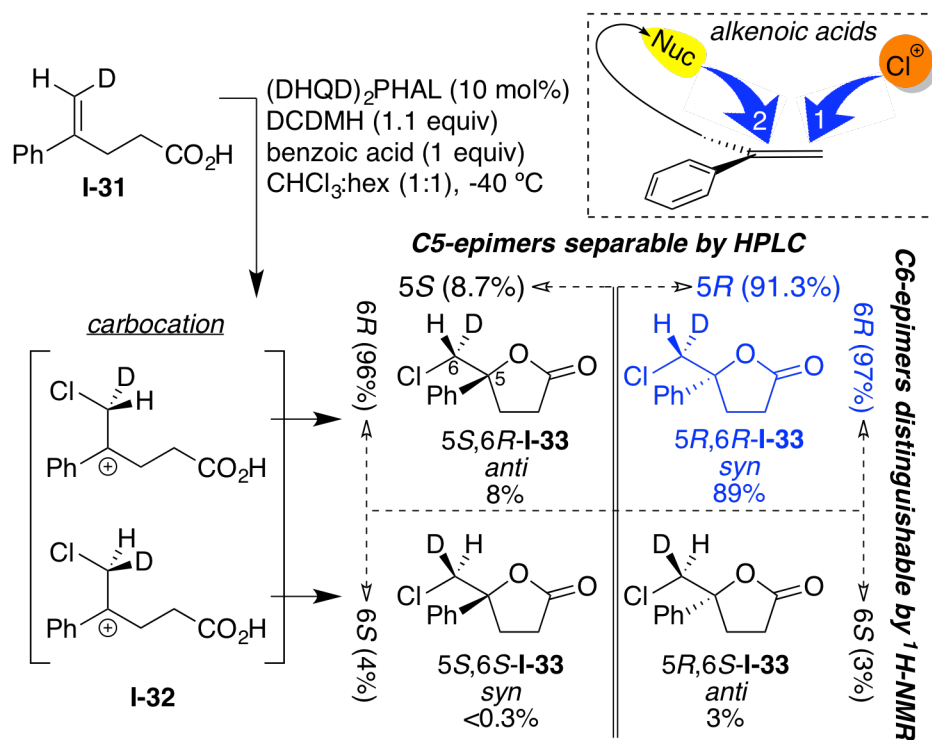
Nonetheless, computational studies predicted that cyclic halonium ions are significantly more stable than the isomerized carbocation ( $\beta$ -bromoethyl and  $\beta$ -chloroethyl carbocations were determined to be 15 kcal/mol higher in energy as compared to the corresponding halonium ions). Consequently, these experiments were revisited.<sup>10</sup> Ohta, Dudley and Scupp propose that the nucleophilicity of the super acid solvents (SO<sub>2</sub>, SO<sub>2</sub>ClF, SO<sub>2</sub>F<sub>2</sub>, etc.) used for the generation of the halonium ions cannot be ignored and that the nucleophilicity of these

molecules could be sufficiently high to intercept the putative halonium ions. In fact the reaction of liquid SO<sub>2</sub> with carbenium ions is well known.<sup>11,12</sup> They were able to demonstrate the theoretical feasibility of a '*syn*'-selective opening of the putative chloronium and bromonium ions to give species **I-29** and **I-30** (the *syn* selectivity was attributed to an intermolecular Cl-S interaction between the chloronium ion and S atom of the incoming SO<sub>2</sub> nucleophile). These species can better account for the observed chemical shifts of these halonium ions in solution. The initially observed temperature dependent equilibrium of different species by Olah and co-workers (see structures **I-10** and **I-11** in Scheme I-2) are now postulated to be a manifestation of a temperature dependent equilibrium between species analogous to **I-29** and **I-30**. Furthermore, the species **I-29** and **I-30** are neither halonium ions nor carbenium ions and are better described as sulfonium ions. They are postulated to be energetically comparable to the cyclic halonium ions and hence more stable than the corresponding β-halocarbenium ions. Although insightful, alternate systems are required to analyze halonium ions **I-26** that either account for or completely avoid the presence of competent nucleophiles in solution.

Recent results from our lab that suggests that face-selectivity in alkene halogenation may not even be *necessary* in certain instances of halocyclization reactions where the chiral catalyst can 'template' the cyclization of the nucleophile on to a β-chlorocarbenium ion.<sup>13</sup> The asymmetric chlorolactonization of the D-labeled substrate **I-31** under our previously optimized conditions<sup>14</sup> helped in determining both, the face selectivity in alkene chlorination as well as the % *syn* vs. *anti* addition across the alkene (see Figure I-4). Three of the four possible stereoisomers of the product **I-33** were formed in quantifiable amounts in this reaction. The fact that products obtained from the *syn* as well as *anti* additions were seen indicated that the classical notion of an *anti* specific opening of a chloronium ion might not be the only available

reaction pathway. Furthermore, 89% of the product came from a net *syn* addition across the alkene as opposed to only 11% from the classically expected *anti* addition. DFT calculations (B3LYP/6-31G\* basis set) have confirmed that the  $\beta$ -chlorocarbenium ion is the likely intermediate for this reaction; no minima could be found for the classical bridged chloronium ion intermediate even in the gas phase (where the only mode of stabilization for the carbocation is the neighboring non-bonding electron pairs on the chlorine atom that could lead to a bridged structure).

**Figure I-4.** Dissecting the stereochemical elements of the asymmetric chlorolactonization reaction by employing D-labeled substrate



These results confirm that the enantioselectivity of the quaternary stereocenter in the product (C5 in **I-33**) originates, not from a face selective chlorine delivery, but by the catalyst-controlled templating of the cyclization of the nucleophile on to a carbocation (i.e. the non-deuterated analogue of **I-32**) that is devoid of any stereocenter. Intriguingly, the face-selectivity of the chloronium delivery to the alkene was determined to be 97:3 favoring the *si*-face; but this

selectivity has no bearing on the determination of the C5 stereochemistry since any remnants of selectivity in the first step is lost during the formation of the open carbocation.

As evident from the studies above, a unified theory that explains the racemization and isomerization processes of chiral halonium ions has remained elusive till date. The choice of the system used for the study as well as the experimental approach employed have often led to conflicting notions regarding these phenomena. Perhaps the greatest discovery that has emerged from these studies is that asymmetric alkene halogenation reactions are mechanistically far more complex than previously imagined. Any approach to achieve this elusive transformation ought to address one or more challenges outlined above.

#### **I.4. Development of enantioselective halocyclization reactions.**

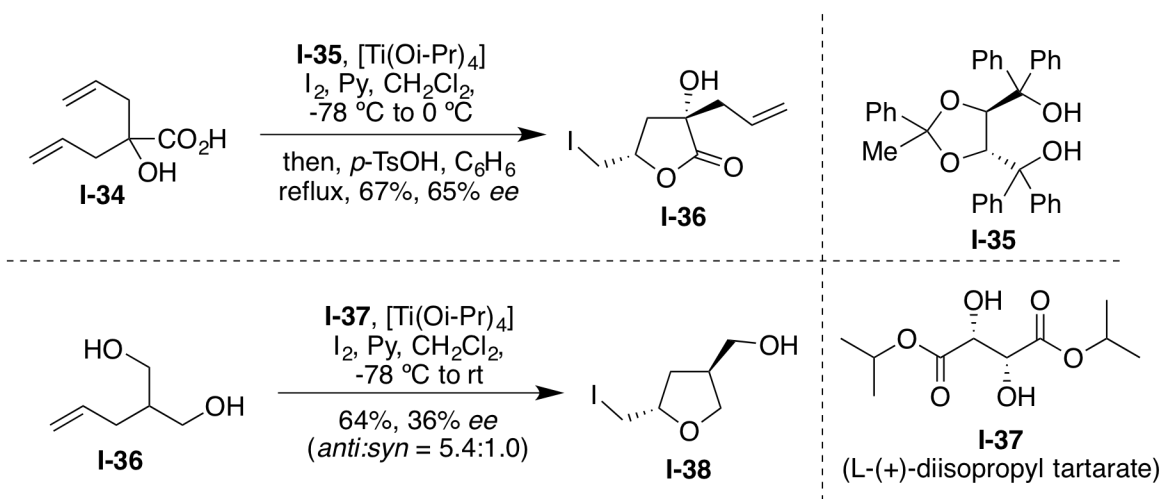
Many of the early reports of asymmetric alkene halogenation reactions relied on the use of chiral auxiliaries or stoichiometric quantities of chiral promoters for overcoming the challenges mentioned above. The chiral auxiliary based approaches will not be presented in this chapter. Instead, a brief overview of *reagent controlled* asymmetric halofunctionalization of alkenes will be presented in the subsequent sections. It is beyond the scope of this chapter to give an exhaustive survey of all asymmetric alkene halogenation reactions developed till date; instead, reactions that showcase the mechanistic underpinnings and diversity encountered in the development of such reactions will be highlighted. Halocyclization reactions that employ stoichiometric amounts of chiral promoters will be presented first followed by catalytic asymmetric variants. Emphasis will be placed on the intermolecular interaction between the substrate-catalyst or the halonium source-catalyst that was exploited for inducing enantioselectivity (for example hydrogen bonding, ion-pairing, phase transfer, etc.). Finally, some recent developments in the *intermolecular* capture of chiral halonium ions will be highlighted.

## I.4.1. Asymmetric halocyclizations that employ stoichiometric quantities of chiral promoters.

### I.4.1.1. Metal mediated enantioselective halocyclization.

Taguchi and co-workers reported the first reagent controlled halocyclization reaction (see Scheme I-6). The iodolactonization of **I-34** proceeded in 65% *ee* in the presence of stoichiometric amounts of  $\text{Ti}(i\text{-OPr})_4$  and the chiral diol ligand **I-35**.<sup>15</sup> Only one substrate was evaluated in that study. Although no binding model was proposed, the authors suggest that the hydroxy acid substrate could form a rigid five membered ring chelate with Ti, thereby anchoring the alkene in the chiral pocket of the Ti-diol complex. An attempted desymmetrization in an iodoetherification reaction of substrate **I-36** using a similar catalytic system (stoichiometric quantity of **I-37** as the chiral promoter instead of **I-35**) gave only 36% *ee* for the cyclized product and a moderate *anti:syn* ratio of 5.4:1.

**Scheme I-6.** First examples of reagent controlled asymmetric halocyclization reactions



### I.4.1.2. Chiral Lewis base mediated halocyclizations.

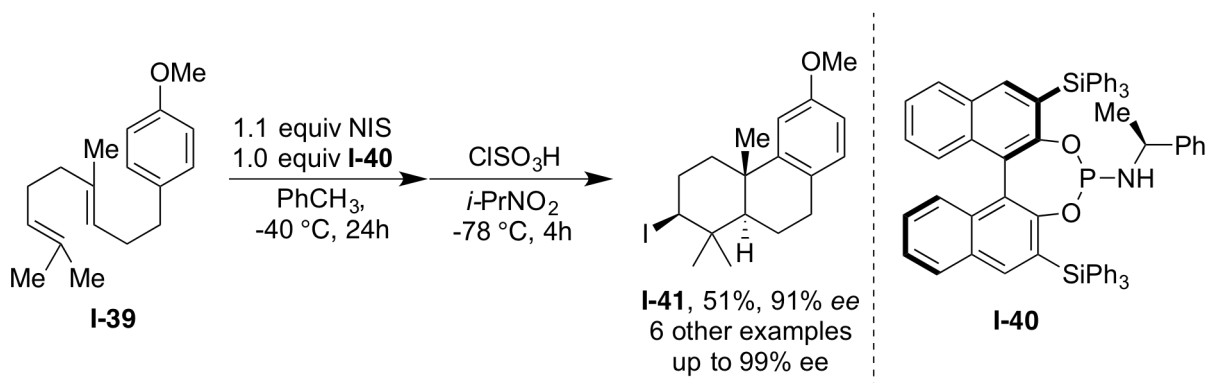
Many subsequent reports that utilized stoichiometric amounts of chiral promoters relied on a chiral Lewis base activation of the halonium source. The working hypothesis in these

instances was that the transfer of the halonium ion from the terminal halogen source to the Lewis basic site of the chiral catalyst should lead to a more active halonium source; face-selective transfer of the halonium ion to the alkene functional group will be dictated by the chirality confining the Lewis basic site.

Although seemingly simple and elegant, this approach has met with little success. The Ishihara and Gouverneur research groups have reported two of the more successful examples in this respect.

In 2007, Ishihara and co-workers disclosed a polyene cyclization cascade initiated by a chiral iodonium ion (see Scheme I-7).<sup>16</sup> In the presence of stoichiometric quantities of **I-40** as the chiral Lewis base promoter and NIS as the iodonium source, numerous polyene substrates underwent highly enantioselective iodocyclization cascade reactions to afford terpene-type skeletons in one step.

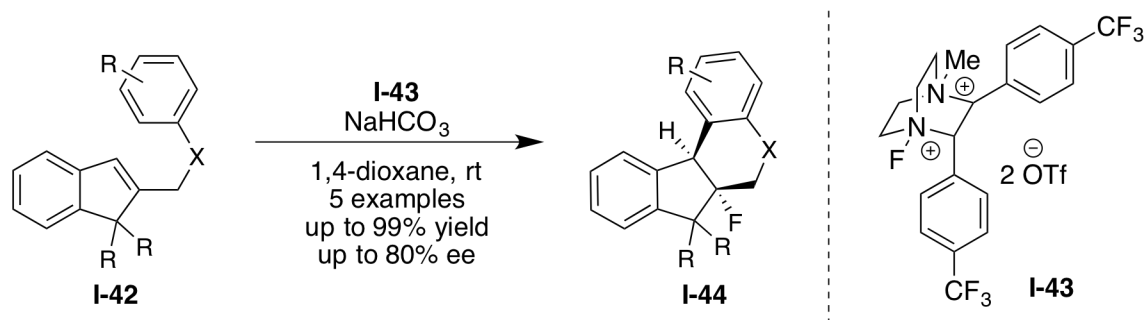
**Scheme I-7.** An asymmetric iodocarbocyclization cascade mediated by a stoichiometric chiral Lewis base



More recently, Gouverneur and coworkers have demonstrated that chiral analogs of Selectfluor® (see **I-43** in Scheme I-8) can be synthesized and employed as a stoichiometric chiral fluorenum source in carbocyclization reactions.<sup>17</sup> Although the substrate scope is

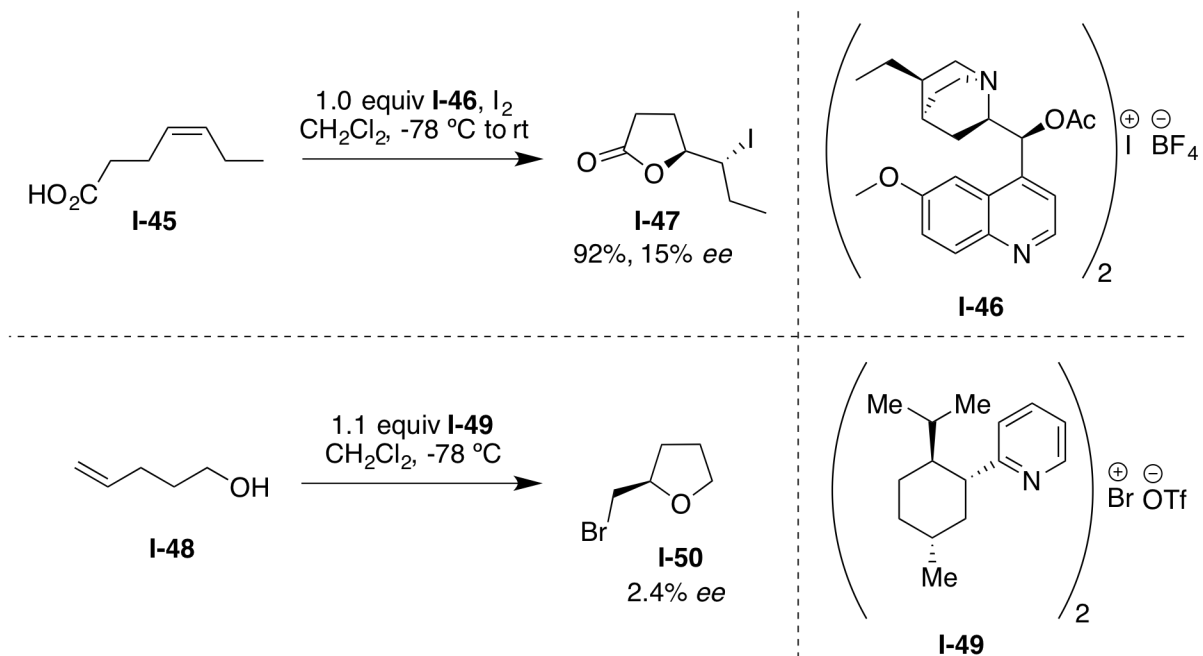
relatively narrow and enantioselectivities are moderate to high, this reaction showcases a rare example of a chiral Lewis base mediated asymmetric alkene halogenation reaction.

**Scheme I-8.** Chiral Selectfluor<sup>®</sup> analogs for asymmetric fluorocarbocyclization reactions



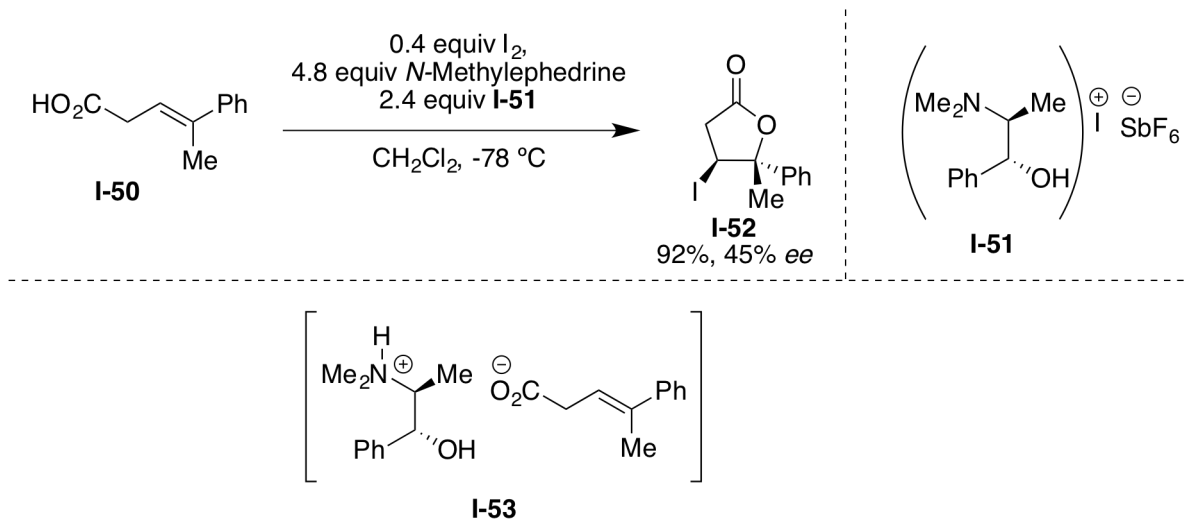
The two results presented above are especially impressive given that numerous attempts to use stoichiometric chiral halonium sources by Lewis base activation have met with little success in asymmetric alkene halogenation reactions. For example, Grossman and Trupp have shown that the iodolactonization reaction of **I-45** mediated a stoichiometric hydroquinidine- $\text{I}_2$  complex **I-46** proceeds in only 15% *ee* (see Scheme I-9).<sup>18</sup>

**Scheme I-9.** Early examples of stoichiometric chiral Lewis base promoted asymmetric halocyclization reactions



Likewise, Cui and Brown were unable to develop highly enantioselective variants of a bromoetherification reaction in the presence of stoichiometric quantities of the bromonium salt **I-49**. Substrate **I-48** was bromocyclized to **I-50** in only 2.4% *ee* in the presence of stoichiometric amounts of the chiral bromonium salt **I-49**.<sup>19</sup>

### Scheme I-10. 5-*endo*-iodolactonization promoted by I-51



Rousseau and co-workers disclosed that superstoichiometric quantities (2.4 equiv) of the chiral iodonium salt **I-51** derived from *N*-methylephedrine can promote iodolactonization reactions with moderate levels of enantioinduction (up to 45% *ee*, see Scheme I-10).<sup>20</sup> The authors rule out the possibility that the chiral ammonium salt **I-53** leads to the observed enantioselectivity; racemic product was isolated when **I-53** was synthesized and subjected to reaction conditions.

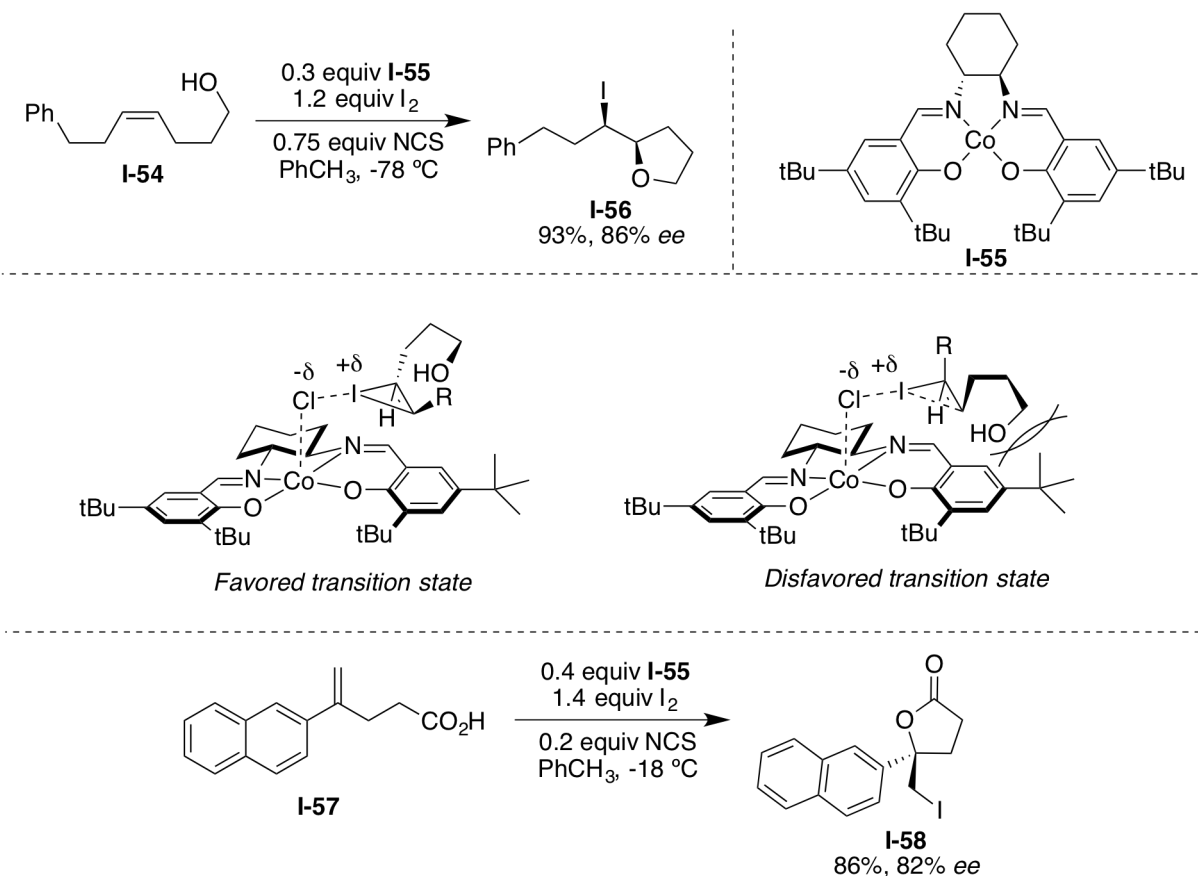
#### I.4.2. Catalytic asymmetric halocyclization reactions.

##### I.4.2.1. Transition metal catalyzed enantioselective halocyclizations.

Chiral metal-salen complexes have been employed in substoichiometric quantities to promote highly enantioselective iodocyclization reactions. Kang and co-workers used the Co-Salen complex **I-55** to mediate highly enantioselective iodoetherification reactions in the presence of molecular iodine as the iodonium precursor (see transformation of **I-54** to **I-56** in Scheme I-11).<sup>21</sup> Substoichiometric amount of NCS was employed as an additive to promote an in-situ generation of ICl. It was postulated that the metal in the salen complex is capable of activating iodine monochloride (ICl), generated in-situ from the reaction of molecular  $I_2$  with the

NCS additive.<sup>22</sup> The face selectivity for the delivery of the iodonium ion to the alkene functionality is governed by the salen diamine backbone, which dictates the approach of the substrate in to the chiral pocket of the catalytic complex (see Scheme I-11). The bulky *t*-butyl groups on the salen aryl rings prevent the approach of the substrate with the nucleophile posited over the catalyst backbone. Subsequently, a Cr-salen complex was developed for mediating the same transformation with comparable levels of enantioinduction at significantly lower catalyst loading (as low as 7 mol%, result not shown).<sup>22</sup>

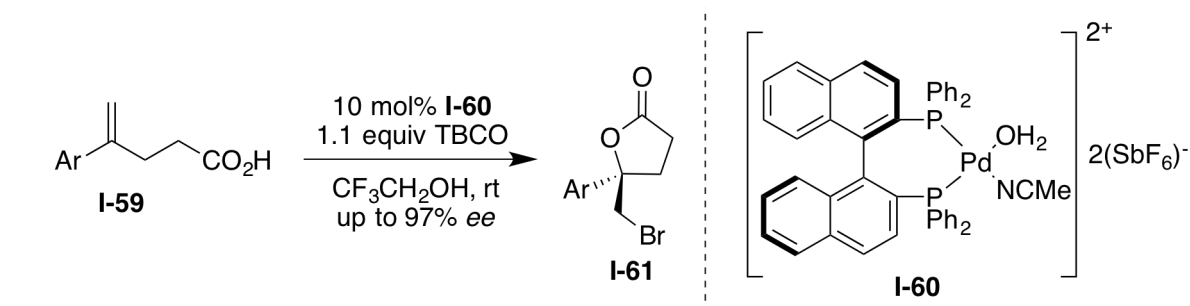
**Scheme I-11.** Co-salen (**I-55**) catalyzed asymmetric iodoetherification and iodolactonization reactions



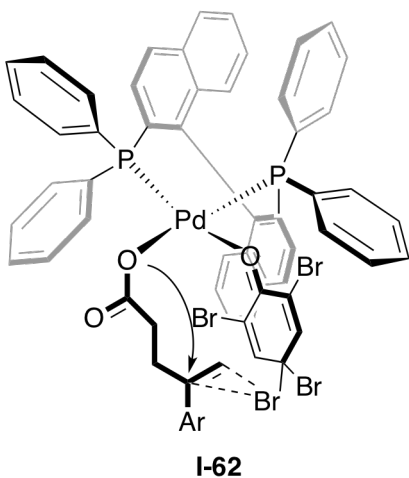
Gao and co-workers were able to demonstrate that **I-55** was also capable of mediating enantioselective iodolactonization reactions (see transformation of **I-57** to **I-58** in Scheme I-11) with minor variations to the conditions reported by Kang *et. al.*<sup>23</sup>

Kim and Lee have reported that a cationic Pd-BINAP complex **I-60** is capable of catalyzing highly enantioselective bromolactonization reactions of alkenoic acids in the presence of 2,4,4,6-tetrabromo-2,5-cyclohexadienone (TBCO) as the terminal bromonium source.<sup>24</sup> A highly organized ternary complex aided by the displacement of the ligands on Pd by the carboxylic acid and TBCO was proposed to lead to the face-selective bromination of the alkene motif (see **I-62** in Scheme I-12).

**Scheme I-12.** Catalytic asymmetric bromolactonization of alkenoic acids mediated by TBCO/**I-60**



**Proposed stereochemical model:**



#### **I.4.2.2. Organocatalytic enantioselective halocyclizations.**

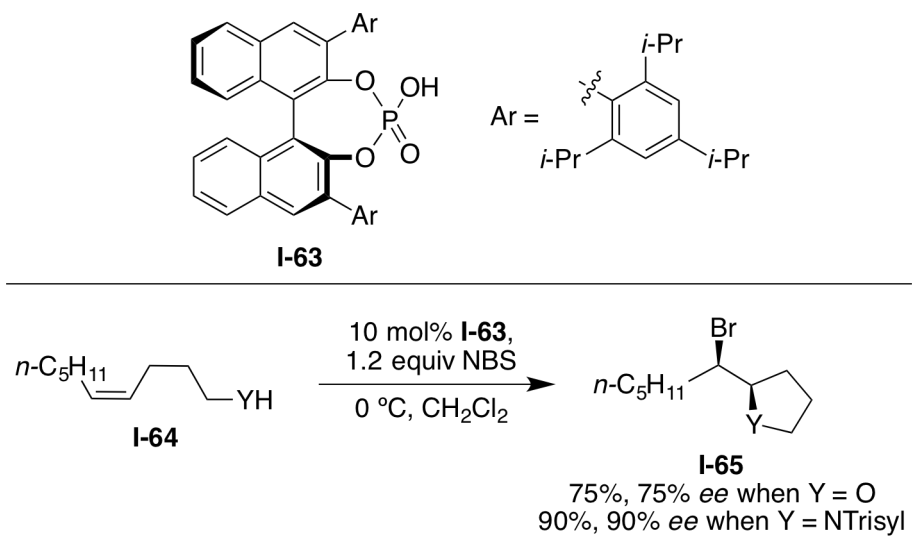
Chiral polyfunctional organocatalysts have proven to be the most well explored subset of chiral catalysts for asymmetric alkene halogenation reactions. For the sake of brevity, only those transformations whose mechanistic underpinnings have been explored in detail are discussed in this section.

##### **I.4.2.2.1. Chiral Bronsted acid catalyzed enantioselective halocyclizations.**

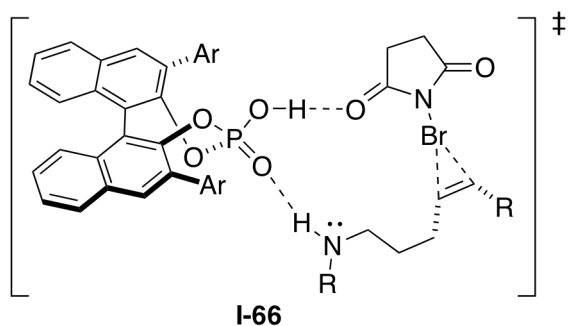
Chiral Bronsted acid **I-63** [(*S*)-TRIP] has proven to be a versatile catalyst for the asymmetric bromocyclization reaction of alkenes (see **I-63** in Scheme I-13). Although the Shi and Denmark groups have independently developed enantioselective bromocyclization reactions catalyzed by **I-63**, they have put forward two distinct mechanistic proposals.

Shi and co-workers propose that **I-63** is capable of acting as both- a H-bond donor and a H-bond acceptor. Highly enantioselective bromoetherification as well as bromoaminocyclization were realized using practically identical conditions (see transformation of **I-64** to **I-65** in Scheme I-13).<sup>25</sup> It was postulated NBS is activated by a hydrogen bonding interaction of the carbonyl group of NBS and the OH group of the phosphoric acid catalyst (the H-bond donor in the catalyst). Additionally, the substrate is held in the catalyst's chiral pocket by the hydrogen bonding interaction between the H-bond donor of the substrate (OH or NH) and the phosphate group of the catalyst (P=O, the H-bond acceptor in the catalyst). This leads to an ordered ternary complex (see **I-66**) that leads to the face-selective delivery of the bromonium ion to the alkene functionality.<sup>25</sup>

**Scheme I-13.** Structure of (*S*)-TRIP (**I-63**) and **I-63**/NBS mediated asymmetric bromocyclization reactions



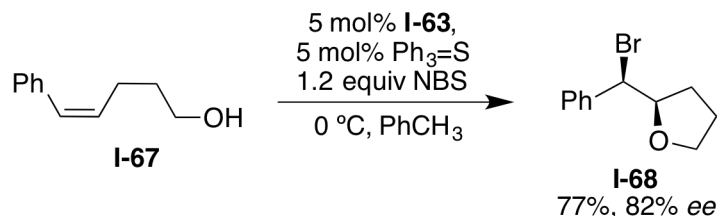
**Proposed transition state:**



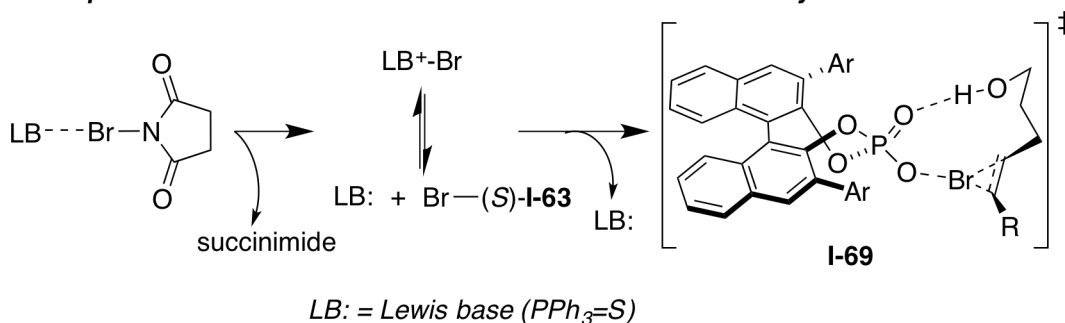
Denmark's group employed **I-63** along with a co-catalyst, namely triphenylphosphine sulfide, as an achiral Lewis base additive for achieving highly enantioselective bromoetherification reactions.<sup>26</sup> *Z*-alkenols gave exclusively the 5-*exo* cyclized products whereas *E*-alkenols gave poor 5-*exo* vs. 6-*endo* selectivity and poor enantioselectivities for the 6-*endo* cyclized products (Scheme I-14 shows a representative example of a *Z*-alkenol bromocyclization). They propose a co-operative activation of NBS by the achiral Lewis base and the chiral Bronsted acid leading to a chiral hypobromite species (see **I-69** in Scheme I-14) that serves as the active bromonium source. An ordered transition state, that does not involve

either the Lewis base additive or the counter anion of the halonium source, is proposed to be the catalytically relevant species.

**Scheme I-14.** Cooperative asymmetric catalysis of **I-63**/ $\text{PPh}_3=\text{Se}$  in the bromoetherification of alkenols



**Proposed activation of NBS and transition state for bromocycloetherification**



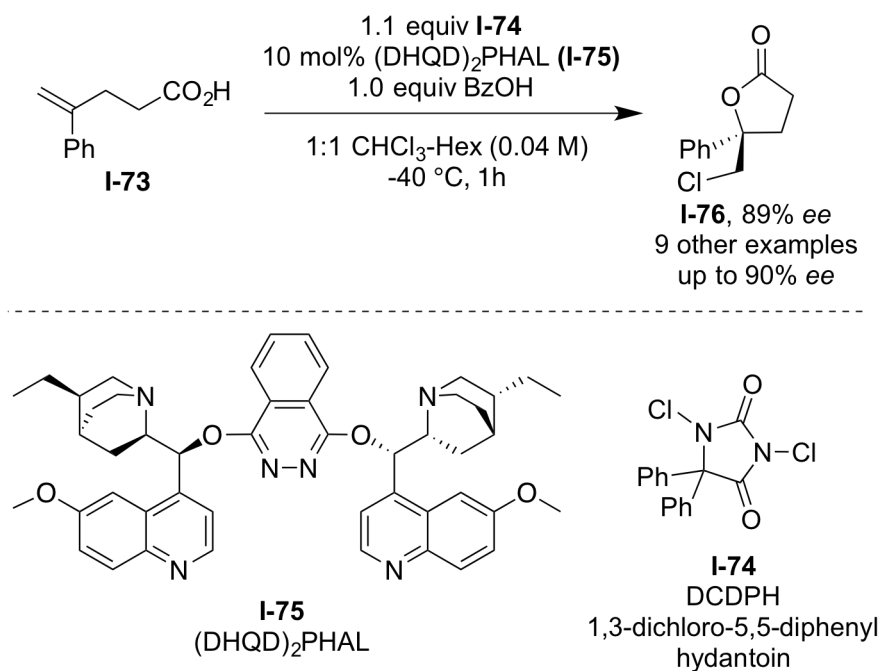
Although the two mechanisms proposed by Shi and Denmark may be distinguished readily by the determination of the rate limiting step as well as the molecularity of the reactions, neither group has disclosed any conclusive studies in this regard till date. Denmark and Burk have reported their preliminary kinetic studies of the bromocycloetherification reaction; nonetheless, the experimental methods employed were unable to identify the rate-limiting step of the reaction.<sup>27</sup>



#### I.4.2.2.2. Chiral Lewis bases and polyfunctional catalysts for enantioselective halocyclizations.

The first highly enantioselective catalytic protocol for asymmetric halolactonization reactions was reported by our group in 2010 (Scheme I-16). The Sharpless ligand (DHQD)<sub>2</sub>PHAL (**I-75**) was found to mediate the asymmetric chlorolactonization reaction of a series of 4-aryl-4-pentenoic acids in the presence of 5,5-diphenyl-1,3-dichlorohydantoin (**I-74**) as the terminal chlorenium source with enantioselectivities of up to 90% *ee* levels for selected substrates. Subsequent mechanistic studies have revealed that (DHQD)<sub>2</sub>PHAL plays multiple roles in imparting enantioselectivity to the reaction.

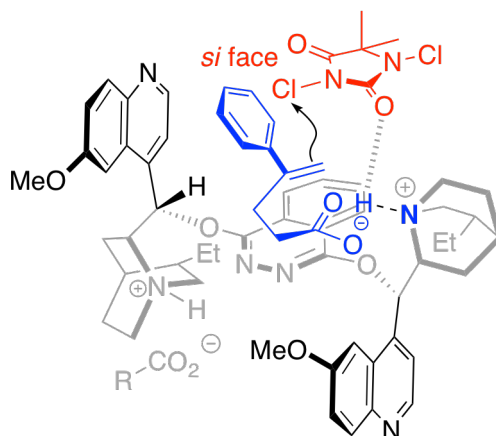
**Scheme I-16.** An asymmetric chlorolactonization reaction mediated by **I-74**/(DHQD)<sub>2</sub>PHAL



The binding model for this reaction has undergone constant refinements over the last two years with the aid of numerous mechanistic investigations. A battery of experiments support the binding model proposed in Figure I-5. They include <sup>1</sup>H NMR ROESY (to determine

catalyst conformation and substrate-catalyst interactions), kinetic analysis (using RPKA studies to determine the molecularity of the reaction) and deuterium labeling studies. At least two key interactions are proposed to promote a highly organized ternary complex of the substrate, catalyst and chlorine source – an ion pair interaction between the carboxylic acid substrate and the Lewis base catalyst [(DHQD)<sub>2</sub>PHAL] and a H-bonding interaction between the chlorohydantoin carbonyl group and the protonated catalyst that serves to activate the chlorohydantoin to deliver the chloronium ion more readily and selectively to the *si* face.

**Figure I-5.** Ternary complex of alkenoic acid substrate, **I-74** and **I-75** leads to rate acceleration and highly face-selective chloronium delivery to alkene

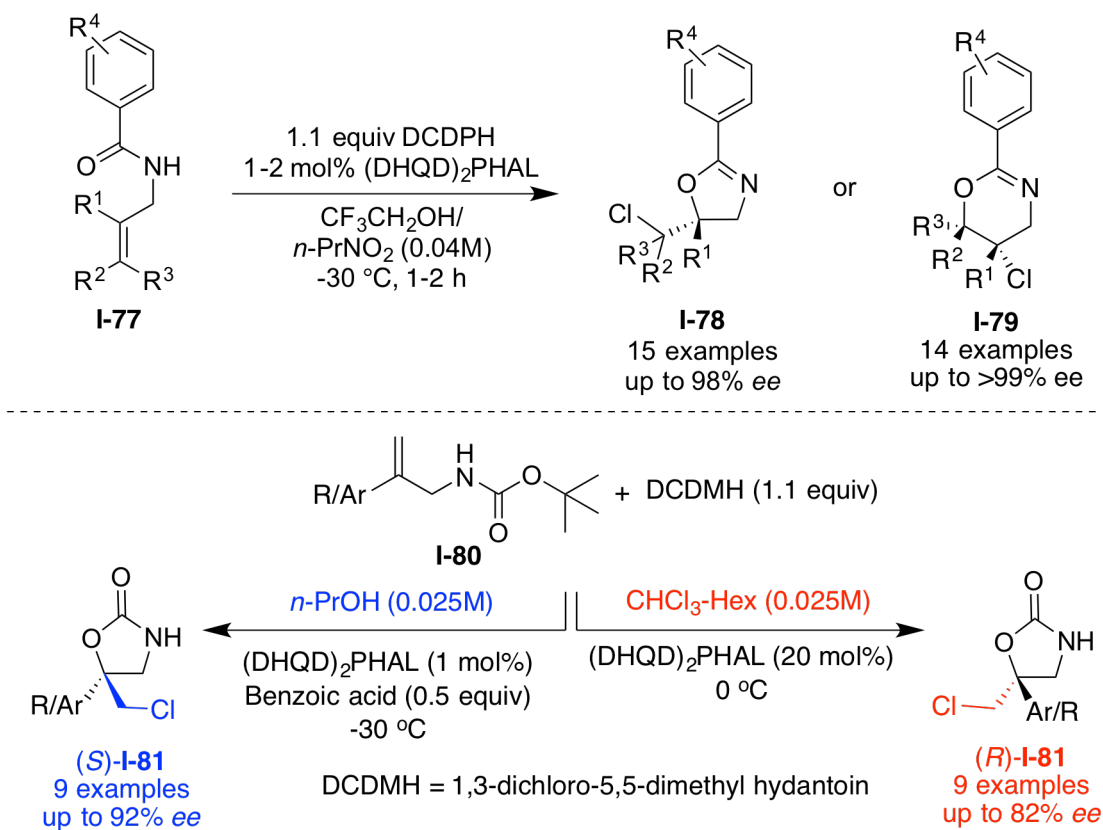


Additionally, experimental and theoretical kinetic isotope effects (KIE) are being used to determine the rate-limiting step for this reaction.

Following this initial discovery, our group was able to extend the scope of asymmetric chlorocyclization reactions to include amides and carbamates as viable nucleophiles in this chemistry (see Scheme I-17).<sup>29,30</sup> The amide chlorocyclization chemistry that yields oxazoline and dihydrooxazine heterocycles was found to be more general with regards to the alkene substituents and the substitution pattern of the olefin. While 1,1-disubstituted alkene substrates yielded oxazoline products, *trans*-disubstituted and trisubstituted alkenes yielded the

dihydrooxazine heterocycles (see **I-77** to **I-78** or **I-79** in Scheme I-17). The carbamate chlorocyclization, while restricted to 1,1-disubstituted allylic carbamates, exhibited an intriguing solvent-dependent enantiodivergence (see **I-80** to **I-81**). The discovery, optimization and mechanistic studies pertaining to these two reactions will be discussed in detail in Chapter 2.

**Scheme I-17.** (DHQD)<sub>2</sub>PHAL catalyzed asymmetric chlorocyclization of allylic amides and carbamates



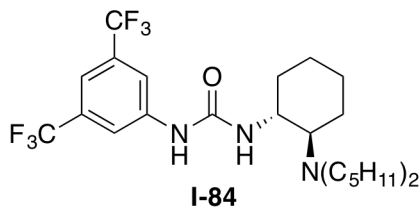
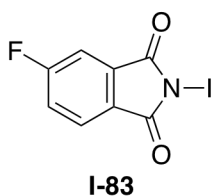
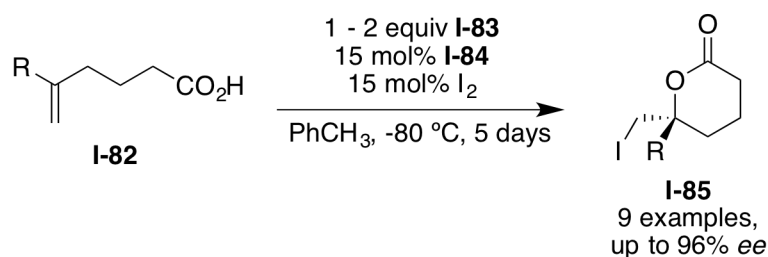
Numerous groups have since reported on the discovery and development of polyfunctional organocatalysts for asymmetric halocyclization reactions. The reader's attention is drawn to numerous early as well as comprehensive reviews dedicated to these reactions.<sup>31-34</sup>

Rather than providing an elaborate list of all the discovered reactions, only examples that highlight the mechanistic basis for successful reactions are presented in this section. This

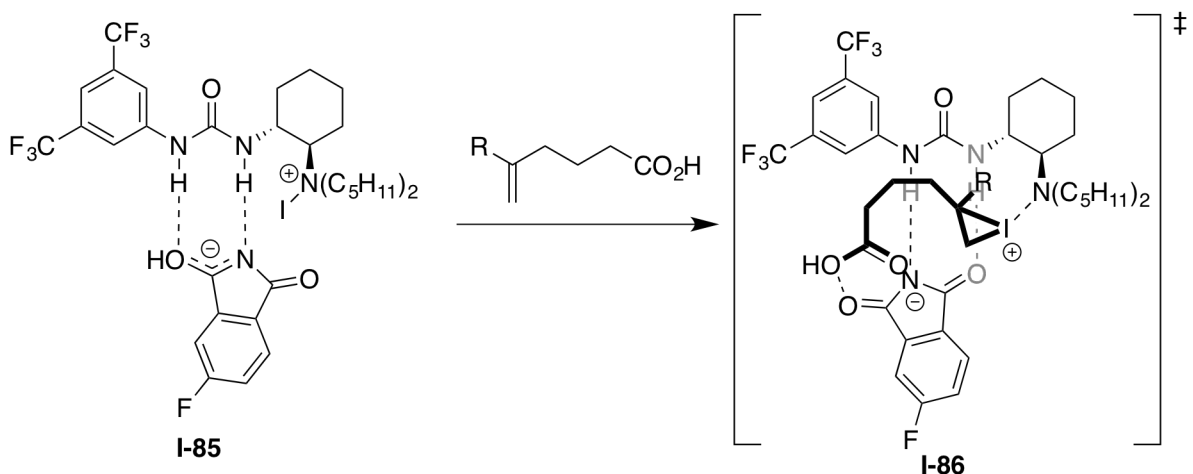
should allow for a straightforward comparison of these reactions with those developed in our lab from a mechanistic standpoint.

Many of the chiral Lewis base catalysts employed in halocyclization reactions have an additional functional group (another Lewis base, urea, thiourea, thiocarbamate, etc) remote from the Lewis basic site that helps in orienting the substrate for a face selective capture of the Lewis base activated halonium ion. Veitch and Jacobsen reported an elegant example of this design strategy in the asymmetric iodolactonization of alkenoic acids catalyzed by the aminourea catalyst **I-84** (see Scheme I-18).<sup>35</sup>

**Scheme I-18.** The **I-83/I-84** mediated asymmetric iodolactonization of 5-aryl-5-hexenoic acids



*Proposed activation of **I-83** and transition state for **I-84** catalyzed iodolactonization*



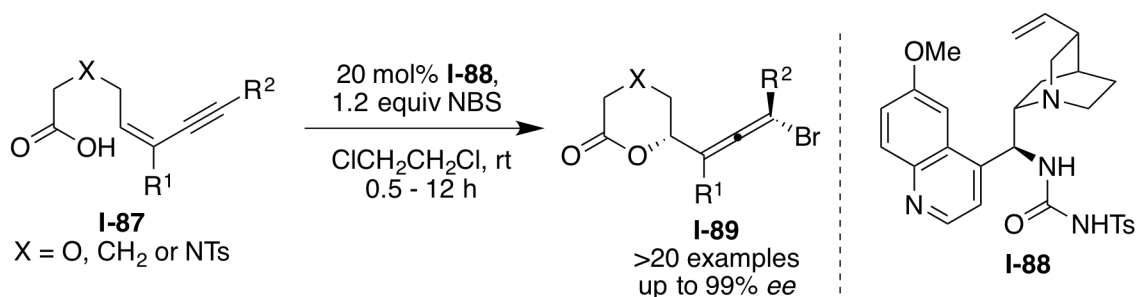
It was proposed that iodenium transfer from **I-83** to the tertiary amine motif of the **I-84** (observed by low temperature proton NMR studies) leads to the intermediate **I-85**. The counteranion of the **I-83** remains bound to the urea motif. The incoming alkenoic acid is oriented within the catalyst chiral pocket by H-bonding interactions of the carboxylic acid functional group with the catalyst bound phthalimide anion (see **I-86** – the proposed transition state for this reaction). The urea functional group in the catalyst plays a pivotal role in enabling this preorganization.

A complementary mode of activating carboxylic acid substrates and the halonium source is also possible with such bifunctional catalysts, whereby, the chiral Lewis base serves to orient the carboxylic acid substrate (rather than activate the halonium source) within the chiral pocket by a tight ion pair interaction and the ancillary functional group activates the halonium reagent. The Tang and Yeung groups have independently disclosed asymmetric bromolactonization reactions that were proposed to exploit such a mode of activation.

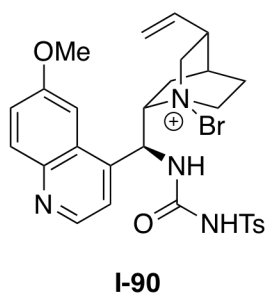
Tang's group reported a highly enantioselective bromolactonization of *Z*-1,3-enynes to bromoallene products catalyzed by the quinine derived chiral urea **I-88** (see Scheme I-19).<sup>36,37</sup> As seen in their proposed stereochemical model **I-91**, the carboxylic acid substrate is bound to the catalyst's quinuclidine moiety.<sup>37</sup> The pendant urea functional group was proposed to activate NBS via H-bonding interactions to the carbonyl group of NBS. The authors rule out the *N*-brominated catalyst **I-90** as the chiral bromonium source based on incubation studies of NBS and **I-88** prior to substrate addition; significant decrease in enantioselectivity with longer incubation times suggest that the formation of **I-90** likely leads to the loss in enantioselectivity (although no isolation/ characterization of **I-90** was provided). Furthermore, the enantioselectivity was dependent on the identity of the bromonium precursor (NBS gave significantly higher enantioinduction as compared to other bromonium sources); this result is not

consistent with the formation of an intermediate such as **I-90** unless the counterion is intimately associated with **I-90**.

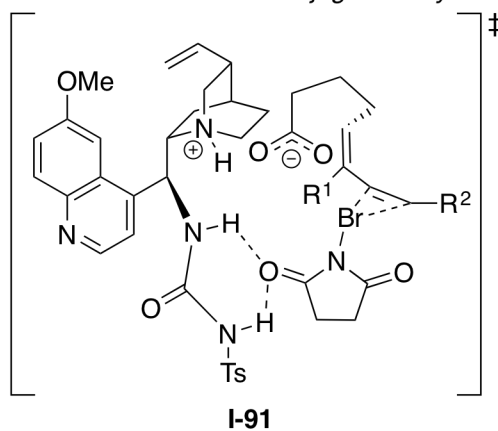
**Scheme I-19.** Enantioselective bromolactonization of *Z*-1,3-enynes catalyzed by **I-88**



*N*-brominated catalyst **I-90** was ruled out as the chiral bromenium source

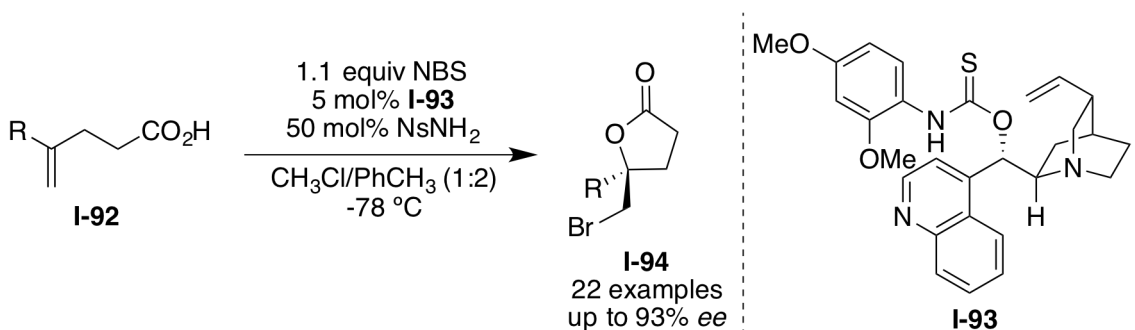


Proposed transition state for **I-88** catalyzed bromolactonization of conjugated enynes

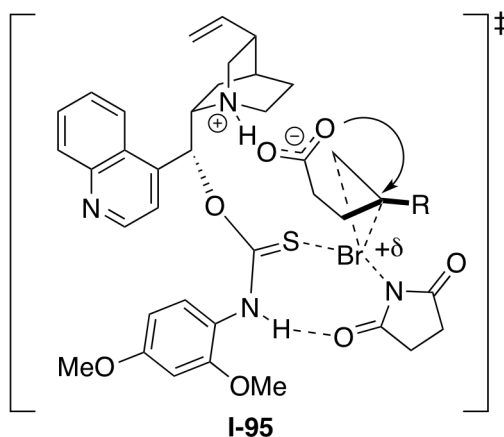


Yeung's group reported an asymmetric bromolactonization reaction catalyzed by the bifunctional catalyst **I-93** (see Scheme I-20).<sup>38</sup> The proposed transition state (see **I-95**) is similar to that proposed by Tang and co-workers. The aminothiobarbamate motif in the catalyst activates NBS by means of a simultaneous H-bonding/ Lewis base activation; the carboxylic acid substrate remains bound to the catalyst after protonating the quinuclidine nitrogen.

### Scheme I-20. I-93 catalyzed enantioselective bromolactonization



Proposed transition state for **I-93** catalyzed bromolactonization

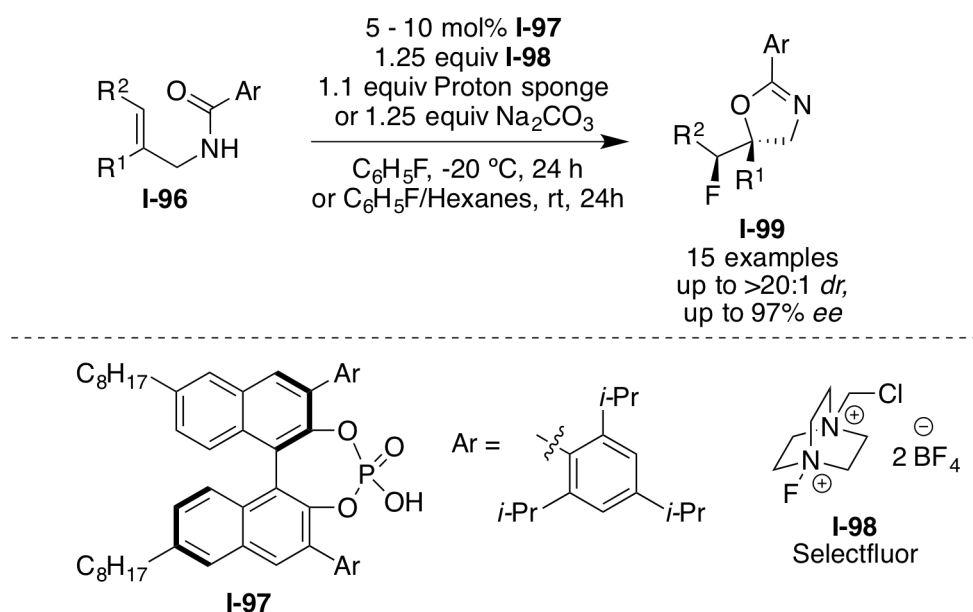


Although Denmark has proposed that all cinchona alkaloid derived catalysts activate the halenium source by the *N*-halogenation of the quinuclidine *N* atom,<sup>33</sup> this proposal seems highly unlikely based on the control experiments of the Tang group (see Scheme I-19) as well as many experiments in our lab. Both theoretical and experimental means seem to rule out *N*-halogenated catalysts to be the chiral halenium source. A detailed description of these experiments is beyond the scope of this chapter; one is instead directed to the doctoral thesis of Dr. Roozbeh Yousefi – a former member of our group who performed many of the preliminary mechanistic studies of the chlorolactonization reaction.<sup>39</sup>

#### I.4.2.2.3. Chiral phase transfer catalyzed enantioselective halocyclizations.

Toste and co-workers have exploited chiral anionic phase transfer catalysis for the asymmetric fluorocyclization of allylic amides (see Scheme I-21).<sup>40</sup> The chiral phosphoric acid phase transfer catalyst **I-97** serves to solubilize Selectfluor® (**I-98**) in non-polar solvents by means of an ion exchange of the phosphate ion of **I-97** and the tetrafluoroborate anion of Selectfluor®. All alkenes that were evaluated possessed cation-stabilizing groups to aid the stabilization of the putative  $\beta$ -fluorocarbenium ion. The group has recently expanded the reaction scope to include fluoroaminocyclization<sup>41</sup> and bromo- and iodocyclization reactions<sup>42</sup> using the same approach.

**Scheme I-21.** Chiral anionic phase transfer catalyzed fluorocyclization of unsaturated amides



#### I.4.3. Intermolecular nucleophilic capture of chiral halonium ions.

Two serious issues associated with the development of synthetically useful asymmetric alkene halogenations are the rapid stereochemical degradation of chiral halonium ions by diffusion controlled olefin-to-olefin halonium transfer and halonium ion isomerization processes (see sections I.3.1 and I.3.2 for a detailed discussion of these phenomena). Not surprisingly

therefore, most examples till date have reported on the *intramolecular* capture of the putative chiral halonium ions *via* tethered nucleophiles (i.e., halocyclization reactions); the proximity driven rate enhancement of the cyclization step presumably outcompetes the stereochemical degradation *via* degenerate halonium transfer among alkenes and also attenuates any isomerization of the halonium ion prior to nucleophilic capture.

The development of an *intermolecular* capture of chiral halonium ions is therefore, an even bigger challenge. Any stereoelectronic effects that contribute to the success of intramolecular variants are absent for analogous intermolecular variants. Also, the requirement for accommodating an additional entity in the diastereo- and/or enantioselectivity determining step imposes entropic constraints that are absent in halocyclization reactions where the nucleophile is predisposed (for better or for worse); any optimizations for halocyclization reactions need not account for nucleophile trajectory or predisposition.

Nonetheless, a few reports of enantioselective vicinal difunctionalization of alkenes initiated by chiral halonium ions have appeared in literature.

#### **I.4.3.1. Stereoselective interception of chiral halonium ions by alcohols, carboxylic acids and amine derivatives.**

Shibasaki and coworkers have disclosed the synthesis of chiral chlorohydrins from cycloalkenes by a formal addition of chlorine and hydroxyl groups across the alkene in a stereospecific manner (see Scheme I-22).<sup>43</sup> An in-situ generated Sn-diisopropyl tartarate complex catalyzes this reaction in the presence of bis-trimethylsilylperoxide (BTSP) and trimethylsilyl chloride (TMSCl). Upto 58% *ee* was obtained for the chlorohydrin derived from cyclohexene (the only other substrate evaluated was cyclopentene that returned the corresponding chlorohydrin in 56% *ee*). The reaction does not involve an electrophilic activation of the alkene by a chloronium ion despite the formation of Cl<sub>2</sub> in this reaction; instead the

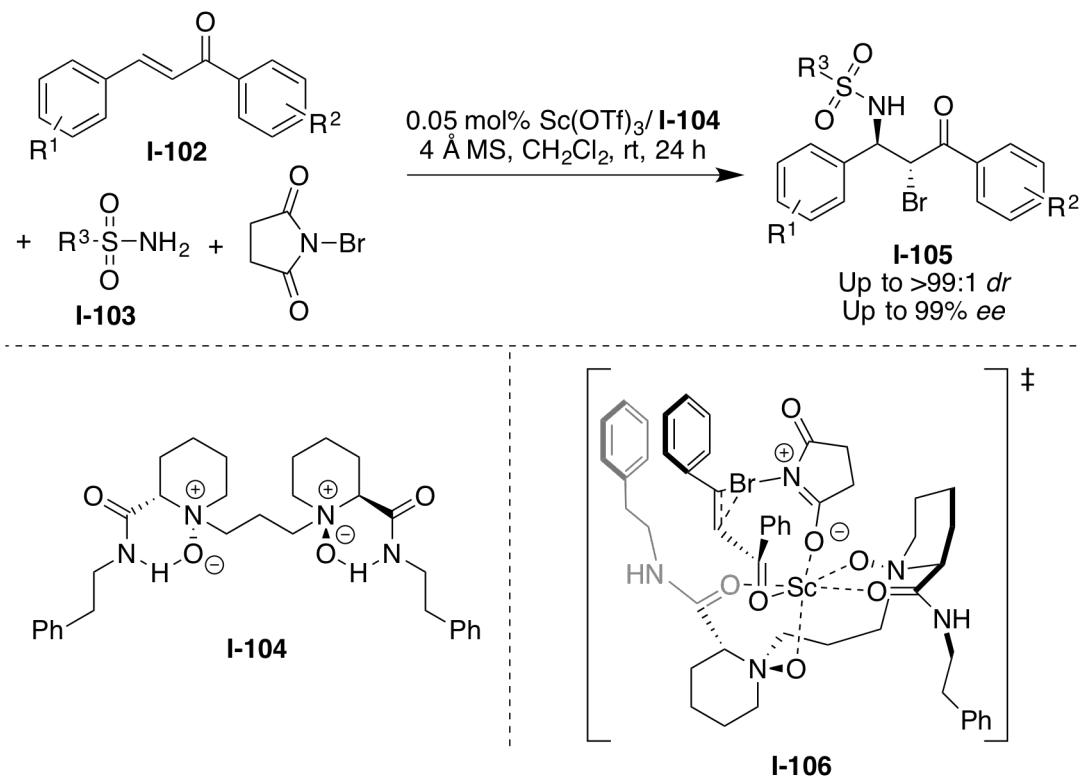
authors propose a *syn*-selective oxystannylation followed by the intramolecular nucleophilic cleavage of the C-Sn bond by a chloride anion and subsequent hydrolysis to give the halohydrin product.  $^{18}\text{O}$  labeled BTSP gave  $^{18}\text{O}$  labeled product thereby confirming the origin of the OH group.

**Scheme I-22.**  $\text{SnCl}_4$ /DIPT catalyzed chiral halohydrin synthesis from cycloalkenes in the presence of TMSCl and BTSP



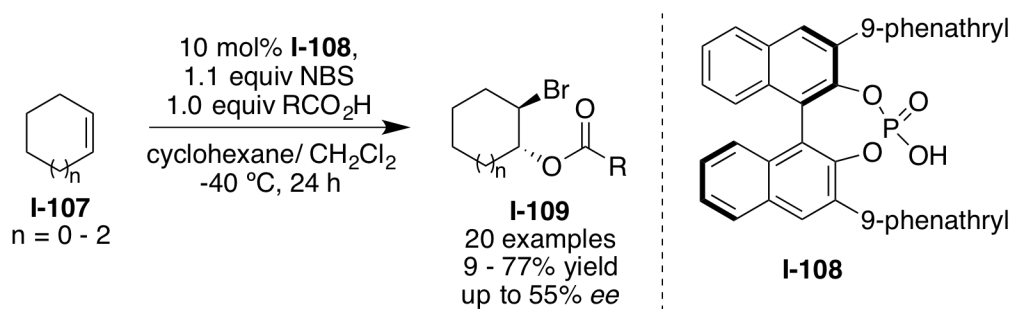
Feng's group has reported a chiral Sc-*N*-oxide complex **I-104** that enables an intermolecular bromoamination of chalcones with excellent diastereo- and enantioselectivity at catalyst loadings as low as 0.05 mol%.<sup>44</sup> The proposed transition state **I-106** is shown in Scheme I-23. The chalcone is held in the chiral pocket of Sc/ **I-104** by means of Lewis acid-base interaction between the Sc and carbonyl oxygen of the chalcone as well as  $\pi$ -stacking interactions between the substrate and catalyst aryl rings. A concomitant Lewis acid activation of NBS by Sc is also proposed. This organized transition state accounts for the *Re*-face selective bromonium delivery. Slight modifications of this catalyst and reaction conditions were subsequently used for developing related chloroamination and iodoamination reactions as well.<sup>45,46</sup> All reactions were postulated to involve the nucleophilic opening of cyclic halonium ion intermediates in order to account for the exquisite diastereoselectivity.

**Scheme I-23.** Sc(OTf)<sub>3</sub>/ **I-104** catalyzed intermolecular asymmetric bromoamination of chalcones



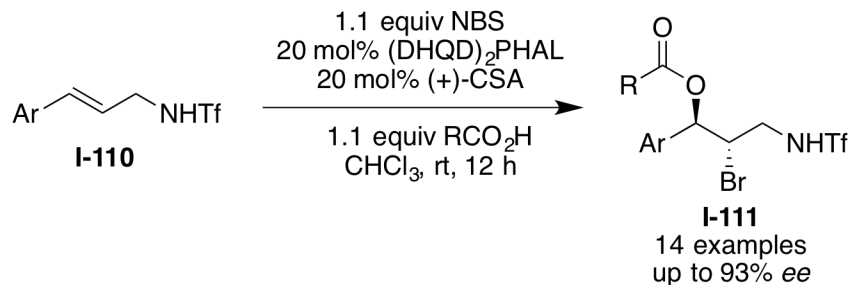
Two examples of intermolecular asymmetric bromoesterification reactions have also appeared in literature. Tang, Zhang and co-workers have disclosed a chiral phosphoric acid catalyzed intermolecular bromoesterification of cyclic alkenes (see Scheme I-24).<sup>47</sup> The substrate scope was restricted to cycloalkenes. Numerous aromatic and aliphatic carboxylic acids were employed as nucleophiles. Low to moderate yields and enantioinduction was observed for all substrates.

**Scheme I-24.** The first catalytic enantioselective intermolecular bromoesterification reaction



Following this report, Tang and co-workers reported an enantioselective intermolecular bromoesterification reaction of allylic sulfonamides catalyzed by  $(\text{DHQD})_2\text{PHAL}$  (see Scheme I-25).<sup>48</sup> The reaction gave good enantioselectivities for *trans*-aryl disubstituted alkenes. Nucleophiles other than carboxylic acids were not evaluated in the study.

**Scheme I-25.**  $(\text{DHQD})_2\text{PHAL}$  catalyzed intermolecular bromoesterification of allylic sulfonamides

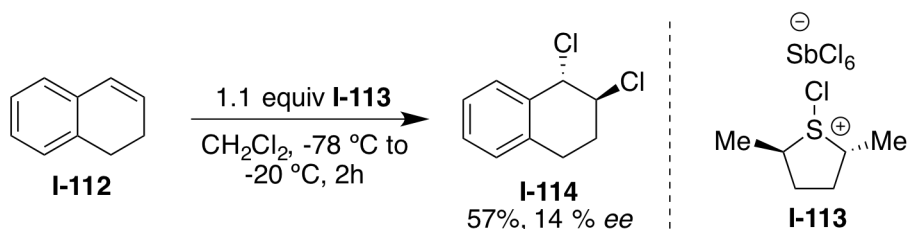


#### I.4.3.2. Stereoselective interception of chiral halonium ions by halide anions – asymmetric vicinal dihalogenation of alkenes.

Catalytic as well as stoichiometric asymmetric dihalogenation reactions of alkenes have been reported. Snyder and co-workers have demonstrated that a chiral chlorosulfonium antimonate salt **I-113** can mediate the asymmetric dichlorination of **I-112** with low levels of stereoselection (14% *ee* for the product **I-114**, see Scheme I-26).<sup>49</sup> Nonetheless, this was the only example that exhibited any enantioinduction. Other substrates gave racemic dichlorides on

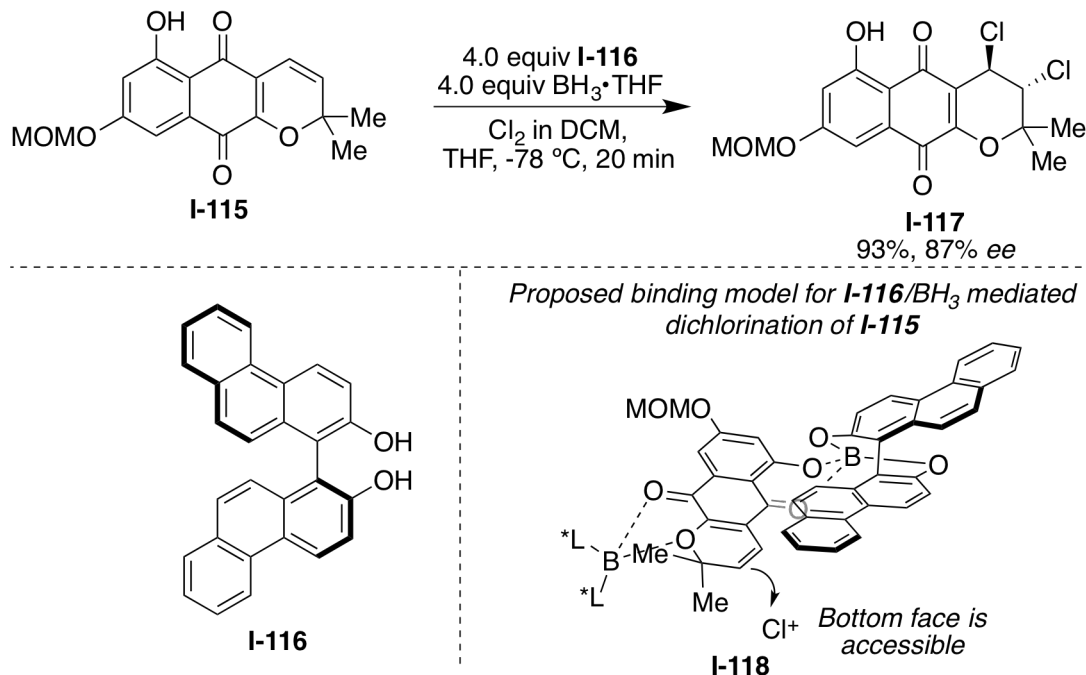
exposure to **I-113**. Also, analogous bromenium and iodenium sources returned racemic products.

**Scheme I-26.** Asymmetric dichlorination of **I-112** mediated by **I-113**



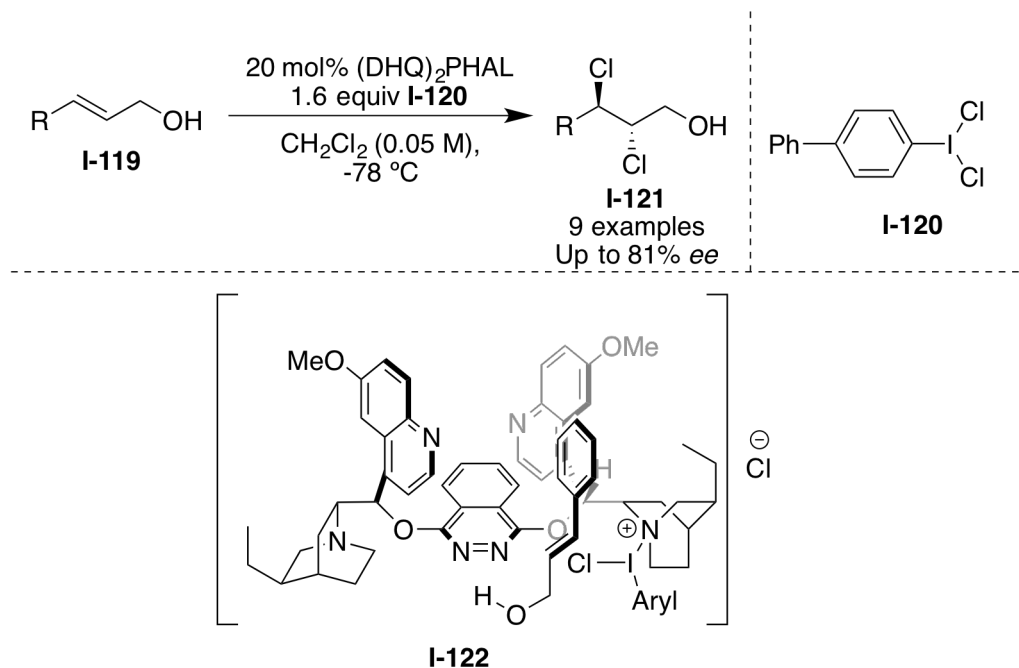
The same group has also reported a highly enantioselective dichlorination of the cyclic alkene **I-115** (see Scheme I-27) in the presence of super stoichiometric quantities of a chiral promoter generated *in-situ* from the reaction of BINOL ligand **I-116** and  $\text{BH}_3$  (4.0 equiv. of each).<sup>50</sup> The dichloride product **I-117** was isolated in 87% *ee* and served as one of the key intermediates in their synthesis of Napyradiomycin A1. The requirement of the large excess of the chiral promoter likely stems from the weak  $\pi$ -stacking interaction between the substrate and the aryl rings of the catalyst that anchors the substrate in the chiral pocket of the catalytic complex; presumably, the association constant for this binary complex (see **I-118** in Scheme I-27) is sufficiently low to require a large excess of the chiral promoter. The chiral ligand **I-116** was recovered from the reaction mixture by column chromatography. The substrate scope for this reaction has not been explored; although based on the proposed stereochemical model, it is likely that the scope might be restricted to cyclic alkenes with adjacent oxygenated functionalities that can chelate to the Lewis acidic boron atom.

**Scheme I-27.** Enantioselective vicinal dichlorination of **I-115** mediated by **I-116**/ $\text{BH}_3$  complex



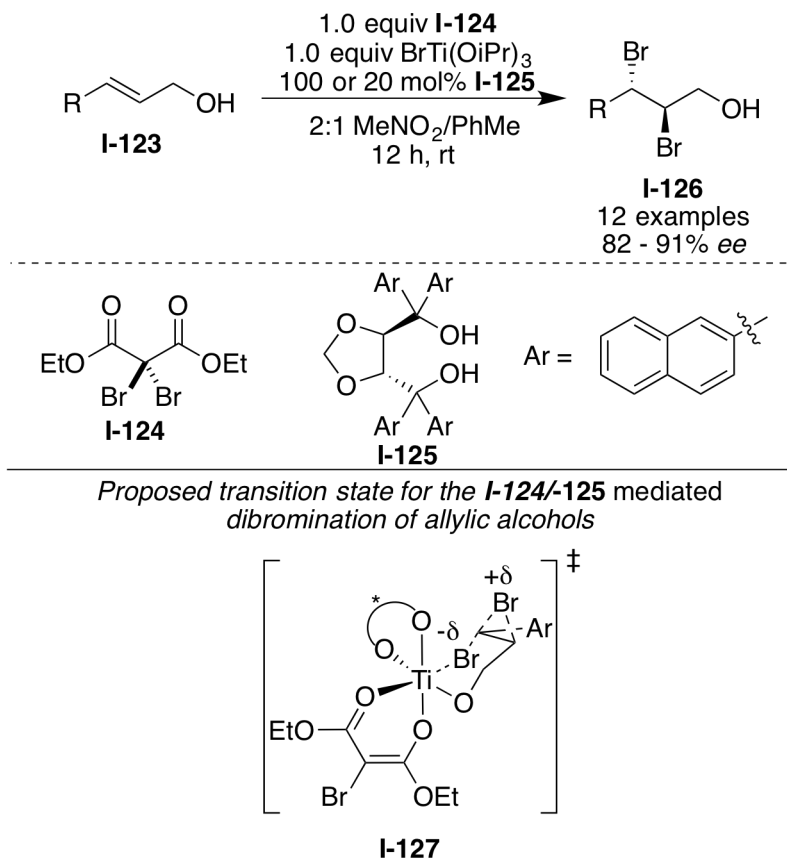
*Catalytic* asymmetric dihalogenations of allylic alcohols have also been reported. Nicolaou and co-workers have reported a catalytic asymmetric dichlorination of cinammyl alcohols by employing  $(\text{DHQ})_2\text{PHAL}$  as the chiral Lewis base catalyst in the presence of dichloro-iodoarenes that serve as both the nucleophilic as well as the electrophilic chlorine source (see Scheme I-28).<sup>51</sup> The proposed model to account for the stereochemical outcome invokes a H-bonding interaction of the substrate's OH group to the phthalazine *N*-atoms of the catalyst (see **I-122**). The quinuclidine *N*-atom is postulated to covalently bind to the hypervalent iodine reagent to aid in the delivery of the chloronium ion to the alkene. The reaction scope was narrow and only unsubstituted cinammyl alcohol gave the corresponding dichloride in 81% *ee*. Substrates with aliphatic alkene substituents (43 – 54% *ee*, 2 substrates), *Z*-allylic alcohols (1 example, 25% *ee*), and *O*-protected allylic alcohols (1 example, <5% *ee*) gave poor results.

**Scheme I-28.** (DHQ)<sub>2</sub>PHAL/**I-120** mediated enantioselective dichlorination of cinnamyl alcohols



More recently, the Burns research group has reported an asymmetric dibromination of allylic alcohols that is more general with regards to the substrate scope (see Scheme I-29).<sup>52</sup> In the presence of **I-125** as the chiral promoter, the dibromomalonate **I-124** as the bromonium source and (*i*-PrO)<sub>3</sub>TiBr as the bromide source, numerous allylic alcohols underwent a facile and enantioselective dibromination at ambient temperature. The proposed transition state **I-127** for this reaction is shown Scheme I-29. Although stoichiometric amounts of **I-125** gave the best results (82 – 91% *ee*), the enantioselectivity was moderate to high when 20 mol% of **I-125** was employed (71 – 85% *ee*). Preliminary results with alkyl substituted allylic alcohols (55% *ee*), homoallylic alcohols (75% *ee*) and *Z*-allylic alcohols (52% *ee*) were also encouraging, although a full disclosure of substrate scope and limitations has not appeared till date.

**Scheme I-29.** Enantioselective dibromination of allylic alcohols mediated by **I-124/I-125** complex



**I.5. Challenges and future directions.**

Despite the significant strides made over the last few years, catalytic asymmetric alkene halogenation reactions are only just beginning to make a mark in the field of organic chemistry. Numerous shortcomings and limitations are evident in the current state of the art. The emphasis during the early stages of any novel reaction methodology development lies in exploring the scope and utility of the reaction. These forays are eventually complemented by mechanistic investigations to decipher the factors that contribute to the success (or failure) of the reaction. It is perhaps a fair assessment that the progress in asymmetric alkene halogenation chemistry has mirrored this trend seen with any other well-established catalytic asymmetric reaction methodology. Much of the early forays have been curiosity-driven with

focus more on developing highly enantioselective variants of halocyclizations rather than on understanding the mechanistic underpinnings that contribute to the success of the reaction. Detailed mechanistic studies of some of these reactions are now emerging. This 2-prongged approach to reaction discovery that includes an initial '*screen-and-select*' approach to zero in on optimal conditions followed by in-depth mechanistic studies will be central to the progress of this chemistry.

From the mechanistic standpoint, there is significant discord in the accepted notions of stability and reactivity of halonium ions – the key intermediates in all these reactions. A comprehensive theory that accounts for the reactivity of halonium ions will go a long way in enabling rational reaction discovery and significantly reduce the need to resort to trial-and-error approaches that are currently rampant.

From a practical standpoint, this research area still lacks generality with regards to diverse nucleophiles and electrophiles employed. Indeed, the potential to adopt this mix-and-match strategy for different halonium ion activation of alkenes (Cl, Br, I and F) coupled with different nucleophiles provides virtually endless opportunities for reaction discovery and mechanistic studies (and in this regard asymmetric alkene halogenations are uniquely more versatile than other asymmetric alkene functionalization reactions). Exploration of late stage alkene halogenation reactions in total synthesis of complex natural products has remained unexplored thus far, as have target driven reaction discovery endeavors.

Many potentially useful but challenging transformations such as enantioselective C-C bond formation reactions and intermolecular nucleophilic capture of chiral halonium ions are yet to witness the generality of reactions such as halolactonizations. Additionally, the development of protocols that are more amenable to preparatory scale applications (lower catalyst loadings, cost effective reagents, reaction concentrations, temperature, etc.) ought to receive more attention; in fact, these efforts, often undertaken as a natural progression to improve upon the

initially developed conditions, lead to the development of more active catalysts and provide valuable mechanistic information. Significant portions of this thesis will be dedicated to the description of efforts in our lab to address some of these challenges.

The explosive growth of research in this area over the last 3 years has been characterized by the discovery of a wide variety of catalysts and transformations. A diverse array in the modes of asymmetric catalysis ranging from chiral Lewis base and Bronsted acid catalysis, hydrogen bonding, ion pairing and even phase transfer catalysis have been exploited in these reactions. With constant innovations, it is likely that catalytic asymmetric alkene halogenation reactions will continue gaining in prominence.

## REFERENCES

## REFERENCES

- (1) Cockerill, A. F.; Harrison, R. G. In *Double-Bonded Functional Groups (1977)*; John Wiley & Sons, Ltd.: **2010**, p 149.
- (2) Roberts, I.; Kimball, G. E. *J. Am. Chem. Soc.* **1937**, *59*, 947.
- (3) Olah, G. A.; Bollinger, J. M. *J. Am. Chem. Soc.* **1968**, *90*, 947.
- (4) Olah, G. A.; Bollinger, J. M.; Brinich, J. *J. Am. Chem. Soc.* **1968**, *90*, 6988.
- (5) Olah, G. A.; Bollinger, J. M.; Brinich, J. *J. Am. Chem. Soc.* **1968**, *90*, 2587.
- (6) Brown, R. S.; Nagorski, R. W.; Bennet, A. J.; McClung, R. E. D.; Aarts, G. H. M.; Klobukowski, M.; McDonald, R.; Santarsiero, B. D. *J. Am. Chem. Soc.* **1994**, *116*, 2448.
- (7) Strating, J.; Wieringa, J. H.; Wynberg, H. *J. Chem. Soc. D: Chem. Commun.* **1969**, 907.
- (8) Neverov, A. A.; Brown, R. S. *J. Org. Chem.* **1996**, *61*, 962.
- (9) Ohta, B. K.; Hough, R. E.; Schubert, J. W. *Org. Lett.* **2007**, *9*, 2317.
- (10) Ohta, B. K.; Scupp, T. M.; Dudley, T. J. *J. Org. Chem.* **2008**, *73*, 7052.
- (11) Peterson, P. E.; Brockington, R.; Vidrine, D. W. *J. Am. Chem. Soc.* **1976**, *98*, 2660.
- (12) Olah, G. A.; Donovan, D. J. *J. Am. Chem. Soc.* **1978**, *100*, 5163.
- (13) Yousefi, R.; Ashtekar, K. D.; Whitehead, D. C.; Jackson, J. E.; Borhan, B. *J. Am. Chem. Soc.* **2013**, *135*, 14524.
- (14) Whitehead, D. C.; Yousefi, R.; Jaganathan, A.; Borhan, B. *J. Am. Chem. Soc.* **2010**, *132*, 3298.
- (15) Kitagawa, O.; Hanano, T.; Tanabe, K.; Shiro, M.; Taguchi, T. *J. Chem. Soc., Chem. Commun.* **1992**, 1005.
- (16) Sakakura, A.; Ukai, A.; Ishihara, K. *Nature* **2007**, *445*, 900.
- (17) Wolstenhulme, J. R.; Rosenqvist, J.; Lozano, O.; Ilupeju, J.; Wurz, N.; Engle, K. M.; Pidgeon, G. W.; Moore, P. R.; Sandford, G.; Gouverneur, V. *Angew. Chem. Int. Ed.* **2013**, *52*, 9796.

- (18) Grossman, R. B.; Trupp, R. J. *Can. J. Chem.* **1998**, *76*, 1233.
- (19) Cui, X.-L.; Brown, R. S. *J. Org. Chem.* **2000**, *65*, 5653.
- (20) Garnier, J. M.; Robin, S.; Rousseau, G. *Eur. J. Org. Chem.* **2007**, *2007*, 3281.
- (21) Kang, S. H.; Lee, S. B.; Park, C. M. *J. Am. Chem. Soc.* **2003**, *125*, 15748.
- (22) Kwon, H. Y.; Park, C. M.; Lee, S. B.; Youn, J.-H.; Kang, S. H. *Chem. Eur. J.* **2008**, *14*, 1023.
- (23) Ning, Z.; Jin, R.; Ding, J.; Gao, L. *Synlett* **2009**, 2291.
- (24) Lee, H. J.; Kim, D. Y. *Tetrahedron Lett.* **2012**, *53*, 6984.
- (25) Huang, D.; Wang, H.; Xue, F.; Guan, H.; Li, L.; Peng, X.; Shi, Y. *Org. Lett.* **2011**, *13*, 6350.
- (26) Denmark, S. E.; Burk, M. T. *Org. Lett.* **2011**, *14*, 256.
- (27) Denmark, S. E.; Burk, M. T. *Chirality* **2013**, n/a.
- (28) Dobish, M. C.; Johnston, J. N. *J. Am. Chem. Soc.* **2012**, *134*, 6068.
- (29) Garzan, A.; Jaganathan, A.; Salehi Marzijarani, N.; Yousefi, R.; Whitehead, D. C.; Jackson, J. E.; Borhan, B. *Chem. Eur. J.* **2013**, *19*, 9015.
- (30) Jaganathan, A.; Garzan, A.; Whitehead, D. C.; Staples, R. J.; Borhan, B. *Angew. Chem. Int. Ed.* **2011**, *50*, 2593.
- (31) Hennecke, U. *Chem. Asian J.* **2012**, *7*, 456.
- (32) Tan, C. K.; Zhou, L.; Yeung, Y. Y. *Synlett* **2011**, 1335.
- (33) Denmark, S. E.; Kuester, W. E.; Burk, M. T. *Angew. Chem. Int. Ed.* **2012**, *51*, 10938.
- (34) Chen, G.; Ma, S. *Angew. Chem. Int. Ed.* **2010**, *49*, 8306.
- (35) Veitch, G. E.; Jacobsen, E. N. *Angew. Chem. Int. Ed.* **2010**, *49*, 7332.
- (36) Zhang, W.; Zheng, S.; Liu, N.; Werness, J. B.; Guzei, I. A.; Tang, W. *J. Am. Chem. Soc.* **2010**, *132*, 3664.
- (37) Zhang, W.; Liu, N.; Schienebeck, C. M.; Decloux, K.; Zheng, S.; Werness, J. B.; Tang, W. *Chem. Eur. J.* **2012**, *18*, 7296.

- (38) Zhou, L.; Tan, C. K.; Jiang, X.; Chen, F.; Yeung, Y.-Y. *J. Am. Chem. Soc.* **2010**, *132*, 15474.
- (39) Yousefi, R., Michigan State University, 2012.
- (40) Rauniyar, V.; Lackner, A. D.; Hamilton, G. L.; Toste, F. D. *Science* **2011**, *334*, 1681.
- (41) Shunatona, H. P.; Früh, N.; Wang, Y.-M.; Rauniyar, V.; Toste, F. D. *Angew. Chem. Int. Ed.* **2013**, *52*, 7724.
- (42) Wang, Y.-M.; Wu, J.; Hoong, C.; Rauniyar, V.; Toste, F. D. *J. Am. Chem. Soc.* **2012**, *134*, 12928.
- (43) Sakurada, I.; Yamasaki, S.; Gvättlich, R.; Iida, T.; Kanai, M.; Shibasaki, M. *J. Am. Chem. Soc.* **2000**, *122*, 1245.
- (44) Cai, Y.; Liu, X.; Hui, Y.; Jiang, J.; Wang, W.; Chen, W.; Lin, L.; Feng, X. *Angew. Chem. Int. Ed.* **2010**, *49*, 6160.
- (45) Cai, Y.; Liu, X.; Jiang, J.; Chen, W.; Lin, L.; Feng, X. *J. Am. Chem. Soc.* **2011**, *133*, 5636.
- (46) Cai, Y.; Liu, X.; Li, J.; Chen, W.; Wang, W.; Lin, L.; Feng, X. *Chem. Eur. J.* **2011**, *17*, 14916.
- (47) Li, G.X.; Fu, Q.-Q.; Zhang, X.M.; Jiang, J.; Tang, Z. *Tetrahedron-Asymmetry* **2012**, *23*, 245
- (48) Zhang, W.; Liu, N.; Schienebeck, C. M.; Zhou, X.; Izhar, I. I.; Guzei, I. A.; Tang, W. *Chem. Sci.* **2013**, *4*, 2652.
- (49) Snyder, S. A.; Treitler, D. S.; Brucks, A. P. *J. Am. Chem. Soc.* **2010**, *132*, 14303.
- (50) Snyder, S. A.; Tang, Z.-Y.; Gupta, R. *J. Am. Chem. Soc.* **2009**, *131*, 5744.
- (51) Nicolaou, K. C.; Simmons, N. L.; Ying, Y.; Heretsch, P. M.; Chen, J. S. *J. Am. Chem. Soc.* **2011**, *133*, 8134.
- (52) Hu, D. X.; Shibuya, G. M.; Burns, N. Z. *J. Am. Chem. Soc.* **2013**, *135*, 12960.

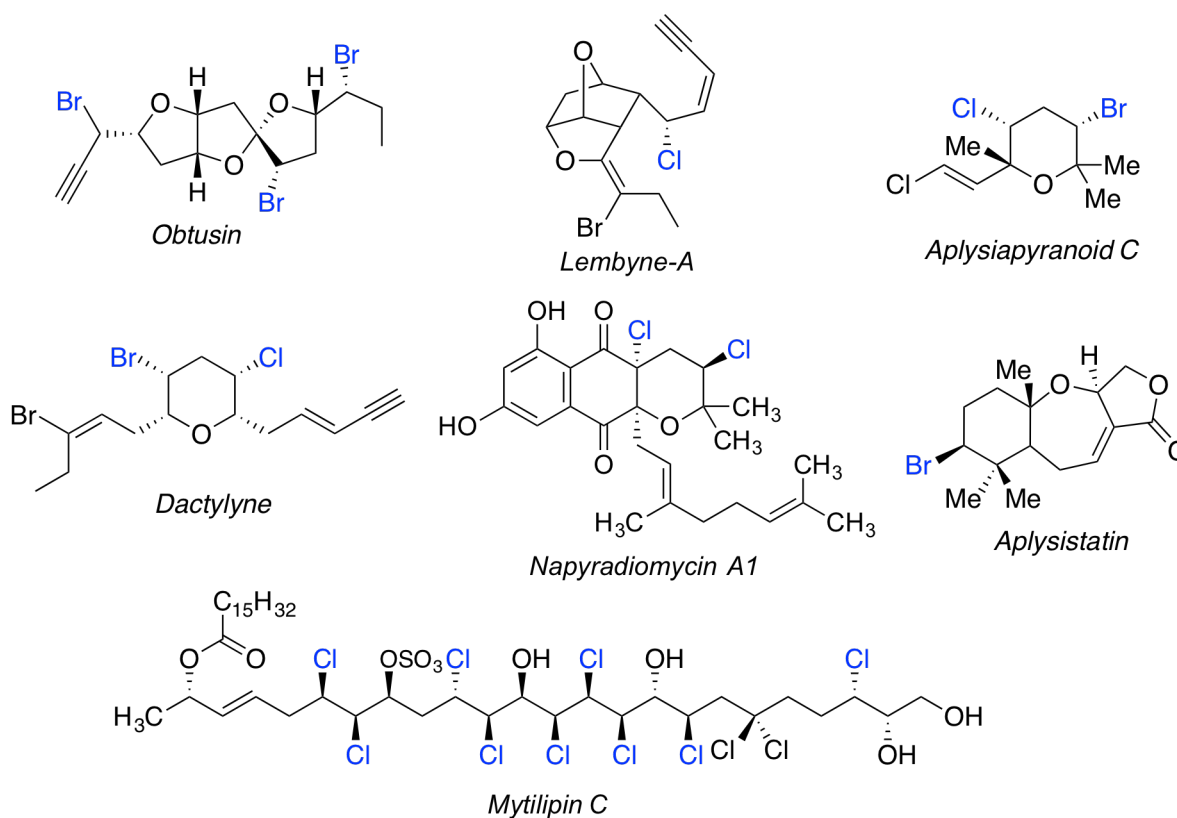
## Chapter II

### ***Organocatalytic asymmetric chlorocyclization of unsaturated amides***

#### II.1. Introduction.

C-halogen bonds are ubiquitous in nature with some estimates suggesting that over 4000 naturally occurring compounds exhibit this unique functionality.<sup>1,2</sup> A representative list of some of these natural products are shown in Figure II-1.

**Figure II-1.** Some natural products with stereodefined C-halogen bonds



As evident, a wide diversity is seen in the complexity of halogen-containing natural products. The biogenetic origin of this unique functionality has been a subject of several investigations in the past. Consequently, five major classes of halogenase enzymes have been discovered.<sup>3-5</sup>

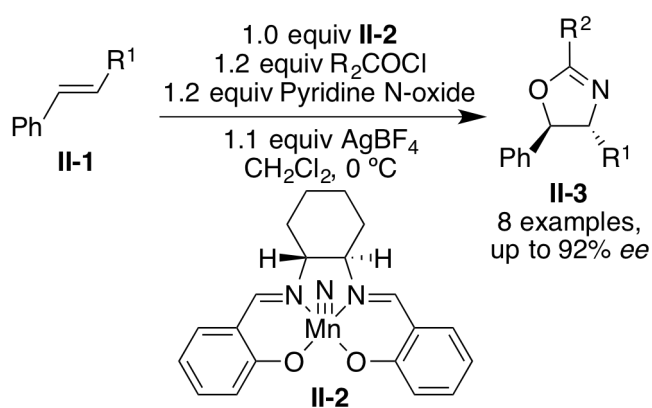
Three of these enzymes classes (Heme-iron dependent haloperoxidases, Vanadium dependent haloperoxidases and Flavin dependent halogenases) are responsible for the halogenation of electron rich aryl rings and alkenes by the formal addition of  $X^+$  to the substrate. The non-heme iron dependent halogenases are responsible for the halogenation of unactivated aliphatic substrates via radical halogenation ( $X^\bullet$ ). Nucleophilic halogenases lead to halide ( $X^-$ ) displacement of good leaving groups in a precursor substrate. Thus, nature has at her disposal, a remarkably diverse and efficient set of tools for incorporating halogen atoms into primary and secondary metabolites.

In contrast, attempts by organic chemists to forge the C-halogen bond stereoselectively have met with little success until recently. After the recent report of a highly enantioselective chlorolactonization reaction by our group in 2010,<sup>6</sup> this research area has witnessed a renewed interest. A myriad of transformations that hinge on the asymmetric alkene halogenation event as the pivotal transformation have been reported over the last three years. Many of these transformations were summarized in Chapter 1. These efforts have uncovered facile routes to a variety of chiral heterocyclic products.

Stereodefined heterocycles such dihydrooxazoles and dihydrooxazines are commonly encountered motifs in natural products, molecules of pharmaceutical interest<sup>7-10</sup> and in several chiral ligands.<sup>11-13</sup> They have also been exploited as useful synthetic intermediates in organic synthesis. However, their syntheses are non-trivial and usually employ stoichiometric quantities of chiral amino alcohols. Some of these amino alcohols are easily derived from naturally occurring amino acids. However, this imposes a serious constraint on the substrate scope. Since the synthesis of enantioenriched amino alcohols often involves non trivial, multi-step syntheses (Asymmetric aminohydroxylation of olefins is not as general as the SAD), the arsenal

of starting materials available for the syntheses of the stereodefined heterocycles is rather limited. As such the synthetic utility of chiral dihydrooxazoles and dihydrooxazines remains untapped. Although numerous reports of the synthesis of racemic oxazolines are known in literature,<sup>14-18</sup> a catalytic asymmetric entry to such class of molecules is highly desirable; however there have been very few successful attempts.

**Scheme II-1.** Komatsu's synthesis of chiral oxazolines *via* interrupted asymmetric nitrene transfer to olefins

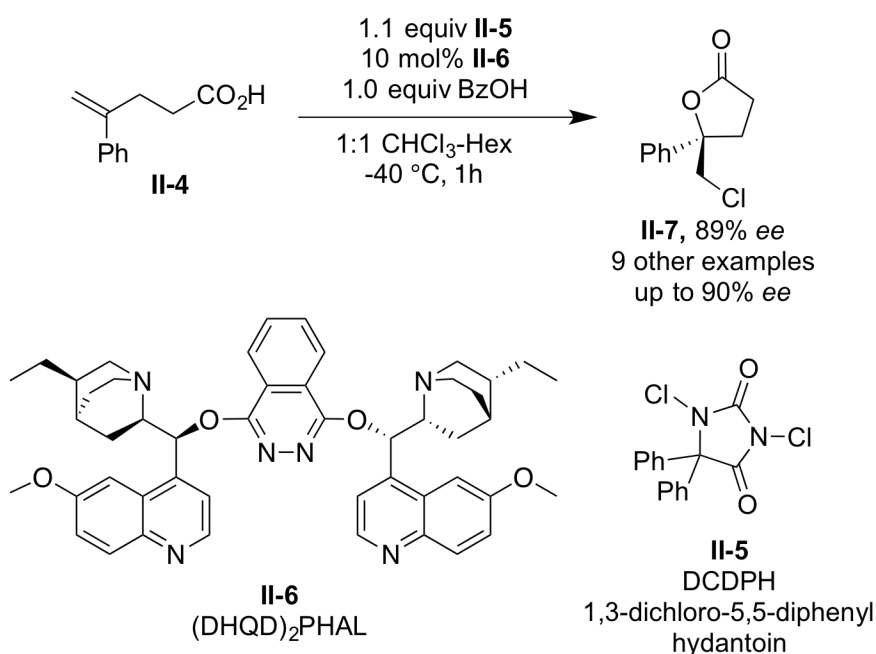


Minakata, Komatsu and co-workers have reported a Mn salen mediated nitrene transfer to olefins in the presence of an acid chloride to give enantioenriched oxazolines in moderate to good yields and good enantioselectivities.<sup>19</sup> It must be emphasized that stoichiometric quantities of the chiral nitrene source **II-2** was employed along with stoichiometric quantities of AgBF<sub>4</sub> and Pyridine *N*-oxide for good results. The scope was limited to *trans*-alkyl substituted styrenes **II-1** (styrene, *cis*-disubstituted and 1,1-disubstituted alkenes gave enantioselectivities in the range of 6 to 32% *ee*). At the commencement of this project, this report was the solitary example of an enantioselective synthesis of oxazolines starting from olefins.

In 2010, our group had disclosed a catalyst system that was capable of promoting highly enantioselective chlorolactonization of alkenoic acids (see Scheme II-2).<sup>6</sup> The commercially

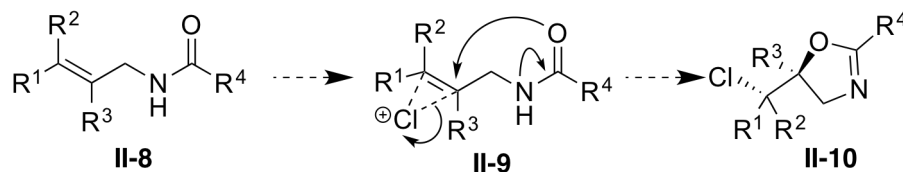
available catalyst **II-6** was employed along with **II-5** as the terminal chlorenium source. While chiral catalyst **II-6** has been used as the chiral promoter in the Sharpless asymmetric dihydroxylation reaction, the chlorenium source **II-5** (5,5-diphenyl-1,3-dichlorohydantoin; abbreviated as DCDPH) is not commercially available. Nonetheless, our lab has devised a one-step synthesis of DCDPH from the corresponding commercially available hydantoin precursor.<sup>20</sup>

**Scheme II-2.** An organocatalytic asymmetric chlorolactonization reaction reported by Whitehead *et.al*



It was envisioned that the same catalytic system (**II-5** with **II-6**) or a slight modification thereof, would enable the enantioselective halocyclization of unsaturated amides as well and thereby enable a facile, one step access to chiral dihydrooxazoles (see Figure 1) starting from alkenes. The halocyclization approach to synthesize these molecules can overcome many of the aforementioned problems - most notably avoiding the use of stoichiometric quantities of chiral amino alcohols or chiral promoters.

**Figure II-2.** Proposed asymmetric chlorocyclization of unsaturated amides to oxazoline heterocycles

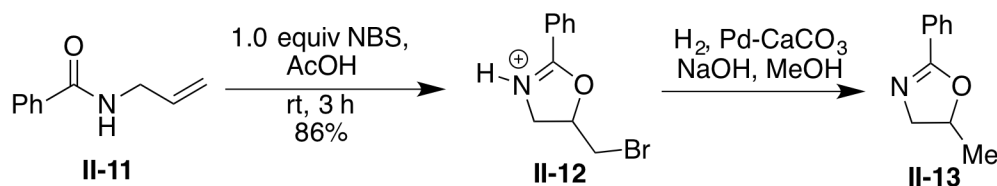


Although the rest of this chapter will deal with the efforts in discovering and optimizing an asymmetric chlorocyclization reaction of unsaturated amides, it merits mention that functional groups other than amides were also evaluated as potentially compatible nucleophiles for this chemistry. These endeavors were met with varying degrees of success. A detailed account of the evaluated reactions will be provided at the end of this chapter.

### II.1.1. Literature precedence for chemoselectivity in the halocyclization of amides.

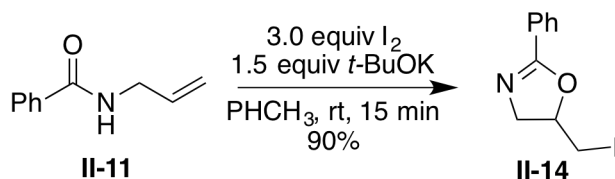
Halocyclization of unsaturated amides finds some precedence in literature.<sup>21-23</sup> The amide nucleophile is ambiphilic in that both the nitrogen atom and the carbonyl oxygen may serve as the nucleophile. Bergmann postulated the formation of oxazoline heterocycles on treatment of N-allyl benzamides with molecular bromine in 1921.<sup>24,25</sup> Over 35 years later, Goodman and Winstein were able to isolate and unambiguously assign the structure of the salts of the cyclized oxazolines heterocycles.<sup>26</sup> Structure assignment of the product **II-12** was initially made on the basis of elemental analysis of the picrate salts of the cyclized products. The structure was further confirmed by chemical transformation of **II-12** into **11-13**.

**Scheme II-3.** Goodman and Winstein's demonstration of bromocyclization of *N*-allylbenzamide to oxazoline heterocycles



More recently, Taguchi and co-workers have demonstrated that exposing **II-11** to molecular I<sub>2</sub> in the presence of a base affords the corresponding iodocyclized oxazoline product **II-14** in good yield.<sup>27</sup>

**Scheme II-4.** Taguchi's iodocyclization of **II-11** to **II-14**



In both instances described above, no aziridine product was detected. The required *N*-allyl amides can be accessed readily and substituents at almost all sites of the molecule can be varied in a straightforward manner. Surprisingly, the stereoselective synthesis of oxazolines using a halocyclization approach has remained virtually unexplored.

Given the utility of these heterocycles and a definitive advantage of this synthetic approach, a systematic study was undertaken to explore this reaction.

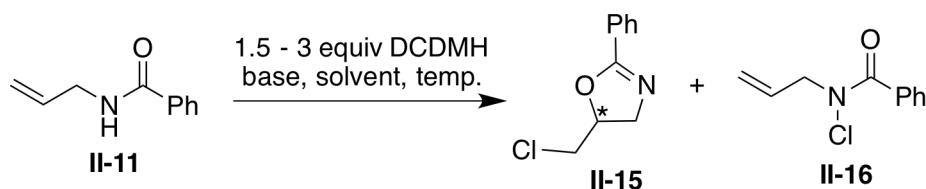
## II.2. Results and discussions.

### II.2.1. Preliminary results.

Although efficient protocols for the bromo- and iodocyclization of **II-11** have been discovered (see Schemes **II-3** and **II-4** above), analogous chlorocyclization reactions find no

precedence. Given that the (DHQD)<sub>2</sub>PHAL catalyst was shown to promote highly enantioselective chlorolactonization (but not the analogous bromo- or iodolactonization reactions), pilot studies aimed to uncover conditions that will lead to the efficient chlorocyclization of substrate **II-11** to give the racemic product **II-15**.

**Table II-1.** Preliminary studies of the non-catalyzed chlorocyclization of **II-11**



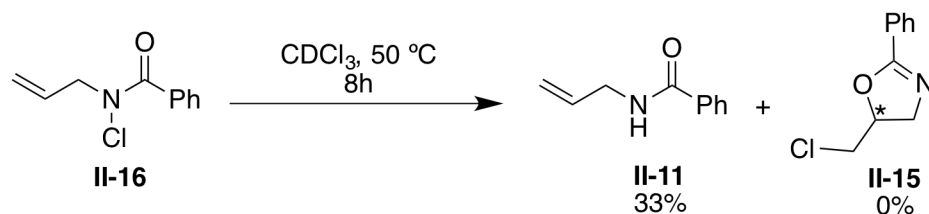
| Entry. | Base                     | Solvent/ Temp                                   | II-15 | II-16 |
|--------|--------------------------|---|-------|-------|
| 1.     | 1.5 equiv <i>t</i> -BuOK | 5:1 CHCl <sub>3</sub> - <i>t</i> BuOH, rt, 13 h | 28%   | 41%   |
| 2.     | None                     | CHCl <sub>3</sub> , rt to 55 °C, 13 h           | 87%   | <2%   |

Note: Yields refer to isolated yields  
Mass balance for Entry 1 was the unreacted substrate

Based on the report by Taguchi and co-workers,<sup>27</sup> the **II-11** was treated with an excess of DCDMH in the presence of *t*-BuOK in a CHCl<sub>3</sub>-*t*-BuOH (5:1) mixed solvent system. In the event, the major product that was isolated was not the desired product **II-15** (28%), but the *N*-chlorinated amide **II-6** (41% yield). 27% of the unreacted substrate was recovered (Entry 1, Table II-1). Postulating that *N*-chlorination may be favored in the presence of a base and a protic solvent, the reaction was run in CHCl<sub>3</sub> as the only solvent and in the absence of *t*-BuOK and *t*-BuOH (Entry 2, Table II-1). These simple measures effectively suppressed the undesired

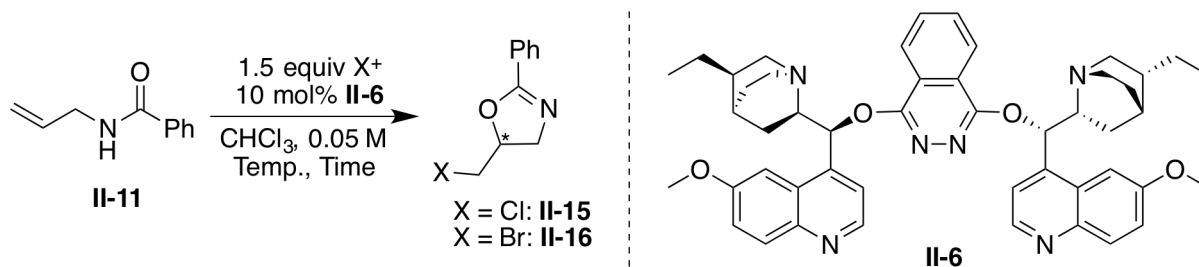
*N*-chlorination. After stirring overnight at 50 °C, the desired oxazoline was obtained as the only product in 87% yield. While this result was encouraging, it could not rule out the possibility of **II-6** being an intermediate that eventually gets transformed to **II-5** either via an intra- or intermolecular chlorine transfer to the olefin. In order to verify whether this was indeed the case, the isolated *N*-chloroamide **II-6** was heated overnight in a CDCl<sub>3</sub> solution (see Scheme II-5). NMR analysis revealed that no oxazoline was formed; in fact the only other compound detected was the dechlorinated amide **II-5** (the mechanism of the dechlorination and the fate of the chlorine atom is unclear at present). This experiment revealed that two different pathways are in operation that leads to either **II-5** or **II-6**. This observation was encouraging given that *N*-chlorination could have precluded the development of an enantioselective variant of this reaction.

**Scheme II-5.** Ruling out **II-16** as a precursor to **II-15**



It merits mention that analogous bromocyclization reaction of **II-11** to the corresponding oxazoline **II-17** was also clean and afforded the cyclized product exclusively. Having found a suitable solvent and conditions that lead predominantly to the desired cyclized product, this reaction was then run in the presence of (DHQD)<sub>2</sub>PHAL. The choice of this particular bis cinchona alkaloid catalyst was dictated by its excellent performance in the chlorolactonization reaction. The screening of other chiral catalysts was to be undertaken in due course.

The following table is a summary of some of the preliminary results with this catalytic system. All reactions were run in micro scale using 0.05 mmol of the amide in 1 mL  $\text{CHCl}_3$  using 10 mol% catalyst loading. Conversions were determined by crude NMR analysis and were determined only when TLC analysis showed unreacted substrate.

**Table II-2.** Enantioselective chloro- and bromocyclization of **II-11** catalyzed by **II-6**

| Entry. | "X <sup>+</sup> " Source | Temp. (°C); Time | Conv. <sup>a</sup> | ee <sup>b</sup> |
|--------|--------------------------|------------------|--------------------|-----------------|
| 1.     | DCDMH                    | 0 °C, 36 h       | < 10%              | - 6%            |
| 2.     | DCDMH                    | 24 °C, 11 h      | 50%                | - 4%            |
| 3.     | NCS                      | 24 °C, 11 h      | < 2%               | nd              |
| 4.     | NCS                      | 60 °C, 72 h      | < 10%              | -8%             |
| 5.     | TCCA                     | - 40 °C, 1.5 h   | ~ 60%              | 10%             |
| 6.     | TCCA                     | -15 °C 12 h      | > 95%              | 11%             |
| 7.     | DBDMH                    | - 40 °C, 90 min. | ~ 20%              | 0%              |
| 8.     | DBDMH                    | -15 °C 8 h       | 40%                | 2%              |
| 9.     | NBS                      | 0 °C, 10h        | Trace              | 6%              |
| 10.    | NBS                      | 24 °C, 10h       | < 10%              | 8%              |
| 11.    | NBS                      | 60 °C, 4.5 h     | > 95%              | 2%              |

Note: Conversions were determined by <sup>1</sup>H NMR analysis and ee values were determined by chiral GC analysis; TCCA = trichloroisocyanuric acid; DBDMH = 1,3-dibromo-5,5-dimethyl hydantoin; NBS = *N*-bromosuccinimide; NCS = *N*-chlorosuccinimide

The reaction with DCDDMH as the chlorenium source was very sluggish and only a trace quantity of the cyclized product was formed even after 36 h at 0 °C (entry 1, Table II-2). The enantioselectivity was also very poor (-6% ee). Conversion was significantly better if the

resaction was run at ambient temperature (50% conv aft 11 h; see entry 2, Table II-2) although there was no improvement in the enantioselectivity (-4% *ee*). Not surprisingly, the less reactive *N*-chlorosuccinimide (NCS) gave even more sluggish reactions and the desired product was isolated in trace quantities even after 3 days at 60 °C (entries 3 and 4, Table II-2). Disappointingly, there was no improvement in enantioselectivity either. On employing the highly reactive TCCA as the terminal chlorenium source, the reactions could be driven to completion within 12 h at -15 °C. Nonetheless, the enantioselectivity was still very poor (>95% conversion, 11% *ee*, entry 6, Table II-2). Intriguingly, TCCA gave enantioinduction that was opposite to that observed with NCS and DCDMH.

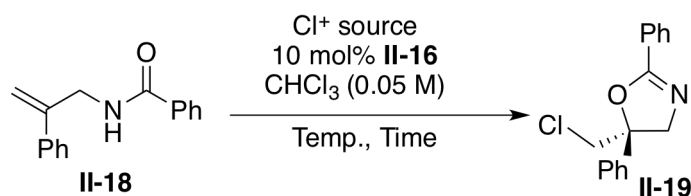
Attempted bromocyclization reaction with NBS and DBDMH as the bromenium sources at various temperatures also led to disappointing results (see entries 7 – 11 in Table II-2).

Two plausible hypotheses could be put forward from these preliminary studies – First, **II-6** [(DHQD)<sub>2</sub>PHAL], that had performed excellently in the chlorolactonization reaction of alkenoic acids) is a poor catalyst for this transformation and second, terminal alkenes may be poor substrates for (DHQD)<sub>2</sub>PHAL. The first hypothesis could be verified by a catalyst-screening endeavor in order to discover a better catalyst for this transformation. The second hypothesis on the other hand, could be easily verified by evaluating a 1,1-disubstituted alkene substrate with the same catalyst. Indeed, 1,1-aryl substituted olefins were the best substrates for the chlorolactonization methodology and not terminal alkenes. It was postulated that 1,1-disubstituted olefins might bind better with the catalyst and thereby afford a more stereoselective reaction.

Gratifyingly, when amide **II-18** was exposed to various chlorenium sources in the presence of 10 mol% (DHQD)<sub>2</sub>PHAL, significant increases in both conversions and *ee*'s were realized. DCDMH and TCCA gave quantitative conversions of the starting material. While DCDMH

returned **II-19** in 57% *ee*, TCCA gave 18% *ee* (entries 1 and 2, Table II-3). Higher temperatures and longer reaction times were needed with the less reactive NCS. An intriguing temperature dependent enantioselectivity was discerned with NCS. **II-19** was formed in trace quantities and 20% *ee* after stirring at 0 °C for 36 h (entry 3, Table II-3). At ambient temperature after 6 days, **II-19** was formed in 50% *ee*. Chloramine-•3H<sub>2</sub>O also gave a significant level of stereinduction (43% *ee*, entry 5, Table II-2); although the conversion to product was very low.

**Table II-3.** Preliminary studies of the asymmetric chlorocyclization of **II-18** to **II-19**



| Entry | X <sup>+</sup> source, Temp., Time | Conv. | <i>ee</i> |
|-------|------------------------------------|-------|-----------|
| 1.    | DCDMH, -20 °C, 10 h                | >95%  | 57%       |
| 2.    | TCCA, -20 °C, 1 h                  | >95%  | 18%       |
| 3.    | NCS, 0 °C, 36 h                    | Trace | 20%       |
| 4.    | NCS, 24 °C, 144 h                  | 65%   | 50%       |
| 5.    | ChloramineT•3H <sub>2</sub> O      | Trace | 43%       |

Note: Conversion was determined by <sup>1</sup>H NMR and *ee* was determined by chiral HPLC analysis

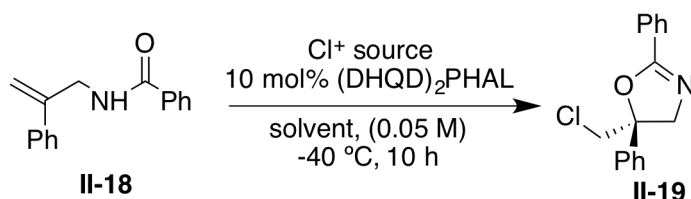
## II.2.2. Optimization of reaction variables.

### II.2.2.1. Retracing the optimization of the asymmetric chlorolactonization reaction.

With a preliminary hit of 57% *ee*, efforts were directed at optimizing it to synthetically useful levels. Extensive optimization data for the asymmetric chlorolactonization methodology was at our disposal at this stage. It was hoped that changes in the reaction conditions would

show similar trends as those seen in the chlorolactonization methodology. We were cognizant that drawing parallels between these two reactions with regards to their mechanisms was premature. However, a quick survey of the previously optimized conditions would reveal the generality of these conditions.

**Table II-4.** Preliminary optimizations guided by the results of the asymmetric chlorolactonization reaction



| Entry | X <sup>+</sup> source, Solvent        | Conv. | ee  |
|-------|---------------------------------------|-------|-----|
| 1.    | DCDMH, CHCl <sub>3</sub>              | >95%  | 57% |
| 2.    | DCDPH, CHCl <sub>3</sub>              | >95%  | 63% |
| 3.    | DCDPH, 1:1 CHCl <sub>3</sub> -Hexanes | >95%  | 69% |

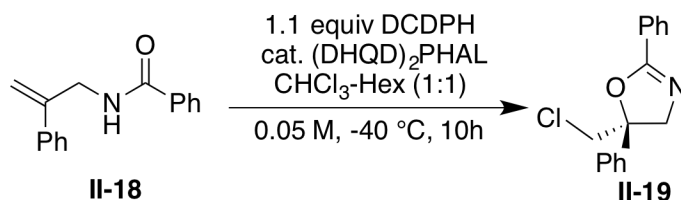
Note: Conversion was determined by <sup>1</sup>H NMR and *ee* was determined by chiral HPLC analysis

The optimized conditions for the chlorolactonization chemistry calls for the use of DCDPH in a 1:1 CHCl<sub>3</sub>-Hexanes solvent system at -40 °C. Changing the chlorine source from DCDMH that was used in the pilot studies to the more bulky DCDPH returned **II-19** in a slightly improved 63% *ee* (entry 2, Table II-4). A further increase in stereoselectivity to 69% *ee* was observed on changing the solvent system from CHCl<sub>3</sub> to a 1:1 CHCl<sub>3</sub>-Hexane co-solvent mixture (entry 3, Table II-4). While these increments in the enantioselectivity were encouraging, the numbers were significantly lower than the ~90% *ee* that was observed for the chlorolactonization reaction.

### II.2.2.2. Catalyst and chlorine source loading studies.

The effect of catalyst loading was then studied. It was evident that increasing the catalyst loading did not affect the *ee*'s significantly. The *ee*'s remained almost constant at ~65% *ee* on systematically increasing the catalyst loading from 10 mol% to 50 mol% (entries 1 – 5, Table II-5). In order to get a feel for the upper limit with this catalytic system, stoichiometric quantities of the catalyst were also evaluated (see entries 5 and 6 in Table II-5). While improved enantioselectivity of 74% *ee* was seen at 0.01 M substrate concentration, the gain in *ee* was deemed too insignificant to warrant such a high catalyst loading. The lower limit for catalyst loading was established much later in the optimization process; this will be discussed in a subsequent section.

**Table II-5.** Catalyst loading studies



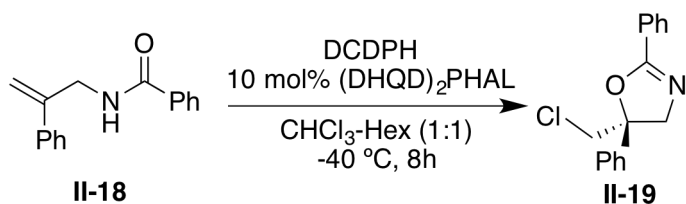
| Entry | Catalyst loading | <i>ee</i>        | Entry | Catalyst loading   | <i>ee</i> |
|-------|------------------|------------------|-------|--------------------|-----------|
| 1.    | 10 mol%          | 66%              | 4.    | 50 mol%            | 65%       |
| 2.    | 20 mol%          | 65%              | 5.    | 100 mol% (0.01 M)  | 74%       |
| 3.    | 30 mol%          | 64% <sup>b</sup> | 6.    | 100 mol% (0.005 M) | 70%       |

Note: *ee* was determined by chiral HPLC analysis

Following this study, the effect of the hydantoin concentration was studied. Once again, no significant improvement of stereoselectivity was observed; the *ee*'s remained almost constant at

70% going from 1.1 equivalents to 5.0 equivalents of DCDPH for each equivalent of the substrate (see Table II-6).

**Table II-6.** Effect of DCDPH stoichiometry on the enantioselectivity of asymmetric chlorocyclization of **II-18**



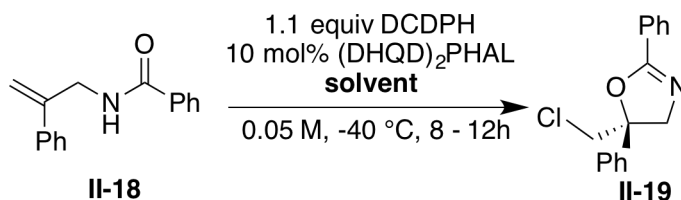
| Entry | Equiv. of DCDPH | <i>ee</i> |
|-------|-----------------|-----------|
| 1.    | 1.1 equiv       | -71%      |
| 2.    | 2.0 equiv       | -68%      |
| 3.    | 3.0 equiv       | -71%      |
| 4.    | 5.0 equiv       | -70%      |

Note: *ee* was determined by chiral HPLC analysis

At this stage, we had arrived at conditions that were very similar to that used in the chlorolactonization methodology after extensive optimization. However, the enantioselectivity was still quite far away from the 91% *ee* realized with this system. It was becoming apparent that the best reaction condition for the chlorolactonization methodology was far from the optimal condition for this reaction. Further modifications would increasingly delineate from the established optimal system. The available data demanded an exhaustive optimization of all reagents involved in this reaction rather than merely retracing the successes achieved with the chlorolactonization. A hypothesis driven approach was imperative.

Since the results so far indicated that the most significant increases in *ee*'s had resulted from changes in the solvent system, an exhaustive screen of solvents was undertaken. The results are presented in Table II-7 below.

**Table II-7.** Solvent screen for the asymmetric chlorocyclization of **II-18** to **II-19**



| Entry | Solvent         | <i>ee</i> (%) | Entry | Solvent                       | <i>ee</i> (%) |
|-------|-----------------|---------------|-------|-------------------------------|---------------|
| 1.    | Hexane          | 26            | 10.   | Isopropanol                   | -15           |
| 2.    | Dioxane         | 0             | 11.   | Nitromethane                  | 79            |
| 3.    | Benzene         | 52            | 12.   | Dimethylformamide             | 38            |
| 4.    | Toluene         | 37            | 13.   | Acetonitrile                  | 67            |
| 5.    | Diethyl ether   | 35            | 14.   | Dimethylsulfoxide             | NR            |
| 6.    | Chloroform      | 57            | 15.   | Ethanol                       | Nd            |
| 7.    | Ethyl acetate   | 44            | 16.   | Methyl- <i>t</i> -Butyl ether | 36            |
| 8.    | Tetrahydrofuran | 27            | 17.   | 1,2-Dichloroethane            | 8             |
| 9.    | Dichloromethane | 17            | 18.   | Acetone                       | 69            |

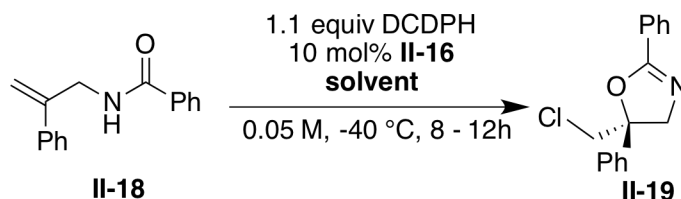
Note: Conversions were not determined for the reactions above; *ee* value was determined by chiral HPLC analysis

Non-polar solvents such as hexane (26% *ee*) , toluene (37% *ee*), benzene (52% *ee*), and ethyl acetate (44% *ee*) gave only modest levels of enantioselectivity for **II-19**. Ethereal solvents such as THF (27% *ee*), MTBE (36% *ee*) and diethylether (35% *ee*) were all equally poor solvents. Dioxane returned the racemic product. Amongst halogenated solvents,

dichloromethane (DCM) (17% *ee*) was significantly inferior to chloroform (56% *ee*), while dichloroethane (DCE) (8% *ee*) was the worst. Reactions in alcoholic solvents such as ethanol and isopropanol (IPA) were messy (presumably due to the competing intermolecular nucleophilic capture of the putative chloronium ion intermediate by the solvent) and the enantioselectivities were poor. Interestingly, IPA gave the product with the opposite stereoselection (-15% *ee*) and remains the solitary example amongst the solvents that were screened that gave an opposite stereoselection. Dimethyl formamide (DMF) gave an *ee* of 38% (the low enantioselectivity is perhaps due to a competing background reaction mediated by DMF itself which is known to be a good catalyst for halocyclization reactions) while DMSO shut down the reaction completely. Acetone gave 69% *ee*. The polar aprotic solvents MeCN (67% *ee*) and MeNO<sub>2</sub> (79% *ee*) emerged as the best solvents for this transformation. It was noteworthy that reactions with MeNO<sub>2</sub> were highly temperature dependent with regards to both yields and enantioselectivities of the reaction. Low temperatures gave cleaner and more stereoselective reactions (these observations along with others pertaining to temperature dependence of this reaction will be discussed later).

A few mixed solvent systems were also evaluated as seen in Table II-8. First, *t*-BuOH-H<sub>2</sub>O solvent system commonly used in the Sharpless asymmetric dihydroxylation reaction (that also employs catalyst (DHQD)<sub>2</sub>PHAL as the source of chirality) was evaluated. Product **II-19** was formed in only 26% *ee* (entry 1, Table II-8). Drastic improvements in the enantioselectivity were observed in the chlorolactonization reaction with the inclusion of non-polar co-solvents such as hexanes and toluene. The decision to pursue mixed solvent systems was largely inspired by the optimization efforts of the chlorolactonization reaction.

**Table II-8.** Evaluation of mixed solvent systems for the asymmetric chlorocyclization of **II-18**



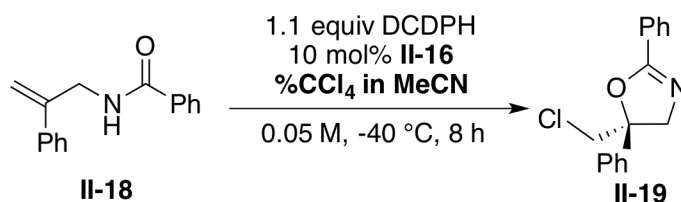
| Entry | Solvent                                   | ee (%) | Entry | Solvent                      | ee (%) |
|-------|---|--------|-------|------------------------------|--------|
| 1.    | <i>t</i> -BuOH-H <sub>2</sub> O (1:1)     | 26     | 4.    | MeCN-Hexane (1:1)            | 67     |
| 2.    | CHCl <sub>3</sub> -Hexane (1:1)           | 68     | 5.    | MeCN-CCl <sub>4</sub> (1:1)  | 79     |
| 3.    | CHCl <sub>3</sub> -CCl <sub>4</sub> (1:1) | 70     | 6.    | MeCN-MeNO <sub>2</sub> (1:1) | 78     |

Note: Conversion was >95% for all reactions as determined by <sup>1</sup>H NMR analysis

Chloroform-Hexane solvent system gave a 68% *ee* (entry 2, Table II-8). Substituting hexane with an equally non polar CCl<sub>4</sub> gave a slightly enhanced *ee* of 70% (entry 3, Table II-8). Since MeCN and MeNO<sub>2</sub> had emerged as the best solvents from the solvent screen (see Table II-7), a similar co-solvent study was undertaken with these two solvents as well. While MeCN-Hexane (1:1) gave a 67% *ee* (entry 4, Table II-8), it must be emphasized that MeCN and hexane are immiscible and the result is perhaps a reflection of the *ee* obtained using MeCN by itself (also 67% *ee*). Likewise, MeNO<sub>2</sub>-CCl<sub>4</sub> (1:1) also forms a heterogenous solvent system and gives an *ee* of 77% (not shown in the table), which is quite similar to that obtained in MeNO<sub>2</sub> by itself (entry 11, Table II-7, 79% *ee*). Significant gains in *ee* were seen with 1:1 MeCN-CCl<sub>4</sub> co-solvent system (entry 5, Table II-8, 79% *ee* as opposed 67% *ee* in MeCN alone).

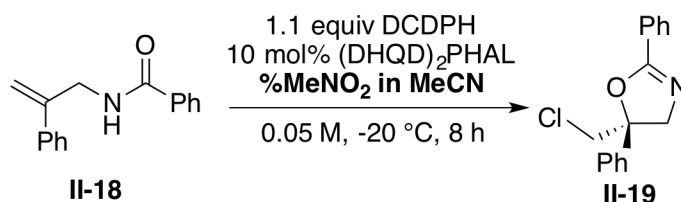
A systematic co-solvent study of the MeCN-CCl<sub>4</sub> system indicated that addition of merely 10 volume % of CCl<sub>4</sub> increases the *ee* to 78% (from 67% with MeCN alone, entry 1, Table II-9). A maximum *ee* of 80% was achieved when 40% CCl<sub>4</sub> in MeCN was employed as the solvent. Any further increase in CCl<sub>4</sub> concentration proved detrimental to enantioselectivities (entries 5 – 9, Table II-9).

**Table II-9.** CCl<sub>4</sub>-MeCN co-solvent study



| Entry | % of CCl <sub>4</sub> in MeCN | <i>ee</i> (%) | Entry | % of CCl <sub>4</sub> in MeCN | <i>ee</i> (%) |
|-------|-------------------------------|---------------|-------|-------------------------------|---------------|
| 1.    | 10                            | 78            | 5.    | 50                            | 78            |
| 2.    | 20                            | 77            | 6.    | 60                            | 75            |
| 3.    | 30                            | 79            | 7.    | 70                            | 70            |
| 4.    | 40                            | 80            | 8.    | 80                            | 63            |

Note: Conversion was >95% for all reactions as determined by <sup>1</sup>H NMR analysis

**Table II-10.** MeNO<sub>2</sub>-MeCN co-solvent study

| Entry | % of MeNO <sub>2</sub> in MeCN | ee (%) | Entry | % of MeNO <sub>2</sub> in MeCN | ee (%) |
|-------|--------------------------------|--------|-------|--------------------------------|--------|
| 1.    | 10                             | 76     | 4.    | 40                             | 78     |
| 2.    | 20                             | 75     | 5.    | 50                             | 78     |
| 3.    | 30                             | 77     | 6.    | 100                            | 79     |

Note: Conversion was >95% for all reactions as determined by <sup>1</sup>H NMR analysis

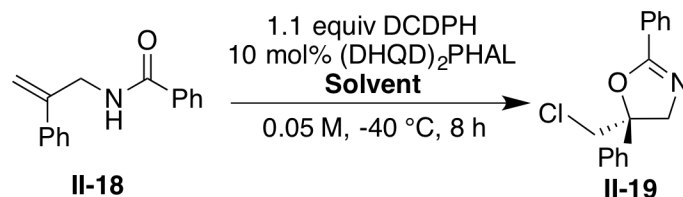
A similar study of MeNO<sub>2</sub>-MeCN co-solvent system was also undertaken (Table II-10).

However, the *ee*'s for all compositions were between those seen for MeCN and MeNO<sub>2</sub>.

### II.2.2.3. *ee* as a function of solvent polarity.

The evaluation of numerous solvents (detailed in the previous section) showed that solvents with higher dielectric constants consistently gave better enantioselectivities than those with lower dielectric constants. In order to determine whether this was a reliable trend, a series of homologous solvents were evaluated for this transformation. The results with homologous solvents are presumably more reliable than comparison across different solvent classes given the same functional group present in each class of homologous solvents. Assuming similar properties of solvation and charge stabilization (admittedly an oversimplification), one could investigate the role of dielectric constant independent of other parameters of the solvents in influencing enantioselectivity. For this purpose, a homologous series of nitroalkanes and alkyl nitriles were evaluated as the solvents for the test reaction.

**Table II-11.** Enantioselectivity as a function of the dielectric constant of the reaction medium



| Entry | Solvent                          | Dielectric constant ( $\epsilon_R$ ) | ee (%) |
|-------|----------------------------------|--------------------------------------|--------|
| 1.    | MeCN                             | 37.5                                 | 67%    |
| 2.    | C <sub>2</sub> H <sub>5</sub> CN | 25.0                                 | 60%    |
| 3.    | <i>i</i> -PrCN                   | 22.0                                 | 60%    |
| 4.    | CCl <sub>3</sub> CN              | 7.85                                 | 40%    |
| 5.    | MeNO <sub>2</sub>                | 35.9                                 | 79%    |
| 6.    | <i>i</i> -PrNO <sub>2</sub>      | 25.5                                 | 80%    |
| 7.    | <i>n</i> -PrNO <sub>2</sub>      | 22.7                                 | 70%    |

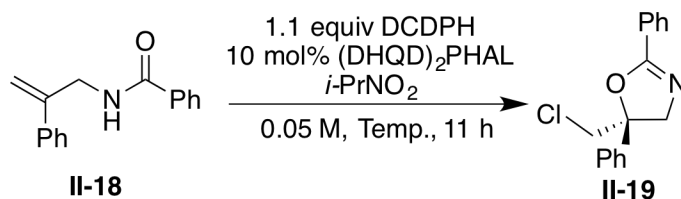
Note: Conversion was >95% for all reactions as determined by <sup>1</sup>H NMR analysis

As evident from the Table II-11, there is a noticeable trend of increasing enantioselectivity with increasing dielectric constants. Amongst alkyl nitriles (entries 1 – 5, Table II-11), MeCN with a dielectric constant of 37.5 gave the highest enantioselectivity (67% *ee*) whereas CCl<sub>3</sub>CN, which had the lowest dielectric constant of 7.85, gave 40% *ee*. C<sub>2</sub>H<sub>5</sub>CN and *i*-PrCN with comparable dielectric constants returned the product in an identical 60% *ee*. A less pronounced trend was seen in the nitroalkane series of solvents (see entries 6 – 9 in Table II-12). The mechanistic implications of this trend are not clear at this stage. It is well

established that hydrophobic interactions between solute molecules are enhanced in polar solvents. It is plausible that polar solvents could be increasing hydrophobic interactions between the substrate and catalyst (such as  $\pi$ -stacking interactions) and thereby promoting a more stereoselective reaction to a stronger substrate-catalyst complex. Such hypotheses cannot be confirmed until more detailed mechanistic studies are undertaken.

Entry 6 in the table above was especially interesting. *i*-PrNO<sub>2</sub> has a melting point of -93 °C. This gives an opportunity to evaluate the reaction at significantly lower temperatures. Indeed, when the test reaction was repeated at lower temperatures, higher enantioselectivities were obtained. The *ee* value steadily improved from 80% to 87% on going from -40 °C to -80 °C (see Table II-12). Although the cryogenic temperatures were somewhat unappealing from a practical stand-point, these studies demonstrated for the first time that enantioselectivities approaching those obtained in the chlorolactonization reaction (ca. 90% *ee*) were indeed achievable with the DCDPH/II-16 catalytic system for the amide chlorocyclization reaction as well.

**Table II-12.** Temperature dependence of enantioselectivity in *i*-PrNO<sub>2</sub>



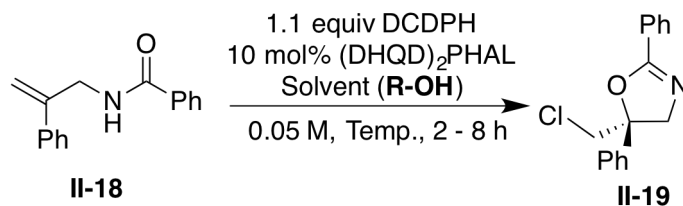
| Entry | Temperature | ee (%) |
|-------|-------------|--------|
| 1.    | -40 °C      | 80     |
| 2.    | -60 °C      | 83     |
| 3.    | -80 °C      | 87     |

Note: Conversion was >95% for all reactions as determined by <sup>1</sup>H NMR analysis

#### II.2.2.4. Serendipitous discovery of CF<sub>3</sub>CH<sub>2</sub>OH as the optimal solvent.

At this stage, a fortuitous set of events led to the identification of the optimal solvent for this transformation. In the preliminary solvent screen for this reaction, alcohols had proven to be poor solvents for this reaction. One of the major side products observed was the chloroether products **II-20** obtained by the intermolecular capture of the putative chloronium ion intermediate by the alcoholic solvent (see entry 1, Table II-13). In an effort to uncover whether the decreased nucleophilicity of alcohols might promote intramolecular cyclization preferentially over the intermolecular nucleophilic capture of the chloronium ion, CF<sub>3</sub>CH<sub>2</sub>OH (trifluoroethanol, TFE) and (CF<sub>3</sub>)<sub>2</sub>CHOH (hexafluoroisopropanol, HFIP) were evaluated as reaction solvents. Delightfully, both solvents gave exclusively the cyclized product (entries 2 and 3, Table II-13). Furthermore, the enantioselectivity for **II-19** was the best observed till date (90% *ee*) when TFE was employed as the reaction solvent. HFIP returned **II-19** in 82% *ee* even at ambient temperature (entry 3, Table II-13)

**Table II-13.** Enantioselectivity of chlorocyclization of **II-18** in alcohol solvents



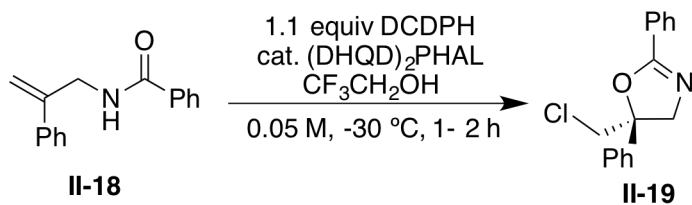
| Entry | Solvent, Temp.                              | II-19:II-20 | ee of II-19 (%) |
|-------|---|-------------|-----------------|
| 1.    | MeOH, -40 °C                                | 2:1         | nd              |
| 2.    | CF <sub>3</sub> CH <sub>2</sub> OH, -40 °C  | >20:1       | 90              |
| 3.    | (CF <sub>3</sub> ) <sub>2</sub> CHOH, 24 °C | >20:1       | 82              |

Note: Conversion was >95% for all reactions as determined by <sup>1</sup>H NMR analysis  
Product ratios were determined by crude <sup>1</sup>H NMR analysis

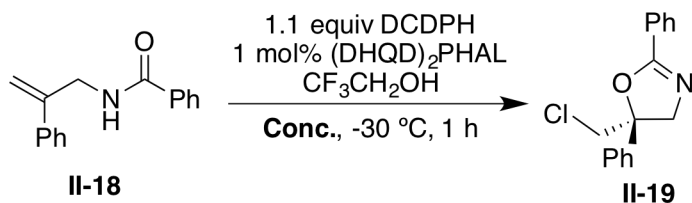
All further attempts to improve the enantioselectivity utilized TFE as the reaction solvent.

#### II.2.2.5. Catalyst loading reaction concentration studies.

Although preliminary studies in the CHCl<sub>3</sub>-Hexanes solvent system had shown negligible improvements in the enantioselectivity with increased catalyst loadings (see Table II-5), it was deemed necessary to revisit the studies in TFE. Delightfully, the reaction exhibited no loss in enantioselectivity when the catalyst loading was progressively decreased from 10 mol% to 1.0 mol% (see entries 1 – 4, Table II-14). At 0.5 mol% loading, a small decrease in enantioselectivity to 86% *ee* was seen (entry 5, Table II-14).

**Table II-14.** Catalyst loading studies for chlorocyclization of **II-18** in  $\text{CF}_3\text{CH}_2\text{OH}$ 

| Entry | Catalyst loading | Conversion | ee  |
|-------|------------------|------------|-----|
| 1.    | 10.0 mol%        | >95%       | 90% |
| 2.    | 5.0 mol%         | >95%       | 90% |
| 3.    | 2.0 mol%         | >95%       | 90% |
| 4.    | 1.0 mol%         | >95%       | 90% |
| 5.    | 0.5 mol%         | 93%        | 86% |

**Table II-15.** Effect of initial substrate concentration on the enantioselectivity of the chlorocyclization reaction of **II-18**

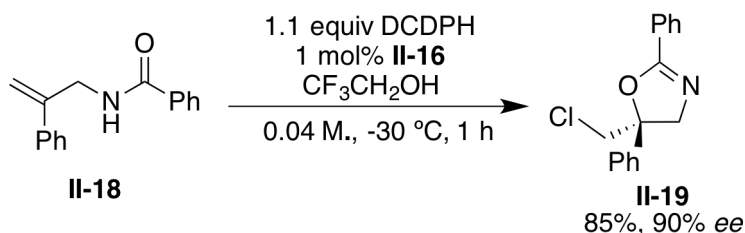
| Entry | Concentration | ee of <b>II-19</b> |
|-------|---------------|--------------------|
| 1.    | 0.04 M        | 90%                |
| 2.    | 0.08 M        | 87%                |
| 3.    | 0.10 M        | 86%                |
| 4.    | 0.15 M        | 82%                |
| 5.    | 0.20 M        | 83%                |

Note: Concentration refers to initial substrate concentration; Conversion was >95% for all substrates

Higher reaction concentrations led to lower enantioselectivities. As seen in Table II-15, the best enantioselectivity (90% *ee*) was obtained at a concentration of 0.04 M. The enantioselectivity progressively decreased to 83% *ee* when the reaction concentration was increased to 0.20 M with respect to the substrate.

On combining the optimal catalyst loading and reaction concentration, the desired product **II-19** was isolated in 85% yield and 90% *ee*. It must be emphasized that reactions were intentionally run at -30 °C instead of -40 °C because of the slightly variable results obtained at -40 °C (perhaps due to the increased viscosity and poor sample mixing at temperatures close to the melting point of TFE: -43 °C).

**Scheme II-6.** Asymmetric chlorocyclization of **II-18** under optimized reaction conditions



Although this result matches the performance of the DCDPH/(DHQD)<sub>2</sub>PHAL system in terms of the enantioselectivity imparted for the chlorolactonization reaction, avenues for further improvements were still available.

### II.2.3. Steric and electronic fine-tuning of the chlorocyclization substrates.

The oxazoline heterocycles obtained from the chlorocyclization reaction are essentially masked vicinal amino-alcohol motifs. The aryl group at C2 acts as a nascent ‘protecting group’ and is ultimately revealed as the acid-labile functionality of the oxazoline product. As such, it could be viewed as a sacrificial entity. The hydrolysis or hydrogenolysis of the oxazoline ring will unveil the embedded amino-alcohol.

Optimization of the reaction through alteration of the aryl group at C2 could provide the opportunity for electronic and steric fine-tuning – a luxury that was absent for the optimization of the analogous chlorocyclization reaction of alkenoic acids. A series of electronically and sterically diverse amides were synthesized and evaluated in the chlorocyclization reaction. These results are summarized in Figure II-3.



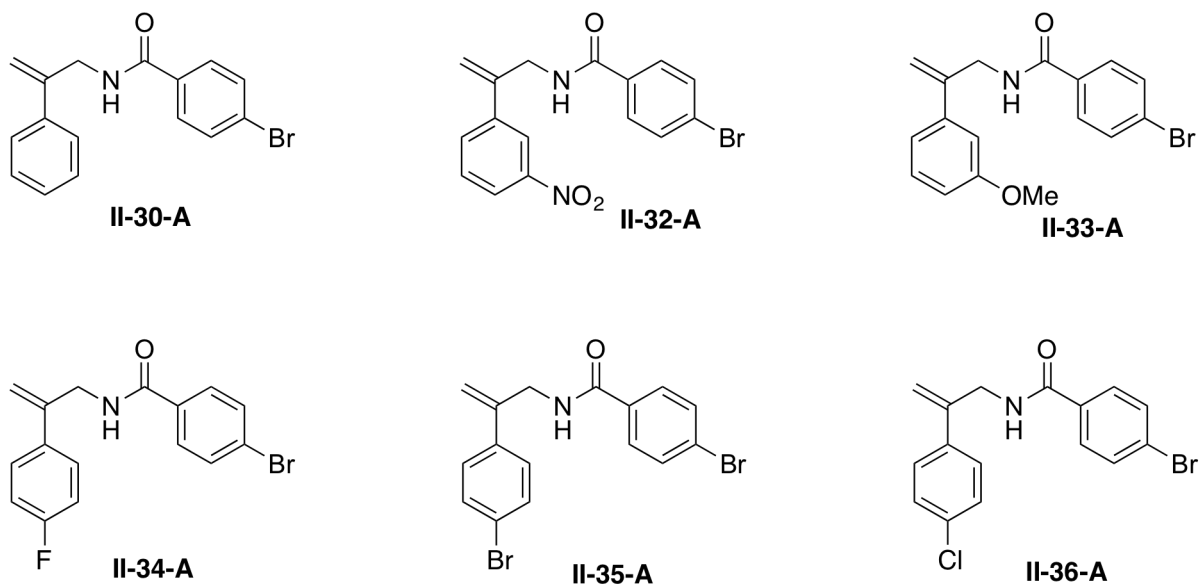
The precise nature of the substrate–catalyst interaction is still under investigation, however, we believe that *para* substituents on the C2 aryl ring provide a steric (rather than electronic) bias for better catalyst–substrate interaction. Substituents at the *para* position of the aryl ring at C2 increased the *ee* value regardless of their electron-donating/- withdrawing properties. For example, when the C2 substituent was an unsubstituted phenyl ring, the product **II-19** was formed in 90 % *ee*. However, the 4-NO<sub>2</sub>C<sub>6</sub>H<sub>4</sub> and the 4-OMeC<sub>6</sub>H<sub>4</sub> substituted products, **II-23-B** and **II-22-B**, were both formed in a slightly enhanced 93 % *ee*. Likewise, comparison of **II-26-B** and **II-27-B** is also indicative of the crucial role of the *para* substituent of the aryl ring. The 3,5-dinitrophenyl substituent (86 % *ee*) is clearly inferior to the 3,5-dinitro-4-methylphenyl substituent (98 % *ee*), thus indicating that the methyl group at the *para* position is essential for good stereoselectivity in the latter case. The methyl substituent led to near complete loss in the enantioselectivity (**II-21-B**, <5% *ee*). The 4-BrC<sub>6</sub>H<sub>4</sub> substituted product **II-30-B** was also formed with an excellent 98 % *ee*. The significantly more bulky *t*Bu group gave the corresponding product **II-25-B** with a lower *ee* value (88 % *ee*). Heterocyclic rings such as 2-pyridyl (**II-28-B**, 79 % *ee*) and 3-pyridyl (**II-29-B**, 92 % *ee*) were also well tolerated as the C2 substituent in this reaction. The sterically demanding 2,4,6-triethylphenyl substituent significantly diminished the stereoselectivity of the reaction to give the product **II-24-B** in only 55 % *ee*. It merits mention that the yields for all these reactions were excellent (79–97%) with no significant quantities of side products. The 4-Br-C<sub>6</sub>H<sub>4</sub> substituent was ultimately chosen as the optimal aryl group at C2 for further studies.

#### **II.2.4. Substrate scope evaluation for the synthesis of chiral oxazolines by asymmetric chlorocyclization of 1,1-disubstituted allyl amides.**

Having thus arrived at the 4-Br-C<sub>6</sub>H<sub>4</sub> benzamide as the optimal ‘protecting group’, the substrate scope for this transformation with regards to the alkene substituent could now be

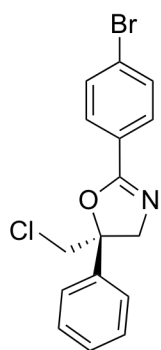
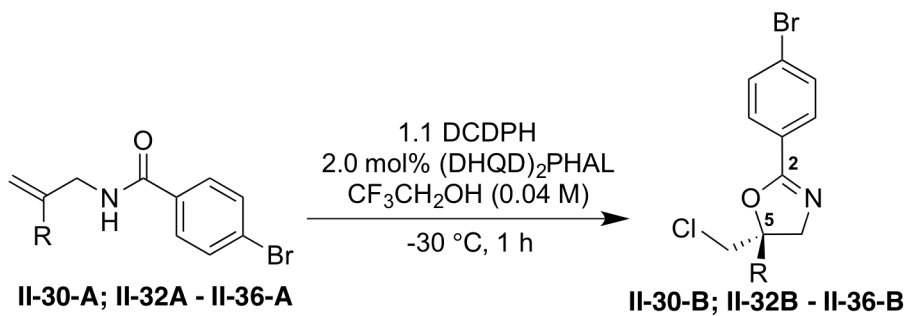
probed. In order to probe the substrate scope for this reaction, a series of 1,1-disubstituted allylic amides were synthesized.

**Figure II-4.** 1,1-disubstituted allylic amide substrates for asymmetric chlorocyclization reaction

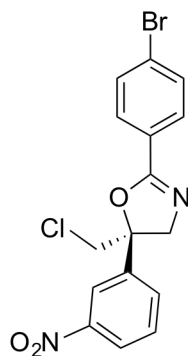


For the substrate scope evaluation, 2.0 mol% of (DHQD)<sub>2</sub>PHAL was used in order to drive the reaction to completion in under 1 hour for all the substrates. The strongly electron-withdrawing NO<sub>2</sub> group at the *meta* position significantly decreased the enantioselectivity of the reaction. The desired product **II-32-B** was isolated in 75 % yield and a modest 68 % *ee* (see Figure II-5). Interestingly, switching the NO<sub>2</sub> group with the electron-donating OMe group at the *meta* position restored the stereoselectivity of the reaction to give the product **II-33-B** in 93 % *ee*. Halogenated aryl rings were well tolerated (**II-34-B** to **II-36-B**)

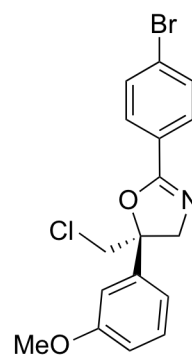
**Figure II-5.** Substrate scope for the asymmetric chlorocyclization of *N*-2-aryl-2-propenylbenzamides



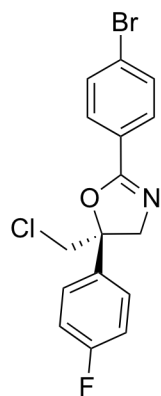
**II-30-B**  
93% yield  
98% ee



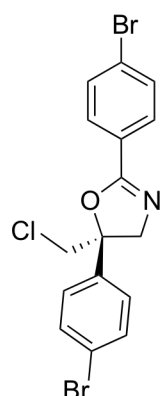
**II-32-B**  
75% yield  
68% ee



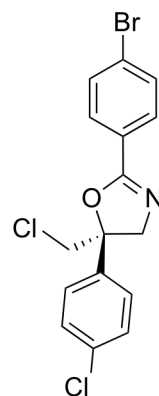
**II-33-B**  
72% yield  
93% ee



**II-34-B**  
65% yield  
87% ee



**II-35-B**  
89% yield  
84% ee

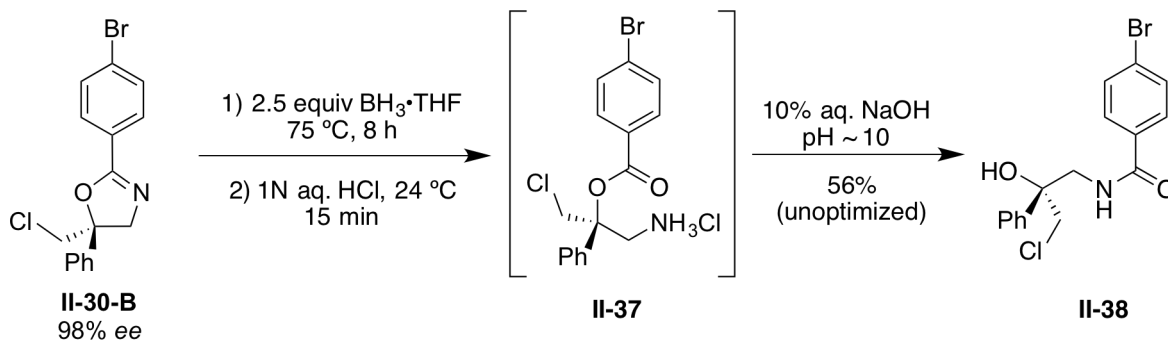


**II-36-B**  
94% yield  
87% ee

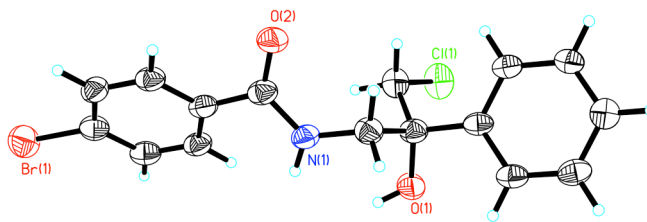
## II.2.5. Determination of absolute stereochemistry of cyclized products.

Although numerous oxazoline products were isolated as waxy solids, attempts to grow diffraction quality crystals were met with no success. It was hoped that chemical transformation of the oxazoline products might provide a crystalline entity.

### Scheme II-7. Establishment of the absolute stereochemistry of **II-30-B** after hydrolysis



*Crystal structure of II-38*



An attempted reduction of the oxazoline **II-30-B** by the action of  $\text{BH}_3 \cdot \text{THF}$  gave the undesired (but highly crystalline) hydrolysis product **II-38**. Presumably,  $\text{BH}_3 \cdot \text{THF}$  acts as a Lewis acid that promotes the hydrolysis of the oxazoline ring rather than as a reducing agent in this instance. The intermediacy of the hydrochloride salt **II-37** was confirmed by  $^1\text{H}$  NMR analysis of crude **II-37**. Upon addition of base, a facile O to N benzoate transposition ensued to

give the chlorohydrin **II-38**. The crystal structure of **II-38** served to confirm the absolute stereochemistry of the cyclized product.

### **II.2.6. Evaluation of *trans*-disubstituted alkenes as viable substrates for asymmetric chlorocyclization of allyl amides.**

One of the major limitations of the chiral halenium chemistry developed in our lab and that of others' has been the relatively narrow substrate scope. The inability to translate this chemistry to other olefin systems such as *cis*- and *trans*- 1,2-disubstituted olefin containing substrates was yet to be addressed. The asymmetric chlorolactonization reaction of alkenoic acids reported by our group in 2010 was restricted to 1,1-disubstituted alkenes.

Having demonstrated that the amide chlorocyclization reaction also works well for 1,1-disubstituted alkenes, attention was then turned to exploring the scope and limitations of this transformation especially with other substitution patterns for alkenes.

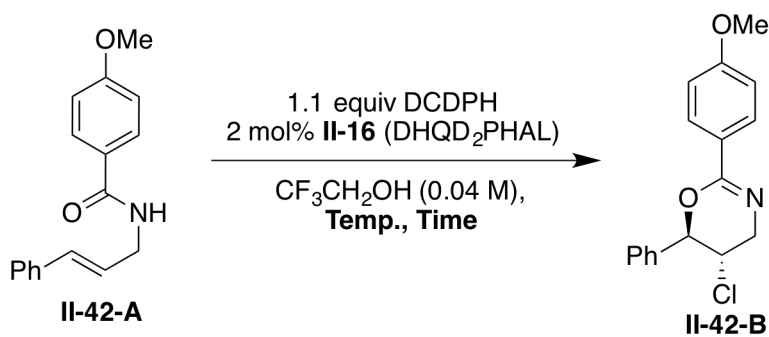
We were delighted to discover that the same reaction conditions could be extended to *trans*-disubstituted and trisubstituted olefin substrates, which yielded the corresponding dihydro-4-H-1,3-oxazines. These reactions were inherently more stereoselective; the corresponding dihydrooxazine heterocycles were obtained in excellent yields and enantioselectivities with the DCDPH-(DHQD)<sub>2</sub>PHAL catalytic system even when the reactions were run under 'sub-optimized' reaction conditions. For example, the chlorocyclization of **II-39** to **II-40** gave good enantioselectivities (87% to 90% *ee*) even when the reactions were run in solvents other than CF<sub>3</sub>CH<sub>2</sub>OH (see entries 1 – 3, Table II-16). On switching to CF<sub>3</sub>CH<sub>2</sub>OH as the reaction medium, nearly complete enantioselectivity was seen for the chlorocyclization (99% *ee*, entry 4, Table II-16).



Unlike the 1,1-disubstituted alkene substrates, the steric and/or electronic fine-tuning of the C2 substituent seemed unnecessary for these substrates. Nonetheless, a few different benzamide motifs were evaluated purely out of scientific curiosity (see Figure II-6). Electron rich, electron deficient and heteroaryl substituents were all compatible with this reaction; the cyclized product was formed in excellent enantioselectivities in all instances.

Next, influence of temperature was investigated. The enantioselectivity was not affected significantly with changes in the reaction temperature (see Table II-17). Remarkably, chlorocyclization of **II-42-A** proceeded to completion in less than 5 min at ambient temperature when 2 mol% of the catalyst was used. More importantly, the product was isolated in 91% yield and 96% *ee* (entry 4, Table II-17).

**Table II-17.** Influence of temperature on the asymmetric chlorocyclization of **II-42-A**

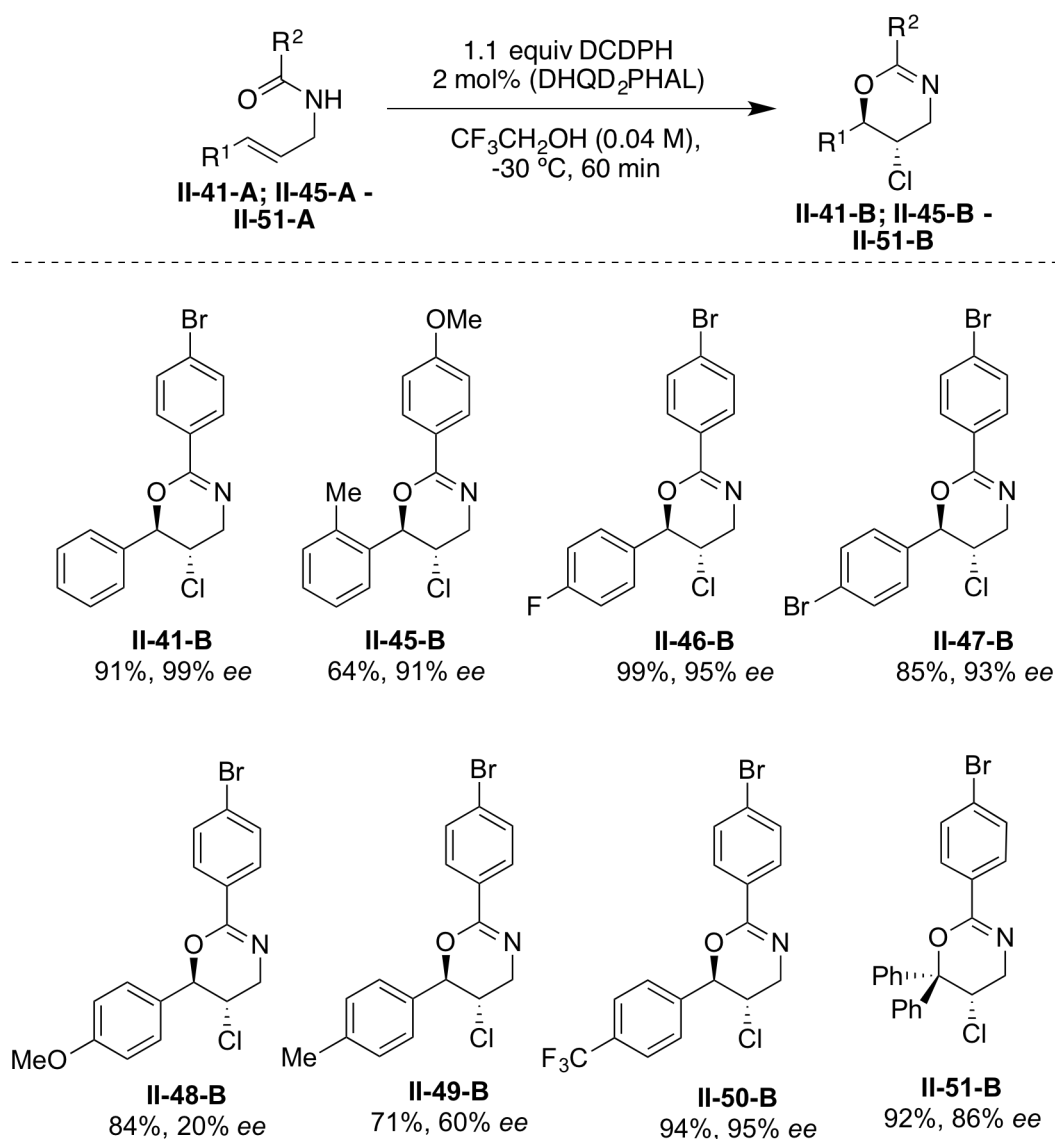


| Entry | Temp., Time    | Conversion (Yield) | <i>ee</i> |
|-------|----------------|--------------------|-----------|
| 1.    | -30 °C, 60 min | >95%               | >99%      |
| 2.    | -20 °C, 60 min | >95%               | >99%      |
| 3.    | 0 °C, 20 min   | >95%               | 99%       |
| 4.    | 24 °C, 5 min   | >95% (91%)         | 96%       |

Note: Reactions were quenched when no starting material was seen by TLC analysis

This was followed by substrate scope evaluation for *trans*-disubstituted alkene substrates. Having already determined that the 4-BrC<sub>6</sub>H<sub>4</sub> was the optimal amide end functionality for the 1,1-disubstituted olefin substrates, the same functionality was retained for these substrates as well. All other reaction variables that were optimized for the 1,1-disubstituted alkene substrates were retained i.e. reaction temperature of -30 °C and 0.04 M initial substrate concentration.

**Figure II-7.** Substrate scope evaluation for the asymmetric chlorocyclization of *trans*-disubstituted allyl amide substrates

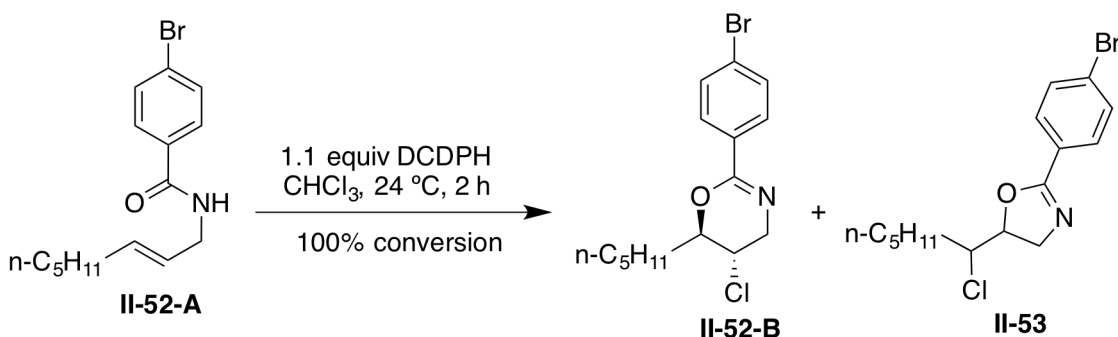


## II.2.7. Rendering substrates with aliphatic alkene substituents compatible with the asymmetric chlorocyclization chemistry.

All substrates evaluated thus far in the chlorocyclization reaction shared a common attribute – the presence of an aryl ring as one of the alkene substituents. This substituent serves to impart exquisite regioselectivity for these transformations, presumably by the stabilization of the developing positive charge at the benzylic position.

On the other hand, alkenes that possess alkyl substituents are electronically unbiased and therefore present an additional challenge of controlling the regiochemistry in addition to the stereoselectivity of these reactions. Additionally, the chloronium ion (or the isomerized  $\beta$ -chlorocarbenium ion) is likely to be more reactive owing to the lower stabilization and therefore be susceptible to decomposition/isomerization processes more so than the analogous arene stabilized intermediates. These fears were confirmed by experimental results that showed that the chlorocyclization of **II-52-A** in the absence of any catalyst in  $\text{CHCl}_3$  gave two constitutional isomers **II-52-B** and **II-53** in a 1:1.2 ratio i.e. an unbiased system such as **II-52-A** shows no preference for a 6-*endo* or a 5-*exo* mode of cyclization (see Scheme II-8).

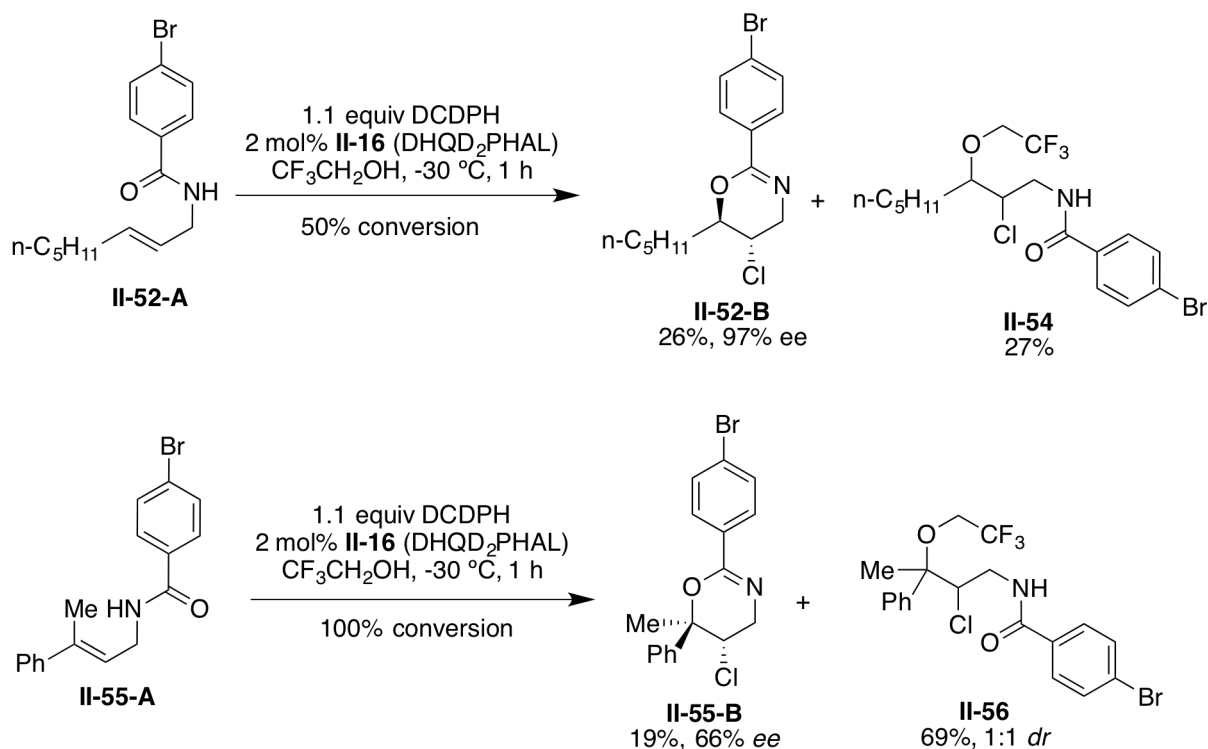
**Scheme II-8.** Non-catalyzed chlorocyclization of **II-52-A**



When the reaction was run under optimized reaction conditions, two aspects became evident straight away. First, the chloroether **II-54** was a major side product of this reaction

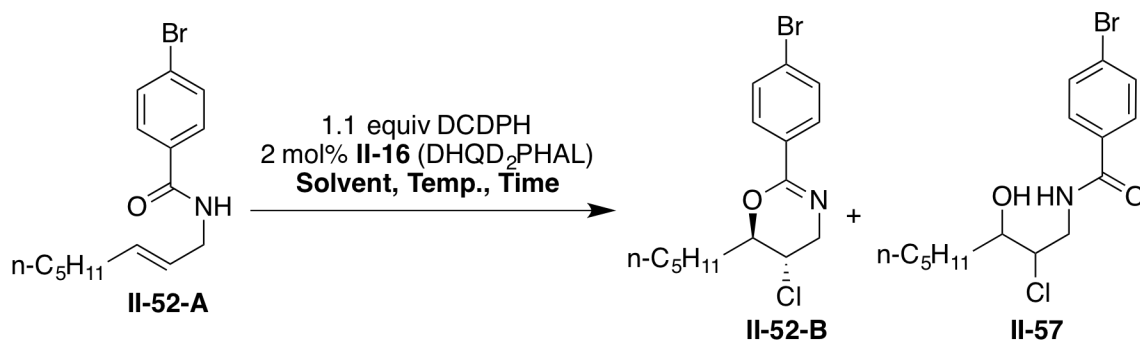
indicating that *intermolecular* capture of the chloronium ion intermediate can occur at rates that compete with the intramolecular interception of the intermediate. Second, the desired cyclized product as well as the chloroether side product were formed with exquisite regioselectivity i.e. catalyst control can override any inherent substrate bias for the site-selectivity of the nucleophilic attack in these substrates. Encouraging was the fact that the desired cyclized product was formed in 97% *ee* indicating that this reaction could be synthetically useful if the formation of the side-product can be suppressed. A similar problem was encountered when trisubstituted alkene substrate **II-55-A** was exposed to the optimized reaction conditions. The desired product was isolated in only 19% yield and a moderate 66% *ee*. The mass balance for this reaction was the chloroether product **II-56** that was isolated as a ~1:1 diastereomeric mixture of *syn* and *anti* products in ~70% yield.

**Scheme II-9.** Asymmetric chlorocyclization of **II-52** and **II-55-A** under ‘optimized’ reaction conditions



In order to prevent the formation of the chloroether side-products, the idea of evaluating other non-nucleophilic solvents was entertained. The transformation of **II-52-A** to **II-52-B** was chosen as the test reaction for this purpose (see Table II-18).

**Table II-18.** Identification of optimal reaction conditions for the asymmetric chlorocyclization of **II-52-A**



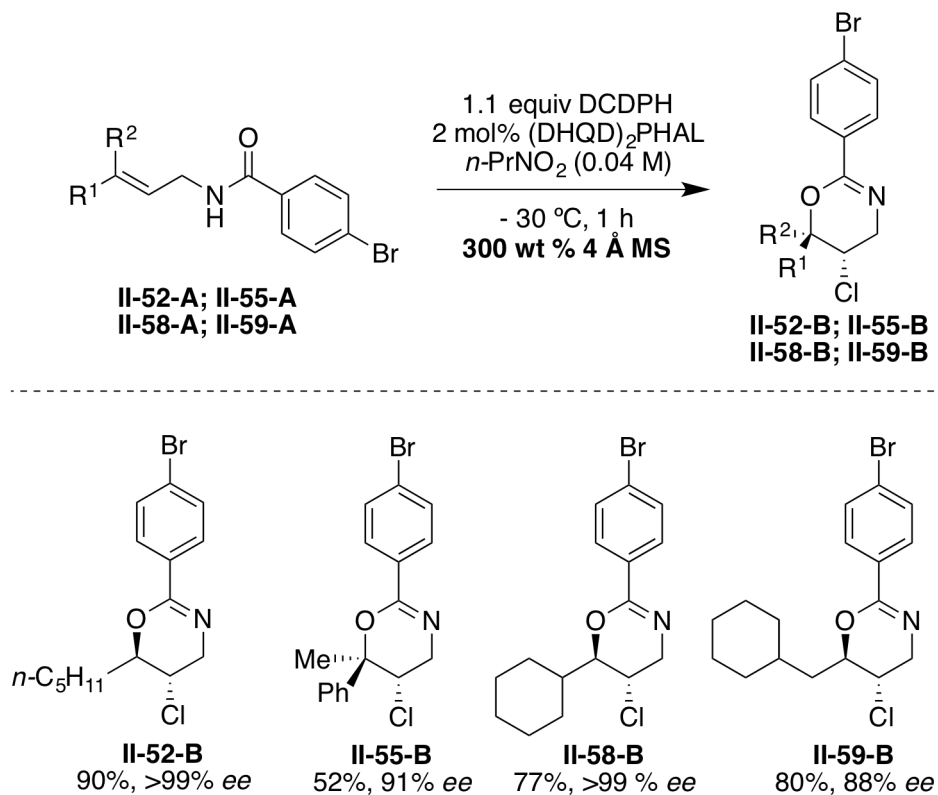
| Entry | Solvent, Temp., Time                         | Conv. (Yield) | II-52B:II-57 | ee (II-52-B) |
|-------|--|---------------|--------------|--------------|
| 1.    | CHCl <sub>3</sub> , -30 °C, 16 h             | 15%           | >15:1        | 42%          |
| 2.    | 1:1 CHCl <sub>3</sub> -hexanes, -30 °C, 16 h | 30%           | >15:1        | 64%          |
| 3.    | MeNO <sub>2</sub> , -30 °C, 24 h             | 75% (33%)     | 1.2:1.0      | 95%          |
| 4.    | <i>n</i> -PrNO <sub>2</sub> , -30 °C, 3 h    | >95% (77%)    | >15:1        | >99%         |

Note: Reaction in *n*-PrNO<sub>2</sub> was run in the presence of 4 Å molecular sieves.

The reaction was sluggish when CHCl<sub>3</sub> or 1:1 CHCl<sub>3</sub> –hexanes co-solvent mixture was employed as the solvent; significant amounts of unreacted starting material was seen even after 16 hours at -30 °C. The enantioselectivity was also only moderate with these two solvent systems (42% and 64% *ee*, respectively; entries 1 and 2, Table II-18). Significant improvement in the enantioselectivity was observed in MeNO<sub>2</sub> (entry 3, Table II-18). The desired product was isolated in 33% yield and an impressive 95% *ee*. Surprisingly, the halohydrin product **II-57** was

also isolated in ~30% yield. Residual amount of moisture in the solvent is apparently sufficient for promoting the formation of this product. The use of MeNO<sub>2</sub> that was stored overnight over 4Å molecular sieves also failed to suppress the formation of **II-57** completely (results not shown). Given the relatively high miscibility of water in MeNO<sub>2</sub> (~10g/ 100 mL), it was postulated that turning to other nitroalkane solvents in which the miscibility of water is lower should help prevent the formation of **II-57**. Water has a much lower lower miscibility in *n*-PrNO<sub>2</sub> (~1.7g/ 100 mL of *n*-PrNO<sub>2</sub>) as compared to MeNO<sub>2</sub>. Not surprisingly, when *n*-PrNO<sub>2</sub> was used as the reaction solvent (in the presence of added 4 Å molecular sieves; 300 weight % of the substrate), **II-52-B** was isolated in 77% yield and >99% *ee* (see entry 4, Table II-18; no significant quantity of **II-57** was seen under these conditions). These conditions were used for the chlorocyclization of other alkyl-substituted and trisubstituted alkene substrates. These results are collected in Figure II-8.

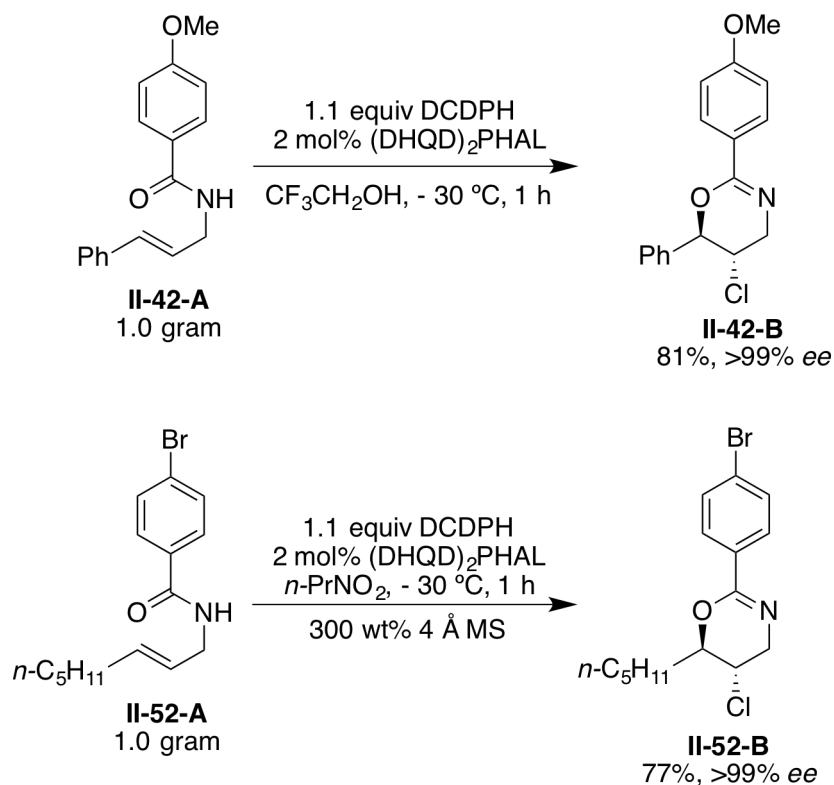
**Figure II-8.** Substrate scope evaluation of trisubstituted and alkyl substituted allyl amides



### II.2.8. Synthetic utility of the amide chlorocyclization reaction and the cyclized products.

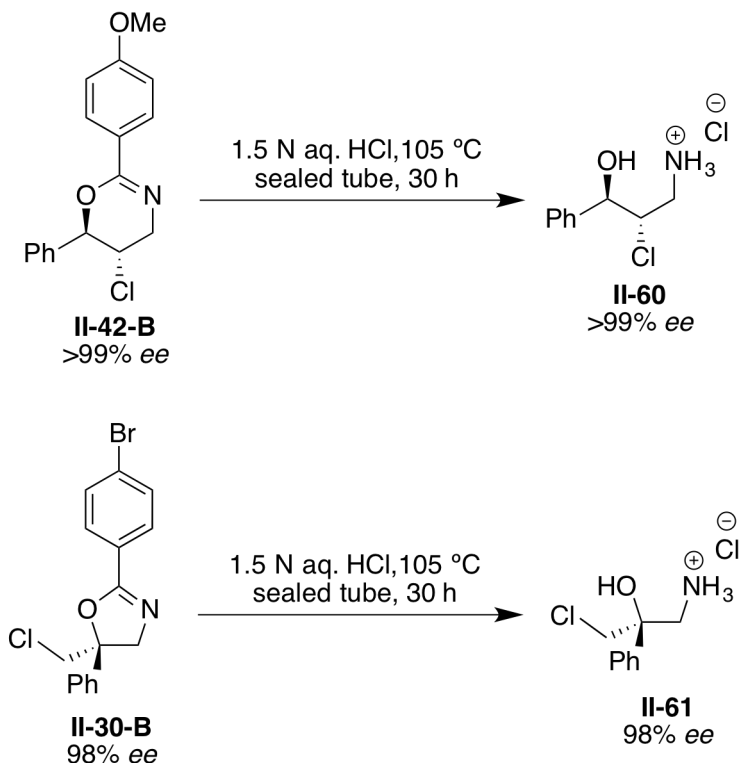
The results disclosed in this chapter represent an unprecedented route to chiral heterocyclic products such as oxazolines and dihydrooxazines. These heterocycles could serve as valuable chiral building blocks. In order to demonstrate the synthetic utility of this reaction on preparative scales, gram scale transformations of substrates **II-42-A** and **II-52-A** were examined. As seen in Scheme II-10, **II-42-A** and **II-52-A** were both transformed into the corresponding cyclized products in good yields and excellent enantioselectivity.

**Scheme II-10.** Gram-scale asymmetric chlorocyclization reactions



While the chiral products of the amide chlorocyclization are of interest in their own right, they are adorned with several functional handles, which can be manipulated and converted into useful synthetic building blocks. Compounds **II-42-B** and **II-30-B** were efficiently transformed into their corresponding 1,2- and 1,3- chiral amino alcohols **II-60** and **II-61**, respectively, by a simple acid hydrolysis of the cyclic imidate functionality (Scheme II-11). These reactions proceed with complete stereochemical fidelity.

**Scheme II-11.** Acid hydrolysis of oxazoline and dihydrooxazine heterocycles



**II.2.9. Development of more cost-effective and ambient temperature conditions for the highly enantioselective chlorocyclization of amides.**

**II.2.9.1. Chloramine salts as superior electrophilic chlorine precursors.**

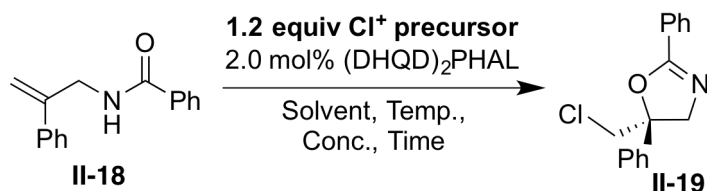
Although highly enantioselective variants of many halocyclizations have appeared in recent years, these initial forays in reaction discovery were largely driven by the desire to understand and address the challenges associated with enantioselective alkene halogenation reactions. From a practical standpoint, the use of readily available, stable and cheap reagents on preparatory scales with no compromise on the stereoselectivity of the reaction is highly desirable. If realized, these measures will bring alkene halogenation reactions at par with some of the well-established asymmetric alkene functionalization reactions such as epoxidations, aziridinations and dihydroxylations.

Optimization studies had identified DCDPH (synthesized in one step from the corresponding hydantoin)<sup>20</sup> as the best candidate after evaluating numerous chlorenium sources. Typical reaction time of an hour was sufficient for completion of most reactions. Nonetheless, cryogenic temperatures (-30 °C) and relatively high dilutions (0.04M) were still required for obtaining the best results. Moreover, modification of the benzamide moiety was paramount to obtaining the best enantioselectivity (the optimal group for a given olefin substituent was established by a trial and error approach). We hoped to improve upon some of these limitations. Of specific interest were the discovery of an inexpensive, stable and commercially available chlorenium source as well as the development of reaction conditions that are amenable to preparatory scale applications in order to improve the generality and usefulness of this transformation.

Preliminary studies had revealed that chloramine-T·3H<sub>2</sub>O results in the formation of the desired oxazoline product in trace quantities but with appreciable level of stereinduction in the presence of (DHQD)<sub>2</sub>PHAL as the chiral catalyst in CHCl<sub>3</sub> (<10% yield; 43% *ee* after 8 hours; entry 1, Table 1). This result was intriguing since chloramine-T is known to serve as an electrophilic chlorine source only in *protic* solvents (in fact, there is ample precedence for the use of chloramine-T to generate metallo-nitrenes under anhydrous conditions in aprotic solvents). We had initially ascribed this result to trace quantities of moisture or protic impurities in the reaction medium. Two major developments prompted us to reevaluate chloramine-T·3H<sub>2</sub>O in CF<sub>3</sub>CH<sub>2</sub>OH as the reaction solvent. First, having previously demonstrated that CF<sub>3</sub>CH<sub>2</sub>OH is the optimal solvent for this transformation, we surmised that the use of CF<sub>3</sub>CH<sub>2</sub>OH as the protic solvent in lieu of CHCl<sub>3</sub> should accelerate the reaction with chloramine-T·3H<sub>2</sub>O. Second, recent studies from our group have shown that catalyst

protonation by fluorinated alcohols enables better substrate-catalyst interactions via hydrogen bonding interactions.

**Table II-19.** Evaluation of chloramine salts as the terminal chlorenium source for the asymmetric chlorocyclization of **II-18**



| Entry           | Solvent/ Temp./ Conc.              | Cl <sup>+</sup> source                                   | Time          | Yield <sup>a</sup> | ee <sup>b</sup> |
|-----------------|------------------------------------|--|---------------|--------------------|-----------------|
| 1.              | CHCl <sub>3</sub> / -40 °C/ 0.04 M | TsNNaCl·3H <sub>2</sub> O                                | 8 h           | <10%               | 43%             |
| 2.              | TFE/ -40 °C/ 0.04 M                | TsNNaCl·3H <sub>2</sub> O                                | 8 h           | 15%                | 93%             |
| 3. <sup>c</sup> | TFE/ 24 °C/ 0.10 M                 | TsNNaCl·3H <sub>2</sub> O                                | 24 h          | 60%                | 93%             |
| 4.              | HFIP/ 24 °C/ 0.10M                 | TsNNaCl·3H <sub>2</sub> O                                | 15 min        | >95%               | 60%             |
| <b>5.</b>       | <b>9:1 TFE-HFIP/ 24 °C/ 0.10M</b>  | TsNNaCl·3H <sub>2</sub> O                                | <b>15 min</b> | <b>95%</b>         | <b>92%</b>      |
| 6.              | 9:1 TFE-HFIP/ 24 °C/ 0.10M         | PhSO <sub>2</sub> NNaCl                                  | 15 min        | 95%                | 89%             |
| 7.              | 9:1 TFE-HFIP/ 24 °C/ 0.10M         | CH <sub>3</sub> SO <sub>2</sub> NNaCl ·xH <sub>2</sub> O | 60 min        | 90%                | 89%             |

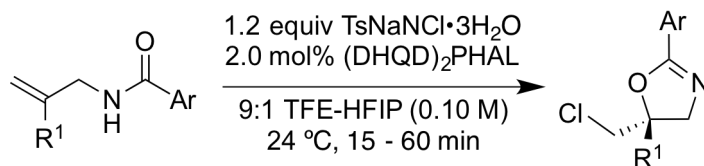
<sup>a</sup>Determined by <sup>1</sup>H NMR using MTBE as external standard; <sup>b</sup>Determined by chiral HPLC; <sup>c</sup>2.0 equiv of TsNNaCl·3H<sub>2</sub>O was used; TFE = 2,2,2-trifluoroethanol; HFIP = 1,1,1,3,3,3-hexafluoro-2-propanol

Employing 1.2 equivalents of chloramine-T·3H<sub>2</sub>O in CF<sub>3</sub>CH<sub>2</sub>OH in the presence of 2 mol% of (DHQD)<sub>2</sub>PHAL gave significant improvements in both conversion and enantioselectivity of this transformation. The desired oxazoline was isolated in 93% *ee* at 15% conversion of the

olefin into product (entry 2, Table II-19). It must be highlighted that this was the highest stereoselection obtained for this particular substrate till date. Emboldened by the negligible background reaction even at ambient temperatures, the reaction was run using 2.0 equivalents of chloramine-T·3H<sub>2</sub>O at 24 °C. To our delight, the conversion improved to 60% with no loss in enantioselectivity although a long reaction time of 24 hours was still required (entry 3, Table II-19). Further increase in reaction times did not improve conversions. Marginal improvements in conversions were realized by using a large excess of chloramine-T·3H<sub>2</sub>O (up to 10 equivalents) or a much higher catalyst loading (10 mol%; results not shown). However, these measures were deemed excessive for the improvement garnered from these changes. On running the reaction in hexafluoroisopropanol (HFIP) as the solvent, the reaction was complete in less than 15 minutes! Although the enantioselectivity of the reaction was significantly lower (60% *ee*; entry 4, Table II-19). This dramatic rate acceleration prompted us to evaluate HFIP as a co-solvent additive for this reaction. The reaction times could be decreased to around 15 min if the reactions were run in a 9:1 TFE:HFIP mixture at 0.10 M concentration to give the product in 92% *ee* (entry 5, Table II-19). Similar level of stereoselection was obtained with chloramine-B and chloramine-M as the chloronium precursors (both chloramine salts returned the product in 89% *ee*, entries 6 and 7, Table II-19). The last result with chloramine-M is particularly appealing due to the high water solubility of the methane sulfonamide by-product that facilitates purification *via* an aqueous extractive work-up.

This new protocol is more general with regards to substrate scope and gave comparable yields and improved enantioselectivities for all substrates evaluated in our previous study. As seen in Table II-20, all 1,1-disubstituted olefin substrates furnished the corresponding chiral oxazoline heterocycles in good to excellent yields and enantioselectivity. Comparison of entries 1 – 5 in Table II-20 indicate a narrow distribution of enantioselectivity as a function of the

benzamide group if chloramine-T·3H<sub>2</sub>O is used (92 → 99% *ee*) as opposed to DCDPH (83 – 98% *ee*). Entries 6 – 8 indicate that for a given nucleophile (i.e. 4-Bromobenzamide motif), the enantioselectivities are consistently about 5 – 6% *ee* higher with various alkene substituents using the new protocol.

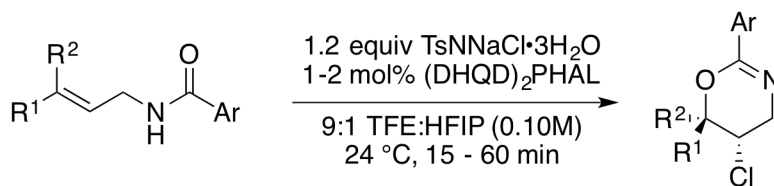
**Table II-20.** Substrate scope evaluation with (DHQD)<sub>2</sub>PHAL/TsNNaCl•3H<sub>2</sub>O system

| Entry | R <sup>1</sup>                      | Ar  | Yield, <i>ee</i>            |                    |
|-------|-------------------------------------|---|-----------------------------|--------------------|
|       |                                     |   | (TsNNaCl•3H <sub>2</sub> O) | (DCDPH)            |
| 1.    | C <sub>6</sub> H <sub>5</sub>       | C <sub>6</sub> H <sub>5</sub>   | 85%, 92% <i>ee</i>          | 96%, 90% <i>ee</i> |
| 2.    | C <sub>6</sub> H <sub>5</sub>       | 4-Br-C <sub>6</sub> H <sub>4</sub>                                    | 87%, 97% <i>ee</i>          | 93%, 98% <i>ee</i> |
| 3.    | C <sub>6</sub> H <sub>5</sub>       | 4-CH <sub>3</sub> -C <sub>6</sub> H <sub>4</sub>                      | 92%, 92% <i>ee</i>          | 90%, 83% <i>ee</i> |
| 4.    | C <sub>6</sub> H <sub>5</sub>       | 2-F-C <sub>6</sub> H <sub>4</sub>                                     | 87%, 99% <i>ee</i>          | 86%, 88% <i>ee</i> |
| 5.    | C <sub>6</sub> H <sub>5</sub>       | 3-Pyr   | 85%, >99% <i>ee</i>         | 84%, 92% <i>ee</i> |
| 6.    | 4-Br-C <sub>6</sub> H <sub>4</sub>  | 4-Br-C <sub>6</sub> H <sub>4</sub>                                    | 87%, 90% <i>ee</i>          | 89%, 84% <i>ee</i> |
| 7.    | 4-Cl-C <sub>6</sub> H <sub>4</sub>  | 4-Br-C <sub>6</sub> H <sub>4</sub>                                    | 88%, 92% <i>ee</i>          | 94%, 87% <i>ee</i> |
| 8.    | 3-OMe-C <sub>6</sub> H <sub>4</sub> | 4-Br-C <sub>6</sub> H <sub>4</sub>                                    | ND                          | 72%, 93% <i>ee</i> |
| 9.    | 4-Cl-C <sub>6</sub> H <sub>4</sub>  | 3,5-NO <sub>2</sub> -4-CH <sub>3</sub> -C <sub>6</sub> H <sub>2</sub> | 90%, 87% <i>ee</i>          | ND                 |

Note: Yields refer to isolated yields after column chromatography

Likewise, *trans*- disubstituted and trisubstituted alkene substrates also furnished the corresponding dihydrooxazine heterocycles in consistently higher enantioselectivities as compared to the first generation protocol (see Table II-21)

**Table II-21.** Chlorocyclization of *trans*-disubstituted and trisubstituted alkene substrates by (DHQD)<sub>2</sub>PHAL/TsNNaCl



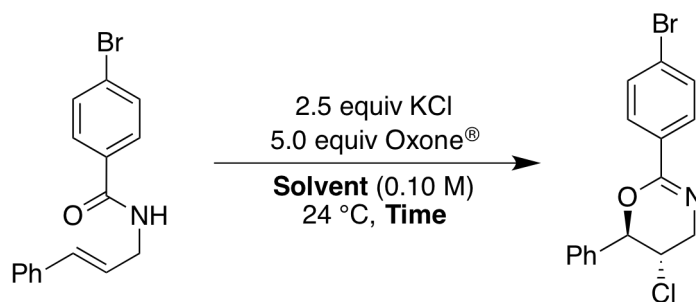
| Entry | R <sup>1</sup>                                   | R <sup>2</sup>                | Ar  | Yield, <i>ee</i><br>(TsNNaCl·3H <sub>2</sub> O) | Yield, <i>ee</i><br>(DCDPH) |
|-------|--|-------------------------------|---|---|-----------------------------|
| 1.    | C <sub>6</sub> H <sub>5</sub>                    | H                             | 4-OCH <sub>3</sub> -C <sub>6</sub> H <sub>4</sub> | ND  | 93%, >99% <i>ee</i>         |
| 2.    | 4-CF <sub>3</sub> -C <sub>6</sub> H <sub>4</sub> | H                             | 4-Br-C <sub>6</sub> H <sub>4</sub>                | 90%, 97% <i>ee</i>                              | 94%, 95% <i>ee</i>          |
| 3.    | 4-Br-C <sub>6</sub> H <sub>4</sub>               | H                             | 4-Br-C <sub>6</sub> H <sub>4</sub>                | 83%, 95% <i>ee</i>                              | 85%, 93% <i>ee</i>          |
| 4.    | 4-F-C <sub>6</sub> H <sub>4</sub>                | H                             | 4-Br-C <sub>6</sub> H <sub>4</sub>                | 93%, 95% <i>ee</i>                              | 99%, 95% <i>ee</i>          |
| 5.    | 2-Me-C <sub>6</sub> H <sub>4</sub>               | H                             | 4-Br-C <sub>6</sub> H <sub>4</sub>                | ND  | 99%, 87% <i>ee</i>          |
| 6.    | C <sub>6</sub> H <sub>5</sub>                    | C <sub>6</sub> H <sub>5</sub> | 4-Br-C <sub>6</sub> H <sub>4</sub>                | 84%, 92% <i>ee</i>                              | 92%, 86% <i>ee</i>          |
| 7.    | C <sub>6</sub> H <sub>5</sub>                    | CH <sub>3</sub>               | 4-Br-C <sub>6</sub> H <sub>4</sub>                | ND  | 52%, 91% <i>ee</i>          |
| 8.    | 4-CH <sub>3</sub> -C <sub>6</sub> H <sub>4</sub> | H                             | 4-Br-C <sub>6</sub> H <sub>4</sub>                | ND  | 93%, 60% <i>ee</i>          |

### II.2.9.2. Oxone®/KCl as the chlorenium source.

Oxone®/KCl could potentially serve as a means of generating the putative chlorenium source in situ. Given the low cost and stability of both reagents, the development of an asymmetric chlorocyclization reaction using the Oxone®/KCl system could have far reaching

implications. In contrast to traditional haloamine reagents such as DCDMH and NCS that tend to lose activity on storage, the practical ease of handling the Oxone®/KCl system, in-situ generation of the active chloronium source and the simplified work-up procedures to remove the inorganic salt by-products are all potential merits. In any event, halocyclization reactions using in-situ halide oxidation are yet to be realized.

**Table II-22.** Evaluation of Oxone®/KCl as a chloronium precursor in the asymmetric chlorocyclization of **II-41-A**



| Entry | Solvent                            | Catalyst                    | Time | Conversion | <i>ee</i>     |
|-------|------------------------------------|-----------------------------|------|------------|---------------|
| 1.    | MeCN                               | None                        | 24 h | 95%        | -             |
| 2.    | MeCN                               | 5% (DHQD) <sub>2</sub> PHAL | 15 h | 29%        | 14% <i>ee</i> |
| 3.    | CF <sub>3</sub> CH <sub>2</sub> OH | 5% (DHQD) <sub>2</sub> PHAL | 15 h | >95%       | 18% <i>ee</i> |

Note: Conversion was determined by crude <sup>1</sup>H NMR analysis

The chlorocyclization of **II-41-A** proceeds cleanly at ambient temperature in MeCN when an excess of KCl and Oxone® (2.5 equiv and 5.0 equiv respectively) was employed (entry 1, Table II-22). On running the reaction in the presence of 5 mol% (DHQD)<sub>2</sub>PHAL, the reaction was only 29% complete in MeCN after 15 hours. The product **II-41-B** was formed in 14% *ee*. When the solvent was switched to CF<sub>3</sub>CH<sub>2</sub>OH, the reaction was complete in 15 hours. A small improvement in the enantioselectivity to 18% *ee* was observed. Although the enantioselectivities

are poor, the reactions were clean and no major side-products were observed. More importantly, these results represent the first example of a direct halocyclization reaction using an in-situ oxidation of halide ions. The substrate and reaction scope as well as further optimizations are ongoing pursuits.

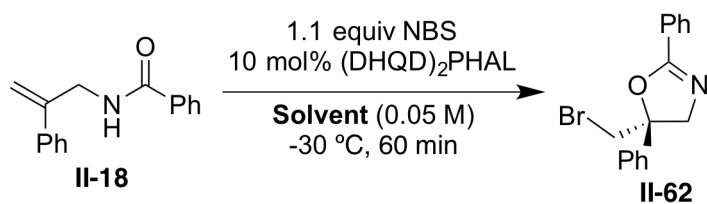
## **II.2.10. Attempted asymmetric bromo- and selenocyclization of unsaturated amides.**

After tasting success with the asymmetric chlorocyclization reaction of unsaturated amides, attempts were made to extend this chemistry to analogous bromo- and selenocyclization reactions.

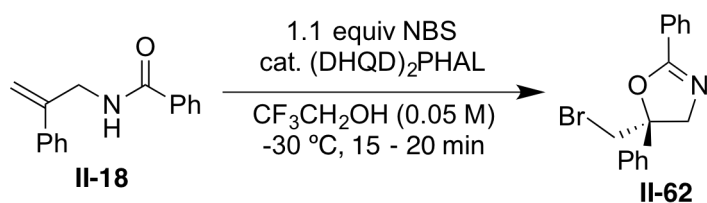
### **II.2.10.1. (DHQD)<sub>2</sub>PHAL catalyzed enantioselective bromocyclization of unsaturated amides.**

In order to verify whether the conditions used for the asymmetric chlorocyclization chemistry could be seamlessly adapted for the analogous bromocyclization reaction, **II-18** was exposed to 1.1 equiv of NBS under conditions that gave moderate to good enantioselectivities for the chlorocyclization reaction.

As seen from the results in Table II-23, conditions that gave >75% *ee* for the chlorocyclization reaction gave only low to moderate levels of enantioinduction for the analogous bromocyclization reaction. While a 1:1 MeCN-CCl<sub>4</sub> solvent mixture gave the product in 28% *ee*, CF<sub>3</sub>CH<sub>2</sub>OH returned **II-62** in 40% *ee*. Although the trend in enantioselectivity is similar to that observed for the chlorocyclization chemistry, the values were not synthetically useful.

**Table II-23.** Asymmetric bromocyclization of **II-18**

| Entry | Solvent                            | Conversion | ee  |
|-------|------------------------------------|------------|-----|
| 1.    | 1:1 MeCN-CCl <sub>4</sub>          | 90%        | 28% |
| 2.    | CF <sub>3</sub> CH <sub>2</sub> OH | >95%       | 40% |

**Table II-24.** Catalyst loading studies for the asymmetric bromocyclization of **II-18**

| Entry | Catalyst loading | Conversion | ee  |
|-------|------------------|------------|-----|
| 1.    | 10 mol%          | >95%       | 40% |
| 2.    | 25 mol%          | >95%       | 48% |
| 3.    | 50 mol%          | >95%       | 40% |
| 4.    | 100 mol%         | >95%       | 49% |
| 5.    | 200 mol%         | >95%       | 49% |

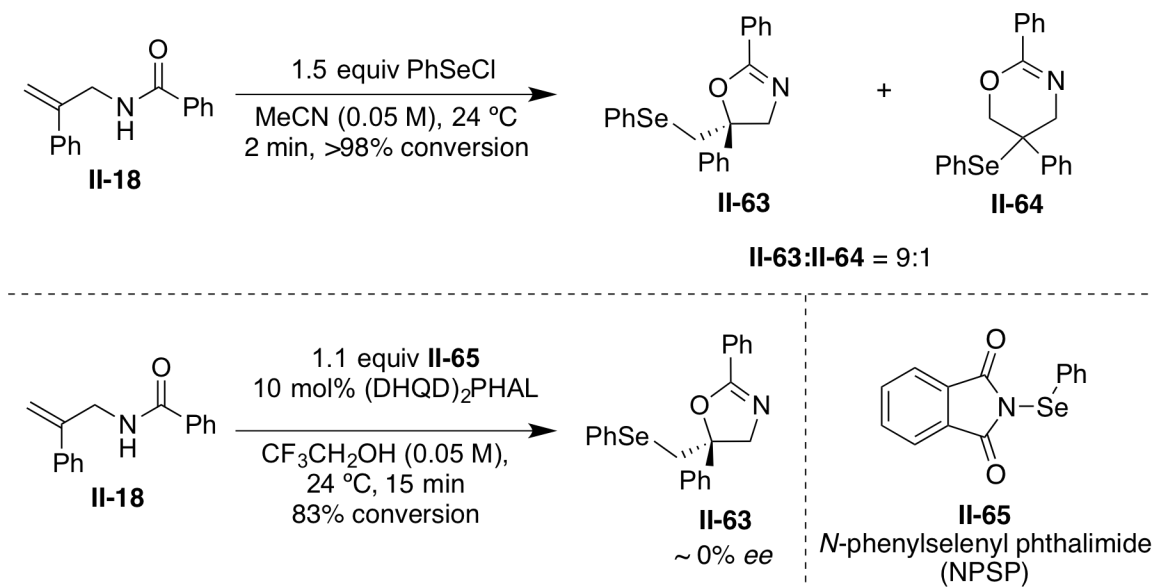
It was noted that the reactions were rapid and that both reactions showed high conversions in under 10 minutes even at -30 °C. Postulating that the non-catalyzed background reaction might be contributing to the low enantioselectivities, the effect of increasing the catalyst loading was studied. As evident from the data in Table II-24, a small improvement in the enantioselectivity was seen with increased catalyst loadings. Nonetheless, even in the presence of superstoichiometric quantities of the catalyst (200 mol%, see entry 5 in Table II-24), only 49% *ee* was observed for the product **II-62**. Clearly, reasons other than the background reaction must be contributing to the low enantioselectivities. Given the low enantioselectivities, the optimization of the bromocyclization reaction was not pursued any further.

#### **II.2.10.2. Attempted enantioselective selenocyclization of unsaturated amides.**

Asymmetric selenocyclization reactions are yet to witness the scope or the success seen with the analogous halocyclization reactions. In order to determine whether asymmetric alkene selenylation can be achieved, substrate **II-18** was exposed to electrophilic selenium sources (see Scheme II-12). The reaction with 1.5 equiv of PhSeCl was complete in less than 2 min at ambient temperature in MeCN. Along with the desired product **II-63**, 10% of a by-product, tentatively assigned as the constitutional isomer **II-64**, was also isolated in this reaction. Given the rapid reaction rates, it seemed logical to move away from PhSeCl as the electrophilic selenium source and instead use a reagent that has attenuated reactivity. For the evaluation of enantioselective variants, *N*-phenylselenyl phthalimide (NPSP, **II-65**) was employed. Nicolaou and co-workers have reported a convenient 1-step synthesis of **II-65** from potassium phthalimide and PhSeCl.

On exposing **II-18** to 1.1 equiv of **II-65** in the presence of 10 mol% of (DHQD)<sub>2</sub>PHAL, the reaction was 83% complete after 15 min. Disappointingly, the cyclized product was found to be practically racemic (see Scheme II-12).

### Scheme II-12. Selenocyclization reaction of II-18



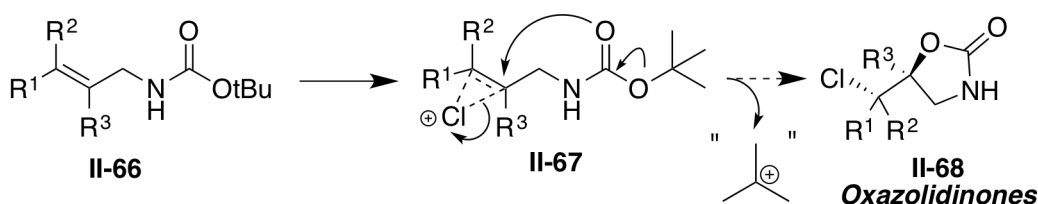
These initial forays into attempted bromo- and selenocyclization reactions are by no means indicators that such transformations will not meet with success eventually. Nonetheless, the results establish that **II-16** is unlikely to be playing a role of merely a Lewis base catalyst in all these reactions. If indeed all these reactions proceeded via a transfer of the electrophile to the quinuclidine nitrogen of the chiral catalyst prior to the delivery to the alkene, one would have expected similar levels of stereoselection for all these transformations (provided the background reactions are negligible). Clearly, in-depth mechanistic studies aimed at teasing out the factors that contribute to the high enantioselectivity in the chlorocyclization reactions are required. Lessons learnt from these studies could then be parlayed into a rational development of other asymmetric electrophilic alkene functionalization reactions.

#### II.2.11. Asymmetric chlorocyclization of unsaturated carbamates.

Having demonstrated that both carboxylic acids and amides are both compatible nucleophiles in highly enantioselective chlorocyclization reactions, other potential nucleophiles were also evaluated concurrent and subsequent to these successful efforts. In this regard,

rendering carbamates as viable nucleophiles seemed like an attractive proposition (see Figure II-9). Firstly, the substrates bear close resemblance to those used in the amide chlorocyclization chemistry and therefore it seemed likely that the development highly enantioselective variants should be possible with minimal variations to the optimized reaction conditions. Secondly, the products of such a transformation will be oxazolidinones – a versatile heterocyclic motif with well-established utility as a chiral building block. With an unprecedented and potentially facile catalytic asymmetric route to these heterocycles, this reaction was studied in detail.

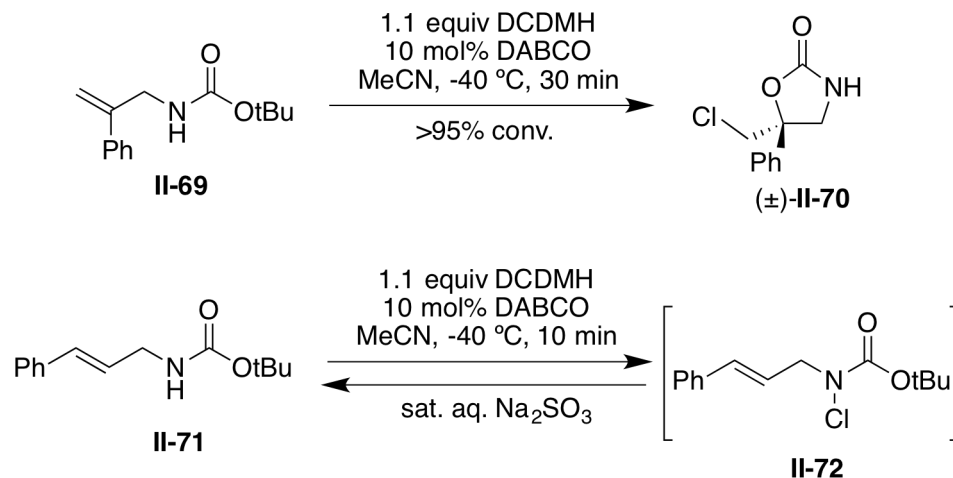
**Figure II-9.** Proposed asymmetric chlorocyclization of unsaturated carbamates



Some of the pilot studies for this reaction were performed during the course of the optimization studies for the amide chlorocyclization reaction. These studies will be presented in the following sections. Detailed reaction optimization and kinetic studies were pursued as a collaborative study with Dr. Atefeh Garzan, a former graduate student in our group.

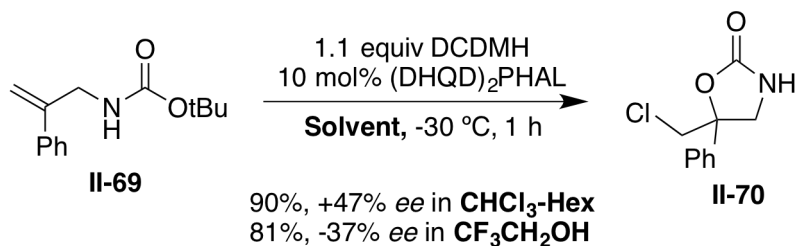
The studies commenced with the chlorocyclization of the two test substrates **II-69** and **II-71** with DCDMH as the chloronium source in MeCN in the presence of 10 mol% of DABCO as the non-chiral Lewis base catalyst (see Scheme II-13). While **II-69** cleanly afforded the desired oxazolidinone product **II-70**, the *trans*-disubstituted alkene substrate **II-71** gave rapid and quantitative *N*-chlorination (see **II-72** in Scheme II-12; this tentative assignment was based on LC-MS and NMR analysis of crude reaction mixture prior to quenching). The starting material was recovered after quenching the reaction with saturated aq.  $\text{Na}_2\text{SO}_3$ . This spectacular divergence in the reaction pathways with these two substrates is not understood as present.

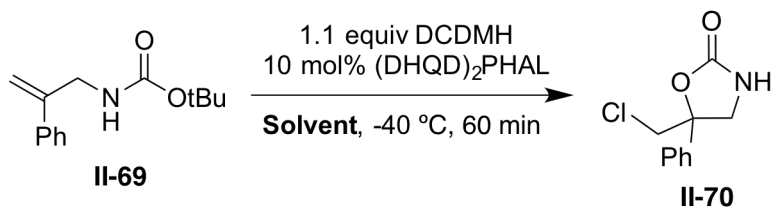
**Scheme II-13.** Preliminary studies of the chlorocyclization of carbamates **II-69** and **II-71**



Turning to enantioselective variants, the first reaction variable to be examined was the reaction solvent. Disappointingly, 1:1  $\text{CHCl}_3$ -hexanes and  $\text{CF}_3\text{CH}_2\text{OH}$  (the two optimal solvents for the asymmetric chlorocyclization of carboxylic acids and amides, respectively) returned the product in only low to moderate levels of enantioselectivity. Also surprising, was the opposite stereinduction in the two solvents with a preference for the (*S*)-enantiomer (-37% *ee*) in  $\text{CF}_3\text{CH}_2\text{OH}$  and the (*R*)-enantiomer (+47% *ee*) in 1:1  $\text{CHCl}_3$ -Hexanes (see Scheme II-14).

**Scheme II-14.** Solvent dependent enantiodivergence in the chlorocyclization of **II-69**



**Table II-25.** Evaluation of different solvents for the asymmetric chlorocyclization of **II-69**

| Solvent                              | Yield (%) | ee (%) | Solvent                            | Yield (%) | ee (%) |
|--------------------------------------|-----------|--------|------------------------------------|-----------|--------|
| CH <sub>3</sub> CN                   | 92        | 14     | CF <sub>3</sub> CH <sub>2</sub> OH | 81        | -37    |
| CHCl <sub>3</sub>                    | 76        | 42     | MeOH                               | 87        | -36    |
| CHCl <sub>3</sub> -Hexane            | 90        | 77     | EtOH                               | 78        | -52    |
| CHCl <sub>3</sub> -PhCH <sub>3</sub> | 50        | 63     | <i>n</i> -PrOH                     | 86        | -74    |
| CHCl <sub>3</sub> -Pentane           | 68        | 57     | IPA                                | 75        | -50    |
| CHCl <sub>3</sub> -Benzene           | 72        | 52     | <i>i</i> -BuOH                     | 81        | -65    |

With an intention of unraveling whether this enantiodivergence was a result of using a protic versus aprotic solvent, **II-69** was exposed to DCDMH in the presence 10 mol% (DHQD)<sub>2</sub>PHAL in a variety of solvents at -40 °C. Indeed, reaction of **II-69** in aprotic solvents led to the formation of (*R*)-**II-70**, with the highest stereinduction observed in a 1:1 CHCl<sub>3</sub>-PhCH<sub>3</sub>

solvent mixture (63% *ee*, see Table II-25). In contrast, when the reaction was carried out in alcoholic solvents, (*S*)-**II-70** was obtained with *n*-PrOH giving the highest *S* selectivity (-74% *ee*). Gratifyingly, synthetically useful levels of enantioselectivity for the formation of either enantiomer using the same catalyst (but different solvents) could be identified after exhaustive optimization efforts. While a detailed description of these efforts can be found in published work from our group,<sup>28</sup> some of the crucial results/conclusions are presented below:

- Eyring plot studies have determined that the enantioselectivity is enthalpy-driven in *n*-PrOH whereas, it is entropy-driven in 1:1 CHCl<sub>3</sub>-hexanes.
- A direct consequence of the entropy driven enantioselectivity in 1:1 CHCl<sub>3</sub>-hexanes is the counterintuitive phenomenon of increase in enantioselectivity with an increase in temperature; the optimal temperature for the reaction in CHCl<sub>3</sub>-hexanes was determined to be 0 °C; The reaction showed much lower enantioselectivity at -40 °C. The optimal temperature for the enthalpy-driven enantioselectivity in *n*-PrOH was -40 °C with a further decrease in temperature not resulting in significant improvements in stereoselectivity.
- The carbamate structure plays a crucial role in the CHCl<sub>3</sub>-hexanes solvent system with the N-Boc carbamates performing significantly better than the N-Cbz or the N-carboxycumyl groups (perhaps not a surprising observation given that *entropy* driven stereoselectivity in reactions is sensitive to steric parameters of the substrate and catalyst). On the other hand, enantioselectivity was unaffected by the nature of the carbamate group for the reaction in *n*-PrOH.

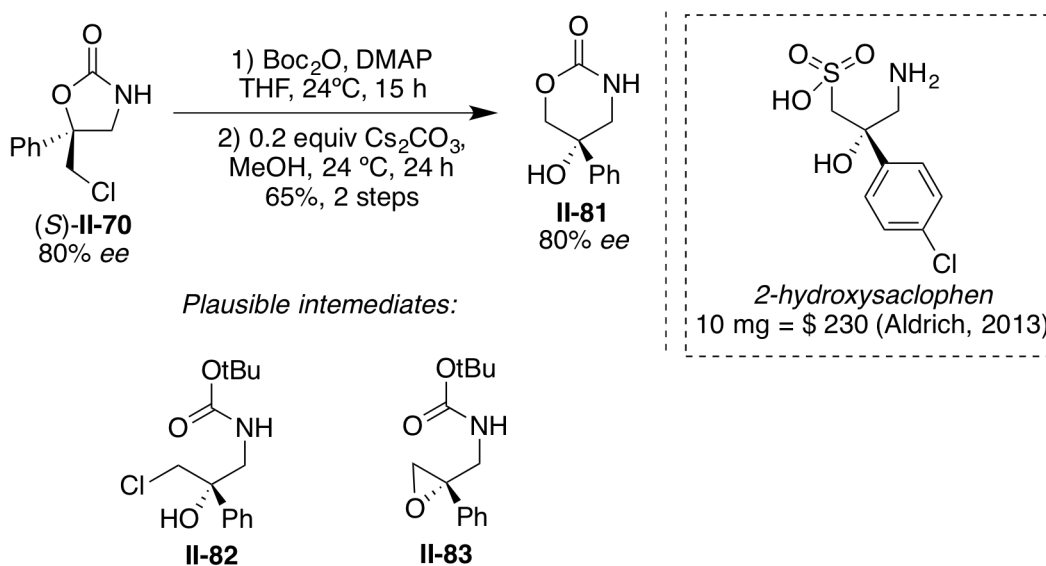
- Certain carboxylic acid additives led to significant enhancement of enantioselectivity in the *n*-PrOH solvent system. Acid and base additives alike were deleterious to the enantioselectivity in the CHCl<sub>3</sub>-hexanes system.
- Stoichiometric <sup>1</sup>H NMR ROESY studies of the catalyst in CD<sub>3</sub>OD and CDCl<sub>3</sub> indicated that the catalyst conformation was practically identical in solution in both protic and aprotic solvents i.e., the origin of enantiodivergence is likely *not* attributable to different catalyst conformations. It emerged much later from deuterium-labeling studies that the observed enantiodivergence is a direct manifestation of the *syn* versus *anti* addition of the chlorine and the nucleophile across the alkene. The role of the solvent in dictating the net *syn* or *anti* addition across the alkene is currently being investigated. The intermediacy of a β-chlorocarbenium ion is highly likely based on both the experimental results as well as theoretical calculations. These studies will be reported in due course.

The substrate scope studies for this transformation are collected in Table II-26. As evident by the data, the enantioselectivity for the cyclization reaction of numerous substrates in *n*-PrOH (condition **A**) proceed with more or less similar enantioselectivity (uniformly greater than 80% *ee* with the exception of substrate **II-80-A** that gave a moderate 51% *ee*. On the contrary, when the same substrates were exposed to the optimized conditions in the CHCl<sub>3</sub>-hexanes solvent (condition **B**), the enantioselectivity was strongly dependent on the steric impediments of the substrate; a wide range of enantioselectivities (from -6% *ee* to +82% *ee*) was observed for these substrates depending on the substituents of the aryl ring on the alkene.



The oxazolidinone product **II-70** was readily transformed into the corresponding oxazinan-2-one **II-81** via a two-step protocol with no loss in the stereospecificity (see Scheme II-15). Boc protection of the oxazolidinone nitrogen, followed by Cs<sub>2</sub>CO<sub>3</sub> mediated opening of the oxazolidinone ring leads to the formation of the corresponding 6-membered cyclic carbamate **II-81**. Although no intermediates were isolated, it is likely that the halohydrin **II-82** or the epoxide **II-83** is the intermediate in this transformation. This reaction is now being used for an expedited synthesis of 2-hydroxysaclophen – a potent and selective antagonist at GABAB receptors (this transformation is being pursued by one of the current lab members - Mr. Hadi Nayebi).

**Scheme II-15.** Chemical transformation of oxazolidinone product **II-70**



### II.3. Summary and future work.

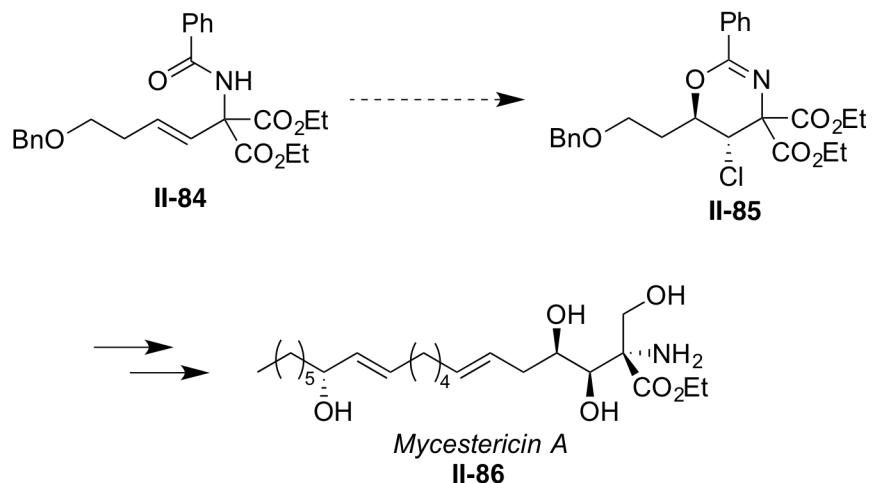
A highly stereoselective chlorocyclization of unsaturated amides to chiral heterocycles mediated by catalytic amounts (1–2 mol %) of the commercially available (DHQD)<sub>2</sub>PHAL was developed. The reaction is operationally simple with no need to resort to strictly anhydrous or inert reaction conditions. A second-generation protocol that employs chloramine salts as the terminal chlorenium source has further improved the practical applicability of this reaction by

enabling ambient temperature reactions at high concentrations. The reaction scope is fairly general with regards to the substitution pattern of the olefin. Both aliphatic and aromatic residues on the olefin are well tolerated.

Mechanistic studies that might enable the understanding of substrate-catalyst as well as reagent-catalyst interactions and also the molecularity with respect to each component will be pivotal in understanding the origins of the enantioselectivity. Additionally, isotope-labeling studies have already established the stereoelectronic outcomes of the alkene chlorination event and the subsequent nucleophilic capture by the pendant amide nucleophile. Some of these studies have been instrumental in enabling the development of related transformations such as asymmetric carbamate chlorocyclizations<sup>28</sup> and kinetic resolution in chlorocyclization reactions.<sup>29</sup> The carbamate chlorocyclization chemistry has been briefly described in the previous section. Studies directed towards the kinetic resolution in halocyclization reactions will be disclosed in subsequent chapters.

Application of this chemistry in the context of natural products' synthesis will also be pursued. For example, the densely functionalized 'head' groups of numerous sphingolipids such as those found in the Mycestericin family of natural products can come from the straightforward manipulation of an appropriately substituted dihydrooxazine precursor. A proposed route to Mycestericin A is shown in Scheme II-16. Efforts are underway to synthesize the precursor **II-84** and evaluate the key asymmetric chlorocyclization reaction to **II-85**.

**Scheme II-16.** Proposed synthesis of Mycestericin A from dihydrooxazine **II-84**



#### II.4. Acknowledgements.

Thanks are due to Dr. Atefeh Garzan who has served as an excellent collaborator in the development of the asymmetric amide chlorocyclization and carbamate chlorocyclization reactions. Dr. Garzan is also acknowledged for running HR-MS analysis for many of the substrates and products presented in this chapter. Ms. Heather Pillsbury, Ms. Yanmen Yang and Mr. Adam Ryske were undergraduate research assistants in the lab during the duration of this project and are thanked for assistance in executing numerous control experiments and for the synthesis of some of the substrates. Dr. Daniel Whitehead is also acknowledged for valuable inputs in the preparation of two published manuscripts detailing the work presented in this chapter. The College of Natural Sciences at Michigan State University is acknowledged for the Dissertation Continuation Fellowship that provided financial support to me during the course of this project.

## II.5. Experimental section.

### II.5.1. General information.

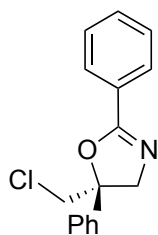
All reagents were purchased from commercial sources and used without purification. Trifluoroethanol and 1-nitropropane were purchased from Aldrich or Alfa Aesar and used without further purification. TLC analyses were performed on silica gel plates (pre-coated on aluminum; 0.20 mm thickness with fluorescent indicator UV<sub>254</sub>) and were visualized by UV, I<sub>2</sub> complex formation or charring in anisaldehyde or PMA stains. <sup>1</sup>H and <sup>13</sup>C NMR spectra were collected on 300, 500 or 600 MHz NMR spectrometers (VARIAN INOVA) using CDCl<sub>3</sub>, or CD<sub>3</sub>CN. Chemical shifts are reported in parts per million (ppm) and are referenced to residual solvent peaks. Flash silica gel (32-63 mm) was used for column chromatography. Enantiomeric excess for all products was judged by HPLC analysis using DAICEL CHIRALPAK OJ-H, OD-H or AS-H columns. Optical rotations were measured in chloroform. All known compounds were characterized by <sup>1</sup>H and <sup>13</sup>C NMR and are in complete agreement with samples reported elsewhere. All new compounds were characterized by <sup>1</sup>H and <sup>13</sup>C NMR, HRMS, optical rotation, and melting point (where appropriate). The absolute stereochemistry of **II-30-B** was established after chemical transformation to the halohydrin which could be crystallized and analyzed by X-ray diffraction analysis. The absolute stereochemistry was inferred by analogy for other oxazolines. The absolute stereochemistry of **II-48-B** and **II-58-B** were established by X-ray diffraction analysis and were inferred by analogy for other dihydrooxazines.

### II.5.2. General procedure for the catalytic asymmetric chlorocyclization of unsaturated amides.

DCDPH (35 mg, 0.11 mmol, 1.1 equiv.) was suspended in 2.2 mL trifluoroethanol (TFE) in a screw capped vial equipped with a stir bar. The resulting suspension was cooled to -30 °C in an immersion cooler. (DHQD)<sub>2</sub>PHAL (1.56 mg, 312 mL of a 5 mg/mL solution in TFE, 2 mol%) was then introduced. After stirring vigorously for 10 min, the substrate (0.10 mmol, 1.0 equiv) was added in a single portion. The vial was capped and the stirring was continued at -30 °C till the reaction was complete (TLC). The reaction was quenched by the addition of 3 mL 10% aq. Na<sub>2</sub>SO<sub>3</sub> and diluted with 3 mL DCM. The organics were separated and the aqueous layer was extracted with DCM (3 x 3mL). The combined organics were dried over Na<sub>2</sub>SO<sub>4</sub> and concentrated in the presence of a small quantity of silica gel. Pure products were isolated by column chromatography on silica gel using EtOAc in hexanes as the eluent.

### II.5.3. Characterization of cyclized products.

**II-19**, (*R*)-5-(chloromethyl)-2,5-diphenyl-4,5-dihydrooxazole



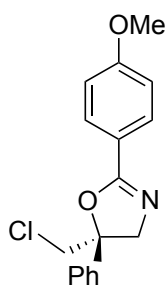
Colorless film; R<sub>f</sub> : 0.38 (30% EtOAc in hexanes) (UV, PMA)

<sup>1</sup>H NMR (500 MHz, CDCl<sub>3</sub>) δ 7.67 (d, *J* = 8.5 Hz, 2H), 7.44 – 7.48 (m, 3H), 7.27 – 7.40 (m, 5H), 6.15 (br s, 1H), 5.51 (s, 1H), 5.31 (d, *J* = 1.0 Hz, 1H), 4.53 (d, *J* = 6.0 Hz, 2H); <sup>13</sup>C NMR

(125 MHz, CDCl<sub>3</sub>)  $\delta$  167.3, 144.3, 138.3, 134.5, 131.5, 128.6, 128.5, 128.1, 126.9, 126.1, 114.1, 43.8; HRMS (ESI): Calculated for [M+H] C<sub>16</sub>H<sub>14</sub>NOCl 271.0764, Found: 271.0755.

Resolution of enantiomers: CHIRALCEL OD-H, 5% IPA-Hexane, 0.8 mL/min, 265 nm, RT1 = 30.2 min, RT2 = 34.6 min;  $[\alpha]_D^{20} = -98.5$  (c 0.50, CHCl<sub>3</sub>, 90% ee)

**II-22-B**, (*R*)-5-(chloromethyl)-2-(4-methoxyphenyl)-5-phenyl-4,5-dihydrooxazole

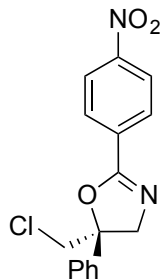


Colorless film; R<sub>f</sub> : 0.24 (30% EtOAc in hexanes) (UV, PMA)

<sup>1</sup>H NMR (500 MHz, CDCl<sub>3</sub>)  $\delta$  (d, *J* = 8.5 Hz, 2H), 7.40 – 7.45 (m, 5H), 6.90 (d, *J* = 8.5 Hz, 2H), 4.57 (d, *J* = 15.3 Hz, 1H), 4.29 (d, *J* = 15.3 Hz, 1H), 3.95 (d, *J* = 12.0 Hz, 1H), 3.83 (s, 3H), 3.85 (d, *J* = 12.0 Hz, 1H); <sup>13</sup>C NMR (125 MHz, CDCl<sub>3</sub>)  $\delta$  162.9, 162.3, 141.6, 134.8, 129.3, 128.6, 124.9, 119.7, 113.8, 87.5, 64.7, 55.4, 51.0; HRMS (ESI): Calculated for [M+H] C<sub>17</sub>H<sub>16</sub>NO<sub>2</sub>Cl 301.0870, Found: 301.0860.

Resolution of enantiomers : CHIRALCEL OJ-H, 7% IPA-Hexane, 0.9 mL/min, 254 nm, RT1 = 23.0 min, RT2 = 51.6 min;  $[\alpha]_D^{20} = -34.0$  (c 0.09, CHCl<sub>3</sub>)

**II-23-B**, (*R*)-5-(chloromethyl)-2-(4-nitrophenyl)-5-phenyl-4,5-dihydrooxazole

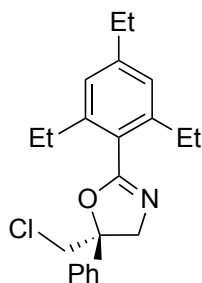


Colorless film;  $R_f$  : 0.34 (30% EtOAc in hexanes) (UV, PMA)

$^1\text{H}$  NMR (300 MHz,  $\text{CDCl}_3$ )  $\delta$  8.30 (d,  $J$  = 9.0 Hz, 2H), 8.20 (d,  $J$  = 9.0 Hz, 2H), 7.32 – 7.44 (m, 5H), 4.57 (d,  $J$  = 15.3 Hz, 1H), 4.29 (d,  $J$  = 15.3 Hz, 1H), 3.95 (d,  $J$  = 12.0 Hz, 1H), 3.85 (d,  $J$  = 12.0 Hz, 1H);  $^{13}\text{C}$  NMR (125 MHz,  $\text{CDCl}_3$ )  $\delta$  161.2, 149.6, 140.9, 133.1, 129.2, 128.8, 126.8, 124.8, 123.6, 88.5, 65.0, 51.1; HRMS (ESI): Calculated for  $[\text{M}+\text{H}]$   $\text{C}_{16}\text{H}_{13}\text{N}_2\text{O}_3\text{Cl}$  316.0615, Found: 316.0628.

Resolution of enantiomers: CHIRALCEL OD-H, 5% IPA-Hexane, 0.8 mL/min, 265 nm, RT1 = 30.2 min, RT2 = 34.6 min;  $[\alpha]_D^{20}$  = -144.8 (c 0.50,  $\text{CHCl}_3$ , 93% *ee*)

**II-24-B**, (*R*)-5-(chloromethyl)-5-phenyl-2-(2,4,6-triethylphenyl)-4,5-dihydrooxazole



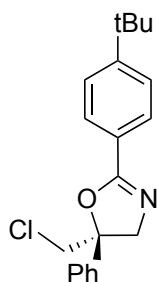
Colorless liquid;  $R_f$  : 0.39 (30% EtOAc in hexanes) (UV, Anisaldehyde)

$^1\text{H}$  NMR (300 MHz,  $\text{CDCl}_3$ )  $\delta$  7.25 - 7.45 (m, 5H), 6.93 (s, 2H), 4.56 (d,  $J$  = 15.0 Hz, 1H), 4.32 (d,  $J$  = 15.0 Hz, 1H), 3.90 (d,  $J$  = 12.0 Hz, 1H), 3.80 (d,  $J$  = 12.0 Hz, 1H), 2.60 – 2.67 (m, 6H),

1.15 – 1.24 (m, 9H);  $^{13}\text{C}$  NMR (125 MHz,  $\text{CDCl}_3$ )  $\delta$  171.2, 167.0, 163.6, 146.0, 138.1, 128.9, 127.7, 125.4, 124.6, 87.6, 64.3, 51.1, 28.8, 26.6, 15.8, 14.1; HRMS (ESI): Calculated for  $[\text{M}+\text{H}]$   $\text{C}_{22}\text{H}_{26}\text{NOCl}$  355.1703, Found: 355.1708.;

Resolution of enantiomers: CHIRALCEL OD-H, 5% IPA-Hexane, 0.8 mL/min, 230 nm, RT1 = 8.1 min, RT2 = 9.0 min;  $[\alpha]_{\text{D}}^{20} = +0.80$  (c 0.50,  $\text{CHCl}_3$ )

**II-25-B**, (R)-2-(4-tert-butylphenyl)-5-(chloromethyl)-5-phenyl-4,5-dihydrooxazole

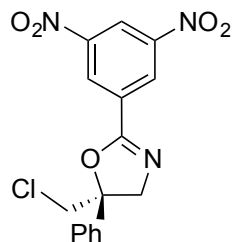


Colorless film ;  $R_f$  : 0.52 (30% EtOAc in hexanes) (UV, PMA)

$^1\text{H}$  NMR (300 MHz,  $\text{CDCl}_3$ )  $\delta$  7.96 (d,  $J = 8.4$  Hz, 1H), 7.46 (d,  $J = 8.4$  Hz, 1H), 7.25 – 7.43 (m, 5H), 4.48 (d,  $J = 14.7$  Hz, 1H), 4.20 (d,  $J = 14.7$  Hz, 1H), 3.92 (d,  $J = 12.0$  Hz, 1H), 3.84 (d,  $J = 12.0$  Hz, 1H), 1.31 (s, 9H);  $^{13}\text{C}$  NMR (125 MHz,  $\text{CDCl}_3$ )  $\delta$  171.1, 163.0, 155.1, 141.7, 128.7, 128.2, 125.4, 124.9, 124.6, 87.4, 65.0, 51.0, 35.0, 31.1; HRMS (ESI): Calculated for  $[\text{M}+\text{H}]$   $\text{C}_{20}\text{H}_{22}\text{NOCl}$  327.1390, Found: 327.1374.

Resolution of enantiomers: Resolution of enantiomers: CHIRALCEL OJ-H, 5% IPA-Hexane, 1.0 mL/min, 254 nm, RT1 = 8.6 min, RT2 = 11.0 min;  $[\alpha]_{\text{D}}^{20} = -65.5$  (c 0.33,  $\text{CHCl}_3$ )

**II-26-B**, (R)-5-(chloromethyl)-2-(3,5-dinitrophenyl)-5-phenyl-4,5-dihydrooxazole

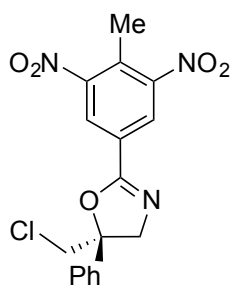


Colorless film;  $R_f$  : 0.46 (30% EtOAc in hexanes) (UV, PMA)

$^1\text{H}$  NMR (300 MHz,  $\text{CDCl}_3$ )  $\delta$  9.16 (s, 2H), 7.37 – 7.44 (m, 5H), 4.64 (d,  $J$  = 15.6 Hz, 1H), 4.36 (d,  $J$  = 15.6 Hz, 1H), 3.97 (d,  $J$  = 12.3 Hz, 1H), 3.84 (d,  $J$  = 12.3 Hz, 1H);  $^{13}\text{C}$  NMR (125 MHz,  $\text{CDCl}_3$ )  $\delta$  159.2, 148.7, 140.4, 131.1, 129.3, 128.7, 128.0, 124.9, 121.1, 89.5, 64.9, 51.1; HRMS (ESI): Calculated for  $[\text{M}+\text{H}]^+$   $\text{C}_{16}\text{H}_{12}\text{N}_3\text{O}_5\text{Cl}$  361.0465, Found: 361.0462.

Resolution of enantiomers: CHIRALCEL OD-H, 3% IPA-Hexane, 1.0 mL/min, 254 nm,  $\text{RT}_1$  = 34.9 min,  $\text{RT}_2$  = 44.2 min;  $[\alpha]_D^{20}$  = -129.1 (c 0.33,  $\text{CHCl}_3$ )

**II-27-B**, (*R*)-5-(chloromethyl)-2-(4-methyl-3,5-dinitrophenyl)-5-phenyl-4,5-dihydrooxazole



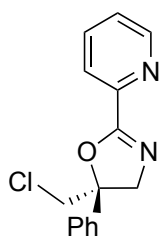
Yellow film;  $R_f$  : 0.61 (30% EtOAc in hexanes) (UV, PMA)

$^1\text{H}$  NMR (300 MHz,  $\text{CDCl}_3$ )  $\delta$  8.59 (s, 2H), 7.30 – 7.43 (m, 5H), 4.58 (d,  $J$  = 15.6 Hz, 1H), 4.30 (d,  $J$  = 15.6 Hz, 1H), 3.94 (d,  $J$  = 12.0 Hz, 1H), 3.82 (d,  $J$  = 12.0 Hz, 1H), 2.62 (s, 3H);  $^{13}\text{C}$  NMR

(125 MHz, CDCl<sub>3</sub>)  $\delta$  171.1, 159.2, 151.6, 140.5, 129.8, 128.7, 127.7, 126.5, 124.7, 89.2, 64.8, 51.1, 21.0, HRMS (ESI): Calculated for [M+H] C<sub>17</sub>H<sub>14</sub>N<sub>3</sub>O<sub>5</sub>Cl 375.0622, Found: 375.0620.

Resolution of enantiomers : CHIRALCEL OD-H, 3% IPA-Hexane, 1.0 mL/min, 254 nm, RT1 = 46.5 min, RT2 = 55.9 min;  $[\alpha]_D^{20} = -115.5$  (c 1.00, CHCl<sub>3</sub>)

**II-28-B**, (*R*)-5-(chloromethyl)-5-phenyl-2-(pyridin-2-yl)-4,5-dihydrooxazole

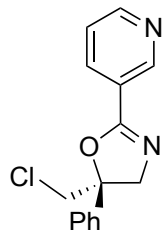


Yellow film; R<sub>f</sub> : 0.30 (50% EtOAc in hexanes; UV, PMA)

<sup>1</sup>H NMR (300 MHz, CDCl<sub>3</sub>)  $\delta$  8.76 (ddd, *J* = 5.1, 1.8, 1.2 Hz, 1H), 8.09 (td, *J* = 6.6, 1.2 Hz, 1H), 7.80 (dt, *J* = 8.1, 1.8 Hz, 1H), 7.30 – 7.47 (m, 6H), 4.58 (d, *J* = 15.6 Hz, 1H), 4.27 (d, *J* = 15.6 Hz, 1H), 3.98 (d, *J* = 12.0 Hz, 1H), 3.86 (d, *J* = 12.0 Hz, 1H); <sup>13</sup>C NMR (150 MHz, CDCl<sub>3</sub>)  $\delta$  162.2, 149.9, 146.4, 141.3, 136.7, 128.8, 128.4, 125.7, 125.0, 124.0, 88.4, 64.9, 50.9; HRMS (ESI): Calculated for [M+H] C<sub>15</sub>H<sub>13</sub>N<sub>2</sub>OCl 272.0716, Found: 272.0730.

Resolution of enantiomers: CHIRALCEL OD-H, 15% IPA-Hexane, 0.7 mL/min, 260 nm, RT1 = 18.0 min, RT2 = 34.0 min;  $[\alpha]_D^{20} = -108.2$  (c 1.0, CHCl<sub>3</sub>)

**II-29-B**, (*R*)-5-(chloromethyl)-5-phenyl-2-(pyridin-3-yl)-4,5-dihydrooxazole

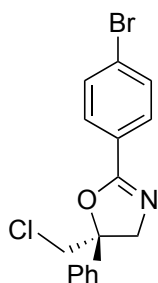


Colorless film;  $R_f$  : 0.20 (50% EtOAc in hexanes; UV, PMA)

$^1\text{H}$  NMR (500 MHz,  $\text{CDCl}_3$ )  $\delta$  9.24 (d,  $J$  = 1.5 Hz, 1H), 8.73 (dd,  $J$  = 5.0, 1.5 Hz, 1H), 8.30 (td,  $J$  = 8.0, 2.0 Hz, 1H), 7.37 – 7.41 (m, 5H, 7.34 (dd,  $J$  = 8.0, 5.0 Hz), 4.53 (d,  $J$  = 15.0 Hz, 1H), 4.26 (d,  $J$  = 15.0 Hz, 1H), 3.93 (d,  $J$  = 12.5 Hz, 1H), 3.84 (d,  $J$  = 12.5 Hz, 1H);  $^{13}\text{C}$  NMR (125 MHz,  $\text{CDCl}_3$ )  $\delta$  161.0, 152.2, 149.4, 141.1, 135.6, 128.9, 128.5, 124.8, 123.3, 88.0, 64.8, 51.1; HRMS (ESI): Calculated for  $[\text{M}+\text{H}]$   $\text{C}_{15}\text{H}_{13}\text{N}_2\text{OCl}$  272.0716, Found: 272.0704.

Resolution of enantiomers: CHIRALCEL AS-H, 5% IPA-Hexane, 0.8 mL/min, 254 nm, RT1 = 34.5 min, RT2 = 41.2 min;  $[\alpha]_D^{20}$  = -123.2 (c 1.0,  $\text{CHCl}_3$ )

**II-30-B**, (*R*)-2-(4-bromophenyl)-5-(chloromethyl)-5-phenyl-4,5-dihydrooxazole



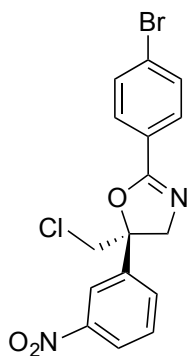
Colorless film;  $R_f$  : 0.48 (30% EtOAc in hexanes)

$^1\text{H}$  NMR (300 MHz,  $\text{CDCl}_3$ )  $\delta$  7.90 (d,  $J$  = 8.4 Hz, 2H), 7.58 (d,  $J$  = 8.4 Hz, 2H), 7.31 – 7.40 (m, 5H), 4.48 (d,  $J$  = 15.3 Hz, 1H), 4.20 (d,  $J$  = 15.4 Hz, 1H), 3.91 (d,  $J$  = 12.0 Hz, 1H), 3.82 (d,  $J$  = 12.0 Hz, 1H);  $^{13}\text{C}$  NMR (125 MHz,  $\text{CDCl}_3$ )  $\delta$  162.3, 141.3, 131.9, 131.6, 129.9, 128.7, 128.5,

126.3, 125.0, 87.9, 64.9, 51.0; HRMS (ESI): Calculated for [M+H] C<sub>16</sub>H<sub>13</sub>NOBrCl 348.9869, Found: 348.9856.

Resolution of enantiomers: CHIRALCEL OJ-H, 5% IPA-Hexane, 1.0 J = mL/min, 254 nm, RT1 = 16.2 min, RT2 = 28.4 min;  $[\alpha]_D^{20} = -110.0$  (c 1.00, CHCl<sub>3</sub>)

**II-32-B**, (R)-2-(4-bromophenyl)-5-(chloromethyl)-5-(3-nitrophenyl)-4,5-dihydrooxazole

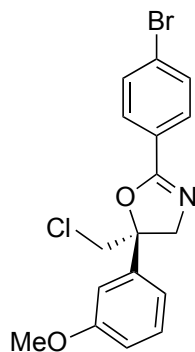


Colorless film; R<sub>f</sub> : 0.28 (30% EtOAc in hexanes) (UV)

<sup>1</sup>H NMR (600 MHz, CDCl<sub>3</sub>) δ 8.29 (t, J = 1.8 Hz, 1H), 8.21 (ddd, J = 8.4, 2.4, 1.2 Hz, 1H), 7.89 (d, J = 8.4 Hz, 2H), 7.74 (ddd, J = 7.8, 1.8, 1.2 Hz, 1H), 7.59 – 7.61 (m, 2H), 4.52 (d, J = 15.6 Hz, 1H), 4.21 (d, J = 15.6 Hz, 1H), 3.92 (d, J = 12.0 Hz, 1H), 3.87 (d, J = 12.0 Hz, 1H); <sup>13</sup>C NMR (150 MHz, CDCl<sub>3</sub>) δ 162.1, 148.5, 143.4, 131.9, 131.2, 130.0, 129.8, 126.7, 125.8, 123.5, 120.4, 87.3, 65.3, 50.3; HRMS (ESI): Calculated for [M+H] C<sub>16</sub>H<sub>12</sub>N<sub>2</sub>O<sub>3</sub>ClBr 393.9720, Found: 393.9704.

Resolution of enantiomers: CHIRALCEL OJ-H, 10% IPA-Hexane, 1.0 mL/min, 254 nm, RT1 = 47.1 min, RT2 = 54.5 min;  $[\alpha]_D^{20} = -95.0$  (c 1.0, CHCl<sub>3</sub>)

**II-33-B**, (R)-2-(4-bromophenyl)-5-(chloromethyl)-5-(3-methoxyphenyl)-4,5-dihydrooxazole

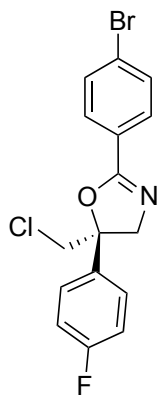


Colorless film;  $R_f$ : 0.21 (15% EtOAc- Hex)(UV)

$^1\text{H}$  NMR (500 MHz,  $\text{CDCl}_3$ )  $\delta$  7.89 (d,  $J = 8.5$  Hz, 2H), 7.57(d,  $J = 8.5$  Hz, 2H), 7.31 (t,  $J = 7.5$  Hz, 1H), 6.93 – 6.95 (m, 2H), 6.84 – 6.87 (m, 1H), 4.46 (d,  $J = 14.5$  Hz, 1H), 4.19 (d,  $J = 14.5$  Hz, 1H), 3.90 (d,  $J = 11.5$  Hz, 1H), 3.82 (d,  $J = 11.5$  Hz, 1H), 3.80 (s, 3H), ;  $^{13}\text{C}$  NMR (125 MHz,  $\text{CDCl}_3$ )  $\delta$  162.2, 159.9, 143.0, 131.7, 130.0, 129.8, 128.5, 126.3, 117.1, 113.1, 111.4, 87.8, 65.0, 55.3, 51.0 ; HRMS (ESI): Calculated for  $[\text{M}+\text{H}]$   $\text{C}_{17}\text{H}_{15}\text{NO}_2\text{ClBr}$  378.9975, Found: 378.9994.

Resolution of enantiomers: CHIRALCEL AS-H, 5% IPA-Hexane, 1.0 mL/min, 254 nm, RT1 = 10.7 min, RT2 = 16.6 min;  $[\alpha]_D^{20} = -134.0$  (c 1.0,  $\text{CHCl}_3$ )

**II-34-B**, (R)-2-(4-bromophenyl)-5-(chloromethyl)-5-(4-fluorophenyl)-4,5-dihydrooxazole

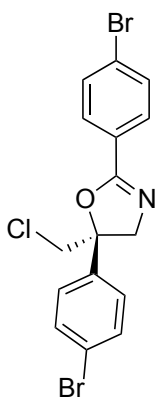


Colorless oil;  $R_f$  : 0.50 (30% EtOAc in hexanes)(UV)

$^1\text{H}$  NMR (600 MHz,  $\text{CDCl}_3$ )  $\delta$  7.87 (d,  $J = 9.0$  Hz, 2H), 7.58 (d,  $J = 9.0$  Hz, 2H), 7.37 (dd,  $^3J_{\text{H-H}} = 9.0$  Hz,  $^4J_{\text{H-F}} = 5.4$  Hz, 2H), 7.08 (t,  $^3J_{\text{H-H}} = ^3J_{\text{H-F}} = 9.0$  Hz, 2H), 4.46 (d,  $J = 14.4$  Hz, 1H), 4.18 (d,  $J = 14.4$  Hz, 1H), 3.87 (d,  $J = 12.0$  Hz, 1H), 3.80 (d,  $J = 12.0$  Hz, 1H);  $^{13}\text{C}$  NMR (150 MHz,  $\text{CDCl}_3$ )  $\delta$  162.5 (d,  $^1J_{\text{C-F}} = 246.0$  Hz), 162.2, 137.1 (d,  $^4J_{\text{C-F}} = 3.0$  Hz), 132.0, 131.8, 129.8, 128.5, 126.8 (d,  $^3J_{\text{C-F}} = 8.7$  Hz), 126.4, 126.2, 115.8 (d,  $^2J_{\text{C-F}} = 21.8$  Hz), 87.6, 65.1, 50.8; HRMS (ESI): Calculated for  $[\text{M}+\text{H}]$   $\text{C}_{16}\text{H}_{12}\text{NOClBrF}$  366.9775, Found: 366.9759.

Resolution of enantiomers: CHIRALCEL OJ-H, 5% IPA-Hex, 1.0 mL/min,  $\text{RT}_1 = 12.5$  min,  $\text{RT}_2 = 23.1$  min.;  $[\alpha]_{\text{D}}^{20} = -87.8$  (c 1.0,  $\text{CHCl}_3$ )

**II-35-B**, (R)-2,5-bis(4-bromophenyl)-5-(chloromethyl)-4,5-dihydrooxazole



Colorless gum;  $R_f$  : 0.53 (30% EtOAc in hexanes)

$^1\text{H}$  NMR (600 MHz,  $\text{CDCl}_3$ )  $\delta$  7.87 (d,  $J = 8.4$  Hz, 2H), 7.57 (d,  $J = 8.4$  Hz, 2H), 7.51 (d,  $J = 8.5$  Hz, 2H), 7.27 (d,  $J = 8.5$  Hz, 2H), 4.45 (d,  $J = 15.0$  Hz, 1H), 4.15 (d,  $J = 15.0$  Hz, 1H), 3.86 (d,  $J = 12.0$  Hz, 1H), 3.79 (d,  $J = 12.0$  Hz, 1H);  $^{13}\text{C}$  NMR (150 MHz,  $\text{CDCl}_3$ )  $\delta$  162.2, 140.3, 132.0,

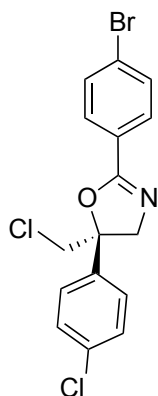
131.8, 129.8, 126.7, 126.5, 126.1, 122.5, 87.6, 65.0, 50.6 ; HRMS (ESI): Calculated for [M+H]

$C_{16}H_{12}NOClBr_2$  426.8782, Found: 426.8786.;

Resolution of enantiomers: CHIRALCEL OJ-H, 5% IPA-Hex, 1.0 mL/min, RT1 = 14.8 min, RT2 =

20.5 min;  $[\alpha]_D^{20} = -96.7$  (c 1.0,  $CHCl_3$ )

**II-36-B**, (R)-2-(4-bromophenyl)-5-(chloromethyl)-5-(4-chlorophenyl)-4,5-dihydrooxazole



Yellow gum;  $R_f$  : 0.48 (30% EtOAc in hexanes)

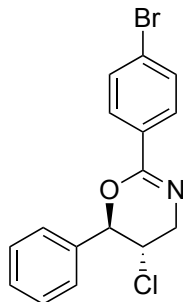
$^1H$  NMR (600 MHz,  $CDCl_3$ )  $\delta$  7.87 (d,  $J = 8.0$  Hz, 2H), 7.57 (d,  $J = 8.0$  Hz, 2H), 7.36 (d,  $J = 8.4$  Hz, 2H), 7.33 (d,  $J = 8.4$  Hz, 2H), 4.46 (d,  $J = 15.0$  Hz, 1H), 4.16 (d,  $J = 15.0$  Hz, 1H), 3.87 (d,  $J = 12.0$  Hz, 1H), 3.80 (d,  $J = 12.0$  Hz, 1H);  $^{13}C$  NMR (150 MHz,  $CDCl_3$ )  $\delta$  162.2, 139.8, 134.4,

131.8, 129.8, 129.0, 128.9, 128.5, 126.4, 126.1, 87.5, 65.0, 50.7; HRMS (ESI): Calculated for [M+H]  $C_{16}H_{12}NOCl_2Br$  382.9479, Found: 382.9484.

Resolution of enantiomers: CHIRALCEL OJ-H, 5% IPA-Hex, 1.0 mL/min, RT1 = 12.9 min, RT2 =

18.9 min;  $[\alpha]_D^{20} = -58.8$  (c 1.0,  $CHCl_3$ )

**II-41-B**, (5S,6R)-2-(4-bromophenyl)-5-chloro-6-phenyl-5,6-dihydro-4H-1,3-oxazine



Colorless needles; M.P.: 93 – 95 °C;  $R_f$  : 0.50 (15% EtOAc in hexanes)

$^1\text{H}$  NMR (300 MHz,  $\text{CDCl}_3$ )  $\delta$  7.81 (d,  $J = 8.4$  Hz, 2H), 7.50 (d,  $J = 8.4$  Hz, 2H), 7.34 – 7.42 (m, 5H), 5.21 (d,  $J = 7.2$  Hz, 1H), 4.19 (dt,  $J = 7.5, 4.8$  Hz, 1H), 3.95 (dd,  $J = 17.1, 4.8$  Hz, 1H), 3.75 (ddd,  $J = 17.1, 7.5, 0.9$  Hz, 1H);  $^{13}\text{C}$  NMR (75 MHz,  $\text{CDCl}_3$ )  $\delta$  154.4, 137.0, 131.5, 131.4, 129.1, 128.9, 128.7, 126.7, 125.6, 80.7, 53.8, 49.8 ; HRMS (ESI): Calculated for  $[\text{M}+\text{H}]$   $\text{C}_{16}\text{H}_{13}\text{NOBrCl}$  348.9869, Found: 348.9853.

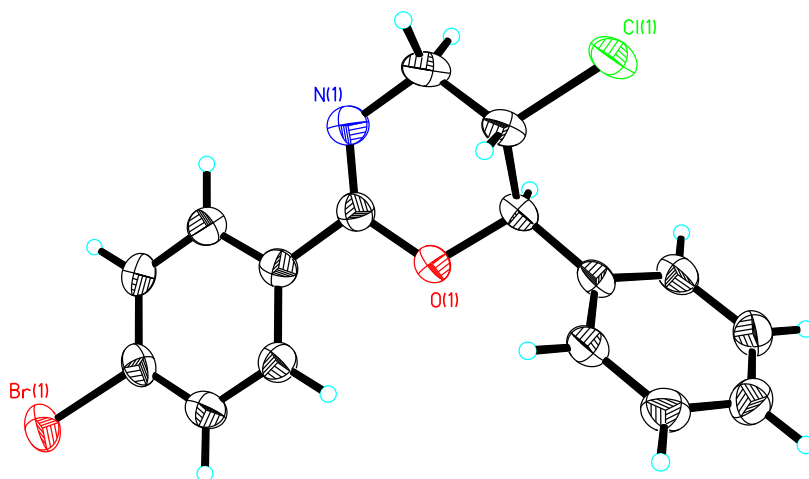
Resolution of enantiomers: CHIRALCEL AS-H, 3% IPA-Hexane, 1.0 mL/min, 254 nm, RT1 = 6.7 min, RT2 = 10.7 min;  $[\alpha]_{\text{D}}^{20} = -17.8$  (c 0.50,  $\text{CHCl}_3$ )

The compound could be crystallized from  $\text{CHCl}_3$  – hexanes using the vapor diffusion technique.

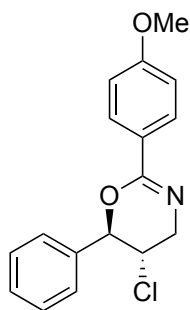
Absolute stereochemistry was determined by X-ray crystallography.

ORTEP drawing (at 50% ellipsoids)

**Figure II-10.** Crystal structure of II-41-B



**II-42-B,** (5*S*,6*R*)-2-(4-methoxyphenyl)-5-chloro-6-phenyl-5,6-dihydro-4*H*-1,3-oxazine

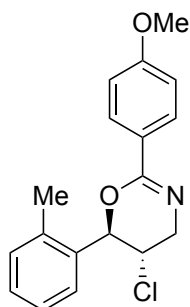


White solid; M.P.: 98 – 100 °C;  $R_f$  : 0.25 (20% EtOAc-Hex) (UV)

$^1\text{H}$  NMR (300 MHz,  $\text{CDCl}_3$ )  $\delta$  7.91 (d,  $J = 9.0$  Hz, 2H), 7.36 – 7.41 (m, 5H), 6.87 (d,  $J = 9.0$  Hz, 2H), 5.23 (d,  $J = 8.0$  Hz, 1H), 4.21 (dt,  $J = 8.0, 4.5$  Hz, 1H), 3.93 (dd,  $J = 16.5, 4.5$  Hz, 1H), 3.82 (s, 3H), 3.76 (dd,  $J = 16.5, 8.0$  Hz, 1H);  $^{13}\text{C}$  NMR (125 MHz,  $\text{CDCl}_3$ )  $\delta$  162.1, 156.2, 137.0, 129.2, 129.1, 128.7, 127.8, 126.7, 113.6, 80.9, 55.4, 55.3, 49.4; HRMS (ESI): Calculated for  $[\text{M}+\text{H}] \text{C}_{16}\text{H}_{13}\text{NOBrCl}$  348.9869, Found: 348.9853.

Resolution of enantiomers: CHIRALCEL AS-H, 4% IPA-Hexane, 0.7 mL/min, 254 nm, RT1 = 16.7 min, RT2 = 22.5 min;  $[\alpha]_D^{20} = -45.9$  (c 1.0, CHCl<sub>3</sub>)

**II-45-B**, (5S,6R)-5-chloro-2-(4-methoxyphenyl)-6-*o*-tolyl-5,6-dihydro-4H-1,3-oxazine

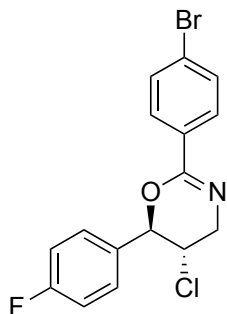


Yellowish solid; M.P. : 87 – 90 °C

<sup>1</sup>H NMR (500 MHz, CDCl<sub>3</sub>) δ 7.93 (d, *J* = 9.0 Hz, 2H), 7.23 – 7.29 (m, 5H), 6.88 (d, *J* = 9.0 Hz, 2H), 5.53 (d, *J* = 7.0 Hz, 1H), 4.27 (dt, *J* = 7.0, 5.0 Hz, 1H), 3.99 (dd, *J* = 17.0, 5.0 Hz, 1H), 3.78 – 3.83 (m, 4H), 2.45 (s, 3H); <sup>13</sup>C NMR (125 MHz, CDCl<sub>3</sub>) δ 161.8, 155.3, 136.1, 135.6, 130.8, 129.0, 128.8, 125.5, 126.2, 125.1, 113.4, 77.4, 55.3, 53.6, 50.0, 19.4 ; HRMS (ESI): Calculated for [M+H] C<sub>18</sub>H<sub>18</sub>ClNO<sub>2</sub> : 315.1026, Found: 315.1030

Resolution of enantiomers: CHIRALCEL OD-H, 1% IPA-Hexane, 0.8 mL/min, 250 nm, RT1 = 25.8 min, RT2 = 27.7 min;  $[\alpha]_D^{20} = -1.7$  (c 1.0, CHCl<sub>3</sub>)

**II-46-B**, (5S,6R)-2-(4-bromophenyl)-5-chloro-6-(4-fluorophenyl)-5,6-dihydro-4H-1,3-oxazine

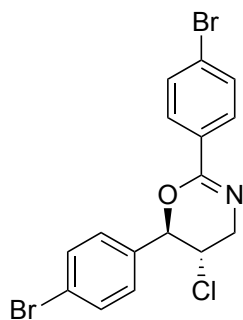


White film;  $R_f$  : 0.54 (15% EtOAc- Hex) (UV)

$^1\text{H}$  NMR (500 MHz,  $\text{CDCl}_3$ )  $\delta$  7.78 (d,  $J$  = 8.5 Hz, 2H), 7.49 (d,  $J$  = 8.5 Hz, 2H), 7.36 (dd,  $^2J_{\text{H-H}}$  = 8.5 Hz,  $^3J_{\text{F-H}}$  = 5.0 Hz, 2H), 7.11 (t,  $^2J_{\text{H-H}}$  =  $^2J_{\text{F-H}}$  = 8.5 Hz, 2H), 5.15 (d,  $J$  = 8.5 Hz, 1H), 4.13 (dt,  $J$  = 8.5, 5.0 Hz, 1H), 3.98 (dd,  $J$  = 17.5, 5.0 Hz, 1H), 3.75 (dd,  $J$  = 17.5, 8.5 Hz, 1H);  $^{13}\text{C}$  NMR (150 MHz,  $\text{CDCl}_3$ )  $\delta$  163.1 (d,  $^1J_{\text{C-F}}$  = 247.1 Hz), 154.4, 132.7 (d,  $^4J_{\text{C-F}}$  = 2.9 Hz), 131.4, 131.3, 128.9, 128.7 ( $^3J_{\text{C-F}}$  = 8.7 Hz), 125.7, 115.7 ( $^2J_{\text{C-F}}$  = 21.8 Hz), 80.2, 53.8, 50.3; HRMS (ESI): Calculated for  $[\text{M}+\text{H}]$   $\text{C}_{16}\text{H}_{12}\text{NOBrClF}$  366.9775, Found: 366.9767.

Resolution of enantiomers: CHIRALCEL AS-H, 5% IPA-Hexane, 1.0 mL/min, 250 nm,  $\text{RT}_1$  = 7.0 min,  $\text{RT}_2$  = 9.3 min;  $[\alpha]_{\text{D}}^{20}$  = -29.4 (c 1.0,  $\text{CHCl}_3$ )

**II-47-B**, (5S,6R)-2,6-bis(4-bromophenyl)-5-chloro-5,6-dihydro-4H-1,3-oxazine

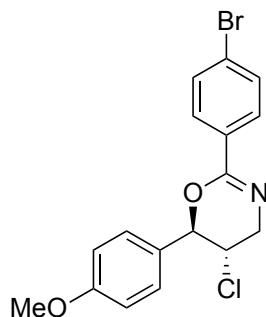


Colorless film;  $R_f$  : 0.50 (15% EtOAc- Hex) (UV)

$^1\text{H}$  NMR (500 MHz,  $\text{CDCl}_3$ )  $\delta$  7.78 (d,  $J = 8.5$  Hz, 2H), 7.55 (d,  $J = 8.5$  Hz, 2H), 7.48 (d,  $J = 8.5$  Hz, 2H), 7.26 (d,  $J = 8.5$  Hz, 2H), 5.13 (d,  $J = 8.0$  Hz, 1H), 4.11 (dt,  $J = 8.0, 4.5$  Hz, 1H), 3.97 (dd,  $J = 17.5, 5.0$  Hz, 1H), 3.75 (dd,  $J = 17.5, 8.0$  Hz, 1H);  $^{13}\text{C}$  NMR (125 MHz,  $\text{CDCl}_3$ )  $\delta$  154.3, 135.9, 131.9, 131.4, 131.3, 128.9, 128.6, 125.8, 123.3, 80.2, 53.6, 50.2; HRMS (ESI): Calculated for  $[\text{M}+\text{H}] \text{C}_{16}\text{H}_{12}\text{NOBr}_2\text{Cl}$  426.8974, Found: 426.8982.

Resolution of enantiomers: CHIRALCEL AS-H, 5% IPA-Hexane, 1.0 mL/min, 250 nm, RT1 = 6.4 min, RT2 = 8.6 min;  $[\alpha]_{\text{D}}^{20} = -9.6$  (c 1.0,  $\text{CHCl}_3$ )

**II-48-B**, (5S,6R)-2-(4-bromophenyl)-5-chloro-6-(4-methoxyphenyl)-5,6-dihydro-4H-1,3-oxazine

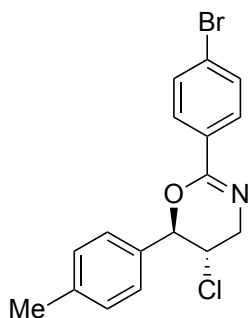


Colorless film;  $R_f$  : 0.44 (15% EtOAc – Hex) (UV)

$^1\text{H}$  NMR (300 MHz,  $\text{CDCl}_3$ )  $\delta$  7.79 (d,  $J = 8.4$  Hz, 2H), 7.48 (d,  $J = 8.4$  Hz, 2H), 7.29 (d,  $J = 9.0$  Hz, 2H), 6.93 (d,  $J = 9.0$  Hz, 2H), 5.14 (d,  $J = 8.1$  Hz, 1H), 4.16 (dt,  $J = 8.1, 4.8$  Hz, 1H), 3.97 (dd,  $J = 17.1, 4.8$  Hz, 1H), 3.82 (s, 3H), 3.74 (dd,  $J = 17.1, 8.1$  Hz, 1H);  $^{13}\text{C}$  NMR (125 MHz,  $\text{CDCl}_3$ )  $\delta$  160.2, 154.6, 131.6, 131.3, 129.0, 128.9, 128.2, 125.6, 114.1, 80.5, 55.3, 54.0, 50.2; HRMS (ESI): Calculated for  $[\text{M}+\text{H}] \text{C}_{17}\text{H}_{15}\text{NO}_2\text{BrCl}$  378.9975, Found: 378.9982.

Resolution of enantiomers: CHIRALCEL AS-H, 3% IPA-Hexane, 1.0 mL/min, 254 nm, RT1 = 8.5 min, RT2 = 12.3 min;  $[\alpha]_{\text{D}}^{20} = +4.7$  (c 0.75,  $\text{CHCl}_3$ )

**II-49-B**, (5S,6R)-2-(4-bromophenyl)-5-chloro-6-p-tolyl-5,6-dihydro-4H-1,3-oxazine



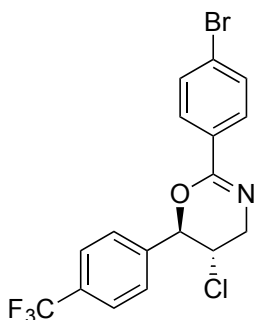
Colorless film;  $R_f$  : 0.56 (15% EtOAc- Hex) (UV)

$^1\text{H}$  NMR (600 MHz,  $\text{CDCl}_3$ )  $\delta$  7.80 (d,  $J$  = 8.4 Hz, 2H), 7.49 (d,  $J$  = 8.4 Hz, 2H), 7.25 (d,  $J$  = 8.4 Hz, 2H), 7.22 (d,  $J$  = 8.4 Hz, 2H), 5.17 (d,  $J$  = 7.8 Hz, 1H), 4.18 (dt,  $J$  = 7.8, 4.8 Hz, 1H), 3.96 (dd,  $J$  = 17.4, 4.8 Hz, 1H), 3.74 (dd,  $J$  = 17.4, 7.8 Hz, 1H), 2.37 (s, 3H);  $^{13}\text{C}$  NMR (150 MHz,  $\text{CDCl}_3$ )  $\delta$  154.5, 139.1, 134.1, 131.6, 131.4, 129.4, 128.9, 126.7, 125.6, 80.7, 53.9, 50.0, 21.2 ;

HRMS (ESI): Calculated for  $[\text{M}+\text{H}]$   $\text{C}_{17}\text{H}_{15}\text{NOBrCl}$  363.0026, Found: 363.0037.

Resolution of enantiomers: CHIRALCEL AS-H, 3% IPA-Hexane, 1.0 mL/min, 254 nm,  $\text{RT}_1$  = 5.7 min,  $\text{RT}_2$  = 7.4 min;  $[\alpha]_D^{20}$  = -4.3 (c 1.0,  $\text{CHCl}_3$ )

**II-50-B**, (5S,6R)-2-(4-bromophenyl)-5-chloro-6-[4-(trifluoromethyl)phenyl]-5,6-dihydro-4H-1,3-oxazine

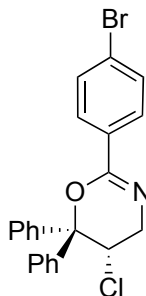


White film;  $R_f$ : 0.48 (15% EtOAc – Hex) (UV)

$^1\text{H}$  NMR (500 MHz,  $\text{CDCl}_3$ )  $\delta$  7.79 (d,  $J = 8.5$  Hz, 2H), 7.69 (d,  $J = 8.5$  Hz, 2H), 7.49 – 7.53 (m, 4H), 5.22 (d,  $J = 8.5$  Hz, 1H), 4.14 (dt,  $J = 8.5, 5.0$  Hz, 1H), 3.99 (dd,  $J = 17.5$  Hz, 5.0 Hz, 1H), 3.77 (dd,  $J = 17.5, 8.5$  Hz, 1H);  $^{13}\text{C}$  NMR (125 MHz,  $\text{CDCl}_3$ )  $\delta$  154.1, 140.7, 131.5, 131.4 (q,  $^2J_{\text{C-F}} = 32.5$  Hz), 131.2, 128.9, 127.4, 125.9, 125.8 (q,  $^3J_{\text{C-F}} = 3.8$  Hz), 123.7 (q,  $^1J_{\text{C-F}} = 270.9$  Hz), 80.1, 53.5, 50.3; HRMS (ESI): Calculated for  $[\text{M}+\text{H}]$   $\text{C}_{17}\text{H}_{12}\text{NOF}_3\text{BrCl}$  416.9743, Found: 416.9721.

Resolution of enantiomers: CHIRALCEL AS-H, 3% IPA-Hexane, 0.8 mL/min, 254 nm, RT1 = 7.2 min, RT2 = 9.1 min;  $[\alpha]_{\text{D}}^{20} = -30.7$  (c 1.0,  $\text{CHCl}_3$ )

**II-51-B**, (S)-2-(4-bromophenyl)-5-chloro-6,6-diphenyl-5,6-dihydro-4H-1,3-oxazine

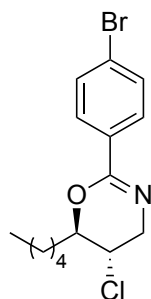


White film;  $R_f$ : 0.35 (15% EtOAc- Hex) (UV)

$^1\text{H}$  NMR (500 MHz,  $\text{CDCl}_3$ )  $\delta$  8.05 (d,  $J = 8.5$  Hz, 2H), 7.60 (d,  $J = 8.5$  Hz, 2H), 7.35 – 7.39 (m, 4H), 7.20 – 7.30 (m, 6H), 5.19 (dd,  $J = 3.8, 2.0$  Hz, 1H), 3.89 (dd,  $J = 18.0, 2.0$  Hz, 1H), 3.75 (dd,  $J = 18.0, 3.8$  Hz, 1H);  $^{13}\text{C}$  NMR (125 MHz,  $\text{CDCl}_3$ )  $\delta$  153.5, 131.6, 129.2, 128.9, 128.4, 128.2, 127.8, 125.2, 124.5, 56.1, 49.4 ; HRMS (ESI): Calculated for  $[\text{M}+\text{H}]$   $\text{C}_{22}\text{H}_{17}\text{NOBrCl}$  425.0182, Found: 425.0166.

Resolution of enantiomers: CHIRALCEL AS-H, 5% IPA-Hexane, 1.0 mL/min, 254 nm, RT1 = 8.3 min, RT2 = 14.8 min;  $[\alpha]_D^{20} = +44.7$  (c 0.50, CHCl<sub>3</sub>)

**II-52-B**, (5S,6R)-2-(4-bromophenyl)-5-chloro-6-pentyl-5,6-dihydro-4H-1,3-oxazine

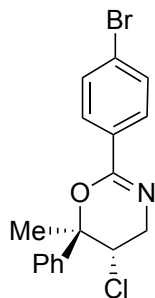


Colorless liquid;  $R_f$  : 0.63 (15% EtOAc- Hex) (UV, PMA)

<sup>1</sup>H NMR (500 MHz, CDCl<sub>3</sub>)  $\delta$  7.75 (d,  $J = 9.0$  Hz, 2H), 7.49 (d,  $J = 9.0$  Hz, 2H), 4.17 (dt,  $J = 8.5$ , 3.0 Hz, 1H), 3.91 – 3.97 (m, 2H), 3.62 (dd,  $J = 10.0$ , 18.5 Hz, 1H), 1.87 – 2.03 (m, 1H), 1.65 – 1.71 (m, 1H), 1.31 – 1.37 (m, 3H), 1.24 – 1.27 (m, 3H), 0.91 (t,  $J = 7.4$  Hz, 3H); <sup>13</sup>C NMR (125 MHz, CDCl<sub>3</sub>)  $\delta$  165.6, 133.6, 131.3, 128.8, 126.1, 125.6, 125.4, 78.7, 52.8, 50.6, 32.3, 31.5, 24.3, 22.5, 14.0; HRMS (ESI): Calculated for [M+H] C<sub>15</sub>H<sub>19</sub>NOBrCl 343.0339, Found: 343.0319.

Resolution of enantiomers: CHIRALCEL OD-H, 100% Hexane, 1 mL/min, RT1 = 52.1 min; RT2 = 62.2 min;  $[\alpha]_D^{20} = +33.9$  (c 0.50, CHCl<sub>3</sub>)

**II-55-B**, (5S,6R)-2-(4-bromophenyl)-5-chloro-6-methyl-6-phenyl-5,6-dihydro-4H-1,3-oxazine

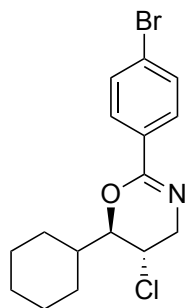


White solid; M.P.: 108 – 111 °C;  $R_f$  : 0.50 (15% EtOAc- Hex) (UV)

$^1\text{H}$  NMR (500 MHz,  $\text{CDCl}_3$ )  $\delta$  7.92 (d,  $J$  = 8.5 Hz, 2H), 7.54 (d,  $J$  = 8.5 Hz, 2H), 7.27 – 7.35 (m, 5H), 4.44 (t,  $J$  = 4.0 Hz, 1H), 3.72 (dd,  $J$  = 18.0, 4.0 Hz, 1H), 3.56 (dd,  $J$  = 18.0, 4.0 Hz, 1H), 1.78 (s, 3H);  $^{13}\text{C}$  NMR (125 MHz,  $\text{CDCl}_3$ )  $\delta$  153.6, 142.6, 131.9, 131.4, 128.9, 128.2, 125.6, 124.3, 80.7, 58.2, 49.2, 25.5 ; HRMS (ESI): Calculated for  $[\text{M}+\text{H}]$   $\text{C}_{17}\text{H}_{15}\text{NOBrCl}$  363.0026, Found: 363.0032.

Resolution of enantiomers: CHIRALCEL AS-H, 5% IPA-Hexane, 1 mL/min, RT1 = 5.9 min; RT2 = 11.5 min;  $[\alpha]_D^{20}$  = +86.8 (c 1.0,  $\text{CHCl}_3$ )

**II-58-B**, (5S,6R)-2-(4-bromophenyl)-5-chloro-6-cyclohexyl-5,6-dihydro-4H-1,3-oxazine



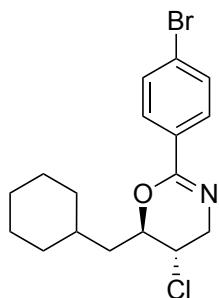
White solid;  $R_f$  : 0.33 (15% EtOAc- Hex) (UV, PMA)

$^1\text{H}$  NMR (500 MHz,  $\text{CDCl}_3$ )  $\delta$  7.75 (d,  $J$  = 8.5 Hz, 2H), 7.49 (d,  $J$  = 8.5 Hz, 2H), 4.12 – 4.17 (m, 1H), 4.02 (dd,  $J$  = 8.0, 4.0 Hz, 1H), 3.94 (dd,  $J$  = 16.5, 4.0 Hz, 1H), 3.63 (dd,  $J$  = 16.5, 8.0 Hz,

1H), 1.85 – 1.95 (m, 1H), 1.60 – 1.84 (m, 6H), 1.22 – 1.45 (m, 4H); <sup>13</sup>C NMR (150 MHz, CDCl<sub>3</sub>)  
δ 154.7, 131.9, 131.4, 128.8, 126.9, 125.4, 82.4, 50.5, 50.2, 38.5, 29.7, 29.5, 26.3, 26.2, 25.8,  
25.7; HRMS (ESI): Calculated for [M+H] C<sub>16</sub>H<sub>19</sub>NOBrCl 355.0339, Found: 355.0333.

Resolution of enantiomers: CHIRALCEL AS-H, 1% IPA-Hexane, 1 mL/min, RT1 = 5.5 min; RT2  
= 7.8 min; [α]<sub>D</sub><sup>20</sup> = +50.3 (c 0.50, CHCl<sub>3</sub>)

**II-59-B**, (5S,6R)-2-(4-bromophenyl)-5-chloro-6-(cyclohexylmethyl)-5,6-dihydro-4H-1,3-oxazine

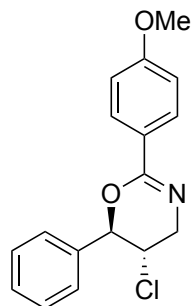


Colorless oil ; R<sub>f</sub> : 0.66 (20% EtOAc- Hex)

<sup>1</sup>H NMR (600 MHz, CDCl<sub>3</sub>) δ 7.74 (d, *J* = 8.4 Hz, 2H), 7.50 (d, *J* = 8.4 Hz, 2H), 4.26 – 4.30 (m,  
1H), 3.89 – 3.97 (m, 2H), 3.63 (dd, *J* = 16.8, 7.8 Hz, 1H), 1.81 – 1.86 (m, 2H), 1.61 – 1.74 (m,  
6H), 1.55 – 1.59 (m, 1H), 1.15 – 1.33 (m, 3H), 0.93 – 1.07 (m, 2H); <sup>13</sup>C NMR (125 MHz, CDCl<sub>3</sub>)  
δ 154.2, 131.9, 131.4, 128.8, 125.4, 76.7, 53.4, 50.3, 40.2, 34.1, 33.8, 32.4, 26.4, 26.2, 26.1;  
HRMS (ESI): Calculated for [M+H] C<sub>17</sub>H<sub>21</sub>NOBrCl 369.0495, Found: 369.0487.

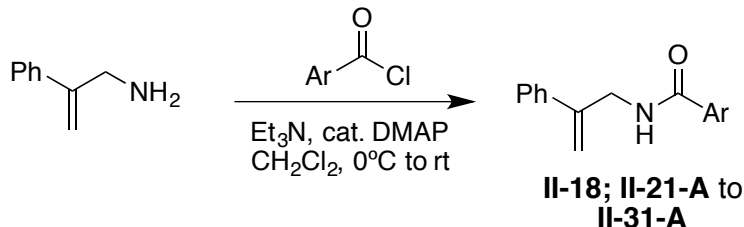
Resolution of enantiomers: CHIRALCEL OD-H, 100% Hexane, 1 mL/min, RT1 = 30.0 min; RT2  
= 48.5 min; [α]<sub>D</sub><sup>20</sup> = +69.9 (c 1.0, CHCl<sub>3</sub>)

**Procedure for gram scale synthesis of II-42-B :**



DCDPH (1.44 g, 4.49 mmol, 1.2 equiv.) was suspended in 93 mL trifluoroethanol (TFE) in a 500 mL round bottom flask equipped with a mechanical stirrer. The resulting suspension was cooled to -45 °C in an immersion cooler. (DHQD)<sub>2</sub>PHAL (29 mg dissolved in 2 mL MeNO<sub>2</sub>, 2 mol%) was then introduced (dissolution of the catalyst in MeNO<sub>2</sub> prior to addition is necessary to obtain consistent results as the catalyst is very sparingly soluble in TFE). After stirring vigorously for 45 min, the substrate (**II-42**) (1.0 g, 3.74 mmol, 1.0 equiv) was added in a single portion. The reaction was stirred for one hour. The reaction was quenched by the addition of 50 mL 10% aq. Na<sub>2</sub>SO<sub>3</sub> and diluted with 50 mL DCM. The organics were separated and the aqueous layer was extracted with DCM (3 x 15mL). The combined organics were dried over Na<sub>2</sub>SO<sub>4</sub> and concentrated in the presence of a small quantity of silica gel. Column chromatography (10% EtOAc - Hexanes) gave the desired product in 81% (0.92 g) yield as a white solid.

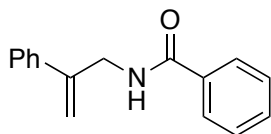
#### II.5.4. General procedure for the synthesis of substrates II-18 and II-21-A – II-31-A.



The following procedure for the synthesis of **II-18** (Ar = Ph) can be regarded a general protocol for the synthesis of substrates **II-21-A** to **II-31-A** as well.

A solution of 2-phenylprop-2-en-1-amine (1.20 g, 9.0 mmol, 1.0 equiv.), triethyl amine (1.04 mL, 18.0 mmol, 2.0 equiv.) and a catalytic amount of DMAP in DCM (50 mL) was cooled in an ice bath. To it was added benzoyl chloride (1.57 mL, 13.5 mmol, 1.5 equiv.) drop wise. After the addition was complete, the reaction was allowed to warm to RT. After 2 h, the reaction was diluted with an equal amount of water and extracted with DCM (3 x 25 mL). The combined organics were washed with brine (1 x 30 mL), dried over Na<sub>2</sub>SO<sub>4</sub> and concentrated under reduced pressure to give the product as a yellow solid. It was recrystallized from MeOH to obtain the pure product as a colorless solid in 1.85 g yield (87%) after collection of three crops of crystals. Compounds **II-21-A** to **II-31-A** were purified by column chromatography.

#### **II-18**, N-(2-phenylallyl)benzamide

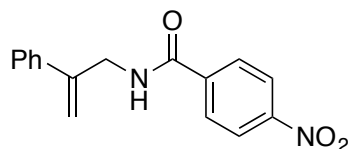


MP: 123 – 125 °C.; R<sub>f</sub> : 0.46 (30% EtOAc-Hexane)

<sup>1</sup>H NMR (600 MHz, CDCl<sub>3</sub>) δ 7.56 (d, *J* = 9.0 Hz, 2H), 7.52 (d, *J* = 9.0 Hz, 2H), 7.45 (d, *J* = 8.4 Hz, 2H), 7.32 (d, *J* = 8.4 Hz, 2H), 6.15 (br s, 1H), 5.49 (s, 1H), 5.31 (s, 1H), 4.48 (d, *J* = 5.4 Hz,

2H);  $^{13}\text{C}$  NMR (150 MHz,  $\text{CDCl}_3$ )  $\delta$  166.3, 143.2, 137.0, 133.0, 132.1, 131.9, 131.5, 128.5, 127.7, 114.9, 43.6; HRMS (ESI): Calculated for  $[\text{M}+\text{H}] \text{C}_{16}\text{H}_{15}\text{NO}$  237.1154, Found: 237.1154.

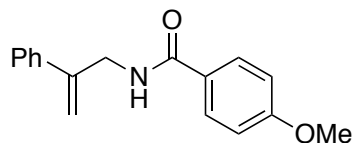
**II-23-A**, 4-nitro-N-(2-phenylallyl)benzamide



M.P.: 136 – 139 °C;  $R_f$  : 0.38 (30% EtOAc in hexanes)

$^1\text{H}$  NMR (600 MHz,  $\text{CDCl}_3$ )  $\delta$  7.55 (d,  $J$  = 8.4 Hz, 2H), 7.52 (d,  $J$  = 8.4 Hz, 2H), 7.38 (d,  $J$  = 9.0 Hz, 2H), 7.29 (d,  $J$  = 9.0 Hz, 2H), 6.14 (br s, 1H), 5.49 (d,  $J$  = 1.2 Hz, 1H), 5.30 (d,  $J$  = 0.6 Hz, 1H), 4.48 (dd,  $J$  = 6.0, 0.6 Hz, 2H);  $^{13}\text{C}$  NMR (150 MHz,  $\text{CDCl}_3$ )  $\delta$  166.3, 143.1, 136.5, 133.0, 131.9, 128.8, 128.5, 127.4, 114.8, 43.6; HRMS (ESI): Calculated for  $[\text{M}+\text{H}] \text{C}_{16}\text{H}_{15}\text{N}_2\text{O}_3$  282.1004, Found: 282.0998.

**II-22-A**, 4-methoxy-N-(2-phenylallyl)benzamide

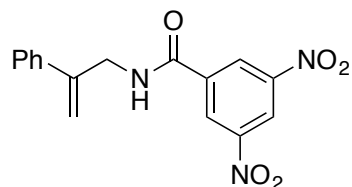


White solid.; MP.: 152 – 154 °C;  $R_f$  : 0.31 (30% EtOAc in hexanes)

$^1\text{H}$  NMR (500 MHz,  $\text{CDCl}_3$ )  $\delta$  7.75 (d,  $J$  = 8.5 Hz, 2H), 7.40 – 7.45 (m, 5H), 6.90 (d,  $J$  = 8.5 Hz, 2H), 5.49 (d,  $J$  = 1.2 Hz, 1H), 5.30 (d,  $J$  = 0.6 Hz, 1H), 4.48 (dd,  $J$  = 6.0, 0.6 Hz, 2H), 3.83 (s, 3H);  $^{13}\text{C}$  NMR (125 MHz,  $\text{CDCl}_3$ )  $\delta$  162.9, 162.3, 141.6, 134.8, 129.3, 128.6, 124.9, 119.7, 113.8,

87.5, 64.7, 55.4, 51.0; HRMS (ESI): Calculated for [M+H] C<sub>17</sub>H<sub>17</sub>NO<sub>2</sub> 267.1259, Found: 267.1253

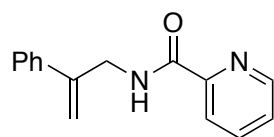
**II-26-A**, 3,5-dinitro-N-(2-phenylallyl)benzamide



R<sub>f</sub> : 0.50 (30% EtOAc in hexanes); Yellow gum

<sup>1</sup>H NMR (300 MHz, CDCl<sub>3</sub>) δ 9.10 (t, *J* = 2.1 Hz, 1H), 8.84 (d, *J* = 2.1 Hz, 2H), 7.43 – 7.44 (m, 2H), 7.30 – 7.39 (m, 3H), 6.40 (s br, 1H), 5.65 (s, 1H), 5.35 (s, 1H), 4.60 (d, *J* = 5.7 Hz, 2H); <sup>13</sup>C NMR (150 MHz, CDCl<sub>3</sub>): δ 162.6, 148.6, 143.3, 137.7, 137.6, 128.8, 128.5, 127.1, 126.0, 121.1, 115.2, 44.4 ; HRMS (ESI): Calculated for [M+H] C<sub>16</sub>H<sub>13</sub>N<sub>3</sub>O<sub>5</sub> 327.0855, Found: 327.0869.

**II-28-A**, N-(2-phenylallyl)picolinamide

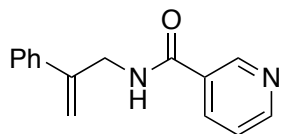


Brown oil ; R<sub>f</sub> : 0.38 (30% EtOAc in hexanes)

<sup>1</sup>H NMR (600 MHz, CDCl<sub>3</sub>) δ 8.48 – 8.49 (m, 1H), 8.21 (br s, 1H), 8.19 (d, *J* = 7.8 Hz, 2H), 7.80 (dt, *J* = 8.4, 1.8 Hz, 1H), 7.40 (d, *J* = 7.8 Hz, 2H), 7.36 – 7.38 (m, 1H), 7.31 – 7.34 (m, 2H), 7.26 (t, *J* = 7.2 Hz, 1H), 5.49 (s, 1H), 5.30 (s, 1H), 4.52 (dd, *J* = 6.0, 1.2 Hz, 2H); <sup>13</sup>C NMR (150 MHz,

CDCl<sub>3</sub>):  $\delta$  164.1, 149.7, 148.0, 144.1, 138.6, 137.3, 128.4, 127.9, 126.1, 126.0, 122.2, 113.6, 42.9 ; HRMS (ESI): Calculated for [M+H] C<sub>15</sub>H<sub>14</sub>N<sub>2</sub>O 238.1106, Found: 238.1105.

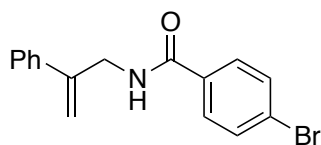
**II-29-A**, N-(2-phenylallyl)nicotinamide



Yellow-brown solid; MP: 125 – 128 °C

<sup>1</sup>H NMR (600 MHz, CDCl<sub>3</sub>)  $\delta$  8.85 (d, *J* = 1.8 Hz, 1H), 8.66 (dd, *J* = 4.8, 1.8 Hz, 1H), 8.03 (td, *J* = 7.8, 1.8 Hz, 1H), 7.60 – 7.64 (m, 1H), 7.43 – 7.45 (m, 2H), 7.27 – 7.35 (m, 3H), 6.34 (br s, 1H), 5.51 (s, 1H), 5.31 (s, 1H), 4.53 (6.0 Hz, 2H); <sup>13</sup>C NMR (125 MHz, CDCl<sub>3</sub>)  $\delta$  165.4, 152.2, 147.8, 143.9, 138.1, 135.1, 130.1, 128.7, 128.5, 128.5, 128.2, 126.1, 123.5, 114.4, 43.8 ; HRMS (ESI): Calculated for [M+H] C<sub>15</sub>H<sub>14</sub>N<sub>2</sub>O 238.1106, Found: 238.1105.

**II-30-A**, 4-bromo-N-(2-phenylallyl)benzamide



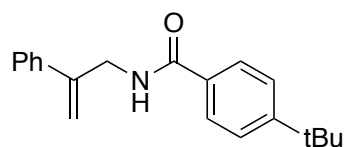
White solid

M.P.: 157 – 159 °C; R<sub>f</sub> : 0.54 (30% EtOAc in hexanes)

<sup>1</sup>H NMR (600 MHz, CDCl<sub>3</sub>)  $\delta$  7.55 (d, *J* = 9.0 Hz, 2H), 7.51 (d, *J* = 9.0 Hz, 2H), 7.44 (d, *J* = 7.5 Hz, 2H), 7.34 (t, *J* = 7.5 Hz, 2H), 7.27 – 7.30 (m, 1H), 6.13 (br s, 1H), 5.50 (s, 1H), 5.29 (s, 1H), 4.51 (d, *J* = 5.4 Hz, 2H); <sup>13</sup>C NMR (150 MHz, CDCl<sub>3</sub>)  $\delta$  166.4, 144.1, 138.2, 133.2, 131.8, 131.6,

128.6, 128.5, 128.2, 128.0, 126.2, 126.1, 114.3, 43.8; HRMS (ESI): Calculated for [M+H]  
C<sub>16</sub>H<sub>14</sub>NOBr 315.0259, Found: 315.0273.

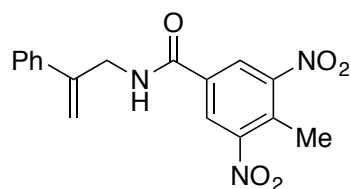
**II-25-A**, 4-*t*-butyl-N-(2-phenylallyl)benzamide



Yellowish solid; M.P.: 135 – 136 °C; R<sub>f</sub> : 0.40 (30% EtOAc in hexanes)

<sup>1</sup>H NMR (600 MHz, CDCl<sub>3</sub>) δ 7.63 (d, *J* = 8.4 Hz, 2H), 7.46 (d, *J* = 8.4 Hz, 2H), 7.40 (dd, *J* = 7.2, 2.0 Hz, 2H), 7.32 – 7.35 (m, 2H), 7.27 – 7.30 (m, 1H), 6.1 (br s, 1H), 5.49 (d, *J* = 0.6 Hz, 1H), 5.30 (d, *J* = 1.2 Hz, 1H), 4.52 (d, *J* = 6.0 Hz, 2H), 1.30 (s, 9H); <sup>13</sup>C NMR (150 MHz, CDCl<sub>3</sub>) δ 167.2, 155.0, 144.4, 138.3, 131.6, 128.6, 128.1, 126.7, 126.1, 125.5, 114.0, 43.7, 34.9, 31.1; HRMS (ESI): Calculated for [M+H] C<sub>20</sub>H<sub>23</sub>NO 293.1780, Found: 293.1772.

**II-27-A**, 4-methyl-3,5-dinitro-N-(2-phenylallyl)benzamide

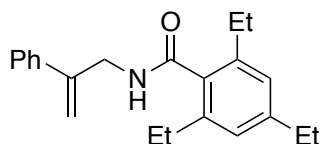


Yellow solid; M.P.: 113 – 115 °C; R<sub>f</sub> : 0.40 (30% EtOAc in hexanes)

<sup>1</sup>H NMR (600 MHz, CDCl<sub>3</sub>) δ 8.27 (s, 2H), 7.42 – 7.44 (m, 2H), 7.33 – 7.36 (m, 2H), 7.29 – 7.31 (m, 1H), 6.29 (br s, 1H), 5.54 (s, 1H), 5.32 (s, 1H), 4.54 (d, *J* = 6.0 Hz, 2H), 2.57 (s, 3H); <sup>13</sup>C

NMR (150 MHz, CDCl<sub>3</sub>) δ 162.6, 151.6, 143.4, 137.7, 134.2, 130.2, 128.8, 125.5, 126.0, 125.6, 115.1, 44.3, 15.1; HRMS (ESI): Calculated for [M+H] C<sub>17</sub>H<sub>15</sub>N<sub>3</sub>O<sub>5</sub> 341.0351, Found: 341.0346.

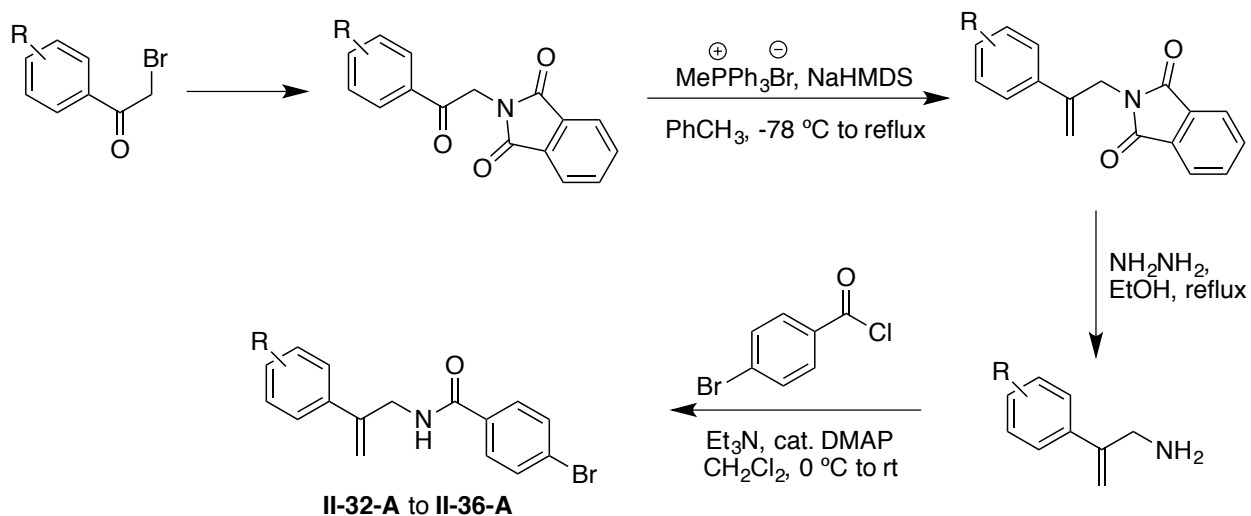
**II-24-A**, 2,4,6-triethyl-N-(2-phenylallyl)benzamide



White solid; M.P.: 74 – 76 °C; R<sub>f</sub> : 0.71 (30% EtOAc in hexanes)

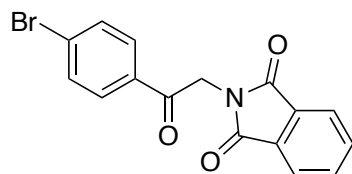
<sup>1</sup>H NMR (300 MHz, CDCl<sub>3</sub>) δ 7.48 (d, *J* = 4.8 Hz, 2H), 7.27 – 7.35 (m, 5H), 5.64 (br s, 1H), 5.46 (s, 1H), 5.31 (d, *J* = 1.2 Hz, 1H), 4.55 (d, *J* = 5.4 Hz, 2H), 2.55 (q, *J* = 7.2 Hz, 2H), 2.44 (q, *J* = 7.8 Hz, 4H), 1.17 (t, *J* = 7.2 Hz, 3H), 1.08 (t, *J* = 7.8 Hz, 6H); <sup>13</sup>C NMR (150 MHz, CDCl<sub>3</sub>) δ 170.1, 145.1, 144.5, 140.5, 138.2, 134.0, 128.5, 128.1, 126.3, 125.3, 115.0, 43.6, 28.7, 26.1, 26.1, 15.8, 15.5 ; HRMS (ESI): Calculated for [M+H] C<sub>22</sub>H<sub>27</sub>NO 321.2093, Found: 321.2101.

**II.5.5. General procedure for the synthesis of substrates for substrate scope evaluation.**



$\alpha$ -Phthalimido aryl ketones were synthesized from commercially available  $\alpha$ -bromo acetophenones by previously reported methods.<sup>30,31</sup>

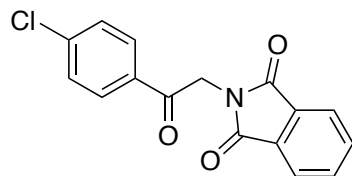
#### 1-phthalimido-2-(4-bromophenyl)-2-ethanone



M.P.: 229 – 233 °C

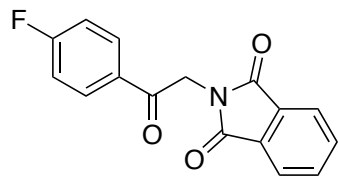
$^1\text{H}$  NMR (300 MHz,  $\text{CDCl}_3$ )  $\delta$  7.89 (dd,  $J = 5.4, 3.0$  Hz, 2H), 7.85 (d,  $J = 8.7$  Hz, 2H), 7.74 (dd,  $J = 5.4, 3.0$  Hz, 2H), 7.65 (d,  $J = 8.7$  Hz, 2H), 5.06 (s, 2H);  $^{13}\text{C}$  NMR (125 MHz,  $\text{CDCl}_3$ )  $\delta$  190.5, 168.2, 134.6, 133.5, 132.7, 132.6, 130.0, 129.8, 124.0, 44.5

#### 1-phthalimido-2-(4-chlorophenyl)-2-ethanone



$^1\text{H}$  NMR (500 MHz,  $\text{CDCl}_3$ )  $\delta$  7.93 (d,  $J = 8.5$  Hz, 2H), 7.88 (dd,  $J = 5.5, 3.0$  Hz, 2H), 7.74 (dd,  $J = 5.5, 3.0$  Hz, 2H), 7.48 (d,  $J = 8.5$  Hz, 2H), 5.07 (s, 2H);  $^{13}\text{C}$  NMR (125 MHz,  $\text{CDCl}_3$ )  $\delta$  189.9, 167.8, 140.6, 134.3, 134.2, 132.7, 132.2, 129.5, 129.3, 123.6, 44.1

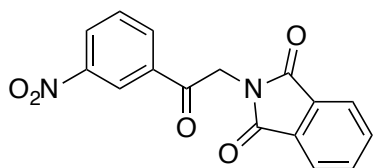
#### 1-phthalimido-2-(4-fluorophenyl)-2-ethanone



M.P.: 151 – 152 °C

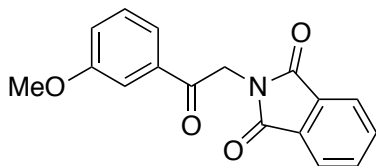
$^1\text{H}$  NMR (300 MHz,  $\text{CDCl}_3$ )  $\delta$  8.02-7.99 (m, 2H), 7.87-7.85 (m, 2H), 7.73-7.71 (m, 2H), 7.15 (t,  $J$  = 8.5 Hz, 2H), 5.07 (s, 2H);  $^{13}\text{C}$  NMR (125 MHz,  $\text{CDCl}_3$ )  $\delta$  189.9, 168.2, 134.6, 132.6, 131.2, 123.9, 116.7, 116.5, 116.4, 44.4; HRMS (ESI): Calculated for  $[\text{M}+\text{H}]$   $\text{C}_{16}\text{H}_{10}\text{FNO}_3$  : 283.0645; Found : 283.0639

1-phthalimido-2-(3-nitrophenyl)-2-ethanone



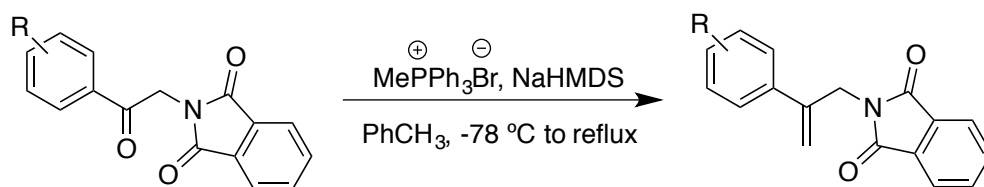
$^1\text{H}$  NMR (500 MHz,  $\text{CDCl}_3$ )  $\delta$  8.83 (t,  $J$  = 2.0 Hz, 1H), 8.49 (ddd,  $J$  = 8.5, 2.0, 1.0 Hz, 1H), 8.32 (ddd,  $J$  = 8.5, 1.0, 0.5 Hz, 1H), 7.90 (dd,  $J$  = 5.5, 3.0 Hz, 2H), 7.72 – 7.78 (m, 3H), 5.15 (s, 2H);  $^{13}\text{C}$  NMR (125 MHz,  $\text{CDCl}_3$ )  $\delta$  189.3, 167.6, 135.6, 134.3, 133.6, 132.1, 130.3, 128.3, 123.7, 123.1, 44.3

1-phthalimido-2-(3-methoxyphenyl)-2-ethanone



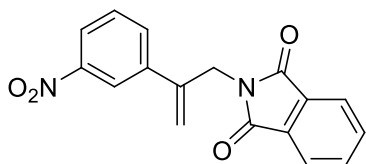
$^1\text{H}$  NMR (500 MHz,  $\text{CDCl}_3$ )  $\delta$  7.88 (dd,  $J = 5.5, 3.0$  Hz, 2H), 7.74 (dd,  $J = 5.5, 3.0$  Hz, 2H), 7.58 (td,  $J = 7.5, 1.5$  Hz, 1H), 7.49 (dd,  $J = 2.5, 1.5$  Hz, 1H), 7.41 (t,  $J = 7.5$  Hz, 1H), 7.15 (ddd,  $J = 7.5, 2.5, 1.5$  Hz, 1H), 5.09 (s, 2H), 3.84 (s, 3H);  $^{13}\text{C}$  NMR (125 MHz,  $\text{CDCl}_3$ )  $\delta$  190.9, 167.9, 160.0, 135.7, 134.1, 132.3, 129.9, 123.6, 120.6, 120.5, 112.4, 55.5, 44.3

### II.5.6. Wittig olefination of II: General procedure.



$\text{MeP}^+\text{Ph}_3\text{Br}^-$  (1.07g, 3 mmol, 1.5 equiv.) was suspended in 10 mL anhydrous toluene and cooled in an ice bath. NaHMDS (3 mL of 1.0 M solution in THF, 3 mmol, 1.5 equiv.) was added drop wise under  $\text{N}_2$  and the resulting yellow slurry was stirred for 0.5 h at  $0^\circ\text{C}$ . The reaction vessel was then cooled to  $-78^\circ\text{C}$  (dry ice- acetone) and the ketone (2 mmol, 1.0 equiv.) was added in a single portion under  $\text{N}_2$ . After a further 10 min. the cooling bath was removed and the reaction was allowed to warm to ambient temperature. A reflux condenser was attached and the reaction was refluxed (bath temp.  $\sim 120^\circ\text{C}$ ) for 24 -36 h (till reaction was complete by TLC). The reaction was poured into 100 mL water and extracted with EtOAc (3 x 25 mL). The combined organics were washed sequentially with water (1 x 20 mL) and brine (1 x 20 mL) and then dried over  $\text{Na}_2\text{SO}_4$  and concentrated *in vacuo* to give the crude products. Pure products were obtained after column chromatography on silica gel using EtOAc-Hexane gradient elution.

2-(3-nitrophenyl)-3-phthalimido-1-propene

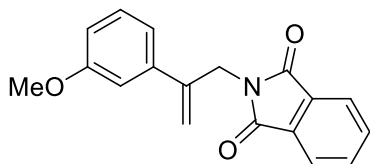


50% yield (white solid);  $R_f$  : 0.43 (30% EtOAc-Hex) (UV, PMA)

$^1\text{H}$  NMR (600 MHz,  $\text{CDCl}_3$ )  $\delta$  8.34 (t,  $J$  = 2.0 Hz, 2H), 8.12 (ddd,  $J$  = 8.4, 2.0, 1.0 Hz, 1H), 7.81 – 7.84 (m, 3H), 7.70 (dd,  $J$  = 5.4, 2.5 Hz, 2H), 5.56 (s, 1H), 5.34 (t,  $J$  = 1.5 Hz, 1H), 4.17 (t,  $J$  = 1.5 Hz, 2H);  $^{13}\text{C}$  NMR (150 MHz,  $\text{CDCl}_3$ )  $\delta$  167.8, 148.4, 140.7, 140.2, 134.2, 132.3, 131.8, 129.4, 123.5, 122.9, 121.5, 117.1, 41.1

HRMS (ESI): Calculated for  $[\text{M}+\text{H}] \text{C}_{17}\text{H}_{12}\text{N}_2\text{O}_4$  : 308.0797; Found : 308.0797

2-(3-methoxyphenyl)-3-phthalimido-1-propene

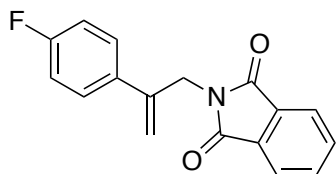


75% (84% brsm) yield (Yellowish solid);  $R_f$  : 0.19 (15% EtOAc- Hex)

$^1\text{H}$  NMR (500 MHz,  $\text{CDCl}_3$ )  $\delta$  7.82 (dd,  $J$  = 4.5, 3.0 Hz, 2H), 7.69 (dd,  $J$  = 4.5, 3.0 Hz, 2H), 7.21 (d,  $J$  = 7.5 Hz, 1H), 7.06 – 7.08 (m, 1H), 7.02 (t,  $J$  = 2.5 Hz, 1H), 6.80 – 6.83 (m, 1H), 5.43 (s, 1H), 5.15 (d,  $J$  = 1.5 Hz, 1H), 4.67 (t,  $J$  = 1.5 Hz, 2H), 3.80 (s, 3H);  $^{13}\text{C}$  NMR (125 MHz,  $\text{CDCl}_3$ )  $\delta$  167.9, 159.5, 142.3, 139.9, 134.0, 132.0, 129.4, 123.4, 118.9, 114.7, 114.2, 113.8, 111.9, 55.3, 41.5

HRMS (ESI): Calculated for  $[\text{M}+\text{H}] \text{C}_{18}\text{H}_{15}\text{NO}_3$  : 293.1052; Found : 293.1046

2-(4-fluorophenyl)-3-phthalimido-1-propene

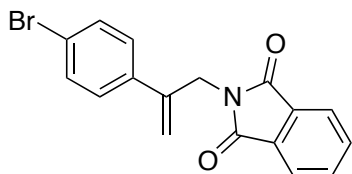


71% (82% brsm) yield (white solid);  $R_f$  : 0.52 (30% EtOAc-Hex) (UV, PMA); M.P.: 85 – 87 °C

$^1\text{H}$  NMR (600 MHz,  $\text{CDCl}_3$ )  $\delta$  7.82 (dd,  $J = 5.4, 3.0$  Hz, 2H), 7.69 (dd,  $J = 5.4, 3.0$  Hz, 2H), 7.44 (dd,  $^2J_{\text{H-H}} = 9.0$  Hz,  $^3J_{\text{H-F}} = 5.4$  Hz, 2H), 6.99 (dd,  $^2J_{\text{H-H}} = ^2J_{\text{H-F}} = 9.0$  Hz, 2H), 5.37 (s, 1H), 5.16 (t,  $J = 1.5$  Hz, 1H), 4.65 (t,  $J = 1.5$  Hz, 2H);  $^{13}\text{C}$  NMR (150 MHz,  $\text{CDCl}_3$ )  $\delta$  167.9, 162.6 (d,  $^1J_{\text{C-F}} = 245.6$  Hz), 141.6, 134.5 (d,  $^4J_{\text{C-F}} = 3.5$  Hz), 134.0, 131.9, 128.1 (d,  $^3J_{\text{C-F}} = 6.6$  Hz), 123.4, 115.2 (d,  $^2J_{\text{C-F}} = 21.1$  Hz), 114.3 (d,  $^5J_{\text{C-F}} = 1.1$  Hz), 41.5

HRMS (ESI): Calculated for  $[\text{M}+\text{H}] \text{C}_{17}\text{H}_{12}\text{NO}_2\text{F}$  :281.0852, Found: 281.0842

2-[2-(4-bromophenyl)allyl]isoindoline-1,3-dione

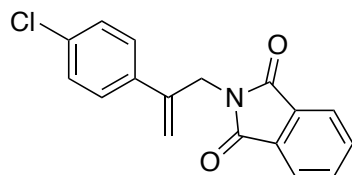


95% Yield (White solid);  $R_f$  : 0.32 (20% EtOAc in hexanes) (UV, PMA) ; M.P.: 125-128 °C

$^1\text{H}$  NMR (300 MHz,  $\text{CDCl}_3$ )  $\delta$  7.82 (dd,  $J = 5.7, 3.0$  Hz, 2H), 7.68 (dd,  $J = 5.7, 3.0$  Hz, 2H), 7.43 (d,  $J = 8.7$  Hz, 2H), 7.34 (d,  $J = 8.7$  Hz, 2H), 5.42 (s, 1H), 5.21 (d,  $J = 0.9$  Hz, 1H), 4.65 (t,  $J = 0.9$  Hz, 2H);  $^{13}\text{C}$  NMR (150 MHz,  $\text{CDCl}_3$ )  $\delta$  190.1, 167.8, 134.2, 133.1, 132.3, 132.2, 129.6, 129.4, 123.6, 44.0

HRMS (ESI): Calculated for [M+H] C<sub>17</sub>H<sub>12</sub>BrNO<sub>2</sub> : 341.0051; Found : 341.0047

2-(4-chlorophenyl)-3-phthalimido-1-propene

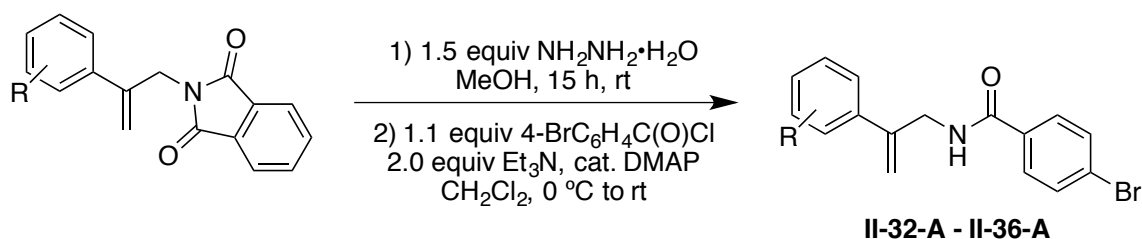


77% Yield (White solid); R<sub>f</sub> : 0.52 (30% EtOAc in hexanes) (UV, PMA); M.P.: 114-119 °C

<sup>1</sup>H NMR (300 MHz, CDCl<sub>3</sub>) δ 7.80 (dd, *J* = 5.5, 3.0 Hz, 2H), 7.67 (dd, *J* = 5.5, 3.0 Hz, 2H), 7.39 (d, *J* = 8.5 Hz, 2H), 7.26 (d, *J* = 8.5 Hz, 2H), 5.40 (s, 1H), 5.19 (s, 1H), 4.64 (s, 2H); <sup>13</sup>C NMR (125 MHz, CDCl<sub>3</sub>) δ 167.8, 141.5, 136.8, 134.0, 131.9, 128.5, 127.7, 123.3, 114.8, 41.3

HRMS (ESI): Calculated for [M+H] C<sub>17</sub>H<sub>12</sub>NO<sub>2</sub>Cl : 297.0557, Found: 297.0558

### II.5.7. General procedure for synthesis of substrates II-32-A to II-36-A.

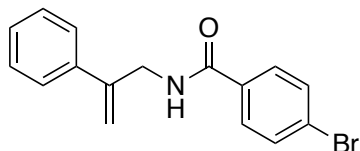


3-Phthalimido-2-aryl-1-propene (1 mmol, 1.0 equiv.) was dissolved in 5 mL MeOH. NH<sub>2</sub>NH<sub>2</sub>·H<sub>2</sub>O (98 mL, 1.5 mmol, 1.5 equiv.) was introduced into the reaction vessel and the resulting suspension was stirred overnight. The reaction was then diluted with 5 mL water and most of the MeOH was removed by rotary evaporation. Concentrated HCl (1mL) was added and the resulting suspension was stirred for a further 30 min at ambient temperature. The precipitated solids were filtered and the filter cake was washed with water (2 x 2 mL). The

combined filtrates were basified with solid NaOH and extracted with ether (3 x 5mL) and concentrated to give the crude 2-arylprop-2-en-1-amines which were used in the next reaction without any purification.

The made substrates were synthesized by reacting the crude amine from previous step with *p*BrBzCl using the same procedure described before for the synthesis of **II-18**. The pure products were obtained by column chromatography of the crude products using silica gel as the stationary phase and EtOAc in hexanes as the eluent.

**II-30-A**, 4-bromo-N-(2-phenylallyl)benzamide

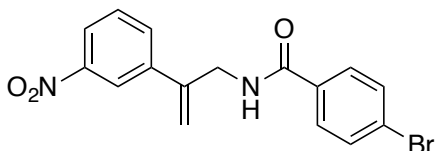


White solid; M.P. : 157 – 159 °C;  $R_f$  : 0.54 (30% EtOAc in hexanes)

$^1\text{H}$  NMR (600 MHz,  $\text{CDCl}_3$ )  $\delta$  7.55 (d,  $J = 9.0$  Hz, 2H), 7.51 (d,  $J = 9.0$  Hz, 2H), 7.44 (d,  $J = 7.5$  Hz, 2H), 7.34 (t,  $J = 7.5$  Hz, 2H), 7.27 – 7.30 (m, 1H), 6.13 (br s, 1H), 5.50 (s, 1H), 5.29 (s, 1H), 4.51 (d,  $J = 5.4$  Hz, 2H);  $^{13}\text{C}$  NMR (150 MHz,  $\text{CDCl}_3$ )  $\delta$  166.4, 144.1, 138.2, 133.2, 131.8, 131.6, 128.6, 128.5, 128.2, 128.0, 126.2, 126.1, 114.3, 43.8

HRMS (ESI): Calculated for  $[\text{M}+\text{H}]$   $\text{C}_{16}\text{H}_{14}\text{NOBr}$  315.0259, Found: 315.0273.

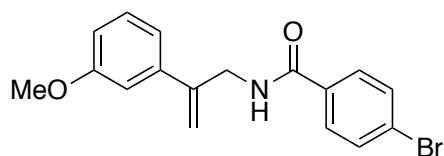
**II-32-A**, 4-bromo-N-[2-(3-nitrophenyl)allyl]benzamide



Brown solid; M.P.: 124 -125 °C;  $R_f$  : 0.33 (30% EtOAc in hexanes) (UV,  $\text{I}_2$ , anisaldehyde)

$^1\text{H}$  NMR (600 MHz,  $\text{CDCl}_3$ )  $\delta$  8.32 (t,  $J = 2.4$  Hz, 1H), 8.12 – 8.14 (m, 1H), 7.77 – 7.79 (m, 1H), 7.58 (d,  $J = 8.4$  Hz, 2H), 7.53 (d,  $J = 8.4$  Hz, 2H), 7.50 (d,  $J = 7.8$  Hz, 1H), 6.23 (br s, 1H), 5.62 (s, 1H), 5.45 (t,  $J = 1.4$  Hz, 1H), 4.54 (d,  $J = 5.4$  Hz, 2H);  $^{13}\text{C}$  NMR (150 MHz,  $\text{CDCl}_3$ )  $\delta$  166.4, 142.5, 140.0, 132.8, 132.0, 131.9, 129.6, 128.5, 126.5, 122.9, 121.1, 116.6, 43.4  
HRMS (ESI): Calculated for  $[\text{M}+\text{H}]$   $\text{C}_{16}\text{H}_{13}\text{N}_2\text{O}_3\text{Br}$  360.0110, Found: 360.0127.

**II-33-A**, 4-bromo-N-[2-(3-methoxyphenyl)allyl]benzamide

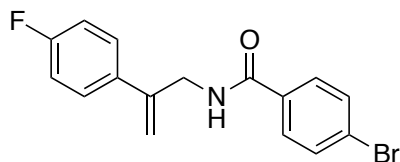


$R_f$  : 0.21 (30% EtOAc- Hex) (UV,  $\text{I}_2$ , anisaldehyde)

$^1\text{H}$  NMR (500 MHz,  $\text{CDCl}_3$ )  $\delta$  7.54 (d,  $J = 8.5$  Hz, 2H), 7.50 (d,  $J = 8.5$  Hz, 2H), 7.25 (t,  $J = 8.0$  Hz, 1H), 7.02 (qd,  $J = 7.5, 1.0$  Hz, 1H), 6.98 (t,  $J = 2.0$  Hz, 1H), 6.84 (ddd,  $J = 7.5, 2.5, 1.0$  Hz, 1H), 6.16 (br s, 1H), 5.49 (d,  $J = 0.5$  Hz, 1H), 5.28 (d,  $J = 1.0$  Hz, 1H), 4.48 (d, 6.0 Hz, 2H), 3.79 (s, 3H);  $^{13}\text{C}$  NMR (125 MHz,  $\text{CDCl}_3$ )  $\delta$  166.3, 159.8, 144.0, 139.7, 133.2, 131.8, 129.6, 128.5, 126.2, 118.5, 114.5, 113.7, 111.9, 55.3, 43.9

HRMS (ESI): Calculated for  $[\text{M}+\text{H}]$   $\text{C}_{17}\text{H}_{16}\text{NO}_2\text{Br}$  345.0365, Found: 345.0352.

**II-34-A**, 4-bromo-N-[2-(4-fluorophenyl)allyl]benzamide

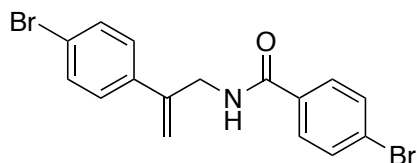


White solid; M.P.: 155 – 157  $^\circ\text{C}$ ;  $R_f$  : 0.50 (30% EtOAc in hexanes) (UV,  $\text{I}_2$ , anisaldehyde)

$^1\text{H}$  NMR (600 MHz,  $\text{CDCl}_3$ )  $\delta$  7.55 (d,  $J = 8.4$  Hz, 2H), 7.52 (d,  $J = 8.4$  Hz, 2), 7.42 (dd,  $J_{\text{H-H}} = 8.4$  Hz,  $^4J_{\text{H-F}} = 5.4$  Hz, 2H), 7.02 (t,  $J_{\text{H-H}} = ^4J_{\text{H-F}} = 8.4$  Hz, 2H), 6.10 (br s, 1H), 5.44 (s, 1H), 5.27 (s, 1H), 4.48 (d,  $J = 5.4$  Hz, 2H);  $^{13}\text{C}$  NMR (150 MHz,  $\text{CDCl}_3$ )  $\delta$  162.7 (d,  $^1J_{\text{C-F}} = 246.6$  Hz), 163.5, 143.2, 134.2 (d,  $^4J_{\text{C-F}} = 3.5$  Hz), 133.1, 128.5, 127.8 (d,  $^3J_{\text{C-F}} = 8.0$  Hz), 126.3, 115.5 (d,  $^2J_{\text{C-F}} = 21.3$  Hz), 114.2, 43.8

HRMS (ESI): Calculated for  $[\text{M}+\text{H}] \text{C}_{16}\text{H}_{13}\text{NOBrF}$  333.0165, Found: 333.0154.

**II-35-A**, 4-bromo-N-[2-(4-bromophenyl)allyl]benzamide

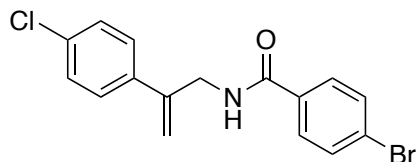


Yellowish solid; M.P.: 152 – 154 °C;  $R_f$ : 0.50 (30% EtOAc in hexanes) (UV,  $I_2$ , anisaldehyde)

$^1\text{H}$  NMR (600 MHz,  $\text{CDCl}_3$ )  $\delta$  7.56 (d,  $J = 9.0$  Hz, 2H), 7.52 (d,  $J = 9.0$  Hz, 2H), 7.45 (d,  $J = 8.4$  Hz, 2H), 7.32 (d,  $J = 8.4$  Hz, 2H), 6.15 (br s, 1H), 5.49 (s, 1H), 5.31 (s, 1H), 4.48 (d,  $J = 5.4$  Hz, 2H);  $^{13}\text{C}$  NMR (150 MHz,  $\text{CDCl}_3$ )  $\delta$  166.3, 143.2, 137.0, 133.0, 132.1, 131.9, 131.5, 128.5, 127.7, 114.9, 43.6

HRMS (ESI): Calculated for  $[\text{M}+\text{H}] \text{C}_{16}\text{H}_{13}\text{NOBr}_2$  392.9364, Found: 392.9376.

**II-36-A**, 4-bromo-N-[2-(4-chlorophenyl)allyl]benzamide

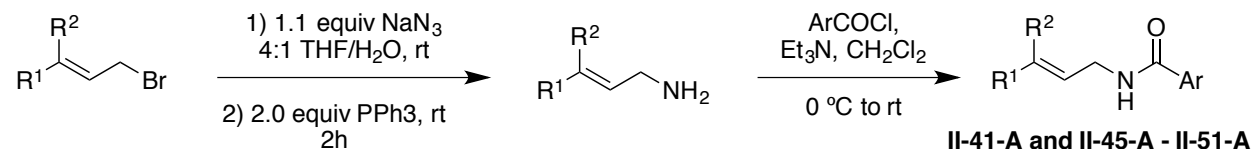


White solid; M.P.: 152 – 154 °C;  $R_f$  : 0.50 (30% EtOAc in hexanes) (UV,  $I_2$ , anisaldehyde)

$^1\text{H}$  NMR (600 MHz,  $\text{CDCl}_3$ ) d 7.55 (d,  $J$  = 8.4 Hz, 2H), 7.52 (d,  $J$  = 8.4 Hz, 2H), 7.38 (d,  $J$  = 9.0 Hz, 2H), 7.29 (d,  $J$  = 9.0 Hz, 2H), 6.14 (br s, 1H), 5.49 (d,  $J$  = 1.2 Hz, 1H), 5.30 (d,  $J$  = 0.6 Hz, 1H), 4.48 (dd,  $J$  = 6.0, 0.6 Hz, 2H);  $^{13}\text{C}$  NMR (150 MHz,  $\text{CDCl}_3$ ) d 166.3, 143.1, 136.5, 133.0, 131.9, 128.8, 128.5, 127.4, 114.8, 43.6

HRMS (ESI): Calculated for  $[\text{M}+\text{H}]$   $\text{C}_{16}\text{H}_{13}\text{NOBrCl}$  348.9869, Found: 348.9865

### II.5.8. General procedure for synthesis of substrates II-41-A and II-45-A – II-51-A.

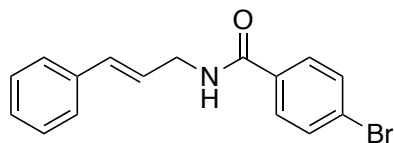


The  $\text{PBr}_3$  bromination of the allylic alcohols gave the corresponding allyl bromides which were used without purification in the subsequent one pot azide displacement – Staudinger reduction sequence.

Allyl bromide (1.0 equiv.) dissolved in THF- $\text{H}_2\text{O}$  (4:1) (5 mL/mmol) was treated with 1.1 equivalents of  $\text{NaN}_3$  at rt. After TLC analysis revealed the complete consumption of starting material (~ 20 min.), 2.0 equivalents of  $\text{PPh}_3$  was added to the reaction vessel. After 2 h at ambient temperature, the reaction was concentrated to remove most of the THF. The resulting suspension was diluted with aq. HCl and extracted with ether (3x). The aqueous layer was then basified by adding solid KOH and extracted with ether (3x). The combined organics were dried ( $\text{Na}_2\text{SO}_4$ ) and concentrated to give the crude amine which was used in the next step. Typical yield over three steps was 55 – 60%.

The crude amines from the previous step were reacted with the appropriate acid chlorides using the same protocol as described for the synthesis of II-18.

**II-41-A**, N-cinnamyl-4-bromobenzamide

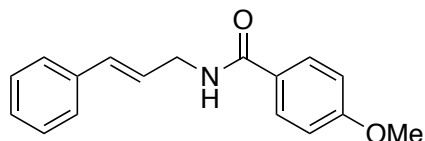


White solid; M.P.: 148 – 150 °C;  $R_f$  : 0.50 (30% EtOAc in hexanes)

$^1\text{H}$  NMR (300 MHz,  $\text{CDCl}_3$ )  $\delta$  7.66 (d,  $J = 9.0$  Hz, 2H), 7.56 (d,  $J = 9.0$  Hz, 2H), 7.21 – 7.38 (m, 5H), 6.59 (d,  $J = 15.9$  Hz, 1H), 6.27 (td,  $J = 15.9, 3.3$  Hz, 1H), 6.18 (br s, 1H), 4.22 (dt,  $J = 4.8, 1.5$  Hz, 2H);  $^{13}\text{C}$  NMR (150 MHz,  $\text{CDCl}_3$ )  $\delta$  166.3, 136.3, 133.2, 132.8, 131.8, 128.6, 128.5, 127.9, 126.4, 126.2, 125.1, 42.2

HRMS (ESI): Calculated for  $[\text{M}+\text{H}] \text{C}_{16}\text{H}_{14}\text{NOBr}$  315.0259, Found: 315.0241.

**II-42-A**, N-cinnamyl-4-methoxybenzamide

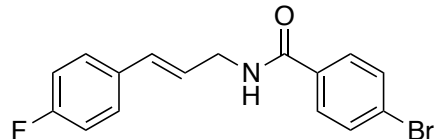


White solid; M.P.: 131 – 132 °C;  $R_f$  : 0.31 (20% EtOAc- Hex)

$^1\text{H}$  NMR (500 MHz,  $\text{CDCl}_3$ )  $\delta$  7.75 (d,  $J = 9.0$  Hz, 2H), 7.35 (d, 7.0 Hz, 2H), 7.29 (t,  $J = 7.0$  Hz, 2H), 7.20 – 7.24 (m, 1H), 6.91 (d,  $J = 9.0$  Hz, 2H), 6.57 (d,  $J = 16.0$  Hz, 1H), 6.27 (td,  $J = 16.0, 6.0$  Hz, 1H), 6.17 (br s, 1H), 4.22 (t,  $J = 6.0$  Hz, 2H), 3.83 (s, 3H);  $^{13}\text{C}$  NMR (150 MHz,  $\text{CDCl}_3$ )  $\delta$  166.8, 162.2, 136.5, 132.4, 128.7, 128.6, 127.7, 126.7, 126.4, 125.7, 113.8, 55.4, 42.1

HRMS (ESI): Calculated for  $[\text{M}+\text{H}] \text{C}_{17}\text{H}_{17}\text{NO}_2$ : 267.1259, Found: 267.1263

**II-46-A, (E)-4-bromo-N-[3-(4-fluorophenyl)allyl]benzamide**

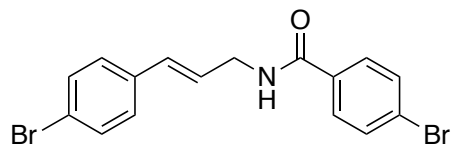


Yellowish solid; M.P.: 164 – 165 °C;  $R_f$  : 0.42 (30% EtOAc in hexanes)

$^1\text{H}$  NMR (300 MHz,  $\text{CDCl}_3$ )  $\delta$  7.65 (d,  $J = 8.7$  Hz, 2H), 7.56 (d,  $J = 8.7$  Hz, 2H), 7.32 (dd,  $J_{\text{H-H}} = 8.7$  Hz,  $^4J_{\text{H-F}} = 5.4$  Hz, 2H), 6.99 (t,  $^2J_{\text{H-H}} = ^3J_{\text{H-F}} = 8.7$  Hz), 6.54 (d,  $J = 15.3$  Hz, 1), 6.13 – 6.23 (m, 2H), 4.21 (dt,  $J = 6.0, 1.5$  Hz, 2H);  $^{13}\text{C}$  NMR (150 MHz,  $\text{CDCl}_3$ )  $\delta$  166.1, 162.2 (d,  $^1J_{\text{C-F}} = 245.6$  Hz), 133.0, 132.3 (d,  $^4J_{\text{C-F}} = 3.5$  Hz), 131.7, 131.4, 128.3, 127.7 (d,  $^3J_{\text{C-F}} = 8.5$  Hz), 126.1, 124.6 (d,  $^5J_{\text{C-F}} = 2.2$  Hz), 115.4 (d,  $^2J_{\text{C-F}} = 21.8$  Hz), 41.9

HRMS (ESI): Calculated for  $[\text{M}+\text{H}] \text{C}_{16}\text{H}_{13}\text{NOBrF}$  333.0165, Found: 333.0169.

**II-47-A, (E)-4-bromo-N-[3-(4-bromophenyl)allyl]benzamide**

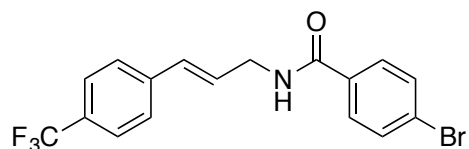


M.P.: 170 – 173 °C;  $R_f$  : 0.42 (30% EtOAc in hexanes)

$^1\text{H}$  NMR (600 MHz,  $\text{CDCl}_3$ )  $\delta$  7.65 (d,  $J = 8.4$  Hz, 2H), 7.56 (d,  $J = 8.4$  Hz, 2H), 7.41 (d,  $J = 8.4$  Hz, 2H), 7.21 (d,  $J = 8.4$  Hz, 2H), 6.50 (d,  $J = 16.2$  Hz, 1H), 6.25 (td,  $J = 16.2, 6.6$  Hz, 1H), 6.20 (br s, 1H), 4.21 (dt,  $J = 6.6, 1.2$  Hz, 2H);  $^{13}\text{C}$  NMR (150 MHz,  $\text{CDCl}_3$ )  $\delta$  166.3, 135.3, 133.1, 131.9, 131.8, 131.5, 128.5, 127.9, 126.3, 126.0, 121.7, 42.1

HRMS (ESI): Calculated for  $[\text{M}+\text{H}] \text{C}_{16}\text{H}_{13}\text{NOBr}_2$  392.9364, Found: 392.9369.

**II-50-A, (E)-4-bromo-N-(3-[4-(trifluoromethyl)phenyl]allyl)benzamide**

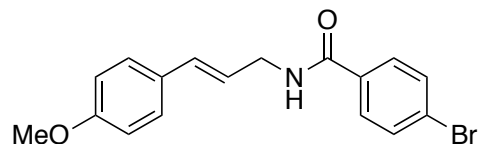


M.P.: 156 – 158 °C;  $R_f$  : 0.38 (30% EtOAc in hexanes)

$^1\text{H}$  NMR (600 MHz,  $\text{CDCl}_3$ )  $\delta$  7.66 (d,  $J$  = 8.4 Hz, 2H), 7.56 (d,  $J$  = 8.4 Hz, 2H), 7.54 (d,  $J$  = 8.4 Hz, 2H), 7.43 (d,  $J$  = 8.4 Hz, 2H), 6.59 (d,  $J$  = 15.6 Hz, 1H), 6.36 (td,  $J$  = 15.6, 6.6 Hz, 1H), 6.32 (br s, 1H), 4.25 (t,  $J$  = 6.0 Hz, 2H);  $^{13}\text{C}$  NMR (75 MHz,  $\text{CDCl}_3$ )  $\delta$  166.4, 139.8, 133.0, 131.9, 131.6, 131.1, 129.6 (q,  $^2J_{\text{C-F}}$  = 32.7 Hz), 128.6, 128.5, 128.0, 126.4, 125.5 (q,  $^3J_{\text{C-F}}$  = 4.1 Hz), 42.0

HRMS (ESI): Calculated for  $[\text{M}+\text{H}]$   $\text{C}_{17}\text{H}_{13}\text{NOF}_3\text{Br}$  383.0133, Found: 383.0139.

**II-48-A, (E)-4-bromo-N-[3-(4-methoxyphenyl)allyl]benzamide**

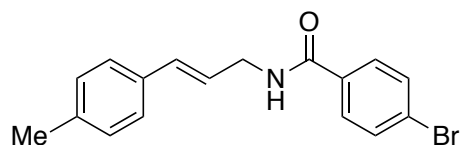


M.P.: 156 – 158 °C;  $R_f$  : 0.38 (30% EtOAc in hexanes)

$^1\text{H}$  NMR (600 MHz,  $\text{CDCl}_3$ )  $\delta$  7.64 (d,  $J$  = 9.0 Hz, 2H), 7.54 (d,  $J$  = 9.0 Hz, 2H), 7.27 (d,  $J$  = 8.4 Hz, 2H), 6.83 (d,  $J$  = 8.4 Hz, 2H), 6.51 (d,  $J$  = 16.2 Hz, 1H), 6.30 (br s, 1H), 6.10 (td,  $J$  = 16.2, 6.6 Hz, 1H), 4.17 (d,  $J$  = 6.4 Hz, 2H), 3.78 (s, 3H);  $^{13}\text{C}$  NMR (150 MHz,  $\text{CDCl}_3$ )  $\delta$  166.3, 159.4, 133.3, 132.4, 131.8, 129.1, 128.6, 127.6, 126.1, 122.7, 114.0, 55.3, 42.3

HRMS (ESI): Calculated for  $[\text{M}+\text{H}]$   $\text{C}_{17}\text{H}_{16}\text{NO}_2\text{Br}$  345.0364, Found: 345.0382.

**II-49-A, (E)-4-bromo-N-(3-p-tolylallyl)benzamide**

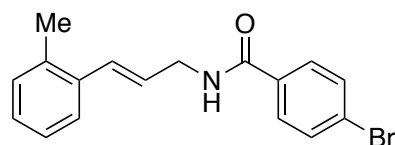


M.P.: 136 – 138 °C;  $R_f$  : 0.47 (30% EtOAc in hexanes)

$^1\text{H}$  NMR (500 MHz,  $\text{CDCl}_3$ )  $\delta$  7.65 (d,  $J = 8.5$  Hz, 2H), 7.54 (d,  $J = 8.5$  Hz, 2H), 7.23 (d,  $J = 7.5$  Hz, 2H), 7.10 (d,  $J = 7.5$  Hz, 2H), 6.53 (d,  $J = 16.0$  Hz, 1H), 6.27 (br s, 1H), 6.19 (td,  $J = 16.0$ , 6.0 Hz, 1H), 4.19 (dt,  $J = 6.0$ , 1.5 Hz, 2H), 2.31 (s, 3H);  $^{13}\text{C}$  NMR (125 MHz,  $\text{CDCl}_3$ )  $\delta$  166.3, 137.7, 133.6, 133.3, 132.7, 131.8, 129.3, 128.6, 126.3, 126.2, 124.0, 42.3, 21.2

HRMS (ESI): Calculated for  $[\text{M}+\text{H}] \text{C}_{17}\text{H}_{16}\text{NOBr}$  329.0415, Found: 329.0414

**(E)-4-bromo-N-(3-o-tolylallyl)benzamide**

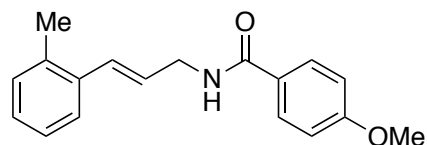


M.P.: 130 – 132 °C;  $R_f$  : 0.50 (30% EtOAc in hexanes)

$^1\text{H}$  NMR (600 MHz,  $\text{CDCl}_3$ )  $\delta$  7.65 (d,  $J = 9.0$  Hz, 2H), 7.56 (d,  $J = 9.0$  Hz, 2H), 7.40 – 7.42 (m, 1H), 7.11 – 7.15 (m, 3H), 6.81 (d,  $J = 15.6$  Hz, 1H), 6.19 (br s, 1H), 6.14 (td,  $J = 15.6$ , 6.0 Hz, 1H), 4.24 (t,  $J = 6.0$  Hz, 2H), 2.33 (s, 3H);  $^{13}\text{C}$  NMR (150 MHz,  $\text{CDCl}_3$ )  $\delta$  166.3, 135.4, 135.3, 133.3, 131.8, 130.8, 130.3, 128.5, 127.8, 126.3, 126.2, 126.1, 125.7, 42.5, 19.8

HRMS (ESI): Calculated for  $[\text{M}+\text{H}] \text{C}_{17}\text{H}_{16}\text{NOBr}$  329.0415, Found: 329.0399.

**II-45-A, (E)-4-methoxy-N-(3-o-tolylallyl)benzamide**



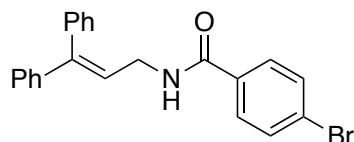
M.P.: 145-148 °C;  $R_f$  : 0.50 (30% EtOAc in hexanes)

$^1\text{H}$  NMR (600 MHz,  $\text{CDCl}_3$ )  $\delta$  7.75 (d,  $J = 8.5$  Hz, 2H), 7.40 – 7.42 (m, 1H), 7.11 – 7.14 (m, 3H), 6.91 (d,  $J = 8.5$  Hz, 2H), 6.79 (d,  $J = 15.6$  Hz, 1H), 6.17 (br s, overlapped with olefin proton), 6.15 (td,  $J = 15.6, 6.6$  Hz, 1H), 4.24 (dt,  $J = 6.6, 1.2$  Hz, 2H), 3.83 (s, 3H), 2.32 (s, 3H);  $^{13}\text{C}$

NMR (150 MHz,  $\text{CDCl}_3$ )  
 $\delta$  166.8, 162.2, 135.6, 135.4, 130.3, 130.3, 128.7, 127.6, 126.9, 126.8, 126.1, 125.7, 113.8, 55.4, 42.4, 19.8

HRMS (ESI): Calculated for  $[\text{M}+\text{H}] \text{C}_{18}\text{H}_{19}\text{NO}_2$  : 281.1416, Found: 281.1417

**II-51-A, 4-bromo-N-(3,3-diphenylallyl)benzamide**

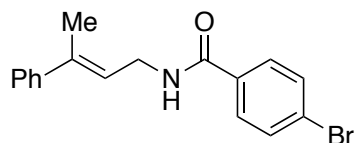


M.P.: 191 – 192 °C;  $R_f$  : 0.63 (30% EtOAc in hexanes)

$^1\text{H}$  NMR (300 MHz,  $\text{CDCl}_3$ )  $\delta$  7.59 (d,  $J = 9.0$  Hz, 2H), 7.53 (d,  $J = 9.0$  Hz, 2H), 7.31 – 7.41 (m, 3H), 7.18 – 7.30 (m, 7H), 6.16 (t,  $J = 6.9$  Hz, 1H), 6.09 (br s, 1H), 4.13 (dd,  $J = 6.9, 5.4$  Hz, 2H);  $^{13}\text{C}$  NMR (125 MHz,  $\text{CDCl}_3$ )  $\delta$  166.2, 145.1, 141.5, 138.9, 133.3, 131.8, 129.6, 128.5, 128.5, 128.2, 127.7, 127.4, 126.1, 124.0, 39.5

HRMS (ESI): Calculated for  $[\text{M}+\text{H}] \text{C}_{22}\text{H}_{18}\text{NOBr}$  391.0572, Found: 391.0576.

**II-55-A**, (E)-4-bromo-N-(3-phenylbut-2-enyl)benzamide

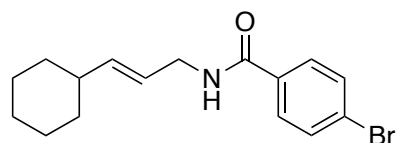


M.P.: 129 – 130 °C;  $R_f$  : 0.54 (30% EtOAc in hexanes)

$^1\text{H}$  NMR (500 MHz,  $\text{CDCl}_3$ )  $\delta$  7.66 (d,  $J = 8.5$  Hz, 2H), 7.55 (d,  $J = 8.5$  Hz, 2H), 7.38 – 7.40 (m, 2H), 7.31 – 7.35 (m, 2H), 7.26 – 7.29 (m, 1H), 6.45 (br s), 5.85 (dt,  $J = 7.0, 1.0$  Hz, 1H), 4.25 (t,  $J = 7.0$  Hz, 2H), 2.13 (d,  $J = 1.0$  Hz, 3H);  $^{13}\text{C}$  NMR (125 MHz,  $\text{CDCl}_3$ )  $\delta$  166.5, 142.6, 138.9, 133.3, 131.7, 128.6, 128.3, 127.3, 126.1, 125.7, 122.9, 38.7, 16.1

HRMS (ESI): Calculated for  $[\text{M}+\text{H}]$   $\text{C}_{17}\text{H}_{16}\text{NOBr}$  329.0415, Found: 329.0403.

**II-58-A**, (E)-4-bromo-N-(3-cyclohexylallyl)benzamide

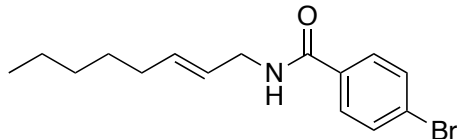


M.P.: 108 – 112 °C;  $R_f$  : 0.54 (30% EtOAc in hexanes)

$^1\text{H}$  NMR (500 MHz,  $\text{CDCl}_3$ )  $\delta$  7.62 (d,  $J = 9.0$  Hz, 2H), 7.54 (d,  $J = 9.0$  Hz, 2H), 6.03 (br s, 1H), 5.62 (dd,  $J = 15.5, 6.5$  Hz, 1H), 5.43 – 5.49 (m, 1H), 3.98 (t,  $J = 6.5$  Hz, 2H), 1.94 (m, 1H), 1.61 – 1.71 (m, 5H), 1.10 – 1.28 (m, 5H);  $^{13}\text{C}$  NMR (125 MHz,  $\text{CDCl}_3$ )  $\delta$  166.1, 140.3, 133.5, 131.8, 128.5, 126.0, 122.8, 42.2, 40.4, 32.8, 26.1, 26.0

HRMS (ESI): Calculated for  $[\text{M}+\text{H}]$   $\text{C}_{16}\text{H}_{20}\text{NOBr}$  321.0728, Found: 321.0726.

**II-52-A, (E)-4-bromo-N-(oct-2-enyl)benzamide**

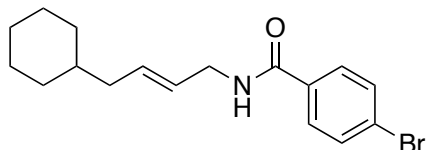


M.P.: 75 – 76 °C;  $R_f$  : 0.54 (30% EtOAc in hexanes)

$^1\text{H}$  NMR (500 MHz,  $\text{CDCl}_3$ )  $\delta$  7.61 (d,  $J = 8.5$  Hz, 2H), 7.50 (d,  $J = 8.5$  Hz, 2H), 6.34 (br s, 1H), 5.62 – 5.67 (m, 1H), 5.45 – 5.51 (m, 1H), 3.95 (dt,  $J = 6.0, 1.0$  Hz, 2H), 1.96 – 2.00 (m, 2H), 1.21 – 1.36 (m, 6H), 0.85 (t,  $J = 7.0$  Hz, 3H);  $^{13}\text{C}$  NMR (125 MHz,  $\text{CDCl}_3$ )  $\delta$  166.2, 134.4, 133.4, 131.7, 128.5, 125.9, 125.1, 42.1, 32.2, 31.3, 28.7, 22.4, 13.9

HRMS (ESI): Calculated for  $[\text{M}+\text{H}]$   $\text{C}_{15}\text{H}_{20}\text{NOBr}$  309.0728, Found: 309.0735.

**II-59-A, (E)-4-bromo-N-(4-cyclohexylbut-2-enyl)benzamide**

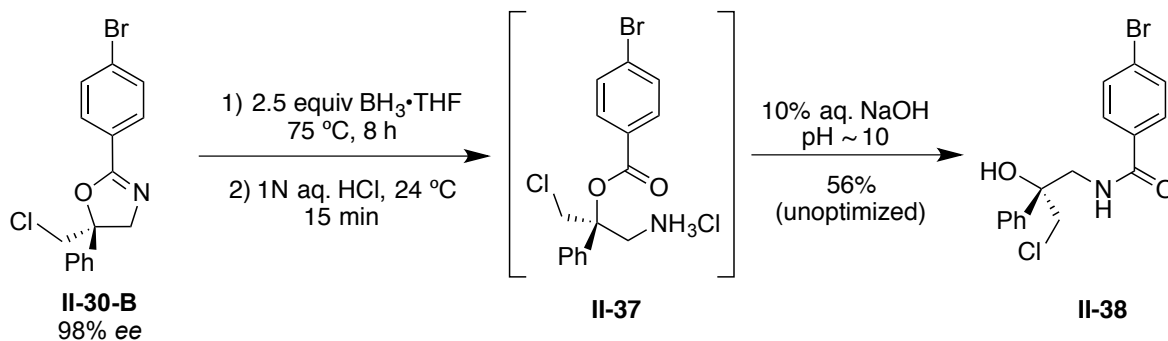


Waxy solid;  $R_f$  : 0.45 (20% EtOAc- Hex)

$^1\text{H}$  NMR (500 MHz,  $\text{CDCl}_3$ )  $\delta$  7.62 (d,  $J = 8.5$  Hz, 2H), 7.54 (d,  $J = 8.5$  Hz, 2H), 6.02 (br s, 1H), 5.63 – 5.69 (m, 1H), 5.46 – 5.52 (m, 1H), 3.99 (dt,  $J = 6.0, 1.0$  Hz, 2H), 1.92 (t,  $J = 6.5$  Hz, 2H), 1.61 – 1.68 (m, 5H), 1.07 – 1.32 (m, 4H), 0.83 – 0.90 (m, 2H);  $^{13}\text{C}$  NMR (125 MHz,  $\text{CDCl}_3$ )  $\delta$  166.2, 133.5, 133.2, 131.8, 128.5, 126.2, 126.0, 42.1, 40.2, 37.7, 33.1, 26.5, 26.3

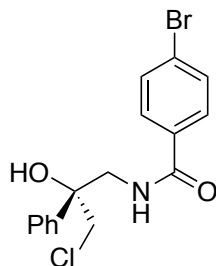
HRMS (ESI): Calculated for  $[\text{M}+\text{H}]$   $\text{C}_{17}\text{H}_{22}\text{NOBr}$  335.0885, Found: 335.0866.

### II.5.9. Determination of absolute stereochemistry of oxazolines.



(*R*)-2-(4-bromophenyl)-5-(chloromethyl)-5-phenyl-4,5-dihydrooxazole (35 mg, 0.10 mmol, >99% ee after chiral chromatographic separation) was dissolved in 500 mL of dry THF in a sealable glass tube. After purging with  $\text{N}_2$ , 1.0M solution of  $\text{BH}_3 \cdot \text{THF}$  solution in THF (250 mL, 0.25 mmol, 2.5 equiv.) was introduced into the reaction vessel at ambient temperature. The reaction vessel was then sealed with a Teflon cap and heated at 65 °C in a sand bath for 8 hours. After cooling to ambient temperature, the reaction was quenched by the addition of 1 mL 10% aq. HCl solution and stirred for a further 0.5 h. The pH was then adjusted to 9 by the drop wise addition of 10% aq. NaOH solution. The aqueous layer was extracted with ether (3x 3 mL). The organics were dried ( $\text{Na}_2\text{SO}_4$ ), concentrated and purified by column chromatography (20% EtOAc in hexanes) to give 20 mg of the desired halohydrin as a waxy solid (54% yield). Crystals for X-ray diffraction analysis were grown by dissolving the product in a minimum amount of  $\text{CHCl}_3$  in a silicone coated vial and layering it with Hexanes. The ee of the halohydrin was also determined to be >99% by chiral HPLC analysis (*vide infra*).

**II-38**, (*R*)-4-bromo-N-(3-chloro-2-hydroxy-2-phenylpropyl)benzamide



White solid; M.P.: 121 – 123 °C;  $R_f$  : 0.21 (20% EtOAc- Hex)

$^1\text{H}$  NMR (500 MHz,  $\text{CDCl}_3$ )  $\delta$  7.44 – 7.53 (m, 5H), 7.38 (t,  $J = 8.0$  Hz, 2H), 7.29 – 7.32 (m, 1H), 6.43 (br s, 1H), 4.08 (dd,  $J = 14.5, 6.5$  Hz, 1H), 3.91 (d,  $J = 12.0$  Hz, 1H), 3.84 (d,  $J = 12.0$  Hz, 1H), 3.80 (br s, 1H), 3.75 (dd,  $J = 14.5, 5.5$  Hz, 1H)

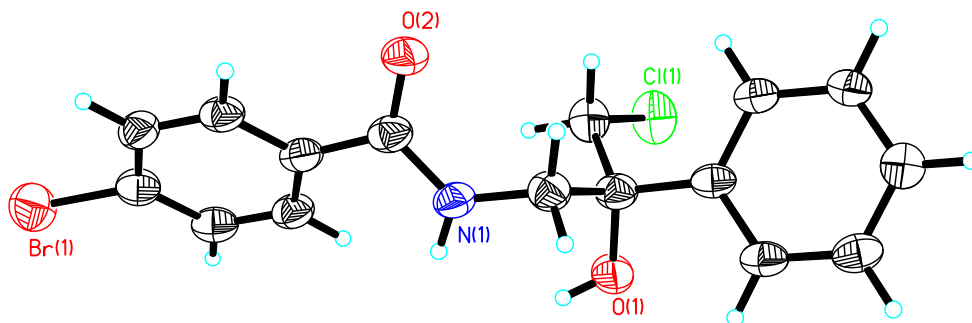
$^{13}\text{C}$  NMR (125 MHz,  $\text{CDCl}_3$ )  $\delta$  167.7, 140.8, 132.6, 131.8, 128.7, 128.5, 128.1, 126.5, 125.4, 76.6, 52.0, 47.9

HRMS (ESI): Calculated for  $[\text{M}+\text{H}]$   $\text{C}_{16}\text{H}_{15}\text{NO}_2\text{ClBr}$  : 366.9975, Found: 366.9988

Resolution of enantiomers: CHIRALCEL OJ-H, 10% IPA-Hex, 1.0 mL/min, 254 nm, RT1 = 25.1 min, RT2 = 34.3 min

ORTEP drawing of the product (at 50% ellipsoids):

**Figure II-11.** Crystal structure of II-38



## REFERENCES

## REFERENCES

- (1) Gribble, G. W. *Acc. Chem. Res.* **1998**, *31*, 141.
- (2) Gribble, G. W. *Chemosphere* **2003**, *52*, 289.
- (3) Blasiak, L. C.; Drennan, C. L. *Acc. Chem. Res.* **2008**, *42*, 147.
- (4) Neumann, C. S.; Fujimori, D. G.; Walsh, C. T. *Chemistry & Biology* **2008**, *15*, 99.
- (5) Wagner, C.; El Omari, M.; Kol`nig, G. M. *J. Nat. Prod.* **2009**, *72*, 540.
- (6) Whitehead, D. C.; Yousefi, R.; Jaganathan, A.; Borhan, B. *J. Am. Chem. Soc.* **2010**, *132*, 3298.
- (7) Bode, H. B.; Irschik, H.; Wenzel, S. C.; Reichenbach, H.; Muller, R.; Hofle, G. *J. Nat. Prod.* **2003**, *66*, 1203.
- (8) Davidson, B. S. *Chem. Rev.* **2002**, *93*, 1771.
- (9) Kline, T.; Andersen, N. H.; Harwood, E. A.; Bowman, J.; Malanda, A.; Endsley, S.; Erwin, A. L.; Doyle, M.; Fong, S.; Harris, A. L.; Mendelsohn, B.; Mdluli, K.; Raetz, C. R. H.; Stover, C. K.; Witte, P. R.; Yabannavar, A.; Zhu, S. *J. Med. Chem.* **2002**, *45*, 3112.
- (10) Pirrung, M. C.; Tumey, L. N.; McClerren, A. L.; Raetz, C. R. H. *J. Am. Chem. Soc.* **2003**, *125*, 1575.
- (11) Ghosh, A. K.; Mathivanan, P.; Cappiello, J. *Tetrahedron: Asymmetry* **1998**, *9*, 1.
- (12) Helmchen, G.; Pfaltz, A. *Acc. Chem. Res.* **2000**, *33*, 336.
- (13) Johnson, J. S.; Evans, D. A. *Acc. Chem. Res.* **2000**, *33*, 325.
- (14) Rajaram, S.; Sigman, M. S. *Org. Lett.* **2002**, *4*, 3399.
- (15) Schwekendiek, K.; Glorius, F. *Synthesis-Stuttgart* **2006**, 2996.
- (16) Wuts, P. G. M.; Northuis, J. M.; Kwan, T. A. *J. Org. Chem.* **2000**, *65*, 9223.
- (17) Zhou, P. W.; Blubaum, J. E.; Burns, C. T.; Natale, N. R. *Tetrahedron Lett.* **1997**, *38*, 7019.
- (18) Badiang, J. G.; Aube, J. *J. Org. Chem.* **1996**, *61*, 2484.
- (19) Nishimura, M.; Minakata, S.; Takahashi, T.; Oderaotoshi, Y.; Komatsu, M. *J. Org. Chem.* **2002**, *67*, 2101.

- (20) Whitehead, D. C.; Staples, R. J.; Borhan, B. *Tetrahedron Lett.* **2009**, *50*, 656.
- (21) Avenoza, A.; Cativiela, C.; Peregrina, J. M. *Tetrahedron* **1994**, *50*, 10021.
- (22) Cardillo, G.; Orena, M.; Sandri, S. *J. Chem. Soc., Chem. Commun.* **1983**, 1489.
- (23) Commerçon, A.; Ponsinet, G. *Tetrahedron Lett.* **1990**, *31*, 3871.
- (24) Bergmann, M.; Dreyer, F.; Radt, F. *Chem. Ber.* **1921**, *54*, 2139.
- (25) Bergmann, M.; Radt, F.; Brand, E. *Chem. Ber.* **1921**, *54*, 1645.
- (26) Goodman, L.; Winstein, S. *J. Am. Chem. Soc.* **1957**, *79*, 4788.
- (27) Kitagawa, O.; Suzuki, T.; Taguchi, T. *J. Org. Chem.* **1998**, *63*, 4842.
- (28) Garzan, A.; Jaganathan, A.; Salehi Marzijarani, N.; Yousefi, R.; Whitehead, D. C.; Jackson, J. E.; Borhan, B. *Chem. Eur. J.* **2013**, *19*, 9015.
- (29) Jaganathan, A.; Staples, R. J.; Borhan, B. *J. Am. Chem. Soc.* **2013**, *135*, 14806.
- (30) Lei, A.; Wu, S.; He, M.; Zhang, X. *J. Am. Chem. Soc.* **2004**, *126*, 1626.
- (31) Wang, Y.-Q.; Lu, S.-M.; Zhou, Y.-G. *Org. Lett.* **2005**, *7*, 3235.

## Chapter III

### *Kinetic Resolution of Unsaturated Amides in a Chlorocyclization*

#### *Reaction: Concomitant Enantiomer Differentiation and Face Selective*

#### *Alkene Chlorination by a Single Catalyst.*

##### III.1. Introduction.

Nature relies on enzyme catalysis to effect formidable reactions with astonishing efficiency. The remarkable chemo- and stereospecificity of enzymatic reactions lead to rapid generation of complex architectures from simple precursors. Key to the success of these reactions is the extensive preorganization of the substrate into reactive conformations as well as a multitude of covalent and/or non-covalent substrate-enzyme interactions. The combined effect of differential entropy and enthalpy modulations serve to distinguish between numerous reaction pathways that would have all been equally accessible in the absence of the enzyme.<sup>1,2</sup> Efforts by synthetic chemists to develop small-molecule catalysts that mimic enzymes have led to a better appreciation for the power of enzyme catalysis as well as the development of novel chemistry (examples include the polyene cascade reactions that generate terpenes, the putative cascade cyclization reactions that yield polyheterocyclic natural products, and products of the polyketide biosynthesis to name a few).<sup>3,4</sup> But despite these advances, biasing reactions exclusively into one of the multitude of available reaction pathways remains a daunting challenge within the realm of small-molecule catalysis; this is especially true when many of these pathways are energetically accessible under reaction conditions. Unlike enzymes, small molecule catalysts do not enjoy large decreases in the differential entropy and enthalpy of activation for mediating reactions.<sup>5</sup> Nonetheless, small-molecule catalysts are generally more promiscuous in terms of substrate specificity and are easily manipulated by means of modular

syntheses. Consequently, the pursuit to discover catalysts that are capable of mimicking enzymes by reducing the available reaction pathways for any given reaction is a worthwhile endeavor.

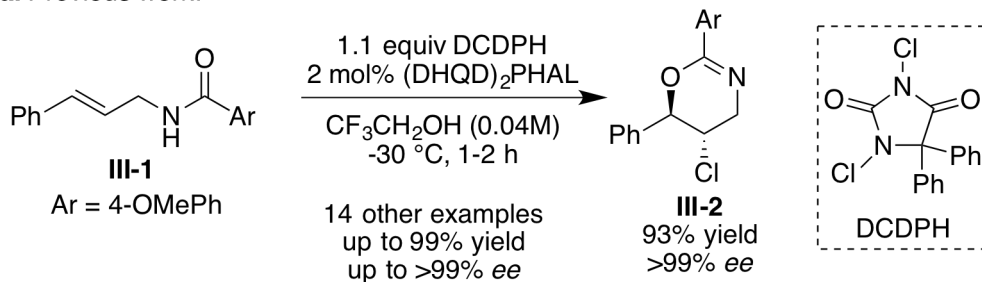
Advances in synthetic chemistry have led to robust 'chemical' equivalents for numerous reactions that are traditionally perceived as the domain of enzyme catalysis. Arguably, the most mimicked of these transformations is the kinetic resolution of racemic mixtures, whereby an enzyme can selectively function on one of two enantiomers.<sup>6,7</sup> Kinetic resolution of racemic molecules has proven to be a powerful transformation for the synthesis of enantiopure compounds in both industrial and academic settings. Either enantiomer of a desired molecule can be theoretically accessed starting from the racemic mixture provided both enantiomers of the catalyst are available. Furthermore, even resolutions that possess low or moderate selectivity factors can be of great value if allowed to proceed to sufficiently high conversions; this is especially true if the racemic substrate is readily accessible on scale and no straightforward means to access the chiral molecule are available. In contrast, resolutions are seldom used for the synthesis of enantioenriched *products* due the requirement of exceptionally high selectivity factors. Additionally, most kinetic resolutions do not create additional stereocenters in the product. From an intellectual standpoint, kinetic resolutions hold great interest because they enable proposals or validations of theoretically predicted 'molecular-recognition' phenomena. Often, they can also serve as a practical means for the synthesis of enantioenriched molecules despite the inherent limitation of the 50% theoretical yield provided the transformations meet certain requirements. Jacobsen and co-workers have elegantly summarized the criteria for an 'ideal kinetic resolution'. The numerous requirements include the ready availability of the catalyst and substrates, paucity of methods to access the desired chiral

molecules using alternate methods, the cost of the catalyst, substrate scope and practical ease in recovery of products and catalysts.

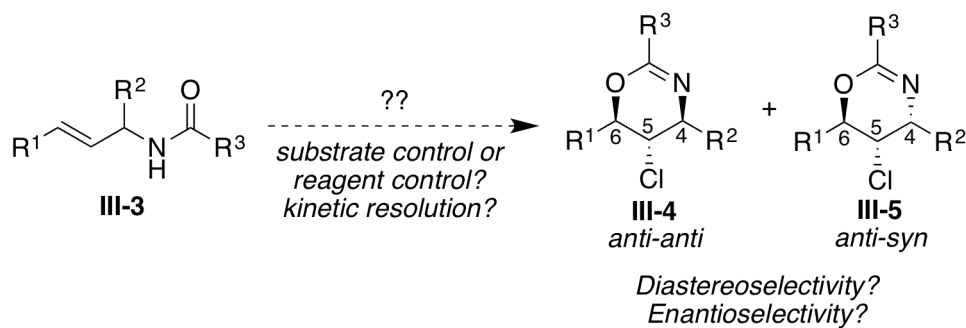
The previous chapter had detailed the discovery and optimization of an enantioselective chlorocyclization of unsaturated amides. It was demonstrated that unsaturated amides can be subjected to a highly enantioselective chlorocyclization reaction to afford corresponding dihydro-oxazine heterocycles with excellent stereoselectivities (Scheme III-1a, typically greater than 95% *ee*). These findings indicated that in the presence of the chiral catalyst the two diastereomeric transition states are sufficiently well differentiated energetically to allow for high levels of enantioinduction. With these results in hand, we had the occasion to examine the possibility of a double stereoselection by an organocatalyst in the context of an asymmetric alkene halogenation reaction.<sup>8-12</sup>

**Scheme III-1.** Enantioselective chlorocyclization of unsaturated amides

a. Previous work:



b. Proposed stereoselective chlorocyclization of racemic unsaturated amides:  
Reagent or substrate control may predominate:

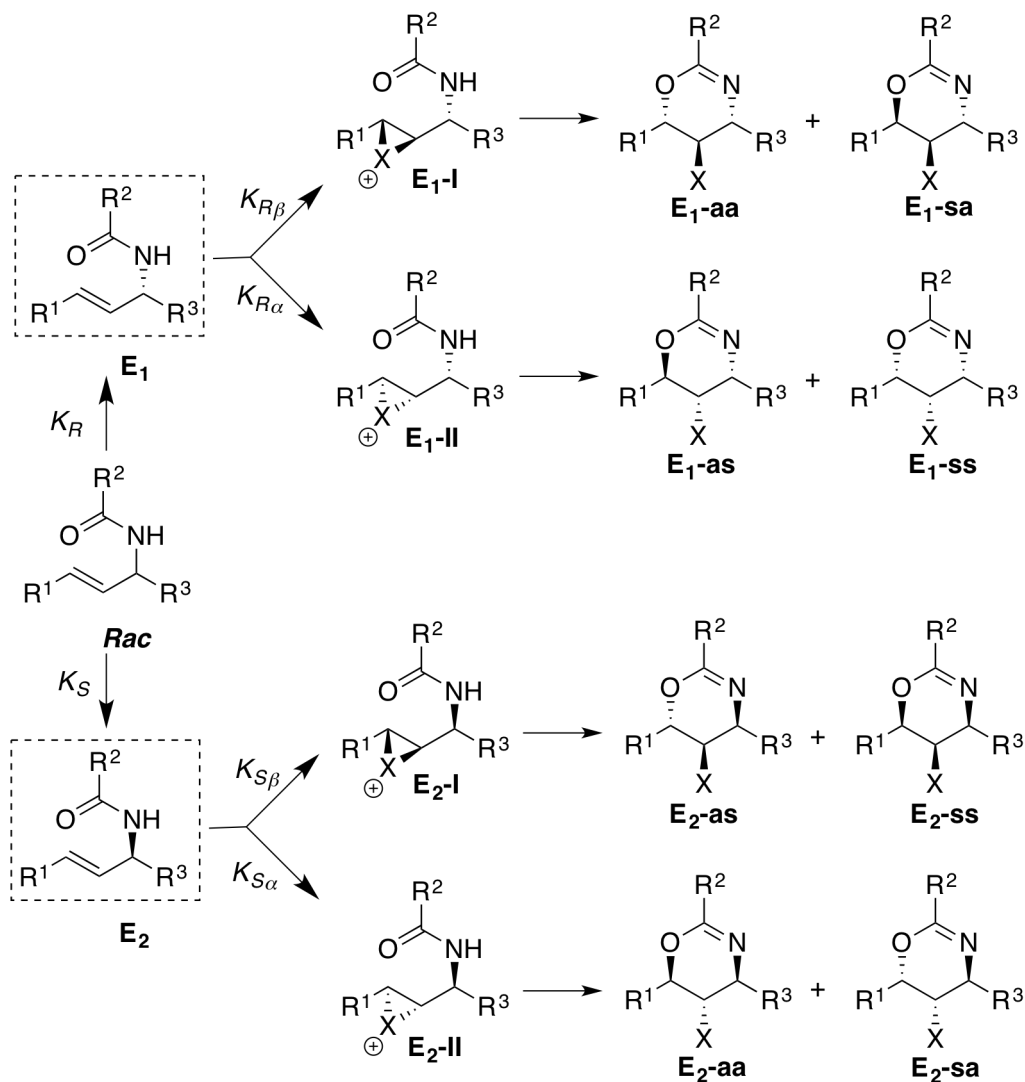


In the presence of pre-existing chirality in the substrate (Scheme III-b), the challenge of controlling the absolute stereochemistry of products is compounded by the additional requirement of controlling the relative stereochemistry of the two newly created stereocenters. Furthermore, the propensity of chloronium ions to readily isomerize to the corresponding carbocations<sup>13-18</sup> followed subsequently by a 'syn' or 'anti' capture of the carbocation by the pendant amide nucleophile results in two additional diastereomeric transition states. The capacity to achieve the required level of selectivity with the catalyst system was in doubt, until recent mechanistic studies with an analogous reaction system, which demonstrated the ability of the catalytic complex to not only dictate face selectivity of chloronium transfer, but also exquisitely control the stereochemistry of cyclization.<sup>19</sup> The capability to control the stereochemical outcome of two independent events by the same catalytic system piqued our

interest in challenging this system to further stereodifferentiate a racemic substrate as a result of preferential binding, much like that in enzymatic systems.

The chlorocyclization of a generic chiral amide, such as one depicted in Figure III-1, can yield eight distinct stereoisomeric products **E<sub>1</sub>-aa** to **E<sub>2</sub>-sa** in the presence of a chiral catalyst. Preliminary studies revealed that there was no evidence of the 'syn' opening pathway for both the non-catalyzed or the catalyzed chlorocyclization of racemic substrates (i.e. **E<sub>1</sub>-sa** to **E<sub>2</sub>-sa**, which would arise from a 'syn' opening were not detected in the reaction). Also, there was no inherent bias for the pathways that lead to the *anti-syn* (**E<sub>1</sub>-as** + **E<sub>2</sub>-as**) and the *anti-anti* (**E<sub>1</sub>-aa** + **E<sub>2</sub>-aa**) diastereomers at ambient temperature (non-catalyzed reactions had an *anti-syn:anti-anti* ratio of ~60:40; vide infra). We were intrigued by the possibility of using a single chiral catalyst that could promote the formation of predominantly one diastereomer of the product with high enantioselectivity. In order to meet this challenge, the catalyst must serve to 'sense chirality' of the substrate in the first stage and enable highly face selective chlorenium delivery to the 'matched' catalyst-bound substrate in the second stage. If the catalyst can selectively accelerate the reaction of one of the two enantiomers (i.e. promote a kinetic resolution of the racemate), then only two of the four pathways will be accessible. The two remaining pathways are defined by the face selectivity in the chlorenium delivery to the olefin moiety. If the same catalyst could further enable a highly face selective chlorenium delivery to the fast reacting enantiomer of the substrate, then one would expect a single stereoisomer of the cyclized product. It is evident that high levels of stereoselection at two stages must operate in concert to enable a diastereoselective kinetic resolution. This enzyme-like catalysis will be manifested as a kinetic resolution of the racemate that also leads to stereotriad products with high diastereoselectivity.

**Figure III-1.** Mechanistic possibilities for the enantioselective chlorocyclization of racemic unsaturated amides

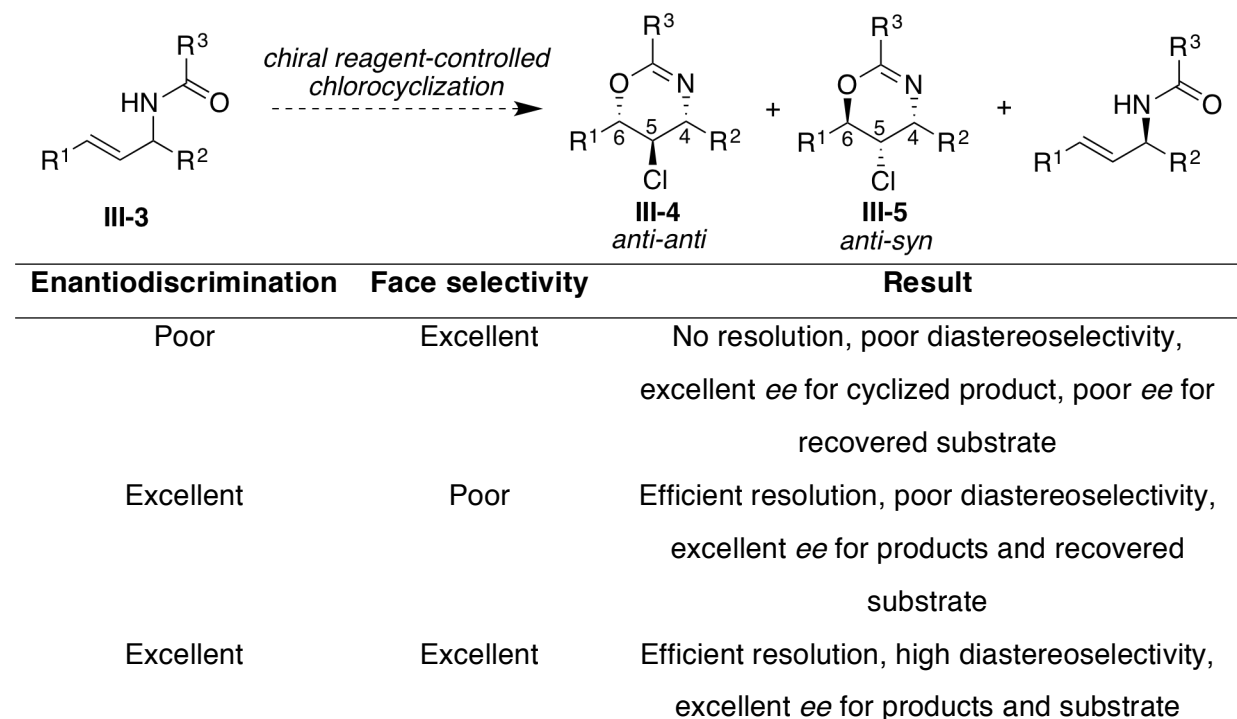


Kinetic resolution *via* alkene halofunctionalization is captivating for many reasons. First, the products are stereotriads (with two new stereocenters being created in the process) adorned with numerous functional handles for further elaboration. Resolutions that create additional stereocenters in the products are relatively rare and are challenging due to the additional requirement of controlling the product diastereoselectivity.<sup>20-23</sup> Second, the kinetic resolution would necessitate the discovery of an intermolecular catalyst-substrate interaction that will serve

to 'sense' chirality of racemic amides (in the current study, an unprecedented interaction of amides with a Lewis base). Finally, a kinetic resolution *via* chlorofunctionalization of olefins was an unrealized transformation at the commencement of this work.<sup>24-26</sup> It must be emphasized that high face selectivity in the delivery of a halonium ion on to the olefin moiety is neither a necessary nor a sufficient condition for achieving an efficient resolution. The crucial requirement is for the chiral catalyst to sufficiently differentiate the reaction rates of the two enantiomers of the racemate. The face selectivity merely dictates the diastereoselectivity of the cyclized products.

The Table III-2 shows the possible outcomes as a result of the synergistic effects of the individual stereodetermining steps.

**Figure III-2.** Synergistic effects of the individual stereodetermining steps

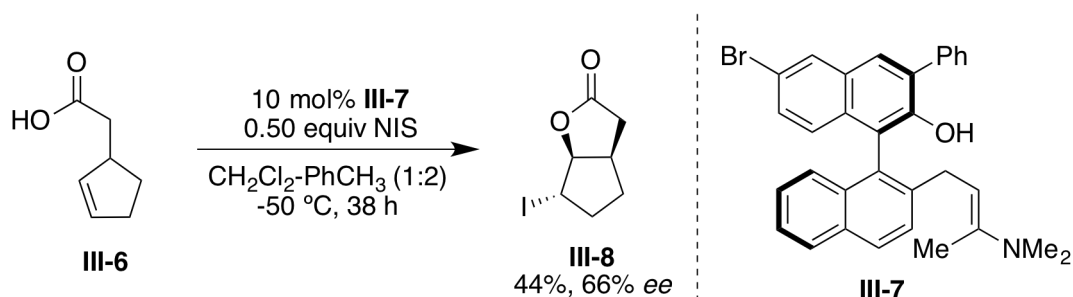


### III.2. Literature precedence for kinetic resolution in halofunctionalization reactions.

During the completion of this project, two reports of kinetic resolution of racemic substrates in halolactonization reactions appeared in literature. Both studies showcased a single substrate with moderate to good selectivity factors.

Martin and co-workers had discovered that **III-7** was an excellent catalyst for the enantioselective iodolactonization of alkenoic acids.<sup>24</sup> In the same study, they evaluated whether catalyst **III-7** could resolve the racemic substrate **III-6**. In the presence of 0.50 equiv of NIS, the bicyclic iodolactone **III-8** was isolated in 44% yield and 66% *ee*. The enantioselectivity of the recovered starting material was not provided. A detailed substrate scope evaluation or further improvements to this protocol have not been reported till date.

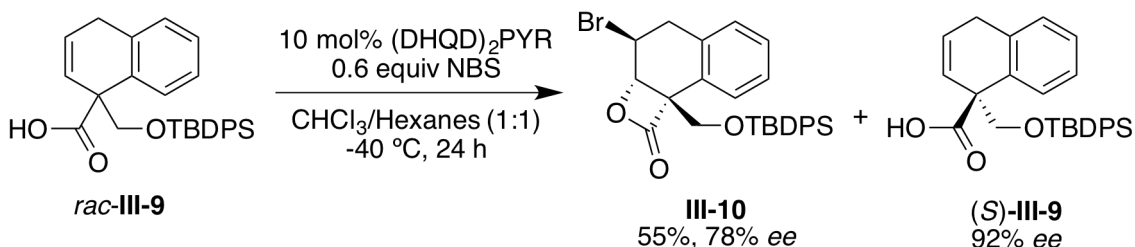
**Scheme III-2.** Kinetic resolution in an iodolactonization reaction



Kan, Hamashima and co-workers were able to show that  $(\text{DHQD})_2\text{PHAL}$  could be used in the desymmetrization of cyclohexadienes via bromolactonization reaction.<sup>25</sup> In fact, with the exception of the halenium source, their optimized conditions including the catalyst, reaction solvent (1:1  $\text{CHCl}_3$ -hexanes co-solvent mixture) and reaction temperature ( $-40\text{ }^\circ\text{C}$ ) were identical to those reported by our group for the chlorolactonization reaction.<sup>27</sup> Attempted extension of their desymmetrization methodology to kinetic resolution of substrate **III-9** was however, not successful. Instead, the authors were able to show that  $(\text{DHQD})_2\text{PYR}$  (also

commercially available) was able to resolve the substrate **III-9** with good levels of stereoselection. The cyclized product **III-10** was isolated in 55% yield and 78% *ee*, whereas the recovered substrate was determined to have 92% *ee* after derivatization into the corresponding methyl ester. The only substrate evaluated in the study was **III-9**; there have been no disclosures with regards to expanding the substrate scope.

**Scheme III-3.** Kinetic resolution in a 4-*exo*-bromolactonization reaction



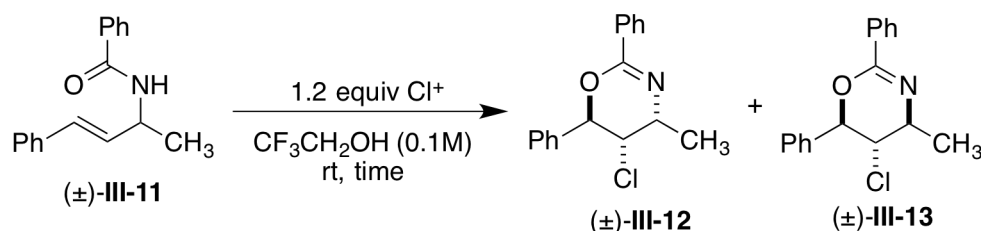
### III.3. Results and Discussion.

#### III.3.1. Investigation of substrate control: Non-catalyzed halocyclization of unsaturated amides.

The studies commenced with the evaluation of the inherent diastereoselectivity of this transformation in the absence of any catalyst (i.e. mapping the substrate control). The racemic test substrate **III-11** was exposed to 1.2 equiv of the chlorenium source in  $\text{CF}_3\text{CH}_2\text{OH}$  (0.10 M concentration with respect to substrate) at ambient temperature. Marginal preference for the formation of **III-12** over **III-13** was observed with numerous chlorenium sources that were evaluated (see Table III-1). Notably, the diastereoselectivity was nearly the same with all the evaluated reagents (~65:35) indicating that the counter anion of the halonium precursor might not be playing a significant role in the non-catalyzed process. The reaction times suggested that background reaction could be a potential problem for the development of enantioselective variants with the more reactive chlorenium sources (entries 1-3, Table III-1, >99% conversion in

less than 10 min). DCDMH, and NCS also gave the cyclized products in comparable diastereoselectivity but at reaction rates that seemed ideal to develop enantioselective variants (see entries 4 and 5 in Table III-1). HCCHD (2,3,4,5,6,6-hexachlorocyclohexa-2,4-dienone) was an incompetent chloronium source for this reaction under non-catalyzed conditions (<5% conversion after 15 h, entry 6, Table III-1).

**Table III-1.** Diastereoselectivity of the non-catalyzed chlorocyclization of **III-11**



| Entry | Cl <sup>+</sup> source | Time   | Conversion | <i>dr</i> (III-12:III-13) |
|-------|------------------------|--------|------------|---------------------------|
| 1.    | TCCA <sup>b</sup>      | 10 min | >99%       | 62:38                     |
| 2.    | TsNCl <sub>2</sub>     | 10 min | >99%       | 69:31                     |
| 3.    | NCSach                 | 10 min | >99%       | 70:30                     |
| 4.    | DCDMH                  | 60 min | 85%        | 66:34                     |
| 5.    | NCS                    | 15 h   | 20%        | 63:37                     |
| 6.    | HCCD                   | 15 h   | trace      | nd                        |

Note: Conversion and *dr* values were determined by GC analysis; TCCA = Trichloroisocyanuric acid; HCCHD = 2,3,4,5,6,6-hexachlorocyclohexa-2,4-dienone; NCSach = N-Chlorosaccharin; DCDMH = 1,3-dichloro-5,5-dimethyl hydantoin

Analogous bromo- and iodocyclization reactions were also evaluated. Intriguingly, the diastereopreference switches going from chloro- to iodocyclization. As evident from Table III-2, as the size of the halonium ion increases, the reaction progressively favors the formation of the *anti-anti* diastereomer. The *syn:anti* ratio was 63:37, 36:64 and 12:88, respectively for the chloro-, bromo-, and iodocyclization reactions. Additionally, the bromo- and iodocyclization

reactions were significantly faster (>99% conversion in 15 min) than the corresponding chlorocyclization reaction (20% conversion after 15 h).

**Table III-2.** Comparison of chloro-, bromo- and iodocyclization reactions of **III-11**

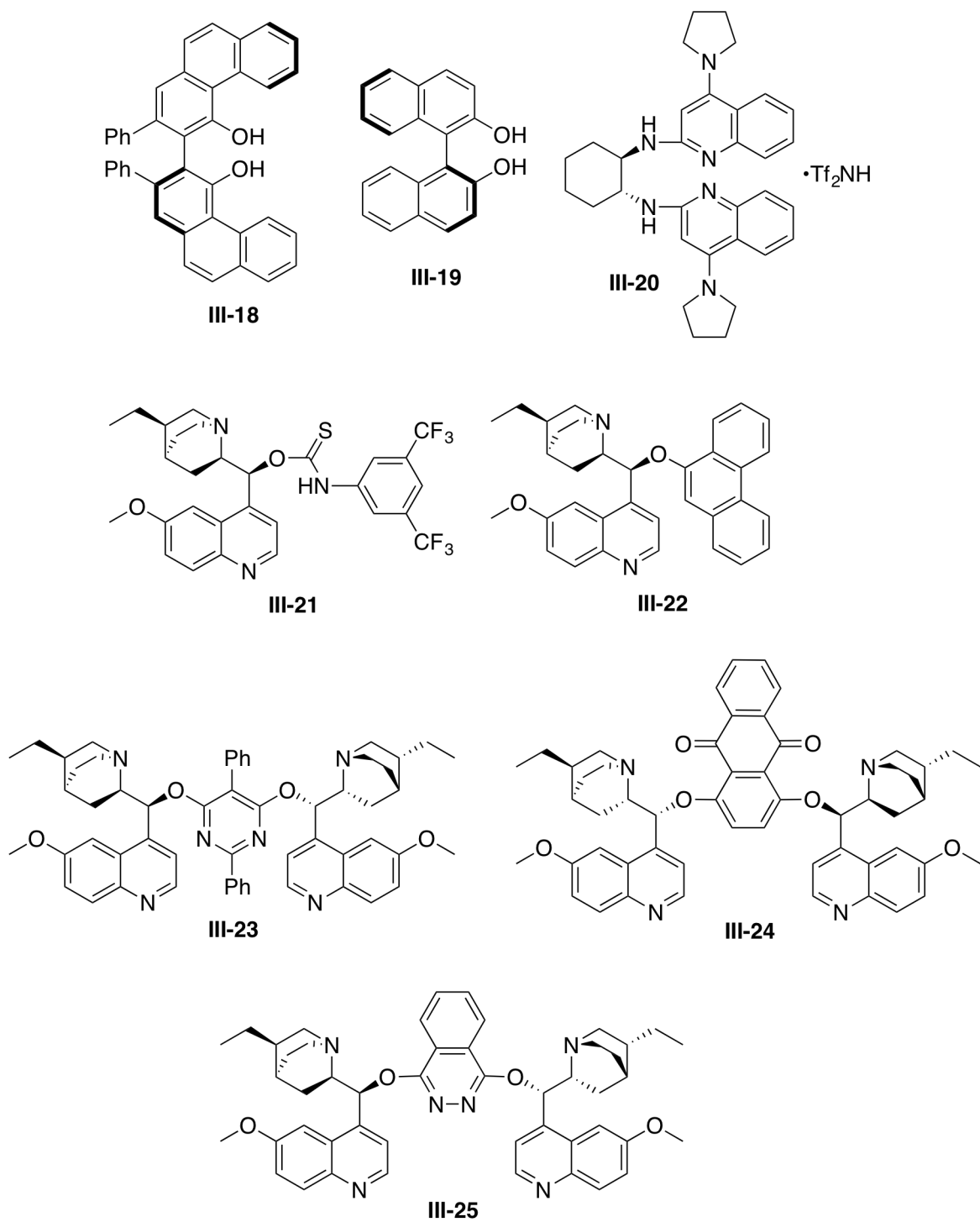
| Entry | $X^+$ source | Time   | Conversion | <i>dr</i> ( <i>anti</i> : <i>syn</i> ) |
|-------|--------------|--------|------------|--|
| 1.    | NCS          | 15 h   | 20%        | 63:37                                  |
| 2.    | NBS          | 15 min | >99%       | 36:64                                  |
| 3.    | NIS          | 15 min | >99%       | 12:88                                  |

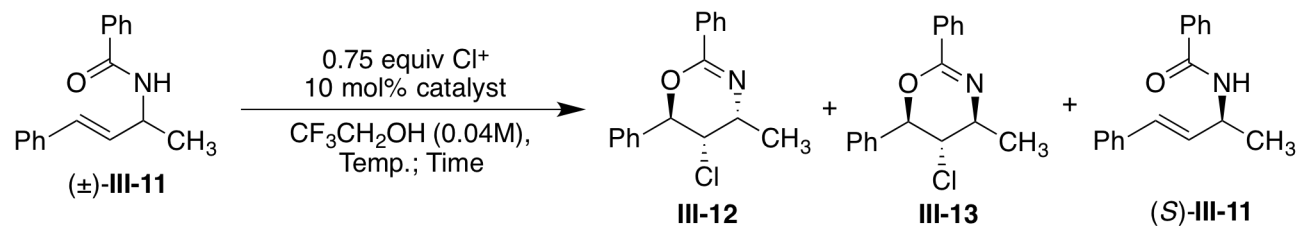
Note: *dr* and conversion were determined by GC analysis with internal standard

### III.3.2. Reagent controlled chlorocyclization of racemic unsaturated amides:

Having mapped out the substrate control, numerous organocatalysts were evaluated at 10 mol% loading in order to determine whether a) substrate control could be significantly amplified or overridden and b) if competent catalysts for a kinetic resolution could be identified. Consequently, reactions were stopped at incomplete conversions and the enantioselectivity of the products and the unreacted substrate were measured. The list of organocatalysts that were evaluated is shown in Figure III-2

**Figure III-3.** Catalysts evaluated for kinetic resolution of test substrate



**Table III-3.** Catalyst screen for the enantioselective chlorocyclization of **III-11**

| Entry | Catalyst | Temp/Time (h) | $\text{Cl}^+$ source | Conv. | <i>dr</i> (12:13) | <i>ee</i> (III-12) | <i>ee</i> (III-13) | <i>ee</i> (S)-III-11 |
|-------|----------|---------------|----------------------|-------|-------------------|--------------------|--------------------|----------------------|
| 1     | None     | 4 °C/4.5      | DCDMH                | 42%   | 65:35             | -                  | -                  | -                    |
| 2     | III-18   | 4 °C/4.5      | DCDMH                | 44%   | 71:29             | -6%                | 2%                 | 8%                   |
| 3     | III-19   | 4 °C/4.5      | DCDMH                | 47%   | 70:30             | 2%                 | 0%                 | 0%                   |
| 4     | III-20   | 4 °C/4.5      | DCDMH                | 28%   | 66:34             | 2%                 | 0%                 | 0%                   |
| 5     | III-21   | 4 °C/4.5      | DCDMH                | 69%   | 44:56             | 14%                | 6%                 | 10%                  |
| 6     | III-22   | -30 °C/1      | DCDMH                | 49%   | 24:76             | -8                 | -40%               | -4%                  |
| 7     | III-23   | -30 °C/1      | DCDMH                | 56%   | 22:78             | -24%               | 4%                 | 6%                   |
| 8     | III-24   | -30 °C/1      | DCDMH                | 60%   | 18:82             | 24%                | 20%                | 18%                  |
| 9     | III-25   | -30 °C/1      | DCDMH                | 61%   | 92:8              | 88%                | 96%                | 94%                  |

Note: Conv. and *dr* values were determined by NMR or GC analysis; (-) sign indicates formation of opposite enantiomer

The studies commenced with the evaluation of numerous hydrogen-bonding catalysts such as BINOL and its derivatives in the hope that they may preferentially associate with one enantiomer of the substrate.<sup>28,29</sup> However, the results with catalysts **III-18** (VAPOL) and **III-19** (BINOL) were disappointing (entries 2 and 3, Table III-3). This was followed by the evaluation of other catalysts that have shown promise in enantioselective alkene halogenation reactions in recent years. The bis-amidine derived Bronsted acid catalyst **III-20** pioneered by Johnston and co-workers<sup>30</sup> and the thiocarbamate catalyst **III-21** analogous to those used by Yeung's group<sup>31</sup> also proved ineffective in resolving the racemic substrate (entries 4 and 5, Table III-3). Catalysts **III-18** to **III-21**, failed to catalyze the reaction as evidenced by the lack of rate acceleration, little to no enantioselectivity, and similar diastereoselectivity as the non-catalyzed reaction (compare entries 2 – 5 to entry 1 in Table III-3). Better results were obtained when cinchona alkaloid derived chiral Lewis bases were screened. Four catalysts (catalysts **III-22** to **III-25**) that significantly altered the substrate control (and thereby confirmed their participation in the stereo-determining step)<sup>32</sup> were identified. Catalysts **III-22**, **III-23** and **III-24** gave the *anti-anti* diastereomer **III-13** as the predominant diastereomer (entries 6-8, Table III-3). But despite overriding substrate control, the enantioselectivities of the cyclized products and the unreacted olefin were poor with all three catalysts; i.e. these catalysts were neither competent in resolving the racemic substrate nor capable of imparting face selectivity to the chlorenium ion delivery to the olefin. In sharp contrast, catalyst **III-25** [(DHQD)<sub>2</sub>PHAL] served to significantly amplify the substrate control by affording the *anti-syn* product **III-12** as the major diastereomer (**III-12:III-13** = 92:8, entry 9, Table III-3). More importantly, when the reaction was stopped at 61% conversion, the major diastereomer **III-12** was isolated in 88% *ee* and the unreacted olefin was highly enriched in the *S*-enantiomer (94% *ee*).<sup>33</sup> While tremendous rate acceleration was

observed with all four catalysts, only (DHQD)<sub>2</sub>PHAL was identified as a competent catalyst for kinetic resolution. Stoichiometric NMR experiments revealed that (DHQD)<sub>2</sub>PHAL was likely behaving as a hydrogen bonding catalyst (rather than a chiral Lewis base) to promote the kinetic resolution (these experiments will be discussed in a subsequent section).

### III.3.3. Optimization of reaction variables.

Having identified a promising catalyst for the kinetic resolution of the test substrate, further studies focused on improving some of the practical aspects of this reaction such as the reaction temperature, concentration and catalyst loading.

#### III.3.3.1. Effect of the chlorenium source and temperature on the stereoselectivity of the reaction.

The identity of the chlorenium source did not significantly influence the diastereo- and enantioselectivity of this transformation provided that sufficient precautions were taken to prevent any background reaction. A detailed survey of the influence of the chlorenium source is shown in Table III-4. All reactions were run in the presence of 3 mol% of (DHQD)<sub>2</sub>PHAL and at the indicated temperatures and concentrations.

On using the significantly more reactive TCCA (0.25 equiv) in lieu of DCDMH (0.75 equiv), the *dr* and *ee* for **III-12** was practically identical to that obtained with DCDMH (compare entries 1 and 2 in Table III-4) although the conversion was only 41%. From a practical standpoint, controlling the conversions to around 50% with TCCA was found to be problematic (due to the 3 equivalents of electrophilic chlorines associated with each TCCA molecule). Using the less reactive chloramine-T as the terminal chlorenium source predictably led to sluggish reactions – only 15% conversion after 60 minutes; although near complete diastereoselectivity for the formation of **III-12** was seen (>99:1 *dr*, see entry 3 in Table III-4). Dichloramine-T (TsNCl<sub>2</sub>, 0.50 equiv) gave excellent diastereoselectivity (*dr* = 99:1) and enantioselectivity for **III-**

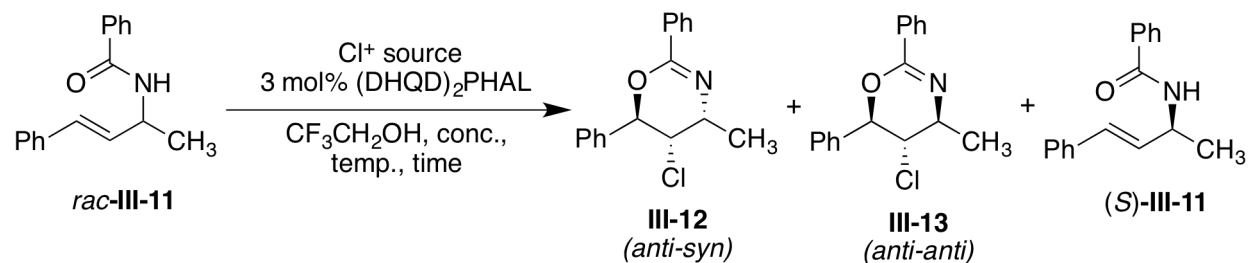
**12** (98% *ee*) at 31% conversion (entry 4, Table III-4); controlling the conversion of the reaction turned out to be problematic with TsNCl<sub>2</sub> as well (>80% conversion was seen with 0.50 equiv of TsNCl<sub>2</sub> if the reaction was allowed to run for 5 h indicating that both chlorine atoms could be transferred to the substrate). *N*-chlorosaccharin afforded the cyclized product is good *dr* and enantioselectivity (92:8 *dr*, 90% *ee*, entry 5, Table III-4). Nonetheless, the unreacted substrate was recovered in only 62% *ee* even at 63% conversion. *N*-chlorosuccinimide (NCS) and *N*-chlorophthalimide (NCP) were eventually identified as the two best chlorine precursors for this reaction (entries 6 and 7 in Table III-4; ≥98:2 *dr*, ≥96% *ee* for the cyclized product). The reaction with NCP was slower than that with NCS (38% conversion with NCP as compared to 53% conversion with NCS after 60 min). This difference is likely due to the poor solubility of NCP in CF<sub>3</sub>CH<sub>2</sub>OH at -30 °C. Having noted that background reaction with NCP and NCS were negligible even at ambient temperatures (<15% conversion after 15 h), it was hoped that these reactions could be run at room temperature and higher concentrations (leading to practically more appealing reaction conditions).

Indeed, the reactions with both NCS and NCP could be run at 23 °C and 0.10 M concentration (with respect to substrate) with practically no loss in the efficiency of the resolution (see entries 10 and 11 in Table III-4; ≥95:5 *dr*, 96% *ee* for **III-12** and ≥94% *ee* for unreacted substrate).

It merits mention that other haloamine salts such as Chloramine-T (TsNNaCl) and Chloramine-M (CH<sub>3</sub>NNaCl) performed just as well as NCS and NCP under these optimized reaction conditions (see entries 8 and 9 in Table III-4). *N*-chlorophthalimide (NCP) was eventually chosen for further studies due to the practical ease of removing the phthalimide by-

product using a basic work-up as well as the consistently higher isolated yields of the cyclized products.

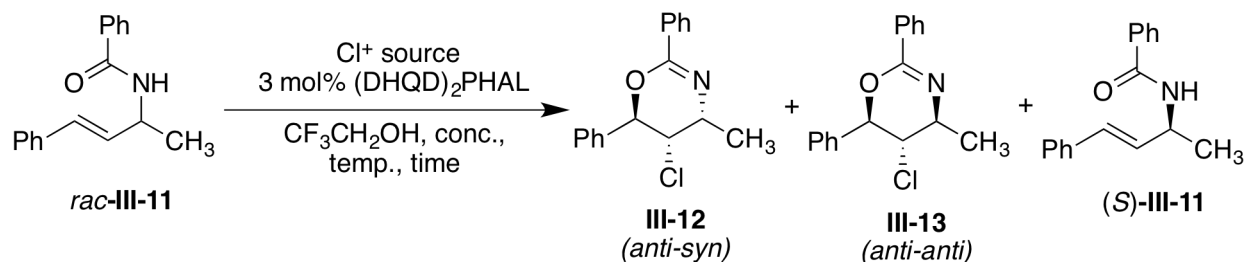
**Table III-4.** Influence of chlorenium precursor and reaction variables on the stereoselectivity of kinetic resolution of **III-11**



| Entry | Cl <sup>+</sup> source        | Conc.  | Temp, Time     | Conv. | dr    | ee (III-12) | ee (III-13) | ee ( <i>S</i> )-III-11 |
|-------|-------------------------------|--------|----------------|-------|-------|-------------|-------------|------------------------|
| 1.    | 0.75 equiv DCDMH              | 0.04 M | -30 °C, 20 min | 62%   | 92:8  | 88%         | >99%        | 94%                    |
| 2.    | 0.25 equiv TCCA               | 0.04 M | -30 °C, 15 min | 41%   | 92:8  | 98%         | 32%         | 30%                    |
| 3.    | 0.75 equiv TsNNaCl            | 0.04 M | -30 °C, 60 min | 15%   | >99:1 | ND          | ND          | ND                     |
| 4.    | 0.50 equiv TsNCl <sub>2</sub> | 0.04 M | -30 °C, 15 min | 31%   | 99:1  | 98%         | ND          | 24%                    |
| 5.    | 0.75 equiv NCSach             | 0.04 M | -30 °C, 15 min | 63%   | 92:8  | 90%         | 58%         | 62%                    |
| 6.    | 0.75 equiv NCS                | 0.04 M | -30 °C, 60 min | 53%   | 98:2  | 96%         | 56%         | 88%                    |
| 7.    | 0.75 equiv NCP                | 0.04 M | -30 °C, 60 min | 38%   | >99:1 | 98%         | ND          | 34%                    |

Note: *dr* values and conversion were determined by GC analysis with undecane as internal standard

Table III-4 (Cont'd)



| Entry            | Cl <sup>+</sup> source | Conc.  | Temp, Time    | Conv. | dr   | ee (III-12) | ee (III-13) | ee (S)-III-11 |
|------------------|------------------------|--------|---------------|-------|------|-------------|-------------|---------------|
| 8. <sup>c</sup>  | 0.75 equiv TsNNaCl     | 0.10 M | 23 °C, 60 min | 53%   | 96:4 | 96%         | 40%         | 92%           |
| 9. <sup>c</sup>  | 0.75 equiv MeNNaCl     | 0.10 M | 23 °C, 60 min | 60%   | 93:7 | 92%         | 60%         | 98%           |
| 10.              | 0.55 equiv NCS         | 0.10 M | 23 °C, 60 min | 53%   | 96:4 | 94%         | 80%         | 94%           |
| 11.              | 0.55 equiv NCP         | 0.10 M | 23 °C, 60 min | 55%   | 95:5 | 94%         | 84%         | 97%           |
| 12. <sup>d</sup> | 0.55 equiv NCP         | 0.10 M | 23 °C, 60 min | 55%   | 94:6 | (-)94%      | (-)82%      | (-)96%        |

Note: Conv. and *dr* values were determined by GC analysis; (-) sign indicates formation of opposite enantiomer

Finally, the quasi-enantiomeric (DHQ)<sub>2</sub>PHAL catalyst gave practically identical results as (DHQD)<sub>2</sub>PHAL, but favoring the opposite enantiomers of products and the recovered olefin (compare entries 11 and 12 in Table III-4).

### III.3.3.2. Catalyst loading studies.

(DHQD)<sub>2</sub>PHAL was found to be an exceptional catalyst for this transformation. Reactions were routinely complete (i.e. 50% consumption of substrate) in less than 2 minutes at ambient temperature even at catalyst loadings as low as 3 mol% (in fact, reaction rates were primarily dependent on the solubility of the substrate). Having noted this, it was hoped that the catalyst loadings could be decreased further. Kinetic resolutions that employ low catalyst loadings ( $\leq 1.0$  mol%) are rare, especially when conversions approaching 50% are required.

Remarkably, no loss in efficiency was seen for the test reaction even at ambient temperatures while maintaining sub 1.0 mol% catalyst loadings, indicating exquisite specificity of the catalyst for the transformation of the *R* enantiomer of the substrate. When the catalyst loading was progressively decreased from 3.0 mol% to 0.25 mol%, there was negligible loss in the efficiency of the resolution (see entries 1 – 4, Table III-5). Longer reaction time of 60 min was required when 0.25 mol% catalyst loading was employed to drive the reaction to ~50% conversion (entry 4). At 0.10 mol% catalyst loading, the reaction still proceeds with excellent diastereoselectivity (94:6 *dr*) and enantioselectivity for the major diastereomer (97% *ee*); nonetheless, the reaction was only 28% complete even after 60 min (entry 5, Table III-5). Longer reaction times with 0.10 mol% catalyst loading could potentially lead to results similar to that with higher catalyst loadings (this was not pursued any further since it had emerged by then that the optimal catalyst loading was dependent on the substrate employed).

**Table III-5.** Catalyst loading studies

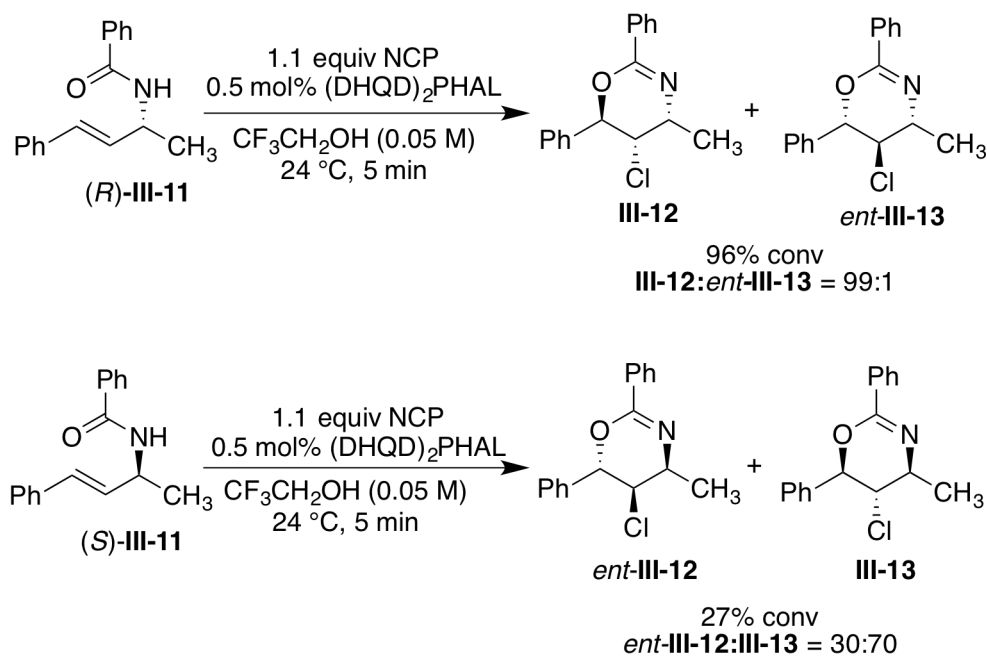
| Entry | Catalyst loading | Time.  | Conv. | dr   | ee (III-12) | ee (S)-III-11 |
|-------|------------------|--------|-------|------|-------------|---------------|
| 1.    | 3.0 mol%         | 15 min | 53%   | 96:4 | 96%         | 92%           |
| 2.    | 1.0 mol%         | 15 min | 51%   | 96:4 | 94%         | 95%           |
| 3.    | 0.50 mol%        | 15 min | 48%   | 94:6 | 93%         | 91%           |
| 4.    | 0.25 mol%        | 60 min | 49%   | 95:5 | 96%         | 86%           |
| 5.    | 0.10 mol%        | 60 min | 28%   | 94:6 | 97%         | 36%           |

Note: *dr* and conversion were determined by GC analysis using undecane as internal standard

### III.3.4. Matched and mismatched substrates for kinetic resolution.

Predictably, a clear preference was observed for the chlorocyclization of enantiomerically pure (*R*)-III-11 in comparison to (*S*)-III-11 under optimized conditions (see Scheme III-4). In the presence of stoichiometric amounts of *N*-chlorophthalimide and 0.50 mol% of (DHQD)<sub>2</sub>PHAL, (*R*)-III-11 was almost completely consumed in 5 min to give exclusively the *anti-syn* diastereomer III-112 (99:1 *dr*) indicating exquisite *a*-face selectivity in the delivery of the chloronium ion to the olefin of (*R*)-III-11. Under identical conditions, (*S*)-III-11 showed only 27% conversion to product. Notably, low olefin face selectivity was seen in the chloronium delivery still favoring the *a*-face by a ratio of 70:30 indicating a much attenuated reagent control for (*S*)-III-11.

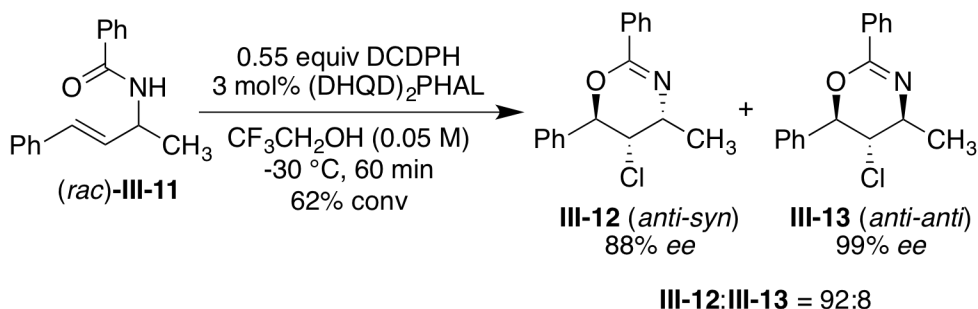
**Scheme III-4.** Matched and mismatched substrates for kinetic resolution with (DHQD)<sub>2</sub>PHAL



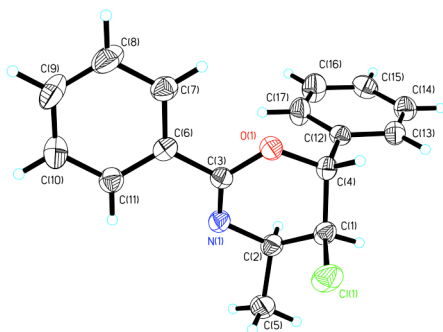
**III.3.5. Determination of absolute stereochemistry of cyclized products.**

The absolute stereochemistry of both diastereomers of the cyclized product was determined by single crystal X-ray diffraction (XRD). The kinetic resolution under conditions detailed in Entry 1, Table III-4 gave both diastereomers in excellent enantioselectivities (92:8 *dr* favoring III-12 over III-13 and 88% *ee* and 99% *ee* respectively, for the two diastereomers at 62% conversion). Preparatory TLC was used to separate the two diastereomers. While III-13 was crystallized from CHCl<sub>3</sub> layered with hexanes, III-12 was crystallized from hot hexanes. Both diastereomers exhibited the same absolute stereochemistry at the chlorinated carbon indicating exquisite reagent control in the alkene chlorination event for this reaction. The absolute stereochemistry of the recovered substrate was determined by comparison of optical rotations to the reported molecule.

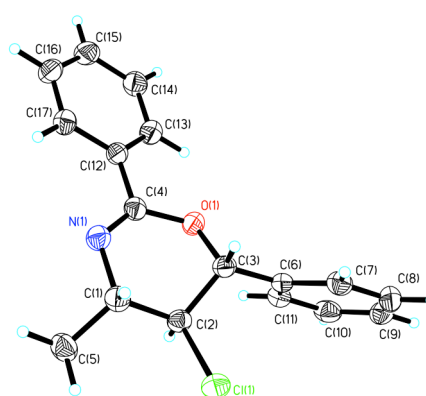
### Scheme III-5. Determination of absolute stereochemistry of cyclized products



Crystal structure of III-12



Crystal structure of III-13



#### III.3.6. Substrate scope.

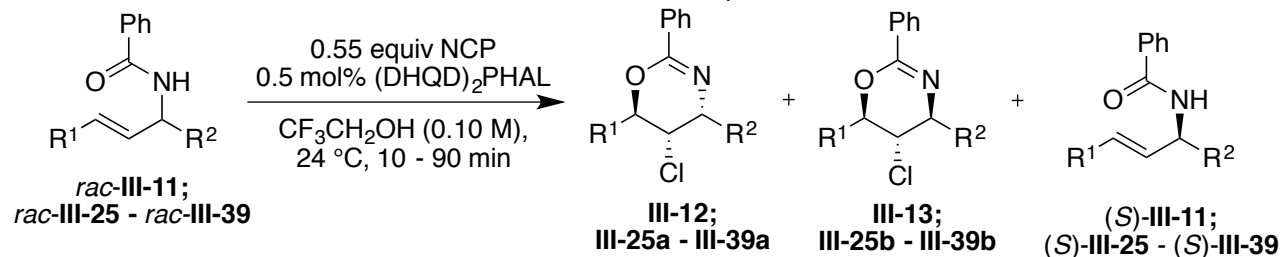
The generality of the kinetic resolution was investigated by subjecting numerous *trans* disubstituted allylic amides to optimized reaction conditions. As seen in Table III-6, the reaction was tolerant of electronically and sterically diverse aryl substituents on the olefin. Electron deficient and halogenated aryl rings presented no difficulties, nor did substrates with *ortho* substituents on the aromatic ring. These substrates were resolved in comparable efficiency as the test substrate (entries 1–6, 8 and 9 Table III-6). In all these instances the cyclized products were formed with excellent diastereoselectivity (93:7 to >99:1 *dr*) at ~50% conversion. Furthermore, the *ee* values for the major diastereomer was >90% for most products and the

unreacted substrates were isolated in >80% *ee* for most substrates (a single crystallization was usually sufficient to upgrade the enantioselectivity to >95% *ee*).

The effect of increasing steric demand of the olefin substituent as well as the substituent at the  $\alpha$ -carbon (i.e. the C3 and C5 substituents of the cyclized products) was then studied. Substrate **III-34** with a sterically demanding naphthyl substituent was efficiently resolved (84% *ee* for unreacted substrate at 55% conversion), albeit the diastereoselectivity of the cyclized product was poor (entry 10, 74:26 *dr*). This result indicates that the catalyst effectively discriminates the enantiomers of the racemic substrate; but a poor facial selectivity in the chlorenium delivery to the olefin leads to the diminished diastereoselectivity.

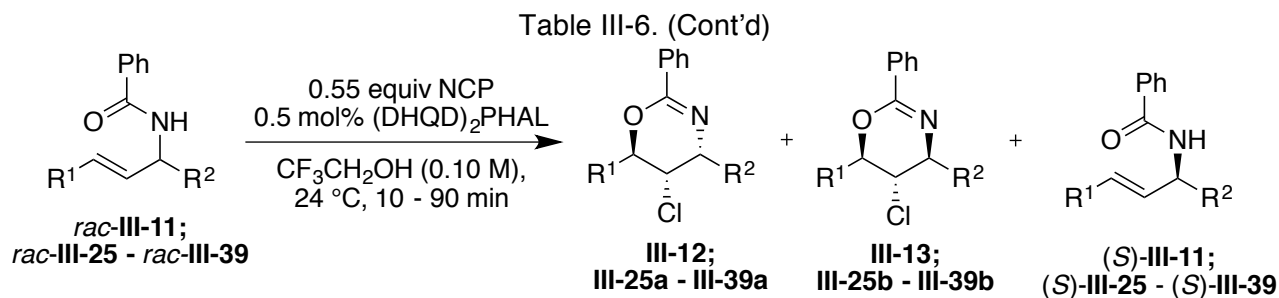
The effect of increasing steric demand of the substituent at  $\alpha$ -position of the amide had a more dramatic effect. Substrates **III-35** and **III-36** with conformationally flexible allyl and *n*-C<sub>5</sub>H<sub>11</sub> substituent, respectively, were excellent substrates for the resolution (entries 11 and 12, Table 2). Much diminished efficiency was observed when the  $\alpha$ -substituent was a homobenzyl, phenyl or a *t*-butyl substituent (entries 13 to 15, Table 2). Cyclization of substrates **III-37**, **III-38** and **III-39** required higher catalyst loadings (3.0 mol%) and longer reaction times (90 min) to reach ~50% conversion. In case of substrate **III-38** with a C<sub>6</sub>H<sub>5</sub>  $\alpha$ -substituent, practically no resolution of the racemic substrate was seen (**III-38** was recovered in 20% *ee* at 55% conversion). The cyclization exhibited poor diastereoselectivity (*dr* = 60:40) and the products exhibited only moderate levels of enantioselectivity (68% *ee* for **III-38a** and 38% *ee* for **III-38b**). Likewise, substrate **III-39** with the bulky *t*-Bu substituent also fared poorly (entry 15, Table III-6). The lower reaction rates and resolution efficiency with these substrates is attributed to poor substrate-catalyst interaction due to increased steric impediments (stoichiometric substrate-catalyst NMR studies support this hypothesis; see below for discussion and the NMR studies).

**Table III-6.** Substrate scope evaluation



| Entry          | Substrate | R <sup>1</sup>                                   | R <sup>2</sup>  | Conversion <sup>a</sup><br>(Yield of prod) <sup>b</sup> | dr <sup>c</sup> | ee (product) <sup>d</sup> | ee (substrate) <sup>d</sup> |
|----------------|-----------|--|-----------------|---|-----------------|---------------------------|-----------------------------|
| 1              | III-11    | C <sub>6</sub> H <sub>5</sub>                    | CH <sub>3</sub> | 57% (55%)   | 95:5            | 94%                       | 97%                         |
| 2              | III-26    | 4-Cl-C <sub>6</sub> H <sub>4</sub>               | CH <sub>3</sub> | 55% (54%)   | 95.5:4.5        | 92%                       | 99%                         |
| 3              | III-27    | 4-F-C <sub>6</sub> H <sub>4</sub>                | CH <sub>3</sub> | 55% (46%)   | 95:5            | 87%                       | 98%                         |
| 4              | III-28    | 2-Cl-C <sub>6</sub> H <sub>4</sub>               | CH <sub>3</sub> | 50% (50%)   | 97:3            | 93%                       | 82%                         |
| 5 <sup>e</sup> | III-29    | 3-OMe-C <sub>6</sub> H <sub>4</sub>              | CH <sub>3</sub> | 42% (36%)   | >99:1           | 97%                       | 70%                         |
| 6              | III-30    | 4-CF <sub>3</sub> -C <sub>6</sub> H <sub>4</sub> | CH <sub>3</sub> | 55% (45%)   | 96:4            | 92%                       | 78%                         |
| 7 <sup>f</sup> | III-31    | 4-CH <sub>3</sub> -C <sub>6</sub> H <sub>4</sub> | CH <sub>3</sub> | 54% (36%)   | 80:20           | 64%                       | 52%                         |

<sup>a</sup>Based on GC yields of the unreacted substrate using undecane as internal standard. <sup>b</sup>Combined isolated yield of products after column chromatography. <sup>c</sup>Determined by crude NMR and/or GC analysis. <sup>d</sup>Determined by chiral HPLC. <sup>e</sup>Reaction was run at -30 °C for 1 h and then at 0 °C for 2 h. <sup>f</sup>3.0 mol% catalyst was used.



| Entry               | Substrate | R <sup>1</sup>                                   | R <sup>2</sup>  | Conversion <sup>a</sup><br>(Yield of prod) <sup>b</sup> | <i>dr</i> <sup>c</sup> | <i>ee</i> (product) <sup>d</sup> | <i>ee</i> (substrate) <sup>d</sup> |
|---------------------|-----------|--|---|---|------------------------|----------------------------------|------------------------------------|
| 8                   | III-32    | 2-CH <sub>3</sub> -C <sub>6</sub> H <sub>4</sub> | CH <sub>3</sub>   | 55% (52%)   | 93:7                   | 92%                              | 84%                                |
| 9                   | III-33    | 2-F-C <sub>6</sub> H <sub>4</sub>                | CH <sub>3</sub>   | 55% (48%)   | 93:7                   | 88%                              | 98%                                |
| 10 <sup>f,g,h</sup> | III-34    | 1-Naphthyl                                       | CH <sub>3</sub>   | 53% (44%)   | 74:26                  | ND                               | 84%                                |
| 11                  | III-35    | C <sub>6</sub> H <sub>5</sub>                    | CH <sub>2</sub> =CHCH <sub>2</sub>                            | 54% (51%)   | 98:2                   | 96%                              | 76%                                |
| 12                  | III-36    | C <sub>6</sub> H <sub>5</sub>                    | <i>n</i> -C <sub>5</sub> H <sub>11</sub>                      | 54% (49%)   | 97:3                   | 88%                              | 84%                                |
| 13 <sup>f,g,h</sup> | III-37    | C <sub>6</sub> H <sub>5</sub>                    | CH <sub>2</sub> CH <sub>2</sub> C <sub>6</sub> H <sub>5</sub> | 50% (45%)   | 89:11                  | 76% (III-37a)                    | 54%                                |
| 14 <sup>f,g,h</sup> | III-38    | C <sub>6</sub> H <sub>5</sub>                    | C <sub>6</sub> H <sub>5</sub>                                 | 55% (52%)   | 60:40                  | 68% (III-38a)/38% (III-38b)      | 20%                                |
| 15 <sup>f,g</sup>   | III-39    | C <sub>6</sub> H <sub>5</sub>                    | <i>t</i> -Bu  | 50% (46%)   | 80:20                  | 44% (III-39a)/20% (III-39b)      | 40%                                |

<sup>a</sup>Based on GC yields of the unreacted substrate using undecane as internal standard. <sup>b</sup>Combined isolated yield of products after column chromatography. <sup>c</sup>Determined by crude NMR and/or GC analysis. <sup>d</sup>Determined by chiral HPLC. <sup>f</sup>3.0 mol% catalyst was used. <sup>g</sup>Reaction time was 90 min. <sup>h</sup>Reaction was run in (CF<sub>3</sub>)<sub>2</sub>CHOH to improve solubility of substrate.

The substrate scope analysis was also repeated with 0.65 equiv of chloaramine-T $\square$ 3H $_2$ O in a 9:1 CF $_3$ CH $_2$ OH/(CF $_3$ ) $_2$ CHOH co-solvent mixture. Chloramine salts were determined to improve the enantioselectivity of the amide chlorocyclization reaction. The details of this discovery and optimization have been provided in the previous chapter. The results for the kinetic resolution reaction employing NCP or chloaramine-T $\square$ 3H $_2$ O were practically identical for most substrates. Slightly longer reaction times (60 – 90 min) were required for the reactions employing chloaramine-T $\square$ 3H $_2$ O as the terminal chlorenium source.

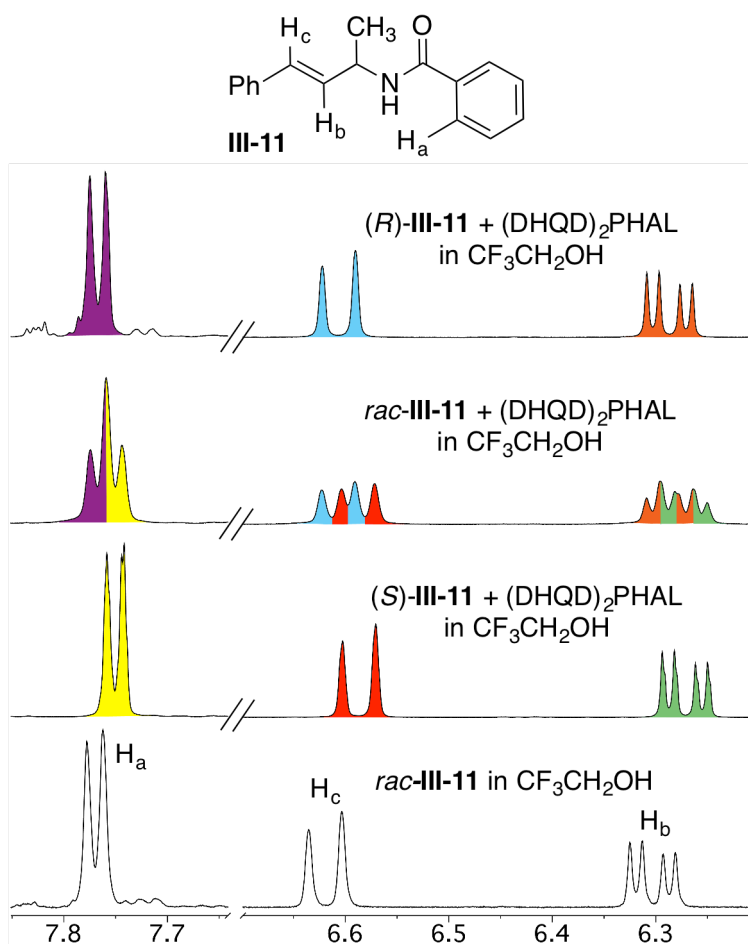
### III.3.7. Mechanistic studies.

#### III.3.7.1. NMR analysis of stoichiometric substrate-catalyst mixtures.

As outlined in Figure III-1, the first and crucial level of selectivity is defined by the catalyst's ability to preferentially accelerate (or inhibit) the reaction of one of the two enantiomers presumably *via* hydrogen-bonding interactions. The absolute magnitudes as well as the relative difference in the association constants ( $K_{aR}$  vs  $K_{aS}$ ) of the two enantiomers with the chiral catalyst are crucial in enabling the kinetic resolution. Implicit is the assumption that only the 'bound' enantiomer will react regardless of whether it is the stronger or the weaker bound enantiomer (scenarios where the stronger bound olefin enantiomer is stereoelectronically incapable of capturing the halenium ion cannot be ruled out at this stage). Given the excellent selectivity factors even at ambient temperatures, stoichiometric mixtures of the test substrate *rac*-III-11 and catalyst (DHQD) $_2$ PHAL were evaluated by  $^1$ H NMR in CF $_3$ CH $_2$ OH in order to elucidate the nature of substrate-catalyst interactions that lead to differential reaction rates for the two enantiomers.<sup>34</sup> Most of the protons of *rac*-III-11 exhibited up field shifts suggesting an intimate association of the substrate and the catalyst. Surprisingly, a clean formation of diastereomeric complexes (in a 1:1 ratio) was seen even at ambient temperatures (see Figure

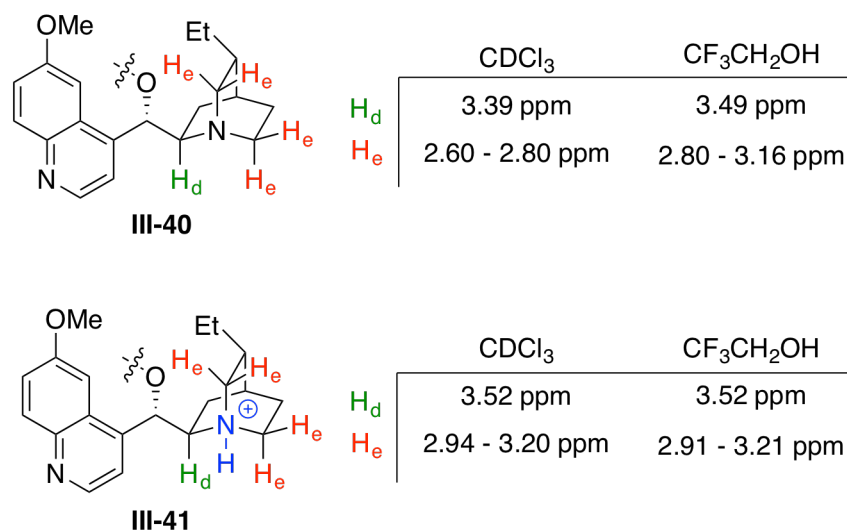
III-4). With enantiomerically pure (*R*)-**1a** and (*S*)-**1a**, diastereomerically pure complexes were seen, ruling out the possibility of non-enantiospecific fluxional processes on a NMR time scale. Diminished or no diastereotopicity was observed in other deuterated solvents such as CDCl<sub>3</sub>, C<sub>6</sub>D<sub>6</sub>, acetone-*d*<sub>6</sub> and CD<sub>3</sub>CN (these spectra are compiled in the experimental section). It is perhaps not surprising that other solvents fare poorly as a reaction medium.

**Figure III-4.** NMR analysis of stoichiometric substrate-catalyst mixtures



It is postulated that the quinuclidine nitrogen atoms of the chiral catalyst ( $pK_a \sim 10$ ) are protonated in CF<sub>3</sub>CH<sub>2</sub>OH ( $pK_a$  of CF<sub>3</sub>CH<sub>2</sub>OH = 12.5; mole ratio of catalyst: CF<sub>3</sub>CH<sub>2</sub>OH  $\geq 1:25,000$  for reactions and  $\sim 1:1,000$  for NMR studies).

**Figure III-5.** NMR of free and protonated (DHQD)<sub>2</sub>PHAL in CDCl<sub>3</sub> and CF<sub>3</sub>CH<sub>2</sub>OH



This hypothesis is supported by NMR studies that reveal little change in the chemical shifts of the methylene and methine protons adjacent to the quinuclidine nitrogen atoms of the catalyst before and after addition of stoichiometric quantities (2.0 equiv) of benzoic acid (see right side column in Figure III-5; methine proton H<sub>d</sub> shows negligible shift from 3.49 ppm to 3.52 ppm after catalyst protonation. Likewise, small downfield shift is seen for the methylene protons H<sub>e</sub>). This behavior is in sharp contrast to that seen in CDCl<sub>3</sub> where H<sub>d</sub> and H<sub>e</sub> have distinct chemical shifts depending on the protonation state of the catalyst. Catalyst protonation leads to significant down field shifts of H<sub>d</sub> and H<sub>e</sub> (H<sub>d</sub> shifts from 3.39 ppm to 3.52 ppm; H<sub>e</sub> protons shift from 2.60-2.80 ppm to 2.94-3.20 ppm, see CDCl<sub>3</sub> column in Figure III-5). Furthermore, the chemical shifts for H<sub>d</sub> and H<sub>e</sub> in CF<sub>3</sub>CH<sub>2</sub>OH *without* the benzoic acid additive are similar to those of the *protonated* catalyst in CDCl<sub>3</sub> (3.52 ppm for H<sub>d</sub> and 2.94–3.20 ppm for H<sub>e</sub>); also there is no further downfield shift in the presence of stoichiometric quantities of benzoic acid in

CF<sub>3</sub>CH<sub>2</sub>OH. These results suggest that the catalyst is protonated in CF<sub>3</sub>CH<sub>2</sub>OH even without an external proton source.

### III.3.7.2. Effect of protic additives.

The protonation of the quinuclidine nitrogen atoms may cause a change in the conformation of the catalyst and allow for better substrate-catalyst interactions in CF<sub>3</sub>CH<sub>2</sub>OH as opposed to other solvents. Although significant, catalyst protonation cannot be the only role for CF<sub>3</sub>CH<sub>2</sub>OH, since mere incorporation of protic additives in different solvents does not recapitulate the results with CF<sub>3</sub>CH<sub>2</sub>OH.

As seen in Table III-7, all Bronsted acid additives (evaluated at 50 mol% loading) led to strong inhibition of the reaction. While benzoic acid and acetic acid additives still gave the products in 21% and 31% conversions respectively (and >95:5 *dr*), other acid additives such as *p*-toluenesulfonic acid, citric acid, *N*-acetyl glycine, CF<sub>3</sub>CO<sub>2</sub>H and *p*-nitrophenol shut down the reaction. Besides its enhanced acidity, CF<sub>3</sub>CH<sub>2</sub>OH is a good hydrogen bond donor, a weak nucleophile, a non-coordinating counteranion, and also a highly polar solvent. The latter set of features is not easily duplicated with other solvent systems.

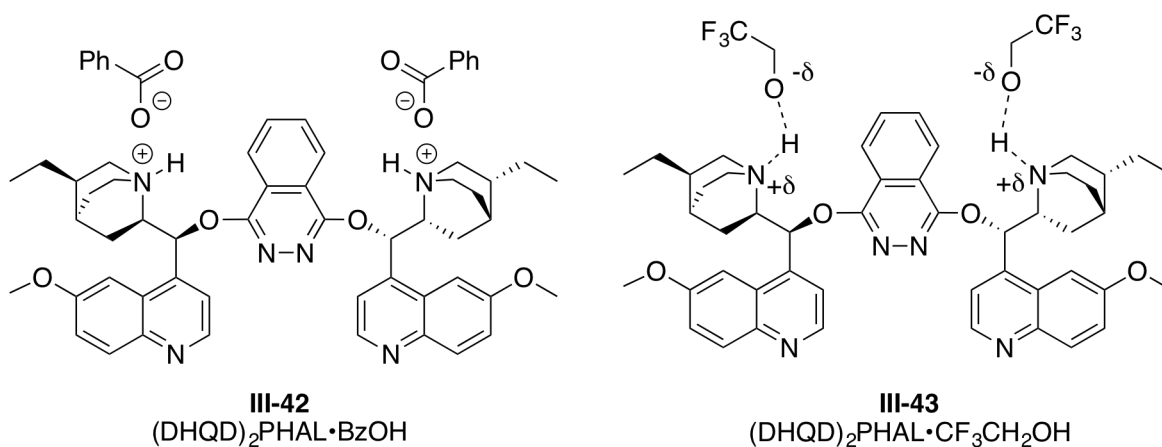
Protic additives that have strongly coordinating counteranions (such as benzoates) may prevent interaction of the amide substrates with the protonated catalyst due to the much larger binding affinity for the ion pair as opposed to a hydrogen bonded association of the amide and the catalyst (see structure **III-42** in Figure III-5). In contrast, the H-bonded complex of (DHQD)<sub>2</sub>PHAL with CF<sub>3</sub>CH<sub>2</sub>OH (see structure **III-43**) can still serve as a H-bond donor to the amide substrate.

**Table III-7.** Inhibitory effects of protic additives

| Entry | Additive                 | Conversion | <i>dr</i> (2a:3a) |
|-------|--------------------------|------------|-------------------|
| 1     | none                     | 55%        | 97:3              |
| 2     | BzOH                     | 21%        | 96:4              |
| 3     | AcOH                     | 31%        | 95:5              |
| 4     | <i>p</i> -TSA            | <1%        | nd                |
| 5     | Citric acid              | <1%        | nd                |
| 6     | <i>N</i> -Acetyl glycine | 3%         | nd                |
| 7     | <i>p</i> -Nitrophenol    | 8%         | 95:5              |

Note: Conversion was determined by crude  $^1\text{H}$  NMR and *dr* was determined by GC

**Figure III-6.** Plausible protonated forms of (DHQD)<sub>2</sub>PHAL in the presence of protic additives



In any event, the protonated catalyst can serve as a hydrogen bond donor to bind to the amide functional group (whereas the non-protonated catalyst can only serve as a hydrogen bond acceptor). These NMR studies support the hypothesis that stereodiscrimination likely results from asymmetric *general acid catalysis* (i.e. hydrogen-bonding catalysis) by protonated (DHQD)<sub>2</sub>PHAL in CF<sub>3</sub>CH<sub>2</sub>OH, although a chiral Lewis-base assisted Bronsted acid catalysis (LBBA) by CF<sub>3</sub>CH<sub>2</sub>OH cannot be ruled out at this stage.<sup>35</sup>

Numerous characteristics of enzyme-type catalysis is evident – a remarkable selectivity for binding one enantiomer of the substrate, extensive preorganization of the substrate-catalyst-reagent triad leading to rapid reaction rates for the catalyzed process for the ‘matched’ enantiomer and finally, exquisite levels of face selectivity in the delivery of the chlorenium ion on to the olefin functionality of the substrates. An in-depth analysis of the enthalpic and entropic drivers for this transformation is currently under way.

### **III.3.8. Features and utility of the resolution.**

#### **III.3.8.1. Determination of selectivity factors.**

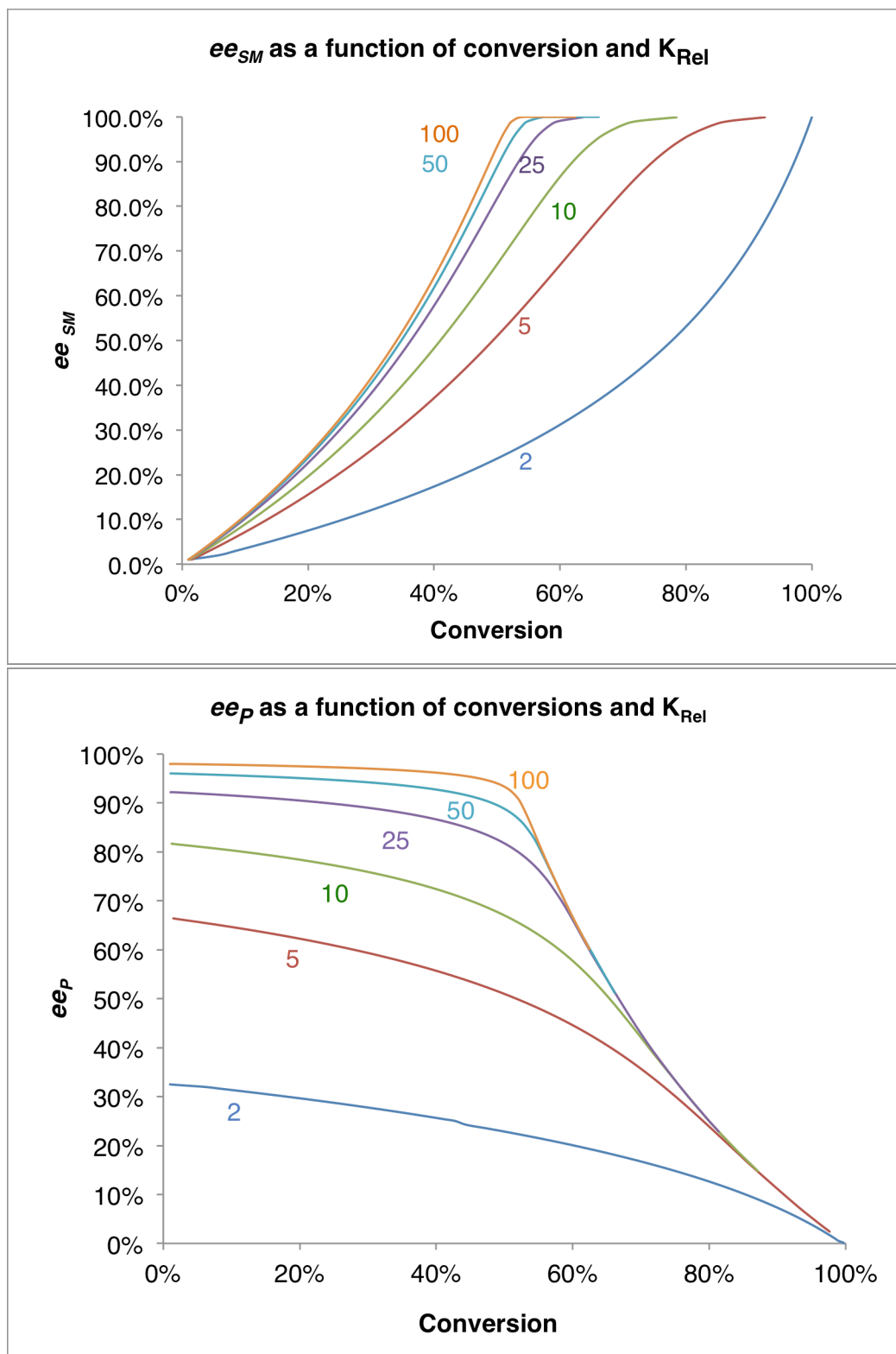
A number of aspects of this kinetic resolution warrant emphasis. Kinetic resolutions are seldom used for the synthesis of the enantioenriched products (as opposed to the unreacted substrate in enantioenriched form). This is because  $K_{Rel}$  values (selectivity factors) of ~50 are required to obtain products with >90% *ees* and in yields approaching 50%. For example, for a  $K_{Rel}$  value of 10, the theoretical maximum *ee* for the products is only ~80% even at conversions as low as 10%. At 65% conversion for the same reaction, the unreacted substrate can be recovered in 94% *ee* and 35% yield (see Figure III-6 and associated discussion).

The resolution presented here can lead to the formation of diastereomeric mixture of products. The excellent diastereo- and enantioselectivity for the cyclized products and recovered

substrates at <1 mol% catalyst loading suggests that high selectivity factors are in operation in addition to exquisite face selectivity in the chlorenium delivery. In order to quantify the efficiency of the resolution,  $K_{Rel}$  values were calculated for four of these reactions on the basis of the yields and *ees* of the cyclized products.<sup>36</sup>

A brief discussion regarding the calculation of selectivity factors and their significance is in order. The graphs shown in Figure III-6 depict  $K_{Rel}$  values as a function of conversions and *ee* of the recovered substrate and the cyclized product. As seen in the graph on the bottom, *ee* values for the cyclized products dramatically decrease at conversions exceeding 50% (this is manifested as a steep slope at higher conversions as opposed to negligible slopes at < 25% conversions). From a statistical viewpoint, a small error in the determination of conversions and/or *ees* will lead to large errors in the estimation of  $K_{Rel}$  values at higher conversions. Consequently, the results obtained at ~25% conversion was used for the determination of  $K_{Rel}$  values for selected substrates. Additionally, at less than 25% conversions, the *dr* for all reactions was at least 98:2, thereby minimizing the influence of the minor diastereomer in impacting the  $K_{Rel}$  value estimation. Furthermore, the reactions were run on 2.0 mmol scale (~0.5 g scale)  $K_{Rel}$  order to ascribe greater confidence to the isolated yields.

**Figure III-7.** Conversion-enantioselectivity- $K_{Rel}$  value correlations for substrates and products for a typical kinetic resolution reaction



The  $K_{Rel}$  values were calculated using the following formula:<sup>37</sup>

$$K_{Rel} = \ln[1 - C(1+ee_P)] / \ln[1 - C(1- ee_P)]$$

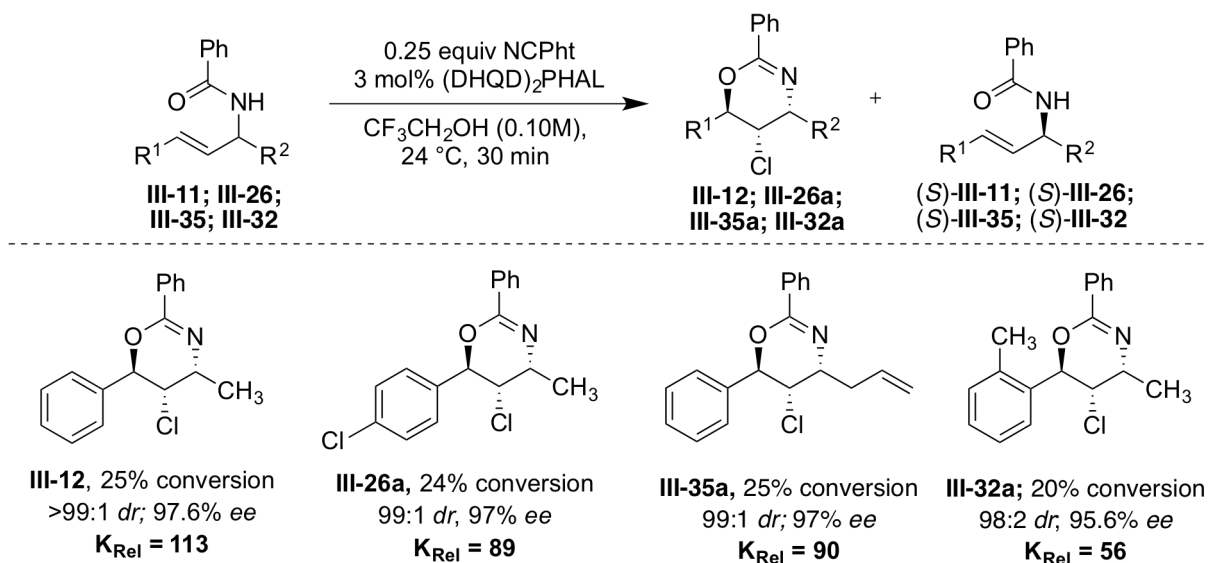
where C = conversion (isolated yield of the products was assumed to represent the conversion in order to obtain the lower limits of  $K_{Rel}$ )

and  $ee_P$  = enantiomeric excess of the cyclized product.

It must be emphasized that the derivation of the above equation assumes a first order dependence with respect to the substrate. Resolutions that proceed *via* a kinetic saturation mechanism will likely exhibit a zero-order dependence with respect to the substrate early on in the reaction and 1<sup>st</sup> order dependence as the substrate is consumed. Nonetheless, this is true in case of most kinetic resolutions (i.e. a preferential binding of one enantiomer of the racemate to a chiral catalyst). A detailed evaluation of the reaction rates and orders with respect to reactants are ongoing pursuits. Instead, the  $K_{Rel}$  value calculations presented here assume 1st order dependence in substrate.

The resolution of substrate **III-11** proceeded with a  $K_{rel}$  value of 113. Likewise,  $K_{rel}$  values of 89, 90 and 56 were calculated for substrates **III-26**, **III-35** and **III-32**, respectively. It must also be emphasized that conversions used in the calculations were based on *isolated yields* of the products on 2.0 mmol (~0.5 g) scale reactions, and therefore, the values obtained for  $K_{rel}$  represent the lower limits. As such, this kinetic resolution has the potential to *simultaneously* access the products and the substrates in highly enantioenriched form and at yields approaching 50% on a preparative scale.

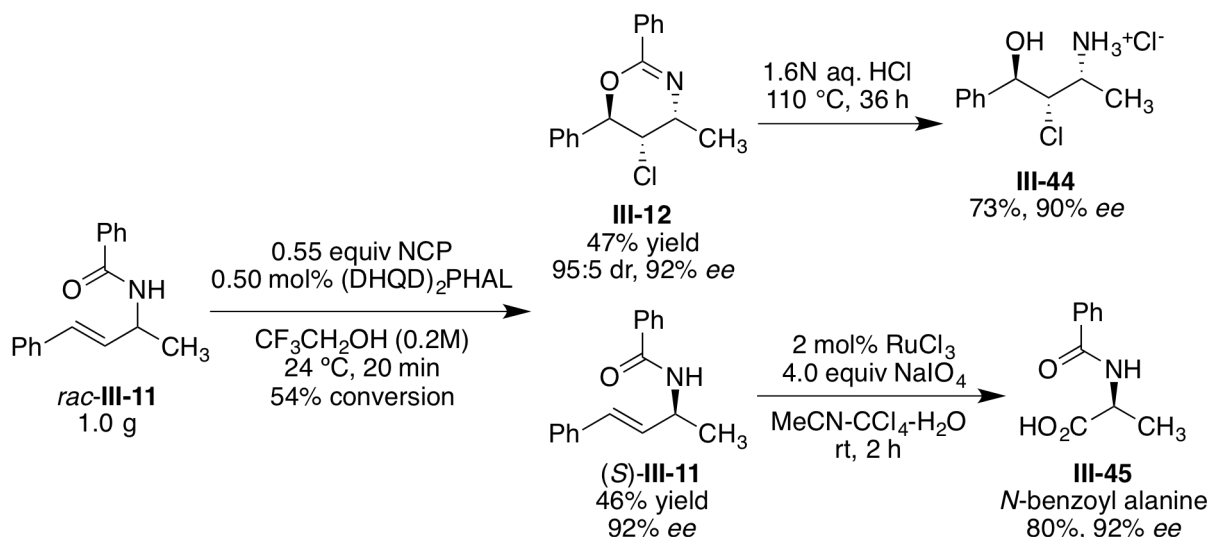
**Figure III-8.** Determination of  $K_{Rel}$  values for selected transformations



### III.3.9. Chemical transformation of products and recovered substrates.

Most of the reactions were rapid (~10 min) and run in open reaction vessels at up to 200 mM concentrations. The resolution is conveniently scaled to gram quantities with no detrimental effect on the *drs* and *ers* (Scheme III-6). Routine hydrolytic and oxidative transformations of the products and the unreacted substrates are shown in Scheme III-6. Acid hydrolysis of **III-12** gave amino alcohol **III-44**. The oxidative cleavage of the recovered olefin (*S*)-**III-11** gave protected alanine **III-45**.

### Scheme III-6. Chemical transformations of products and recovered substrates

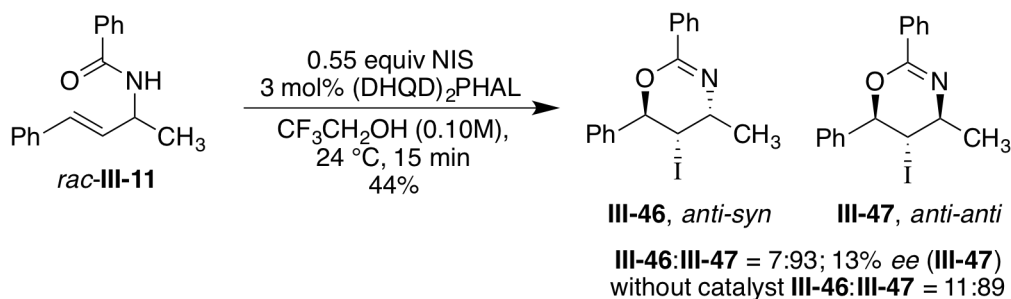


#### III.3.10. Development of a tandem kinetic resolution/diastereoselective iodocyclization cascade.

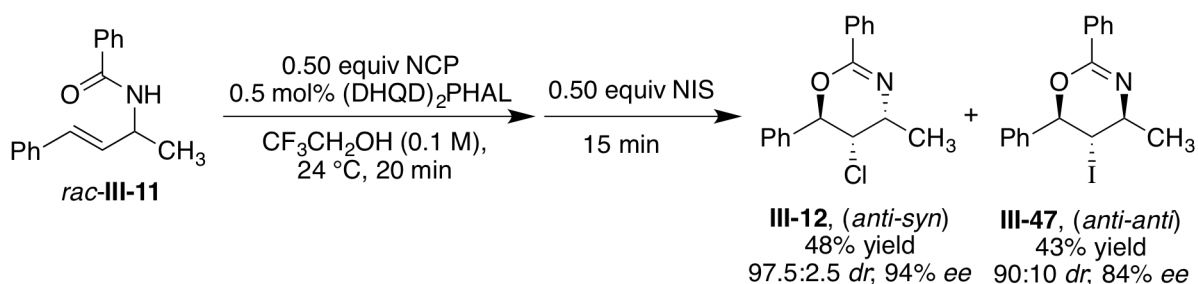
Attempts to uncover analogous kinetic resolution phenomena in iodocyclization reactions of the racemic compounds led to intriguing results. While the resolution was inefficient, the cyclization exhibited a complementary diastereoselectivity to the chlorocyclization reaction and favored the formation of the *anti-anti* diastereomer in a 93:7 ratio (Scheme III-7a).<sup>38</sup> The iodocyclized products **III-46** and **III-47** exhibited low enantioenrichment. Notably, unlike the chlorocyclization reaction, the non-catalyzed and catalyzed reactions exhibited similar levels of diastereoselectivity for the iodocyclization (89:11 *dr* without catalyst as opposed to 93:7 *dr* with catalyst). The transformation was rapid; no significant rate acceleration or change in product distribution was observed even at up to 3 mol% catalyst loadings.

**Scheme III-7.** Development of a tandem one-pot kinetic resolution/diastereoselective iodocyclization cascade

**a.** Iodocyclization of **III-11** in the presence and absence of (DHQD)<sub>2</sub>PHAL



**b.** One-pot kinetic resolution/diastereoselective iodocyclization cascade



Taken together with the complementary diastereoselectivity and negligible reagent control at ambient temperatures, a tandem one-pot kinetic resolution/diastereoselective iodocyclization cascade was conceptualized (Scheme III-7) that would allow for a 100% conversion of the racemic substrate into densely functionalized stereotriads. *rac*-**III-11** was resolved *via* a chlorocyclization reaction under optimized reaction conditions; this was followed by the addition of 0.50 equiv of NIS in to the reaction vessel to initiate the diastereoselective iodocyclization of the enantioenriched substrate. This tandem protocol gave chlorocyclized product **III-12** in 97.5:2.5 *dr* with the major *anti-syn* diastereomer being formed in 94% *ee* and the iodocyclized product **III-47** in a 90:10 *dr* with the major *anti-anti* diastereomer being formed in 84% *ee* (Scheme III-7b). Products **III-12** and **III-47** were readily separable by column chromatography and were isolated in 48% and 43% yields, respectively.

### III.3.11. Catalyst recycling studies.

The catalyst was found to be stable to the reaction conditions and was isolated using routine silica gel chromatography. The catalyst could be recycled up to three times with negligible loss in activity. After elution of the cyclized product (5% EtOAc in hexanes) and the unreacted substrate (20% EtOAc in hexanes), the column was flushed with EtOAc-MeOH-Et<sub>3</sub>N (100:10:1) to recover the catalyst. The eluent fractions containing the catalyst were concentrated *in vacuo* in a vial. The resulting gummy solid was redissolved in ~ 2 mL CH<sub>2</sub>Cl<sub>2</sub> and concentrated *in vacuo*. The residue thus obtained was left under high vacuum (~50 mtorr) for 2 hours at ambient temperature. The next reaction was run in the vial containing the recovered catalyst. No significant loss was observed in the efficiency of the kinetic resolution even after 3 recycles using the procedure outlined above.

**Table III-8.** Catalyst recycle studies

The reaction scheme shows the cyclization of *rac*-III-11 to a mixture of III-12, III-13, and (*S*)-III-11. The starting material *rac*-III-11 is a chiral auxiliary with a phenyl group, a methyl group, and a chlorine atom. The reaction conditions are 0.55 equiv NCPht, 3 mol% (DHQD)<sub>2</sub>PHAL, and CF<sub>3</sub>CH<sub>2</sub>OH (0.1M) at 24 °C for 60 min. The products are III-12, III-13, and (*S*)-III-11.

| Cycle | Conv. (Isolated yield) | dr   | ee (III-12) | ee of ( <i>S</i> )-III-11 |
|-------|------------------------|------|-------------|---------------------------|
| 1     | 55% (52%)              | 95:5 | 96%         | 92%                       |
| 2     | 53% (46%)              | 96:4 | 95%         | 84%                       |
| 3     | 50% (44%)              | 96:4 | 94%         | 83%                       |

Note: Conversion and *dr* values were determined by GC using undecane as internal std.

Taken together with the recyclability of the catalyst and solvent, this reaction paves the way for efficient, multi-gram scale synthesis of densely functionalized chiral building blocks.

### III.3.12. Attempted kinetic resolution in the bromo- and iodocyclization reactions.

If the catalyst is able to resolve the racemic compound by differential hydrogen bonding to the two enantiomers, it seemed plausible that the resolution efficiency should be independent of the halonium source. In other words, the enantioselectivity-determining step is *not* the alkene halogenation event, but is instead, the alkene-catalyst binding interaction that will presumably remain constant regardless of the stereoselectivity of the alkene functionalization event. With enantioselectivity already determined by differential hydrogen bonding affinities, the stereoselectivity of the alkene functionalization event can only affect the diastereoselectivity of the transformation but *not* the enantioselectivity; both diastereomers should be formed in exquisite enantioselectivity if there is negligible background reaction.

With this premise, analogous bromo- and iodocyclization reactions were evaluated. If the face selectivity of halonium delivery were poor with bromonium and iodonium sources, one would expect a poor diastereoselectivity but excellent enantioselectivity for both diastereomers of the cyclized product. Disappointingly, experimental results suggest otherwise. Although the bromo- and iodocyclization reactions were not accompanied by efficient resolution of the racemate, these results are provided here for the sake of completeness as well as to provide some food for mechanistic musings for this transformation regarding the qualitative differences amongst the different halocyclizations.

**Table III-9.** Attempted kinetic resolution in the bromo- and iodocyclization reactions of **III-11**

| Entry | X <sup>+</sup> source/<br>Temp., Time | Conv. | dr<br>(syn:anti) | ee<br>(syn) | ee<br>(anti) | ee of (S)-1a |
|-------|---------------------------------------|-------|------------------|-------------|--------------|--------------|
| 1     | NBS, 24 °C, 15 min                    | 55%   | 57:43            | 84%         | 6%           | 54%          |
| 2     | BCDMH, -40 °C, 30 min                 | 50%   | 62:38            | 84%         | 48%          | 65%          |
| 3     | NIS, 24 °C, 15 min                    | 44%   | 7:93             | 20%         | 7%           | nd           |

Note: Conversion and *dr* values were determined by GC using undecane as internal std

When NCP was replaced with NBS under otherwise identical optimized reaction conditions, the reaction cleanly proceeded to 55% conversion in 15 min., albeit in much lower diastereoselectivity (57:43 favoring the *anti-syn* product, see entry 1 in Table III-9). Notably, the *anti-syn* diastereomer **III-14** was formed in 84% *ee* whereas the *anti-anti* diastereomer **III-15** was found to have only 6% *ee*. The recovered substrate was moderately enantioenriched (54% *ee*). Improved results were obtained when the reaction employed 3-bromo-1-chloro-5,5-dimethylhydantoin (BCDMH) as the bromenium source. The reaction was run at -40 °C to minimize any background reaction with the significantly more reactive BCDMH (entry 2, Table III-9). A small improvement was seen in the diastereoselectivity (**III-14:III-15** = 62:38). The *anti-syn* product **III-14** had 84% *ee* whereas the *anti-anti* diastereomer has a much-improved 48% *ee*. Analogous reaction with NIS under optimized conditions gave high diastereoselectivity favoring the *anti-anti* diastereomer (**III-17:III-16** = 93:7, entry 3, Table III-9). Unfortunately, both diastereomers showed poor enantioselectivity (7% and 20% *ee*, respectively).

The lack of efficient resolution of the substrate during bromo- and iodocyclization reactions is likely attributable to the significantly faster background reaction that may outcompete any stereoselectivity of the catalyzed process leading to less predictable outcomes. This is manifested by the much-reduced reagent control in these reactions whereby the non-catalyzed and catalyzed reactions show similar diastereoselectivities unlike the chlorocyclization reactions. Alternately, one could propose that the rate-determining step for the chlorocyclization is the chloronium delivery to the alkene whereas the enantioselectivity-determining step is the substrate-catalyst binding event i.e. regardless of the rate of cyclization, the enantioselectivity is determined by the population of the [matched substrate][catalyst] concentration. In case of the bromo- and iodocyclization variant the alkene halogenation reaction may be rapid enough that both – the substrate-catalyst binding event and the halonium delivery steps can act as the rate and enantioselectivity determining steps. With more than one rate and enantioselectivity determining steps, the analysis of synergistic or antagonistic existence of these steps becomes much less straightforward.

Detailed kinetic and mechanistic investigations are required for the validation of these proposals as well as to arrive at a binding model and transition state. Quantitative reaction rate data as well as heavy atom isotope labeling studies should allow for elucidation of mechanistic nuances such as the order, molecularity and the rate determining steps for this reaction. Our lab has extensively explored these avenues in other related transformations such as the chlorolactonization reaction<sup>39</sup> and enantioselective chlorocyclization of carbamates and amides.<sup>40</sup>

### III.3.13. Limitations of the kinetic resolution protocol.

The substrate scope was one of the major limitations of this methodology. *trans*-disubstituted olefins were excellent substrates. Nonetheless, attempted resolution of a trisubstituted alkene substrate gave poor results.

Additionally, the  $\alpha$ -substituent cannot be bulky as evidenced by the poor results with substrates **III-38** ( $\alpha$ -Ph substituent) and **III-39** ( $\alpha$ -*t*-Bu substituent). NMR studies suggest that these bulky substrates do not bind well to the chiral catalyst (although quantitative values of binding constants have not been estimated as yet).

Unlike the amide chlorocyclization reaction that was tolerant of aliphatic alkene substituents, the resolution chemistry with substrates having an aliphatic substituent gave complex reaction mixtures. Spectroscopic and mass spectrometry analysis of partially purified fractions suggests that all four possible isomers (resulting from 5-*exo* and 6-*endo* cyclization and the *syn* and *anti* diastereomers for each constitutional isomer) are formed in these reactions along with products arising from the CF<sub>3</sub>CH<sub>2</sub>OH capture of the putative chloronium ion intermediate.

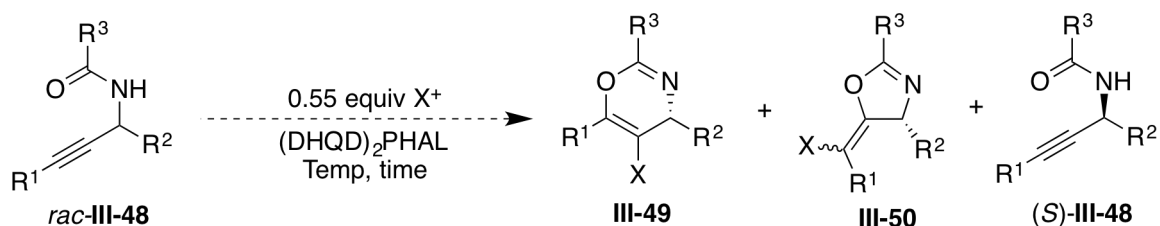
It is likely that significant improvements in terms of the substrate scope will be elusive with this catalytic system. A better understanding of the substrate-catalyst interaction (i.e. the binding model) will be crucial in enabling a rational design of a second generation of catalysts that can accommodate sterically diverse substrates.

### III.3.14. Kinetic resolution of propargyl amides in a chlorocyclization reaction.

Experimental results seem to bolster the two-stage stereoselectivity paradigm outlined in Figure III-1 for the diastereoselective kinetic resolution in the chlorocyclization of racemic allylic amides. If indeed the resolution were a direct manifestation of preferential H-bonding

interactions of the two enantiomers of the substrate, one would predict that an analogous kinetic resolution of propargyl amides should also be feasible (see Figure III-7).

**Figure III-9.** Proposed kinetic resolution of propargyl amides *via* halocyclization

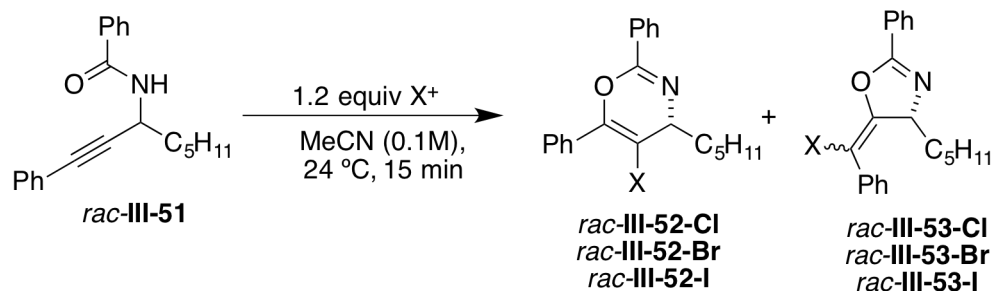


This transformation seemed plausible for numerous reasons. First, it did not seem far-fetched that H-bonding affinities of racemic propargyl amides and allylic amides for protonated Lewis bases could be similar. A matched and mismatched substrate-catalyst complex also seemed plausible with racemic compounds such as **III-48**. If successful, this will validate the hypothesis that differential hydrogen-bonding affinities alone are sufficient to promote kinetic resolution of substrates. In addition, diastereoselectivity arising due to the creation of two additional stereocenters in alkene halogenation is not an issue with analogous alkynyl substrates i.e. there is no face selectivity issue in the halogenation of alkynes indicating that only one level of stereoselection is sufficient for a kinetic resolution in this instance. The cyclized products **III-49** and **III-50** are arguably of much greater synthetic value owing to the embedded cyclic enol ether and the vinyl halide functionalities that are both easily manipulated using diverse chemistry. The only concern at the outset was the possibility of both 5-*exo*-dig and 6-*endo*-dig modes of cyclizations that could give rise to a mixture of constitutional isomers **III-49** and **III-50**.

Preliminary studies of the non-catalyzed reaction revealed that the formation of constitutional isomers was indeed a concern (see Table III-10). While the reaction of **III-51** with TCCA in MeCN was too messy to obtain reliable ratios of the two products, analogous reactions

with NBS and NIS were clean. The bromocyclization with NBS exhibited a preference for the 6-*endo*-dig cyclization over the 5-*exo*-dig cyclization by 84:16 ratio (entry 2, Table III-10). The iodocyclization exhibited practically no selectivity (entry 3, Table III-10, ~50:50).

**Table III-10.** Regioselectivity in the non-catalyzed halocyclization of **III-51**



| Entry | X <sup>+</sup> source | Conv. | rr <sup>a</sup> (III-52:III-53) |
|-------|-----------------------|-------|---------------------------------|
| 1     | TCCA                  | >95%  | nd                              |
| 2     | NBS                   | 66%   | 84:16                           |
| 3     | NIS                   | >99%  | 50:50                           |

Note: Conversion was determined by crude <sup>1</sup>H NMR analysis.

The cyclized products were fairly unstable if left neat on the bench top and chromatographic purification must be performed rapidly. The products could be stored in the refrigerator as solutions in CH<sub>2</sub>Cl<sub>2</sub> or CHCl<sub>3</sub> under Ar (~95% assay after 5 days).

**Table III-11.** Kinetic resolution of **III-51** via halocyclization

| Entry | X <sup>+</sup> source, temp | Conv. | III-52:III-53 | III-54 | ee (III-52) | ee (S)-III-51 |
|-------|-----------------------------|-------|---------------|--------|-------------|---------------|
| 1     | DCDMH, -40 °C               | 55%   | 95:5          | 12%    | 70%         | >99%          |
| 2     | NCP, 24 °C                  | 53%   | >99:1         | 6%     | 88%         | 97%           |
| 3     | NBS, -40 °C                 | 50%   | 96:4          | 7%     | 38%         | 32%           |
| 4     | DBDMH, -40 °C               | 84%   | 96:4          | 10%    | nd          | nd            |

Note: Conversion and product ratios were determined by crude NMR analysis using MTBE as internal standard.

This was followed by exposing substrate **III-51** to conditions optimized for the kinetic resolution of allylic amides (see Table III-11). Gratifyingly, the chlorocyclization reaction proceeded with excellent regio- and enantioselectivity (see **III-51** to **III-52-Cl** in Table III-11) for the cyclized product as well as for the recovered substrate. In the event, the reaction with 0.55 equiv of DCDMH at -40 °C gave the cyclized product in 95:5 regioselectivity (**III-52-Cl**:**III-53-Cl**) and 70% *ee* (entry 1, Table 7). The unreacted substrate was recovered in >99% *ee*. The reaction with NCP at ambient temperature afforded much better results (entry 2, Table III-11,

>99:1 *rr*, 88% *ee* for the major regioisomer and 97% *ee* for recovered substrate at 53% conversion). The analogous bromocyclization with NBS, although highly regioselective (96:4 *rr*), proceeded with much diminished enantioselectivity for the product (38% *ee*) and the recovered substrate (32% *ee* at 50% conversion, entry 3, Table III-11) even at -40 °C. 1,3-dibromo-5,5-dimethyl hydantoin (DBDMH) was found to be too reactive; the reaction was 84% complete in 15 minutes even when only 0.50 equiv of DBDMH was employed indicating that both bromine atoms are viable electrophiles under the reaction conditions (entry 4, Table III-11).

It merits mention that all reactions were accompanied by the formation of variable amounts of a haloether side-product (see structure **III-54** in Table III-11) that was characterized by <sup>1</sup>H and <sup>13</sup>C NMR and LC-MS analysis. Surprisingly, this enol-ether compound was stable to SiO<sub>2</sub> gel column chromatography. The origin of this product can be attributed to the capture of the putative halirenium intermediate by CF<sub>3</sub>CH<sub>2</sub>OH (the reaction solvent). The stereochemistry of this side-product is yet to be established. Nonetheless, **III-54-CI** was formed in >90% *ee* indicating that kinetic resolution of the racemic substrate is viable even for an *intermolecular* capture of the chlorenium activated alkyne. If optimized to proceed exclusively via an intermolecular capture of the putative halirenium ion, this will represent an attractive methodology to access stereodefined tri- and tetrasubstituted chiral enol ethers – a non-trivial challenge in organic chemistry.<sup>41</sup> The assignment of the absolute stereochemistry of the products and recovered substrates shown in Table III-11 is tentative; it was assumed that the *R*-enantiomer of the substrate would react preferentially when (DHQD)<sub>2</sub>PHAL was used as the catalyst as was observed in the allyl amide chlorocyclization. Conclusive evidence for the absolute stereochemistry of the products by crystallographic methods or chemical transformations is yet to be uncovered. Further optimizations and substrate scope evaluations

are currently under way in a collaborative effort with Ms. Yi Yi (a current graduate student in our lab).

### III.3.15. Desymmetrization of meso dienes via chlorocyclization.

Having tasted success with kinetic resolution of racemic amides, attention was then turned to extending this chemistry to desymmetrization reactions. Diastereoselective desymmetrization of dienes via halocyclization reactions finds ample precedence in literature.<sup>42</sup> Catalytic enantioselective variants on the other hand are yet to witness much success. Under the premise that (DHQD)<sub>2</sub>PHAL may enable such a transformation, the meso compound III-55 was exposed to conditions similar to that used for the kinetic resolution reaction. In the presence of 10 mol% of (DHQD)<sub>2</sub>PHAL and 1.1 equiv of NCP, the reaction afforded the cyclized product III-56 in good diastereoselectivity (>9:1 *dr*) and enantioselectivity (89% *ee*). The low isolated yield is attributed to the reactivity of the alkene functionality in the product that leads to the formation of by-products (see next section for a description and characterization of the by-products). The relative and absolute stereochemistry of **III-56** was established by single crystal XRD and was consistent with those seen for the products of the kinetic resolution chemistry (i.e. formation of the *anti-syn* diastereomer as the major product and a-face selective chlorenium ion delivery).

**Scheme III-8.** Preliminary result of desymmetrization of **III-55** via chlorocyclization

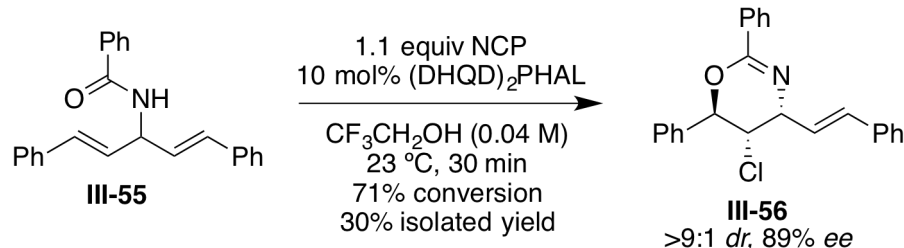
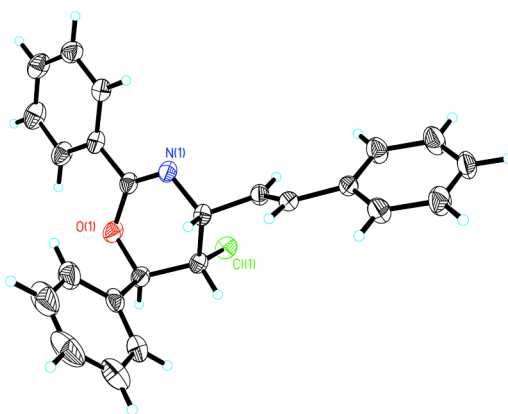


**Figure III-10.** Crystal structure of **III-56**

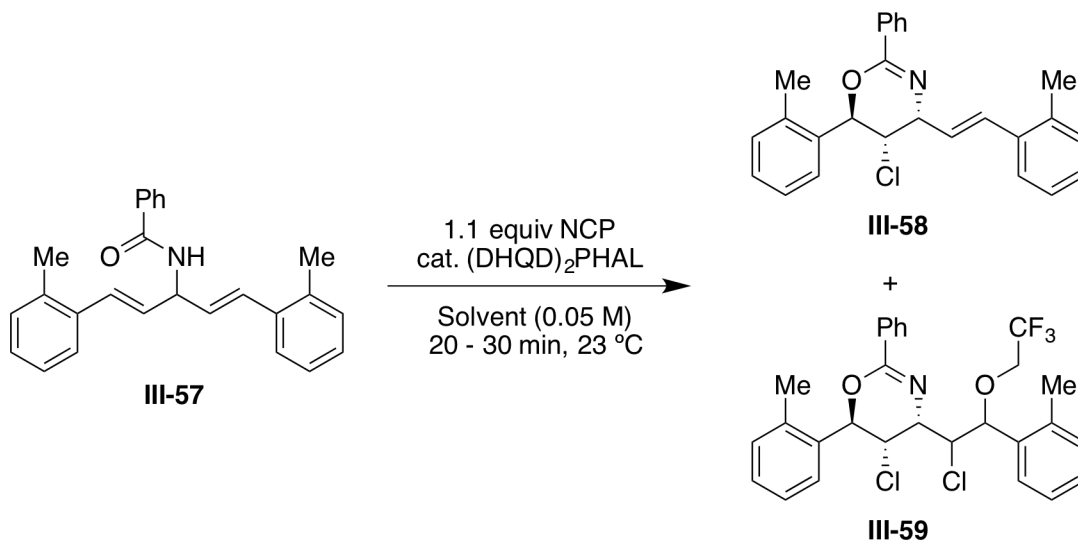


Encouraged by this first unoptimized run, a brief survey of conditions to improve the yield and enantioselectivity was undertaken with substrate **III-57** (the choice of this substrate was governed by the ease in analysis of the products by HPLC as well as a higher yielding synthetic route to **III-57**).

Catalyst loading had a negligible impact on the outcome of the reaction; 2.5 mol% catalyst loading gave practically identical results as a 10 mol% loading (>95:5 *dr*, 90% *ee* and comparable yields; compare entries 1 and 2 in Table III-12). Variable amounts of the chloroether side-product **III-59** was also seen in all these reactions indicating that the product is unstable to the reaction conditions and that CF<sub>3</sub>CH<sub>2</sub>OH can add into the chloronium ion derived from **III-58**. In an attempt to reduce the formation of **III-59**, the less nucleophilic HFIP was

incorporated as a co-solvent (see entries 3 and 4 in Table III-12). While a 3:1 TFE:HFIP had a negligible impact on the product distribution or stereoselectivity (entry 3), a 1:1 co-solvent mixture gave an improved 63% yield for the desired product and a reduced 5% yield of **III-59**. Nonetheless, this latter result came at the expense of compromising the diastereoselectivity of the product (89:11 *dr*, 90% *ee*). Not surprisingly, when the reaction was run in HFIP as the solvent, the *dr* value was significantly eroded (66:34); the major diastereomer was still formed in 91% *ee* (entry 5, Table III-12). A 9:1 co-solvent mixture of TFE-MeCN gave high diastereoselectivity (93:7 *dr*), but the product was formed in only 40% *ee* (entry 6, Table III-12) indicating that TFE or HFIP was crucial for getting high enantioselectivity for the product. Finally, the use of substoichiometric quantities of NCP in an effort to minimize the formation of **III-59** from **III-58** led to a promising 78% yield for the desired product (based on 75% conversion of substrate; see entry 7, Table III-12). More importantly, the diastereo- and enantioselectivity of the product was excellent (>95:5 *dr* and 92% *ee* for **III-58**) and only trace quantity of **III-59** was observed. It is likely that other measures such as gradual/syringe pump addition of NCP will lead to even better results. These studies are ongoing.

**Table III-12.** Preliminary optimization for the desymmetrization of **III-57**



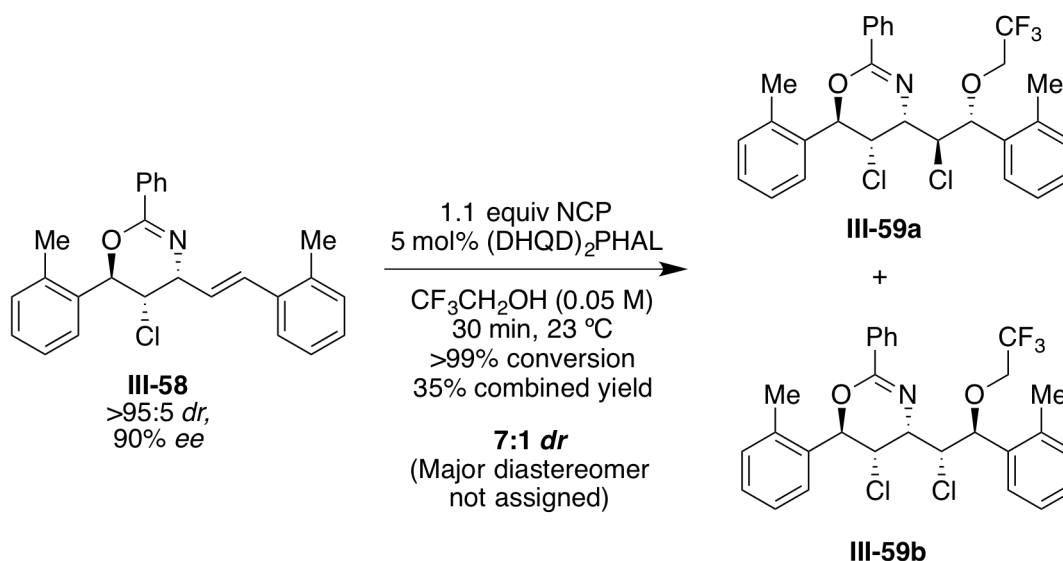
| Entry | Catalyst loading | Solvent                               | Yield (III-58) | <i>dr, ee</i> (III-58) | Yield (III-59) |
|-------|------------------|---------------------------------------|----------------|------------------------|----------------|
| 1.    | 10 mol%          | TFE                                   | 53%            | >95:5, 90% <i>ee</i>   | 6%             |
| 2.    | 2.5 mol%         | TFE                                   | 48%            | >95:5, 90% <i>ee</i>   | 10%            |
| 3.    | 5 mol%           | 3:1 TFE -HFIP                         | 47%            | >95:5, 92% <i>ee</i>   | 13%            |
| 4.    | 5 mol %          | 1:1 TFE -HFIP                         | 63%            | 89:11, 90% <i>ee</i>   | 5%             |
| 5.    | 10 mol%          | HFIP (0 °C, 10 min)                   | 58% (brsm)     | 66:34, 91% <i>ee</i>   | nd             |
| 6.    | 10 mol%          | 9:1 TFE-MeCN                          | 37%            | 93:7, 40% <i>ee</i>    | nd             |
| 7.    | 5 mol%           | TFE (0.75 equiv<br>NCP, 0 °C, 10 min) | 71% (brsm)     | >95:5, 92% <i>ee</i>   | <5%            |

Note: Conversion, yield and *dr* values were determined by crude  $^1\text{H}$  NMR analysis with

MTBE as added external standard; brsm = based on recovered starting material

When **III-58** was isolated and exposed to the reaction conditions, **III-59** was isolated as the major product in a moderate 7:1 *dr* (the major diastereomer has not been assigned as yet). Numerous side products were also formed in this reaction (and hence **III-59** was isolated in only 35% yield even at 100% conversion). The isolation and complete characterization of these side-products has not been undertaken as yet.

**Scheme III-9.** Fate of **III-58** under reaction conditions



#### III.4. Conclusion and future directions.

The first example of a highly diastereoselective kinetic resolution in a chlorofunctionalization reaction of olefins was developed. Two distinct and highly stereoselective events mediated by the *same* catalyst are crucial to the success of this reaction. The catalyst not only ensures rate acceleration for one of the two enantiomers of a chiral substrate, but also serves to impart exceptional stereoselectivity in the alkene chlorination and cyclization events resulting in stereotriad products with excellent relative and absolute stereocontrol starting from easily accessed racemic starting materials. Low catalyst loadings, ambient reaction temperatures, open reaction vessels, short reaction times and recyclability of the catalyst are

some of the features of this chemistry. The  $K_{rel}$  values for many substrates are sufficiently high to permit the use of the resolution protocol for the simultaneous synthesis of products and substrates in highly enantioenriched form.

NMR studies have uncovered a substrate-catalyst hydrogen-bonding interaction as a potentially key molecular recognition event in enabling the resolution; these studies have also hinted at the transformation of a chiral Lewis base catalyst into a hydrogen-bonding catalyst in  $CF_3CH_2OH$ , thereby opening the doors to hitherto unknown modes of activation for this class of catalyst. Attempts to elucidate the binding constants for the two enantiomers with the chiral catalyst using NMR titration experiments (Jobs plot of continuous variations) have not been reliable. The relatively small chemical shifts with respect to the line widths of the peaks have cast serious doubts on the reliability of these estimations i.e. the errors associated with each measurement are large. Although alternate NMR methods such as DOSY could be used for determination of association constants, coupling these experiments to no-D NMR protocols in  $CF_3CH_2OH$  presents practical challenges in suppressing the solvent signals. An alternate approach involving isothermal calorimetry (ITC) could potentially serve us better in accurately estimating the binding constants.

The conditions optimized for the kinetic resolution of allyl amides have been tweaked to allow for efficient resolution of propargyl amides as well as desymmetrization reactions of *meso*-dienes in halocyclization reactions. A detailed substrate scope analysis and mechanistic studies are currently under way for these newly discovered reactions.

### **III.5. Acknowledgements.**

Ms. Heather Pillsbury and Ms. Yanmen Yang are thanked for the experimental assistance in the synthesis of some of the substrates reported in this chapter. Dr. Ramin Vismeh is acknowledged for running HR-MS analyses for most of the compounds presented in

this chapter. Thanks are also due to Dr. Daniel Holmes who assisted in setting up No-D  $^1\text{H}$  NMR experiments for analyzing the substrate-catalyst interactions in  $\text{CF}_3\text{CH}_2\text{OH}$  and other non-deuterated solvents.

### III.6. Experimental section.

#### III.6.1. General information.

All reagents were purchased from commercial sources and were used without purification. THF and Et<sub>2</sub>O were freshly distilled from Na-benzophenone ketyl whereas CH<sub>2</sub>Cl<sub>2</sub> and PhCH<sub>3</sub> were distilled over CaH<sub>2</sub>. Trifluoroethanol (>99%) and hexafluoroisopropanol (>99.5%) were purchased from Aldrich or Synquest Labs, stored over 3Å molecular sieves and used without further purification. TLC analyses were performed on silica gel plates (pre-coated on glass; 0.20 mm thickness with fluorescent indicator UV<sub>254</sub>) and were visualized by UV, I<sub>2</sub> complex formation or charring in anisaldehyde or PMA stains. <sup>1</sup>H and <sup>13</sup>C NMR spectra were collected on 300, 500 or 600 MHz NMR spectrometers (VARIAN INOVA) using CDCl<sub>3</sub>, or CD<sub>3</sub>CN. Chemical shifts are reported in parts per million (ppm) and are referenced to residual solvent peaks. Flash silica gel (32-63 mm, Silicycle 60 Å) was used for column chromatography. Enantiomeric excess for all products was determined by HPLC analysis using DAICEL CHIRALCEL<sup>®</sup> OJ-H and OD-H or CHIRALPAK<sup>®</sup> AS-H and AD-H columns. Diastereomeric ratios were determined by GC and/or crude NMR analysis. Optical rotations were measured in chloroform. All known compounds were characterized by <sup>1</sup>H and <sup>13</sup>C NMR and are in complete agreement with samples reported elsewhere. All new compounds were characterized by <sup>1</sup>H and <sup>13</sup>C NMR, HRMS, optical rotation, and melting point (where appropriate). The absolute stereochemistry of **III-12**, **III-13** and **III-44** was determined by single crystal X-ray diffraction (CCDC 948806-948807 are the Cambridge Structural Database deposition numbers for the crystal structures of **III-12** and **III-13**) and was inferred analogously for the other cyclized products. The absolute stereochemistry of

**III-11** was established by comparison of optical rotation to reported values and was inferred analogously for unreacted substrates.

### **III.6.2. General procedure for screening and optimization of kinetic resolution.**

A 5 mL glass vial equipped with a magnetic stir bar was charged with the substrate (0.15 mmol, 1.0 equiv) and dissolved in a stock solution of (DHQD)<sub>2</sub>PHAL in CF<sub>3</sub>CH<sub>2</sub>OH (1.5 mL of a 0.39 mg/mL solution, 0.58 mg catalyst, 0.005 equiv). The vial was capped and the resulting suspension was stirred at ambient temperature till all the solids had completely dissolved. This was followed by the addition of *N*-chlorophthalimide (15.0 mg, 0.08 mmol, 0.55 equiv) in a single portion. The vial was capped and the reaction was stirred at ambient temperature for 60 min. The reaction was then quenched with saturated aqueous Na<sub>2</sub>SO<sub>3</sub> solution (3.0 mL) and extracted with CH<sub>2</sub>Cl<sub>2</sub> (3 x 2 mL). The combined organics were washed with brine and then dried over anhydrous Na<sub>2</sub>SO<sub>4</sub> and filtered. Conversions and yields were initially determined by GC analysis of the crude reaction mixture (A standard curve for each substrate was obtained with undecane as internal standard; see below for a detailed procedure). Pure products and unreacted substrates were subsequently isolated using column chromatography on silica gel as stationary phase (EtOAc-Hexanes gradient). Isolated yields and GC yields were in good agreement for all substrates; isolated yield of the products was used as conversion for calculation of selectivity factors.

### **III.6.3. General procedure for kinetic resolution of unsaturated amides for substrate scope evaluation.**

The procedures detailed above were followed except all reagents were scaled to 0.50 mmol of substrate.

(Note: Reactions were run in disposable screw-capped vials with no special efforts to maintain anhydrous or inert atmosphere conditions. Practically identical results were obtained when anhydrous solvents were used under an inert atmosphere of Ar gas).

### III.6.4. Characterization of cyclized products.

**III-12:** (4*R*,5*S*,6*R*)-5-chloro-4-methyl-2,6-diphenyl-5,6-dihydro-4*H*-1,3-oxazine

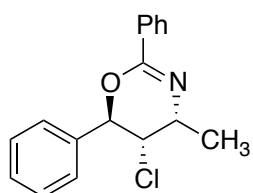
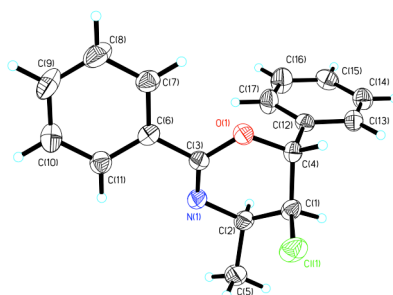


**Figure III-11.** Crystal structure of **III-12**



White solid; M.P.: 102 – 108 °C;  $R_f$  : 0.23 (5% EtOAc in hexanes, UV)

$^1\text{H}$  NMR (500 MHz,  $\text{CDCl}_3$ )  $\delta$  8.03 (d,  $J$  = 8.0 Hz, 2H), 7.47 – 7.44 (m, 1H), 7.41 – 7.33 (m, 5H), 7.31 – 7.29 (m, 2H), 5.56 (d,  $J$  = 4.5 Hz, 1H), 4.31 (dd,  $J$  = 7.0 Hz, 4.5 Hz, 1H), 3.76 – 3.72 (m, 1H), 1.39 (d,  $J$  = 7.0 Hz, 3H);  $^{13}\text{C}$  NMR (125 MHz,  $\text{CDCl}_3$ )  $\delta$  153.2, 138.4, 132.9, 130.8, 128.9, 128.7, 128.2, 127.4, 125.6, 79.6, 59.5, 47.6, 19.4

Resolution of enantiomers: DAICEL Chiralcel<sup>®</sup> OJ-H column, 5% IPA-Hexanes, 1.0 mL/min, 254 nm, RT1 (minor) = 12.8 min, RT2 (major) = 18.4 min

HRMS analysis (ESI): Calculated for (M+H): C<sub>17</sub>H<sub>17</sub>ClNO: 286.0999; Found: 286.1004

$[\alpha]_D^{20} = +13.4$  (c 1.0, CHCl<sub>3</sub>, 94% ee)

Absolute stereochemistry was determined by single crystal X-ray diffraction (XRD). Crystals for XRD were obtained by crystallization from HPLC grade hexanes in a silicone-coated vial.

**III-13:** (4*S*,5*S*,6*R*)-5-chloro-4-methyl-2,6-diphenyl-5,6-dihydro-4*H*-1,3-oxazine

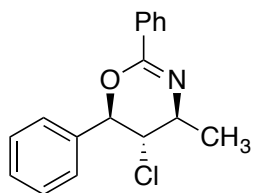
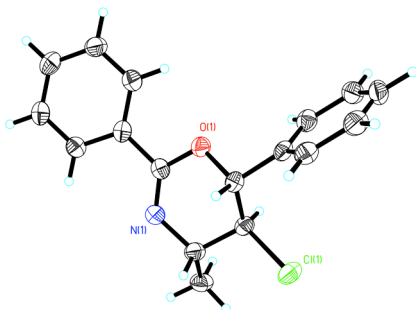


**Figure III-12.** Crystal structure of **III-13**



White solid; M.P.: 130 – 136 °C; R<sub>f</sub>: 0.32 (5% EtOAc in hexanes, UV)

<sup>1</sup>H NMR (500 MHz, CDCl<sub>3</sub>) δ 7.92 (d, *J* = 7.5 Hz, 2H), 7.46 – 7.40 (m, 6H), 7.34 (t, *J* = 7.5 Hz, 2H), 5.08 (d, *J* = 10.5 Hz, 1H), 3.88 – 3.82 (m, 1H), 3.74 (t, *J* = 10.0 Hz, 1H), 1.51 (d, *J* = 6.5 Hz, 3H); <sup>13</sup>C NMR (125 MHz, CDCl<sub>3</sub>) δ 136.8, 130.9, 129.1, 128.9, 128.5, 128.1, 127.7, 127.5, 125.6, 80.7, 61.9, 56.9, 20.7

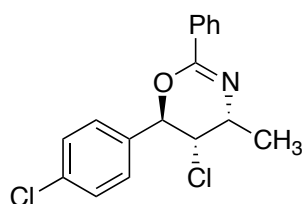
Resolution of enantiomers: DAICEL Chiralcel<sup>®</sup> OJ-H column, 5% IPA-Hexanes, 1.0 mL/min, 254 nm, RT1 (major) = 6.3 min, RT2 (minor) = 8.8 min

$[\alpha]_D^{20} = +17.2$  (c 1.0,  $\text{CHCl}_3$ , 96% *ee*)

HRMS analysis (ESI): Calculated for (M+H):  $\text{C}_{17}\text{H}_{17}\text{ClNO}$ : 286.0999; Found: 286.1003

Absolute stereochemistry was determined by single crystal X-ray diffraction (XRD). Crystals for XRD were obtained by crystallization from  $\text{CHCl}_3$  layered with hexanes in a silicone-coated vial.

**III-26-A**, (4R,5S,6R)-5-chloro-6-(4-chlorophenyl)-4-methyl-2-phenyl-5,6-dihydro-4H-1,3-oxazine



$R_f$  : 0.25 (5% EtOAc in hexanes, UV)

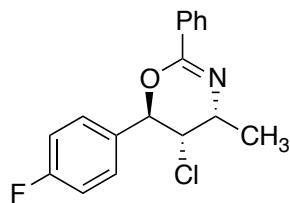
$^1\text{H}$  NMR (500 MHz,  $\text{CDCl}_3$ )  $\delta$  8.00 (d,  $J = 8.0$  Hz, 2H), 7.45 (dd,  $J = 8.5, 1.5$  Hz, 1H), 7.34 – 7.41 (m, 4H), 7.25 (d,  $J = 8.0$  Hz, 2H), 5.48 (d,  $J = 5.0$  Hz, 1H), 4.24 (dd,  $J = 5.0, 4.0$  Hz, 1H), 3.71 – 3.77 (m, 1H), 1.40 (d,  $J = 6.5$  Hz, 3H);  $^{13}\text{C}$  NMR (125 MHz,  $\text{CDCl}_3$ )  $\delta$  153.1, 136.8, 134.7, 132.6, 130.9, 129.1, 128.2, 127.4, 127.3, 78.7, 59.1, 48.1, 19.1

HRMS analysis (ESI): Calculated for (M+H):  $\text{C}_{17}\text{H}_{16}\text{Cl}_2\text{NO}$  320.0609; Found: 320.0610

Resolution of enantiomers: DAICEL Chiralcel<sup>®</sup> OJ-H column, 230 nm, 2% IPA-Hexanes, 0.7 mL/min, 254 nm, RT1 (minor) = 31.2 min, RT2 (major) = 37.7 min.

$[\alpha]_D^{20} = +3.2$  (c 1.0,  $\text{CHCl}_3$ , 90% *ee*)

**III-27-A**, (4R,5S,6R)-5-chloro-6-(4-fluorophenyl)-4-methyl-2-phenyl-5,6-dihydro-4H-1,3-oxazine



R<sub>f</sub> : 0.20 (5% EtOAc in hexanes, UV)

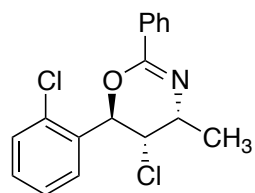
<sup>1</sup>H NMR (500 MHz, CDCl<sub>3</sub>) δ 8.00 (d, *J* = 8.0 Hz, 2H), 7.45 (dd, *J* = 7.0, 1.5 Hz, 1H), 7.37 – 7.40 (m, 2H), 7.27 – 7.30 (m, 2H), 7.06 – 7.10 (m, 2H), 5.49 (d, *J* = 5.0 Hz, 1H), 4.25 (dd, *J* = 5.0, 3.5 Hz, 1H), 3.74 – 3.78 (m, 1H), 1.40 (d, *J* = 7.0 Hz, 3H); <sup>13</sup>C NMR (125 MHz, CDCl<sub>3</sub>) δ 162.8 (d, <sup>1</sup>*J*<sub>C-F</sub> = 246.2 Hz), 153.2, 134.1 (d, <sup>4</sup>*J*<sub>C-F</sub> = 3.3 Hz), 130.9, 128.2, 127.7 (d, <sup>3</sup>*J*<sub>C-F</sub> = 8.3 Hz), 127.4, 115.8 (d, <sup>2</sup>*J*<sub>C-F</sub> = 21.8 Hz), 78.7, 59.3, 48.1, 19.13

HRMS analysis (ESI): Calculated for (M+H): C<sub>17</sub>H<sub>16</sub>ClFNO: 304.0904; Found: 304.0906

Resolution of enantiomers: DAICEL Chiralcel<sup>®</sup> OJ-H column, 5% IPA-Hexanes, 0.7 mL/min, 254 nm, RT1 (minor) = 21.6 min, RT2 (major) = 36.7 min.

[α]<sub>D</sub><sup>20</sup> = +3.9 (c 1.0, CHCl<sub>3</sub>, 87% *ee*)

**III-28-A,** (4R,5S,6R)-5-chloro-6-(2-chlorophenyl)-4-methyl-2-phenyl-5,6-dihydro-4H-1,3-oxazine



R<sub>f</sub> : 0.20 (5% EtOAc in hexanes, UV)

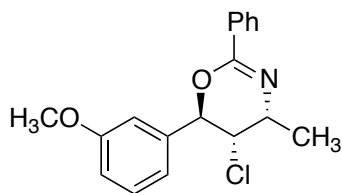
$^1\text{H}$  NMR (500 MHz,  $\text{CDCl}_3$ )  $\delta$  8.04 (d,  $J = 7.5\text{Hz}$ , 2H), 7.46 (dddd,  $J = 7.5, 7.5, 2.0, 2.0$  Hz, 1H), 7.38 – 7.43 (m, 3H), 7.25 – 7.32 (m, 3H), 5.92 (d,  $J = 3.0$  Hz, 1H), 4.46 (t,  $J = 3.0$  Hz, 1H), 3.64 – 3.69 (m, 1H), 1.39 (d,  $J = 7.0\text{Hz}$ , 3H);  $^{13}\text{C}$  NMR (125 MHz,  $\text{CDCl}_3$ )  $\delta$  153.2, 135.9, 132.7, 131.5, 130.9, 130.05, 130.00, 128.2, 127.5, 127.4, 127.0, 78.2, 57.2, 46.9, 19.8

HRMS analysis (ESI): Calculated for (M+H):  $\text{C}_{17}\text{H}_{16}\text{Cl}_2\text{NO}$ : 320.0609; Found: 320.0611

Resolution of enantiomers: DAICEL Chiralcel<sup>®</sup> OJ-H column, 10% IPA-Hexanes, 0.7 mL/min, 254 nm, RT1 (minor) = 14.7 min, RT2 (major) = 30.0 min.

$[\alpha]_{\text{D}}^{20} = +3.9$  (c 1.0,  $\text{CHCl}_3$ , 93% *ee*)

**III-29-A,** (4*R*,5*S*,6*R*)-5-chloro-6-(3-methoxyphenyl)-4-methyl-2-phenyl-5,6-dihydro-4*H*-1,3-oxazine



Colorless film;  $R_f$  : 0.39 (10% EtOAc in hexanes, UV)

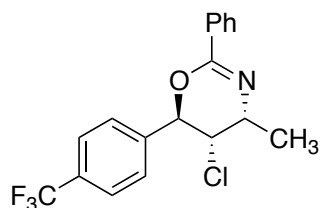
$^1\text{H}$  NMR (500 MHz,  $\text{CDCl}_3$ )  $\delta$  8.02 (d,  $J = 7.5$  Hz, 2H), 7.45 (dddd,  $J = 7.0, 7.0, 2.0, 2.0$  Hz, 1H), 7.41 – 7.37 (m, 2H), 7.30 (t,  $J = 7.5$  Hz, 1H), 6.89 – 6.86 (m, 2H), 6.82 (t,  $J = 2.0$  Hz, 1H), 5.52 (d,  $J = 4.5$  Hz, 1H), 4.30 (dd,  $J = 4.5, 4.0$  Hz, 1H), 3.77 (s, 3H), 3.76 – 3.71 (m, 1H), 1.38 (d,  $J = 6.5$  Hz, 3H);  $^{13}\text{C}$  NMR (125 MHz,  $\text{CDCl}_3$ )  $\delta$  160.0, 153.2, 140.0, 132.9, 130.8, 130.0, 128.2, 127.4, 117.8, 113.8, 111.6, 79.6, 59.4, 55.3, 47.6, 19.4

HRMS analysis (ESI): Calculated for (M+H):  $\text{C}_{18}\text{H}_{19}\text{Cl NO}_2$ : 316.1104; Found: 316.1107

Resolution of enantiomers: DAICEL Chiralpak<sup>®</sup> AD-H column 3% IPA-Hexanes, 0.7 mL/min, 254 nm, RT1 (major) = 12.1 min, RT2 (minor) = 13.1 min.

$[\alpha]_D^{20} = +8.7$  (c 1.0, CHCl<sub>3</sub>, 97% ee)

**III-30-A**, (4R,5S,6R)-5-chloro-4-methyl-2-phenyl-6-[4-(trifluoromethyl)phenyl]-5,6-dihydro-4H-1,3-oxazine



R<sub>f</sub> : 0.25 (5% EtOAc in hexanes, UV)

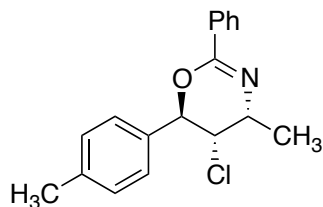
<sup>1</sup>H NMR (500 MHz, CDCl<sub>3</sub>) δ 8.01 (d, *J* = 8.5 Hz, 2H), 7.66 (d, *J* = 8.5 Hz, 2H), 7.47 – 7.44 (m, 3H), 7.42 – 7.38 (m, 2H), 5.56 (d, *J* = 5.5 Hz, 1H), 4.28 (dd, *J* = 5.5, 4.0 Hz, 1H), 3.77 – 3.72 (m, 1H), 1.41 (d, 6.5 Hz, 3H); <sup>13</sup>C NMR (125 MHz, CDCl<sub>3</sub>) δ 152.9, 142.1 (q, <sup>4</sup>*J*<sub>C-F</sub> = 1.2 Hz), 132.5, 131.04 (q, <sup>2</sup>*J*<sub>C-F</sub> = 32.6 Hz), 131.02, 128.2, 127.4, 126.4, 125.9 (q, <sup>3</sup>*J*<sub>C-F</sub> = 3.9 Hz), 123.8 (q, <sup>1</sup>*J*<sub>C-F</sub> = 270.4 Hz), 78.7, 58.9, 48.2, 19.1

HRMS analysis (ESI): Calculated for (M+H): C<sub>18</sub>H<sub>16</sub>ClF<sub>3</sub>NO: 354.0873; Found: 354.0875

Resolution of enantiomers: DAICEL Chiralcel<sup>®</sup> OJ-H column, 3% IPA-Hexanes, 0.5 mL/min, 254 nm, RT1 (minor) = 22.6 min, RT2 (major) = 26.2 min.

$[\alpha]_D^{20} = -6.3$  (c 1.0, CHCl<sub>3</sub>, 92% ee)

**III-31-A**, (4R,5S,6R)-5-chloro-4-methyl-2-phenyl-6-(*p*-tolyl)-5,6-dihydro-4H-1,3-oxazine



R<sub>f</sub> : 0.25 (5% EtOAc in hexanes, UV)

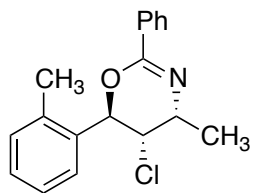
<sup>1</sup>H NMR (500 MHz, CDCl<sub>3</sub>) δ 8.02 (d, *J* = 8.0 Hz, 2H), 7.45 – 7.43 (m, 1H), 7.40 – 7.37 (m, 2H), 7.10 (br s, 4H), 5.51 (d, *J* = 4.5 Hz, 1H), 4.27 (dd, *J* = 4.5, 4.0 Hz, 1H), 3.78 – 3.72 (m, 1H), 2.34 (s, 3H), 1.39 (d, *J* = 6.5 Hz, 3H); <sup>13</sup>C NMR (125 MHz, CDCl<sub>3</sub>) δ 153.4, 138.6, 135.5, 132.9, 130.8, 129.5, 128.2, 127.4, 125.6, 79.6, 59.6, 47.7, 21.1, 19.3

HRMS analysis (ESI): Calculated for (M+H): C<sub>18</sub>H<sub>19</sub>ClNO 300.1155; Found: 300.1157

Resolution of enantiomers: DAICEL Chiralcel<sup>®</sup> OJ-H column, 10% IPA-Hexanes, 0.7 mL/min, 254 nm, RT1 (minor) = 18.7 min, RT2 (major) = 32.8 min

[α]<sub>D</sub><sup>20</sup> = +11.3 (c 1.0, CHCl<sub>3</sub>, 64% ee)

### III-32-A, (4R,5S,6R)-5-chloro-4-methyl-2-phenyl-6-(o-tolyl)-5,6-dihydro-4H-1,3-oxazine



Yellowish film; R<sub>f</sub> : 0.30 (5% EtOAc in Hexanes)

<sup>1</sup>H NMR (500 MHz, CDCl<sub>3</sub>) δ 8.05 (d, *J* = 7.5 Hz, 2H), 7.48 (dddd, *J* = 7.0, 7.0, 1.5, 1.5 Hz, 1H), 7.40 – 7.43 (m, 2H), 7.23 – 7.29 (m, 4H), 5.79 (d, *J* = 3.5 Hz, 1H), 4.27 (t, *J* = 3.5 Hz, 1H), 3.83 (dq, *J* = 6.5, 3.5 Hz, 1H), 1.43 (d, *J* = 6.5 Hz, 3H); <sup>13</sup>C NMR (125 MHz, CDCl<sub>3</sub>) δ 153.7, 136.6,

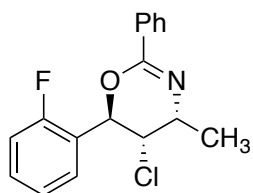
134.5, 132.9, 130.9, 130.8, 128.6, 128.2, 128.1, 127.5, 127.4, 126.6, 125.4, 77.7, 58.2, 47.3, 19.6, 19.0

HRMS analysis (ESI): Calculated for (M+H): C<sub>18</sub>H<sub>19</sub>ClNO 300.1155; Found: 300.1157

Resolution of enantiomers: DAICEL Chiralcel<sup>®</sup> OJ-H column, 2% IPA-Hexanes, 0.7 mL/min, 254 nm, RT1 = 21.3 min, RT2 = 26.6 min.

$[\alpha]_D^{20} = +47.0$  (c 1.0, CHCl<sub>3</sub>, 94% ee)

**III-33-A**, (4*R*,5*S*,6*R*)-5-chloro-6-(2-fluorophenyl)-4-methyl-2-phenyl-5,6-dihydro-4*H*-1,3-oxazine



Colorless solid; R<sub>f</sub>: 0.43 (15% EtOAc in Hexanes)

M.P.: 108 – 114 °C

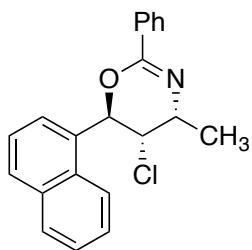
<sup>1</sup>H NMR (500 MHz, CDCl<sub>3</sub>) δ 8.02 (d, *J* = 7.5 Hz, 2H), 7.46 (dd, *J* = 7.5, 7.5 Hz, 1H), 7.41 – 7.38 (m, 2H), 7.37 – 7.32 (m, 1H), 7.26 (d, *J* = 7.0 Hz, 1H), 7.15 – 7.09 (m, 2H), 5.83 (d, *J* = 4.0 Hz, 1H), 4.41 (t, *J* = 4.0 Hz, 1H), 3.76 – 3.71 (m, 1H), 1.41 (d, *J* = 6.5 Hz, 3H); <sup>13</sup>C NMR (125 MHz, CDCl<sub>3</sub>) δ 159.3 (d, <sup>1</sup>*J*<sub>C-F</sub> = 245.8 Hz), 153.1, 132.6, 130.9, 130.5 (d, <sup>3</sup>*J*<sub>C-F</sub> = 8.6 Hz), 128.2, 127.4, 127.2 (d, <sup>1</sup>*J*<sub>C-F</sub> = 3.8 Hz), 125.6 (d, <sup>2</sup>*J*<sub>C-F</sub> = 12.2 Hz), 124.7 (d, <sup>3</sup>*J*<sub>C-F</sub> = 3.9 Hz), 115.8 (d, <sup>2</sup>*J*<sub>C-F</sub> = 20.9 Hz), 74.9 (d, <sup>3</sup>*J*<sub>C-F</sub> = 2.9 Hz), 57.7 (d, <sup>4</sup>*J*<sub>C-F</sub> = 1.9 Hz), 47.8, 19.4

HRMS analysis (ESI): Calculated for (M+H): C<sub>17</sub>H<sub>16</sub>ClFNO: 304.0904; Found: 304.0899

Resolution of enantiomers: DAICEL Chiralpak<sup>®</sup> AD-H column, 5% IPA-Hexanes, 1.0 mL/min, 254 nm, RT1 = 4.7 min, RT2 = 5.9 min.

$[\alpha]_D^{20} = +28.9$  (c 1.0, CHCl<sub>3</sub>, 88% ee)

**III-34-A**, (4*R*,5*S*,6*R*)-5-chloro-4-methyl-6-(naphthalen-1-yl)-2-phenyl-5,6-dihydro-4*H*-1,3-oxazine



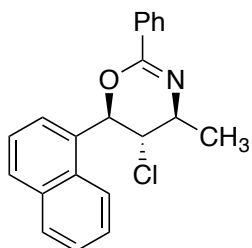
**III-34-A** and **III-34-B** were isolated as a chromatographically inseparable mixture in 75:25 ratio favoring **III-34-A**

R<sub>f</sub> : 0.25 (5% EtOAc in hexanes, UV)

NMR data for **III-34-A**:

<sup>1</sup>H NMR (500 MHz, CDCl<sub>3</sub>) δ 8.03 (d, *J* = 7.5 Hz, 2H), 7.47 – 7.44 (m, 1H), 7.41 – 7.35 (m, 5H), 7.30 – 7.29 (m, 2H), 6.39 (d, *J* = 1.5 Hz, 1H), 4.54 (dd, *J* = 3.0, 3.0 Hz, 1H), 3.72 – 3.67 (m, 1H), 1.36 (d, *J* = 7.0 Hz, 3H)

**III-34-B**, (4*S*,5*S*,6*R*)-5-chloro-4-methyl-6-(naphthalen-1-yl)-2-phenyl-5,6-dihydro-4*H*-1,3-oxazine



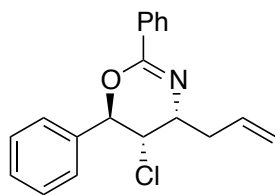
Only the peaks that could be unambiguously assigned to **III-34-B** from the <sup>1</sup>H NMR spectrum of the mixture of **III-34-A** and **III-34-B** are given below:

$^1\text{H}$  NMR (500 MHz,  $\text{CDCl}_3$ )  $\delta$  8.17(d,  $J = 8.5$  Hz, 2H), 5.87 (d,  $J = 10.0$  Hz, 1H), 4.16 (dd,  $J = 10.0, 10.0$  Hz, 1H), 4.01 – 3.97 (m, 1H), 1.57 (d,  $J = 6.5$ Hz, 3H)

HRMS analysis (ESI): Calculated for (M+H):  $\text{C}_{21}\text{H}_{19}\text{ClNO}$  336.1155; Found: 336.1158

Resolution of enantiomers: HPLC conditions to resolve the two diastereomers and the four stereoisomers could not be identified.

**III-35-A**, (4R,5S,6R)-4-allyl-5-chloro-2,6-diphenyl-5,6-dihydro-4H-1,3-oxazine



Colorless oil;  $R_f$ : 0.38 (5% EtOAc in Hexanes, UV, PMA)

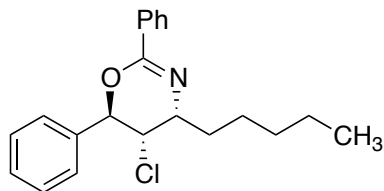
$^1\text{H}$  NMR (500 MHz,  $\text{CDCl}_3$ )  $\delta$  8.07 (d,  $J = 7.0$  Hz, 2H), 7.46 (dddd,  $J = 7.0, 7.0, 1.5, 1.5$  Hz, 1H), 7.31 – 7.42 (m, 5H), 7.24 (d,  $J = 7.0$  Hz, 2H), 5.77 – 5.86 (m, 1H), 5.66 (d,  $J = 2.5$  Hz, 1H), 5.16 (ddd,  $J = 17.5, 3.0, 2.5$  Hz, 1H), 5.07 (dd,  $J = 11.0, 1.0$  Hz, 1H), 4.37 (dd,  $J = 2.5, 2.5$  Hz, 1H), 3.46 – 3.50 (m, 1H), 2.56 – 2.62 (m, 1H), 2.42 – 2.46 (m, 1H);  $^{13}\text{C}$  NMR (125 MHz,  $\text{CDCl}_3$ )  $\delta$  153.2, 138.7, 134.3, 132.9, 130.9, 129.0, 128.6, 128.2, 127.5, 125.0, 117.9, 80.6, 57.8, 50.6, 38.2

HRMS analysis (ESI): Calculated for (M+H):  $\text{C}_{19}\text{H}_{19}\text{ClNO}$  312.1155; Found: 312.1157

Resolution of enantiomers: DAICEL Chiralpak<sup>®</sup> AD-H column, 5% IPA-Hexanes, 1.0 mL/min, 254 nm, RT1 = 5.5 min (major), RT2 = 7.2 min. (minor)

$[\alpha]_D^{20} = +44.6$  (c 1.0,  $\text{CHCl}_3$ , 96% ee)

**III-36-A, (4R,5S,6R)-5-chloro-4-pentyl-2,6-diphenyl-5,6-dihydro-4H-1,3-oxazine**



R<sub>f</sub> : 0.36 (5% EtOAc in hexanes, UV)

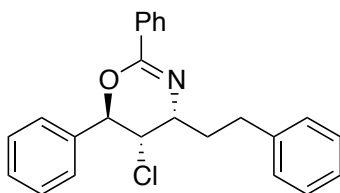
<sup>1</sup>H NMR (500 MHz, CDCl<sub>3</sub>) δ 8.06 (d, *J* = 7.5 Hz, 2H), 7.31 – 7.47 (m, 6H), 7.25 (d, *J* = 8.5 Hz, 2H), 5.63 (d, *J* = 3.0 Hz, 1H), 4.35 (dd, *J* = 3.0, 3.0 Hz, 1H), 3.38 – 3.41 (m, 1H), 1.62 – 1.68 (m, 2H), 1.42 – 1.52 (m, 1H), 1.24 – 1.40 (m, 5H), 0.85 (t, *J* = 7.5 Hz, 3H); <sup>13</sup>C NMR (125 MHz, CDCl<sub>3</sub>) δ 152.7, 138.8, 133.0, 130.8, 129.0, 128.5, 128.2, 127.4, 125.1, 80.4, 58.5, 50.9, 33.8, 31.8, 25.4, 22.6, 14.0

HRMS analysis (ESI): Calculated for (M+H): C<sub>21</sub>H<sub>25</sub>ClNO 342.1625; Found: 342.1627

Resolution of enantiomers: DAICEL Chiralcel<sup>®</sup> OJ-H column, 1% IPA-Hexanes, 0.5 mL/min, 254 nm, RT1 (minor) = 18.5 min, RT2 (major) = 23.3 min.

[α]<sub>D</sub><sup>20</sup> = +19.4 (c 1.0, CHCl<sub>3</sub>, 88% ee)

**III-37-A, (4R,5S,6R)-5-chloro-4-phenethyl-2,6-diphenyl-5,6-dihydro-4H-1,3-oxazine**



Colorless film.

R<sub>f</sub> : 0.46 (10% EtOAc in hexanes, UV)

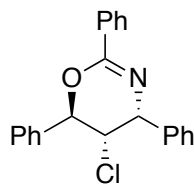
$^1\text{H}$  NMR (500 MHz,  $\text{CDCl}_3$ )  $\delta$  8.03 (d,  $J = 8.0$  Hz, 2H), 7.43 – 7.39 (m, 1H), 7.37 – 7.33 (m, 2H), 7.31 – 7.26 (m, 3H), 7.17 – 7.13 (m, 4H), 7.09– 7.07 (m, 3H), 5.57 (d,  $J = 3.0$  Hz, 1H), 4.30 (dd,  $J = 3.0, 3.0$  Hz, 1H), 3.42 – 3.39 (m, 1H), 2.85 – 2.79 (m, 1H), 2.70 – 2.64 (m, 1H), 2.07 – 1.99 (m, 1H), 1.94 – 1.88 (m, 1H);  $^{13}\text{C}$  NMR (125 MHz,  $\text{CDCl}_3$ )  $\delta$  152.9, 141.7, 138.6, 132.9, 130.8, 128.9, 128.6, 128.4, 128.3, 128.2, 127.4, 125.8, 125.1, 80.4, 58.3, 50.3, 35.5, 32.0

HRMS analysis (ESI): Calculated for (M+H):  $\text{C}_{24}\text{H}_{23}\text{ClNO}$  376.1468; Found: 376.1472

Resolution of enantiomers: Daicel CHIRALPAK<sup>®</sup> AD-H column, 254 nm, 7% IPA in hexane, 0.5 mL/min, RT1 (minor) = 11.2 min, RT2 (major) = 12.0 min.

$[\alpha]_{\text{D}}^{20} = +11.5$  (c 0.42,  $\text{CHCl}_3$ , 76% ee)

### III-38-A, (4*R*,5*S*,6*R*)-5-chloro-2,4,6-triphenyl-5,6-dihydro-4*H*-1,3-oxazine



Colorless oil;  $R_f$ : 0.40 (50%  $\text{CH}_2\text{Cl}_2$  in Hexanes, UV, PMA)

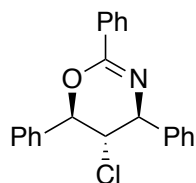
$^1\text{H}$  NMR (500 MHz,  $\text{CDCl}_3$ )  $\delta$  8.23 (d,  $J = 7.5$  Hz, 2H), 7.56 – 7.53 (m, 1H), 7.50 – 7.37 (m, 11H), 7.34 – 7.31 (m, 1H), 5.67 (d,  $J = 4.0$  Hz, 1H), 4.87 (d,  $J = 3.5$  Hz, 1H), 4.58 (dd,  $J = 4.0, 3.5$  Hz, 1H);  $^{13}\text{C}$  NMR (125 MHz,  $\text{CDCl}_3$ )  $\delta$  154.3, 139.4, 138.4, 132.8, 131.1, 129.1, 128.9, 128.2, 128.0, 127.8, 127.6, 127.4, 125.4, 79.8, 59.0, 54.8

HRMS analysis (ESI): Calculated for (M+H):  $\text{C}_{22}\text{H}_{19}\text{ClNO}$  348.1155; Found: 348.1154

Resolution of enantiomers: DAICEL Chiralcel<sup>®</sup> OD-H column, 3% IPA-Hexanes, 0.5 mL/min, 254 nm, RT1 = 12.4 min (minor), RT2 = 16.5 min. (major)

$[\alpha]_D^{20} = -7.0$  (c 0.5,  $\text{CHCl}_3$ , 68% *ee*)

**III-38-B**, (4*S*,5*S*,6*R*)-5-chloro-2,4,6-triphenyl-5,6-dihydro-4*H*-1,3-oxazine



White solid;  $R_f$ : 0.35 (50%  $\text{CH}_2\text{Cl}_2$  in Hexanes, UV, PMA)

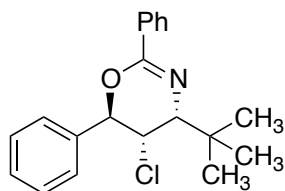
$^1\text{H}$  NMR (500 MHz,  $\text{CDCl}_3$ )  $\delta$  8.00 (d,  $J = 7.5$  Hz, 2H), 7.49 – 7.30 (m, 13H), 5.27 (d,  $J = 10.0$  Hz, 1H), 4.88 (d,  $J = 10.0$  Hz, 1H), 3.96 (dd t,  $J = 10.0, 10.0$  Hz 1H);  $^{13}\text{C}$  NMR (125 MHz,  $\text{CDCl}_3$ )  $\delta$  155.7, 140.6, 136.4, 132.3, 131.1, 129.3, 128.5, 128.3, 128.2, 128.0, 127.84, 127.81, 127.7, 81.0, 65.0, 61.5

HRMS analysis (ESI): Calculated for (M+H):  $\text{C}_{22}\text{H}_{19}\text{ClNO}$  348.1155; Found: 348.1142

Resolution of enantiomers: DAICEL Chiralcel<sup>®</sup> OD-H column, 3% IPA-Hexanes, 0.5 mL/min, 254 nm,  $RT_1 = 13.2$  min (major),  $RT_2 = 14.5$  min. (minor)

$[\alpha]_D^{20} =$  Not determined (38% *ee*)

**III-39-A**, (4*R*,5*S*,6*R*)-4-tert-butyl-5-chloro-2,6-diphenyl-5,6-dihydro-4*H*-1,3-oxazine



White waxy solid. (Eluent for column chromatography: 30%  $\text{CH}_2\text{Cl}_2$  in hexanes)

R<sub>f</sub> : 0.57 (10% EtOAc in hexanes, UV)

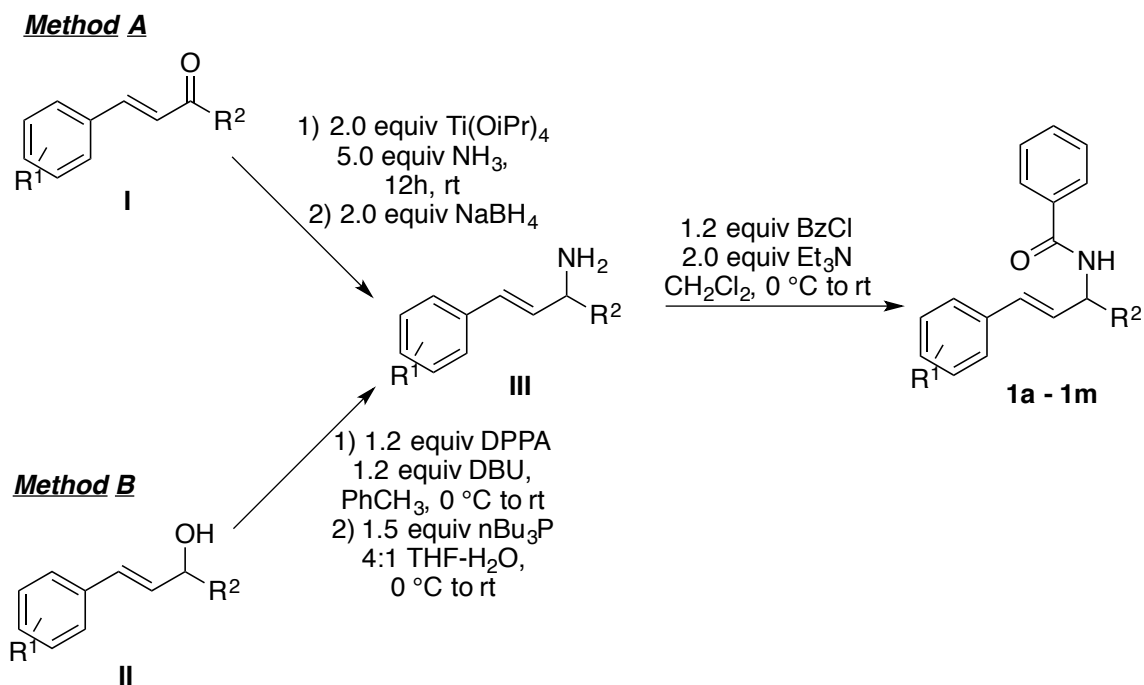
<sup>1</sup>H NMR (500 MHz, CDCl<sub>3</sub>) δ 8.14 (d, *J* = 7.2 Hz, 2H), 7.47 – 7.30 (m, 6H), 7.23 (d, *J* = 7.2 Hz, 2H), 5.62 (s, 1H), 4.53 (t, *J* = 2.5 Hz, 1H), 3.04 (d, 1H, *J* = 2.5 Hz), 1.04 (s, 9H); <sup>13</sup>C NMR (125 MHz, CDCl<sub>3</sub>) δ 152.4, 139.6, 133.3, 130.6, 129.1, 128.4, 128.1, 127.4, 124.6, 82.3, 57.3, 56.3, 34.6, 27.1

HRMS analysis (ESI): Calculated for (M+H): C<sub>20</sub>H<sub>23</sub>CINO 328.1468; Found: 328.1472

Resolution of enantiomers: DAICEL Chiralcel<sup>®</sup> OJ-H column, 254 nm, 5% IPA in hexane, 0.5 mL/min, RT1 (major) = 9.3 min, RT2 (minor) = 12.1 min

[α]<sub>D</sub><sup>20</sup> = -14.3 (c 0.5, CHCl<sub>3</sub>, 50% ee)

### III.6.5. General method for the preparation of substrates for kinetic resolution.



Racemic amines **III** were benzoylated using standard procedures to obtain the substrates for the kinetic resolution. The amines **III** could be synthesized using one of two methods. A direct reductive amination of ketones **I** mediated by  $\text{Ti}(i\text{OPr})_4$  and ethanolic  $\text{NH}_3$  followed by  $\text{NaBH}_4$  reduction gave the racemic amines **III**. Alternately, ketones **I** could be reduced to the corresponding secondary alcohols **II**. The alcohols **II** were converted to the corresponding secondary azides with Diphenylphosphoryl azide (DPPA) and DBU. The crude azides were reduced to amines **III** using  $n\text{-Bu}_3\text{P}$  in aqueous THF.

#### Method A:<sup>43</sup>

3.0 mmol of ketone **I** was dissolved in a 2 M solution of  $\text{NH}_3$  in EtOH (7.5 mL, 15.0 mmol, 5 equiv) under Ar. Freshly distilled  $\text{Ti}(i\text{OPr})_4$  (1.82 mL, 6.0 mmol, 2.0 equiv) was added under Ar and the resulting solution was stirred at ambient temperature for 12 hours.  $\text{NaBH}_4$  (226 mg, 6.0

mmol, 2.0 equiv) was then added under Ar in a single portion and the resulting suspension was rapidly stirred for a further 12 hours at ambient temperature. The reaction was quenched with 2M NH<sub>4</sub>OH (10 mL). The solids were filtered through a celite bed and washed with EtOAc. Concentration of the filtrates in vacuo followed by routine acid-base extraction gave crude amines. The amines thus obtained were benzoylated without further purification (see below for procedure). On 20.0 mmol scale, 2 x 1.5 equiv of NaBH<sub>4</sub> was added at 12 h intervals.

#### Method B:<sup>44</sup>

Alcohol **II** (1.21 mmol) and diphenylphosphoryl azide (314 mL, 1.46 mmol, 1.2 equiv) were dissolved in anhydrous toluene (2.5 mL) under N<sub>2</sub> and cooled in an ice bath. DBU (218 mL, 1.46 mmol, 1.2 equiv) was added drop wise under N<sub>2</sub>. The reaction was allowed to warm to ambient temperature and monitored for consumption of substrate (TLC). On completion, the reaction mixture was directly loaded on a packed silica gel column (5 cm height x 3.5 cm width packed in 100% hexanes) and rapidly flushed with 5% EtOAc in Hexanes (~125 mL) and concentrated to obtain the secondary azide (NOTE: the crude azide was not rigorously dried to reduce explosion hazards associated with handling pure and dry azides). The crude azide was suspended in 5 mL of 4:1 THF-H<sub>2</sub>O and cooled in an ice bath. *n*Bu<sub>3</sub>P (450 mL, 1.80 mmol, 1.5 equiv) was added drop wise. The reaction was then allowed to warm to ambient temperature. On complete consumption of azide (TLC), the reaction mixture was diluted with 10 mL of 1N aq. HCl. Routine acid-base extraction afforded the crude amine **III**, which was benzoylated with no further purification.

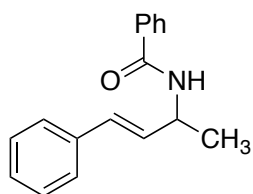
#### General procedure for benzoylation of amines:

A solution of the amine **III** (1.0 equiv) and triethyl amine (2.0 equiv) in CH<sub>2</sub>Cl<sub>2</sub> (5 mL per mmol of amine) was cooled in an ice bath. To it was added benzoyl chloride (1.2 equiv) drop wise under

N<sub>2</sub>. After the addition was complete, the reaction was allowed to warm to ambient temperature. After 2 h, the reaction was diluted with an equal amount of water and extracted with DCM (3x). The combined organics were washed with brine (1x), dried over anhydrous Na<sub>2</sub>SO<sub>4</sub> and concentrated under reduced pressure to give the crude product. Purification was achieved by column chromatography on silica gel as stationary phase and EtOAc-Hexanes gradient as eluent. Further purification by crystallization from hot EtOH gave products of high purity (≥98% GC assay.)

### III.6.6. Analytical data for kinetic resolution substrates.

III-11, (*E*)-N-(4-phenylbut-3-en-2-yl)benzamide<sup>45</sup>



White solid; R<sub>f</sub>: 0.30 (20% EtOAc in Hexanes; UV and anisaldehyde)

M.P.: 127 – 130 °C

<sup>1</sup>H NMR (500 MHz, CDCl<sub>3</sub>) δ 7.79 (d, *J* = 7.5 Hz, 2H), 7.50 (t, *J* = 7.0 Hz, 1H), 7.43 (t, *J* = 7.5 Hz, 2H), 7.37 (d, *J* = 7.0 Hz, 2H), 7.31 (t, *J* = 7.5 Hz, 2H), 7.26 – 7.22 (m, 1H), 6.58 (d, *J* = 16.5 Hz, 1H), 6.27 (dd, *J* = 16.5, 5.5 Hz, 1H), 6.16 (br d, *J* = 7.0 Hz, 1H), 4.99 – 4.95 (m, 1H), 1.45 (d, *J* = 7.0 Hz, 3H); <sup>13</sup>C NMR (125 MHz, CDCl<sub>3</sub>) δ 166.6, 136.6, 134.7, 131.4, 130.8, 130.0, 128.6, 127.6, 126.9, 126.4, 46.9, 20.7

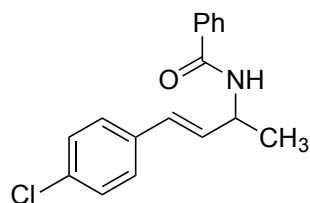
HRMS analysis (ESI): Calculated for (M+H): C<sub>18</sub>H<sub>18</sub>NO 252.1389; Found: 252.1393

Resolution of enantiomers: Daicel Chiralpak AD-H, 15% IPA-Hex, 1 mL/min; 254 nm, RT1 = 7.4 min, RT2 = 10.3 min

$[\alpha]_D^{20}$  for **(S)-III-11** = -31.4 (c 1.0, CHCl<sub>3</sub>, >99% ee) Reported  $[\alpha]_D^{20}$  = -11.0 (c 1.0, CHCl<sub>3</sub>, 90.2:9.8 *er*)<sup>45</sup>

$[\alpha]_D^{20}$  for **(R)-III-11** = +31.2 (c 1.0, CHCl<sub>3</sub>, >99% ee)

**III-26**, (*E*)-N-[4-(4-chlorophenyl)but-3-en-2-yl]benzamide



White solid; 0.26 (20% EtOAc in Hexanes, UV and anisaldehyde)

M.P.: 133 – 135 °C

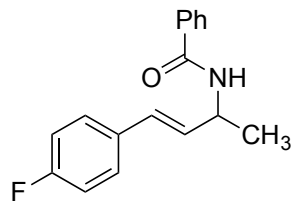
<sup>1</sup>H NMR (500 MHz, CDCl<sub>3</sub>) δ 7.78 (d, *J* = 7.5 Hz, 2H), 7.49 (dd, *J* = 7.5, 7.5 Hz, 1H), 7.42 (dd, *J* = 7.5, 7.5 Hz, 2H), 7.24 – 7.28 (m, 4H), 6.51 (d, *J* = 16.0 Hz, 1H), 6.22 (dd, *J* = 16.0, 5.5 Hz, 1H), 6.13 (br s, 1H), 4.91 – 4.98 (m, 1H), 1.43 (d, *J* = 7.0 Hz, 3H); <sup>13</sup>C NMR (125 MHz, CDCl<sub>3</sub>) δ 166.6, 135.1, 134.5, 133.3, 131.5, 128.8, 128.7, 128.6, 127.6, 126.9, 46.8, 20

HRMS analysis (ESI): Calculated for (M+H): C<sub>17</sub>H<sub>17</sub>ClNO 286.0999; Found: 286.1004

Resolution of enantiomers: Daicel CHIRALPAK<sup>®</sup> AD-H, 15% IPA-Hex, 1 mL/min; 254 nm, RT1 (minor) = 9.0 min, RT2 (major) = 11.9 min.

$[\alpha]_D^{20}$  = -23.8 (c 1.0, CHCl<sub>3</sub>, 95% ee)

**III-27**, (*E*)-N-[4-(4-fluorophenyl)but-3-en-2-yl]benzamide



White solid; 0.22 (20% EtOAc in Hexanes, UV and anisaldehyde)

M.P.: 118 – 121 °C

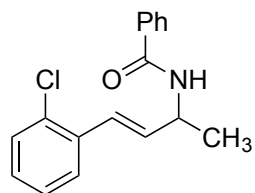
$^1\text{H}$  NMR (500 MHz,  $\text{CDCl}_3$ )  $\delta$  7.77 (d,  $J = 7.5$  Hz, 2H), 7.48 (t,  $J = 7.5$  Hz, 1H), 7.41 (t,  $J = 7.5$  Hz, 2H), 7.30 (dd,  $^2J_{\text{H-H}} = 8.0$  Hz,  $^3J_{\text{H-F}} = 5.5$  Hz, 2H), 6.97 (dd,  $^2J_{\text{H-H}} = ^2J_{\text{H-F}} = 5.5$  Hz, 2H), 6.52 (d,  $J = 16.0$  Hz, 1H), 6.17 (br s, 1H), 6.15 (dd,  $J = 16.0, 5.5$  Hz, 1H), 4.96 – 4.90 (m, 1H), 1.42 (d,  $J = 7.0$  Hz, 3H);  $^{13}\text{C}$  NMR (125 MHz,  $\text{CDCl}_3$ )  $\delta$  166.6, 162.3 (d,  $^1J_{\text{C-F}} = 245.8$  Hz), 134.6, 132.8, 131.5, 130.6, 128.9, 128.6, 127.9 (d,  $^3J_{\text{C-F}} = 7.8$  Hz), 126.9, 115.4 (d,  $^2J_{\text{C-F}} = 21.5$  Hz), 46.9, 20.7

HRMS analysis (ESI): Calculated for (M+H):  $\text{C}_{17}\text{H}_{17}\text{FNO}$  270.1294; Found: 270.1299

Resolution of enantiomers: Daicel Chiralpak<sup>®</sup> AD-H, 15% IPA-Hex, 1 mL/min; 254 nm, RT1 (minor) = 6.6 min, RT2 (major) = 8.9 min

$[\alpha]_{\text{D}}^{20} = -20.9$  (c 1.0,  $\text{CHCl}_3$ , 98% ee)

**III-28**, (E)-N-[4-(2-chlorophenyl)but-3-en-2-yl]benzamide



White solid; 0.30 (20% EtOAc in Hexanes, UV and anisaldehyde); M.P.: 132 – 134 °C

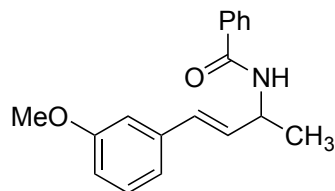
$^1\text{H}$  NMR (500 MHz,  $\text{CDCl}_3$ )  $\delta$  7.78 (d,  $J = 8.0$  Hz, 2H), 7.47 – 7.51 (m, 2H), 7.42 (dd,  $J = 7.5$ , 7.5 Hz, 2H), 7.32 (dd,  $J = 7.5$ , 2.0 Hz, 1H), 7.14 – 7.21 (m, 2H), 6.96 (dd,  $J = 16.0$ , 1.5 Hz, 1H), 6.27 (dd,  $J = 16.0$ , 5.5 Hz, 1H), 6.13 (br s, 1H), 4.99 – 5.01 (m, 1H), 1.46 (d,  $J = 7.0$  Hz, 3H);  $^{13}\text{C}$  NMR (125 MHz,  $\text{CDCl}_3$ )  $\delta$  166.7, 134.8, 134.7, 133.8, 133.1, 131.5, 129.7, 128.7, 128.6, 126.90, 126.87, 126.83, 126.1, 46.8, 20.5

HRMS analysis (ESI): Calculated for (M+H):  $\text{C}_{17}\text{H}_{17}\text{ClNO}$  286.0999; Found: 286.1001

Resolution of enantiomers: Daicel Chiralpak<sup>®</sup> AD-H, 15% IPA-Hex, 1 mL/min; 254 nm, RT1 (minor) = 7.6 min, RT2 (major) = 9.4 min

$[\alpha]_{\text{D}}^{20} = -28.9$  (c 1.0,  $\text{CHCl}_3$ , 82% ee)

### III-29, (*E*)-N-[4-(3-methoxyphenyl)but-3-en-2-yl]benzamide



White solid; 0.22 (20% EtOAc in Hexanes, UV and anisaldehyde)

M.P.: 85 – 87 °C

$^1\text{H}$  NMR (500 MHz,  $\text{CDCl}_3$ )  $\delta$  7.78 (d,  $J = 8.5$  Hz, 2H), 7.46 – 7.50 (m, 1H), 7.40 – 7.44 (m, 2H), 7.20 (dd,  $J = 7.5$ , 7.5 Hz, 1H), 6.95 (d,  $J = 8.0$  Hz, 1H), 6.89 (dd,  $J = 2.0$ , 2.0 Hz, 1H), 6.77 (dd,  $J = 7.5$ , 2.0 Hz, 1H), 6.54 (d,  $J = 16.0$  Hz, 1H), 6.25 (dd,  $J = 16.0$ , 6.0 Hz, 1H), 6.11 (d,  $J = 7.5$  Hz, 1H), 4.92 – 4.98 (m, 1H), 3.79 (s, 3H), 1.43 (d,  $J = 6.0$  Hz, 3H);  $^{13}\text{C}$  NMR (125 MHz,  $\text{CDCl}_3$ )  $\delta$  166.6, 159.8, 138.0, 134.6, 131.5, 131.1, 129.9, 129.5, 128.6, 126.9, 119.0, 113.4, 111.6, 55.2, 46.8, 20.7

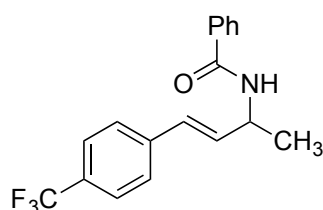
HRMS analysis (ESI): Calculated for (M+H): C<sub>18</sub>H<sub>20</sub>NO<sub>2</sub> 282.1494; Found: 282.1499

Resolution of enantiomers: Daicel Chiralpak<sup>®</sup> AD-H, 15% IPA-Hex, 1 mL/min; 254 nm; RT1

(minor) = 9.6 min, RT2 (major) = 15.4 min

$[\alpha]_D^{20} = -43.3$  (c 1.0, CHCl<sub>3</sub>, 70% ee)

**III-30**, (*E*)-N-[4-[4-(trifluoromethyl)phenyl]but-3-en-2-yl]benzamide



White solid; 0.24 (20% EtOAc in Hexanes, UV and anisaldehyde)

M.P.: 126 – 131 °C

<sup>1</sup>H NMR (600 MHz, CDCl<sub>3</sub>) δ 7.80 (d, *J* = 7.8 Hz, 2H), 7.50 (d, *J* = 7.8 Hz, 2H), 7.45 – 7.48 (m, 1H), 7.37 – 7.39 (m, 4H), 6.54 (d, *J* = 15.6 Hz, 1H), 6.50 (br s, 1H), 6.31 (dd, *J* = 15.6, 5.4 Hz, 1H), 4.93 – 4.96 (m, 1H), 1.41 (d, *J* = 7.2 Hz, 3H); <sup>13</sup>C NMR (150 MHz, CDCl<sub>3</sub>) δ 166.7, 140.1 (q, <sup>4</sup>*J*<sub>C-F</sub> = 1.2 Hz), 134.4, 133.7, 131.5, 129.2 (q, <sup>2</sup>*J*<sub>C-F</sub> = 32.0 Hz), 128.5, 128.4, 126.9, 126.5, 125.4 (q, <sup>3</sup>*J*<sub>C-F</sub> = 3.9 Hz), 124.1 (q, <sup>1</sup>*J*<sub>C-F</sub> = 270.1 Hz), 46.9, 20.4

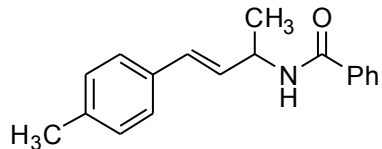
HRMS analysis (ESI): Calculated for (M+H): C<sub>18</sub>H<sub>17</sub>F<sub>3</sub>NO 320.1262; Found: 320.1270

Resolution of enantiomers : Daicel Chiralpak<sup>®</sup> AD-H, 15% IPA-Hex, 1 mL/min; 254 nm, RT1

(minor) = 9.0 min, RT2 (major) = 11.9 min

$[\alpha]_D^{20} = -21.4$  (c 1.0, CHCl<sub>3</sub>, 78% ee)

**III-31, (E)-N-(4-p-tolylbut-3-en-2-yl)benzamide**



White solid; 0.50 (30% EtOAc in Hexanes, UV and anisaldehyde); M.P.: 138 – 140 °C

$^1\text{H}$  NMR (500 MHz,  $\text{CDCl}_3$ )  $\delta$  7.77 (d,  $J = 8.5$  Hz, 2H), 7.50 – 7.47 (m, 1H), 7.43 – 7.40 (m, 2H), 7.26 – 7.24 (m, 2H), 7.09 (d,  $J = 8.5$  Hz, 2H), 6.54 (d,  $J = 16.0$  Hz, 1H), 6.20 (dd,  $J = 16.0, 6.0$  Hz, 1H), 6.10 (br d,  $J = 6.0$  Hz, 1H), 4.96 – 4.93 (m, 1H), 2.31 (s, 3H), 1.43 (d,  $J = 6.5$  Hz, 3H);

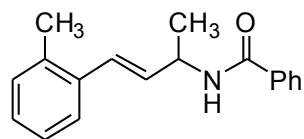
$^{13}\text{C}$  NMR (125 MHz,  $\text{CDCl}_3$ )  $\delta$  166.5, 137.5, 134.7, 133.7, 131.4, 129.9, 129.7, 129.3, 128.6, 126.9, 126.3, 46.9, 21.2, 20.7

HRMS analysis (ESI): Calculated for (M+H):  $\text{C}_{18}\text{H}_{20}\text{NO}_2$  282.1494; Found: 282.1487

Resolution of enantiomers: Daicel Chiralpak<sup>®</sup> AD-H, 15% IPA-Hex, 1 mL/min; 254 nm RT1 (minor) = 7.4 min, RT2 (major) = 8.9 min

$[\alpha]_{\text{D}}^{20} = -33.9$  (c 1.0,  $\text{CHCl}_3$ , 52% ee)

**III-32, (E)-N-(4-o-tolylbut-3-en-2-yl)benzamide**



White solid; 0.50 (30% EtOAc in Hexanes, UV and anisaldehyde)

M.P.: 115 – 118 °C

$^1\text{H}$  NMR (500 MHz,  $\text{CDCl}_3$ )  $\delta$  7.77 (d,  $J = 7.5$  Hz, 2H), 7.48 (dd,  $J = 7.5, 7.5$  Hz, 1H), 7.40 – 7.44 (m, 3H), 7.10 – 7.15 (m, 3H), 6.80 (dd,  $J = 15.5, 1.5$  Hz, 1H), 6.12 (dd,  $J = 15.5, 5.5$  Hz, 1H), 6.09 (br s, 1H), 4.94 – 4.99 (m, 1H), 2.32 (s, 3H), 1.45 (d,  $J = 7.0$  Hz, 3H);  $^{13}\text{C}$  NMR (125 MHz,

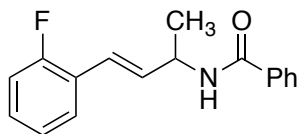
CDCl<sub>3</sub>) δ 166.7, 135.7, 135.5, 132.1, 131.4, 130.3, 128.6, 128.1, 127.6, 126.9, 126.1, 125.6, 47.2, 20.9, 19.8

HRMS analysis (ESI): Calculated for (M+H): C<sub>18</sub>H<sub>20</sub>NO<sub>2</sub> 282.1494; Found: 282.1487

Resolution of enantiomers: Daicel Chiralpak<sup>®</sup> AD-H, 15% IPA-Hex, 1 mL/min; 254 nm RT1 (minor) = 6.9 min, RT2 (major) = 8.4 min

[α]<sub>D</sub><sup>20</sup> = -43.6 (c 1.0, CHCl<sub>3</sub>, 84% ee)

### III-33, (*E*)-*N*-(4-(2-fluorophenyl)but-3-en-2-yl)benzamide



White solid; 0.46 (30% EtOAc in Hexanes, UV and anisaldehyde); M.P.: 110 – 114 °C

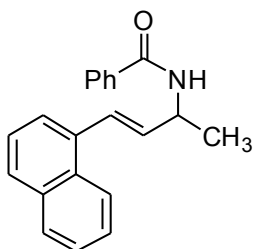
<sup>1</sup>H NMR (600 MHz, CDCl<sub>3</sub>) δ 7.79 (d, *J* = 7.2 Hz, 2H), 7.50 – 7.47 (m, 1), 7.46 – 7.40 (m, 3H), 7.20 – 7.16 (m, 1H), 7.08 – 7.05 (m 1H), 6.71 (d, *J* = 16.2 Hz, 1H), 6.36 (dd, *J* = 16.2, 5.4 Hz, 1H), 6.17 (br s, 1H), 4.99 – 4.95 (m, 1H), 1.44 (d, *J* = 6.6 Hz, 3H); <sup>13</sup>C NMR (150 MHz, CDCl<sub>3</sub>) δ 166.7, 160.2 (d, <sup>1</sup>*J*<sub>C-F</sub> = 247.5 Hz), 134.6, 133.5 (d, <sup>4</sup>*J*<sub>C-F</sub> = 4.9 Hz), 131.5, 128.9 (d, <sup>3</sup>*J*<sub>C-F</sub> = 8.3 Hz), 128.6, 127.5 (d, <sup>4</sup>*J*<sub>C-F</sub> = 3.3 Hz), 126.9, 124.1 (d, <sup>4</sup>*J*<sub>C-F</sub> = 3.9 Hz), 122.5, 115.7 (d, <sup>2</sup>*J*<sub>C-F</sub> = 22.7 Hz), 47.1, 20.6

HRMS analysis (ESI): Calculated for (M+H): C<sub>17</sub>H<sub>17</sub>FNO: 270.1294; Found: 270.1299

Resolution of enantiomers: Daicel Chiralpak<sup>®</sup> AD-H, 15% IPA-Hex, 1 mL/min; 254 nm RT1 (minor) = 7.6 min, RT2 (major) = 9.9 min

[α]<sub>D</sub><sup>20</sup> = -18.8 (c 1.0, CHCl<sub>3</sub>, 98% ee)

**III-34, (E)-N-[4-(naphthalen-1-yl)but-3-en-2-yl]benzamide**



White solid; 0.47 (30% EtOAc in Hexanes, UV and anisaldehyde); M.P.: 148 – 152 °C

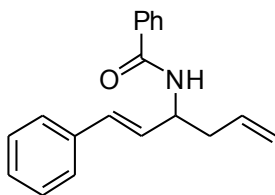
$^1\text{H}$  NMR (500 MHz,  $\text{CDCl}_3$ )  $\delta$  8.07 (d,  $J = 8.0$  Hz, 1H), 7.81 (dd,  $J = 8.5, 9.0$  Hz, 3H), 7.77 (d,  $J = 8.0$  Hz, 1H), 7.56 (d,  $J = 6.5$  Hz, 1H), 7.42- 7.51 (m, 6H), 7.34 (d,  $J = 16.0$  Hz, 1H), 6.27 (dd,  $J = 16.0, 6.0$  Hz, 1H), 6.16 (br d,  $J = 7.5$  Hz, 1H), 5.05 – 5.10 (m, 1H), 1.53 (d,  $J = 7.0$  Hz, 3H);  $^{13}\text{C}$  NMR (125 MHz,  $\text{CDCl}_3$ )  $\delta$  166.7, 134.7, 134.5, 134.2, 133.6, 131.5, 131.2, 128.6, 128.5, 128.0, 127.5, 126.9, 126.1, 125.8, 125.6, 123.9, 123.8, 47.3, 20.9

HRMS analysis (ESI): Calculated for (M+H):  $\text{C}_{21}\text{H}_{20}\text{NO}$ : 302.1545; Found: 302.1549

Resolution of enantiomers: Daicel Chiralpak<sup>®</sup> AD-H, 15% IPA-Hex, 1 mL/min; 254 nm; RT1 (minor) = 6.7 min, RT2 (major) = 10.0 min

$[\alpha]_{\text{D}}^{20} = -33.4$  (c 1.0,  $\text{CHCl}_3$ , 84% ee)

**III-35, (E)-N-(1-phenylhexa-1,5-dien-3-yl)benzamide**



White solid; 0.57 (30% EtOAc in Hexanes, UV and anisaldehyde); M.P.: 98 – 100 °C

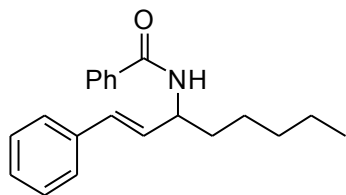
$^1\text{H}$  NMR (600 MHz,  $\text{CDCl}_3$ )  $\delta$  7.77 (d,  $J = 7.8$  Hz, 2H), 7.49 (dd,  $J = 7.2, 7.2$  Hz, 1H), 7.43 (dd,  $J = 7.2, 7.2$  Hz, 2H), 7.34 (d,  $J = 7.2$  Hz, 2H), 7.28 (t,  $J = 7.2$  Hz, 2H), 7.21 (t,  $J = 7.8$  Hz, 1H), 6.57 (d,  $J = 16.2$  Hz, 1H), 6.22 (dd,  $J = 16.2, 6.0$  Hz, 1H), 6.17 (br s, 1H), 5.83 – 5.90 (m, 1H), 5.15 – 5.20 (m, 2H), 4.96 (pentet,  $J = 6.6$  Hz, 1H), 2.51 – 2.55 (m, 2H);  $^{13}\text{C}$  NMR (150 MHz,  $\text{CDCl}_3$ )  $\delta$  166.7, 136.6, 134.7, 133.8, 131.5, 130.8, 129.1, 128.6, 128.5, 127.7, 126.9, 126.4, 118.7, 50.3, 39.5

HRMS analysis (ESI): Calculated for (M+H):  $\text{C}_{19}\text{H}_{20}\text{NO}$  278.1545; Found: 278.1553

Resolution of enantiomers: Daicel Chiralpak<sup>®</sup> AD-H, 15% IPA-Hex, 1 mL/min; 254 nm, RT1 (minor) = 9.8 min, RT2 = 12.2 min

$[\alpha]_{\text{D}}^{20} = -23.6$  (c 1.0,  $\text{CHCl}_3$ , 76% ee)

### III-36, (E)-N-(1-phenyloct-1-en-3-yl)benzamide



White solid; 0.60 (30% EtOAc in Hexanes); M.P.: 102 – 104 °C

$^1\text{H}$  NMR (500 MHz,  $\text{CDCl}_3$ )  $\delta$  7.78 (d,  $J = 8.0$  Hz, 2H), 7.49 (dd,  $J = 7.0, 7.0$  Hz, 1H), 7.36 – 7.44 (m, 2H), 7.35 (d,  $J = 8.0$  Hz, 2H), 7.28 (dd,  $J = 7.0, 7.0$  Hz, 2H), 7.22 (dt,  $J = 7.5, 1.5$  Hz, 1H), 6.57 (d,  $J = 15.5$  Hz, 1H), 6.17 (dd,  $J = 15.5, 6.5$  Hz, 1H), 6.09 (br d,  $J = 8.0$  Hz, 1H), 4.80 – 4.85 (m, 1H), 1.69 – 1.74 (m, 2H), 1.29 – 1.43 (m, 6H), 0.87 (t,  $J = 7.0$  Hz, 3H);  $^{13}\text{C}$  NMR (125 MHz,  $\text{CDCl}_3$ )  $\delta$  166.7, 136.7, 134.8, 131.4, 130.7, 130.0, 128.6, 128.5, 127.6, 126.9, 126.4, 51.5, 35.4, 31.6, 25.6, 22.5, 14.0

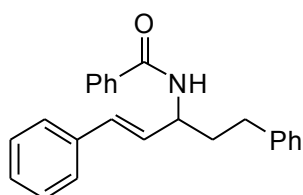
HRMS analysis (ESI): Calculated for (M+H): C<sub>21</sub>H<sub>26</sub>NO 308.2014; Found: 308.2027

Resolution of enantiomers: Daicel Chiralpak<sup>®</sup> AD-H, 15% IPA-Hex, 1 mL/min; 254 nm, RT1

(minor) = 8.8 min, RT2 = 9.8 min

$[\alpha]_D^{20} = -14.2$  (c 1.0, CHCl<sub>3</sub>, 84% ee)

**III-37**, (E)-N-(1,5-diphenylpent-1-en-3-yl)benzamide



White solid; 0.53 (30% EtOAc in Hexanes, UV and anisaldehyde); M.P.: 160 – 166 °C

<sup>1</sup>H NMR (500 MHz, CDCl<sub>3</sub>) δ 7.69 (d, *J* = 7.5 Hz, 2H), 7.45 (tt, *J* = 7.5, 1.5 Hz, 1H), 7.43 – 7.39 (m, 2H), 7.41 (t, *J* = 7.0 Hz, 2H), 7.31 – 7.26 (m, 4H), 7.24 – 7.17 (m, 4H), 6.58 (dd, *J* = 16.0, 1.0 Hz, 1H), 6.21 (dd, *J* = 16.0, 6.5 Hz, 1H), 6.10 (br d, *J* = 8.5 Hz, 1H), 4.94 – 4.88 (m, 1H), 2.79 – 2.76 (m, 2H), 2.09 (dd, *J* = 15.5, 6.5 Hz, 2H); <sup>13</sup>C NMR (125 MHz, CDCl<sub>3</sub>) δ 166.6, 141.5, 136.6, 134.5, 131.5, 131.1, 129.4, 128.58, 128.56, 128.4, 127.7, 126.9, 126.4, 126.1, 51.4, 36.7, 32.3

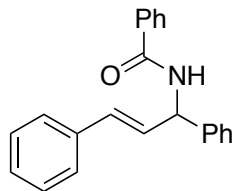
HRMS analysis (ESI): Calculated for (M+H): C<sub>24</sub>H<sub>24</sub>NO 342.1858; Found: 342.1858

Resolution of enantiomers: Daicel Chiralpak<sup>®</sup> AD-H, 15% IPA-Hex, 1 mL/min; 254 nm, RT1

(minor) = 14.0 min, RT2 = 27.7 min

$[\alpha]_D^{20} = -8.4$  (c 1.0, CHCl<sub>3</sub>, 54% ee)

**III-38**, (E)-N-(1,3-diphenylallyl)benzamide



White solid; 0.57 (30% EtOAc in Hexanes); M.P.: 152 - 153°C

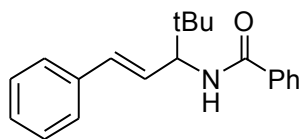
$^1\text{H}$  NMR (500 MHz,  $\text{CDCl}_3$ )  $\delta$  7.81 (d,  $J = 7.5$  Hz, 2H), 7.50 (t,  $J = 7.5$  Hz, 1H), 7.44 – 7.41 (m, 4H), 7.39 – 7.36 (m, 4H), 7.32 – 7.28 (m, 3H), 7.22 (t,  $J = 7.0$  Hz, 1H), 6.61 (d,  $J = 16.0$  Hz, 1H), 6.47 (d,  $J = 7.5$  Hz, 1H), 6.43 (dd,  $J = 16.0, 6.0$  Hz, 1H), 6.02 (t,  $J = 7.0$  Hz, 1H);  $^{13}\text{C}$  NMR (125 MHz,  $\text{CDCl}_3$ )  $\delta$  166.4, 140.8, 136.4, 134.4, 131.8, 131.7, 128.9, 128.7, 128.63, 128.57, 127.85, 127.82, 127.2, 127.0, 126.6, 55.2

HRMS analysis (ESI): Calculated for (M+H):  $\text{C}_{22}\text{H}_{20}\text{NO}$  314.1545; Found: 314.1549

Resolution of enantiomers: Daicel Chiralpak<sup>®</sup> AD-H, 15% IPA-Hex, 1 mL/min; 254 nm, RT1 = 14.3 min, RT2 = 15.8 min

$[\alpha]_{\text{D}}^{20}$ : Not determined (20% ee)

### III-39, (E)-N-(4,4-dimethyl-1-phenylpent-1-en-3-yl)benzamide



White solid;  $R_f$ : 0.29 (15% EtOAc in Hexanes, UV and anisaldehyde); MP : 134 – 136 °C

$^1\text{H}$  NMR (600 MHz,  $\text{CDCl}_3$ )  $\delta$  7.78 (d,  $J = 7.2$  Hz, 2H), 7.50 (dddd,  $J = 7.2, 7.2, 2.0, 2.0$  Hz, 1H), 7.42 – 7.45 (m, 2H), 7.34 – 7.35 (m, 2H), 7.28 (dd,  $J = 8.4, 8.4$  Hz, 2H), 7.21 (dddd,  $J = 8.4, 8.4, 2.0, 2.0$  Hz, 1H), 6.58 (d,  $J = 15.6$  Hz, 1H), 6.23 (dd,  $J = 15.6, 7.2$  Hz, 1H), 6.16 (br d,  $J = 7.2$

Hz, 1H), 4.68 – 4.71 (m, 1H), 1.04 (s, 9H);  $^{13}\text{C}$  NMR (150 MHz,  $\text{CDCl}_3$ )  $\delta$  166.8, 136.8, 135.0,

132.3, 131.4, 128.6, 128.5, 127.6, 126.84, 126.82, 126.4, 59.7, 35.1, 26.5

HRMS analysis (ESI): Calculated for (M+H):  $\text{C}_{20}\text{H}_{24}\text{NO}$  294.1858; Found: 294.1868

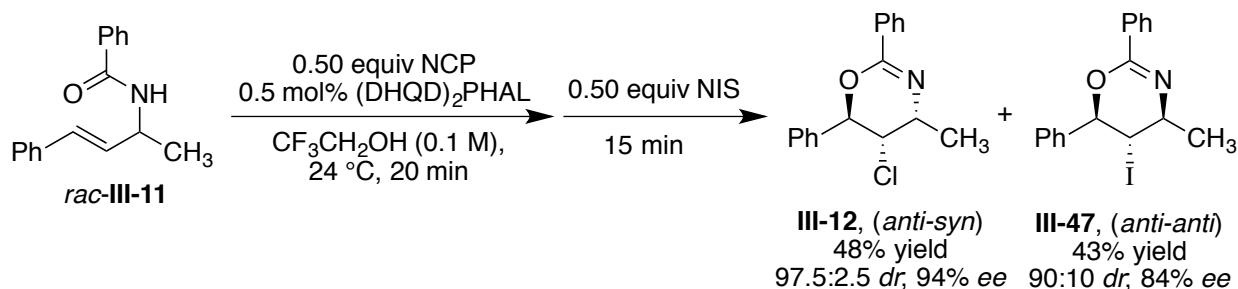
Resolution of enantiomers: DAICEL Chiralcel<sup>®</sup> OD-H column, 250 nm, 5% IPA in hexane, 1.0

mL/min, RT1 = 22.4 min, RT2 = 30.6 min

$[\alpha]_{\text{D}}^{20} = -6.3$  (c 1.0,  $\text{CHCl}_3$ , 40% *ee*)

### III.6.7. Chemical transformations.

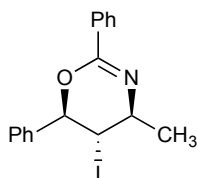
#### A) Sequential one-pot kinetic resolution/diastereoselective iodocyclization reaction:



A 7 mL capacity disposable screw-capped glass vial equipped with a magnetic stir bar was charged with the *rac*-III-11 (38 mg, 0.15 mmol, 1.0 equiv) and (DHQD)<sub>2</sub>PHAL (3.5 mg, 0.03 equiv). This was followed by the addition of CF<sub>3</sub>CH<sub>2</sub>OH (1.5 mL, 0.10 M concentration of substrate). The vial was capped and the resulting suspension was stirred at ambient temperature till all the solids had completely dissolved. This was followed by the addition of *N*-chlorophthalimide (13.7 mg, 0.075 mmol, 0.50 equiv) in a single portion. The vial was capped and the reaction was stirred at ambient temperature. After 60 min, NIS (16.9 mg, 0.075 mmol, 0.50 equiv) was added in a single portion. The reaction was stirred for a further 15 min at ambient temperature and then quenched with sat. aq. Na<sub>2</sub>SO<sub>3</sub> (5 ml). The resulting suspension was diluted with CH<sub>2</sub>Cl<sub>2</sub> (5 mL). The aqueous layer was extracted with CH<sub>2</sub>Cl<sub>2</sub> (2x 5 mL). The combined organics were washed with 1% aq. NaOH (1x 5mL), brine (1x 5 mL) and dried over anhydrous Na<sub>2</sub>SO<sub>4</sub>. GC analysis of a small aliquot gave the *dr* values for the cyclized products. Pure products were isolated by column chromatography on silica gel using 97:3 Hexanes-EtOAc as the eluent.

See above for characterization data of III-12.

**III-47**, (4*S*,5*S*,6*R*)-5-iodo-4-methyl-2,6-diphenyl-5,6-dihydro-4*H*-1,3-oxazine



Slightly yellow solid (progressively darkens if stored at ambient temperature)

R<sub>f</sub> : 0.55 (10% EtOAc in Hexanes, UV, I<sub>2</sub>)

<sup>1</sup>H NMR (500 MHz, CDCl<sub>3</sub>) δ 7.88 (d, *J* = 8.0 Hz, H), 7.41 – 7.39 (m, 6H), 7.34 – 7.30 (m, 2H),

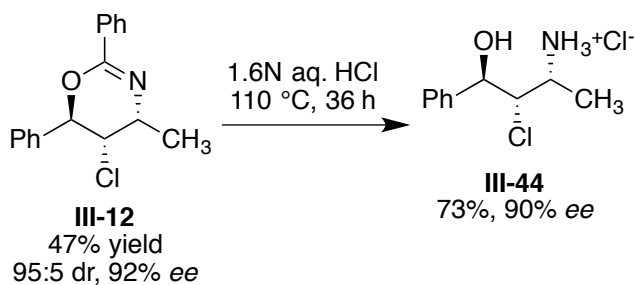
5.31 (d, *J* = 10.5 Hz, 1H), 4.12 – 4.03 (m, 2H), 1.59 (d, *J* = 6.5 Hz, 3H); <sup>13</sup>C NMR (125 MHz,

CDCl<sub>3</sub>) δ 154.8, 138.4, 132.8, 130.8, 129.2, 128.4, 128.1, 127.9, 127.3, 82.1, 58.2, 36.2, 22.5

HRMS analysis (ESI): Calculated for (M+H): C<sub>17</sub>H<sub>17</sub>INO: 378.0355; Found: 378.0356

Resolution of enantiomers: DAICEL Chiralcel OJ-H column, 254 nm, 5% IPA in hexane, 1.0 mL/min, RT1 = 6.4 min, RT2 = 7.4 min

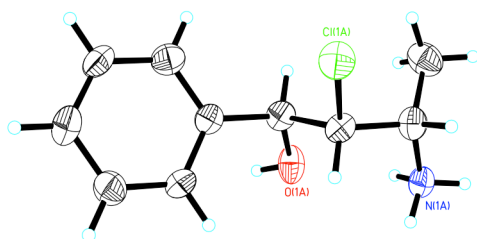
*B* Acid hydrolysis of dihydrooxazine product (**2a**):



**III-12** (100 mg, 0.35 mmol) was suspended in 1.5N aq. HCl (3.5 mL) in a screw-capped glass vial equipped with a magnetic stir bar. The resulting suspension was stirred vigorously at 110 °C (sand bath temperature) for 48 h. After allowing to cool to ambient temperature, the crude reaction mixture was partitioned against 5 mL Et<sub>2</sub>O and 5 mL 1N aq. HCl. The organic layer

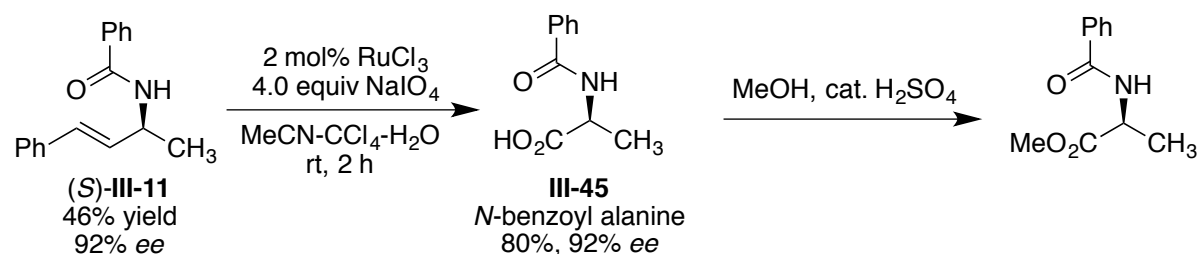
containing benzoic acid was discarded. The aqueous fraction was concentrated to dryness to give the desired hydrochloride salt as a white solid in 73% yield. Crystallization from MeOH-EtOAc gave crystals suitable for single crystal X-ray diffraction analysis. The crystal structure served to confirm the absolute stereochemistry of **III-12**.

**Figure III-13.** Crystal structure of drawing of **III-44**



$^1\text{H}$  NMR (500 MHz,  $\text{CD}_3\text{CN} + 2$  drops  $\text{D}_2\text{O}$ )  $\delta$  7.48 – 7.38 (m, 5H), 5.08 (d,  $J = 5.5$  Hz, 1H), 4.31 (dd,  $J = 5.5, 2.0$  Hz, 1H), 3.79 – 3.75 (m, 1H), 1.35 (d,  $J = 7.0$  Hz, 3H);  $^{13}\text{C}$  NMR (125 MHz,  $\text{CD}_3\text{CN} + 2$  drops  $\text{D}_2\text{O}$ )  $\delta$  141.7, 130.2, 129.9, 128.1, 77.1, 66.3, 49.3, 17.3

C] Oxidative cleavage of recovered olefin substrate:



**III-11** (50 mg, 0.20 mmol, 1.0 equiv) was dissolved in a 2:2:3 mixture of  $\text{MeCN-CCl}_4\text{-H}_2\text{O}$  (3.5 mL) in a screw capped glass vial equipped with a magnetic stir bar.  $\text{NaIO}_4$ , (175 mg, 0.80 mmol, 4.0 equiv) was added in a single portion. The resulting suspension was stirred vigorously till all the  $\text{NaIO}_4$  had dissolved.  $\text{RuCl}_3 \cdot x\text{H}_2\text{O}$  (0.81 mg, 0.004 mmol, 0.02 equiv) was added and

the reaction mixture was stirred at ambient temperature. TLC analysis (20% EtOAc in Hexanes) revealed complete consumption of starting material in 2 hours. The reaction mixture was partitioned against water and EtOAc. Extraction of the aqueous layer with EtOAc followed by concentration of the organics gave the crude acid. Purification by column chromatography on silica gel (1:1 EtOAc-Hexanes to 99.9:0.1 EtOAc-AcOH gradient) gave pure *N*-benzoyl alanine (30 mg, 80% yield, white solid). Characterization data including optical rotation was in complete agreement with those reported elsewhere.<sup>46</sup>

The isolated *N*-benzoyl alanine (**III-45**) was dissolved in MeOH (2 mL). 1 drop of conc. H<sub>2</sub>SO<sub>4</sub> was added and the reaction was stirred at 50 °C for 2 hours in a screw-capped vial. Solid NaHCO<sub>3</sub> (~100 mg) was added to quench the acid catalyst. Filtration of the reaction mixture through a plug of celite followed by removal of the volatiles *in vacuo* gave the methyl ester of *N*-benzoyl alanine in quantitative yield.

Resolution of enantiomers: Agilent Cyclosil b column (At constant pressure of 14.89 psi of He carrier gas) temperature ramp from 90 °C to 220 °C at 5 °C/min and then held at 220 °C for 5 min. RT1 = 26.0 min, RT2 = 26.2 min

### III.6.8. Stoichiometric NMR experiments.

Stoichiometric mixtures of the racemic substrate **III-11** and DHQD<sub>2</sub>PHAL (1:1 molar ratio) were analyzed by <sup>1</sup>H NMR in order to uncover the nature of substrate-catalyst interactions in numerous solvents. Spectra in CF<sub>3</sub>CH<sub>2</sub>OH were recorded by employing no-D <sup>1</sup>H NMR using solvent suppression. All analyses were performed on a 500 MHz NMR machine on 20 mM concentration solutions of **III-11** and DHQD<sub>2</sub>PHAL at 25±0.5 °C temperature and peaks were referenced to tetramethyl silane (TMS) or the residual solvent peaks.

1:1 mixture of racemic olefin and DHQD<sub>2</sub>PHAL showed a binding phenomenon in numerous solvents. Diastereomeric complexes were seen by NMR indicating preferential binding of one enantiomer of **III-11** with the chiral catalyst. Time-averaged distribution of bound and unbound substrate was observed in all instances (i.e. exchange was more rapid than the NMR time scale).

Figure III-14  $^1\text{H}$  NMR of 1:1 III-11: DHQD<sub>2</sub>PHAL in  $\text{CDCl}_3$

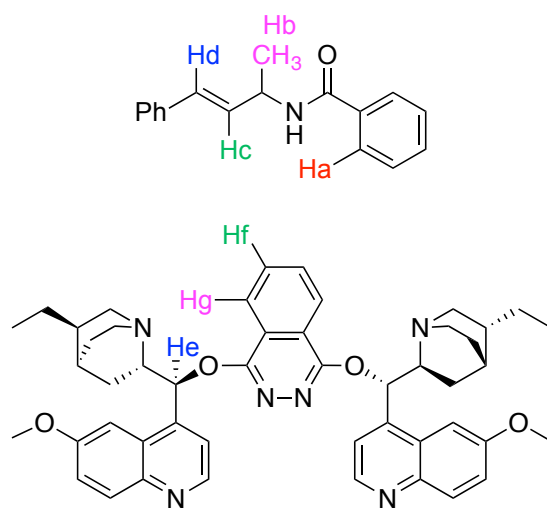
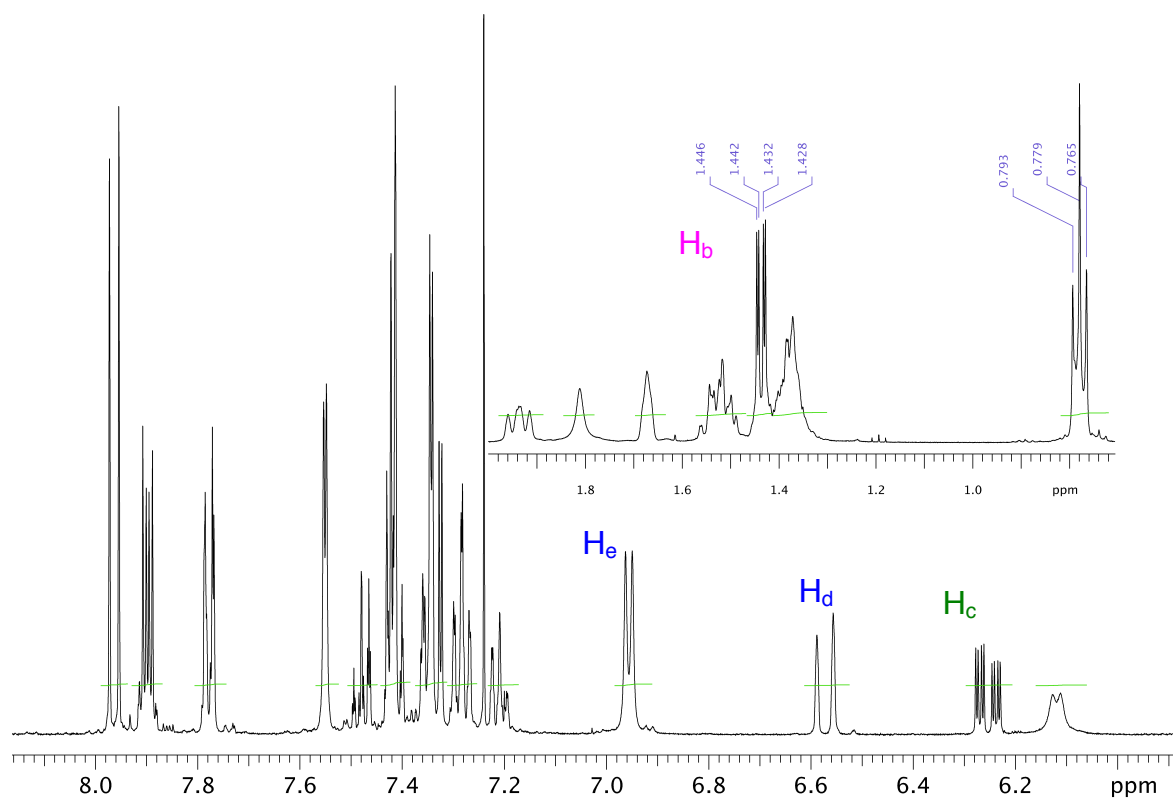


Figure III-15.  $^1\text{H}$  NMR of 1:1 III-11: DHQD<sub>2</sub>PHAL in CD<sub>3</sub>CN:

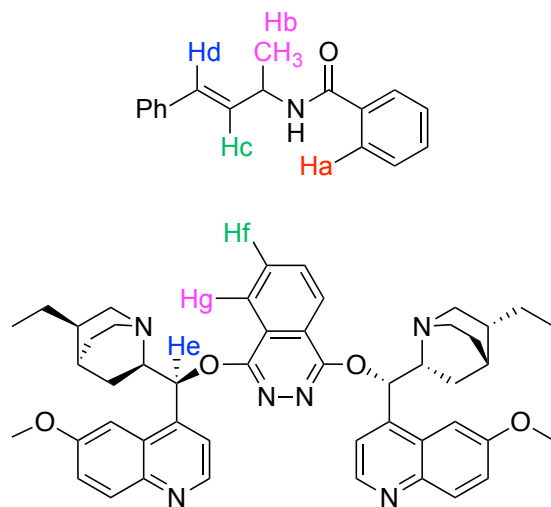
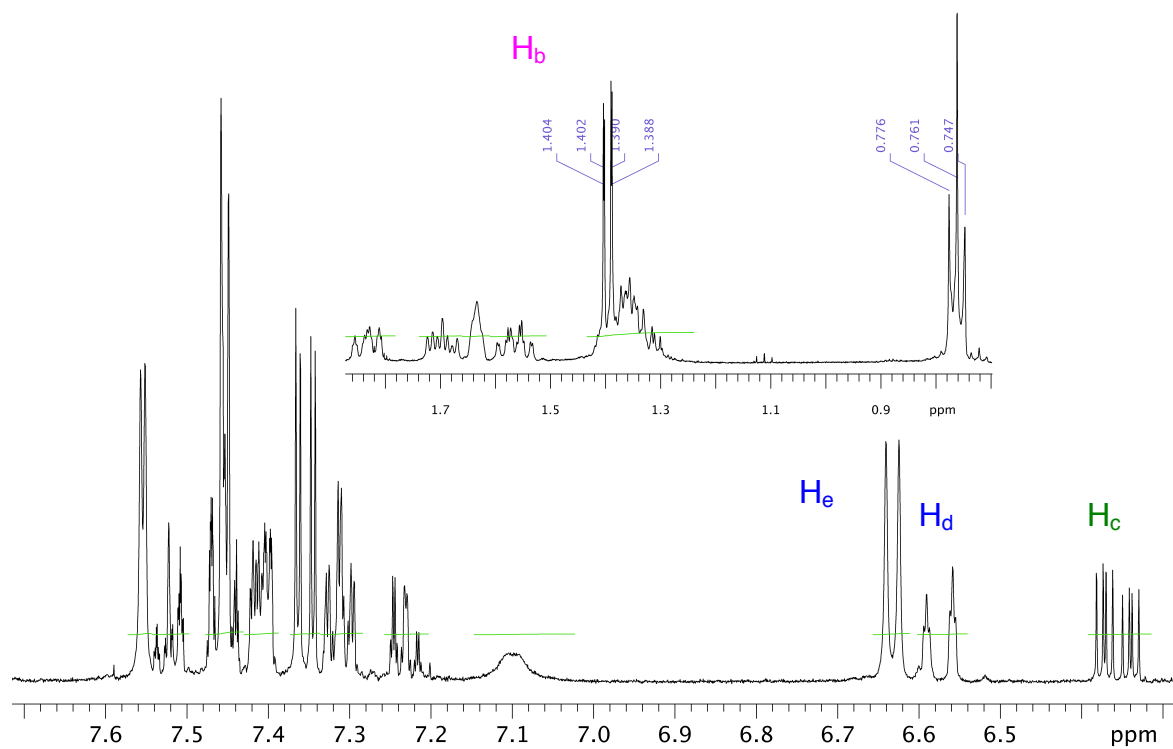


Figure III-16.  $^1\text{H}$  NMR of 1:1 III-11: DHQD<sub>2</sub>PHAL in Acetone-d<sub>6</sub>

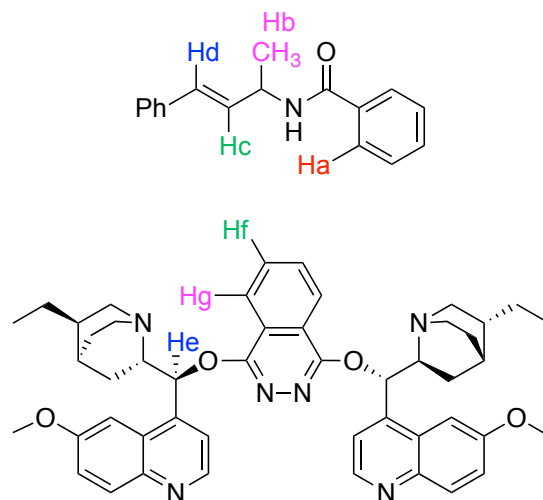
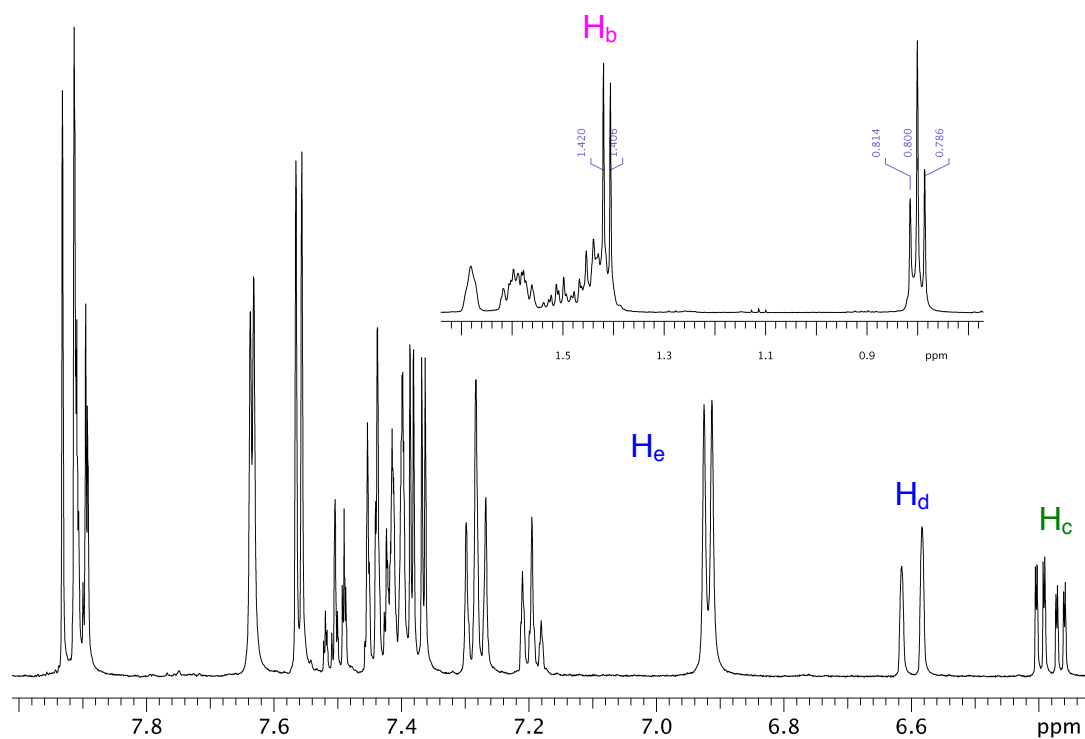


Figure III-17.  $^1\text{H}$  NMR of 1:1 III-11: DHQD<sub>2</sub>PHAL in C<sub>6</sub>D<sub>6</sub>

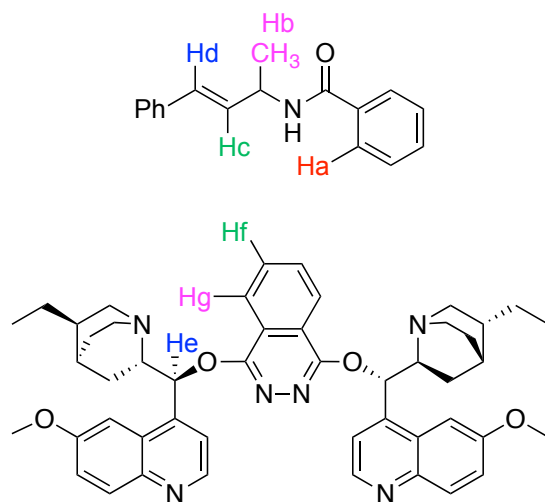
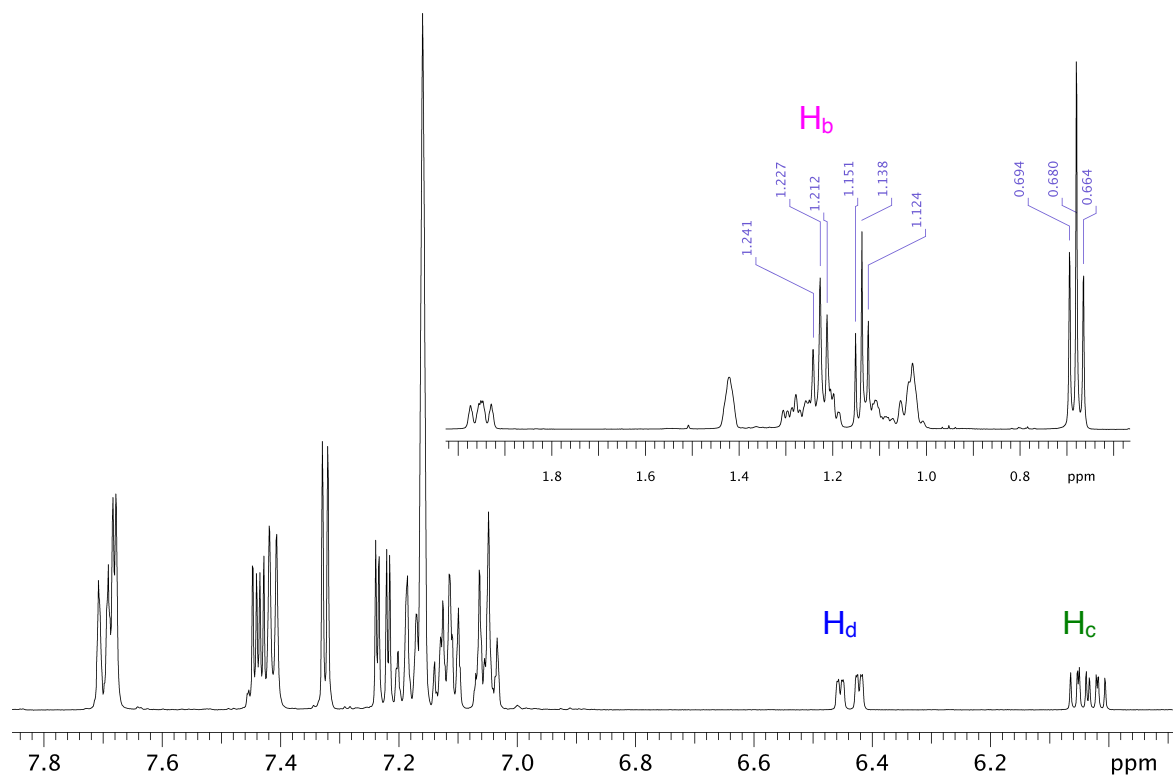


Figure III-18.  $^1\text{H}$  NMR of 1:1 III-11: DHQD<sub>2</sub>PHAL in  $\text{CF}_3\text{CH}_2\text{OH}$

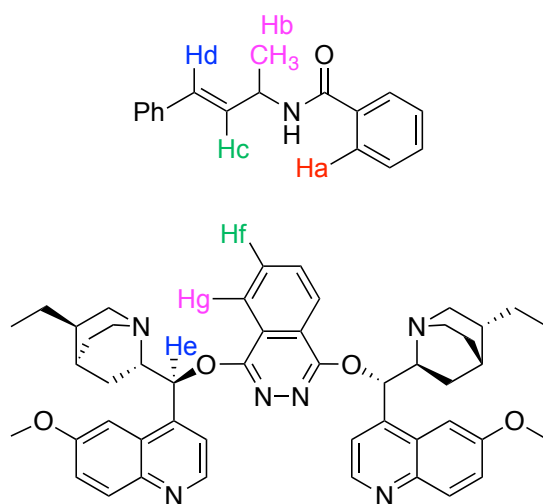
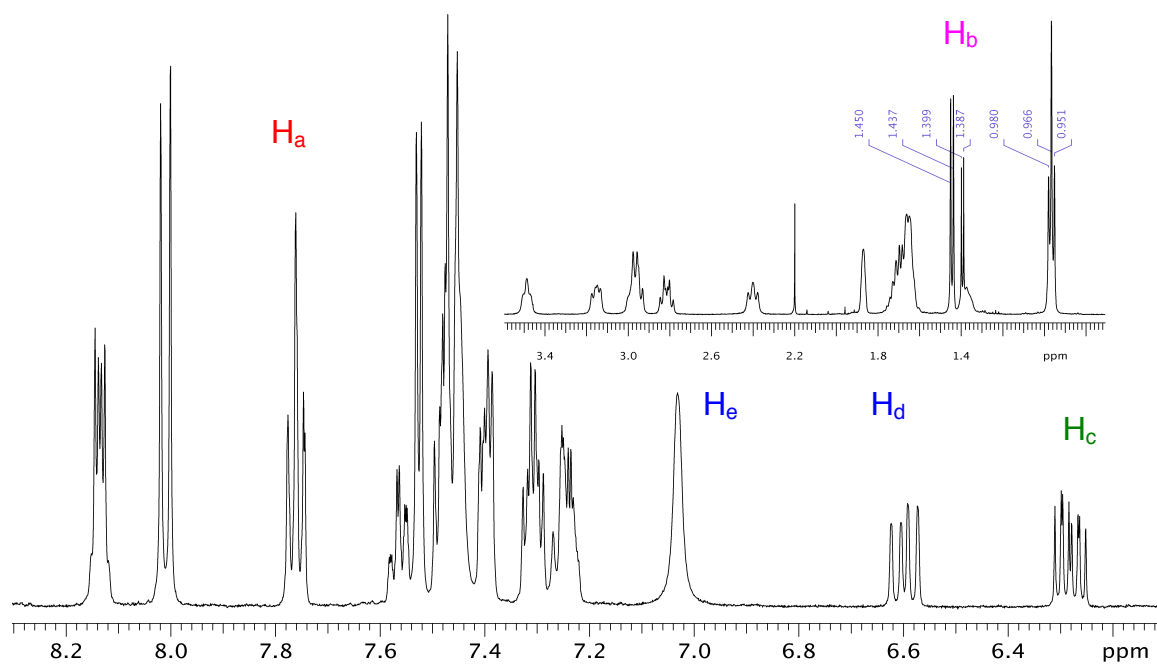


Figure III-19.  $^1\text{H}$  NMR of 1:1 III-38: DHQD<sub>2</sub>PHAL in  $\text{CF}_3\text{CH}_2\text{OH}$

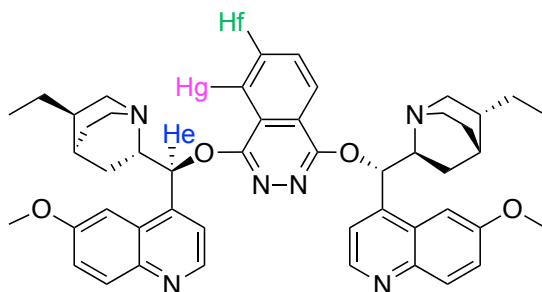
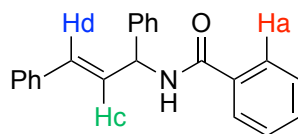
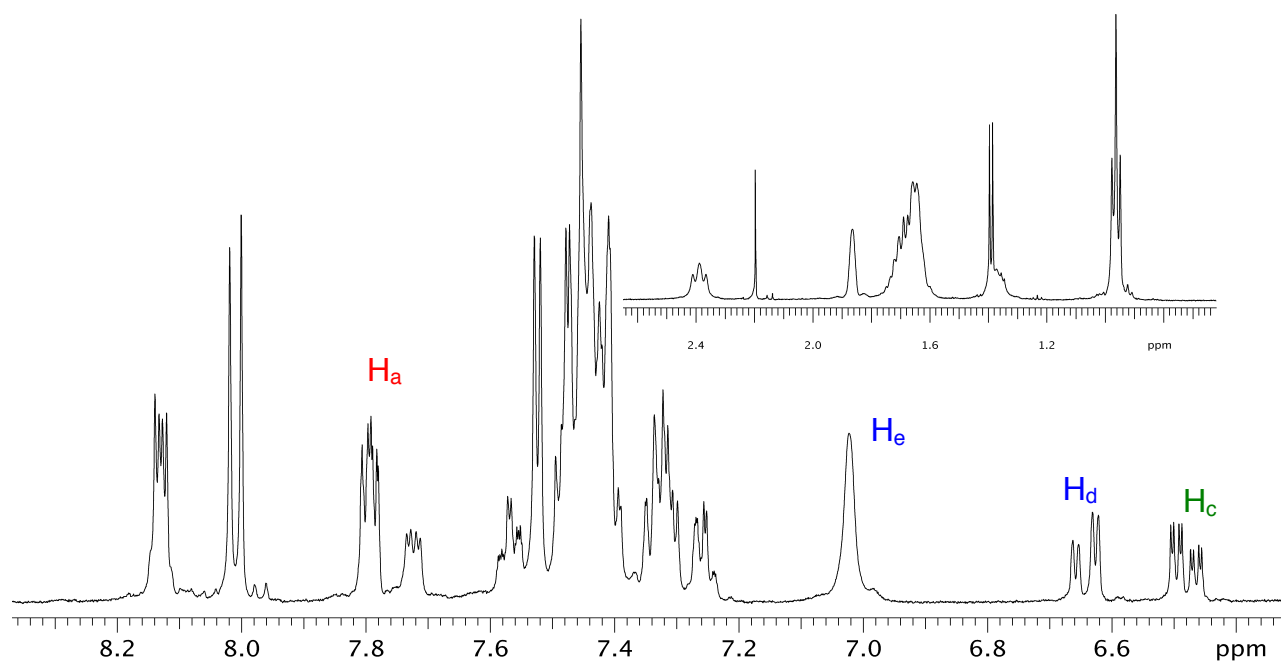
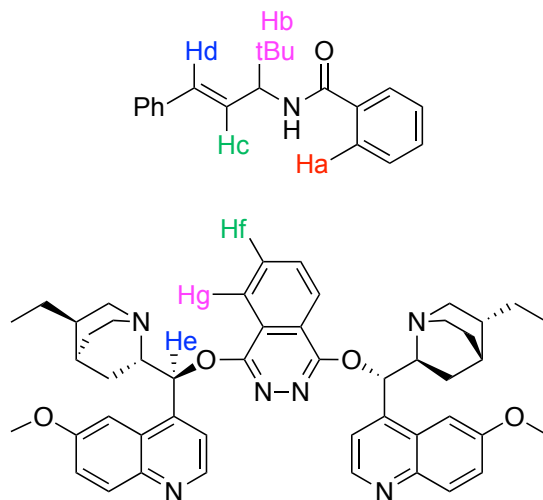
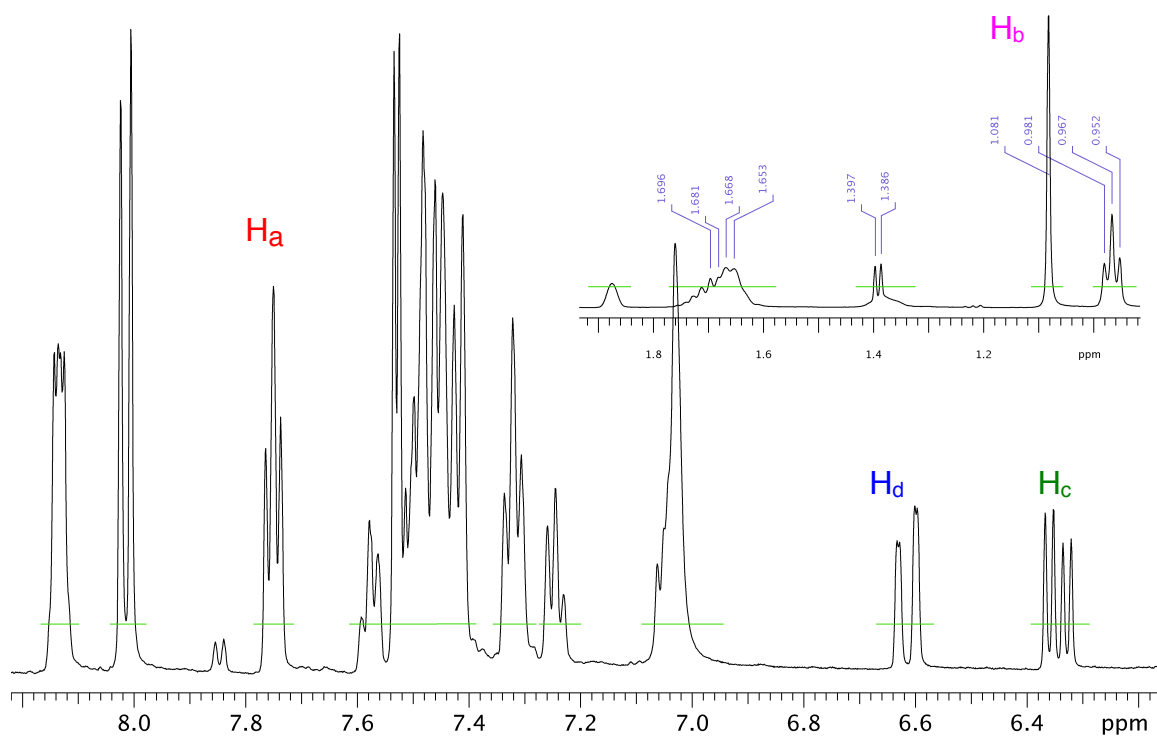


Figure III-20.  $^1\text{H}$  NMR of 1:1 **III-39**: DHQD<sub>2</sub>PHAL in  $\text{CF}_3\text{CH}_2\text{OH}$ :



Note that going from **III-11** to **III-38** to **III-39**, there is a progressive decrease in diastereotopicity of the hydrogen bonded complex of 1:1 complexes of the substrate with (DHQD)<sub>2</sub>PHAL

(compare spectra **Figure III-18** to **Figure III-20** above). This is an indication that bulky substrates do not bind well to the catalyst.

## REFERENCES

## REFERENCES

- (1) Gao, J.; Ma, S.; Major, D. T.; Nam, K.; Pu, J.; Truhlar, D. G. *Chem. Rev.* **2006**, *106*, 3188.
- (2) Warshel, A.; Sharma, P. K.; Kato, M.; Xiang, Y.; Liu, H.; Olsson, M. H. M. *Chem. Rev.* **2006**, *106*, 3210.
- (3) Yoder, R. A.; Johnston, J. N. *Chem. Rev.* **2005**, *105*, 4730.
- (4) Nicolaou, K. C.; Edmonds, D. J.; Bulger, P. G. *Angew. Chem. Int. Ed.* **2006**, *45*, 7134.
- (5) Knowles, R. R.; Jacobsen, E. N. *Proc. Natl. Acad. Sci.* **2010**, *107*, 20678.
- (6) Pellissier, H. *Adv. Synth. Catal.* **2011**, *353*, 1613.
- (7) Robinson, D. E. J. E.; Bull, S. D. *Tetrahedron: Asymmetry* **2003**, *14*, 1407.
- (8) Castellanos, A.; Fletcher, S. P. *Chemistry-a European Journal* **2011**, *17*, 5766.
- (9) Chen, G.; Ma, S. *Angewandte Chemie-International Edition* **2010**, *49*, 8306.
- (10) Denmark, S. E.; Kuester, W. E.; Burk, M. T. *Angew. Chem. Int. Ed.* **2012**, *51*, 10938.
- (11) Hennecke, U. *Chem. Asian J.* **2012**, *7*, 456.
- (12) Murai, K.; Fujioka, H. *Heterocycles* **2013**, *87*, 763.
- (13) Ohta, B. K.; Hough, R. E.; Schubert, J. W. *Org. Lett.* **2007**, *9*, 2317.
- (14) Olah, G. A.; Bollinger, J. M. *J. Am. Chem. Soc.* **1968**, *90*, 947.
- (15) Olah, G. A.; Bollinger, J. M.; Brinich, J. *J. Am. Chem. Soc.* **1968**, *90*, 6988.
- (16) Olah, G. A.; Peterson, P. E. *J. Am. Chem. Soc.* **1968**, *90*, 4675.
- (17) Olah, G. A.; Westerman, P. W.; Melby, E. G.; Mo, Y. K. *J. Am. Chem. Soc.* **1974**, *96*, 3565.
- (18) Solling, T. I.; Radom, L. *Int. J. Mass Spectrom* **1999**, *185*, 263.
- (19) Kang, S. H.; Lee, S. B.; Park, C. M. *J. Am. Chem. Soc.* **2003**, *125*, 15748.

- (20) Corey, E. J.; Noe, M. C.; Guzman-Perez, A. *J. Am. Chem. Soc.* **1995**, *117*, 10817.
- (21) Yun, J.; Buchwald, S. L. *J. Org. Chem.* **2000**, *65*, 767.
- (22) Brimble, M. A.; Johnston, A. D. *Tetrahedron-Asymmetry* **1997**, *8*, 1661.
- (23) Xing, X.; Zhao, Y.; Xu, C.; Zhao, X.; Wang, D. Z. *Tetrahedron* **2012**, *68*, 7288.
- (24) Fang, C.; Paull, D. H.; Hethcox, J. C.; Shugrue, C. R.; Martin, S. F. *Org. Lett.* **2012**, *14*, 6290.
- (25) Ikeuchi, K.; Ido, S.; Yoshimura, S.; Asakawa, T.; Inai, M.; Hamashima, Y.; Kan, T. *Org. Lett.* **2012**, *14*, 6016.
- (26) Wilking, M.; Mück-Lichtenfeld, C.; Daniliuc, C. G.; Hennecke, U. *J. Am. Chem. Soc.* **2013**, *135*, 8133.
- (27) Whitehead, D. C.; Yousefi, R.; Jaganathan, A.; Borhan, B. *J. Am. Chem. Soc.* **2010**, *132*, 3298.
- (28) Brunel, J. M. *Chem. Rev.* **2005**, *105*, 857.
- (29) Chen, Y.; Yekta, S.; Yudin, A. K. *Chem. Rev.* **2003**, *103*, 3155.
- (30) Schaus, S. E.; Brandes, B. D.; Larrow, J. F.; Tokunaga, M.; Hansen, K. B.; Gould, A. E.; Furrow, M. E.; Jacobsen, E. N. *J. Am. Chem. Soc.* **2002**, *124*, 1307.
- (31) Zhou, L.; Tan, C. K.; Jiang, X.; Chen, F.; Yeung, Y.-Y. *J. Am. Chem. Soc.* **2010**, *132*, 15474.
- (32) Denmark, S. E.; Burk, M. T. *Proc. Natl. Acad. Sci.* **2010**, *107*, 20655.
- (33) Nicolaou, K. C.; Simmons, N. L.; Ying, Y.; Heretsch, P. M.; Chen, J. S. *J. Am. Chem. Soc.* **2011**, *133*, 8134.
- (34) Kang, S. H.; Park, C. M.; Lee, S. B. *Bull. Korean Chem. Soc.* **2004**, *25*, 1615.
- (35) Sakakura, A.; Sakuma, M.; Ishihara, K. *Org. Lett.* **2011**, *13*, 3130.
- (36) Kang, S. H.; Park, C. M.; Lee, S. B.; Kim, M. *Synlett* **2004**, 1279.
- (37) Kagan, H. B.; Fiaud, J. C. In *Topics in Stereochemistry*; John Wiley & Sons, Inc.: 2007, p 249.
- (38) Kim, Y. G.; Cha, J. K. *Tetrahedron Lett.* **1989**, *30*, 5721.
- (39) Yousefi, R.; Ashtekar, K. D.; Whitehead, D. C.; Jackson, J. E.; Borhan, B. *J. Am. Chem. Soc.* **2013**, *135*, 14524.

- (40) Marzijarani, N.; Ashtekar, D. K.; Borhan, B. *Unpublished results*.
- (41) Okamoto, N.; Miwa, Y.; Minami, H.; Takeda, K.; Yanada, R. *J. Org. Chem.* **2011**, *76*, 9133.
- (42) Nakahara, K.; Fujioka, H. *Symmetry* **2010**, *2*, 437.
- (43) Miriyala, B.; Bhattacharyya, S.; Williamson, J. S. *Tetrahedron* **2004**, *60*, 1463.
- (44) Thompson, A. S.; Humphrey, G. R.; DeMarco, A. M.; Mathre, D. J.; Grabowski, E. J. J. *J. Org. Chem.* **1993**, *58*, 5886.
- (45) Klauber, E. G.; Mittal, N.; Shah, T. K.; Seidel, D. *Org. Lett.* **2011**, *13*, 2464.
- (46) Miyashita, A.; Takaya, H.; Souchi, T.; Noyori, R. *Tetrahedron* **1984**, *40*, 1245.

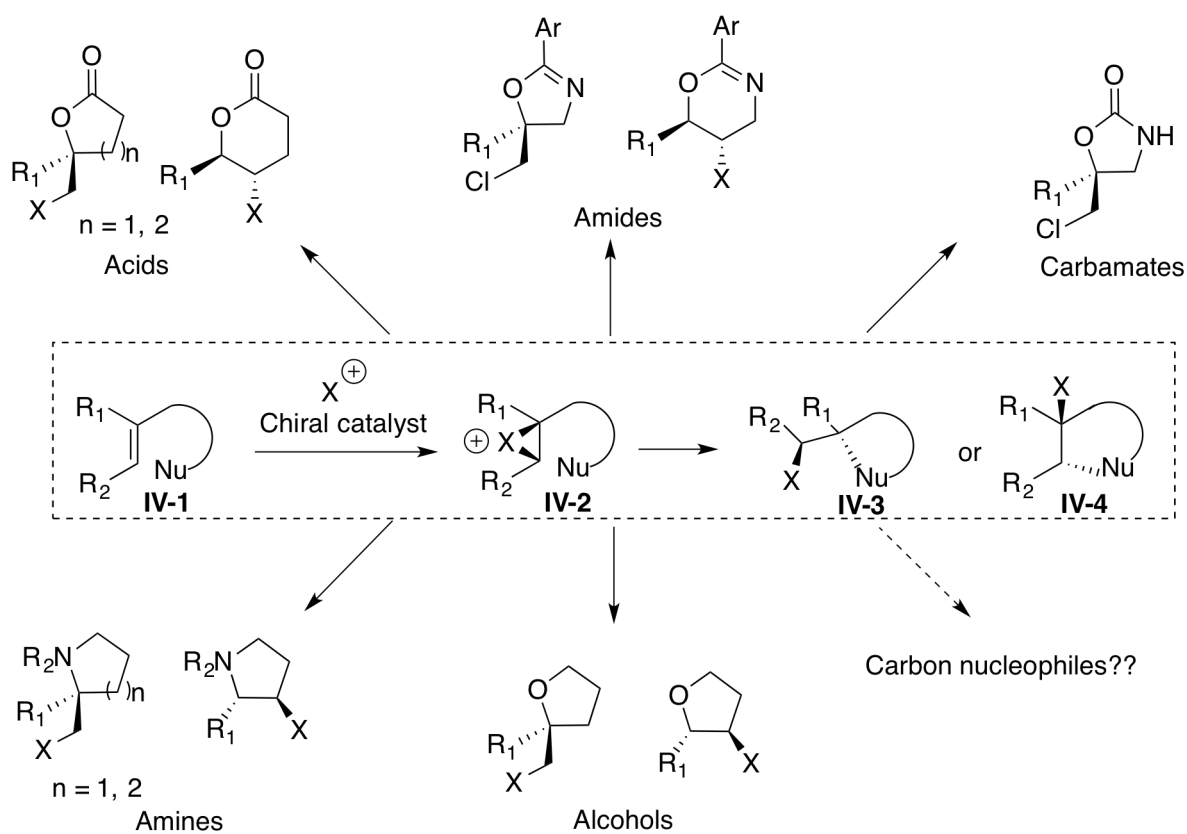
## Chapter IV

### *Organocatalytic arylation of chiral chloronium ions: Parlaying the stereochemistry of an enantioselective C-Cl bond formation to a C-C bond forming reaction.*

#### IV.1. Introduction.

The preceding chapters have described my efforts to utilize asymmetric halogenation of alkenes as a 'lynchpin event' to forge C-heteroatom bonds in a stereoselective fashion. These endeavors have led to the development of many unprecedented asymmetric halocyclization

**Figure IV-1.** Nucleophiles explored thus far (2013) in catalytic asymmetric halocyclization reactions



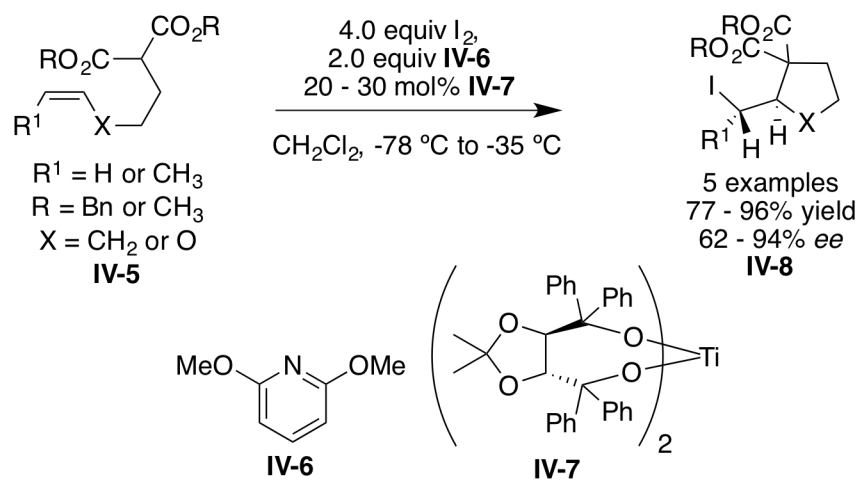
reactions such as the chlorocyclization of unsaturated carboxylic acids, amides and carbamates. Following seminal reports of asymmetric halogenation of alkenes from our group in 2010 this research area has witnessed an explosive growth over the last 3 years. Combined theoretical and experimental approaches have greatly expanded the scope of such transformations with regards to both the halogen sources used to activate olefins as well as the compatible nucleophiles. A review of the recent literature in this area reveals numerous reports of catalytic asymmetric chloro-, bromo-, iodo- and fluorocyclizations of alkenes with a wide variety of nucleophiles such as carboxylic acids, amides, sulfonamides, alcohols, carbamates, oximes and even *N*-acyl hemiaminals (Some representative examples are presented in Figure IV-1). These efforts have paved the way to access a wide variety of chiral heterocycles by the hitherto unavailable means of enantioselective C-O and C-N bond formation reactions initiated by chiral halonium ions. Nonetheless, the translation of the stereoselectivity of the initial alkene halogenation event to a C-C bond formation has thus far remained underdeveloped. In this chapter, our work towards achieving this elusive transformation is described. These efforts have led to the development of the first catalytic asymmetric arylation of chiral chloronium ions. Kinetic studies have uncovered a ligand accelerated catalysis phenomenon that has further spurred research into rational catalyst design. The prediction of the optimal protecting group in the substrate was guided by an unprecedented approach of using Eyring plot analysis. What follows is a detailed account of the motivations, optimization, scope and preliminary mechanistic and kinetic studies for this reaction.

#### **IV.2. Prior work in stereoselective C-C bond formation initiated by halonium ions.**

The first example of a halonium ion initiated enantioselective C-C bond formation reaction was reported by Taguchi and coworkers in 1995.<sup>1</sup> They had disclosed the enantioselective iodocarbocyclization of 4-pentenyl malonates **IV-5** mediated by sub-

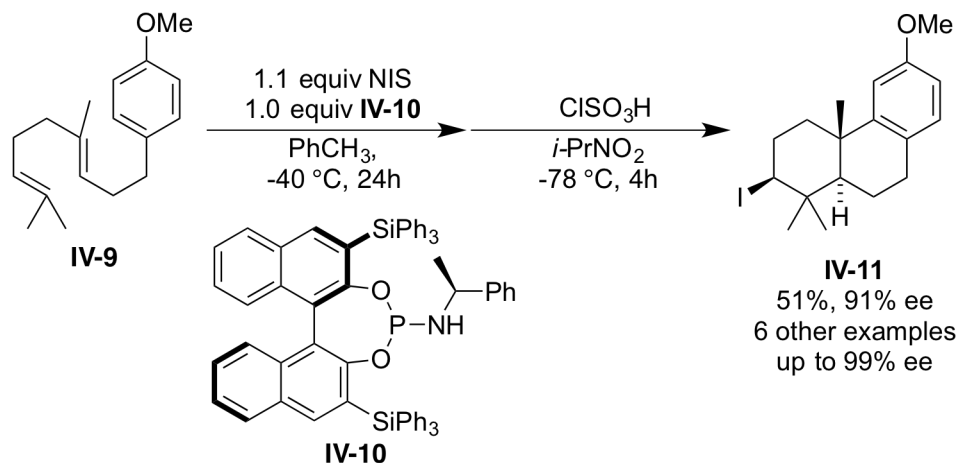
stoichiometric amounts of a chiral Ti-TADDOL complex in the presence of 4 equivalents of molecular iodine (see Figure IV-2). The hindered organic base **IV-6** was also necessary to obtain good enantioselectivities and yields. Despite the narrow substrate scope, exquisite enantioselectivity was observed for selected substrates.

**Figure IV-2.** Taguchi's asymmetric iodocarbocyclization of malonate esters



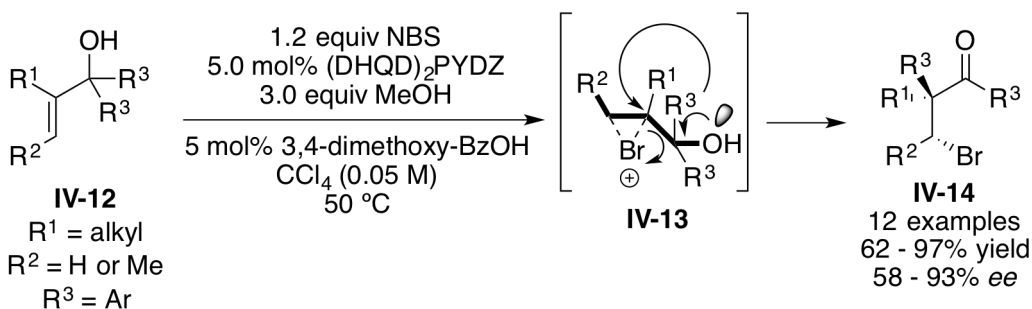
Ishihara and coworkers have demonstrated that enantioselective polyene cyclizations could also be achieved using NIS as the iodine source in the presence of stoichiometric amounts of chiral phosphoramidite promoters such as **IV-10** (Figure 3).<sup>2</sup>

**Figure IV-3.** Ishihara's chiral iodonium ion initiated polyene cascade



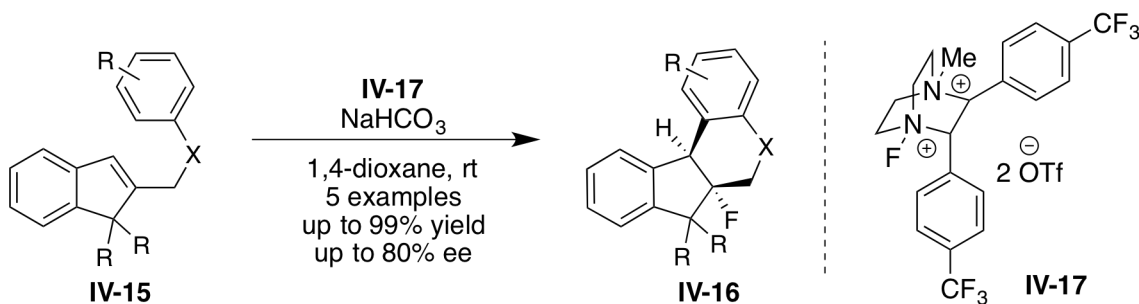
More recently, Tu and coworkers have disclosed an enantioselective bromination-semi-pinacol rearrangement cascade of tertiary allylic alcohols catalyzed by cinchona alkaloid dimers (see Figure IV-4).<sup>3</sup> Although not a halocyclization, this reaction represents a rare example of an enantioselective C-C bond formation reaction initiated by asymmetric halogenation of alkenes.

**Figure IV-4.** Tu's enantioselective alkene bromination/semi-pinacol rearrangement cascade



Most recently, Gouverneur and co-workers have disclosed an asymmetric fluorocyclization reaction that leads to the formation of C-C bonds.<sup>4</sup> Stoichiometric amount of the chiral flourenium source IV-17 was employed in the reaction (see Figure IV-5). Although the substrate scope was limited to 5 examples and the best enantioselectivity was 80% ee, this work demonstrates for the first time that chiral electrophilic fluorinating reagents can be synthesized and used for obtaining fluorinated carbocycles with useful levels of stereoselectivity.

**Figure IV-5.** Gouverneur's IV-17 mediated asymmetric fluorocarbocyclization reaction

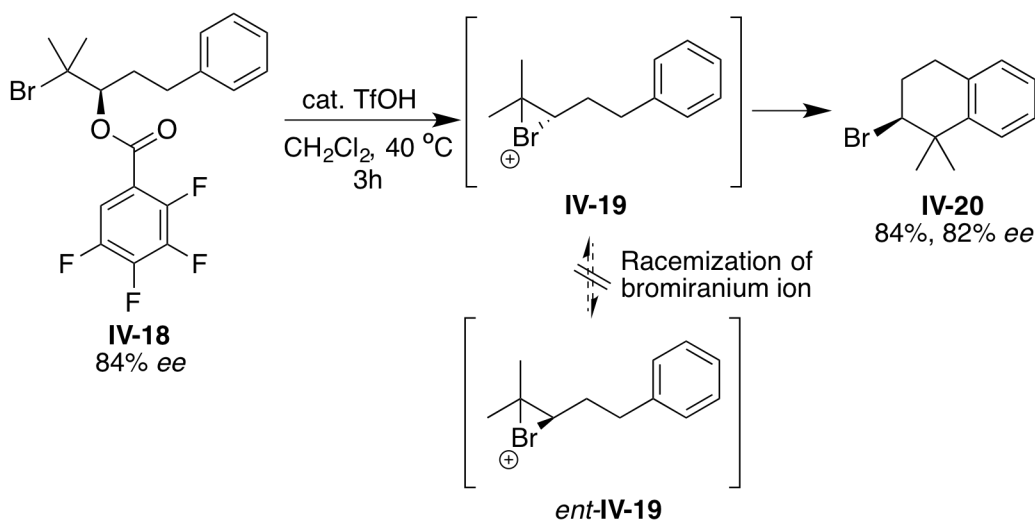


### IV.3. Challenges associated with rendering C-nucleophiles compatible with halonium chemistry.

The development of carbocyclization reactions initiated by halonium ions is a challenging transformation for many reasons. First, the carbon nucleophile can potentially compete with the alkene functionality for the halogen electrophile. Furthermore, this C- halogenation is likely irreversible unlike in the case of halocyclization reactions with heteroatom nucleophiles (notably the sulfonamides, where N-halogenated substrates have been invoked and/or characterized).<sup>5-7</sup> As such, its nucleophilicity must be sufficiently high to render it capable of capturing a tethered halonium ion while at the same time be attenuated with respect to that of the olefin to prevent non-productive C-halogenation pathways. Second, the rate of cyclization must be rapid enough to outcompete the kinetic and stereochemical decomposition pathways available to chiral halonium ions (these pathways have been described in detail in Chapter 1). Braddock and coworkers have elegantly demonstrated that olefin-to-olefin halonium transfer is not a dominant stereochemical erosion pathway for polyene cyclizations initiated by chiral bromonium ions (see Figure IV-6).<sup>8</sup> The capture of an in-situ generated chiral bromonium ion **IV-19** by the pendant aryl ring nucleophile exhibits complete stereochemical fidelity (see Figure IV-6) even in the presence of sacrificial amounts of 1-methylcyclohexene. The product **IV-20** and its precursor **IV-18** have practically identical enantioselectivities. That the enantioselectivity is unperturbed even in the presence of an added trisubstituted alkene rules out the possibility of degenerate bromonium transfer from the bromonium ion to the alkene as a potential stereo-randomizing event for the chiral bromonium ion. Reid and Rodebaugh have calculated the rates for these transfer processes to be as high as  $2 \times 10^7 \text{ M}^{-1} \text{ s}^{-1}$  at 27 °C from adamantalidene adamantane derived bromonium salts to mono- and disubstituted alkenes. In other words, these transfer rates approach the diffusion limit.<sup>9</sup>

It must be emphasized that at first glance, Braddock's results seem to contradict the proposal of Denmark<sup>10</sup> suggesting that chiral bromonium ions undergo rapid racemization in the presence of alkenes *via* degenerate olefin-to-olefin bromonium transfer (a hypothesis that is consistent with the observations of Reid and Rodebaugh stated above); nonetheless, a direct comparison of these two results is invalid given that Denmark's study was restricted to the *intermolecular* capture of halonium ions by weakly nucleophilic carboxylate anions – a process likely to be much slower (and hence more susceptible to racemization *via* bromonium transfer) than any *intramolecular* variants. Clearly, the rates of intramolecular nucleophilic capture of halonium ions are much faster than any racemization pathways. Testament to this fact is the development of numerous highly enantioselective bromocyclization reactions in recent years.

**Figure IV-6.** Braddock's demonstration of negligible racemization rates for chiral bromonium ions in a carbocyclization reaction.



Regardless, Braddock's experiment establishes that racemization *via* olefin-to-olefin halonium transfer may not be diffusion controlled. (It is likely that the steric and electronic parameters of the bromonium ion dictate the rates of bromonium transfers; the transfer rates from the sterically demanding adamantylidene adamantane derived bromonium ion is evidently much faster than those from simpler trisubstituted alkene derived bromonium ions)

Given the paucity of carbocyclization reactions initiated by chiral halonium ions and our lab's interest in the development of asymmetric halogenation reactions, we initiated a project aimed at parlaying the stereochemical information of the initial alkene halogenation event to a C-C bond forming reaction. The exercise would be intellectually stimulating due to the lack of any precedence and guiding principles at our disposal. It was hoped that fundamentally new insights into the mechanistic aspects, reactivity of molecules and reaction design would emerge from this study in addition to tackling an unmet challenge in organic chemistry.

#### **IV.4. Results and discussion.**

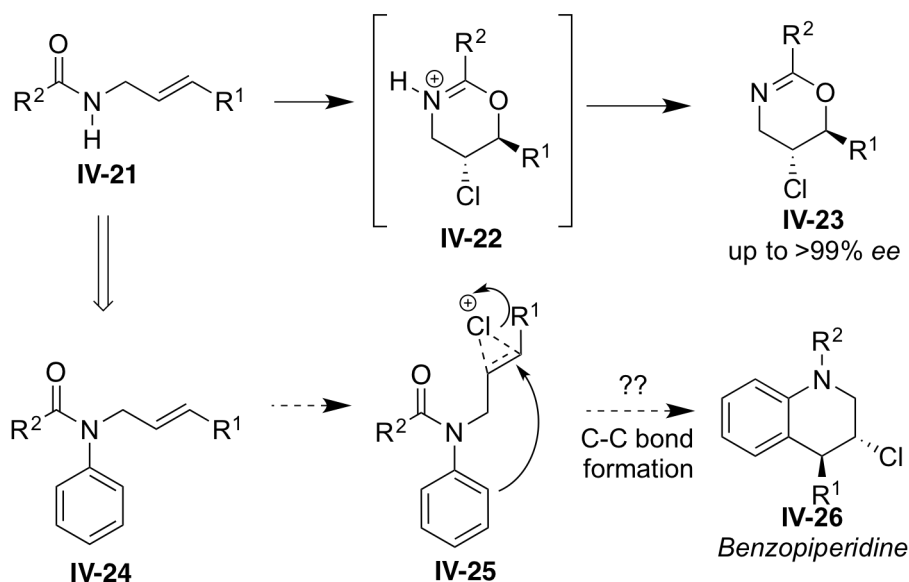
##### **IV.4.1. Preliminary studies: Determination of test reaction and scale.**

As is the case with the development of any new reaction methodology, the first and crucial step was the choice of a test reaction. We decided to pursue the optimization of a Friedel-Crafts type of reaction of arenes initiated by the electrophilic activation of a tethered olefin by halonium ions. The *N*-aryl amide **IV-27** was initially chosen as the test substrate. This choice was partly based on intuition (*vide infra*) and partly on the ease with which the arene ring nucleophilicity and the protecting group on the N tether can be varied. This would enable a systematic evaluation of steric and electronic parameters of the test substrate on the yields and enantioselectivities of this reaction.

The mechanistic hypothesis at the outset is highlighted in Figure IV-7. The test substrate chosen for the carbocyclization reaction bears close resemblance to the substrates used in the amide chlorocyclization chemistry (**IV-21** and **IV-24** in Figure IV-7).<sup>11</sup> It was hoped that the structural similarities between **IV-21** and **IV-24** might provide similar substrate-catalyst interactions that enabled a highly enantioselective chlorocyclization of amides. Once the halonium ion is delivered to the alkene in a face-selective manner, nucleophilic attack by the pendant aryl ring will ensue leading to the product **IV-26**. The enantioselectivity determining

step will be the alkene halogenation event. With the aid of deuterium labeling studies, we have previously demonstrated that the DCDMH-(DHQD)<sub>2</sub>PHAL reagent system is capable of highly face-selective alkene chlorination in the unrelated chlorolactonization reaction of 1,1-disubstituted alkenoic acids; although we were cognizant that the lack of a hydrogen-bonding motif in this substrate, unlike in the secondary amide or alkenoic acid substrates used in prior studies, may significantly alter/diminish substrate-catalyst interactions.

**Figure IV-7.** Mechanistic hypothesis for an asymmetric Friedel-Crafts reaction initiated by a chiral chloronium ion

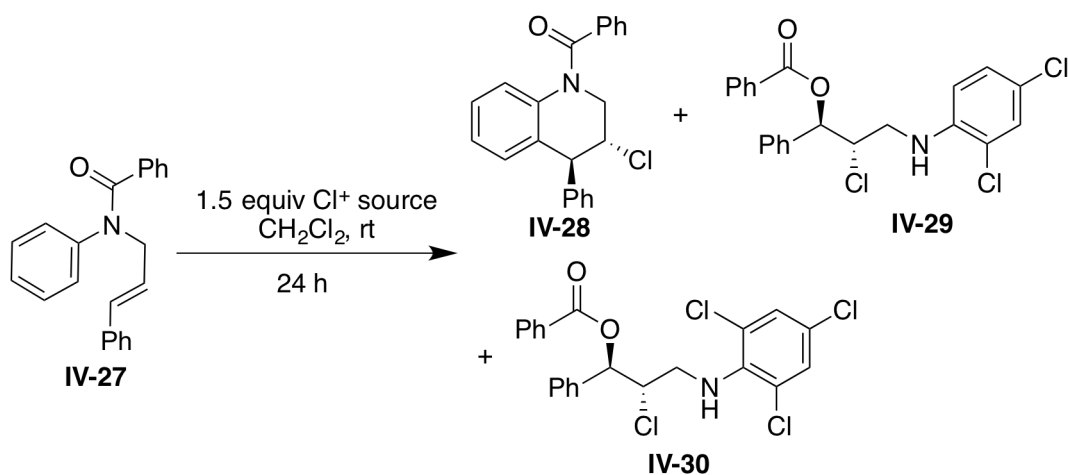


#### IV.4.2. Serendipitous discovery of a halonium ion initiated benzoate transposition of tertiary allylic amides.

Our studies commenced with identifying conditions that promote the efficient chlorocyclization under non-asymmetric conditions (i.e. without any catalysts or with achiral catalysts). The test substrate **IV-27** was treated with 1.5 equiv of the chloronium source (NCS or DCDMH) in CH<sub>2</sub>Cl<sub>2</sub> (entries 1 and 2, Table IV-1). Negligible reaction was seen after 24 h with NCS as the chlorine source. The reaction with the more reactive DCDMH showed about

10% conversion (based on NMR yield of unreacted substrate) over the same duration. When the reaction with DCDMH was repeated in the presence of 10 mol% DABCO as a non chiral catalyst, the starting material was cleanly consumed in 24 h to give two products as judged by TLC analysis (entry 3, Table IV-1). Disappointingly, neither product was the desired benzopiperidine product **IV-28**. Instead, these products were identified as **IV-29** and **IV-30**! On employing an excess of DCDMH, only **IV-30** was isolated (entry 4, Table IV-1). The reaction is formally a 1,4-benzoate transposition that proceeds with the creation of two new stereocenters in the product.

**Table IV-1.** Preliminary attempts to synthesize **IV-28** *via* chlorocyclization of **IV-27**



| Entry | $\text{Cl}^+$ source | Catalyst  | Conv. (Yield) | 28:29:30 |
|-------|----------------------|-----------|---------------|----------|
| 1.    | NCS                  | none      | trace         | nd       |
| 2.    | DCDMH                | none      | 10%           | nd       |
| 3.    | DCDMH                | 10% DABCO | >99%          | 0:5:1    |
| 4.    | DCDMH (4 equiv)      | 10% DABCO | >99% (64%)    | 0:0:1    |

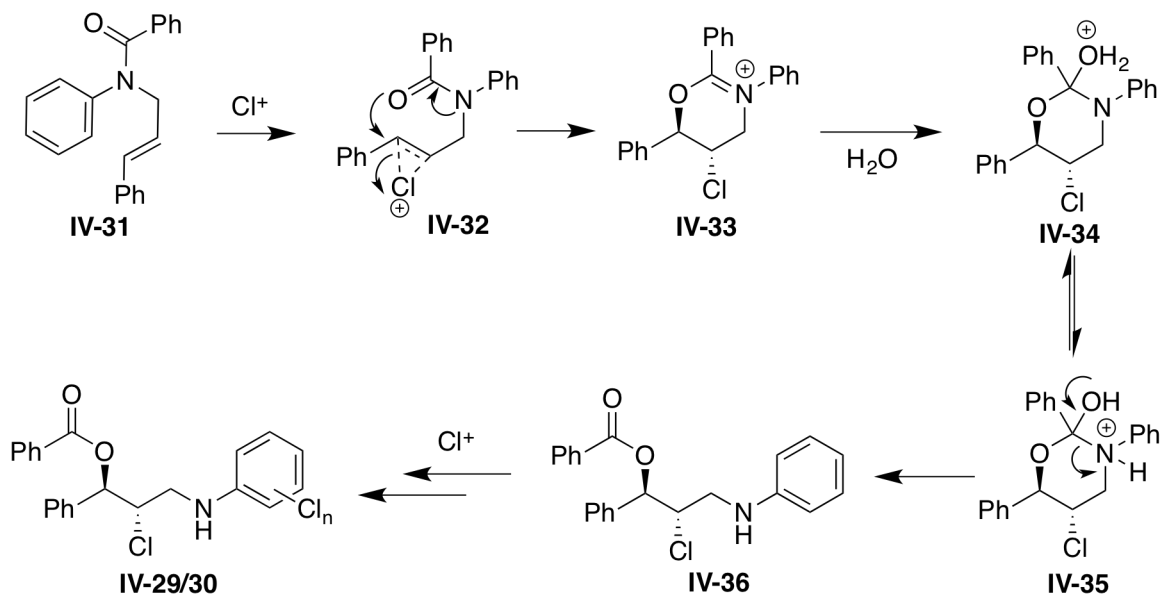
Note: Conversions and product ratios were determined by crude NMR analysis

The formation of these products may be rationalized by the mechanism given in Figure IV-8 shown below. The putative chloronium ion intermediate **IV-32** can be opened by the

neighboring *N*-phenyl benzamide functional group to give intermediate iminium ion **IV-33**. The hydrolysis of this intermediate (presumably by adventitious water in the solvent) can lead to the observed products after the collapse of the tetrahedral intermediate **IV-35**. The electrophilic chlorination of aryl ring in **IV-36** likely follows the rearrangement step (this assumption is based on the fact that the aryl ring does not become electron rich till after the rearrangement has occurred).

Preliminary studies indicate that the rearrangement occurs with comparable efficiency in numerous solvents. Lewis bases such as DABCO significantly increase the rate of the reaction; nonetheless, the reactions do proceed even in the absence of the Lewis base catalyst. Reactions are also significantly faster if fluorinated alcohols are employed as solvents.

**Figure IV-8.** Plausible mechanism for chloronium ion initiated 1,4-benzoate transposition of tertiary allylic amides



The benzoate transposition from the tertiary amide functional group to the alkene also leads to a simultaneous C-O and C-Cl vicinal difunctionalization of the alkene. Exquisite diastereoselectivity (>95:5 *dr*) was observed for this reaction. The diastereoselectivity is likely attributable to the *anti*-selective opening of the chloronium ion intermediate by the tertiary

amide. Anchimeric participation of tertiary amides in alkene halogenation reactions is not without precedence;<sup>12,13</sup> nonetheless, it has never been studied in any detail. Aspects such as the scope, mechanism and utility of this transformation are being currently explored in our lab along with possibilities of developing enantioselective variants of this reaction (this work is being pursued by one of the current group members - Ms. Nastaran Salehi Marzijarani).

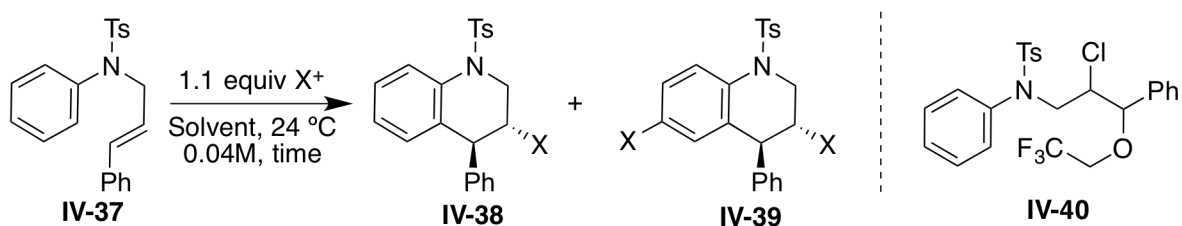
#### **IV.4.3. Development of a halocyclization route to *racemic* benzopiperidines.**

It was hypothesized that switching to a protecting group that is incapable of engaging in anchimeric assistance may alleviate the formation of the by-product. Indeed, substrate **IV-37** with a sulfonamide protecting group cleanly afforded the cyclized product on treatment with TCCA or NBS (see Entries 1 and 2, Table IV-2) even in the absence of any catalyst. Electrophilic aromatic chlorination was observed with TCCA and this led to tedious chromatographic separation of the over halogenated product **IV-39** from the desired product **IV-38**.

The use of the less reactive DCDMH gave negligible conversion to product even after 12 h in CHCl<sub>3</sub> (entry 3, Table IV-2). Nonetheless, in the presence of 5 mol% DABCO, the reaction with DCDMH proceeded to complete conversion with significantly reduced overchlorinated by-product (entry 4, Table IV-2) The reactions were significantly faster in fluorinated alcohol solvents. In fact, the reaction with DCDMH proceeded to completion even in the absence of any catalyst in CF<sub>3</sub>CH<sub>2</sub>OH (compare Entries 3 and 5 in Table IV-2). The low yield obtained in CF<sub>3</sub>CH<sub>2</sub>OH is due to the competing intermolecular nucleophilic interception of the chloronium ion by CF<sub>3</sub>CH<sub>2</sub>OH to give **IV-40**. Not surprisingly, the reaction proceeded cleanly in hexafluoroisopropanol (HFIP) (entry 6, Table IV-2) given its low nucleophilicity. In the presence of 2 mol% DABCO, the reaction proceeded in nearly quantitative yield in under 30 min (entry 7,

Table IV-2). HFIP could also be used as a co-solvent additive. Near quantitative yields were obtained in 9:1 CHCl<sub>3</sub>-hexafluoroisopropanol (HFIP) mixture (entry 8, Table IV-2). A detailed co-solvent study of HFIP with numerous other solvents was also performed; these results will be presented later.

**Table IV-2.** Preliminary results for the non-asymmetric chlorocyclization of **IV-37**



| Entry | X <sup>+</sup> source/ Time | Catalyst | Solvent   | Conv. (Yield) <sup>a</sup> | 38:39 |
|-------|-----------------------------|----------|---|----------------------------|-------|
| 1.    | TCCA, 15 min                | None     | CHCl <sub>3</sub>   | 100%                       | 2:3   |
| 2.    | NBS, 15 min                 | None     | CHCl <sub>3</sub>   | 100%                       | 1:0   |
| 3.    | DCDMH, 12 h                 | None     | CHCl <sub>3</sub>   | <5%                        | nd    |
| 4.    | DCDMH, 12 h                 | 5% DABCO | CHCl <sub>3</sub>   | 100%                       | 10:1  |
| 5.    | DCDMH, 12 h                 | None     | CF <sub>3</sub> CH <sub>2</sub> OH                              | 100% (37%)                 | 5:1   |
| 6.    | DCDMH, 12 h                 | None     | (CF <sub>3</sub> ) <sub>2</sub> CHOH                            | 100% (95%)                 | >10:1 |
| 7.    | DCDMH, 30 min               | 2% DABCO | (CF <sub>3</sub> ) <sub>2</sub> CHOH                            | 100% (99%)                 | >10:1 |
| 8.    | DCDMH, 30 min               | 2% DABCO | 9:1 CHCl <sub>3</sub> -<br>(CF <sub>3</sub> ) <sub>2</sub> CHOH | 100% (99%)                 | >10:1 |

Note: Yields and product ratios were determined by <sup>1</sup>H NMR of crude reaction mixture using MTBE as external standard

It warrants emphasis, that there have been no prior reports of direct synthesis of benzopiperidine heterocycles by employing a halocyclization approach. It emerged much later during the project that the conditions described above are fairly general with regards to substrate scope for the synthesis of racemic functionalized *N*-containing heterocycles.

It must be highlighted that recent efforts by the Gulder and Zhou labs have led to efficient non-asymmetric bromo- and iodo-carbocyclization reactions of *N*-aryl acrylamides by employing hypervalent iodine based reagents.<sup>14,15</sup> Presumably, enantioselective variants of these approaches will also appear in due course.

Having optimized the non-asymmetric protocol for the halonium ion initiated Friedel-Crafts reaction, attention was turned to rendering this transformation enantioselective. The beneficial effects of both fluorinated alcohols and Lewis base catalysts in mediating the non-asymmetric carbocyclization reaction, served as a guiding principle for the preliminary screening of reaction conditions.

#### **IV.4.4. Catalyst screen for asymmetric arylation of chloriranium ions**

The preliminary studies detailed in the preceding section employed compound **IV-37** as the test substrate for the chlorocyclization reaction. For practical reasons such as easier purification and *ee* determination by chiral HPLC, the methoxy-substituted substrate **IV-56** was chosen for optimization of the enantioselective variant (Fortuitously, this electron rich substrate also happened to give significantly better enantioselectivity for the cyclized products as opposed to the electron neutral substrate **IV-37**; this became evident much later during the optimization process)

All reactions were run in micro-scale (0.05 mmol of substrate). Yields of the cyclized product were determined by crude NMR analysis with methyl *t*-butyl ether (MTBE) as an added external standard. Alternately, yields could also be determined by GC analysis of crude extracts

of the reaction mixture using undecane as an internal standard. Enantioselectivity (*ee*) was determined by chiral HPLC analysis (Chiralcel® OD or Chiralpak® AD-H columns).

Given that there were no H-bond donors in the test substrate, it was postulated that any strategy to impart enantioselectivity in the alkene halogenation reaction must involve creating a chiral environment around the halonium ion that will be delivered; in other words, substrate-catalyst interactions (that may potentially lead to discrimination of the two olefin faces) were deemed less crucial than the halonium source-catalyst interactions. Consequently, most of the evaluated catalysts were chiral Lewis bases or bifunctional catalysts that necessarily possessed a chiral Lewis base motif. These catalysts are listed in Figure IV-9. It merits mention that a series of 'in-house' catalysts that incorporated numerous structural variations in the initial 'hit' scaffolds were also synthesized and evaluated for the test reaction after the optimization of reaction variables; these results will be presented later.

The studies commenced with the evaluation of numerous commercially available organocatalysts at a 10 mol% loading in a 9:1 CHCl<sub>3</sub>-HFIP co-solvent mixture. (1*R*, 2*S*)-*N*-methylephedrine (**IV-41**) led to dramatic rate acceleration of the reaction; nonetheless the product was isolated in practically racemic form (entry 1, Table IV-3). Similar results were obtained with quinine derived thiocarbamate and thiourea catalysts **IV-42** and **IV-43** (entries 2 and 3, Table IV-3). Non-functionalized hydroquinidine (**IV-44**) gave significantly slower reaction rates (~60% conversion) and no enantioselectivity (entry 4, Table IV-3). The Hatakeyama catalyst **IV-45**<sup>16</sup> that is derived from quinidine also gave nearly racemic products, although it was significantly more active than hydroquinidine (entry 5, Table IV-3). The cinchonidine derived phase transfer catalyst **IV-46** also gave incomplete conversion (85%) and negligible enantioselectivity (entry 6, Table IV-3). Catalysts other than cinchona alkaloids were also evaluated. Oxazoline catalysts **IV-47** and **IV-48** did not lead to significant rate acceleration

(15% and 10% conversion, respectively). **IV-48** gave no stereinduction, whereas **IV-47** returned the product in 7% *ee* (entries 7 and 8, Table IV-3). The TADDOL derived catalyst **IV-49** returned the product in 17% conversion and 7% *ee* (entry 9, Table IV-3). BINAP **IV-50** was an active catalyst (67% conv.) but gave practically racemic product (entry 10, Table IV-3).

**Figure IV-9.** Catalysts evaluated for the asymmetric carbocyclization reaction

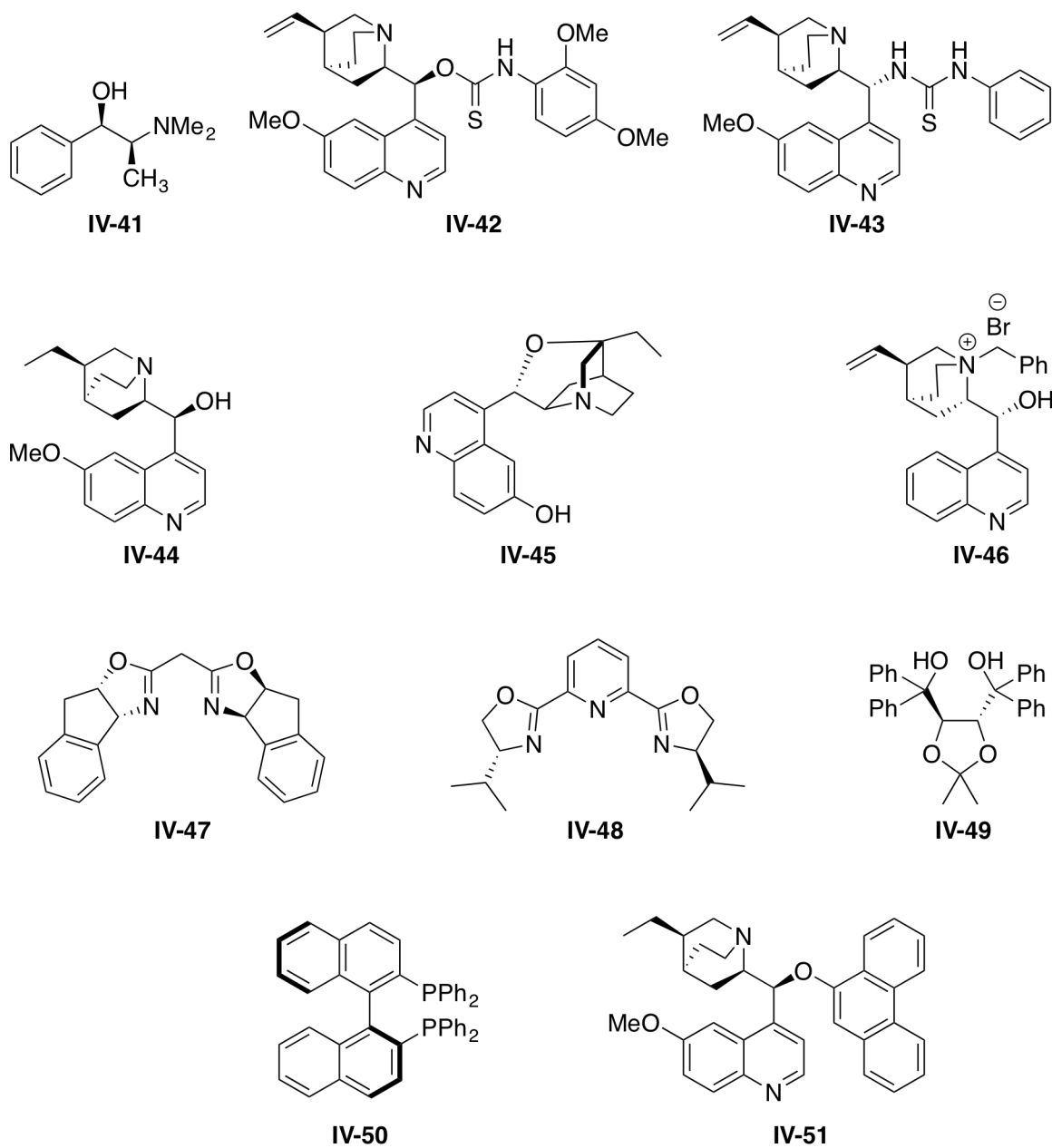
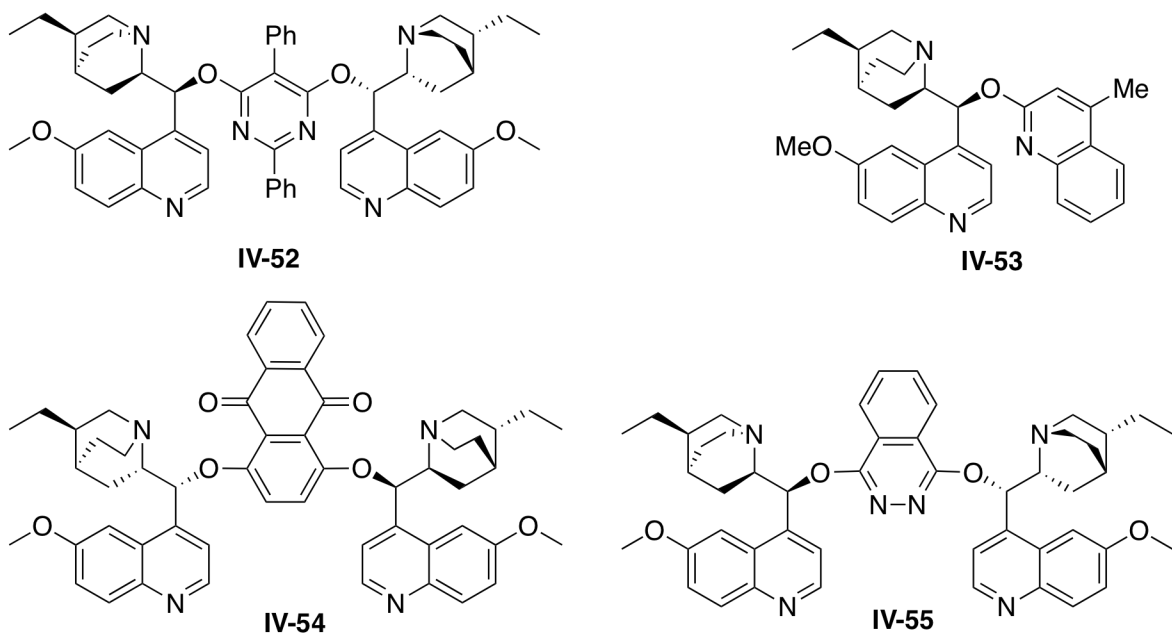
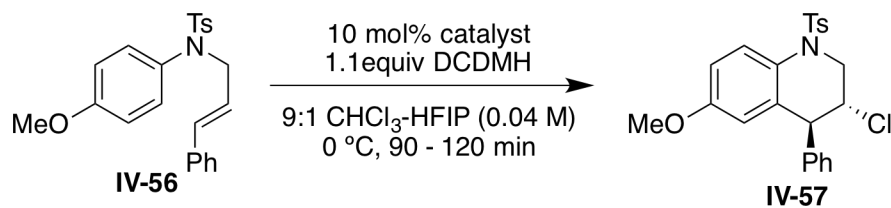


Figure IV-9: (Cont'd)



At this stage, it became apparent that active catalysts did not necessarily lead to good stereinduction; i.e. rate acceleration that was indicative of the catalyst participation in the reaction, was neither a necessary nor a sufficient condition to achieve enantioselective transformation. It was hoped that evaluating catalysts that have shown promise in the asymmetric dihydroxylation of alkenes might prove to be a better strategy given their well-established tendency to bind olefins within the catalyst's chiral pocket. Catalysts **IV-51**, **IV-52** and **IV-53** gave complete conversion to product in under 90 min; but disappointingly, all three catalysts returned the product with little or no enantioselectivity (entries 11 – 13, Table IV-3). Only two catalysts were identified that led to significant levels of enantioinduction (entries 14 and 15, Table IV-3). Catalyst **IV-54** [(DHQ)<sub>2</sub>AQN] gave the product in -40% *ee* (negative sign indicates that the first peak to elute in the chiral HPLC analysis was the major peak). [(DHQD)<sub>2</sub>PHAL] **IV-55** also gave significant enantioinduction (35% *ee*).

**Table IV-3.** Catalyst evaluation for the test reaction

| Entry | Catalyst     | Conv. | ee   |
|-------|--------------|-------|------|
| 1.    | <b>IV-41</b> | >95%  | <5%  |
| 2.    | <b>IV-42</b> | >95%  | <5%  |
| 3.    | <b>IV-43</b> | >95%  | <5%  |
| 4.    | <b>IV-44</b> | 60%   | <5%  |
| 5.    | <b>IV-45</b> | >95%  | <5%  |
| 6.    | <b>IV-46</b> | 85%   | <5%  |
| 7.    | <b>IV-47</b> | 15%   | 7%   |
| 8.    | <b>IV-48</b> | 10%   | <5%  |
| 9.    | <b>IV-49</b> | 17%   | 7%   |
| 10.   | <b>IV-50</b> | 67%   | <5%  |
| 11.   | <b>IV-51</b> | >95%  | <5%  |
| 12.   | <b>IV-52</b> | >95%  | <5%  |
| 13.   | <b>IV-53</b> | >95%  | 5%   |
| 14.   | <b>IV-54</b> | >95%  | -40% |
| 15.   | <b>IV-55</b> | >95%  | 35%  |

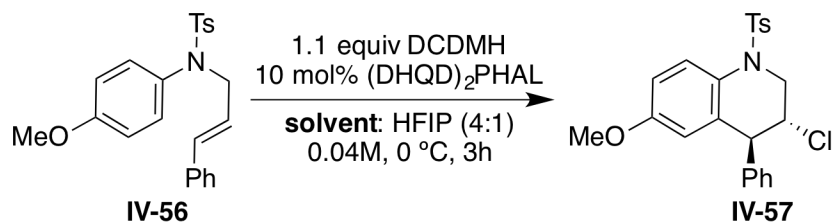
Note: Conversions were determined by crude <sup>1</sup>H NMR analysis

With these two catalysts having emerged as 'hits', efforts to further improve the stereoselectivity of the reaction commenced. It is worth mentioning that much of the optimization work was simultaneously undertaken with both catalysts at the initial stages due to their similar performance. **IV-54** eventually proved to be more intransigent to further improvements due to its relative insensitivity to parameters such as reaction temperature and concentration. Hence, optimization efforts only with **IV-55** will be presented in subsequent sections for the sake of avoiding redundancy.

#### **IV.4.5. Reaction variables' optimization.**

##### **IV.4.5.1. Determination of optimal co-solvent.**

Preliminary studies had already established that the reaction rate was significantly higher in fluorinated alcohols. Numerous solvents were evaluated as co-solvents for this reaction at a constant (and arbitrarily chosen) 20 volume % of HFIP at 0.04 M reaction concentration. This co-solvent study was undertaken in the hope of addressing two major challenges. The first, and most obvious reason was to determine if enantioselectivity could be improved using a specific co-solvent mixture that was better than the 9:1 CHCl<sub>3</sub>-HFIP system used for the catalyst screen. The second reason was to enable evaluation of lower temperature regimes, which is precluded in the absence of the co-solvent (melting point of HFIP = -4 °C). After the discovery of the optimal co-solvent, other aspects such as the co-solvent compositions, reaction concentration and temperatures could be sequentially evaluated.

**Table IV-4.** Evaluation of HFIP-co-solvent mixtures as a reaction medium

| Entry | Co-solvent                           | Yield | ee  |
|-------|--------------------------------------|-------|-----|
| 1.    | CH <sub>2</sub> ClCH <sub>2</sub> Cl | >99%  | 59% |
| 2.    | CH <sub>2</sub> Cl <sub>2</sub>      | 99%   | 55% |
| 3.    | CHCl <sub>3</sub>                    | 92%   | 50% |
| 4.    | CH <sub>3</sub> CCl <sub>3</sub>     | >99%  | 64% |
| 5.    | CHCl <sub>2</sub> CHCl <sub>2</sub>  | 95%   | 59% |
| 6.    | PhCl                                 | >95%  | 44% |
| 7.    | PhCF <sub>3</sub>                    | >95%  | 56% |
| 8.    | <i>n</i> -PrNO <sub>2</sub>          | >99%  | 19% |
| 9.    | MeNO <sub>2</sub>                    | 99%   | 1%  |
| 10.   | MeCN                                 | <5%   | nd  |
| 11.   | <i>i</i> -PrCN                       | <5%   | nd  |

Note: Yields were determined by crude <sup>1</sup>H NMR analysis with MTBE as external standard

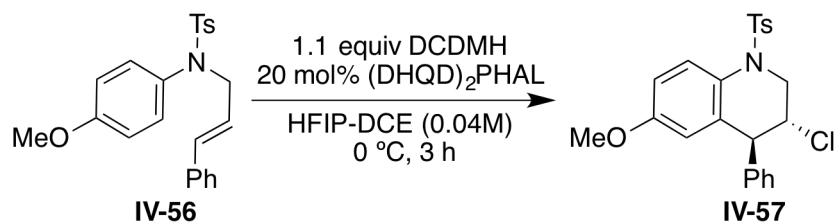
As seen in Table IV-4, the reaction proceeded in excellent yields with many halogenated hydrocarbon co-solvents (up to >99% yield, Entries 1 – 7, Table IV-4). Among these, 1,1,1-trichloroethane co-solvent gave the best enantioselectivity (64% *ee*, entry 4, Table IV-4). 1,2-Dichloroethane, Dichloromethane, chloroform and tetrachloroethane co-solvents furnished the

product in *ees* ranging from 50% to 59% *ee*. PhCl and PhCF<sub>3</sub> were also evaluated as co-solvents. While chlorobenzene co-solvent resulted in an eroded stereoselectivity (44% *ee*, entry 6, Table IV-4), PhCF<sub>3</sub> fared much better (56% *ee*, entry 7, Table IV-4). Nitroalkanes such as MeNO<sub>2</sub> and *n*-PrNO<sub>2</sub> were also compatible co-solvents ( $\geq$  99% yield of product), although in both instances, the product was formed in low enantioselectivity (1% and 19% *ee* respectively; entries 8 and 9, Table IV-4). Alkyl nitriles were poor co-solvents and gave trace quantities (if any) of the desired product (Entries 10 and 11, Table IV-4). 1,2-Dichloroethane (DCE) was chosen as the co-solvent for further optimization studies (the reactions in 4:1 DCE-HFIP were homogenous as opposed to biphasic mixtures that were obtained with CHCl<sub>3</sub> and 1,1,1-trichloroethane co-solvents at lower temperatures).

Next, attention was turned to optimizing the quantity of the co-solvent in the reaction mixture. Varying the quantity of HFIP in the HFIP-DCE binary mixture had a significant impact on the enantioselectivity of the reaction. As evident from Table IV-5, the enantioselectivity progressively increases with an increase in the amount of HFIP co-solvent in DCE. At DCE-HFIP ratio of 95:5, the reaction proceeded in 30% *ee* (entry 1, Table IV-5). This value steadily improved to 73% *ee* as the quantity of HFIP was progressively increased to 50:50 ratio of HFIP-DCE. Separate studies on the impact of reaction concentration on the enantioselectivity of the transformation revealed that higher dilutions gave improved enantioselectivities (compare entries 2, 6 and 7 in Table IV-5). The enantioselectivity significantly improved from 40% *ee* at 0.04 M concentration (entry 2 in Table IV-5) to 48% *ee* at 0.02 M concentration (entry 6, Table IV-5). A further decrease in concentration to 0.01 M resulted in a less pronounced increase in the enantioselectivity to 52% *ee*. The reason for improved enantioselectivity as a result of decreasing reaction concentration is not clear at present. Although catalyst aggregation with

cinchona alkaloid derived catalysts is well established at high concentrations,<sup>17,18</sup> the results with catalyst loading studies detailed below seem to rule out this possibility.

**Table IV-5.** Optimization of reaction concentration and co-solvent composition



| Entry | HFIP:DCE/ conc. | Yield | ee  |
|-------|-----------------|-------|-----|
| 1.    | 5:95/ 0.04M     | >99%  | 30% |
| 2.    | 10:90/ 0.04M    | >99%  | 40% |
| 3.    | 20:80/ 0.04M    | >99%  | 60% |
| 4.    | 30:70/ 0.04M    | >99%  | 70% |
| 5.    | 50:50/ 0.04M    | >99%  | 73% |
| 6.    | 10:90/ 0.02M    | >99%  | 48% |
| 7.    | 10:90/ 0.01 M   | >99%  | 52% |

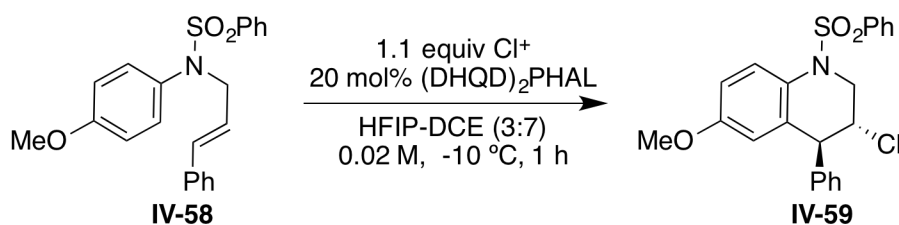
Note: Yields were determined by crude <sup>1</sup>H NMR analysis with MTBE as external standard

#### IV.4.5.2. Identification of the optimal chlorenium source.

The enantioselectivity as a function of the chlorenium source was then evaluated. It emerged that the enantioselectivity was strongly influenced by the identity of the chlorenium source. *N*-chlorosulfonamides fared poorly (entries 1 – 3, Table IV-6); *N*-chlorosaccharin, chloramine-T and dichloramine-T gave 52%, 60% and 55% *ee*, respectively. All the chlorohydantoins evaluated in the study gave practically identical enantioselectivities (see entries 4 – 7 in Table IV-6). It merits mention that the different steric parameters of the hydantoins have a negligible effect on the stereoselectivity of the transformation. Also, the

stoichiometry of the chlorohydantoin seems to play no role in affecting the enantioselectivity (compare entries 5 and 6 in Table IV-6). *N*-chloroimides such as NCS and NCP fared only marginally worse than the chlorohydantoin (66% and 68% *ee*, respectively, entries 8 and 9, Table IV-6). *t*-butyl hypochlorite returned the product in diminished yield and enantioselectivity (70% yield, 15% *ee*; entry 10, Table IV-6)

**Table IV-6.** Evaluation of chlorenium sources



| Entry | Cl <sup>+</sup> source    | Yield            | <i>ee</i> |
|-------|---------------------------|------------------|-----------|
| 1.    | NCSach                    | >95%             | 52%       |
| 2.    | TsNNaCl•3H <sub>2</sub> O | >95%             | 60%       |
| 3.    | TsNCl <sub>2</sub>        | >95%             | 55%       |
| 4.    | DCH                       | 95%              | 74%       |
| 5.    | DCDMH                     | >95%             | 73%       |
| 6.    | DCDMH (2.0 equiv)         | >95%             | 73%       |
| 7.    | DCDPH                     | 91%              | 71%       |
| 8.    | NCP                       | >95%             | 66%       |
| 9.    | NCS                       | 90%              | 68%       |
| 10.   | <i>t</i> -BuOCl           | 70% (100% conv.) | 15%       |

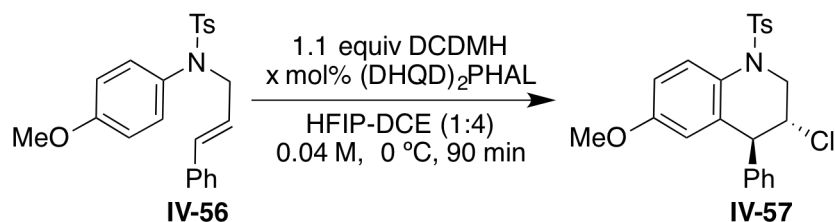
Note: Yields were determined by crude <sup>1</sup>H NMR analysis with MTBE as external standard

Although encouraging, it was hoped that significant improvements could be made with regards to the enantioselectivity of the transformation.

#### IV.4.5.3. Optimization of the catalyst loading.

The catalyst loading had a negligible effect on the enantioselectivity within the limits that were evaluated (2 mol% to 30 mol% loading). As seen in Table IV-7, all reactions proceeded in excellent yields in under 90 min with enantioselectivities ranging between 59% to 63% *ee*. No obvious trend was seen as a function of catalyst loading. It warrants emphasis that similar levels of enantioinduction at 2 mol% and 30 mol% catalyst loadings suggest that there is negligible background reaction in this transformation.

**Table IV-7.** Catalyst loading studies



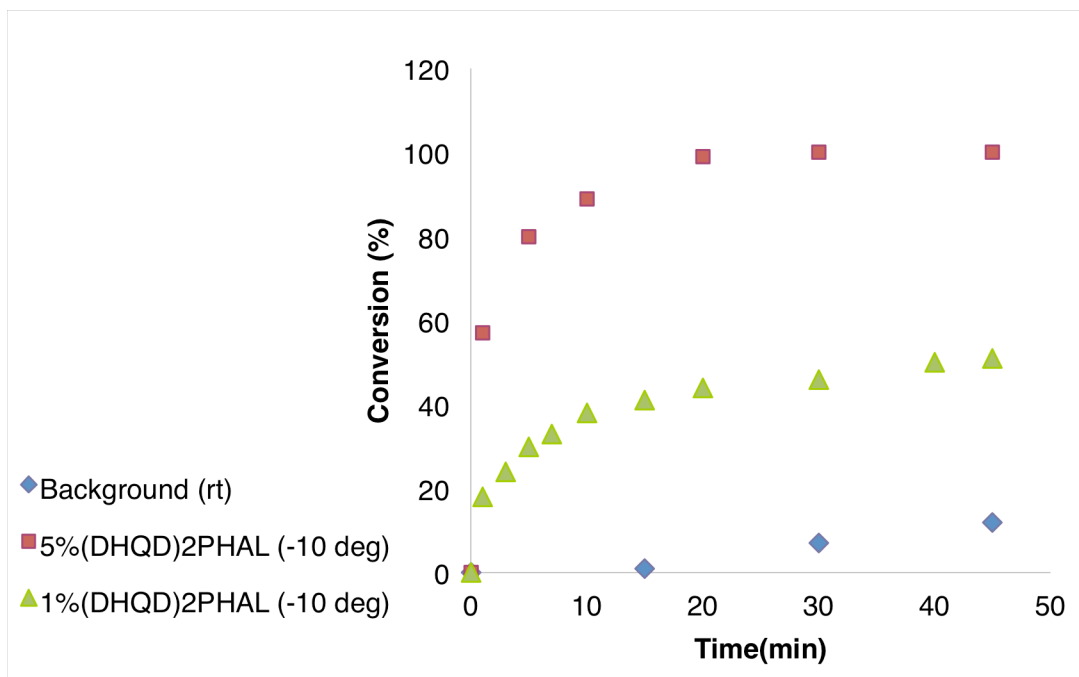
| Entry | Catalyst loading | Yield | <i>ee</i> |
|-------|------------------|-------|-----------|
| 1.    | 30 mol%          | >99%  | 62%       |
| 2.    | 20 mol%          | >99%  | 60%       |
| 3.    | 10 mol%          | >99%  | 59%       |
| 4.    | 5 mol%           | >99%  | 62%       |
| 5.    | 2 mol%           | >99%  | 59%       |

Note: Yields were determined by crude  $^1\text{H}$  NMR analysis with MTBE as external standard

Careful monitoring of the catalyzed and non-catalyzed reactions revealed that at 5 mol% catalyst loading, the reaction is virtually complete (99%) in 20 min. In contrast, the non-catalyzed reaction is less than 5% complete even at ambient temperature under otherwise

identical conditions. In fact, only 12% conversion was seen even after 45 min at ambient temperature in the absence of any catalyst (see Figure IV-10)

**Figure IV-10.** Conversion as a function of time and catalyst loading



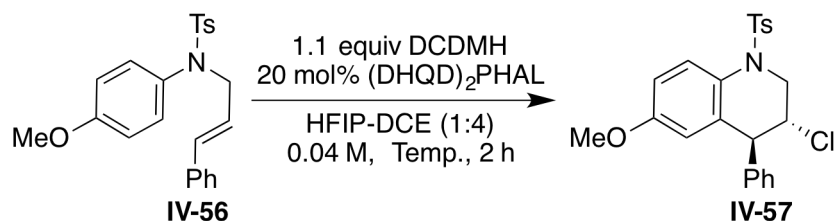
Furthermore, catalyst aggregation is likely absent given that even a 15-fold increase in catalyst concentration leads to almost identical stereoselectivity (compare entries 1 and 5 in Table IV-7). Song and Chin have demonstrated that catalyst aggregation of cinchona alkaloid derived catalysts can adversely affect the enantioselectivity of the reaction.<sup>17,18</sup>

#### **IV.4.5.4. Optimization of the reaction temperature.**

The enantioselectivity of the transformation also showed significant temperature dependence – lower temperatures gave higher enantioselectivities. The reaction proceeded in 50% *ee* at 24 °C. The enantioselectivity progressively improved to 71% *ee* at -20 °C (see Table IV-8). The lower temperature regime was limited by the freezing point of the 4:1 DCE-HFIP co-solvent mixture (~ -20 °C). Efforts to further lower the freezing point of the DCE-HFIP mixture

by the incorporation of additives that may serve as spectator ‘anti-freezes’ will be discussed later.

**Table IV-8.** Enantioselectivity as a function of temperature

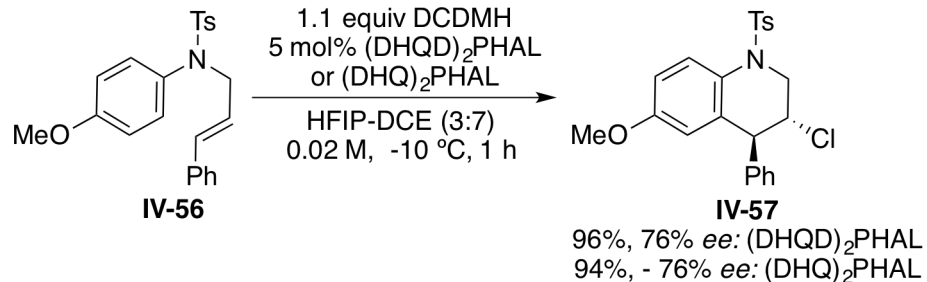


| Entry | Temperature | Yield | ee  |
|-------|-------------|-------|-----|
| 1.    | 24 °C       | 95%   | 50% |
| 2.    | 10 °C       | >95%  | 60% |
| 3.    | 0 °C        | >95%  | 65% |
| 4.    | -10 °C      | >95%  | 71% |
| 5.    | -20 °C      | >95%  | 71% |

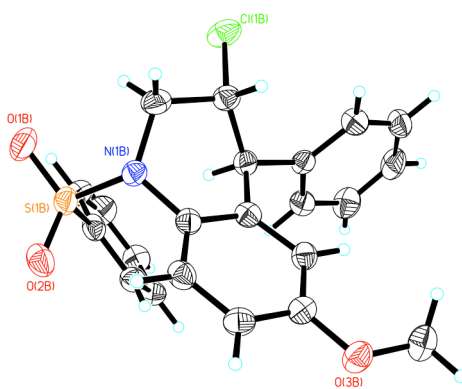
Note: Yields were determined by crude  $^1\text{H}$  NMR analysis with MTBE as external standard

Having thus optimized numerous reaction variables independently (temperature, concentration, catalyst loading and reaction medium), the combined effect of these optimizations was then evaluated. As shown in Scheme IV-1, under conditions obtained after this preliminary optimization, the desired product was obtained in excellent yield and 76% ee. The quasi enantiomeric catalyst (DHQ) $_2$ PHAL was also evaluated under identical conditions; the reaction proceeded in excellent yield and an identical 76% ee favoring the opposite enantiomer of the product thus establishing that either enantiomer of the product can be obtained by an appropriate choice of the catalyst.

**Scheme IV-1.** Results of the test reaction with best conditions thus far



Crystal structure that established the absolute stereochemistry of **IV-57**:  
(50% thermal ellipsoid drawing)



#### IV.4.6. Variation of *N*-protecting group.

##### IV.4.6.1. Screening other protecting groups.

As detailed in Section 4.3.4, the optimization of numerous reaction variables such as catalyst loading, temperature, concentration and chlorenium sources had led to the identification of conditions that led to excellent yields and moderate levels of enantioselectivity (96%, 76% *ee*). At this stage, it was hoped that fine-tuning the substrate catalyst interactions by varying the substrate structure might lead to higher stereoselectivities. This strategy had worked well for the enantioselective chlorocyclization of amides (detailed in Chapter 2) whereby the expendable benzamide functionality was systematically varied to identify the optimal ‘protecting group’. A similar opportunity existed in the context of the current reaction. The variation of the protecting

group on the nitrogen atom of the substrate allowed for an analogous ‘steric and electronic fine-tuning’. The results with a series of *N*-aryl and *N*-alkyl sulfonyl protecting groups are summarized in Figure IV-11.

**Figure IV-11.** Influence of the protecting group structure on enantioselectivity

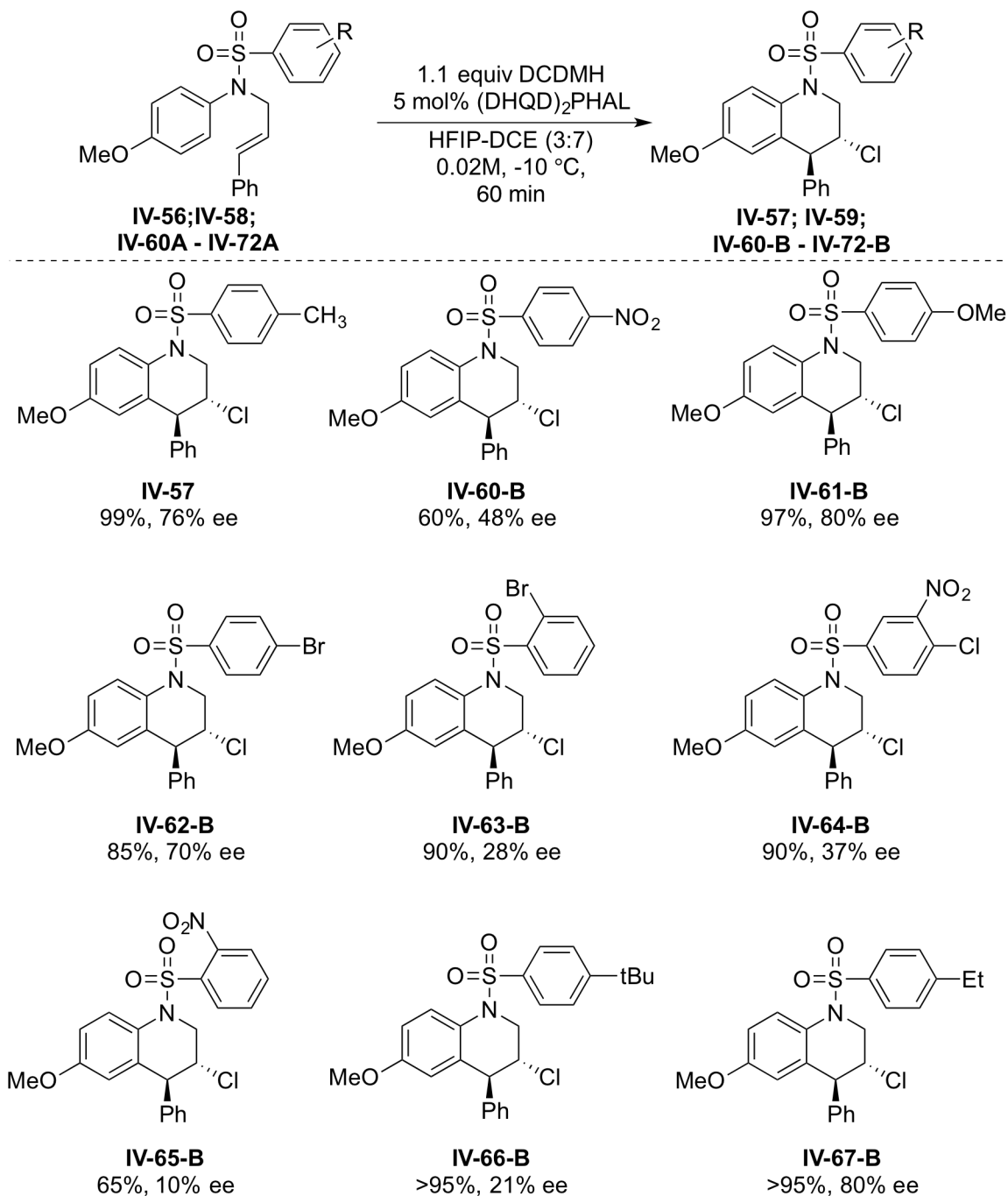
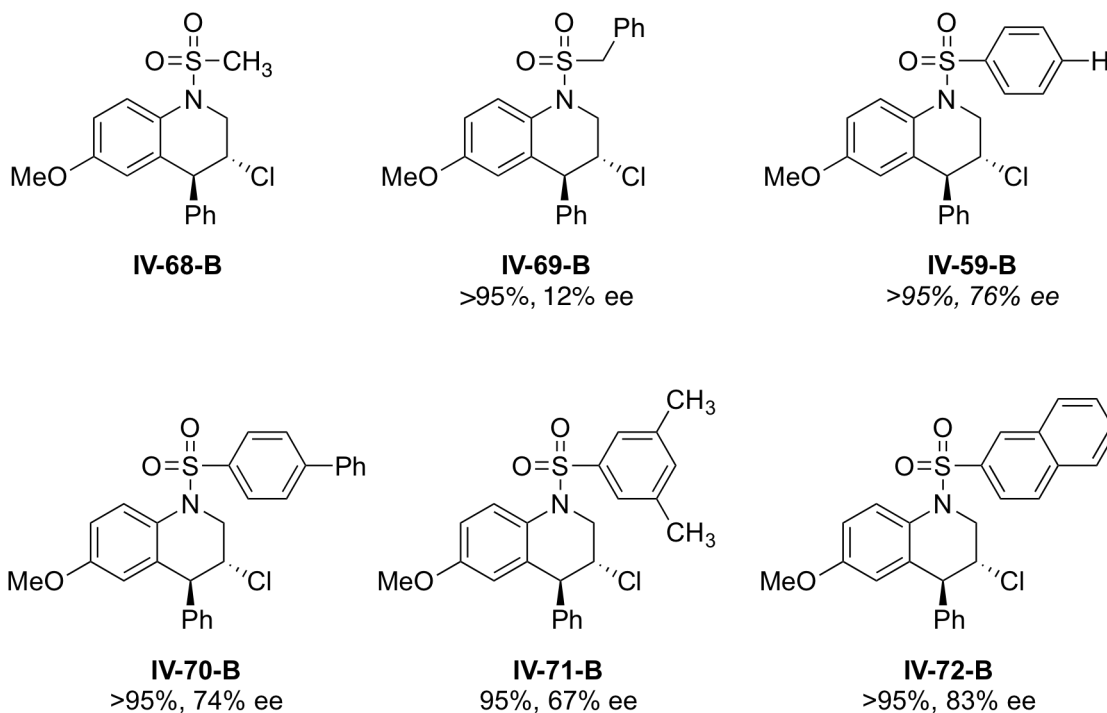


Figure IV-11. (Cont'd)



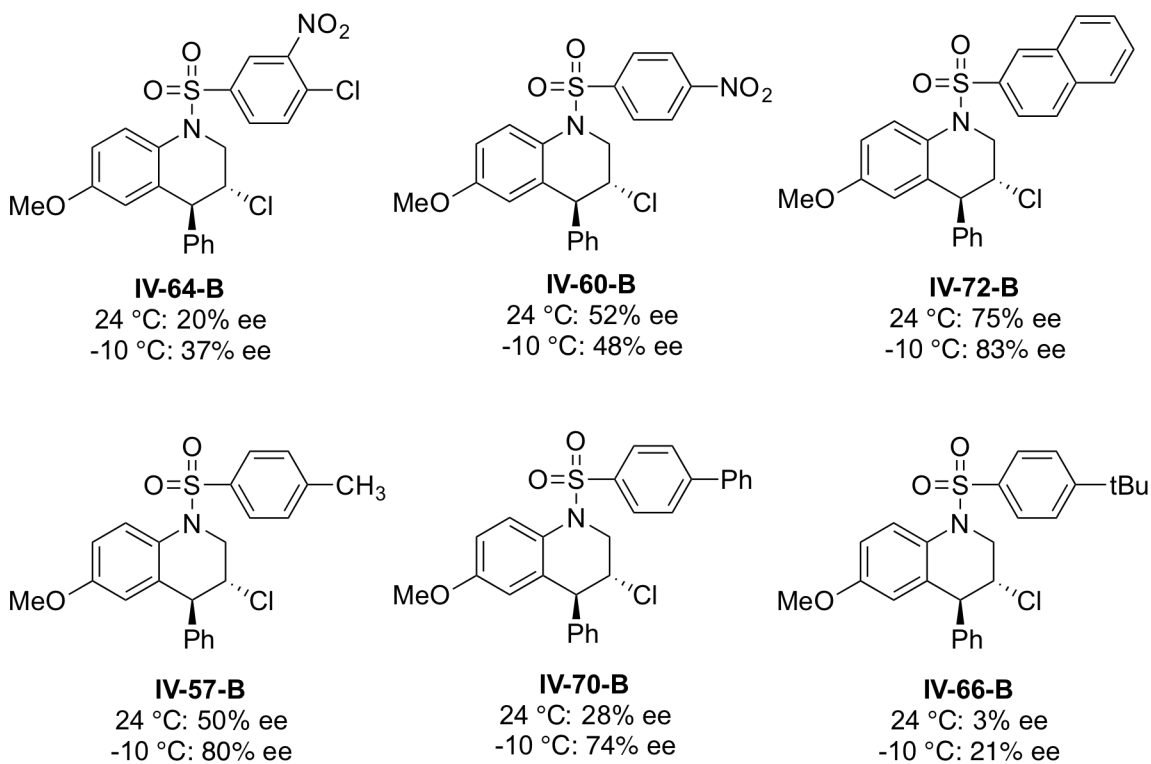
Among *N*-aryl sulfonate protecting groups, those with electron deficient aryl rings gave much diminished enantioselectivity. For example, the *p*-Nosyl and *o*-Nosyl protecting groups gave the cyclized products **IV-60-B** and **IV-65-B** in 48% and 10% *ee*, respectively. In addition, lower isolated yields were obtained with these protecting groups. The electron rich *p*-methoxybenzenesulfonyl group gave a marginal improvement in the enantioselectivity (see **IV-61-B** in Figure IV-11; 97%, 80% *ee*). The *p*-bromobenzenesulfonyl protecting group fared much better (**IV-62-B**: 85%, 70% *ee*) than the *o*-bromobenzenesulfonyl group (**IV-63-B**: 90%, 28% *ee*). Hydrophobic arylsulfonyl groups were also evaluated (see structures **IV-66-B** to **IV-72-B** in Figure IV-11). Among these, the  $\beta$ -naphthyl sulfonyl protecting group fared the best returning the product **IV-72-B** in 83% *ee*. Other protecting groups such as the benzene sulfonyl, biphenylsulfonyl and *p*-ethylbenzenesulfonyl also returned the product in comparable levels of enantioselectivity (76%, 74% and 80% *ee*, respectively). The methanesulfonyl and

benzylsulfonyl groups gave practically racemic products **IV-68-B** and **IV-69-B**. Although these results were frustrating in the sense that significant improvements in the enantioselectivity was not achieved with respect to the initially chosen *N*-toluenesulfonyl protecting group, the diversity in the observed enantioselectivity was a clear indication that the protecting group was a crucial 'recognition element' in the substrate. This observation will likely play a crucial role in unraveling the substrate-catalyst interaction.

#### **IV.4.6.2. Temperature dependence of enantioselectivity as a function of protecting groups.**

Preliminary optimizations with substrate **IV-56** revealed that the reaction was more stereoselective at lower temperatures. During the course of screening various *N*-protecting groups, it became evident that this trend in the temperature dependence of enantioselectivity varied widely for different protecting groups. Some of the evaluated protecting groups gave comparable levels of enantioinduction at room temperature and at -10 °C! In an extreme case, the *p*-nosyl protected substrate returned the cyclized product **IV-60-B** in higher enantioselectivity at ambient temperature (52% *ee*) as opposed to -10 °C (48% *ee*). Results with some of the other protecting groups are summarized in Figure IV-12.

**Figure IV-12.** Temperature dependence of enantioselectivity as a function of protecting groups



Postulating that enthalpy-entropy compensation effects may be contributing to this behavior, an Eyring plot analysis was undertaken for the chlorocyclization reaction of numerous substrates in an effort to better understand the enthalpic and entropic drivers for these reactions. It was hoped that extricating the differential activation parameters ( $\Delta\Delta H^\ddagger$  and  $\Delta\Delta S^\ddagger$ ) for each protecting group from the corresponding Eyring plots would aid in the *predictive* design of protecting groups rather than relying on a brute force screening approach.

#### **IV.4.7. Eyring plot analyses to map the enthalpic and entropic drivers of enantioselectivity with different protecting groups.**

A detailed description of the postulates and limitations of the Eyring equation (and the Eyring plots)<sup>19</sup> as well as its application in the analysis of enantioselective processes can be

found elsewhere.<sup>20-25</sup> Instead, a quick mathematical derivation of the equation associated with the Eyring plots is detailed below:

$$\Delta\Delta G^\ddagger = \Delta\Delta H^\ddagger - T\Delta\Delta S^\ddagger \quad (1)$$

$$\Delta G = -RT\ln(k_S/k_R) \quad (2)$$

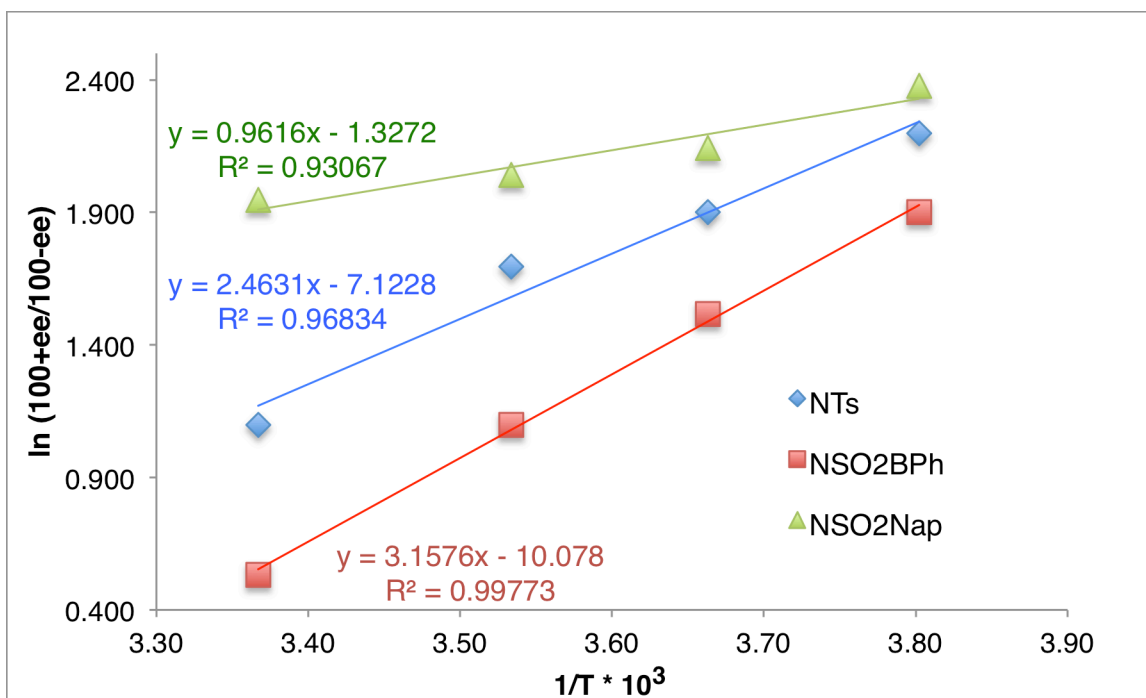
Substituting (2) in equation (1) gives the familiar form of the Eyring equation:

$$\ln(k_S/k_R) = -\Delta\Delta H^\ddagger_{S-R} / RT + \Delta\Delta S^\ddagger_{S-R} / R \quad (3)$$

The equation above enables a direct correlation of the differential reaction rates ( $k_S/k_R$ ) as a function of temperature. In this particular instance, the  $k_S/k_R$  value refers to the rates of formation of the two enantiomers of the product i.e. the enantiomeric ratios (*ers*) of the product. By plotting the natural logarithm of enantiomeric ratio of the reaction as a function of ( $1/T$ ), one will obtain a line with a specific slope and intercept ( $y = mx + c$ ). The slope of such a line will be  $(-\Delta\Delta H^\ddagger_{S-R} / R)$ , whereas the intercept will be  $(\Delta\Delta S^\ddagger_{S-R} / R)$ . Thus, the differential enthalpy and entropy of activation values can be determined for each protecting group. By determining which of the two parameters ( $\Delta\Delta H^\ddagger_{S-R}$  or  $\Delta\Delta S^\ddagger_{S-R}$ ) plays a more dominant role in lowering the  $\Delta\Delta G^\ddagger$ , one might be able to find correlations between the enantioselectivity of the reaction and the steric or electronic parameters of the protecting group. This method is non-empirical and will enable the *quantitative* estimations of the differential activation parameters. For example, with known  $\Delta\Delta G^\ddagger$  for a given reaction, one can predict the temperature at which one may expect to achieve >95% *ee*. Alternately, if the enantioselectivity is entropy driven, modulation of steric parameters (rather than the electronic parameters) of the protecting group will likely have a higher impact in affecting the enantioselectivity.

The Eyring plots were run for three of the better performing protecting groups – the *N*-toluenesulfonyl (NTs), *N*-naphthylsulfonyl (NSO<sub>2</sub>Nap) and the *N*-biphenylsulfonyl (NSO<sub>2</sub>Bph). The temperature range evaluated was from -10 °C to 24 °C. As seen in Figure IV-13, all three sets of Eyring plots showed relatively good correlation coefficients (error analysis of individual data points was not included at this stage).

**Figure IV-13.** Eyring plots for different *N*-protecting groups

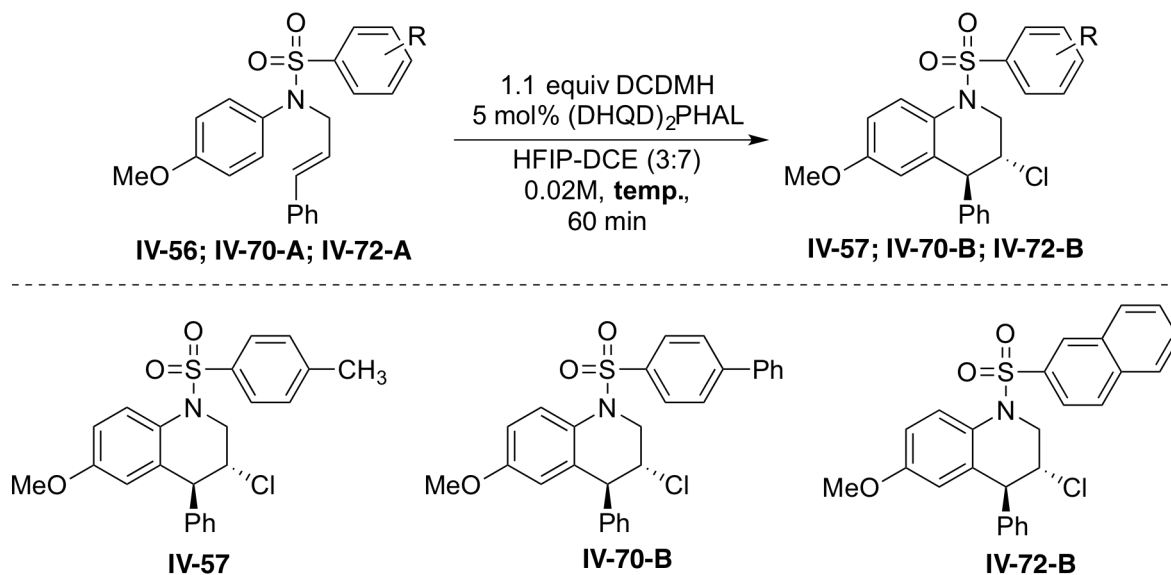


Based on the slopes and the intercepts of these lines (fitted to a linear line equation), the following differential activation parameters can be extracted.

As evident from Table IV-9 below, the calculated  $\Delta\Delta G^\ddagger$  values for all three protecting groups is  $\sim 1$  kcal/mol at 263 K (-10 °C); consequently the observed enantioselectivities at -10 °C are also quite similar (74 – 83% ee). Nonetheless, the surprising aspect that emerges from

the figures in the table is that drastically different  $\Delta\Delta H^\ddagger$  and  $\Delta\Delta S^\ddagger$  values lead to remarkably similar  $\Delta\Delta G^\ddagger$  values.

**Table IV-9:** Segregation of enthalpic and entropic contributions to  $\Delta\Delta G^\ddagger$



| Product      | $\Delta\Delta H^\ddagger$ (kcal/mol) | $\Delta\Delta S^\ddagger$ (cal/mol/K) | $\Delta\Delta G^\ddagger_{(263K)}$ (kcal/mol) | ee (263K) |
|--------------|--------------------------------------|---------------------------------------|---|-----------|
| <b>IV-57</b> | -4.90                                | -14.2                                 | -1.18   | 76%       |
| <b>IV-70</b> | -6.26                                | -20.0                                 | -0.99   | 74%       |
| <b>IV-72</b> | -1.91                                | -2.6                                  | -1.22   | 83%       |

$$\Delta\Delta G^\ddagger = \Delta\Delta H^\ddagger - T\Delta\Delta S^\ddagger$$

The enantioselectivity for all three reactions are enthalpy driven as seen by the negative values for the  $\Delta\Delta H^\ddagger$  values. Among the three, the enantioselectivity is most strongly enthalpy driven for the substrate possessing the biphenylsulphonyl protecting group on the nitrogen (-6.23 kcal/mol). But the same protecting group must also pay a big entropic cost (presumably due to the steric bulk) resulting in -20.0 cal/mol/K differential entropy of activation. On the other

extreme, the enantioselectivity is only weakly enthalpy driven ( $\Delta\Delta H^\ddagger = -1.91$  kcal/mol) for the  $\beta$ -naphthylsulfonyl protecting group. But despite this, it has to pay the lowest entropic cost ( $-2.6$  cal/mol/K) to accommodate a planar naphthyl ring in the transition state. As a result, it outperforms the biphenylsulfonyl protecting group despite being significantly worse off from a purely enthalpic standpoint. The *N*-toluenesulfonyl group represents a tradeoff between these two extremes in terms of both  $\Delta\Delta H^\ddagger$  and  $\Delta\Delta S^\ddagger$  values; the net result of the enthalpy-entropy compensation still leads to a similar performance as the other two groups.

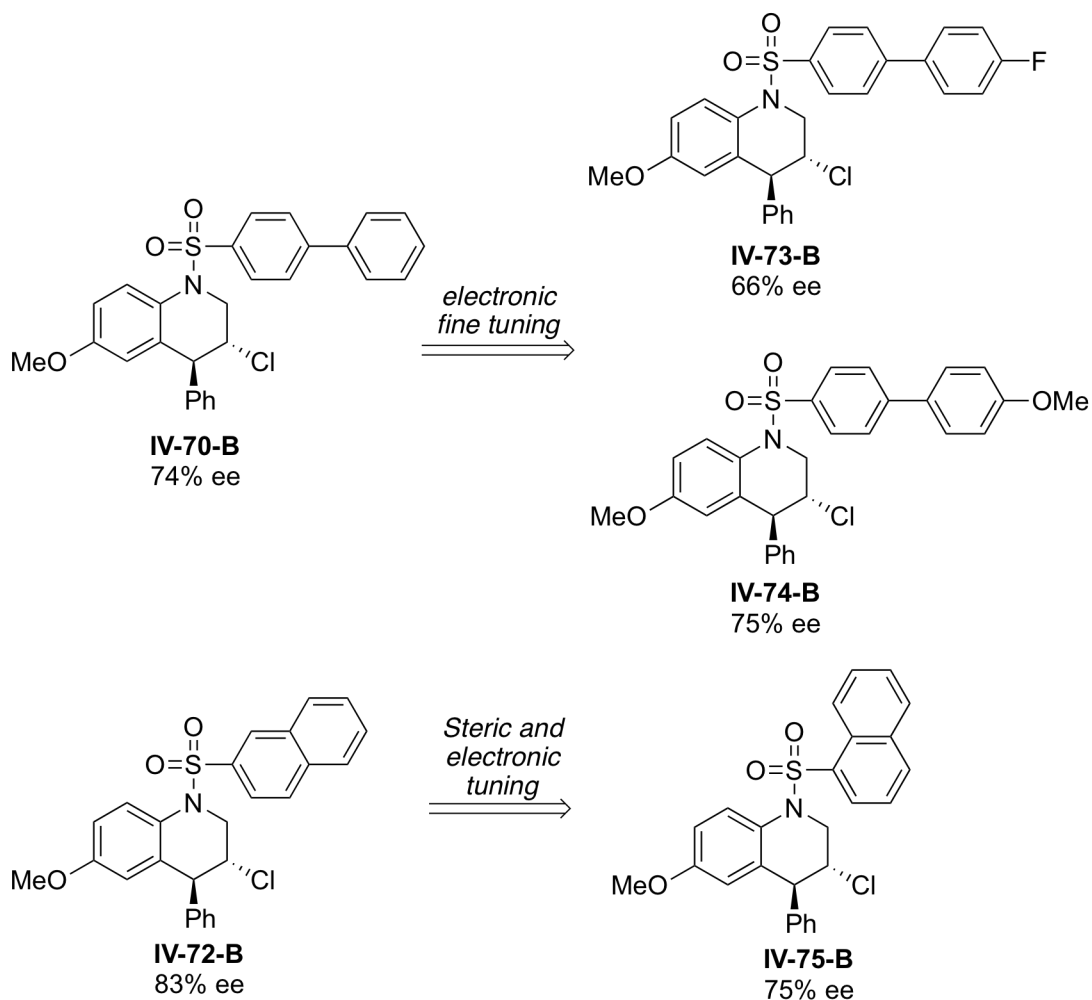
From a practical standpoint, the Eyring plots hold several vital clues for a rational optimization of reaction parameters and protecting group choice. For example, the stereoselectivity with the naphthylsulfonyl group is practically entropy independent ( $\Delta\Delta S^\ddagger = -2.6$  cal/mol/K). Hence the  $(-T\Delta\Delta S^\ddagger)$  term contributes little to the lowering of the  $\Delta\Delta G^\ddagger$  value. In other words, decreasing the temperature will have a negligible effect on the enantioselectivity of the reaction if the protecting group is a naphthylsulfonyl.

On the other hand, the *N*-toluenesulfonyl and *N*-biphenylsulfonyl groups have significant enthalpic ( $\Delta\Delta H^\ddagger$ ) and entropic contributions ( $\Delta\Delta S^\ddagger$ ). As such a decrease in temperature should favor higher enantioselectivities ( $-T\Delta\Delta S^\ddagger$  term becomes less positive at lower temperatures thereby leading to a more negative  $\Delta\Delta G^\ddagger$ ). Intuitively, a decrease in reaction temperature also ought to favor any favorable substrate-catalyst and/or reagent-catalyst interactions. While it is impossible to ascribe mechanistic events by merely analyzing the Eyring plots for a reaction, this study serves to confirm that the protecting group behavior is unique for any given group and that the differential activation parameters can be quantified using the Eyring plots rather than making intuitive/predictive guesses.

#### IV.4.7.1. Rational design of protecting groups based on Eyring plot analyses.

It was hoped that the knowledge from the Eyring plots could be used for a rational design of protecting groups. For example, in the biphenylsulfonyl series of protecting groups, it was envisioned that substitution of the 4-Ph group that leads to **IV-70-B** with electron donating or withdrawing groups could potentially modulate the  $\Delta\Delta H^\ddagger$  component without significantly affecting the  $\Delta\Delta S^\ddagger$  component. With the hope of discerning a trend, the 4'-F-Ph and 4'-OMe-Ph analogues were evaluated in this reaction. The fluorinated protecting group was inferior to the corresponding non-fluorinated one (66% *ee* for **IV-73-B** as opposed to 74% *ee* for **IV-70-B**, see Figure IV-14). The introduction of the electron donating OMe-substituent on the back ring leads to practically no change in the enantioselectivity (75% *ee* for **IV-75-B** as opposed to 74% *ee* for **IV-70-B**). Although qualitatively, these results suggest that electron rich aryl rings at the 4-position of the biphenyl ring might prove to be beneficial, this avenue was not pursued further. An alternate strategy building on the  $\beta$ -naphthylsulfonyl protecting group was also evaluated. It was hoped that resorting to the  $\alpha$ -naphthylsulfonyl group in lieu of its  $\beta$ -isomer could potentially lead to better enantioselectivities by either decreasing the  $\Delta\Delta H^\ddagger$  term or increasing the  $\Delta\Delta S^\ddagger$  term. Frustratingly, this change also led to an inferior result (a decrease of 8% *ee* from 83% *ee* for **IV-72** to 75% *ee* for **IV-75** was seen).

**Figure IV-14.** Steric and electronic fine-tuning of protecting groups



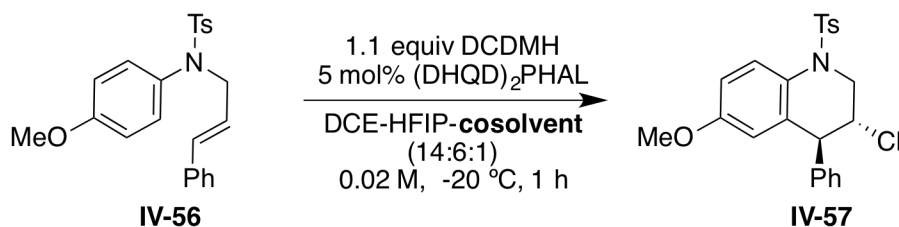
Having thus evaluated numerous protecting groups with only marginal improvements over the initially discovered system, and having deemed that any further improvements would have to come at the expense of the practical appeal of this chemistry, it was decided to abandon any further efforts of discovering an ideal protecting group. The following sections will describe alternate approaches that were evaluated for improving the enantioselectivity of the reaction.

#### **IV.4.8. Sampling lower reaction temperatures with the aid of additional co-solvents.**

It has been highlighted in earlier sections that the relatively high melting point of the 7:3 DCE-HFIP co-solvent mixture (ca. -15 °C) precludes evaluation of the reaction at lower

temperatures. Given the strongly enthalpy dependent enantioselectivity for the test substrate and the resulting improvement in enantioselectivity with decreasing temperature, it was envisioned that incorporation of low melting co-solvents that could aid in maintaining a homogenous reaction mixture will enable the sampling of lower temperature regimes. A crucial attribute for such an 'antifreeze' is that it must serve as an 'ee-neutral' component i.e., it should not lead to deterioration of enantioselectivity. Numerous low-melting solvents were added to the 7:3 DCE-HFIP mixture so that the final ratio of DCE:HFIP:co-solvent ratio was 14:6:1. Reactions were run at -20 °C in order to determine whether enantioselectivities improve significantly over 78% ee that is obtained at -10 °C.

**Table IV-10.** Evaluation of co-solvent anti-freezes



| Entry | Co-solvent                         | Conv. | ee  |
|-------|------------------------------------|-------|-----|
| 1.    | DMSO                               | <2%   | nd  |
| 2.    | <i>n</i> -PrNO <sub>2</sub>        | >95%  | 83% |
| 3.    | MeCN                               | >95%  | 75% |
| 4.    | THF                                | >95%  | 82% |
| 5.    | CF <sub>3</sub> CH <sub>2</sub> OH | >95%  | 81% |
| 6.    | Acetone                            | >95%  | 79% |

Note: Conversion was determined by crude <sup>1</sup>H NMR analysis.

DMSO shut down the reaction and the unreacted substrate was almost quantitatively recovered (entry 1, Table IV-10). Among the other solvents evaluated, *n*-PrNO<sub>2</sub>, THF and CF<sub>3</sub>CH<sub>2</sub>OH gave marginal improvements in enantioselectivity (83%, 82% and 81% *ee*, respectively, see Table IV-10). Acetone (79% *ee*) and acetonitrile (75% *ee*) led to no improvements in the enantioselectivity. Further optimization of the quantity of the co-solvent and temperatures was not undertaken at this stage given the small improvements in enantioselectivities.

#### **IV.4.9. Enantioselectivity as a function of electron density of nucleophile.**

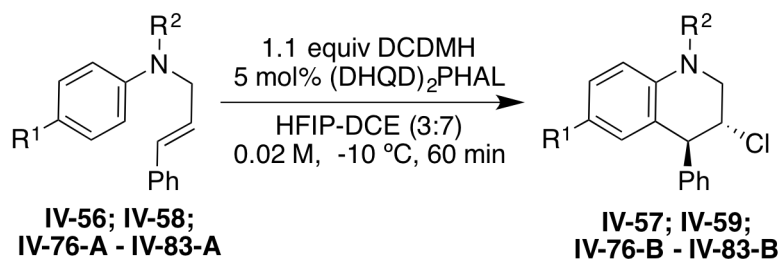
A preliminary substrate scope for this transformation will be presented in a subsequent section. A small subset of those results that is pertinent to the mechanistic underpinnings of the transformation is presented in this section.

At the outset of this project, it seemed reasonable that the conditions optimized for highly enantioselective chlorocyclization of the test substrates **IV-56** and **IV-58** should provide similar levels of enantioinduction for various arene nucleophiles i.e. the nucleophilicity of the aryl ring and the stereoselectivity of the alkene chlorination event are distinct and uncoupled phenomena. One might therefore expect different rates of cyclization, but similar levels of enantioinduction for the cyclized products with varying nucleophilicity of the aryl ring.

This hypothesis was unfounded by experimental results. Both, the rates and the enantioselectivity of the chlorocyclization reaction, was dependent on the electron density of the nucleophilic aryl ring. Decreasing electron density led to slower reactions and lower enantioselectivity (entries 1 – 4, Table IV-11). Similar behavior was seen with substrates possessing the benzenesulfonyl protecting group (entries 5 – 9, Table IV-11).

That the electronic perturbation of a site remote from the alkene halogenation event can influence the enantioselectivity of the chlorination event so profoundly was surprising to say the least. Additionally, this observation was also frustrating in the sense that it seemed to suggest that only substrates with electron rich arene rings will cyclize with high enantioselectivity (and thereby leading to a relatively narrow substrate scope with regards to the nucleophile).

**Table IV-11.** *ee* as a function of nucleophile electron density



| Entry | R <sup>1</sup>     | R <sup>2</sup>                                     | Substrate      | Product        | Yield (Conv.) | <i>ee</i> |
|-------|--------------------|--|----------------|----------------|---------------|-----------|
| 1.    | OMe                | 4-Me-C <sub>6</sub> H <sub>4</sub> SO <sub>2</sub> | <b>IV-56</b>   | <b>IV-57</b>   | >99%          | 76%       |
| 2.    | Me                 | 4-Me-C <sub>6</sub> H <sub>4</sub> SO <sub>2</sub> | <b>IV-76-A</b> | <b>IV-76-B</b> | 78%           | 53%       |
| 3.    | H                  | 4-Me-C <sub>6</sub> H <sub>4</sub> SO <sub>2</sub> | <b>IV-77-A</b> | <b>IV-77-B</b> | >99%          | 36%       |
| 4.    | Cl                 | 4-Me-C <sub>6</sub> H <sub>4</sub> SO <sub>2</sub> | <b>IV-78-A</b> | <b>IV-78-B</b> | 74%           | 11%       |
| 5.    | OMe                | C <sub>6</sub> H <sub>5</sub> SO <sub>2</sub>      | <b>IV-58</b>   | <b>IV-59</b>   | 98%           | 74%       |
| 6.    | CH <sub>3</sub>    | C <sub>6</sub> H <sub>5</sub> SO <sub>2</sub>      | <b>IV-79-A</b> | <b>IV-79-B</b> | nd            | 64%       |
| 7.    | H                  | C <sub>6</sub> H <sub>5</sub> SO <sub>2</sub>      | <b>IV-80-A</b> | <b>IV-80-B</b> | nd            | 35%       |
| 8.    | NHAc               | C <sub>6</sub> H <sub>5</sub> SO <sub>2</sub>      | <b>IV-81-A</b> | <b>IV-81-B</b> | 90%           | 37%       |
| 9.    | CH <sub>2</sub> OH | C <sub>6</sub> H <sub>5</sub> SO <sub>2</sub>      | <b>IV-82-A</b> | <b>IV-82-B</b> | 75% (100%)    | 17%       |
| 10.   | CO <sub>2</sub> Et | C <sub>6</sub> H <sub>5</sub> SO <sub>2</sub>      | <b>IV-83-A</b> | <b>IV-83-B</b> | 72% (75%)     | 3%        |

Note: Yields refer to NMR yields with MTBE as added external standard

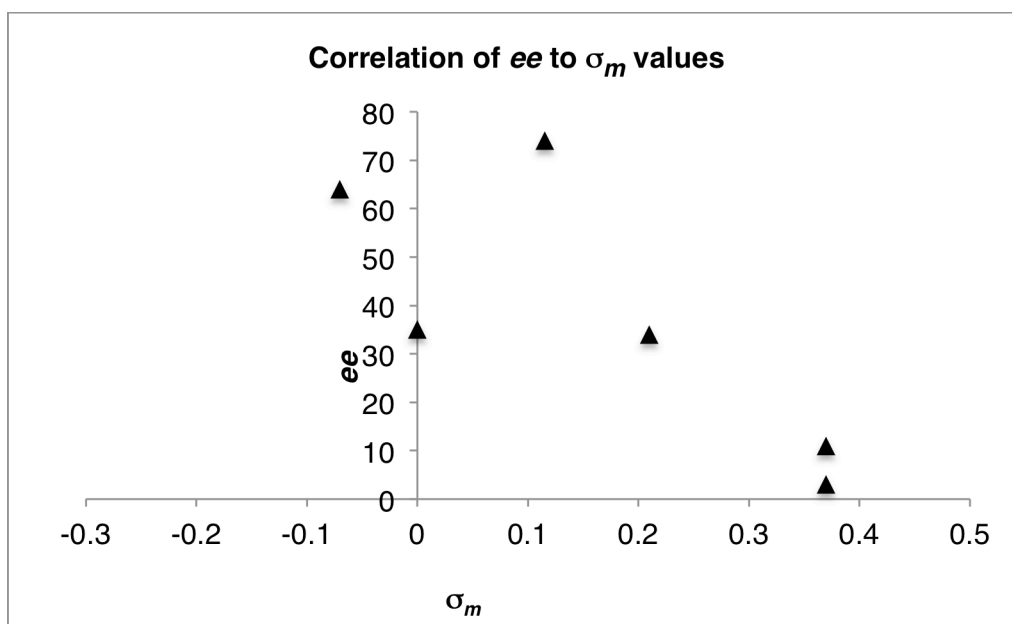
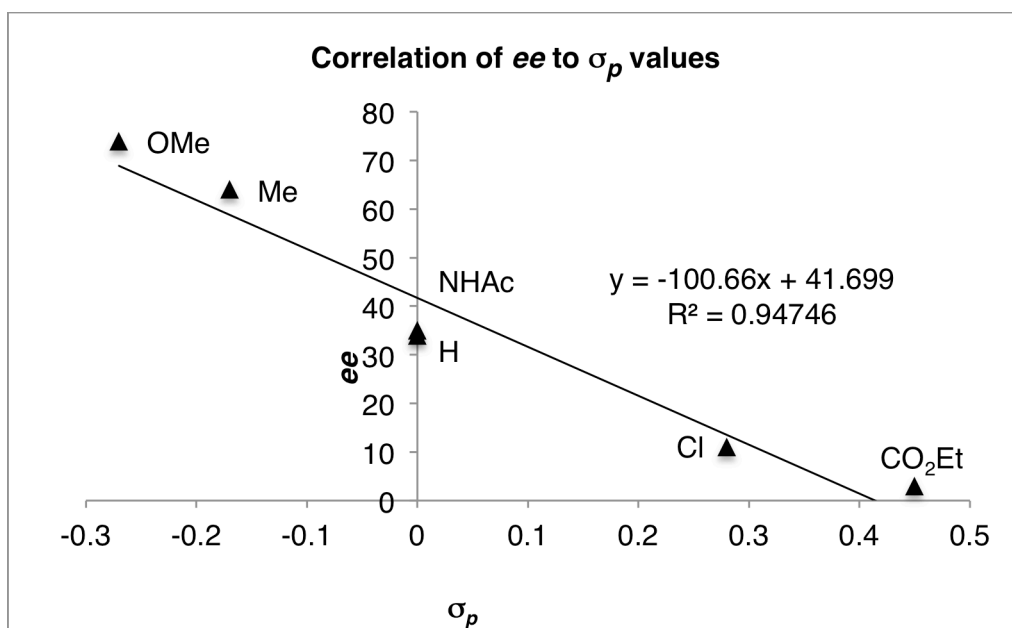
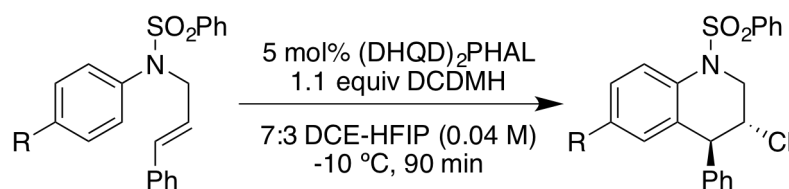
#### IV.4.9.1. Correlation of enantioselectivity and the Hammett constants of substituents on nucleophilic arene ring.

An effort to correlate the observed trend in the enantioselectivity to a fundamental steric or electronic parameter of the substituents seemed like a worthwhile endeavor. Indeed, Sigman and co-workers have demonstrated that such correlations might be used as a *predictive* tool for improving the enantioselectivity of reactions.<sup>26-28</sup>

It emerged that for the reaction under study, a plot of the enantioselectivity of the reaction as a function of Hammett substituent constants ( $\sigma_p$ ) shows a linear dependence with fairly good correlation coefficient ( $R^2 = 0.947$ , see Figure IV-15).<sup>29</sup> The mechanistic implications of this trend are not clear at this stage. Also of note is that there is poor correlation of *ee* with  $\sigma_m$  values despite the fact that the newly formed C-C bond originates at the *meta* position with respect to the substituent on the aryl ring (see Figure IV-15).

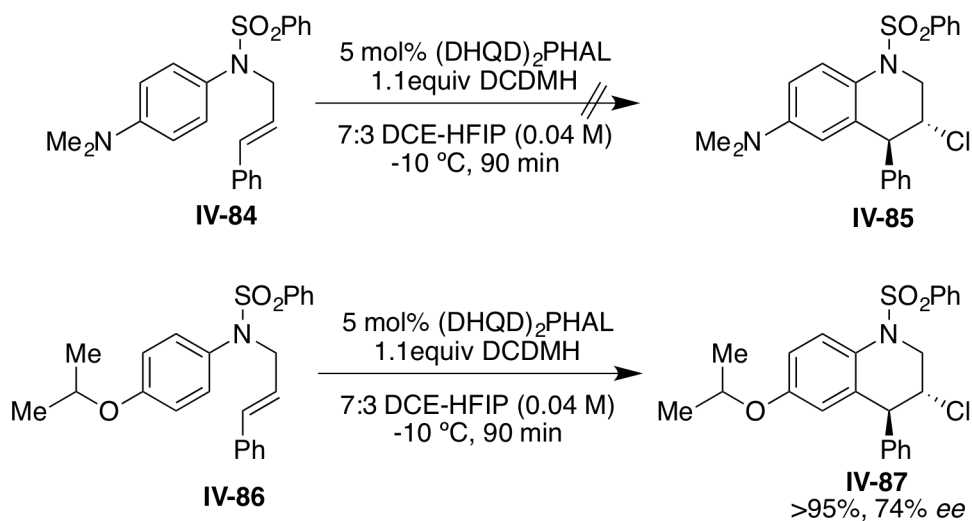
In fact,  $\sigma_p$  values of substituents that are remote from the site of the reaction (i.e. the olefin functionality) may shed little light on the mechanistic nuances. Nonetheless, the trend seems to be reliable and may prove to be useful for a strategic introduction of a cleavable group at the 4-position of the nucleophile.

**Figure IV-15.** Correlation of *ee* and Hammett substituent constants ( $\sigma_p/\sigma_m$ )



At this juncture, it was hoped that substituents that had lower  $\sigma_p$  values than the OMe group could potentially improve the enantioselectivity. The NMe<sub>2</sub> group and *i*-PrO group emerged as plausible candidates. Based on the reported  $\sigma_p$  values for these substituents (-0.83 and -0.45, respectively for NMe<sub>2</sub> and *i*-PrO),<sup>29</sup> the predicted enantioselectivity with these groups was >99% *ee* and 87% *ee* respectively. Disappointingly, when substrate **IV-84** with NMe<sub>2</sub> substituent was exposed to the optimized reaction conditions, no desired product was obtained (see Scheme IV-2). It is likely that the product of this reaction was ring-chlorinated compound resulting from electrophilic aromatic substitution of the electron rich aryl ring; this tentative assignment was based on <sup>1</sup>H NMR that suggested that the product had an intact double bond. LC-MS analysis of the product was consistent with the incorporation of one chlorine atom. Substrate **IV-86** with *i*-PrO substituent returned the product **IV-87** in 74% *ee* (that was practically identical to that of **IV-59** with the OMe substituent). These studies indicated that further increments in enantioselectivity would require modification of other parameters.

**Scheme IV-2.** Evaluation of electronically tuned nucleophiles in the carbocyclization reaction



#### IV.4.10. Design and evaluation of second-generation cinchona alkaloid derived catalysts.

Given the direct correlation between the electron density of the nucleophilic arene ring of the substrate and the rates and enantioselectivity of the reaction, it seems plausible that  $\pi$ -stacking interactions of the arene ring with the numerous aryl rings of the catalyst (most notably the electron deficient phthalazine linker) could be a crucial interaction that anchors the substrate in the catalyst's chiral pocket.

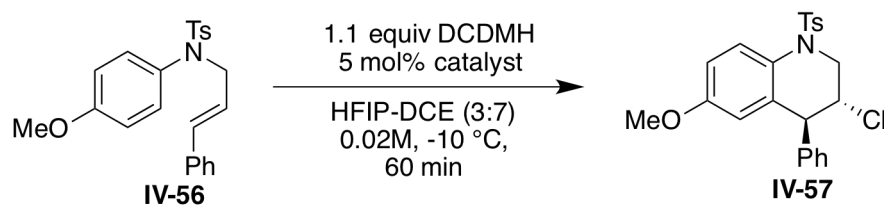
If true, the variation of the steric and electronic parameters of the many aryl rings of the catalyst should exert a pronounced effect on the efficiency of this  $\pi$ -stacking interaction and thereby affect the stereoselectivity of the reaction. A small library of catalysts was synthesized with the aim of probing this hypothesis. Having already demonstrated the superiority of **IV-54** and **IV-55** [(DHQ)<sub>2</sub>AQN and (DHQD)<sub>2</sub>PHAL] over other catalyst frameworks during the preliminary studies (see Section 4.4.4), many of the synthesized catalysts share close resemblance to these initial 'hits'. It was hoped that electronic and steric 'tweaking' of **IV-55** would lead to better enantioselectivities. Additionally, efforts in the area of catalyst design for the asymmetric chlorolactonization reaction had already led to the genesis of a relatively large library of 'in-house' catalysts. Both these catalyst libraries were evaluated in the hope that trends may emerge during the course of this 'Structure-Enantioselectivity-Relationships' study. The list of the evaluated catalysts and the corresponding enantioselectivities are shown in Figure IV-16.

It is well-established in numerous reactions catalyzed by cinchona alkaloid derivatives that the two quasi enantiomers (DHQD)<sub>2</sub>PHAL and (DHQ)<sub>2</sub>PHAL show remarkably dissimilar stereoinductions. This behavior has been observed in the Sharpless asymmetric dihydroxylation reaction (the technology that has led to the genesis of these dimeric catalysts) as well as in the chlorolactonization of alkenoic acids reported by our group. In both reactions,

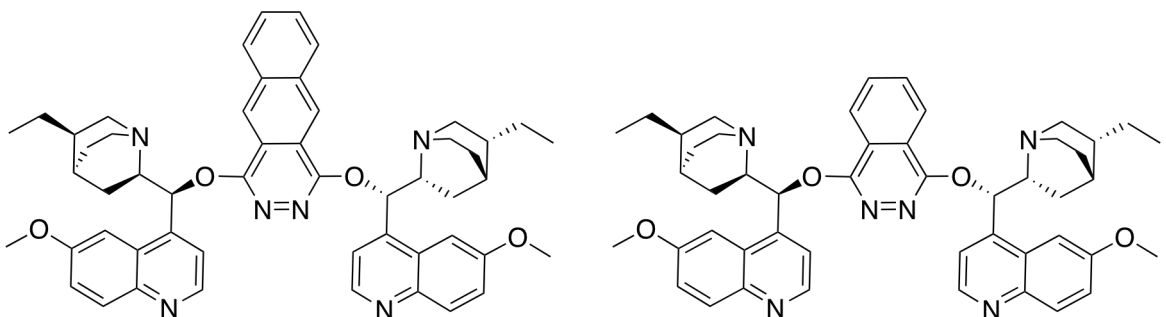
the quinidine derived dimers outperform the quinine derived ones. Nonetheless, in the current reaction, the enantio-complementary (DHQ)<sub>2</sub>PHAL catalyst **IV-90** gave an identical level of enantioinduction (-76% *ee*) in the opposite sense as (DHQD)<sub>2</sub>PHAL catalyst **IV-55** (76% *ee*). Having noted this, it was deemed valid to evaluate either quasi-enantiomer as the monomeric component in these catalysts – the choice was largely governed by the ease of synthesis and purification of the dimeric catalysts and the cost of the commercially available monomers.

Variation of the linker size was initially investigated by retaining the monomeric unit as hydroquinidine. The catalyst **IV-88** with the extended benzo-phthalazine linker led to a noticeable decrease in the enantioselectivity to 68% *ee* from 76% *ee* for catalyst **IV-55** with the phthalazine linker. Chlorination of the phthalazine back ring did not affect the stereochemical outcome as seen in the results with the dichlorophthalazine linked catalyst **IV-89** (76% *ee*). A logical progression was to evaluate catalyst **IV-91** with the truncated pyridazine (PYDZ) linker. A small improvement in the enantioselectivity to 78% *ee* was achieved.

**Figure IV-16.** Evaluation of second generation of cinchona alkaloid dimer catalysts

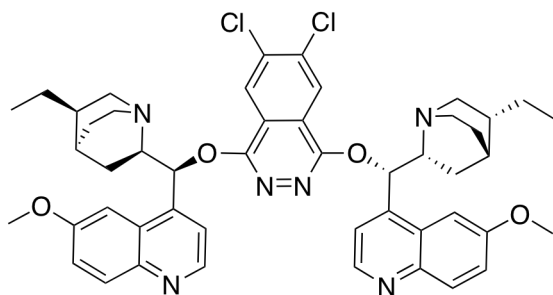


**Variation of linker:**

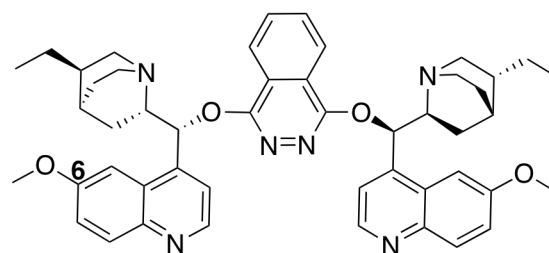


**IV-88**  
(DHQD)<sub>2</sub>(benzo-PHAL)  
> 95%, 68% ee

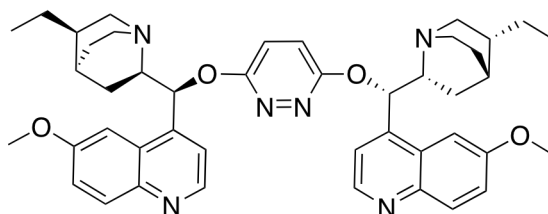
**IV-55**  
(DHQD)<sub>2</sub>PHAL  
99%, 76% ee



**IV-89**  
(DHQD)<sub>2</sub>Cl<sub>2</sub>PHAL  
> 95%, 74% ee

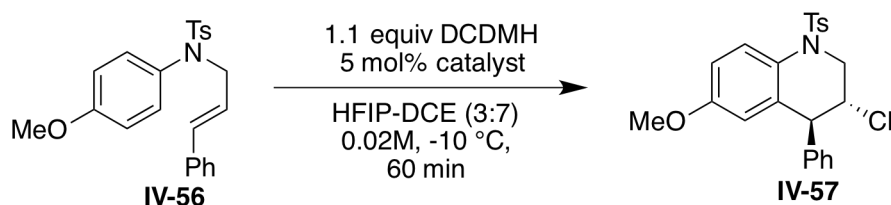


**IV-90**  
(DHQ)<sub>2</sub>PHAL  
99%, -76% ee

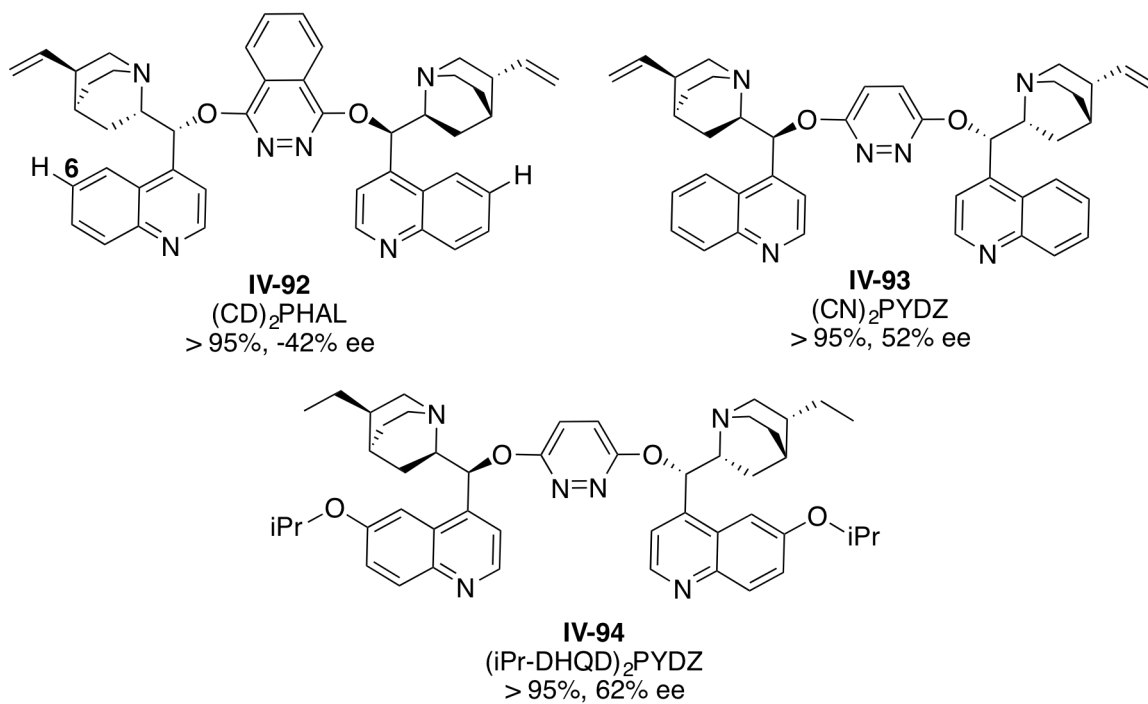


**IV-91**  
(DHQD)<sub>2</sub>(PYDZ)  
> 95%, 78% ee

Figure IV-16. (Cont'd)



**Variation of C6 substituent of monomer:**

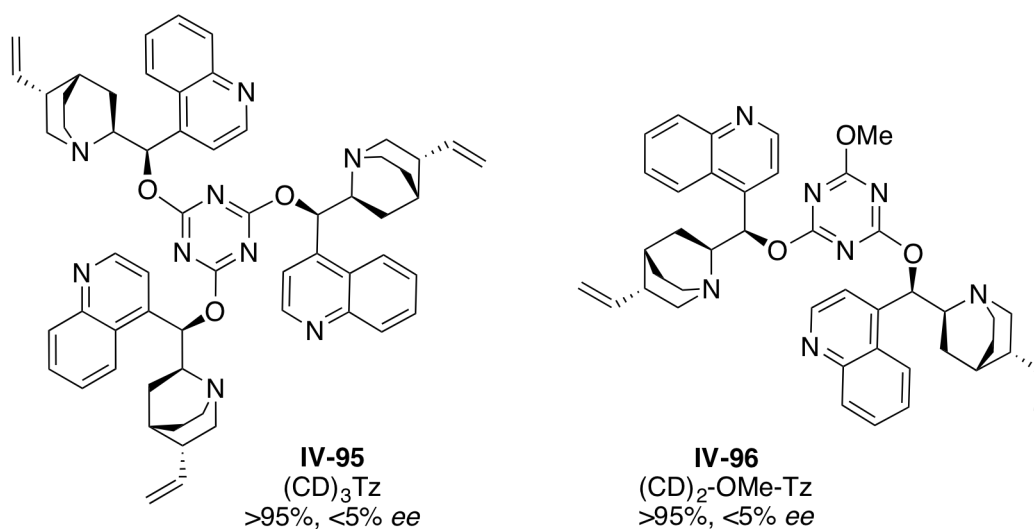


Attention was then turned to changing the structure of the monomer. In this regard, variation of the C6 substituent on the quinoline ring of the monomeric catalyst seemed to be the most straightforward modification. Cinchonidine and quinine are identical in all respects with the exception of the C6 substituent (H in cinchonidine as opposed to OMe in quinine). A similar relationship exists between cinchonine and quinidine. Having established that quinine dimer **IV-90** gives -76% ee, it was surprising that the analogous dimeric cinchonidine catalyst **IV-92** gave the product in only -42% ee. It must be highlighted that the only difference between the two catalysts is the presence of the C6 OMe group in **IV-90**, which is absent in **IV-92**. That a single

substitution on the macromolecular catalyst could lead to such a drastic difference was both surprising and informative. A similar comparison of the catalysts **IV-91** [(DHQD)<sub>2</sub>PYDZ] and **IV-93** [(CN)<sub>2</sub>PYDZ] with the pyridazine linker also revealed the same trend; the **IV-93** (C6-H substituent) gave only 52% *ee* as opposed to **IV-91** (C6-OMe substituent) that gave 78% *ee*. These results confirmed that the C6 substituent is a valuable handle for tweaking the catalyst performance. Indeed, replacing the C6-H substituent in **IV-93** with the C6-*i*PrO substituent in **IV-94** restored some of the performance by leading to product formation in 62% *ee* (although evidently, the *i*-PrO group is still inferior to the OMe group found in the (DHQD)<sub>2</sub>PYDZ catalyst that gives 78% *ee*).

Dimeric and trimeric cinchonidine derived catalysts with the triazine linker were also evaluated. Bradley and co-workers have demonstrated that related catalyst structures with the triazine linker are excellent catalysts for the asymmetric dihydroxylation reaction.<sup>30</sup> Disappointingly, both catalysts **IV-95** and **IV-96** exhibited practically no enantioselectivity (see Figure II-17).

**Figure IV-17.** Evaluation of catalysts with triazine linker

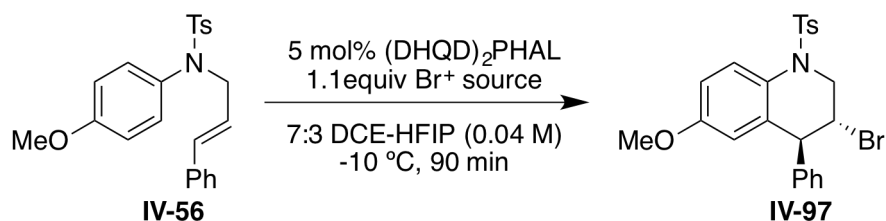


Although these preliminary catalyst libraries had failed to improve on the initially discovered catalyst hits, vital clues for designing the next generation of catalyst library have been gleaned from this study. Noteworthy is the observation that the C6 substituent on the monomer plays a vital role in determining the enantioselectivity. The approaches for designing the 2<sup>nd</sup> generation catalyst library will be disclosed in the concluding sections of this chapter. These approaches will include: 1) Subtle and systematic variation of the monomeric component of these dimeric catalysts and 2) Variation of the linker that connects the two monomeric catalyst units.

#### **IV.4.11. Limitations of the methodology.**

All optimizations notwithstanding, the reaction still shows the hallmarks of an over-engineered process. The scope of the reaction is narrow, both in terms of the electrophilic sources that can be used as well as substrate classes. Results that underscore the limitations of this reaction will be briefly summarized in this section.

The reaction could not be extended to analogous bromocyclization reactions without a complete loss in enantioselectivity. Numerous bromonium sources of varying activities were evaluated for the test reaction as shown in Table IV-12. Although the yields were good, the bromocyclized product **IV-97** was isolated in practically racemic form in every instance. These results are in line with some of the results in other halocyclization reactions developed in our lab, whereby, the initial success with the chlorocyclization reaction could not be translated to enantioselective variants of the bromocyclization reaction.

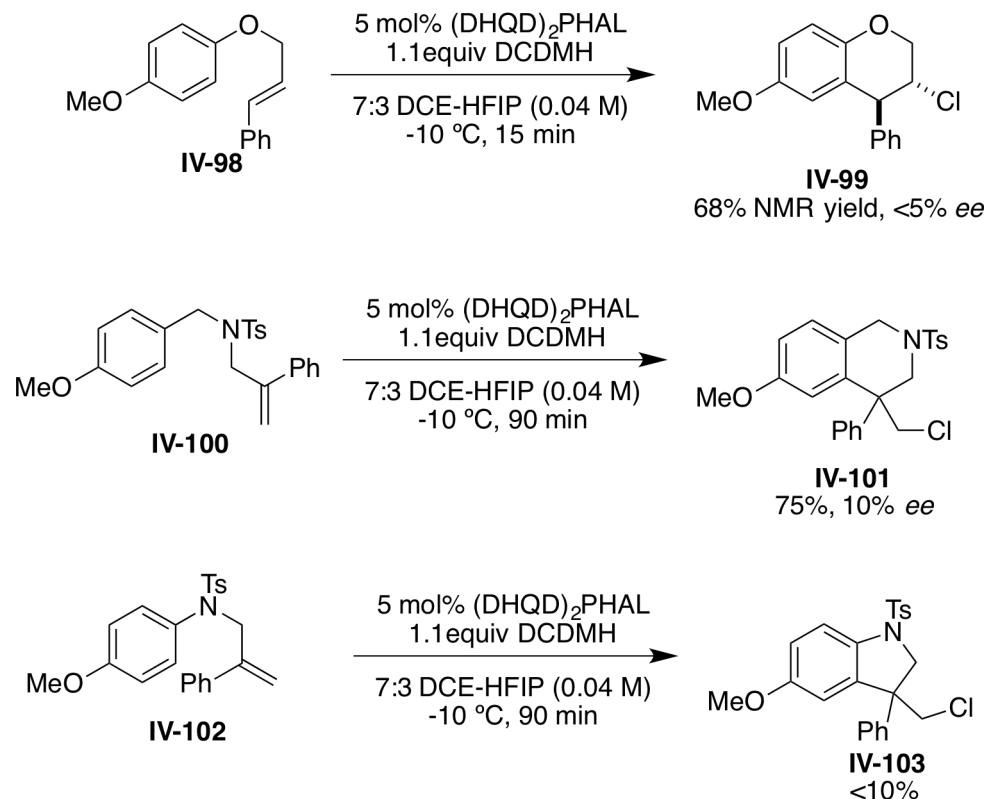
**Table IV-12.** Bromocarbocyclization reaction using Br<sup>+</sup>/ **IV-55** reagent system

| Entry | Br <sup>+</sup> source | Yield                      | ee |
|-------|------------------------|----------------------------|----|
| 1.    | NBS                    | 93%                        | 0% |
| 2.    | DBDMH                  | 96%                        | 0% |
| 3.    | TsNBr <sub>2</sub>     | 70% (20% ring bromination) | nd |
| 4.    | TsNBrNa                | 92%                        | 0% |
| 5.    | BCDMH                  | 90%                        | 0% |

Note: Yields were determined by crude <sup>1</sup>H NMR analysis with MTBE as external standard  
BCDMH = 1-chloro-3-bromo-5,5-dimethyl hydantoin

The chlorocyclization reactions are limited to *N*-sulfonylaryl protected tethers. Reaction of an analogous compound **IV-98** with an O-tether gave a messy reaction and practically no enantioselectivity for the cyclized product **IV-99** (see Figure IV-18). Also incompatible are 1,1-disubstituted alkenes. When substrate **IV-100** was exposed to the optimized reaction conditions, the desired tetrahydroisoquinoline **IV-101** was formed in moderate yield (75%) but only 10% *ee*. Attempted synthesis of dihydroindole derivative **IV-103** via a 5-*exo* chlorocyclization of **IV-102** gave only trace quantities of the product.

**Figure IV-18.** Substrate scope limitations of the current carbocyclization protocol



#### IV.4.12. Synthesis of substrates.

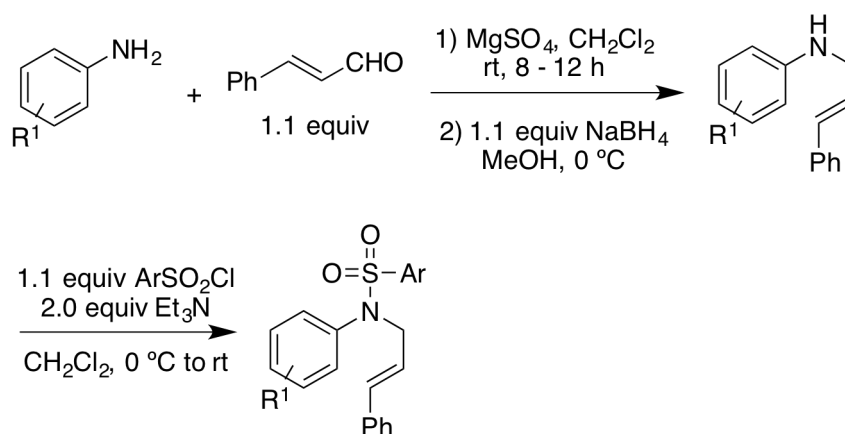
Prior to the presentation of future plans and a summary of this project, a brief digression is in order, to outline the synthetic routes used for accessing the carbocyclization substrates. Two approaches were adopted. The experimental procedures, yields and characterization data can be found in the experimental section. The first approach involved a reductive amination protocol that furnished the free *N*-aryl cinammyl amines (see Scheme IV-3; route 1). The protection of the amine with different functionalities enabled a straightforward evaluation of enantioselectivities as a function of the protecting group for any given olefin substituent and nucleophile.

The second route exploited an unprecedented Mitsunobu reaction of arene sulfonamides with cinnamyl alcohols as a one-step, high yielding route to the carbocyclization substrates

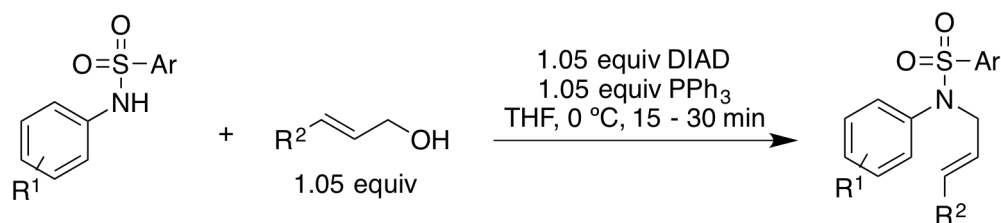
(route 2 in Scheme IV-3). This convergent methodology allows for an expedited route for the simultaneous variation of both the nucleophilic arene moiety as well as the alkene substituent by adopting a 'mix-and-match' strategy. It merits mention that there have been few studies directed towards exploiting arene sulfonamides as *N*-nucleophiles in the Mitsunobu reaction prior to this work.<sup>31</sup> A detailed substrate scope evaluation revealed that unactivated as well as activated (allylic, benzylic or propargyl) primary, secondary and cyclic secondary alcohols were all compatible with this chemistry (>25 examples). These results will be published in due course. Ms. Elizabeth Santos (then an undergraduate research assistant in our laboratory) assisted with the substrate scope evaluation.

**Scheme IV-3.** Synthetic approaches to the substrates for the carbocyclization chemistry

**Route 1: Reductive amination**

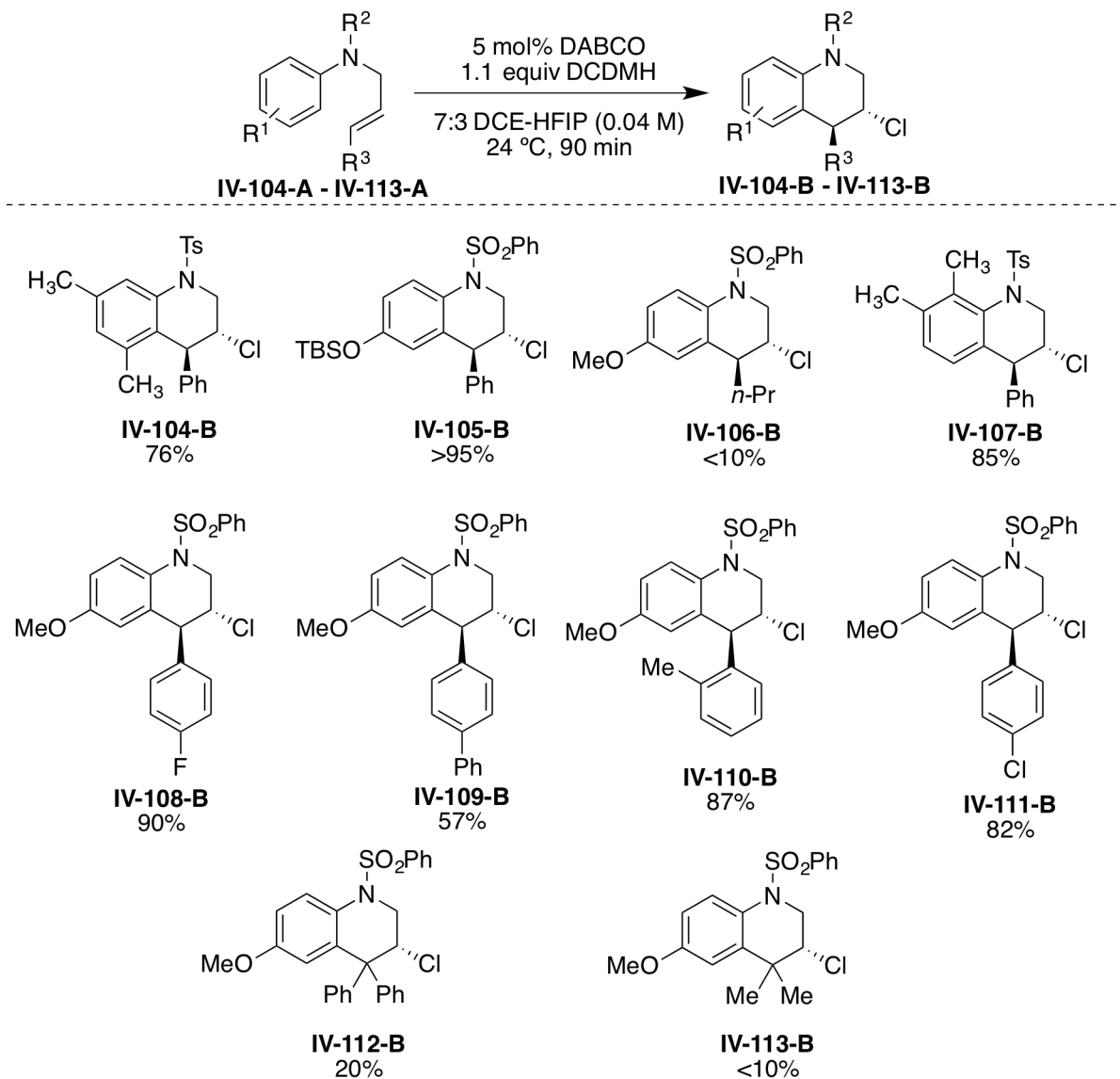


**Route 2: Mitsunobu reaction of arene sulfonamides with allylic alcohols**



It merits mention that numerous other substrates have been synthesized and evaluated in the non-asymmetric chlorocyclization reaction (1.1 equiv of DCDMH and 5 mol% DABCO as the catalyst). These results are summarized in Figure IV-19. Evaluation of the catalytic asymmetric variant will follow.

**Figure IV-19.** The non-asymmetric chlorocyclization of other substrates



#### IV.5. Summary and future work.

As a result of extensive optimization efforts, enantioselectivities of up to 83% *ee* have been realized for the carbocyclization reaction initiated by a chiral chloronium ion. While these results are promising, there is sufficient room for further improvements especially with regards to the enantioselectivity of this reaction. Nonetheless, this work still constitutes the first example a direct chloronium ion mediated Friedel-Crafts reaction of unactivated alkenes – in either enantioselective or racemic fashion.

Till date, close to 20 different protecting groups, numerous co-solvent mixtures, temperatures and concentrations have been evaluated. The key insights gained from these studies are 1) The *N*-protecting group as well as the nucleophilic arene ring are vital catalyst recognition elements present in the substrate that likely ‘anchor’ the substrate in the catalyst’s chiral pocket; 2) The catalyst structure, specifically, the linker and the C6 substituent on the monomer are crucial for obtaining good enantioselectivities.

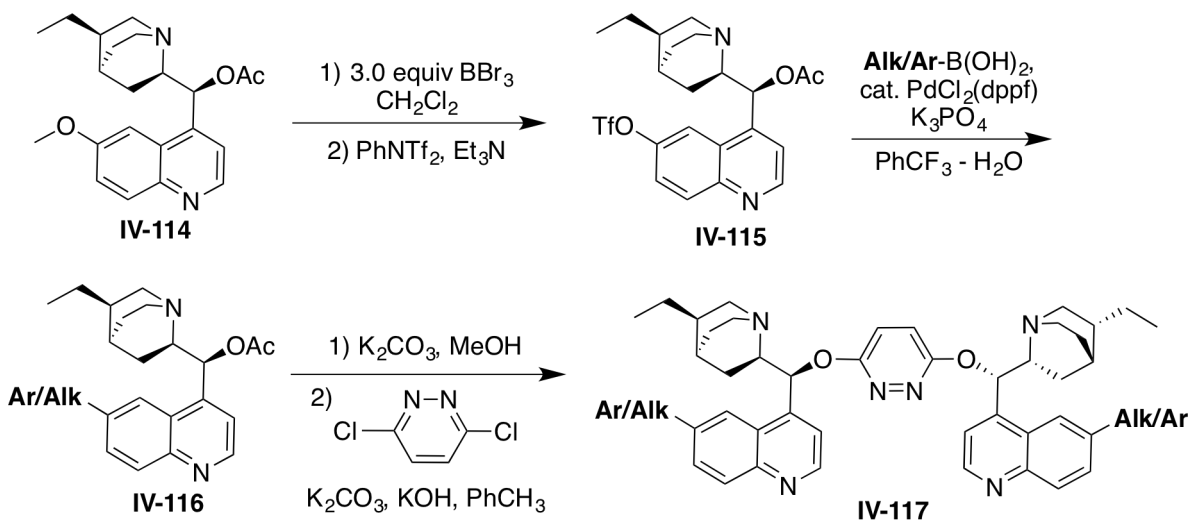
Two key approaches are yet to be evaluated for the reaction optimization. The first approach will involve the synthesis and evaluation of alternate catalyst libraries. It is clear that the best catalyst thus far, (DHQD)<sub>2</sub>PYDZ, must be close to the optimal catalyst structure. Small variations of this catalyst structure especially with regards to the C6 substituent will be pursued. There is sufficient literature precedence for the straightforward substitution of the C6 OMe group of cinchona alkaloids with alkyl/aryl substituents as well as other alkoxy groups (see structures **IV-117** and **IV-119** in Scheme IV-4).

The synthesis of **IV-117** will involve converting the C6-OMe group of **IV-114** to an OTf group *via* a demethylation-triflation sequence (see Scheme IV-4). The aryl triflate **IV-115** thus obtained can be coupled to a wide variety of boronic acids *via* the Suzuki coupling reaction. Waldmann and co-workers have exploited this method to synthesize a library of C6 aryl

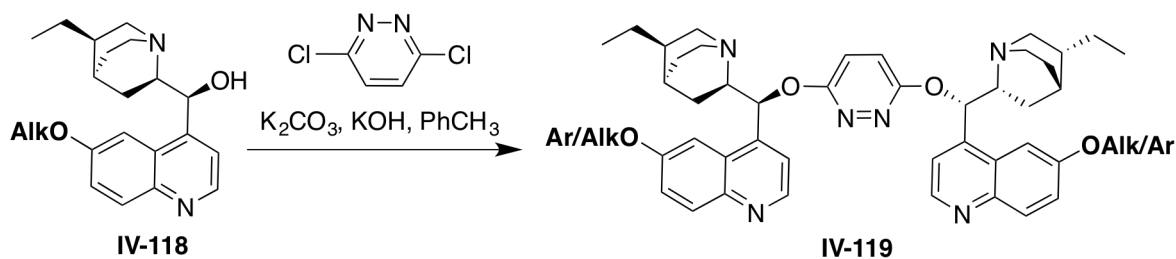
substituted Hatekeyama catalyst (see structure **IV-45** in Figure 8) derivatives.<sup>32</sup> With technology at hand for B-alkyl Suzuki couplings,<sup>33,34</sup> the possibilities for catalyst diversification at the C6 position with aryl and alkyl substituents are endless.

**Scheme IV-4.** Proposed routes for varying C6 substituents of the dimeric catalyst

**Synthesis of C6-substituted cinchona alkaloid dimer libraries:**



**Synthesis of C6-alkoxy substituted cinchona alkaloid dimer libraries:**



An alternate library that will incorporate a variety of alkoxy substituents at C6 (see **IV-119** in Scheme IV-4) will also be synthesized. Sharpless and co-workers have used a 2-step protocol for the synthesis of the O-alkylated cinchona alkaloid derivatives **IV-118** that will be used as precursors for this library.<sup>35</sup> Dimerization of **IV-118** with dichloropyridazine spacer (again using the Sharpless conditions)<sup>35</sup> will give the requisite C6 alkoxy substituted catalysts **IV-119**. Such subtle changes in the catalyst structure have led to much improved

enantioselectivities for the dihydroxylation of terminal olefins in the Sharpless asymmetric dihydroxylation reaction.<sup>35</sup>

The steric and electronic parameters of the C6 substituent can thus be varied systematically using one of the two approaches detailed above. Additionally, statistical methods introduced by Sigman and co-workers can also be exploited once the data from the evaluation of these catalysts become available.<sup>26-28</sup>

The second approach for further improvements will rely on the evaluation of a variety of additives. Our lab has previously demonstrated the beneficial effect of carboxylic acid additives in the chlorocyclization of alkenoic acids and carbamates.<sup>36,37</sup> Unpublished work in the area of intermolecular chloroetherification reactions being pursued in our lab has revealed that inorganic base additives improve diastereo- and enantioselectivity of the products. With these precedents at hand, a series of acidic, basic and neutral additives will be screened for the test reaction. A detailed substrate scope analysis will follow once the optimal conditions are identified.

The overarching goal is to identify catalysts and conditions that will enable a fairly general and robust protocol for C-C bond formation reactions initiated by halonium ions. Key to the success of such endeavors is to identify the substrate-catalyst as well as the halonium-source catalyst interactions. These studies are the main focus of the doctoral thesis work of some of the current group members.

#### **IV.6. Acknowledgements.**

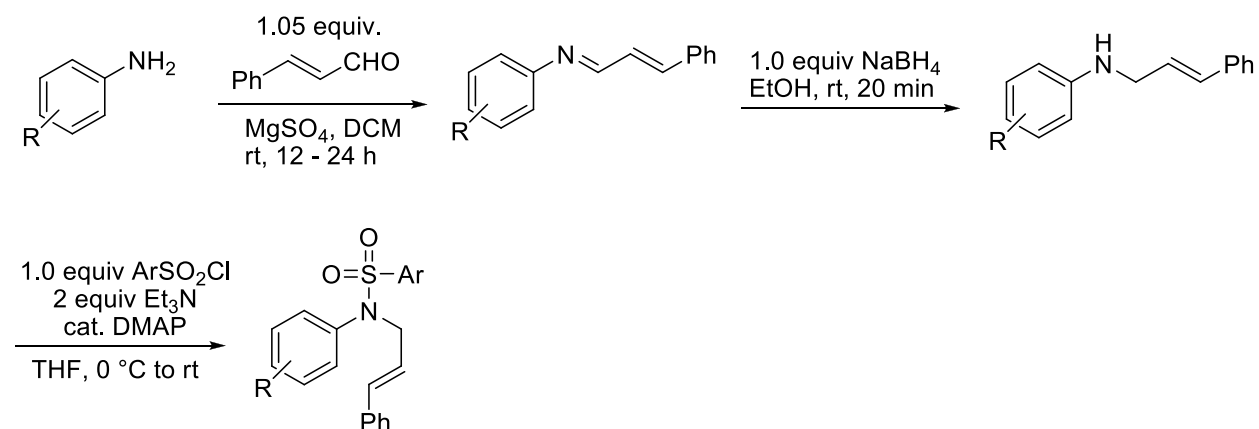
This project has served as a training bed for numerous undergraduates who have worked on many short- and long-term projects in the Borhan lab. Ms. Elizabeth Santos, Ms. Yanmen Yang, Ms. Heather Pillsbury and Mr. Austin Buckley are gratefully acknowledged for their assistance in the synthesis, purification and characterization of numerous substrates presented in this chapter. Insightful discussions with Dr. Carmin Burrell and Dr. Anil Gupta

regarding various aspects of reaction optimizations and mechanistic studies are also acknowledged.

#### IV.7. Experimental section.

##### IV.7.1. General procedure for synthesis of substrates for carbocyclization (Variation of protecting group on N).

The *N*-aryl allylic amines were synthesized using a 2-step reductive amination protocol. The crude imines obtained from the condensation of substituted anilines and cinammaldehyde was reduced with sodium borohydride. The secondary amines thus obtained were reacted with the appropriate sulfonyl chlorides to give the desired substrates for carbocyclization.



##### *Reductive amination :*

An oven dried round bottom flask equipped with a magnetic stir bar was charged with 1.0 equiv of substituted aniline, 1.05 equiv of cinammaldehyde and MgSO<sub>4</sub> (0.3g/mmol of aniline). After purging the reaction vessel with Ar, anhydrous dichloromethane (3mL/mmol of aniline) was introduced. The resulting setup was wrapped in an aluminum foil and stirred at ambient temperature (12 – 24 h with periodic monitoring of small aliquots by <sup>1</sup>H NMR). On complete consumption of starting materials, the reaction was rapidly filtered through a frit funnel. The residual MgSO<sub>4</sub> was washed with DCM. The filtrate thus obtained was diluted with EtOH (2 mL/mmol of aniline). NaBH<sub>4</sub> (1.0 equiv) was then added in small portions over 15-20 min at

ambient temperature. After stirring for a further 20 min, the reaction was diluted with equal amounts of water. The aqueous layer was extracted with DCM (2x). The combined organics was washed with water (2x), dried over anhydrous  $\text{Na}_2\text{SO}_4$  and concentrated to afford the crude amines, which were used without purification in the subsequent step.

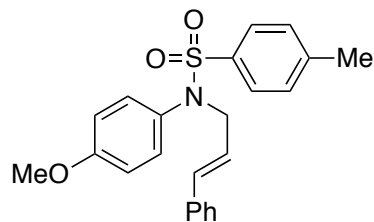
*Alternate protocol:*

To a solution of the substituted aniline in EtOH (5 ml/mmol of aniline) was added at ambient temperature and under  $\text{N}_2$ , cinnamaldehyde (neat, 1.0 equiv) drop wise. The reaction was stirred at 50 °C for 3 hours. The suspension was then cooled in an ice bath and  $\text{NaBH}_4$  (1.0 equiv) was then added portion wise over 15 – 20 min. The work-up and isolation of the crude amine product was identical to the procedure detailed above.

*Protection (sulfonylation) of secondary amines :*

Secondary amine (1.0 equiv) and a catalytic amount of DMAP were charged in an oven dried single neck round bottom flask equipped with a magnetic stir bar and a  $\text{N}_2$  balloon. After purging with  $\text{N}_2$ , anhydrous THF (5 mL/mmol of amine) was introduced under  $\text{N}_2$ . The resulting solution was cooled in an ice bath. This was followed by the sequential addition of dry  $\text{Et}_3\text{N}$  (2.0 equiv) and the appropriate sulfonyl chloride (1.0 equiv) under  $\text{N}_2$ . The reaction was allowed to gradually warm to ambient temperature. On complete consumption of starting material (by TLC analysis), the reaction was diluted with an equal amount of water and extracted with EtOAc (3x). The combined organic layers were washed sequentially with water (2x) and brine (1x) and then dried over anhydrous  $\text{Na}_2\text{SO}_4$ . Concentration in vacuo afforded the crude products, which were then purified by column chromatography ( $\text{SiO}_2$  stationary phase, EtOAc-Hexanes gradient eluent).

**IV-56;** N-cinnamyl-N-(4-methoxyphenyl)-4-methylbenzenesulfonamide



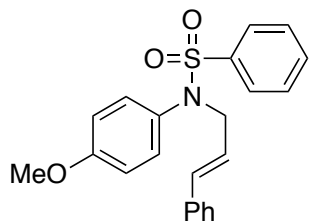
Partial data:

$^1\text{H}$  NMR (500 MHz,  $\text{CDCl}_3$ )  $\delta$  7.51 (d,  $J = 8.5$  Hz, 2H), 7.26 – 7.17 (m, 7H), 6.94 (d,  $J = 9.0$  Hz, 2H), 6.76 (d,  $J = 9.0$  Hz, 2H), 6.34 (d,  $J = 15.5$  Hz, 1H), 6.08 (td,  $J = 15.5, 6.5$  Hz, 1H), 4.27 (dd,  $J = 6.5, 1.5$  Hz, 2H), 3.75 (s, 3H), 2.41 (s, 3H)

$^{13}\text{C}$  NMR (125 MHz,  $\text{CDCl}_3$ )  $\delta$  159.0, 143.3, 136.4, 135.8, 133.7, 131.7, 130.2, 129.4, 128.5, 127.8, 127.7, 126.4, 124.3, 114.1, 55.3, 53.6, 21.5

LR-MS (ESI): calculated for  $[\text{M}+\text{H}]$   $\text{C}_{23}\text{H}_{24}\text{NO}_3\text{S}$ : 394.1; Found: 394.1

**IV-58;** *N*-cinnamyl-*N*-(4-methoxyphenyl)benzenesulfonamide

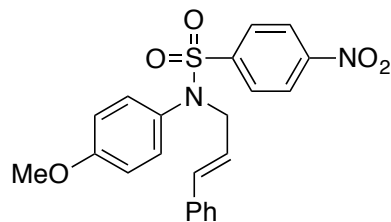


Partial data:

$^1\text{H}$  NMR (500 MHz,  $\text{CDCl}_3$ )  $\delta$  7.67 (d,  $J = 8.5$  Hz, 2H), 7.60 (dd,  $J = 7.5, 7.5$  Hz, 1H), 7.49 (dd,  $J = 8.0, 8.0$  Hz, 2H), 7.32 – 7.21 (m, 5H), 6.97 (d,  $J = 9.0$  Hz, 2H), 6.80 (d,  $J = 9.0$  Hz, 2H), 6.38 (d,  $J = 15.5$  Hz, 1H), 6.12 (td,  $J = 15.5, 6.5$  Hz, 1H), 4.32 (d,  $J = 6.5$  Hz, 2H), 3.78 (s, 3H)

$^{13}\text{C}$  NMR (125 MHz,  $\text{CDCl}_3$ )  $\delta$  159.0, 138.7, 136.3, 133.8, 132.6, 131.5, 130.2, 128.8, 128.5, 127.8, 127.7, 126.4, 124.1, 114.2, 55.3, 53.7

**IV-60-A;** *N*-cinnamyl-*N*-(4-methoxyphenyl)-4-nitrobenzenesulfonamide

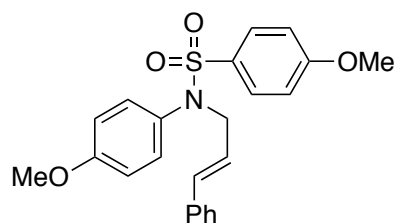


Partial data:

$^1\text{H}$  NMR (500 MHz,  $\text{CDCl}_3$ )  $\delta$  8.28 (d,  $J = 8.5$  Hz, 2H), 7.80 (d,  $J = 8.5$  Hz, 2H), 7.28 – 7.20 (m, 5H), 6.93 (d,  $J = 9.0$  Hz, 2H), 6.79 (d,  $J = 9.0$  Hz, 2H), 6.38 (d,  $J = 15.5$  Hz, 1H), 6.07 (td,  $J = 15.5, 6.5$  Hz, 1H), 4.32 (dd,  $J = 6.5, 1.0$  Hz, 2H), 3.78 (s, 3H)

$^{13}\text{C}$  NMR (125 MHz,  $\text{CDCl}_3$ )  $\delta$  134.6, 130.2, 128.9, 128.6, 128.1, 126.5, 124.0, 123.3, 114.6, 55.4, 54.2

**IV-61-A;** N-cinnamyl-4-methoxy-N-(4-methoxyphenyl)benzenesulfonamide

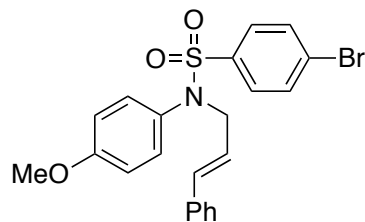


Partial data:

$^1\text{H}$  NMR (500 MHz,  $\text{CDCl}_3$ )  $\delta$  7.57 (d,  $J = 9.0$  Hz, 2H), 7.27 – 7.18 (m, 5H), 6.97 (d,  $J = 8.5$  Hz, 2H), 6.91 (d,  $J = 9.0$  Hz, 2H), 6.77 (d,  $J = 8.5$  Hz, 2H), 6.35 (d,  $J = 15.5$  Hz, 1H), 6.09 (td,  $J = 15.5, 6.5$  Hz, 1H), 4.28 (dd,  $J = 6.5, 1.0$  Hz, 2H), 3.86 (s, 3H), 3.76 (s, 3H)

$^{13}\text{C}$  NMR (125 MHz,  $\text{CDCl}_3$ )  $\delta$  162.8, 158.9, 136.4, 133.7, 131.8, 130.3, 129.8, 128.5, 127.7, 126.4, 124.3, 144.1, 113.9, 55.6, 55.3, 53.5

**IV-62-A;** N-cinnamyl-N-(4-methoxyphenyl)-4-bromo-benzenesulfonamide

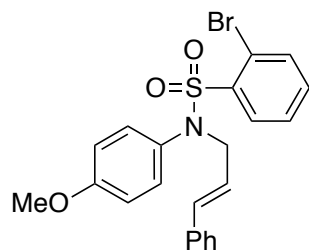


Partial data:

$^1\text{H}$  NMR (500 MHz,  $\text{CDCl}_3$ )  $\delta$  7.58 (d,  $J = 9.0$  Hz, 2H), 7.48 (d,  $J = 9.0$  Hz, 2H), 7.27 – 7.20 (m, 5H), 6.94 (d,  $J = 9.0$  Hz, 2H), 6.77 (d,  $J = 9.0$  Hz, 2H), 6.36 (d,  $J = 16.0$  Hz, 1H), 6.07 (td,  $J = 16.0, 6.5$  Hz, 1H), 4.28 (dd,  $J = 6.5, 1.5$  Hz, 2H), 3.76 (s, 3H)

$^{13}\text{C}$  NMR (125 MHz,  $\text{CDCl}_3$ )  $\delta$  159.2, 137.9, 136.3, 134.1, 132.09, 132.07, 131.3, 130.2, 129.2, 128.5, 127.9, 127.6, 126.47, 126.46, 123.8, 114.3, 55.4, 53.8

**IV-63-A; N-cinnamyl-N-(4-methoxyphenyl)-2-bromo-benzenesulfonamide**

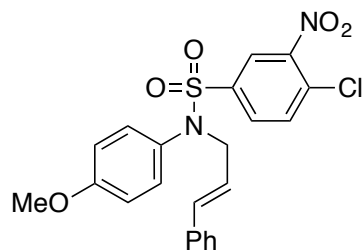


Partial data:

$^1\text{H}$  NMR (500 MHz,  $\text{CDCl}_3$ )  $\delta$  7.80 (dd,  $J = 7.5, 1.5$  Hz, 1H), 7.69 (dd,  $J = 7.5, 1.5$  Hz, 1H), 7.29 – 7.15 (m, 7H), 7.02 (d,  $J = 8.5$  Hz, 2H), 6.67 (d,  $J = 8.5$  Hz, 2H), 6.32 (d,  $J = 16.0$  Hz, 1H), 6.20 (td,  $J = 16.0, 7.0$  Hz, 1H), 4.54 (dd,  $J = 7.0, 1.0$  Hz, 2H), 3.66 (s, 3H)

$^{13}\text{C}$  NMR (125 MHz,  $\text{CDCl}_3$ )  $\delta$  159.1, 138.6, 136.4, 135.3, 133.9, 133.5, 133.0, 131.0, 130.5, 128.5, 127.8, 127.4, 126.5, 124.8, 120.3, 114.2, 55.4, 55.3

**IV-64-A; N-cinnamyl-N-(4-methoxyphenyl)-4-chloro-3-nitrobenzenesulfonamide**

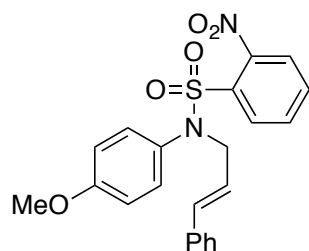


Partial data:

$^1\text{H}$  NMR (500 MHz,  $\text{CDCl}_3$ )  $\delta$  8.10 (d,  $J = 2.0$  Hz, 1H), 7.69 (dd,  $J = 8.5, 2.0$  Hz, 1H), 7.61 (d,  $J = 8.5$  Hz, 1H), 7.28 – 7.20 (m, 5H), 6.97 (d,  $J = 9.0$  Hz, 2H), 6.81 (d,  $J = 9.0$  Hz, 2H), 6.40 (d,  $J = 15.5$  Hz, 1H), 6.06 (td,  $J = 15.5, 6.5$  Hz, 1H), 4.32 (d,  $J = 6.5$  Hz, 2H), 3.77 (s, 3H)

$^{13}\text{C}$  NMR (125 MHz,  $\text{CDCl}_3$ )  $\delta$  159.6, 147.8, 139.4, 136.0, 134.8, 132.5, 131.5, 131.3, 130.6, 130.2, 128.6, 128.1, 126.5, 124.7, 123.0, 114.7, 55.4, 54.3

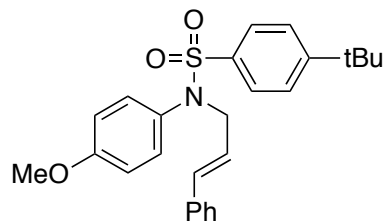
**IV-65-A;** N-cinnamyl-N-(4-methoxyphenyl)-2-nitrobenzenesulfonamide



Partial data:

$^1\text{H}$  NMR (300 MHz,  $\text{CDCl}_3$ )  $\delta$  7.64 – 7.62 (m, 2H), 7.57 – 7.53 (m, 1H), 7.49 – 7.43 (m, 1H), 7.27 – 7.20 (m, 5H), 7.07 (d,  $J = 9.0$  Hz, 2H), 6.76 (d,  $J = 9.0$  Hz, 2H), 6.36 (d,  $J = 15.9$  Hz, 1H), 6.17 (dt,  $J = 15.9, 6.9$  Hz, 1H), 4.47 (dd,  $J = 6.9, 0.9$  Hz, 2H), 3.75 (s, 3H)

**IV-66-A;** N-cinnamyl-N-(4-methoxyphenyl)-4-tert-butyl-benzenesulfonamide

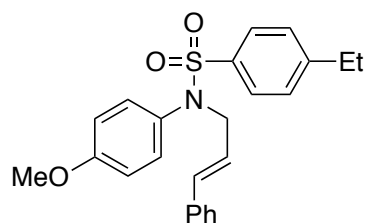


Partial data:

$^1\text{H}$  NMR (500 MHz,  $\text{CDCl}_3$ )  $\delta$  7.56 (d,  $J = 8.5$  Hz, 2H), 7.45 (d,  $J = 8.5$  Hz, 2H), 7.26 – 7.17 (m, 5H), 6.98 (d,  $J = 9.0$  Hz, 2H), 6.77 (d,  $J = 9.0$  Hz, 2H), 6.34 (d,  $J = 16.0$  Hz, 1H), 6.07 (td,  $J = 16.0, 6.5$  Hz, 1H), 4.28 (dd,  $J = 6.5, 1.5$  Hz, 2H), 3.76 (s, 3H), 1.33 (s, 9H)

$^{13}\text{C}$  NMR (125 MHz,  $\text{CDCl}_3$ )  $\delta$  159.0, 156.3, 136.4, 136.0, 133.7, 131.9, 130.3, 128.5, 127.7, 126.4, 125.7, 124.3, 114.1, 55.3, 53.6, 35.1, 31.1, 14.8

**IV-67-A;** *N*-cinnamyl-4-ethyl-*N*-(4-methoxyphenyl)benzenesulfonamide

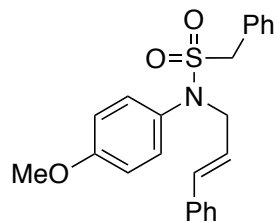


Partial data:

$^1\text{H}$  NMR (500 MHz,  $\text{CDCl}_3$ )  $\delta$  7.54 (d,  $J = 8.0$  Hz, 2H), 7.28 – 7.17 (m, 7H), 6.95 (d,  $J = 9.0$  Hz, 2H), 6.77 (d,  $J = 9.0$  Hz, 2H), 6.33 (d,  $J = 16.0$  Hz, 1H), 6.08 (td,  $J = 16.0, 7.0$  Hz, 1H), 4.27 (dd,  $J = 7.0, 1.0$  Hz, 2H), 3.75 (s, 3H), 2.71 (q,  $J = 7.5$  Hz, 2H), 1.25 (t,  $J = 7.5$  Hz, 3H)

$^{13}\text{C}$  NMR (125 MHz,  $\text{CDCl}_3$ )  $\delta$  159.0, 149.5, 136.4, 136.0, 133.7, 131.7, 130.2, 128.5, 128.2, 127.9, 127.7, 126.4, 124.2, 114.1, 55.3, 53.6, 28.8, 15.0

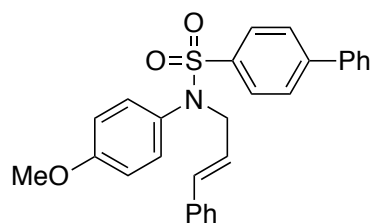
**IV-69-A;** *N*-cinnamyl-*N*-(4-methoxyphenyl)-1-phenylmethanesulfonamide



$^1\text{H}$  NMR (500 MHz,  $\text{CDCl}_3$ )  $\delta$  7.46 – 7.44 (m, 2H), 7.40 – 7.37 (m, 3H), 7.27 – 7.20 (m, 5H), 7.14 (d,  $J = 9.5$  Hz, 2H), 6.83 (d,  $J = 9.5$  Hz, 2H), 6.25 (d,  $J = 15.0$  Hz, 1H), 5.93 (td,  $J = 15.0$ , 6.5 Hz, 1H), 4.28 (s, 2H), 4.10 (d,  $J = 6.5$  Hz, 2H), 3.77 (s, 3H)

$^{13}\text{C}$  NMR (125 MHz,  $\text{CDCl}_3$ )  $\delta$  159.0, 136.3, 133.7, 131.6, 130.9, 130.5, 129.1, 128.8, 128.7, 128.5, 127.8, 126.5, 124.5, 114.5, 57.7, 55.4, 54.5

**IV-70-A;** N-cinnamyl-N-(4-methoxyphenyl)biphenyl-4-sulfonamide

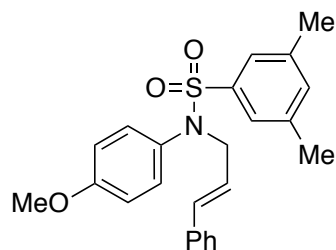


Partial data:

$^1\text{H}$  NMR (500 MHz,  $\text{CDCl}_3$ )  $\delta$  7.70 – 7.65 (m, 4H), 7.60 (d,  $J = 7.5$  Hz, 2H), 7.47 (apparent t,  $J = 8.0$  Hz, 2H), 7.42 – 7.39 (m, 1H), 7.26 – 7.18 (m, 5H), 7.00 (d,  $J = 9.0$  Hz, 2H), 6.78 (d,  $J = 9.0$  Hz, 2H), 6.36 (d,  $J = 16.0$  Hz, 1H), 6.10 (td,  $J = 16.0$ , 7.0 Hz, 1H), 4.33 (dd,  $J = 7.0$ , 1.5 Hz, 2H), 3.76 (s, 3H)

$^{13}\text{C}$  NMR (125 MHz,  $\text{CDCl}_3$ )  $\delta$  159.1, 145.4, 139.3, 137.4, 136.4, 133.8, 131.6, 130.3, 129.0, 128.50, 128.47, 128.27, 127.80, 127.35, 127.30, 126.4, 124.1, 114.2, 55.4, 53.7

**IV-71-A;** N-cinnamyl-N-(4-methoxyphenyl)-3,5-dimethylbenzenesulfonamide

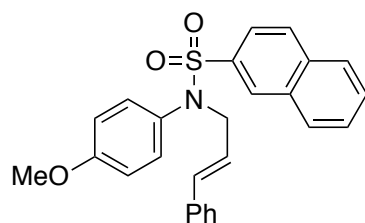


Partial data:

$^1\text{H}$  NMR (500 MHz,  $\text{CDCl}_3$ )  $\delta$  7.27 – 7.17 (m, 8H), 6.95 (d,  $J = 9.0$  Hz, 2H), 6.77 (d,  $J = 9.0$  Hz, 2H), 6.35 (d,  $J = 16.0$  Hz, 1H), 6.10 (td,  $J = 16.0, 7.0$  Hz, 1H), 4.28 (dd,  $J = 7.0, 1.0$  Hz, 2H), 3.76 (s, 3H), 2.31 (s, 6H)

$^{13}\text{C}$  NMR (125 MHz,  $\text{CDCl}_3$ )  $\delta$  159.0, 138.7, 138.4, 136.4, 134.2, 133.7, 131.8, 130.3, 128.5, 127.8, 126.4, 125.3, 124.2, 114.1, 55.4, 53.7, 21.2

**IV-72-A;** *N*-cinnamyl-*N*-(4-methoxyphenyl)naphthalene-2-sulfonamide

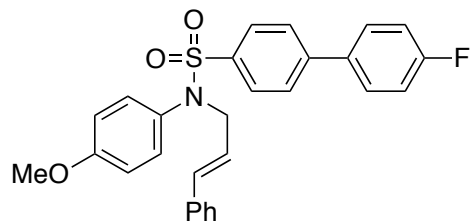


Partial data:

$^1\text{H}$  NMR (500 MHz,  $\text{CDCl}_3$ )  $\delta$  8.21 (s, 1H), 7.90 (d,  $J = 8.5$  Hz, 2H), 7.87 (d,  $J = 8.5$  Hz, 1H), 7.65 – 7.56 (m, 3H), 7.25 – 7.17 (m, 5H), 6.95 (d,  $J = 9.0$  Hz, 2H), 6.74 (d,  $J = 9.0$  Hz, 2H), 6.34 (d,  $J = 15.5$  Hz, 1H), 6.10 (td,  $J = 15.5, 7.0$  Hz, 1H), 4.34 (dd,  $J = 7.0, 1.0$  Hz, 2H), 3.75 (s, 3H)

$^{13}\text{C}$  NMR (125 MHz,  $\text{CDCl}_3$ )  $\delta$  159.0, 136.3, 135.8, 134.8, 133.8, 132.1, 131.6, 130.3, 129.3, 128.9, 128.7, 128.5, 127.86, 127.79, 127.4, 126.4, 124.1, 123.1, 114.2, 55.3, 53.8

**IV-73-A;** *N*-cinnamyl-4'-fluoro-*N*-(4-methoxyphenyl)biphenyl-4-sulfonamide

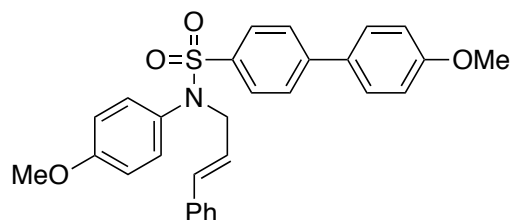


Partial data:

$^1\text{H}$  NMR (500 MHz,  $\text{CDCl}_3$ )  $\delta$  7.68 (d,  $J = 8.5$  Hz, 2H), 7.61 (d,  $J = 8.5$  Hz, 2H), 7.55 – 7.58 (m, 2H), 7.14 – 7.26 (m, 7H), 6.99 (d,  $J = 7.0$  Hz, 2H), 6.77 (d,  $J = 7.0$  Hz, 2H), 6.35 (d,  $J = 15.5$  Hz, 1H), 6.09 (td,  $J = 15.5, 1.5$  Hz, 1H), 4.31 (dd,  $J = 6.5, 1.5$  Hz, 2H), 3.76 (s, 3H)

$^{13}\text{C}$  NMR (125 MHz,  $\text{CDCl}_3$ )  $\delta$  163.2 (d,  $^1J_{\text{C-F}} = 247.5$  Hz), 159.1, 144.4, 137.6, 136.4, 135.4, 133.9, 131.6, 130.3, 129.0 (d,  $^3J_{\text{C-F}} = 8.25$  Hz), 128.5, 128.3, 127.8, 127.2, 126.5, 124.1, 116.0 ( $^2J_{\text{C-F}} = 21.5$  Hz), 114.3, 55.4, 53.7

**IV-74-A;** N-cinnamyl-4'-methoxy-N-(4-methoxyphenyl)biphenyl-4-sulfonamide

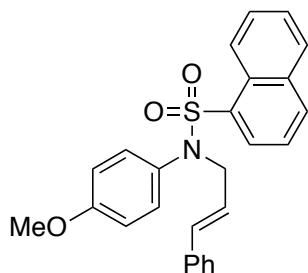


Partial data:

$^1\text{H}$  NMR (500 MHz,  $\text{CDCl}_3$ )  $\delta$  7.65 (d,  $J = 8.5$  Hz, 2H), 7.61 (d,  $J = 8.5$  Hz, 2H), 7.55 (d,  $J = 9.0$  Hz, 2H), 7.17 – 7.26, m, 5H), 6.99 (app dd,  $J = 9.0, 1.0$  Hz, 2H), 6.77 (d,  $J = 9.0$  Hz, 2H), 6.36 (d, 16.0 Hz, 1H), 6.10 (td,  $J = 16.0, 7.0$  Hz, 1H), 4.31 (dd,  $J = 7.0, 1.0$  Hz, 2H), 3.86 (s, 3H), 3.76 (s, 3H)

$^{13}\text{C}$  NMR (125 MHz,  $\text{CDCl}_3$ )  $\delta$  160.1, 159.0, 145.0, 136.6, 136.4, 133.8, 131.65, 131.61, 130.3, 128.5, 128.4, 128.3, 127.8, 126.7, 126.4, 124.2, 114.5, 114.2, 55.40, 55.35, 53.7

**IV-75-A;** *N*-cinnamyl-*N*-(4-methoxyphenyl)naphthalene-1-sulfonamide

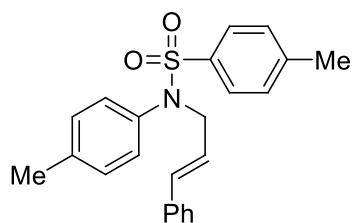


Partial data:

$^1\text{H}$  NMR (500 MHz,  $\text{CDCl}_3$ )  $\delta$  8.53 (d,  $J = 8.0$  Hz, 1H), 8.08 (d,  $J = 7.5$  Hz, 1H), 8.02 (d,  $J = 8.5$  Hz, 1H), 7.90 (dd,  $J = 7.5, 2.0$  Hz, 1H), 7.51 – 7.57 (m, 2H), 7.43 (app t,  $J = 8.5$  Hz, 1H), 7.17 – 7.23 (m, 4H), 6.89 (d,  $J = 7.5$  Hz, 2H), 6.66 (d,  $J = 7.5$  Hz, 2H), 6.28 (d,  $J = 15.5$  Hz, 1H), 6.09 (dt,  $J = 15.5, 6.5$  Hz, 1H), 4.38 (dd,  $J = 6.5, 1.5$  Hz, 2H), 3.71 (s, 3H)

$^{13}\text{C}$  NMR (125 MHz,  $\text{CDCl}_3$ )  $\delta$  159.0, 136.3, 134.3, 133.9, 131.2, 130.94, 130.86, 128.76, 128.74, 127.82, 127.77, 126.7, 126.4, 125.5, 124.3, 114.1, 55.3, 53.7

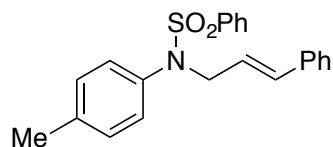
**IV-76-A;** *N*-cinnamyl-4-methyl-*N*-*p*-tolylbenzenesulfonamide



$^1\text{H}$  NMR (500 MHz,  $\text{CDCl}_3$ )  $\delta$  7.51 (d,  $J = 8.0$  Hz, 2H), 7.26 – 7.17 (m, 7H), 7.05 (d,  $J = 8.5$  Hz, 2H), 6.93 (d,  $J = 8.5$  Hz, 2H), 6.35 (d,  $J = 16.0$  Hz, 1H), 6.08 (td,  $J = 16.0, 7.0$  Hz, 1H), 4.29 (dd,  $J = 7.0, 1.5$  Hz, 2H), 2.41 (s, 3H), 2.29 (s, 3H)

$^{13}\text{C}$  NMR (125 MHz,  $\text{CDCl}_3$ )  $\delta$  143.3, 137.8, 136.5, 136.4, 133.6, 129.6, 129.4, 128.7, 128.5, 127.8, 127.7, 126.4, 124.2, 53.4, 21.5, 21.1

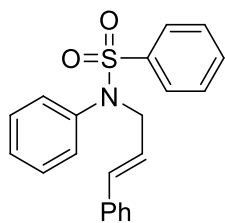
**IV-79-A;** N-cinnamyl-N-p-tolylbenzenesulfonamide



$^1\text{H}$  NMR (500 MHz,  $\text{CDCl}_3$ )  $\delta$  7.67 (d,  $J = 7.5$  Hz, 2H), 7.59 (dd,  $J = 7.5, 7.5$  Hz, 1H), 7.48 (dd,  $J = 7.5, 7.5$  Hz, 2H), 7.29 – 7.21 (m, 5H), 7.08 (d,  $J = 8.0$  Hz, 2H), 6.95 (d,  $J = 8.0$  Hz, 2H), 6.39 (d,  $J = 16.0$  Hz, 1H), 6.11 (td,  $J = 16.0, 7.0$  Hz, 1H), 4.34 (dd,  $J = 7.0, 1.0$  Hz, 2H), 2.32 (s, 3H)

$^{13}\text{C}$  NMR (125 MHz,  $\text{CDCl}_3$ )  $\delta$  138.7, 137.9, 136.3, 133.7, 132.6, 129.6, 128.8, 128.7, 128.5, 127.8, 127.7, 126.4, 124.1, 53.5, 21.0

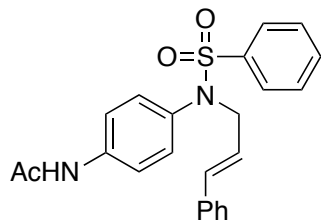
**IV-80-A;** N-cinnamyl-N-phenylbenzenesulfonamide



$^1\text{H}$  NMR (500 MHz,  $\text{CDCl}_3$ )  $\delta$  7.65 (d,  $J = 7.0$  Hz, 2H), 7.59 (dd,  $J = 7.5, 7.5$  Hz, 1H), 7.47 (dd,  $J = 7.5, 7.5$  Hz, 2H), 7.31 – 7.20 (m, 8H), 7.07 (dd,  $J = 7.5, 1.5$  Hz, 2H), 6.38 (d,  $J = 16.0$  Hz, 1H), 6.11 (td,  $J = 16.0, 6.5$  Hz, 1H), 4.36 (dd,  $J = 6.5, 1.0$  Hz, 2H),

$^{13}\text{C}$  NMR (125 MHz,  $\text{CDCl}_3$ )  $\delta$  139.1, 138.6, 136.3, 133.9, 132.6, 129.0, 128.9, 128.8, 128.5, 127.9, 127.8, 127.7, 126.4, 123.9, 53.4

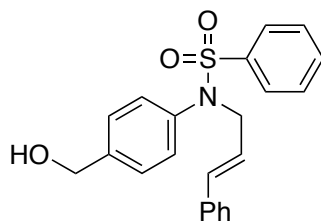
**IV-81-A;** N-(4-(N-cinnamylphenylsulfonamido)phenyl)acetamide



$^1\text{H}$  NMR (500 MHz,  $\text{CDCl}_3$ )  $\delta$  7.64 (d,  $J = 7.5$  Hz, 2H), 7.59 (dd,  $J = 8.0, 8.0$  Hz, 1H), 7.47 (dd,  $J = 7.5, 7.5$  Hz, 2H), 7.43 (d,  $J = 9.0$  Hz, 2H), 7.28 – 7.19 (m, 6H; includes amide NH proton), 7.00 (d,  $J = 9.0$  Hz, 2H), 6.35 (d,  $J = 16.0$  Hz, 1H), 6.08 (td,  $J = 16.0, 7.0$  Hz, 1H), 4.31 (d,  $J = 7.0$  Hz, 2H), 2.15 (s, 3H)

$^{13}\text{C}$  NMR (125 MHz,  $\text{CDCl}_3$ )  $\delta$  168.3, 138.4, 137.6, 136.2, 134.6, 134.0, 132.8, 129.6, 128.9, 128.5, 127.9, 127.6, 126.4, 123.8, 119.8, 53.4, 24.6

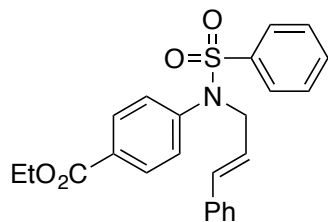
**IV-82-A;** *N*-cinnamyl-*N*-(4-(hydroxymethyl)phenyl)benzenesulfonamide



$^1\text{H}$  NMR (600 MHz,  $\text{CDCl}_3$ )  $\delta$  7.62 (d,  $J = 8.4$  Hz, 2H), 7.56 (dd,  $J = 9.0, 7.5$  Hz, 1H), 7.44 (dd,  $J = 7.8, 7.8$  Hz, 2H), 7.26 – 7.17 (m, 7H), 7.04 (d, 6.0 Hz, 2H), 6.34 (d,  $J = 15.6$  Hz, 1H), 6.07 (td,  $J = 15.6, 7.2$  Hz, 1H), 4.64 (s, 2H), 4.32 (dd,  $J = 6.6, 1.2$  Hz, 2H), 1.75 (br s, 1H)

$^{13}\text{C}$  NMR (150 MHz,  $\text{CDCl}_3$ )  $\delta$  140.6, 138.6, 138.3, 136.2, 133.9, 132.7, 129.0, 128.8, 128.5, 127.8, 127.7, 127.4, 126.4, 123.9, 64.6, 53.4

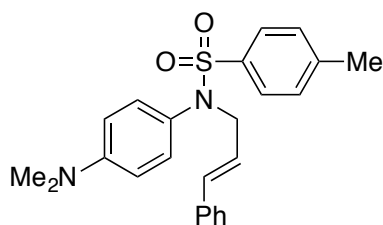
**IV-83-A;** ethyl 4-(*N*-cinnamylphenylsulfonamido)benzoate



$^1\text{H}$  NMR (500 MHz,  $\text{CDCl}_3$ )  $\delta$  7.94 (d,  $J = 8.5$  Hz, 2H), 7.61 – 7.56 (m, 3H), 7.47 – 7.44 (m, 2H), 7.24 – 7.14 (m, 7H), 6.37 (d,  $J = 16.0$  Hz, 1H), 6.05 (td,  $J = 16.0, 6.5$  Hz, 1H), 4.36 (dd,  $J = 6.5, 1.5$  Hz, 2H), 4.33 (q,  $J = 7.0$  Hz, 2H), 1.35 (t,  $J = 7.0$  Hz, 3H)

$^{13}\text{C}$  NMR (150 MHz,  $\text{CDCl}_3$ )  $\delta$  165.8, 143.2, 138.2, 136.0, 134.3, 132.9, 130.3, 129.6, 129.0, 128.5, 128.1, 128.0, 127.6, 126.4, 123.4, 61.1, 52.9, 14.3

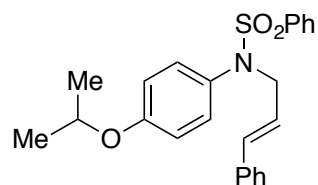
**IV-84;** *N*-cinnamyl-*N*-(4-(dimethylamino)phenyl)-4-methylbenzenesulfonamide



$^1\text{H}$  NMR (500 MHz,  $\text{CDCl}_3$ )  $\delta$  7.56 (d,  $J = 8.0$  Hz, 2H), 7.26 – 7.24 (m, 6H), 7.21 – 7.17 (m, 1H), 6.88 (d,  $J = 9.0$  Hz, 2H), 6.56 (d,  $J = 9.0$  Hz, 2H), 6.38 (d,  $J = 15.5$  Hz, 1H), 6.12 (td,  $J = 15.5, 7.0$  Hz, 1H), 4.28 (dd,  $J = 7.0, 1.0$  Hz, 2H), 2.92 (s, 6H), 2.43 (s, 3H)

$^{13}\text{C}$  NMR (125 MHz,  $\text{CDCl}_3$ )  $\delta$  149.8, 143.0, 136.6, 136.3, 133.3, 129.8, 129.3, 128.4, 127.8, 127.6, 127.5, 126.4, 124.7, 112.1, 53.7, 40.4, 21.5

**IV-86;** *N*-cinnamyl-*N*-(4-isopropoxyphenyl)benzenesulfonamide

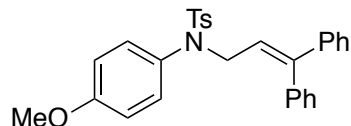


White solid.

$^1\text{H}$  NMR (500 MHz,  $\text{CDCl}_3$ )  $\delta$  7.64 (d,  $J$  = 8.5 Hz, 2H), 7.56 (dd,  $J$  = 8.0, 8.0 Hz, 1H), 7.45 (dd,  $J$  = 7.5, 7.5 Hz, 2H), 7.26 – 7.17 (m, 6H), 6.91 (d,  $J$  = 9.0 Hz, 2H), 6.73 (d,  $J$  = 9.0 Hz, 2H), 6.35 (d,  $J$  = 15.5 Hz, 1H), 6.08 (ddd,  $J$  = 15.5, 7.0, 7.0 Hz, 1H), 4.50 – 4.44 (septet,  $J$  = 6.0 Hz, 1H), 4.28 (d,  $J$  = 7.0 Hz, 2H), 1.29 (d,  $J$  = 6.0 Hz, 6H)

$^{13}\text{C}$  NMR (125 MHz,  $\text{CDCl}_3$ )  $\delta$  157.4, 138.8, 136.4, 133.7, 132.5, 131.2, 130.3, 128.8, 128.5, 127.8, 127.7, 126.4, 124.2, 115.8, 70.0, 53.7, 22.0

**IV-112-A;** *N*-(3,3-diphenylallyl)-*N*-(4-methoxyphenyl)-4-methylbenzenesulfonamide

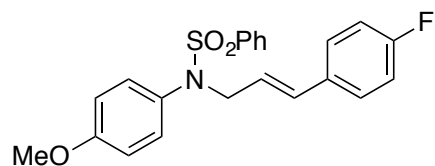


Partial data:

$^1\text{H}$  NMR (500 MHz,  $\text{CDCl}_3$ )  $\delta$  7.61 (d,  $J$  = 7.5 Hz, 2H), 7.55 (dd,  $J$  = 7.5, 7.5 Hz, 1H), 7.43 (dd,  $J$  = 7.5, 7.5 Hz, 2H), 7.29 – 7.23 (m, 6H), 7.10 – 7.09 (m, 2H), 6.88 – 6.84 (m, 4H), .80 (d,  $J$  = 7.5 Hz, 2H), 6.10 (t,  $J$  = 7.0 Hz, 1H), 4.24 (d,  $J$  = 7.0 Hz, 2H), 3.82 (s, 3H)

$^{13}\text{C}$  NMR (125 MHz,  $\text{CDCl}_3$ )  $\delta$  159.0, 145.0, 141.3, 138.7, 138.5, 132.4, 131.4, 130.3, 129.5, 128.7, 128.1, 128.0, 127.56, 127.53, 127.34, 127.29, 123.4, 114.1, 55.4, 50.3

**IV-108-A;** (*E*)-*N*-(3-(4-fluorophenyl)allyl)-*N*-(4-methoxyphenyl)benzenesulfonamide

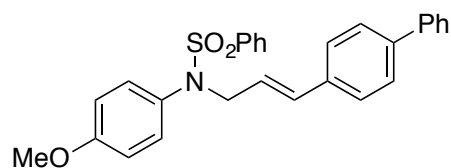


Partial data:

$^1\text{H}$  NMR (500 MHz,  $\text{CDCl}_3$ )  $\delta$  7.63 (d,  $J = 7.5$  Hz, 2H), 7.56 (t,  $J = 7.0$  Hz, 1H), 7.45 (t,  $J = 7.5$  Hz, 1H), 7.19 (dd,  $J = 9.0, 5.5$  Hz, 2H), 6.95 – 6.91 (m, 4H), 6.76 (d,  $J = 9.0$  Hz, 2H), 6.31 (d,  $J = 15.5$  Hz, 1H), 5.99 (td,  $J = 15.5, 6.5$  Hz, 1H), 4.27 (dd,  $J = 6.5, 1.5$  Hz, 2H), 3.75 (s, 3H)

$^{13}\text{C}$  NMR (125 MHz,  $\text{CDCl}_3$ )  $\delta$  162.1 (d,  $^1J_{\text{C-F}} = 246.0$  Hz), 158.8, 138.4, 132.35, 132.20, 131.3, 130.0, 128.5, 127.7 (d,  $^3J_{\text{C-F}} = 8.4$  Hz), 127.4, 123.6 (d,  $^4J_{\text{C-F}} = 2.5$  Hz), 115.1 (d,  $^2J_{\text{C-F}} = 21.8$  Hz), 113.9, 55.1, 53.3,

**IV-109-A;** (*E*)-*N*-(3-([1,1'-biphenyl]-4-yl)allyl)-*N*-(4-methoxyphenyl)benzenesulfonamide

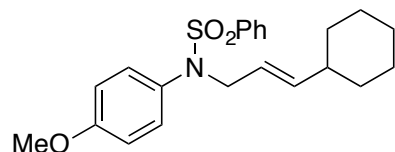


Partial data:

$^1\text{H}$  NMR (500 MHz,  $\text{CDCl}_3$ )  $\delta$  7.64 (d,  $J = 7.0$  Hz, 2H), 7.59 – 7.54 (m, 3H), 7.49 – 7.45 (m, 4H), 7.40 (t,  $J = 7.5$  Hz, 2H), 7.33 – 7.29 (m, 3H), 6.95 (d,  $J = 9.0$  Hz, 2H), 6.77 (d,  $J = 9.0$  Hz, 2H), 6.38 (d,  $J = 16.0$  Hz, 1H), 6.13 (td,  $J = 16.0, 7.0$  Hz, 1H), 4.31 (dd,  $J = 7.0, 1.0$  Hz, 2H), 3.76 (s, 3H)

$^{13}\text{C}$  NMR (125 MHz,  $\text{CDCl}_3$ )  $\delta$  159.0, 140.6, 140.5, 138.7, 135.3, 133.4, 132.6, 132.1, 131.5, 130.3, 128.80, 128.77, 127.7, 127.4, 127.2, 126.90, 126.87, 124.2, 114.2, 55.4, 53.7.

(*E*)-*N*-(3-cyclohexylallyl)-*N*-(4-methoxyphenyl)benzenesulfonamide

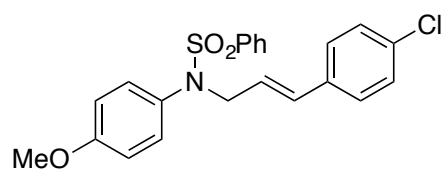


Partial data:

$^1\text{H}$  NMR (500 MHz,  $\text{CDCl}_3$ )  $\delta$  7.61 (d,  $J = 7.5$  Hz, 2H), 7.54 (dddd,  $J = 7.0, 7.0, 1.5, 1.5$  Hz, 1H), 7.44 (dd,  $J = 7.5, 7.5$  Hz, 2H), 6.86 (d,  $J = 9.0$  Hz, 2H), 6.75 (d,  $J = 9.0$  Hz, 2H), 5.32 (dd,  $J = 15.0, 6.5$  Hz, 1H), 5.28 – 5.22 (m, 1H), 4.04 (d,  $J = 6.5$  Hz, 2H), 3.77 (s, 3H), 1.81 – 1.74 (m, 1H), 1.61 – 1.47 (m, 4H), 1.18 – 1.00 (m, 3H), 0.90 – 0.82 (m, 2H)

$^{13}\text{C}$  NMR (125 MHz,  $\text{CDCl}_3$ )  $\delta$  158.9, 141.8, 138.8, 132.4, 131.4, 130.5, 128.7, 127.7, 121.6, 113.9, 55.4, 53.5, 40.1, 32.5, 26.0, 25.7

**IV-111-A;** (*E*)-*N*-(3-(4-chlorophenyl)allyl)-*N*-(4-methoxyphenyl)benzenesulfonamide

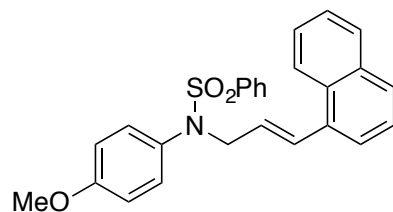


Partial data:

$^1\text{H}$  NMR (500 MHz,  $\text{CDCl}_3$ )  $\delta$  7.62 (d,  $J = 7.5$  Hz, 2H), 7.55 (dd,  $J = 7.5, 7.5$  Hz, 1H), 7.45 (dd,  $J = 7.5, 7.5$  Hz, 2H), 7.20 (d,  $J = 8.0$  Hz, 2H), 7.14 (d,  $J = 8.0$  Hz, 2H), 6.92 (d,  $J = 8.5$  Hz, 2H), 6.76 (d,  $J = 8.5$  Hz, 2H), 6.30 (d,  $J = 16.0$  Hz, 1H), 6.06 (td,  $J = 16.0, 6.5$  Hz, 1H), 4.27 (d,  $J = 6.5$  Hz, 2H), 3.75 (s, 3H)

$^{13}\text{C}$  NMR (125 MHz,  $\text{CDCl}_3$ )  $\delta$  159.1, 138.6, 134.8, 133.5, 132.6, 132.5, 131.5, 130.2, 128.8, 128.7, 127.7, 127.6, 124.9, 114.2, 55.4, 53.6

(*E*)-*N*-(4-methoxyphenyl)-*N*-(3-(naphthalen-1-yl)allyl)benzenesulfonamide

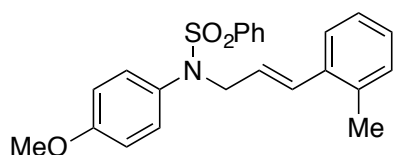


Partial data:

$^1\text{H}$  NMR (600 MHz,  $\text{CDCl}_3$ )  $\delta$  7.78 (d,  $J = 8.5$  Hz, 2H), 7.72 – 7.71 (m, 2H), 7.68 (d,  $J = 8.5$  Hz, 2H), 7.57 (dd,  $J = 8.5, 8.5$  Hz, 1H), 7.46 (dd,  $J = 7.5, 7.5$  Hz, 2H), 7.44 – 7.38 (m, 2H), 7.36 (d,  $J = 4.2$  Hz, 2H), 7.04 (d,  $J = 15.6$  Hz, 1H), 6.99 (d,  $J = 9.0$  Hz, 2H), 6.79 (d,  $J = 9.0$  Hz, 2H), 6.07 (td,  $J = 15.6, 7.2$  Hz, 1H), 4.40 (d,  $J = 7.2, 1.2$  Hz, 2H), 3.76 (s, 3H)

$^{13}\text{C}$  NMR (150 MHz,  $\text{CDCl}_3$ )  $\delta$  159.1, 138.7, 134.3, 133.4, 132.6, 131.8, 131.5, 131.0, 130.4, 128.8, 128.4, 128.1, 127.7, 127.2, 125.9, 125.8, 125.5, 124.0, 123.7, 114.2, 55.4, 53.7.

**IV-110-A;** (*E*)-*N*-(4-methoxyphenyl)-*N*-(3-(*o*-tolyl)allyl)benzenesulfonamide

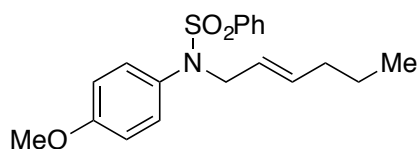


Partial data:

$^1\text{H}$  NMR (600 MHz,  $\text{CDCl}_3$ )  $\delta$  7.65 (d,  $J = 8.4$  Hz, 2H), 7.56 (dd,  $J = 7.2, 7.2$  Hz, 1H), 7.46 (dd,  $J = 7.8, 7.8$  Hz, 2H), 7.22 (d,  $J = 7.2$  Hz, 1H), 7.12 – 7.05 (m, 3H), 6.94 (d,  $J = 8.5$  Hz, 2H), 6.77 (d,  $J = 8.5$  Hz, 2H), 6.52 (d,  $J = 15.6$  Hz, 1H), 5.93 (td,  $J = 15.6, 6.6$  Hz, 1H), 4.31 (dd,  $J = 7.2, 1.2$  Hz, 2H), 3.76 (s, 3H), 2.14 (s, 3H)

$^{13}\text{C}$  NMR (150 MHz,  $\text{CDCl}_3$ )  $\delta$  159.0, 138.7, 135.6, 135.4, 132.6, 132.2, 131.5, 130.3, 130.1, 128.8, 127.72, 127.67, 126.0, 125.9, 125.3, 114.1, 55.4, 53.7, 19.6

**IV-106-A;** (*E*)-*N*-(hex-2-en-1-yl)-*N*-(4-methoxyphenyl)benzenesulfonamide

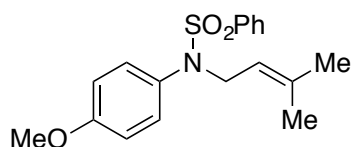


Partial data:

$^1\text{H}$  NMR (500 MHz,  $\text{CDCl}_3$ )  $\delta$  7.61 (d,  $J = 7.5$  Hz, 2H), 7.54 (dddd,  $J = 7.5, 7.5, 1.5, 1.5$  Hz, 1H), 7.44 (dd,  $J = 7.5, 7.5$  Hz, 2H), 6.87 (d,  $J = 9.0$  Hz, 2H), 6.76 (d,  $J = 9.0$  Hz, 2H), 5.41 – 5.27 (m, 1H), 4.06 (s,  $J = 1.5$  Hz, 2H), 3.76 (s, 3H), 1.82 (q,  $J = 7.0$  Hz, 2H), 1.24 – 1.17 (m, 2H), 0.71 (t,  $J = 7.5$  Hz, 3H)

$^{13}\text{C}$  NMR (125 MHz,  $\text{CDCl}_3$ )  $\delta$  158.9, 138.7, 135.8, 132.4, 131.5, 130.3, 128.7, 127.7, 124.3, 114.0, 55.38, 55.36, 53.4, 34.1, 22.0, 13.3

**IV-113-A;** *N*-(4-methoxyphenyl)-*N*-(3-methylbut-2-en-1-yl)benzenesulfonamide

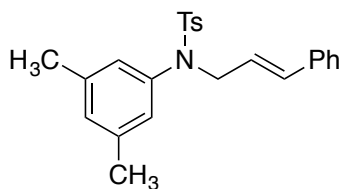


Partial data:

$^1\text{H}$  NMR (500 MHz,  $\text{CDCl}_3$ )  $\delta$  7.62 (dd,  $J = 8.0, 1.5$  Hz, 2H), 7.54 (dddd,  $J = 8.0, 8.0, 1.5, 1.5$  Hz, 1H), 7.47 (dd,  $J = 7.5, 7.5$  Hz, 2H), 6.89 (d,  $J = 9.0$  Hz, 2H), 6.76 (d,  $J = 9.0$  Hz, 2H), 5.08 – 5.05 (m, 1H), 4.10 (d,  $J = 7.0$  Hz, 2H), 3.77 (s, 3H), 1.57 (s, 3H), 1.44 (s, 3H)

$^{13}\text{C}$  NMR (125 MHz,  $\text{CDCl}_3$ )  $\delta$  158.9, 139.0, 36.9, 132.4, 131.8, 130.2, 128.7, 127.7, 118.8, 114.0, 55.4, 48.9, 25.6, 17.7

**IV-104-A;** *N*-cinnamyl-*N*-(3,5-dimethylphenyl)-4-methylbenzenesulfonamide



$^1\text{H}$  NMR (500 MHz,  $\text{CDCl}_3$ )  $\delta$  7.54 (d,  $J = 7.5$  Hz, 2H), 7.27 – 7.18 (m, 7H), 6.87 (s, 1H), 6.67 (s, 2H), 6.38 (d,  $J = 15.5$  Hz, 1H), 6.09 (td,  $J = 15.5, 6.5$  Hz, 1H), 4.27 (dd,  $J = 6.5, 1.0$  Hz, 2H), 2.42 (s, 3H), 2.22 (s, 6H)

$^{13}\text{C}$  NMR (125 MHz,  $\text{CDCl}_3$ )  $\delta$  143.3, 139.1, 138.4, 136.4, 135.9, 133.4, 129.6, 129.2, 128.4, 127.8, 127.7, 126.5, 126.4, 124.4, 53.4, 21.5, 21.1

**IV-105-A;** *N*-(4-(tert-butyldimethylsilyloxy)phenyl)-*N*-cinnamylbenzenesulfonamide

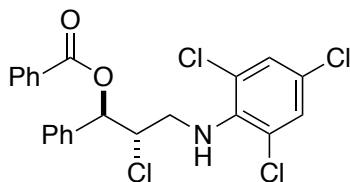


$^1\text{H}$  NMR (500 MHz,  $\text{CDCl}_3$ )  $\delta$  7.63 (d,  $J = 7.5$  Hz, 2H), 7.54 (dd,  $J = 7.5, 7.5$  Hz, 1H), 7.44 (dd,  $J = 7.5$  Hz, 2H), 7.26 – 7.17 (m, 5H), 6.87 (d,  $J = 8.5$  Hz, 1H), 6.70 (d,  $J = 8.5$  Hz, 2H), 6.34 (d,  $J = 17.5$  Hz, 1H), 7.07 (td,  $J = 17.5, 7.0$  Hz, 1H), 4.24 (d,  $J = 7.0$  Hz, 2H), 0.93 (s, 9H), 0.15 (s, 6H)

$^{13}\text{C}$  NMR (125 MHz,  $\text{CDCl}_3$ )  $\delta$  155.3, 138.8, 136.4, 133.9, 132.5, 132.2, 130.2, 128.7, 128.5, 127.8, 127.7, 126.4, 124.2, 120.3, 53.6, 25.6, 18.2, -4.5

**IV.7.2. Characterization of cyclized products.**

**IV-30,** 2-chloro-1-phenyl-3-((2,4,6-trichlorophenyl)amino)propyl benzoate

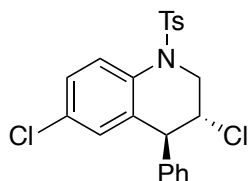


$^1\text{H}$  NMR (500 MHz,  $\text{CD}_3\text{CN}_3 + 1$  drop  $\text{D}_2\text{O}$  to remove exchangeable NH proton) (Note: the 2 proton singlet of the chlorinated aryl ring was overlapping with the residual  $\text{CHCl}_3$  peak if the NMR was run in  $\text{CDCl}_3$ )  $\delta$  8.06 (d,  $J = 7.5$  Hz, 1H), 7.66 (dd,  $J = 7.5, 7.5$  Hz, 1H), 7.54 – 7.48 (m, 4H), 7.41 – 7.36 (m, 3H), 7.29 (s, 2H), 6.13 (d,  $J = 7.0$  Hz, 1H), 4.62 – 4.59 (m, 1H), 3.94 (dd,  $J = 15.0, 3.0$  Hz, 1H), 3.76 (dd,  $J = 15.0, 8.0$  Hz, 1H), 2.78 (1H assumed; HDO peak)

$^{13}\text{C}$  NMR (125 MHz,  $\text{CDCl}_3$ )  $\delta$  164.9, 140.4, 136.4, 133.5, 129.8, 129.5, 128.9, 128.7, 128.6, 128.5, 127.2, 126.5, 126.2, 76.5, 63.9, 49.1

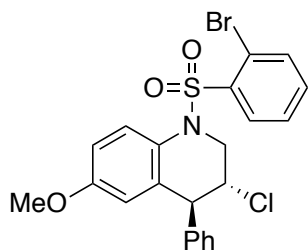
LR-MS (ESI): calculated for  $[\text{M}+\text{H}] \text{C}_{22}\text{H}_{18}\text{Cl}_4\text{NO}_2$ : 468.0; Found: 467.8

**IV-39**; (3*R*,4*S*)-3,6-dichloro-4-phenyl-1-tosyl-1,2,3,4-tetrahydroquinoline



$^1\text{H}$  NMR (500 MHz,  $\text{CDCl}_3$ )  $\delta$  7.85 (d,  $J = 9.0$  Hz, 1H), 7.59 (d,  $J = 8.0$  Hz, 2H), 7.30 (d,  $J = 8.0$  Hz, 2H), 7.24 – 7.14 (m, 4H), 6.64 (dd,  $J = 3.0, 1.0$  Hz, 1H), 6.51 (d,  $J = 8.0$  Hz, 2H), 4.60 (dd,  $J = 14.0, 4.0$  Hz, 1H), 3.92 (d,  $J = 9.0$  Hz, 1H), 3.78 – 3.73 (m, 1H), 3.62 (dd,  $J = 14.0, 11.0$  Hz, 1H), 2.44 (s, 3H);  $^{13}\text{C}$  NMR (125 MHz,  $\text{CDCl}_3$ )  $\delta$  144.6, 140.6, 136.2, 134.4, 133.2, 131.5, 130.2, 130.1, 128.8, 128.6, 127.70, 127.68, 127.4, 126.0, 56.6, 53.9, 51.9, 21.6

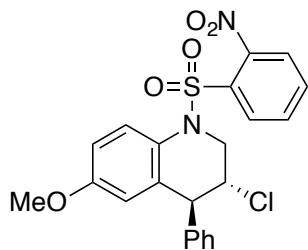
**IV-63-B**; (3*R*,4*S*)-1-((2-bromophenyl)sulfonyl)-3-chloro-6-methoxy-4-phenyl-1,2,3,4-tetrahydroquinoline



$^1\text{H}$  NMR (500 MHz,  $\text{CDCl}_3$ )  $\delta$  8.11 (dd,  $J = 8.0, 2.0$  Hz, 1H), 7.79 (dd,  $J = 7.5, 1.5$  Hz, 1H), 7.50 – 7.43 (m, 2H), 7.29 – 7.24 (m, 3H), 7.13 (d,  $J = 9.0$  Hz, 1H), 7.04 (dd,  $J = 7.5, 1.5$  Hz, 2H), 6.63 (ddd,  $J = 8.0, 3.0, 0.5$  Hz, 1H), 6.26 (dd,  $J = 3.0, 1.0$  Hz, 1H), 4.60 (dd,  $J = 14.0, 4.0$  Hz, 1H), 4.25 – 4.20 (m, 1H), 4.11 (d,  $J = 9.0$  Hz, 1H), 3.75 – 3.67 (m, 1H), 3.58 (s, 3H)

$^{13}\text{C}$  NMR (125 MHz,  $\text{CDCl}_3$ )  $\delta$  157.4, 141.5, 139.8, 136.1, 134.1, 133.4, 132.1, 129.2, 129.1, 128.7, 128.0, 127.5, 124.6, 120.7, 115.3, 113.1, 58.8, 55.3, 54.4, 52.2

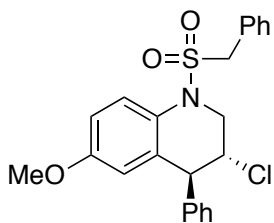
**IV-65-B;** (3*R*,4*S*)-3-chloro-6-methoxy-1-((2-nitrophenyl)sulfonyl)-4-phenyl-1,2,3,4-tetrahydroquinoline



$^1\text{H}$  NMR (500 MHz,  $\text{CDCl}_3$ )  $\delta$  7.86 (d,  $J = 7.5$  Hz, 1H), 7.75 (ddd,  $J = 7.5, 7.5, 1.5$  Hz, 1H), 7.66 (dd,  $J = 7.5, 7.5$  Hz, 2H), 7.45 (d,  $J = 9.0$  Hz, 1H), 7.23 – 7.18 (m, 3H), 6.84 (dd,  $J = 8.0, 2.5$  Hz, 2H), 6.75 (dd,  $J = 9.0, 3.0$  Hz, 1H), 6.26 (d,  $J = 3.0$  Hz, 1H), 4.54 (dd,  $J = 9.0, 3.5$  Hz, 1H), 4.13 – 4.07 (m, 2H), 3.69 (dd,  $J = 14.0, 10.0$  Hz, 1H), 3.62 (s, 3H)

$^{13}\text{C}$  NMR (125 MHz,  $\text{CDCl}_3$ )  $\delta$  157.8, 141.3, 134.1, 133.5, 131.8, 130.9, 128.91, 128.89, 128.6, 128.5, 127.5, 125.4, 124.5, 115.3, 113.4, 58.1, 55.4, 54.2, 52.1

**IV-69-B;** (3*R*,4*S*)-1-(benzylsulfonyl)-3-chloro-6-methoxy-4-phenyl-1,2,3,4-tetrahydroquinoline

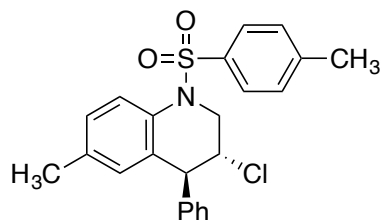


$^1\text{H}$  NMR (500 MHz,  $\text{CDCl}_3$ )  $\delta$  7.38 (s, 5H), 7.32 – 7.24 (m, 3H), 7.21 (d,  $J = 9.0$  Hz, 1H), 7.10 (d,  $J = 8.0$  Hz, 2H), 6.71 (dd,  $J = 9.0, 3.0$  Hz, 1H), 6.32 (d,  $J = 3.0$  Hz, 1H), 4.48 (d,  $J = 2.5$  Hz, 2H), 4.22 – 4.18 (m, 1H), 4.13 – 4.08 (m, 1H), 3.93 (dd,  $J = 14.0, 3.5$  Hz, 1H), 3.61 (s, 3H), 3.51 (dd,  $J = 14.0, 9.0$  Hz, 1H)

$^{13}\text{C}$  NMR (125 MHz,  $\text{CDCl}_3$ )  $\delta$  156.4, 141.7, 130.9, 130.6, 129.3, 129.08, 129.06, 128.9, 128.7, 128.3, 127.6, 122.4, 115.7, 113.4, 59.0, 58.7, 55.4, 53.9, 50.9

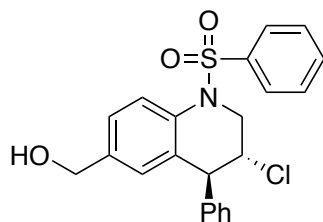
Resolution of enantiomers: DAICEL Chiralpak<sup>®</sup> AD column, 10% IPA-Hexanes, 1.0 mL/min, 254 nm, RT1 = 25.1 min, RT2 = 28.4 min

**IV-76-B;** (3*R*,4*S*)-3-chloro-6-methyl-4-phenyl-1-tosyl-1,2,3,4-tetrahydroquinoline



$^1\text{H}$  NMR (500 MHz,  $\text{CDCl}_3$ )  $\delta$  7.76 (d,  $J$  = 8.5 Hz, 1H), 7.57 (d,  $J$  = 8.0 Hz, 2H), 7.28 – 7.18 (m, 6H), 7.13 (dd,  $J$  = 8.0, 8.0 Hz, 2H), 7.02 (d,  $J$  = 9.0 Hz, 1H), 6.50 (d,  $J$  = 7.0 Hz, 2H), 6.44 (s, 1H), 4.61 (dd,  $J$  = 14.0, 4.0 Hz, 1H), 3.91 (d,  $J$  = 9.5 Hz, 1H), 3.78 – 3.73 (m, 1H), 3.60 (dd,  $J$  = 14.0, 11.5 Hz, 1H), 2.43 (s, 3H), 2.13 (s, 3H)

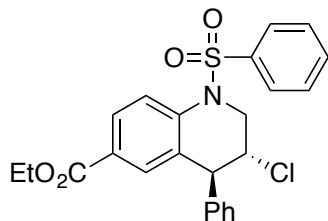
**IV-82-B;** ((3*R*,4*S*)-3-chloro-4-phenyl-1-(phenylsulfonyl)-1,2,3,4-tetrahydroquinolin-6-yl)methanol



$^1\text{H}$  NMR (500 MHz,  $\text{CDCl}_3$ )  $\delta$  7.87 (d,  $J$  = 8.5 Hz, 1H), 7.74 (dd,  $J$  = 8.5, 1.0 Hz, 2H), 7.62 (dd,  $J$  = 7.5, 7.5 Hz, 1H), 7.49 (dd,  $J$  = 7.5, 7.5 Hz, 2H), 7.24 – 7.18 (m, 1H), 7.14 (dd,  $J$  = 7.0, 7.0 Hz, 2H), 6.67 (br s, 1H), 6.55 (d,  $J$  = 8.0 Hz, 2H), 4.59 (dd,  $J$  = 14.0, 4.0 Hz, 1H), 4.49 (d,  $J$  = 5.5 Hz, 2H), 3.97 (d,  $J$  = 9.0 Hz, 1H), 3.83 – 3.78 (m, 1H), 3.66 (dd,  $J$  = 14.0, 11.0 Hz, 1H)

Resolution of enantiomers: DAICEL Chiralcel<sup>®</sup> AS-H column, 40% IPA-Hexanes, 1.0 mL/min, 254 nm, RT1 (major) = 11.5 min, RT2 (minor) = 19.5 min

**IV-83-B**; ethyl (3*R*,4*S*)-3-chloro-4-phenyl-1-(phenylsulfonyl)-1,2,3,4-tetrahydroquinoline-6-carboxylate

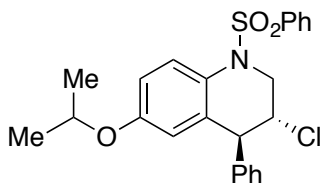


<sup>1</sup>H NMR (500 MHz, CDCl<sub>3</sub>) δ 7.97 (d, *J* = 9.0 Hz, 1H), 7.87 (dd, *J* = 9.0, 2.0 Hz, 1H), 7.78 (dd, *J* = 9.0, 1.5 Hz, 2H), 7.64 – 7.61 (m, 1H), 7.51 – 7.43 (m, 4H), 7.20 – 7.14 (m, 2H), 6.58 (d, *J* = 7.0 Hz, 2H), 4.47 (dd, *J* = 14.0, 4.0 Hz, 1H), 4.29 – 4.21 (m, 2H), 4.10 (d, *J* = 8.5 Hz, 1H), 3.95 – 3.91 (m, 1H), 3.82 (dd, *J* = 14.0, 10.0 Hz, 1H), 1.28 (t, *J* = 7.0 Hz, 3H)

<sup>13</sup>C NMR (125 MHz, CDCl<sub>3</sub>) δ 165.7, 140.9, 139.7, 139.2, 133.5, 132.4, 129.7, 129.6, 128.73, 128.65, 127.6, 127.3, 122.7, 61.0, 56.8, 53.5, 51.0, 14.2 (1 quaternary carbon unaccounted)

Resolution of enantiomers: DAICEL Chiralcel<sup>®</sup> AS-H column, 40% IPA-Hexanes, 1.0 mL/min, 254 nm, RT1 (major) = 8.5 min, RT2 (minor) = 16.3 min

**IV-87**; (3*R*,4*S*)-3-chloro-6-isopropoxy-4-phenyl-1-(phenylsulfonyl)-1,2,3,4-tetrahydroquinoline



Colorless film

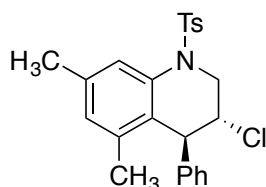
<sup>1</sup>H NMR (500 MHz, CDCl<sub>3</sub>) δ 7.82 (d, *J* = 9.0 Hz, 1H), 7.71 (d, *J* = 8.5 Hz, 2H), 7.65 (dd, *J* = 7.0, 7.0 Hz, 1H), 7.21 (dd, *J* = 7.5, 7.5 Hz, 1H), 7.15 (dd, *J* = 7.5, 7.5 Hz, 2H), 6.80 (dd, *J* = 9.0,

3.0 Hz, 1H), 6.49 (d,  $J = 7.5$  Hz, 2H), 6.14 (d,  $J = 3.0$  Hz, 1H), 4.67 (dd,  $J = 14.0, 4.0$  Hz, 1H), 4.34 (septet,  $J = 6.0$  Hz, 1H), 3.89 (d,  $J = 10.0$  Hz, 1H), 3.76 – 3.71 (m, 1H), 3.64 (dd,  $J = 14.0, 11.5$  Hz, 1H), 1.25 (d,  $J = 6.0$  Hz, 3H), 1.17 (d,  $J = 6.0$  Hz, 3H)

$^{13}\text{C}$  NMR (125 MHz,  $\text{CDCl}_3$ )  $\delta$  155.8, 141.0, 139.4, 133.5, 133.1, 129.5, 128.8, 128.4, 128.3, 127.5, 127.4, 126.4, 117.1, 114.8, 70.0, 57.2, 54.2, 52.4, 21.9, 21.6

Resolution of enantiomers: DAICEL Chiralpak<sup>®</sup> AD column, 5% IPA-Hexanes, 1.0 mL/min, 250 nm, RT1 (minor) = 9.2 min, RT2 (major) = 12.0 min

**IV-104-B;** (3*R*,4*S*)-3-chloro-5,7-dimethyl-4-phenyl-1-tosyl-1,2,3,4-tetrahydroquinoline

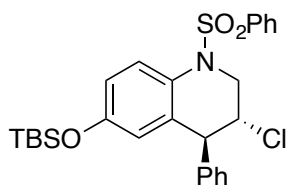


$^1\text{H}$  NMR (500 MHz,  $\text{CDCl}_3$ )  $\delta$  7.74 (s, 1H), 7.68 (d,  $J = 9.0$  Hz, 2H), 7.25 – 7.23 (m, 3H), 7.17 – 7.13 (m 1H), 7.08 (dd,  $J = 7.5, 7.5$  Hz, 2H), 6.60 (d,  $J = 7.5$  Hz, 2H), 4.24 (d,  $J = 5.5$  Hz, 1H), 4.20 – 4.16 (m, 1H), 4.12 – 4.08 (m, 1H), 3.89 (dd,  $J = 13.5, 8.0$  Hz, 1H), 2.40 (s, 3H), 2.37 (s, 3H), 1.87 (s, 3H)

$^{13}\text{C}$  NMR (125 MHz,  $\text{CDCl}_3$ )  $\delta$  144.2, 141.5, 136.0, 135.7, 134.7, 129.9, 129.8, 128.7, 127.9, 127.5, 127.2, 121.6, 58.3, 51.5, 49.3, 21.6, 21.4, 17.5

Resolution of enantiomers: DAICEL Chiralcel<sup>®</sup> AS-H column, 15% IPA-Hexanes, 1.0 mL/min, 250 nm, RT1 (major) = 8.7 min, RT2 (minor) = 18.2 min.

**IV-105-B;** (3*R*,4*S*)-6-((*tert*-butyldimethylsilyl)oxy)-3-chloro-4-phenyl-1-(phenylsulfonyl)-1,2,3,4-tetrahydroquinoline

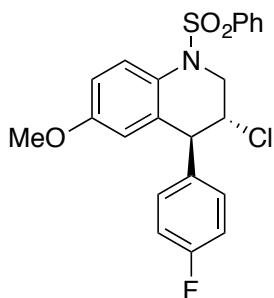


$^1\text{H}$  NMR (500 MHz,  $\text{CDCl}_3$ )  $\delta$  7.76 (d,  $J = 9.0$  Hz, 1H), 7.66 (dd,  $J = 8.5, 1.0$  Hz, 2H), 7.62 (dddd,  $J = 9.0, 9.0, 1.5, 1.5$  Hz, 1H), 7.45 (dd,  $J = 8.5, 8.5$  Hz, 2H), 7.18 (dddd,  $J = 7.5, 7.5, 1.5, 1.5$  Hz, 1H), 7.11 (dd,  $J = 7.5, 7.5$  Hz, 2H), 6.72 (ddd,  $J = 9.0, 3.5, 0.5$  Hz, 1H), 6.41 (d,  $J = 8.0$  Hz, 2H), 6.04 (dd,  $J = 3.0, 1.0$  Hz, 1H), 4.66 (dd,  $J = 14.0, 4.0$  Hz, 1H), 3.84 (d,  $J = 10.0$  Hz, 1H), 3.72 (ddd,  $J = 11.5, 10.0, 4.0$  Hz, 1H), 3.61 (dd,  $J = 14.0, 11.5$  Hz, 1H), 0.81 (s, 9H), 0.00 (s, 3H), -0.04 (s, 3H)

$^{13}\text{C}$  NMR (125 MHz,  $\text{CDCl}_3$ )  $\delta$  153.8, 141.0, 139.4, 133.5, 133.1, 129.4, 129.0, 128.7, 128.4, 127.5, 127.3, 126.3, 121.1, 119.5, 56.9, 54.0, 52.4, 25.6, 18.3, -4.5, -4.7

Resolution of enantiomers: DAICEL Chiralpak<sup>®</sup> OT-(+) column, 5% IPA-Hexanes, 0.8 mL/min, 250 nm, RT1 = 8.6 min, RT2 = 10.0 min

**IV-108-B;** (3*R*,4*S*)-3-chloro-4-(4-fluorophenyl)-6-methoxy-1-(phenylsulfonyl)-1,2,3,4-tetrahydroquinoline

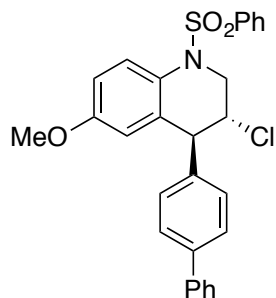


$^1\text{H}$  NMR (600 MHz,  $\text{CDCl}_3$ )  $\delta$  7.80 (d,  $J = 8.4$  Hz, 1H), 7.67 (dd,  $J = 8.0, 1.2$  Hz, 2H), 7.62 (dddd,  $J = 8.0, 8.0, 1.2, 1.2$  Hz, 1H), 7.49 – 7.47 (m, 2H), 6.83 – 6.77 (m, 3H), 6.44 (dd,  $J = 8.5, 5.4$  Hz, 2H), 6.10 (dd,  $J = 2.4, 1.2$  Hz, 1H), 4.64 (dd,  $J = 14.4, 4.2$  Hz, 1H), 3.87 (d,  $J = 10.2$  Hz, 1H), 3.68 – 3.64 (m, 1H), 3.62 (s, 3H), 3.59 (dd,  $J = 14.4, 12.0$  Hz, 1H)

$^{13}\text{C}$  NMR (150 MHz,  $\text{CDCl}_3$ )  $\delta$  162.0 (d,  $^1J_{\text{C-F}} = 245.0$  Hz), 157.6, 139.4, 136.8 (d,  $^4J_{\text{C-F}} = 3.3$  Hz), 133.3, 133.1, 130.3 (d,  $^3J_{\text{C-F}} = 7.7$  Hz), 129.5, 128.6, 127.5, 126.6, 115.4 (d,  $^2J_{\text{C-F}} = 21.5$  Hz), 114.9, 113.3, 57.2, 55.3, 53.5, 52.3

Resolution of enantiomers: DAICEL Chiralcel<sup>®</sup> AS-H column, 10% IPA-Hexanes, 0.5 mL/min, 250 nm, RT1 = 38.7 min, RT2 = 46.4 min.

**IV-109-B;** (3*R*,4*S*)-4-([1,1'-biphenyl]-4-yl)-3-chloro-6-methoxy-1-(phenylsulfonyl)-1,2,3,4-tetrahydroquinoline

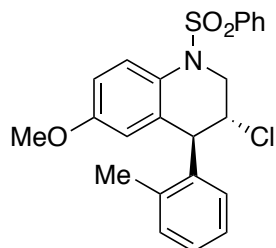


<sup>1</sup>H NMR (600 MHz, CDCl<sub>3</sub>) δ 7.83 (d, *J* = 9.0 Hz, 1H), 7.71 (d, *J* = 8.4 Hz, 2H), 7.64 (dd, *J* = 7.2, 7.2 Hz, 1H), 7.53 – 7.48 (m, 4H), 7.41 (dd, *J* = 7.2, 7.2 Hz, 2H), 7.34 – 7.31 (m, 3H), 6.81 (dd, *J* = 7.2, 2.4 Hz, 1H), 6.54 (d, *J* = 7.8 Hz, 2H), 6.19 (d, *J* = 2.4 Hz, 1H), 4.67 (dd, *J* = 7.8, 3.6 Hz, 1H), 3.93 (d, *J* = 9.6 Hz, 1H), 3.78 – 3.74 (m, 1H), 3.66 – 3.61 (m, 4H; includes OCH<sub>3</sub> singlet at 3.63)

<sup>13</sup>C NMR (150 MHz, CDCl<sub>3</sub>) δ 157.6, 140.5, 140.3, 140.0, 139.4, 133.4, 133.2, 129.5, 129.2, 128.8, 128.7, 127.5, 127.4, 127.2, 127.0, 126.5, 115.1, 113.2, 57.1, 55.4, 53.9, 52.4

Resolution of enantiomers: DAICEL Chiralcel<sup>®</sup> OD-H column, 10% IPA-Hexanes, 0.4 mL/min, 250 nm, RT1 = 37.2 min, RT2 = 41.8 min.

**IV-110-B;** (3*R*,4*S*)-3-chloro-6-methoxy-1-(phenylsulfonyl)-4-(*o*-tolyl)-1,2,3,4-tetrahydroquinoline

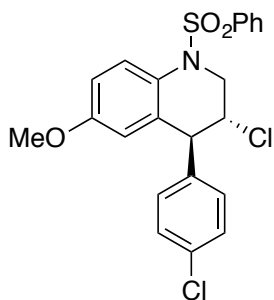


$^1\text{H}$  NMR (600 MHz,  $\text{CDCl}_3$ )  $\delta$  7.82 (d,  $J = 9.0$  Hz, 1H), 7.71 (dd,  $J = 7.2, 1.2$  Hz, 2H), 7.63 (dddd,  $J = 7.2, 7.2, 1.2, 1.2$  Hz, 1H), 7.49 (dd,  $J = 7.8, 7.8$  Hz, 2H), 7.10 (d,  $J = 7.2$  Hz, 1H), 7.06 (ddd,  $J = 7.2, 7.2, 1.2$  Hz, 1H), 6.83 (dd,  $J = 7.2, 7.2$  Hz, 1H), 6.77 (ddd,  $J = 9.0, 3.6, 0.6$  Hz, 1H), 6.01 (dd,  $J = 2.7, 0.9$  Hz, 1H), 5.75 (br d,  $J = 6.0$  Hz, 1H), 4.64 (dd,  $J = 14.4, 4.2$  Hz, 1H), 4.24 (d,  $J = 10.2$  Hz, 1H), 3.86 (ddd,  $J = 10.2, 10.2, 3.6$  Hz, 1H), 3.69 (dd,  $J = 14.4, 10.8$  Hz, 1H), 3.61 (s, 3H), 2.25 (s, 3H)

$^{13}\text{C}$  NMR (150 MHz,  $\text{CDCl}_3$ )  $\delta$  157.5, 139.5, 137.0, 133.9, 133.1, 130.3, 129.5, 128.5, 127.5, 127.2, 126.4, 126.1, 114.9, 112.6, 57.3, 55.3, 52.5, 19.8

Resolution of enantiomers: DAICEL Chiralcel<sup>®</sup> AS-H column, 20% IPA-Hexanes, 1.0 mL/min, 250 nm, RT1 = 10.5 min, RT2 = 15.3 min.

**IV-111-B;** (3*R*,4*S*)-3-chloro-4-(4-chlorophenyl)-6-methoxy-1-(phenylsulfonyl)-1,2,3,4-tetrahydroquinoline



$^1\text{H}$  NMR (600 MHz,  $\text{CDCl}_3$ )  $\delta$  7.81 (d,  $J = 9.0$  Hz, 1H), 7.68 (dd,  $J = 8.4, 1.2$  Hz, 2H), 7.63 (dd,  $J = 7.2, 7.2$  Hz, 1H), 7.48 (dd,  $J = 7.2, 7.2$  Hz, 2H), 7.09 (d,  $J = 8.4$  Hz, 2H), 6.80 (dd,  $J = 9.0, 3.0$  Hz, 1H), 6.40 (d,  $J = 8.4$  Hz, 2H), 6.09 (d,  $J = 3.0$  Hz, 1H), 4.65 (dd,  $J = 13.2, 3.6$  Hz, 1H), 3.87 (d,  $J = 9.6$  Hz, 1H), 3.65 (ddd,  $J = 11.4, 9.6, 3.6$  Hz, 1H), 3.62 (s, 3H), 3.58 (dd,  $J = 13.2, 11.4$  Hz, 1H)

$^{13}\text{C}$  NMR (150 MHz,  $\text{CDCl}_3$ )  $\delta$  157.6, 139.6, 139.4, 133.3, 133.2, 133.0, 130.1, 129.5, 128.7, 128.6, 127.5, 126.6, 114.8, 113.4, 57.0, 55.3, 53.6, 52.3

Resolution of enantiomers: DAICEL Chiralpak® AD-H column, 10% IPA-Hexanes, 1.0 mL/min,  
250 nm, RT1 = 9.6 min, RT2 = 10.6 min.

## REFERENCES

## REFERENCES

- (1) Inoue, T.; Kitagawa, O.; Ochiai, O.; Shiro, M.; Taguchi, T. *Tetrahedron Lett.* **1995**, *36*, 9333.
- (2) Sakakura, A.; Ukai, A.; Ishihara, K. *Nature* **2007**, *445*, 900.
- (3) Li, H.; Zhang, F.-M.; Tu, Y.-Q.; Zhang, Q.-W.; Chen, Z.-M.; Chen, Z.-H.; Li, J. *Chem. Sci.* **2011**, *2*, 1839.
- (4) Wolstenhulme, J. R.; Rosenqvist, J.; Lozano, O.; Ilupeju, J.; Wurz, N.; Engle, K. M.; Pidgeon, G. W.; Moore, P. R.; Sandford, G.; Gouverneur, V. *Angew. Chem. Int. Ed.* **2013**, *52*, 9796.
- (5) Cai, Y.; Liu, X.; Jiang, J.; Chen, W.; Lin, L.; Feng, X. *J. Am. Chem. Soc.* **2011**, *133*, 5636.
- (6) Zhou, L.; Chen, J.; Tan, C. K.; Yeung, Y.-Y. *J. Am. Chem. Soc.* **2011**, *133*, 9164.
- (7) Minakata, S.; Morino, Y.; Oderaotoshi, Y.; Komatsu, M. *Org. Lett.* **2006**, *8*, 3335.
- (8) Braddock, D. C.; Marklew, J. S.; Thomas, A. J. F. *Chem. Commun.* **2011**, *47*, 9051.
- (9) Rodebaugh, R.; Fraser-Reid, B. *J. Am. Chem. Soc.* **1994**, *116*, 3155.
- (10) Denmark, S. E.; Burk, M. T.; Hoover, A. J. *J. Am. Chem. Soc.* **2010**, *132*, 1232.
- (11) Jaganathan, A.; Garzan, A.; Whitehead, D. C.; Staples, R. J.; Borhan, B. *Angew. Chem. Int. Ed.* **2011**, *50*, 2593.
- (12) Tang, Y.; Li, C. *Tetrahedron Lett.* **2006**, *47*, 3823.
- (13) Robin, S.; Rousseau, G. r. *Tetrahedron* **1998**, *54*, 13681.
- (14) Fabry, D. C.; Stodulski, M.; Hoerner, S.; Gulder, T. *Chem. Eur. J.* **2012**, *18*, 10834.
- (15) Wei, H.-L.; Piou, T.; Dufour, J.; Neuville, L.; Zhu, J. *Org. Lett.* **2011**, *13*, 2244.
- (16) Iwabuchi, Y.; Nakatani, M.; Yokoyama, N.; Hatakeyama, S. *J. Am. Chem. Soc.* **1999**, *121*, 10219.
- (17) Oh, S. H.; Rho, H. S.; Lee, J. W.; Lee, J. E.; Youk, S. H.; Chin, J.; Song, C. E. *Angew. Chem. Int. Ed.* **2008**, *47*, 7872.

- (18) Song, E., C. *Cinchona Alkaloids in Synthesis and Catalysis*, 2009.
- (19) Eyring, H. *J. Chem. Phys.* **1935**, *3*, 107.
- (20) Bartook, M. I. *Chem. Rev.* **2009**, *110*, 1663.
- (21) Cainelli, G.; Galletti, P.; Giacomini, D. *Chem. Soc. Rev.* **2009**, *38*, 990.
- (22) Cainelli, G.; Giacomini, D.; Galletti, P. *Chem. Commun.* **1999**, 567.
- (23) Cainelli, G.; Giacomini, D.; Galletti, P.; Quintavalla, A. *Eur. J. Org. Chem.* **2002**, *2002*, 3153.
- (24) Sohtome, Y.; Shin, B.; Horitsugi, N.; Takagi, R.; Noguchi, K.; Nagasawa, K. *Angew. Chem. Int. Ed.* **2010**, *49*, 7299.
- (25) Sohtome, Y.; Tanaka, S.; Takada, K.; Yamaguchi, T.; Nagasawa, K. *Angew. Chem. Int. Ed.* **2010**, *49*, 9254.
- (26) Harper, K. C.; Bess, E. N.; Sigman, M. S. *Nat Chem* **2012**, *4*, 366.
- (27) Harper, K. C.; Sigman, M. S. *Proc. Natl. Acad. Sci.* **2011**, *108*, 2179.
- (28) Sigman, M. S.; Miller, J. J. *J. Org. Chem.* **2009**, *74*, 7633.
- (29) McDaniel, D. H.; Brown, H. C. *J. Org. Chem.* **1958**, *23*, 420.
- (30) McNamara, C. A.; King, F.; Bradley, M. *Tetrahedron Letters* **2004**, *45*, 8527.
- (31) Hughes, D. L. In *Organic Reactions*; John Wiley & Sons, Inc.: 2004.
- (32) Waldmann, H.; Khedkar, V.; Dücker, H.; Schürmann, M.; Oppel, I. M.; Kumar, K. *Angew. Chem. Int. Ed.* **2008**, *47*, 6869.
- (33) Miyaura, N.; Ishiyama, T.; Sasaki, H.; Ishikawa, M.; Sato, M.; Suzuki, A. *J. Am. Chem. Soc.* **1989**, *111*, 314.
- (34) Chemler, S. R.; Trauner, D.; Danishefsky, S. J. *Angew. Chem. Int. Ed.* **2001**, *40*, 4544.
- (35) Arrington, M. P.; Bennani, Y. L.; Gobel, T.; Walsh, P.; Zhao, S.-H.; Sharpless, K. B. *Tetrahedron Letters* **1993**, *34*, 7375.
- (36) Garzan, A.; Jaganathan, A.; Salehi Marzijarani, N.; Yousefi, R.; Whitehead, D. C.; Jackson, J. E.; Borhan, B. *Chem. Eur. J.* **2013**, *19*, 9015.

(37) Whitehead, D. C.; Yousefi, R.; Jaganathan, A.; Borhan, B. *J. Am. Chem. Soc.* **2010**, *132*, 3298.

## Chapter V

### *Cyclic orthoesters as synthetic building blocks for the synthesis of chiral molecules.*

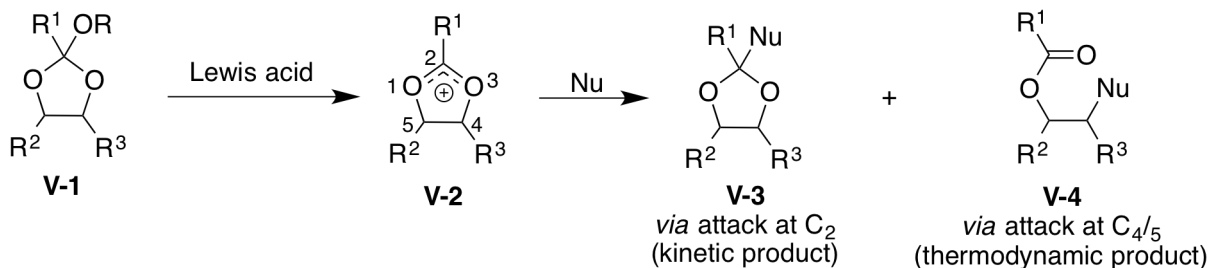
#### V.1. Introduction.

Cyclic orthoesters have found useful applications as intermediates in organic syntheses.<sup>1</sup> However, they still remain a rather ill explored family of synthetic intermediates as compared to some of the more commonly encountered intermediates such as epoxides and aziridines. This may be attributed to several factors such as the poor stability of orthoesters in acidic media and a rather limited means of accessing cyclic orthoesters. These two aspects are detailed in this section.

#### V.1.1. Reactivity of orthoesters.

Little work has been devoted to understanding and tuning the reactivity of orthoesters. Most orthoesters are stable to strongly basic reaction conditions. Nonetheless, they are highly unstable even to mildly acidic conditions. In the presence of Lewis acids, they are transformed to the stabilized oxonium ions that are ambivalent (see structure **V-2** in Scheme V-1). These ions have two electrophilic sites that can be intercepted by a nucleophile.

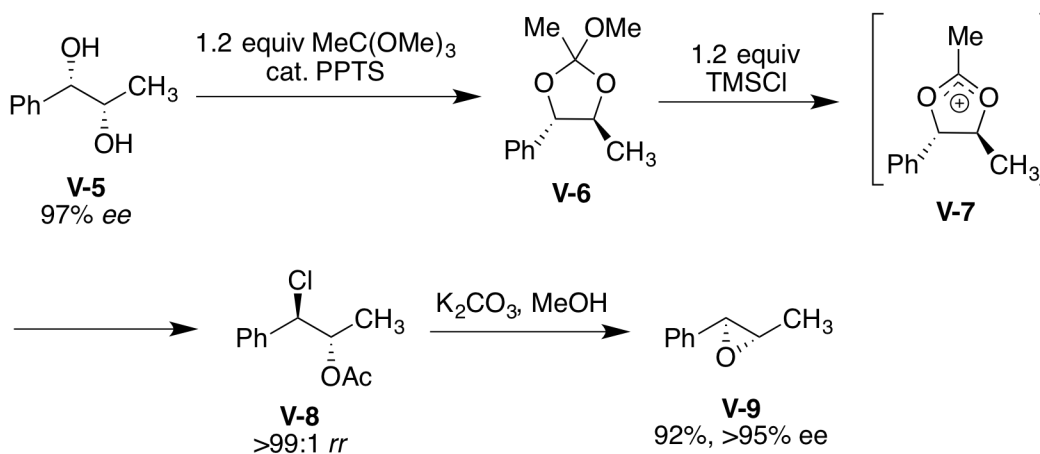
**Scheme V-1.** Reactivity of orthoesters



While there are general guidelines regarding the preference for nucleophilic attack on one or the other electrophilic site<sup>2</sup> (based on the hardness/softness of the nucleophile), they are not universally applicable.<sup>3</sup> The addition into C2 (referred to as the acetoxonium carbon) is proposed to be a kinetically driven process. Many hard nucleophiles such as silyl enol ethers, titanium enolates and cuprates intercept the oxonium ion at the acetoxonium carbon by a kinetically controlled process to give products **V-3**. On the other hand, soft nucleophiles such as alcohols and phenols add to the C4/C5 carbons (the carbinol carbons) under thermodynamic control (see structure **V-4** in Scheme V-1). Furthermore, the transformation of the kinetic product into the thermodynamic product is also possible depending on the duration of the reaction and temperature. Our group and others have observed this mechanistic dichotomy in unrelated transformations that involve cyclic orthoesters.

Sharpless and Kolb were able to demonstrate that treatment of chiral cyclic orthoesters with TMSCl and TMSBr proceeds with a highly *anti*-selective opening of the cyclic acetoxonium ion.<sup>4</sup> This property was exploited for developing a high-yielding, two-step synthesis of chiral epoxides from the corresponding diols (see transformation of **V-5** into **V-9** in Scheme V-2).

**Scheme V-2.** Conversion of chiral diols to epoxides through the intermediacy of cyclic orthoester



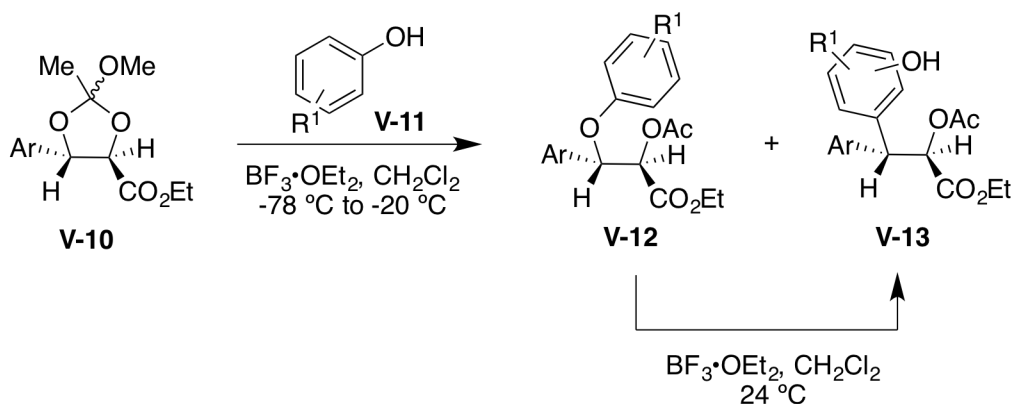
This report had spurred research into exploring other compatible nucleophiles. These efforts have met with varying degrees of success and are briefly summarized in the next section.

### V.1.2. Prior reports of nucleophilic functionalization of cyclic orthoesters.

The use of cyclic orthoesters as chiral building blocks has gained in prominence since the advent of the Sharpless asymmetric dihydroxylation protocol.<sup>5</sup> Cyclic orthoesters are readily synthesized in one step from the corresponding diols. The development of a variety of catalysts and conditions for accessing vicinal diols in highly enantioenriched form has paved the way for exploiting cyclic orthoesters as valuable precursors.

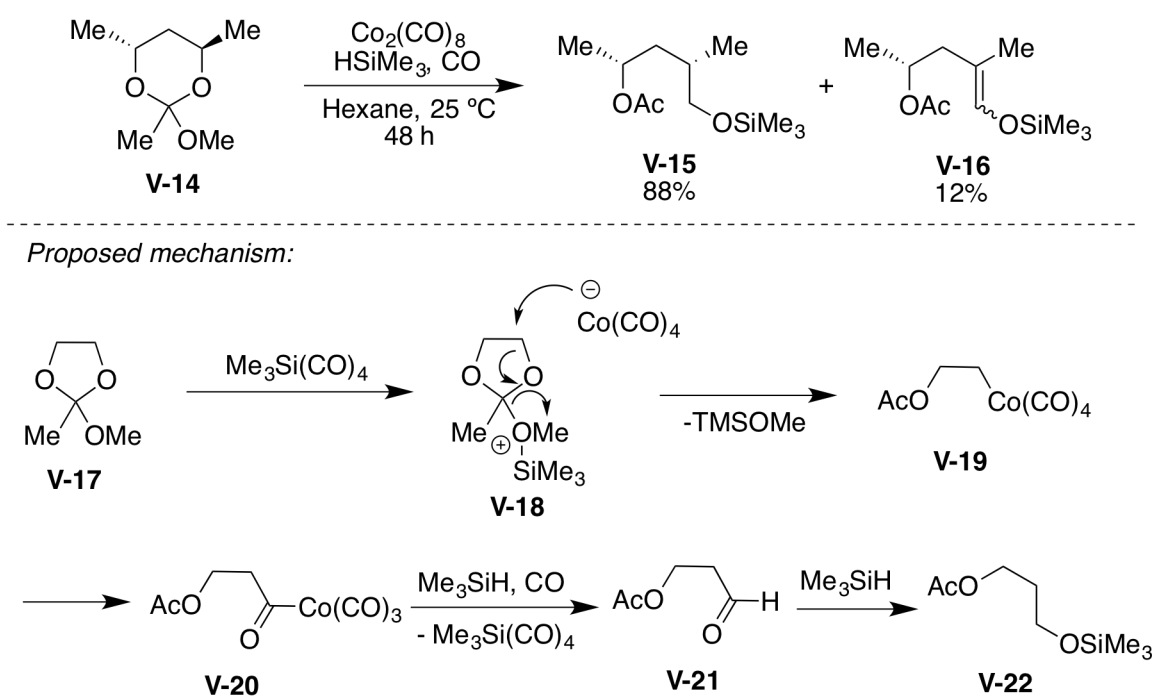
Bozell and co-workers have shown that phenols are capable of intercepting orthoesters in the presence of Lewis acids (see Scheme V-3).<sup>6</sup> Both C-alkylation and O-alkylation products were seen. Furthermore, the isomerization of O-alkylated products to the C-alkylated ones under reaction conditions was also demonstrated indicating that O-alkylation might be a kinetically controlled process. Unlike the Kolb and Sharpless' original report with TMSCl, there was ample evidence for the isomerization of the acetoxonium ions under reaction conditions indicating that the rates of intermolecular nucleophilic capture may not outcompete isomerization processes.

**Scheme V-3.** Interception of acetoxonium ions by phenol nucleophiles



Murai and co-workers have demonstrated that even anionic cobalt complexes are competent nucleophiles that selectively react at the carbinol carbon (see Scheme V-4).<sup>7</sup> The Co catalyzed reaction of cyclic orthoesters with hydrosilanes and carbon monoxide proceeds in moderate to good yields for most substrates. A representative example is shown in Scheme V-4.

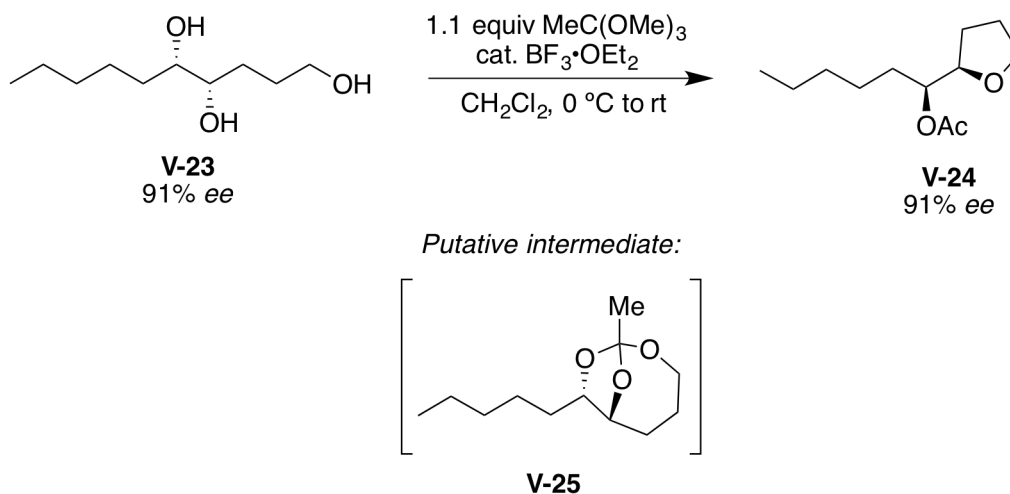
**Scheme V-4.** Anionic cobalt complexes as viable nucleophiles for intercepting acetoxonium ions



Perhaps the most useful synthetic application of orthoesters is the nucleophilic capture of acetoxonium ions by pendant alcohol nucleophiles. The cyclization of 1,2-n-triols to THF and THP rings proceeds in excellent yields and stereospecificity (see Scheme V-5). Fujioka, Kita and co-workers discovered this reaction in 1993;<sup>8</sup> however, it was greatly expanded by our group more recently.<sup>9</sup>

These reactions proceed with exceptional stereoselectivities. The kinetic product in all these reactions is likely the caged orthoester **V-25**. In fact, intermediates analogous to **V-25** have been isolated and characterized. Exposure of these intermediates to the reaction conditions cleanly affords the cyclized products.

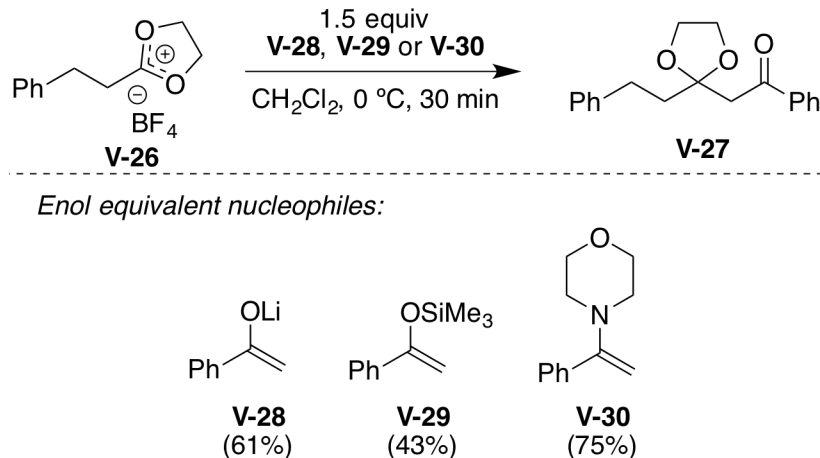
**Scheme V-5.** Intramolecular capture of acetoxonium ions by pendant alcohols



The stereochemistry of chiral diols (obtained in highly enantioenriched form *via* Sharpless Asymmetric Dihydroxylation of olefins) could thus be efficiently translated to the newly formed C-O bond thereby enabling stereoselective syntheses of heterocycles (see transformation of **V-23** to **V-24**).

Nucleophiles such as silyl-enol ethers, enamines and organocuprates are known to selectively react at the acetoxonium carbon. A few examples that have exploited this reactivity of acetoxonium ions are highlighted below.

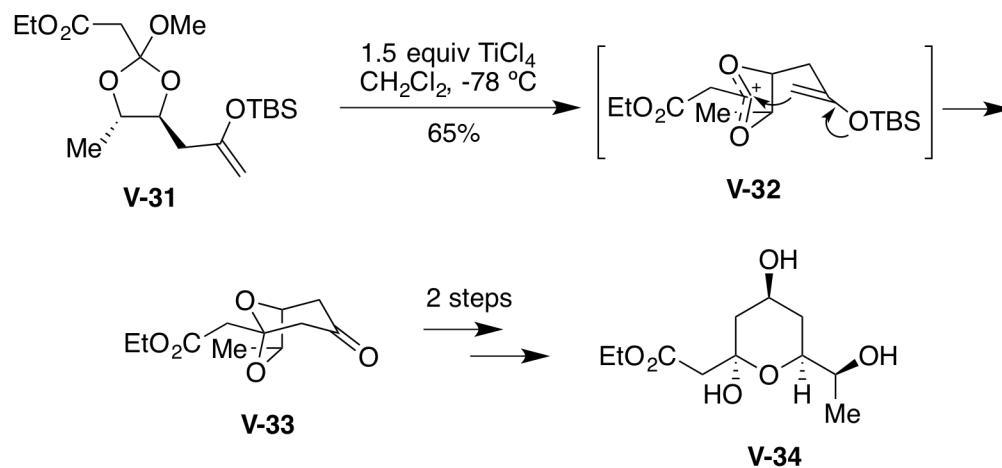
**Scheme V-6.** Nucleophilic addition of enol-equivalents into acetoxonium ions



Mukaiyama and co-workers have shown that the fluoroborate salt of the oxonium ion **V-26** reacts with enamines, enolates and silyl enol ethers to give the corresponding product **V-27** in moderate yields (see Scheme V-6; yield with the respective enol equivalent is given in the parenthesis below the structure of the nucleophile).<sup>10</sup> Other nucleophiles employed successfully in that study included tin enolates and trimethylsilyl cyanide that also exhibited similar reactivity patterns (i.e., attack exclusively at the acetoxonium carbon).

Likewise, Léger and co-workers have exploited an intramolecular nucleophilic capture of an acetoxonium ion by a pendant silyl enol ether as a rapid means to access the C(1)-C(8) segment of the natural product (+)-acutiphycin (see structure **V-34** in Scheme V-7).<sup>11</sup> The acetoxonium ion **V-32** derived from the Lewis acid treatment of **V-31** was intercepted by the pendant silyl-enol ether exclusively at the acetoxonium carbon to give the bicyclic compound **V-33**.

**Scheme V-7.** Intramolecular capture of acetoxonium ions by pendant silyl-enol ethers



Despite these sporadic reports of synthetically useful transformations that involve orthoester intermediates, a plethora of nucleophiles are yet to be evaluated. In this regard, sections of doctoral theses of former members (Dr. Tao Zhang and Mr. Zhihua Shang) of our group were dedicated to evaluating other nucleophiles. While limited success was seen with pendant thiol nucleophiles, other nucleophiles such as acids, esters, amides, sulfonamides and amines were all shown to be incompatible.

At the outset, the aim of this project was to map out the scope and limitations of the orthoester reaction methodology and eventually render this methodology general enough to allow for the use of a variety of heteroatom-based nucleophiles on chiral orthoester scaffolds. This would reveal a novel method for making carbon-heteroatom bonds stereoselectively. Both intra- as well as intermolecular attack of nucleophiles on orthoesters was to be explored. It was also hoped that a better understanding of the reactivities of orthoesters and mechanisms involving these intermediates would emerge from this work.

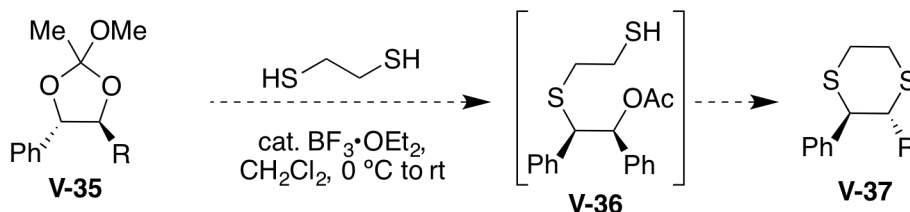
## V.2. Results and discussions.

### V.2.1. Discovery of a 1,2-aryl migration in cyclic orthoesters.

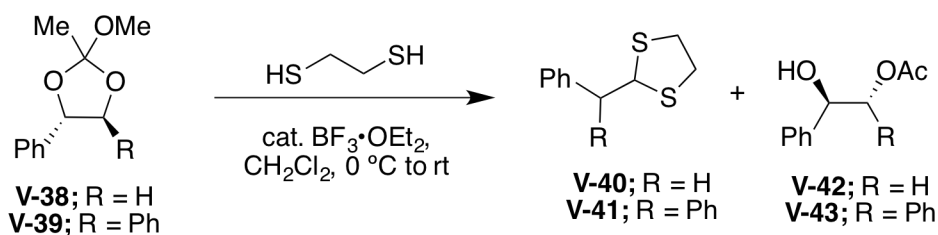
While investigating thiols as potential nucleophiles in the reaction with orthoesters, an interesting rearrangement was discovered. The desired reaction is shown in Scheme V-8. It was hoped that C2-symmetric cyclic 1,4-dithianes (**V-37**) could be accessed by using linear 1,2-dithiols as nucleophiles. With numerous reaction methodologies that exploit sulfur ylides under study in our lab at the time,<sup>12,13</sup> this methodology seemed like an expedient means of accessing chiral sulfur ylides.

**Scheme V-8.** Exploration of dithiols as nucleophiles in orthoester chemistry

*Desired transformation:*



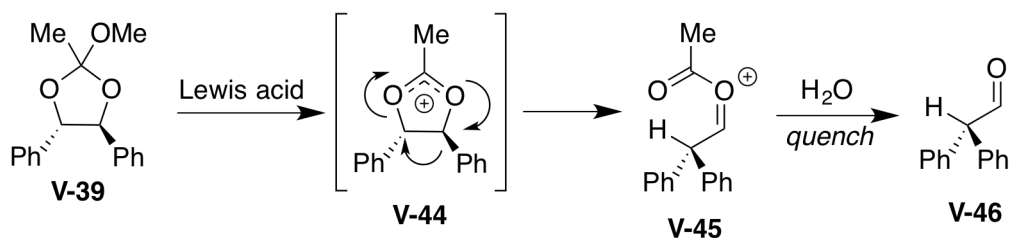
*Observed transformation:*



When orthoesters **V-38** and **V-39** were treated with 1,2-ethanedithiol in the presence of BF<sub>3</sub>·OEt<sub>2</sub>, none of the desired 1,4-dithianes were isolated. Instead, the major products (see structures **V-40** and **V-41**) of both these reactions seem to have arisen from a semi-pinacol rearrangement of the substrates. The mass balance for both reactions was the hydrolyzed

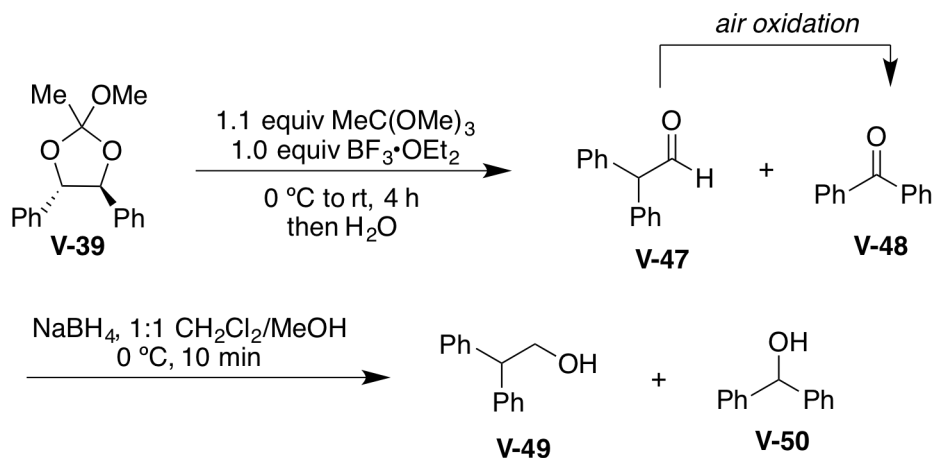
orthoester product (**V-42** and **V-43**, respectively). It merits mention that other nucleophiles such as ethylene diamine, benzyl amine and *p*-toluenesulfonamide were also evaluated as nucleophiles at this stage; no evidence of the desired product was observed in any instance.

**Scheme V-9.** Mechanism of 1,2-aryl ring migration in cyclic acetoxonium ions



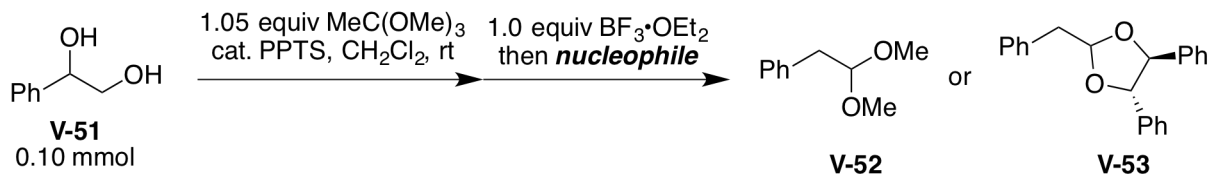
The mechanism for this rearrangement is given in Scheme V-9. It is evident that the thiol plays no role in the rearrangement step. The rearrangement likely occurs at the rigid cyclic acetoxonium ion intermediate **V-44**. Not surprisingly, when ethane dithiol was left out of the reaction, the  $\alpha,\alpha$ -diphenyl acetaldehyde (**V-47**) was isolated along with benzophenone (presumably derived from the air oxidation of **V-47**). It was further established experimentally that **V-47** decomposes to benzophenone if exposed to air for a few hours or if the reaction was performed under dry air. Although a photo-oxidation variant of this reaction has been reported,<sup>14</sup> it was accomplished using a NaY zeolite using irradiation of visible light. The mechanism of this oxidation is unclear at this point in time. The mixture of the diaryl aldehyde and benzophenone (inseparable by column chromatography) was reduced to the corresponding alcohols using  $\text{NaBH}_4$ . Both **V-49** and **V-50** were readily identified by GC-MS analysis.

**Scheme V-10.** Characterization of the primary products of the semi-pinacol rearrangement of **V-39**



The aldehyde product can be intercepted by other nucleophiles under the reaction conditions. Two examples where the reaction was quenched with MeOH and stilbene diol are shown in Table V-1. The products **V-52** and **V-53** were isolated in moderate yields.

**Table V-1.** Exploration of diols and alcohols as nucleophilic traps for rearrangement products



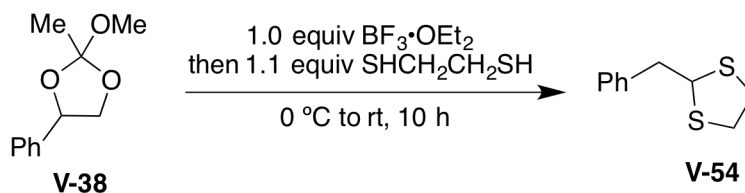
| Entry | Nucleophile             | Product     | Yield |
|-------|-------------------------|-------------|-------|
| 1.    | 1.0 mL MeOH             | <b>V-52</b> | 43%   |
| 2.    | 0.5 equiv stilbene diol | <b>V-53</b> | 59%   |

Note: Yields refer to isolated yields of pure product

A preliminary evaluation of other reaction solvents was undertaken to determine if the yield of the rearrangement reaction could be improved. Compound **V-38** was used as the

orthoester precursor and ethane dithiol was employed as the nucleophile. This data is collected in Table V-2.

**Table V-2.** Identification of optimal solvent for the semi-pinacol rearrangement of **V-38**



| Entry | Solvent                             | GC yield of V-54 |
|-------|-------------------------------------|------------------|
| 1.    | $\text{ClCH}_2\text{CH}_2\text{Cl}$ | 22%              |
| 2     | $\text{MeNO}_2$                     | 56%              |
| 3     | $\text{PhCH}_3$                     | 35%              |
| 4     | $\text{Et}_2\text{O}$               | 37%              |
| 5     | DMSO                                | 0%               |
| 6     | DMF                                 | 3%               |
| 7     | MeCN                                | 25%              |
| 8     | $\text{CHCl}_3$                     | 42%              |
| 9     | $\text{CH}_2\text{Cl}_2$            | 35%              |
| 10    | THF                                 | 31%              |

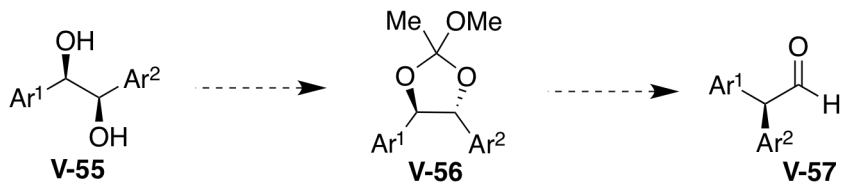
Note: Yields refer to GC yields with 1,4-dichlorobenzene as added external standard

With the exception of DMSO and DMF that returned only trace quantities of the product, all other solvents that were evaluated gave low to moderate yields of the desired product. Amongst the solvents evaluated, MeNO<sub>2</sub> gave the best yield (56% GC yield, 43% isolated yield). Mixed solvent systems were not evaluated.

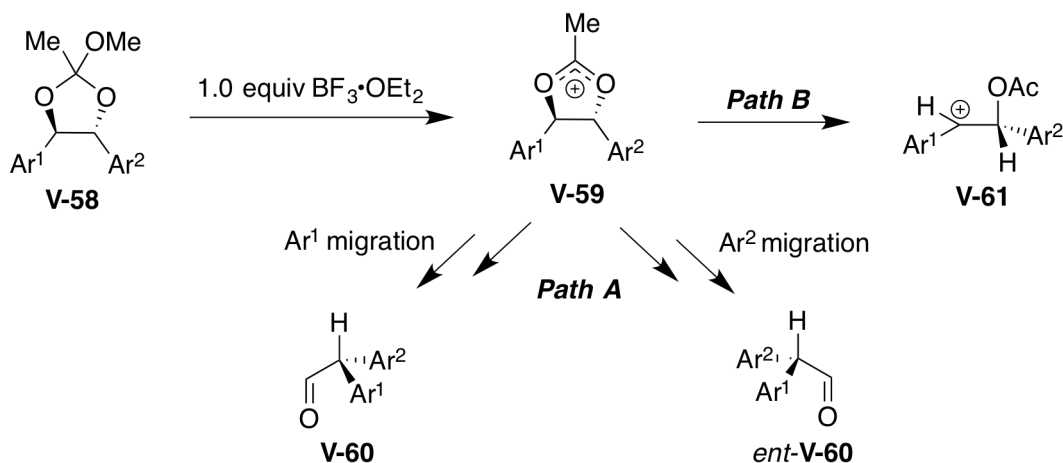
To the best of our knowledge, such rearrangements of cyclic orthoesters have not been documented previously. An analogous rearrangement with epoxides was reported by Mukaiyama and Harada<sup>15</sup> where a catalytic amount of trityl antimonate effects similar 1,2 alkyl and aryl shifts. Several other Lewis acids have been reported since then for this rearrangement of aryl epoxides. Nonetheless, without exception, extensive racemization was observed in these instances and consequently, the stereochemistry of enantioenriched epoxides could not be transferred to the products. It was hoped that the rigid 5-membered ring of the acetoxonium ion should allow for a highly stereoselective 1,2-migration. A potential synthetic application for this rearrangement was identified, namely, the synthesis of  $\alpha,\alpha$ -diaryl chiral aldehydes. The product obtained will be chiral if the two aryl groups in the diol starting compound are different. Furthermore, these chiral diols are easily accessible from the Sharpless asymmetric dihydroxylation (SAD) of the corresponding *trans*-stilbenes. This can provide access to protected chiral  $\alpha,\alpha$ -diaryl aldehydes that are not easy to synthesize using conventional asymmetric catalysis. While Pd catalyzed  $\alpha$ -arylation of aldehydes has been reported by several groups<sup>16</sup> only the intramolecular variant reported by Fortanet and Buchwald is known to give chiral  $\alpha,\alpha$ -diaryl aldehydes (4 examples 68-98% *ee*).<sup>17</sup>

**Figure V-1.** Mechanistic considerations for translation of stereochemistry of vicinal diols to  $\alpha,\alpha$ -diaryl aldehydes

*Accessing chiral  $\alpha,\alpha$ -diarylaldehydes from chiral diols*



*Mechanistic considerations for the semi-pinacol rearrangement*

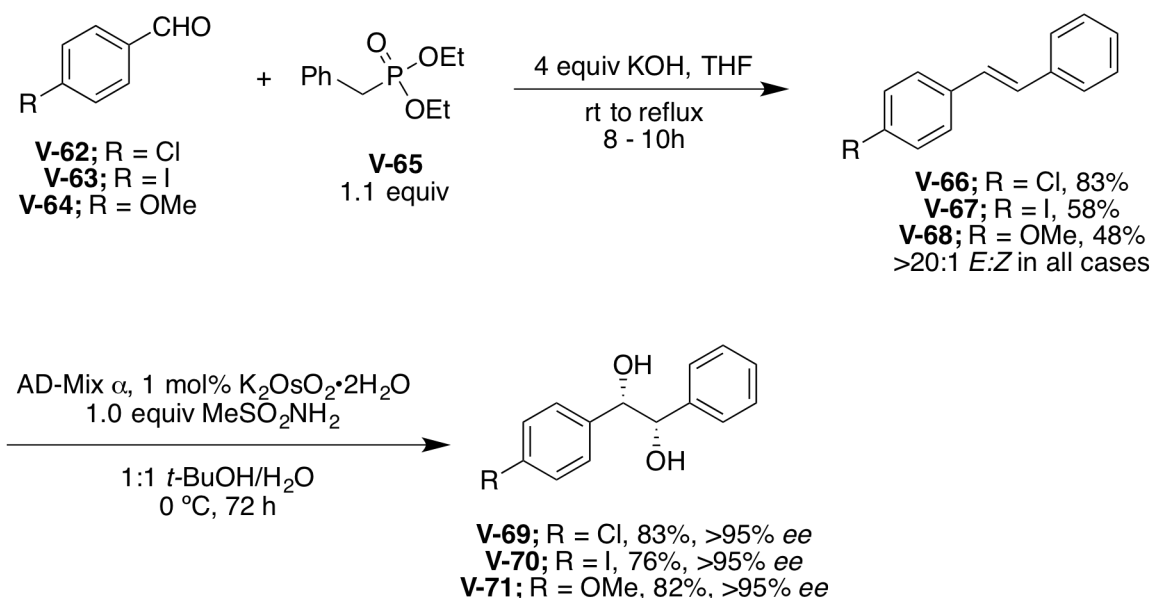


The nature of the 1,2-aryl migration, especially the degree to which the stereochemistry of the diol is eroded during the course of the migration, will dictate if the reaction would be useful in the context of asymmetric synthesis. Furthermore, it is also imperative that the two aryl rings have distinct migrating abilities. If there were no appreciable difference in the migrating group abilities, then extensive racemization would be expected after formation of **V-59** (Path A in Figure V-1; both **V-60** and its enantiomer would be formed in similar quantities). It was hoped that by changing the substituents on the aryl rings, the migrating group ability could be modulated. Another possibility was that this migration might occur in a step-wise manner and might involve a stabilized benzylic carbocation (see **V-61** in Figure V-1) in which case extensive racemization would be expected once again (Path B in Figure V-1). If indeed the products are

formed in high *ee*'s the enantioselectivity will be attributable to the electronic and not the steric impediments of the aryl rings and hence even isosteric aryl rings should, in theory, give enantioenriched products.

In order to deduce which of these mechanisms is in operation, few substituted stilbenes and their corresponding diols were synthesized (Scheme V-11). The stilbenes could be synthesized from the Horner-Wadsworth-Emmons (HWE) reaction of the appropriately substituted aldehyde with the ylide generated from the benzyl phosphonate (Scheme V-11).<sup>18</sup> The Sharpless asymmetric dihydroxylation of the stilbenes furnished the corresponding chiral diols. The racemic diols were also synthesized from the stilbenes by employing the Upjohn dihydroxylation conditions. The rearrangement reactions were simultaneously and under identical conditions run with both, the racemic and chiral diols.

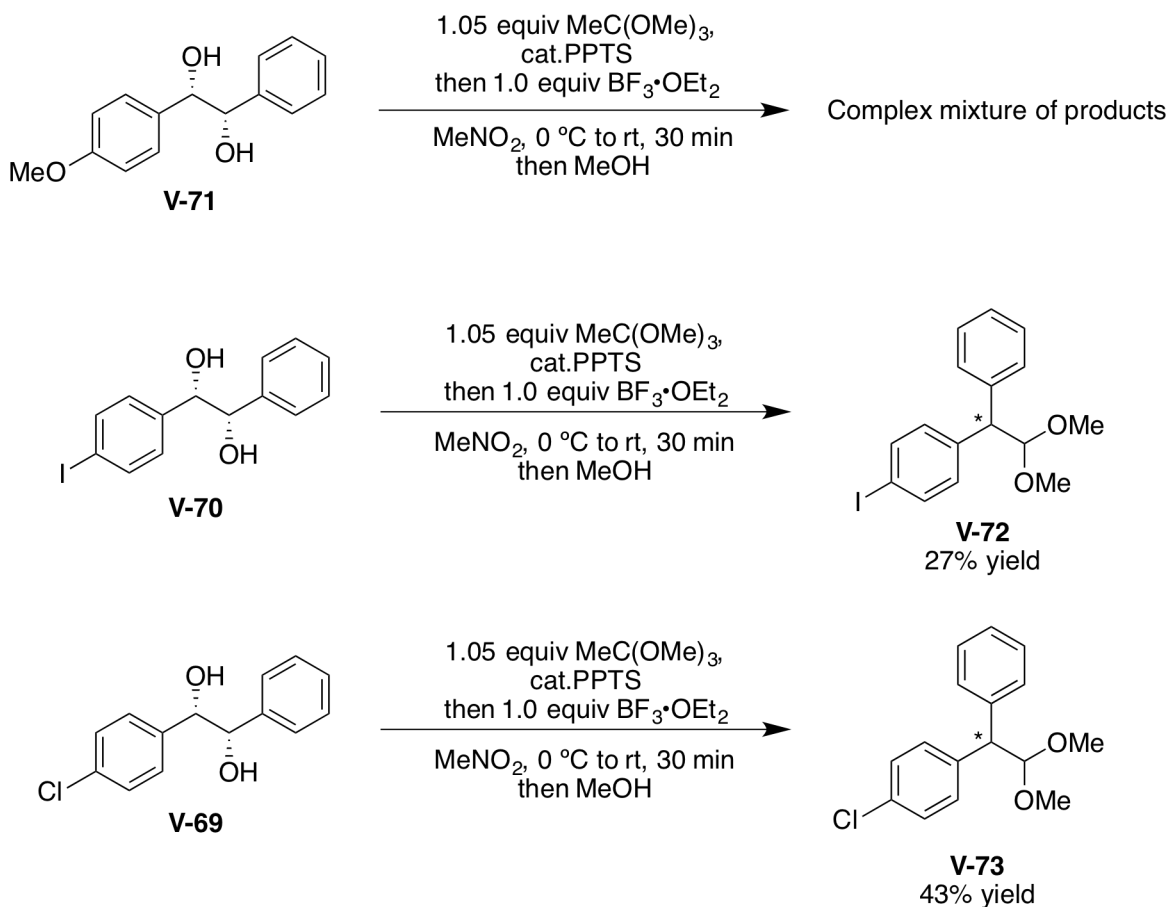
**Scheme V-11.** Synthesis of enantioenriched vicinal diols



When substrate **V-71** was exposed to the rearrangement conditions, a complex mixture of products was obtained. When **V-69** and **V-70** were exposed to the reaction conditions, the

rearranged products were isolated in low yields (see **V-72** and **V-73**). The products were not racemic as evidenced by the optical rotation measurements. Unfortunately conditions to resolve the two enantiomers using a variety of chiral HPLC and GC columns were unsuccessful for both compounds. Chemical derivatization of **V-72** and **V-73** was not pursued.

**Scheme V-12.** Semi-pinacol rearrangements of enantioenriched cyclic acetoxonium ions

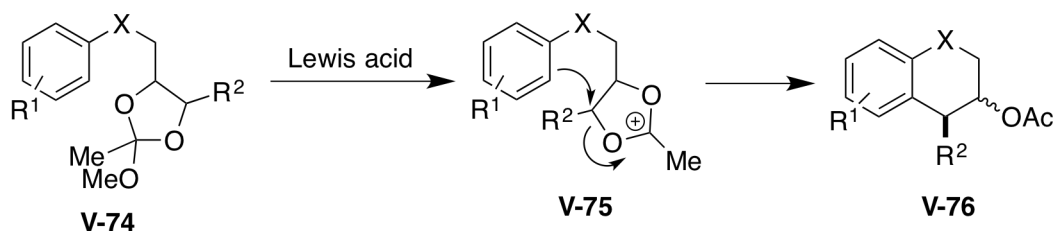


## V.2.2. Attempted arylation of orthoesters: Discovery of a new route to cyclotrimeratrylenes (CTVs).

In our efforts towards stereoselective C–C bond formation using orthoester scaffolds, we became curious about exploring electron rich aromatic rings as potential nucleophiles. While there has been some literature precedence of using this type of chemistry in an intermolecular

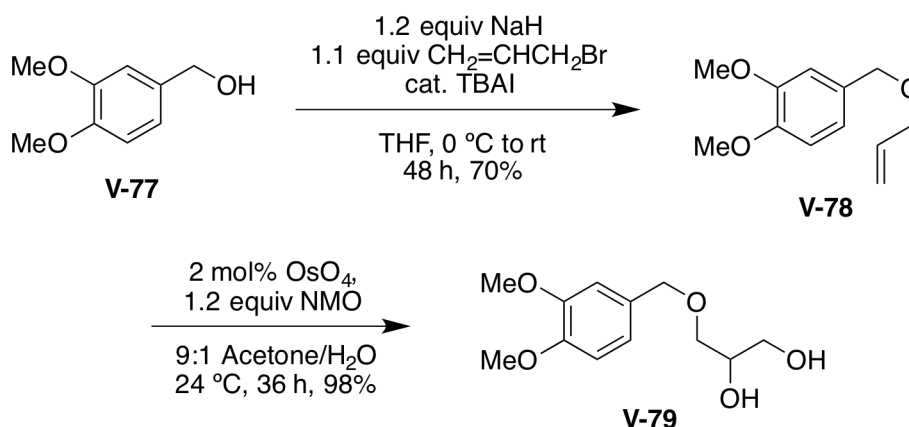
fashion (see **V-10** to **V-13** in Section 5.1.2), the yields and stereoselectivities have been moderate at best. It was envisaged that developing an intramolecular version of this reaction would overcome these problems, besides enabling access to useful heterocyclic scaffolds such as benzopiperidines and benzopyrans. The reaction is formally a Friedel-Crafts alkylation of electron rich arenes (see Scheme V-13).

**Scheme V-13.** Proposed arylation of cyclic acetoxonium ions



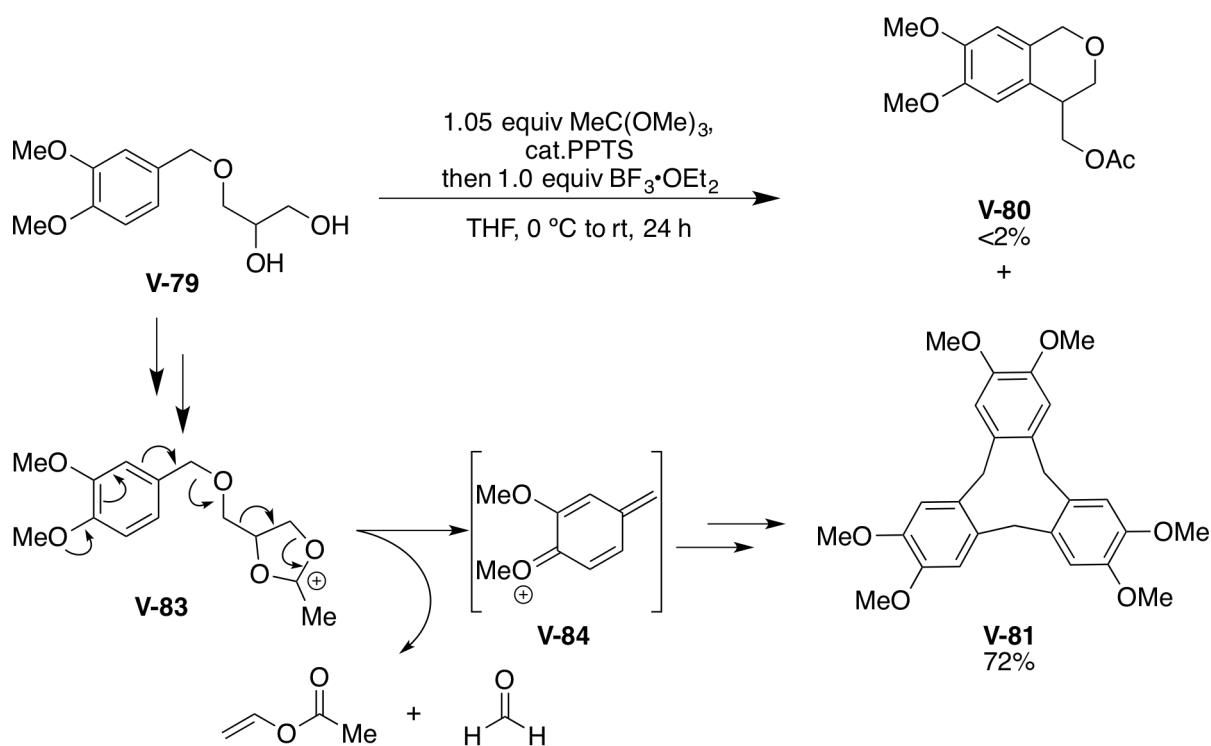
With this idea in mind, compound **V-79** was synthesized from the commercially available 3,4-dimethoxy-benzyl alcohol (**V-77**; veratryl alcohol) in two steps as highlighted in Scheme V-14. The allylation of **V-77** followed by Upjohn dihydroxylation of **V-78** furnished **V-79** in good yield over two steps.

**Scheme V-14.** Synthesis of precursor **V-79** for arylation of acetoxonium ions



However, when **V-79** was converted to the orthoester and then treated with  $\text{BF}_3 \cdot \text{OEt}_2$ , the desired product **V-80** was not formed. Surprisingly, the trimeric product, cyclotrimeratrylene (CTV; **V-81**), was obtained in 72% yield (see Scheme V-15). The identity of this compound was confirmed by NMR, HRMS and single crystal XRD. A plausible mechanism for this transformation has also been proposed in Scheme V-15. Once the acetoxonium ion **V-83** is formed, it can fragment as indicated to give the corresponding *p*-quinone methide **V-84** along with the concomitant loss of vinyl acetate and formaldehyde. The trimerization of **V-84** will give the CTV **V-81**.

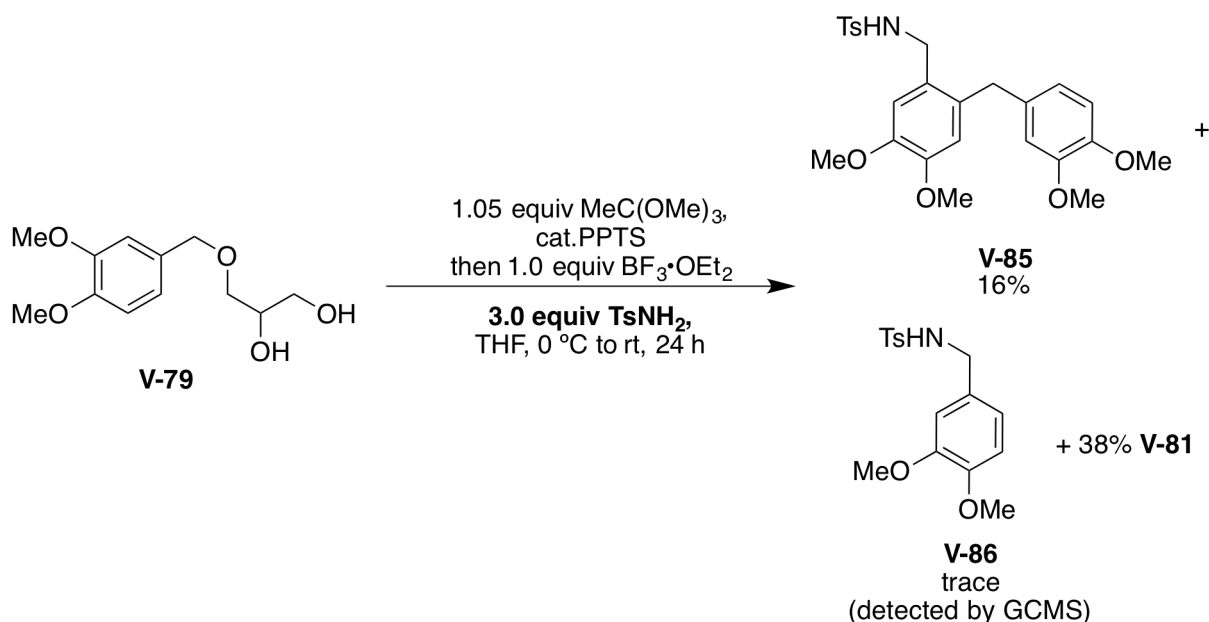
**Scheme V-15.** The unexpected trimerization of **V-79** to **V-81**



The hypothesis that this reaction might involve a *p*-quinone methide **V-84** was experimentally confirmed by running this reaction in the presence of 3 equiv of  $\text{TsNH}_2$  (see Scheme V-16) in the hope of isolating **V-86**. Although the trimerization to **V-81** could not be

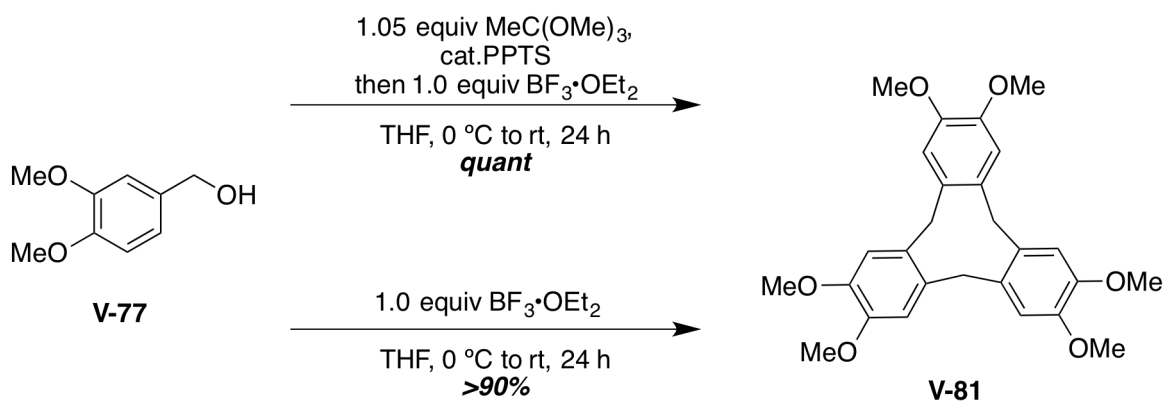
suppressed (38% yield of **V-81**), **V-85** was isolated in 16% yield whereas, **V-86** was detected by GC-MS. There are two ways by which **V-85** could be formed. The putative *p*-quinone methide formed in the 1<sup>st</sup> step can be trapped by the attack of TsNH<sub>2</sub>, resulting in a molecule that is electron rich and can further react with another *p*-quinone methide moiety to give **V-85**. Alternately, the dimerization of the *p*-quinone methide may still be occurring, but the TsNH<sub>2</sub> interrupts the trimerization.

**Scheme V-16.** Attempted nucleophilic interception of putative *p*-quinone methide intermediate

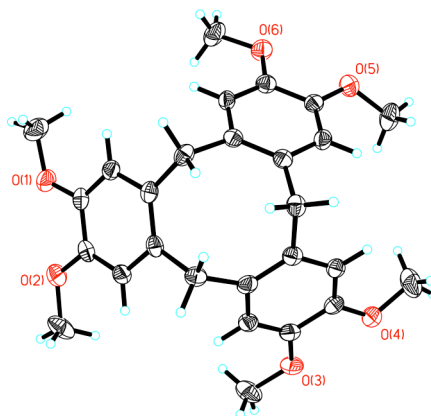


With these results in hand, two more reactions were run (Scheme V-17). Compound **V-77** was subjected to the same conditions as the diol **V-79**. This gave the CTV in quantitative yield indicating that the 3 carbon residue on the benzyl alcohol was not required for this reaction to occur. In the second experiment, **V-77** was treated with BF<sub>3</sub>·OEt<sub>2</sub> alone. This also gave the CTV in >90% yields (average of 2 runs was 92%) indicating the BF<sub>3</sub>·OEt<sub>2</sub> by itself is capable of effecting a dehydrative trimerization of **V-77** to the CTV **V-81**.

**Scheme V-17.**  $\text{BF}_3 \cdot \text{OEt}_2$  mediated dehydrative trimerization of **V-77**



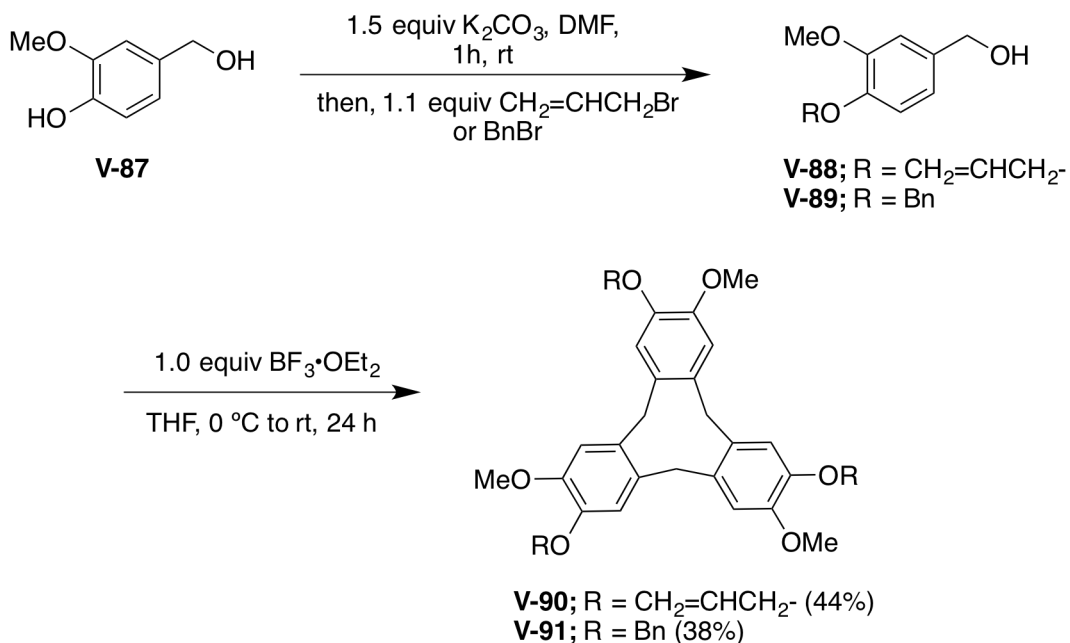
*Crystal structure of V-81*



While the chemistry of dehydrative trimerization of electron rich benzyl alcohols has been fairly well explored over the past several decades, the latter transformation amounts to the most efficient synthesis of this particular CTV (**V-81**). The synthesis of CTVs usually involves treating the appropriate electron rich benzyl alcohol with strong dehydrating agents and Bronsted acids such as  $\text{HClO}_4$ ,<sup>19</sup>  $\text{P}_2\text{O}_5$ ,<sup>20</sup>  $\text{H}_2\text{SO}_4$ <sup>21</sup> and TFA. The use of Lewis acids is also known<sup>22</sup> but not used very commonly. A quick literature survey indicated that these molecules are typically obtained in modest yields (yields typically vary from 35-55%). Furthermore, most

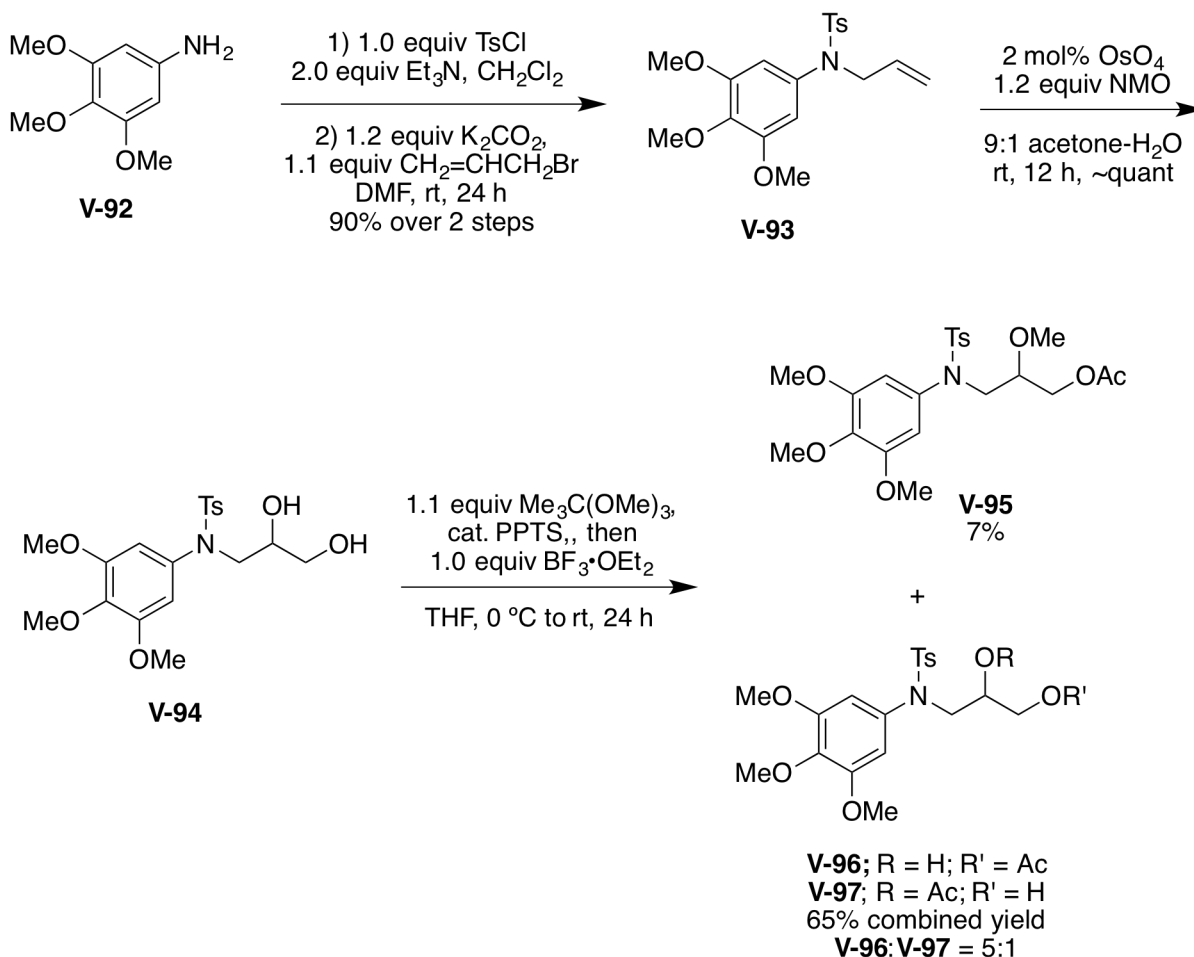
conditions are not applicable to a variety of substrates. CTVs have found useful applications in several areas of research where their rigid bowl shaped conformer of the central 9-member ring has been exploited. They have been used as starting materials in supramolecular chemistry for studying solid inclusion complexes, chiral scaffolds for triple helix formation, self-assembled monolayers on gold surfaces and many other applications. Given the usefulness of these molecules and the lack of a general procedure for accessing many of the CTVs, the plan was to determine the substrate scope for this reaction. Two more substrates were synthesized from the commercially available **V-87** (see Scheme V-18). Allylation and benzylation of 4-hydroxy-3-methoxy benzyl alcohol gave **V-88** and **V-89**, respectively. These substrates were treated with 1.0 equiv of  $\text{BF}_3 \cdot \text{OEt}_2$ . The yields of the corresponding CTVs were 44% and 38%, respectively. These yields are comparable to the best yields obtained for these compounds as reported by Collet and co-workers (50–55%).<sup>23</sup>

**Scheme V-18.** Synthesis and dehydrative trimerization of **V-88** and **V-89**



It was evident from the above results that if the oxygen's lone pair of electrons are 'in conjugation' with the orthoester, the formation of the *p*-quinone methide and its subsequent trimerization is quite facile. In order to circumvent this problem, substrate **V-94** was synthesized as shown in Scheme V-19. The formation of a *p*-quinone methide will not be possible in this case. The diol **V-94** was converted to the corresponding orthoester and then treated with  $\text{BF}_3 \cdot \text{OEt}_2$  *in situ*.

**Scheme V-19.** Synthesis and attempted arylation of orthoester derived from **V-94**



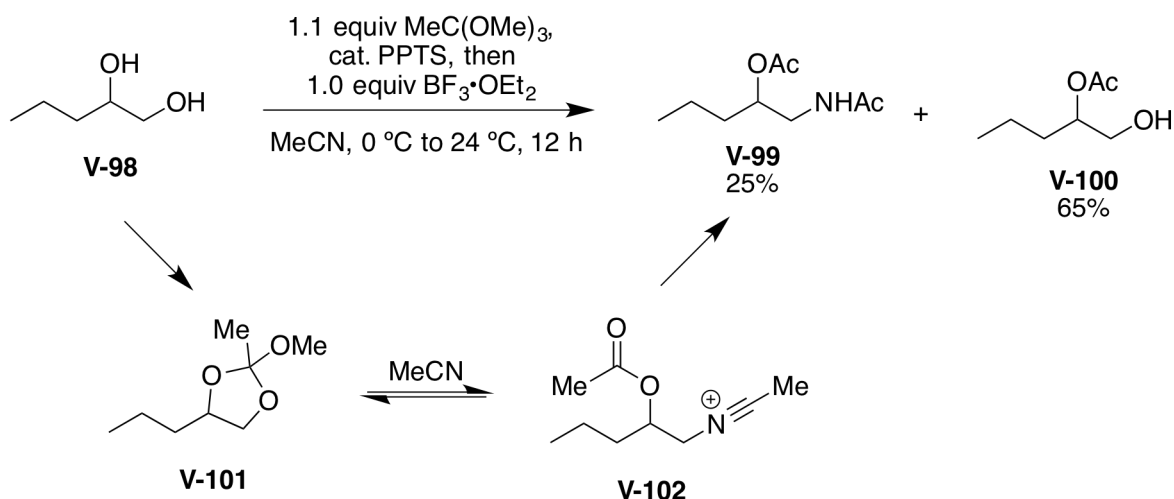
However, this reaction gave the hydrolyzed orthoester (**V-96** and **V-97**) as the major product and some starting material (which was probably derived from the deacetylation of **V-96**

and/or **V-97**, since it could be visualized by TLC only after a period of several hours). A small quantity of **V-95** (7%) was also isolated. This result perhaps hints at the fact that this reaction should be carried out under more forcing conditions.

### V.2.3. Other attempts of C–Heteroatom bond formation reactions on orthoester scaffolds.

Encouraging results were seen in a Ritter-type of reaction. It was postulated that if the acetoxonium ions could be generated in acetonitrile, the solvent should be able to intercept the acetoxonium ion (see structure **V-101** in Scheme V-20), thereby leading to the formation of protected vicinal-amino alcohols. When the orthoester derived from pentane-1,2-diol was exposed to  $\text{BF}_3 \cdot \text{OEt}_2$  in MeCN, the desired ‘Ritter-product’ **V-99** was isolated in appreciable amounts (25% yield) along with significant quantities of the hydrolyzed orthoesters product **V-100**. Disappointingly, this result was not reproducible.

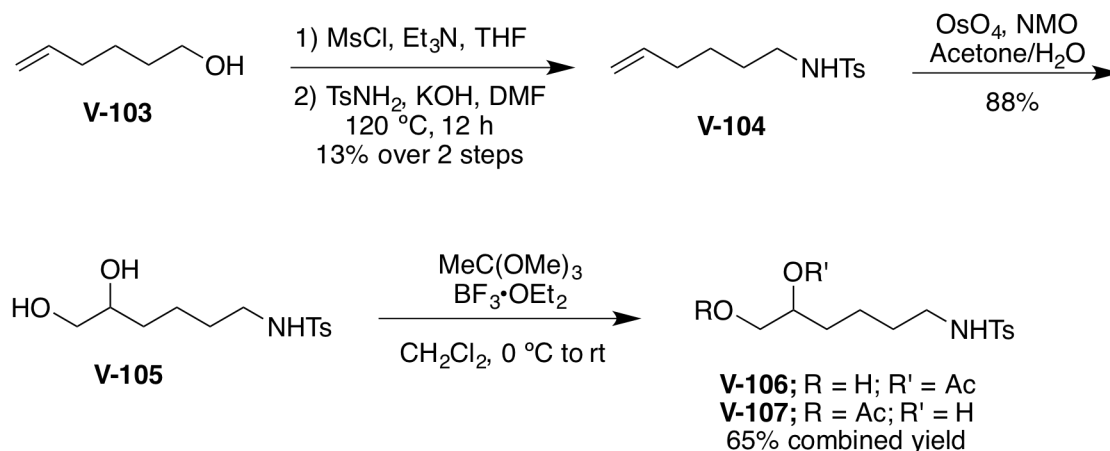
**Scheme V-20.** A Ritter-type reaction of orthoester **V-101**



Several other attempts of C–heteroatom bond formation reactions using orthoester scaffolds were tried but with little or no success. These attempts have been summarized below.

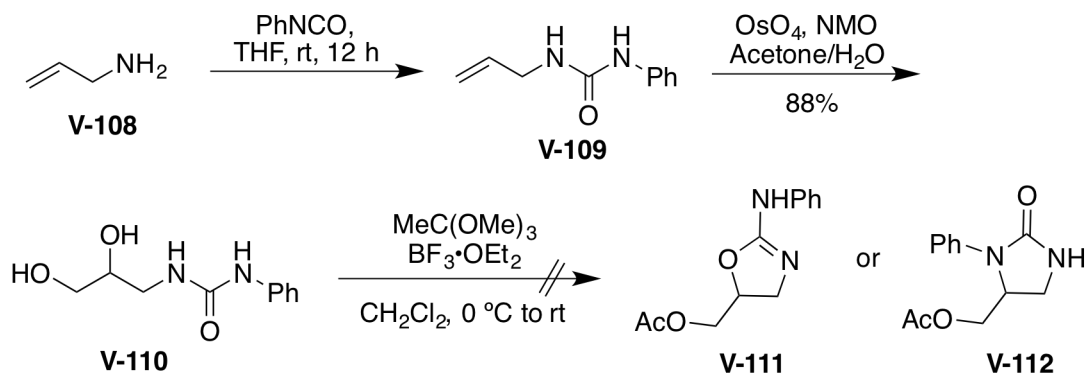
An intramolecular attack of a sulfonamide nucleophile was attempted in an effort to synthesize piperidine heterocycles (see Scheme V-21 for the synthesis of the precursor and attempted cyclization). However, substrate **V-105** gave only the isomeric hydroxy acetates **V-106** and **V-107** arising from the hydrolysis of the orthoester.

**Scheme V-21.** Sulfonamide as an intramolecular nucleophilic trap for acetoxonium ions



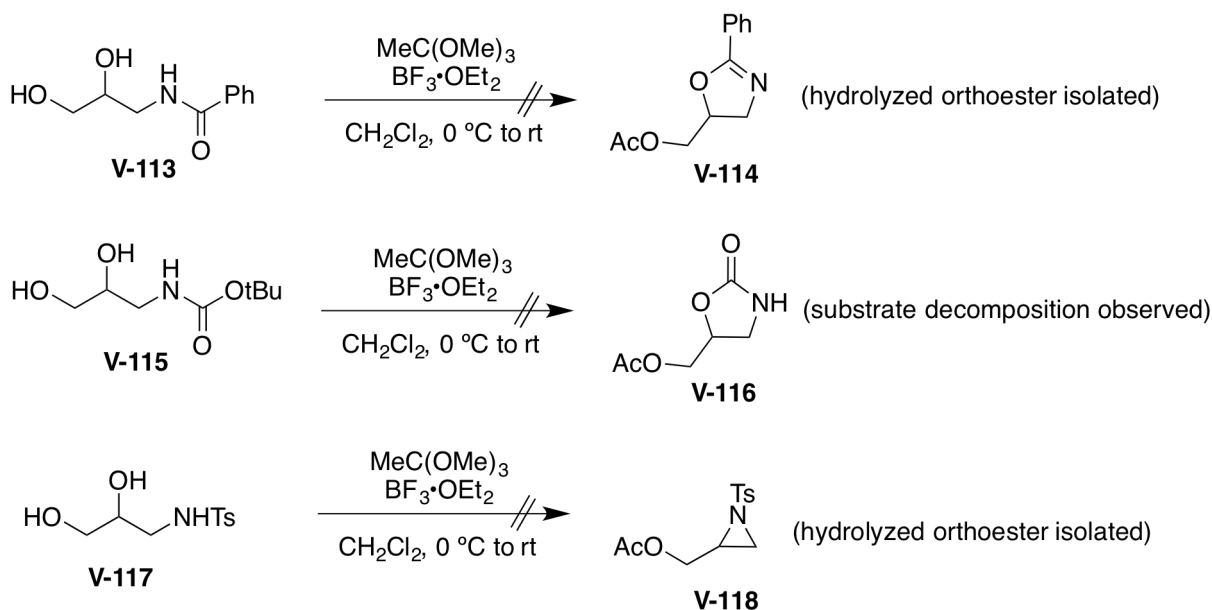
In yet another effort, the compound **V-110** was synthesized from allyl amine in 2 steps as highlighted in Scheme V-22. It was envisioned that the orthoester derived from **V-110** could undergo an intramolecular nucleophilic attack by two plausible ways. If the urea oxygen acted as the nucleophile, then the acetylated oxazole methanol **V-111** would be formed. If the urea nitrogen were to act as the nucleophile then compound **V-112** could be synthesized. Oxazole methanols that resemble **V-111** are found in several pharmaceutically interesting molecules. The synthesis of **V-112** would lead to the formation of vicinal diamines stereoselectively starting from chiral diols. However, neither product was formed when **V-110** was treated with the standard conditions. Extensive decomposition of the substrate was observed.

**Scheme V-22.** Attempted synthesis of oxazoline and imidazolidinone heterocycles from orthoesters



This was followed by the synthesis of substrates **V-113**, **V-115** and **V-117**. It was hoped that these substrates could lead to the synthesis of oxazoline **V-114**, oxazolidinone **V-116** and aziridine **V-118**, respectively. But disappointingly, only substrate decomposition or hydrolysis of the orthoester intermediate was seen in all instances (see Scheme V-23). It merits mention that the results of these single runs do not by any means suggest that such transformations cannot be achieved eventually; nonetheless, transformations analogous to those shown in Scheme V-23 were eventually achieved using the enantioselective alkene halogenation approach. The efforts leading to highly enantioselective variants of such transformations were detailed in Chapters 2, 3 and 4. This alternate strategy was synthetically more appealing since it precluded the need for pre-formed chiral substrates. Consequently, many of these transformations were not pursued any further.

**Scheme V-23.** Investigation of amides, carbamates and sulfonamides as nucleophilic traps for acetoxonium ions



### V.3. Summary and Future work.

Attempts to exploit chiral orthoesters as intermediates in the synthesis of heterocycles were met with little success. While a novel 1,2-aryl shift in cyclic orthoesters has been discovered, its potential applications in synthesis is yet to be proven. Certain aspects of the mechanism of this rearrangement seem to have been elucidated; other aspects such as the stereoselectivity of this migration and the substrate scope are yet to be determined.

During the course of this study,  $\text{BF}_3 \cdot \text{OEt}_2$  in THF was serendipitously discovered as an attractive reagent for the synthesis of cyclotriveratrylenes (CTVs) from the corresponding benzyl alcohols.

Attempted reactions with amides, carbamates, sulfonamides and aryl rings as nucleophiles were all infructuous. Much of this chemistry was eventually abandoned due to

significantly better results obtained for similar transformations using the enantioselective alkene halogenation approach.

#### **V.4. Experimental section.**

##### **V.4.1. General information.**

Methylene chloride was dried over  $\text{CaH}_2$  and freshly distilled prior to use. Nitromethane, acetonitrile and DMSO were dried over  $\text{CaH}_2$  and stored over  $4\text{\AA}$  molecular sieves. Tetrahydrofuran was freshly distilled from Na/benzophenone ketyl. Trimethyl orthoacetate was purchased from Aldrich and was distilled over Na-benzophenone and stored in a rubber septum sealed, flame dried round bottom flask.  $\text{BF}_3 \cdot \text{Et}_2\text{O}$  was treated with a small quantity of ethyl ether, and then distilled under atmospheric pressure and stored over  $4\text{\AA}$  molecular sieves. All the other reagents were used as purchased from commercial sources. NMR spectra were obtained using either a 300 MHz Inova or 500 MHz Varian NMR spectrometer and referenced to residual solvent peaks. Column chromatography was performed using Silicycle (40-60  $\mu\text{m}$ ) silica gel. Pre-coated silica gel 60 F254 plates were used for analytical TLC and visualized using UV light or *p*-anisaldehyde as the stain. GC analyses were performed on an Agilent Technologies 6850 Series II Network GC system. Agilent Tech. J & W Scientific High Resolution Gas Chromatographic Column (HP-1 or DB-5ms) used for GC analysis.

##### **V.4.2. Generation of standard curve used for determination of yield of V-54.**

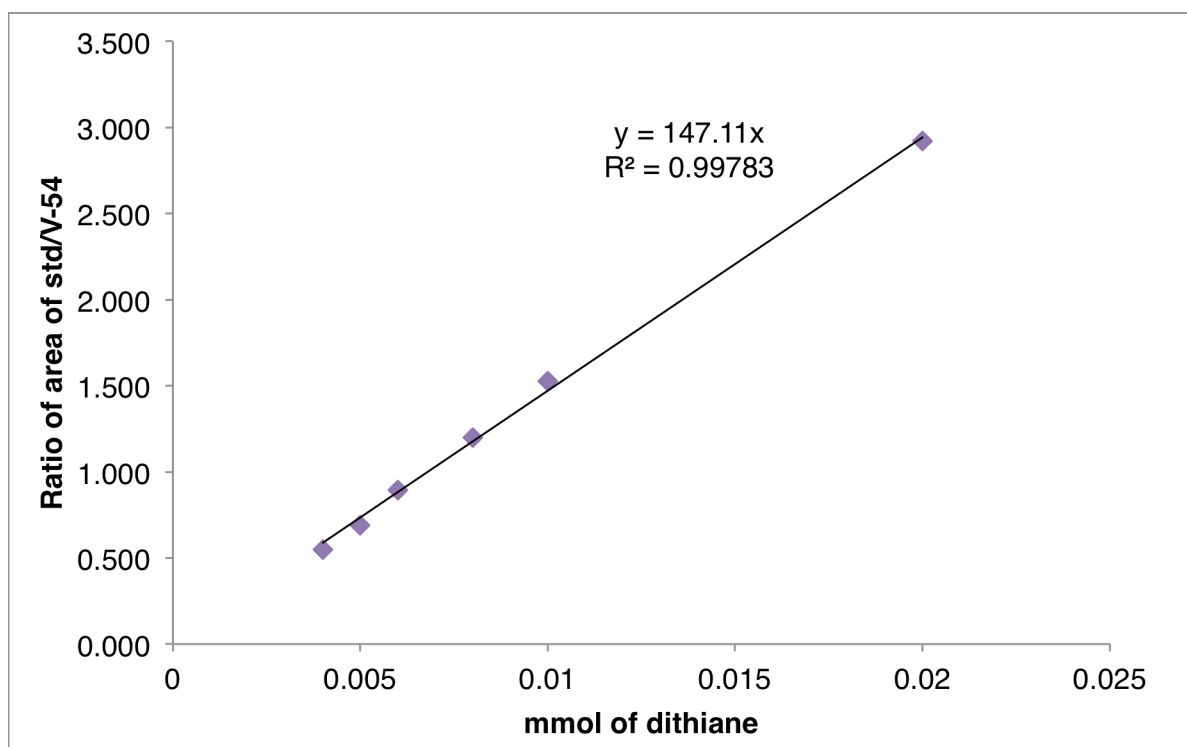
Standard solutions of the dithiane (5 mg/mL in  $\text{MeNO}_2$ ) and *p*-dichlorobenzene (1.0 M solution in  $\text{MeNO}_2$ ) were prepared. The ratio of the peak areas of dithiane and the external standard was obtained for several different mole ratios of the dithiane with respect to the external standard. These ratios were plotted on the Y-axis and the mmol of the dithiane were plotted on the X-axis. The resulting graph was a straight line as shown below. For all reactions analyzed by GC, only

the ratio of the areas of dithiane peak to the external standard peak was obtained. The mmol of dithiane that was formed in the reaction mixture could then conveniently be read off the x-axis.

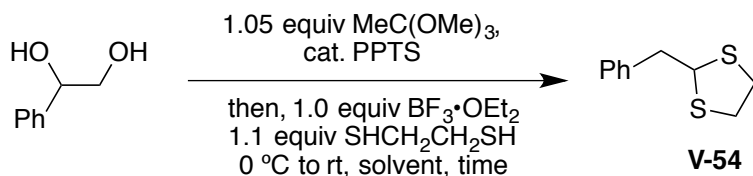
**Table V-3.** Data for standard curve analysis of **V-54**

| Dithiane(Area)<br>(A) | p-dichlorobenzene<br>(Area) (B) | mmol of p-<br>dichlorobenzene | mmol of<br>V-54 | A/B   |
|-----------------------|---------------------------------|-------------------------------|-----------------|-------|
| 35.080                | 64.007                          | 0.01                          | 0.004           | 0.548 |
| 41.008                | 59.620                          | 0.01                          | 0.005           | 0.688 |
| 46.590                | 52.006                          | 0.01                          | 0.006           | 0.896 |
| 53.606                | 44.676                          | 0.01                          | 0.008           | 1.200 |
| 58.131                | 38.060                          | 0.01                          | 0.010           | 1.527 |
| 70.381                | 24.095                          | 0.01                          | 0.020           | 2.921 |

**Figure V-2.** Standard curve for determining GC yields of **V-54**

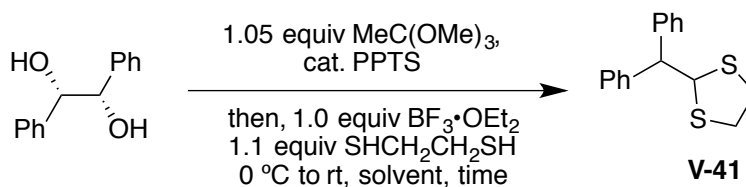


### V.4.3. General protocol for the synthesis of V-54.



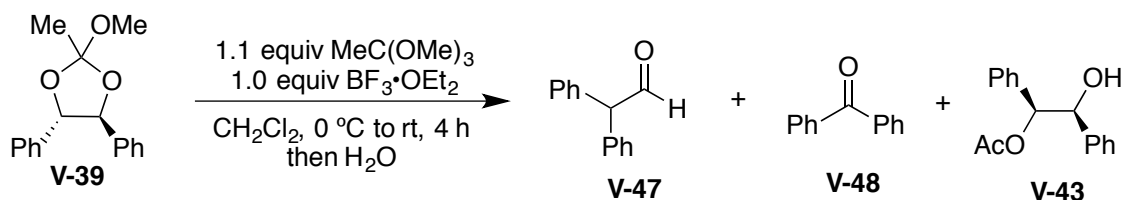
Styrene diol (1.0 equiv) and a catalytic amount of PPTS (3-5 mol%) were taken in a flame dried round bottomed flask equipped with a septum and a magnetic stir bar and dissolved in the solvent (0.04 M in diol concentration). Trimethyl orthoacetate (1.05 equiv) was added in a single portion at ambient temperature *via* a syringe. After orthoester formation was complete (TLC, typically about 30 min), reaction was cooled to 0 °C and BF<sub>3</sub>·OEt<sub>2</sub> (1.0 equiv) was added in a single portion. After stirring for an additional 10 min, the nucleophile (ethane 1,2-dithiol) was added to the reaction mixture in a single portion. The reaction was allowed to warm to ambient temperature and stirred for 4-48 h under N<sub>2</sub> (reaction was monitored by TLC). When reaction was complete, the reaction was quenched with aq. acetone, concentrated *in vacuo* and purified by column chromatography using gradient elution (100% hexane to 5% EtOAc in hexane). In cases where reactions were analyzed by GC, 1 mL of the crude reaction mixture was withdrawn. Conversions were calculated by adding to the 1 mL aliquot a known quantity of a 1.0 M solution of *p*-dichlorobenzene in nitromethane as an external standard and injecting 1-3 μL samples into the GC column. GC yields were interpreted by the standard curve that was obtained as described before. <sup>1</sup>H NMR (500 MHz, CDCl<sub>3</sub>) δ 7.22-7.29 (m, 5H), 4.71 (t, 1H, *J* = 7.2 Hz), 3.13-3.27 (2 x m, 4 H), 3.01 (d, 2 H, *J* = 7.2 Hz). <sup>13</sup>C NMR (75 MHz, CDCl<sub>3</sub>) δ 139.1, 129.1, 128.3, 126.8, 54.9, 45.3, 38.5. Mass (EI): 196.1 (M<sup>+</sup>), 135.2, 105.3, 91.1, 77.3, 61.3, 45.3

#### V.4.4. Characterization of compounds.



**V-41** was prepared using the same protocol that was used for synthesis of **V-54**. In one of the experiments carried out using diol (0.22 mmol, 47 mg), the compound **V-41** was isolated in 40 mg (67%) yield after column chromatography. The product was isolated as a white gum. <sup>1</sup>H NMR (500 MHz, CDCl<sub>3</sub>) δ 7.32-7.33 (m, 2 H), 7.24-7.31 (m, 4 H), 7.19-7.20 (m, 2 H), 5.37 (d, 1H, *J* = 10.5 Hz), 4.16 (d, 1H, 10.5 Hz), 3.15 – 3.24 (m, 4 H). <sup>13</sup>C NMR (125 MHz, CDCl<sub>3</sub>) δ 143.3, 128.5, 127.9, 126.9, 60.4, 58.5, 39.1. Mass (EI): 272.1 (M<sup>+</sup>), 178.2, 165.1, 105.0, 77.1, 61.1, 45.1

#### Attempted Ritter type reaction of orthoesters.



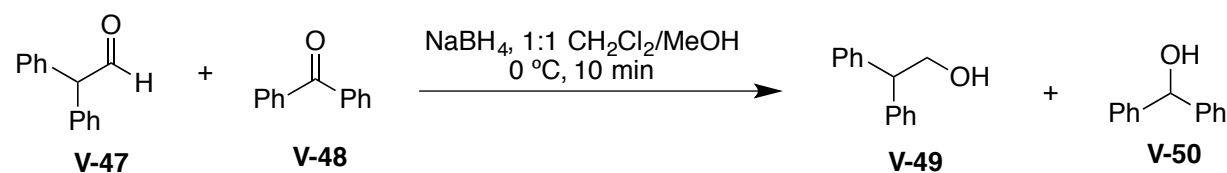
Stilbene diol (50 mg, 0.23 mmol, 1.0 equiv) and a catalytic amount of PPTS were dissolved in 2 mL dry CH<sub>2</sub>Cl<sub>2</sub> and cooled to 0 °C. Me<sub>3</sub>C(OMe)<sub>3</sub> (31 μL, 0.24 mmol, 1.05 equiv) was added in a single portion. After orthoester formation to **V-39** was complete (30 min), BF<sub>3</sub>·OEt<sub>2</sub> (7 μL, 0.05 mmol, 0.2 equiv) was added in a single portion. Reaction was allowed to warm to room temperature and stirred for a further 30 min before quenching with aqueous acetone. After

concentrating the reaction mixture, the crude residue was purified by column chromatography using gradient elution (5% to 10% EtOAc in hexane). The first fraction gave a mixture of **V-47** and **V-48** in 32 mg yield.  $^1\text{H}$  NMR of mixture of **V-47** and **V-48** (500 MHz,  $\text{CDCl}_3$ )  $\delta$  9.94 (d, 1H,  $J = 2.4$  Hz), 7.75 (d, 1H,  $J = 1.0$  Hz), 7.19-7.47 (m, 28H), 4.88 (d, 1.5 H,  $J = 2.4$  Hz). Several other impurities were also seen. GC-MS data: Peak with  $R_t = 17.05$  min 181.9 ( $M^+$  for **V-48**), 104.8, 76.9, 50.9. Peak with  $R_t = 17.73$  min: 195.9 ( $M^+$  for **V-49**), 166.9, 151.9, 114.9, 88.8, 76.9, 62.9

The identity of **V-48** was confirmed by injecting a solution of benzophenone into the GC-MS that had the same retention time ( $R_t = 17.42$  min) and an identical fragmentation as **V-48**.

The hydrolyzed orthoester **V-43** was also isolated in 16 mg (27%) yield as a colorless liquid.  $^1\text{H}$  NMR (500 MHz,  $\text{CDCl}_3$ )  $\delta$  7.20-7.24 (m, 6 H), 7.03-7.10 (m, 4 H), 5.8 (d, 1H,  $J = 7.2$  Hz), 4.9 (d, 1H,  $J = 7.2$  Hz), 2.45 (bs, 1H), 2.11 (s, 3 H)

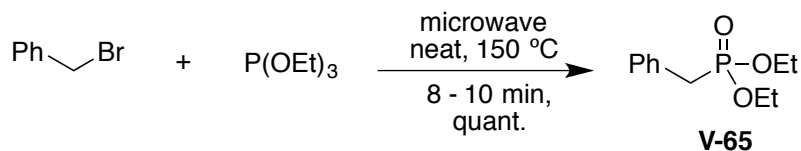
#### Reduction of **V-48** and **V-49**.



To a solution of **V-48** and **V-49** in 1:1  $\text{CH}_2\text{Cl}_2/\text{MeOH}$  (~15 mg in 0.7 mL) was added 10 mg of  $\text{NaBH}_4$  at ambient temperature. After allowing to stand for 5 minutes with intermittent agitation, the reaction mixture was partitioned against water and  $\text{CH}_2\text{Cl}_2$ . Extraction with  $\text{CH}_2\text{Cl}_2$  and analysis of the crude extract by NMR and Mass spectrometry identified the presence of compounds **V-49** and **V-50**.  $^1\text{H}$  NMR of mixture (300 MHz,  $\text{CDCl}_3$ )  $\delta$  6.99 - 7.20 (br m, 19 H),

3.99 (br, s, 1.5 H), 3.93 (t, 2 H,  $J = 5.7$  Hz), 3.1 (s, 0.4 H). GC-MS data: Peak with  $R_t = 15.72$  min : 183.9 ( $M^+$  for **V-49**), 164.9, 151.9, 104.8, 76.9, 50.9. Peak with  $R_t = 17.53$  min: 198.0 ( $M^+$  for **V-50**), 166.9, 151.9, 104.8, 90.9, 76.9, 50.9.

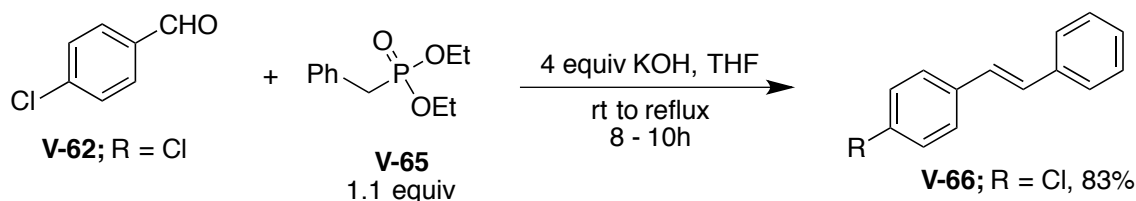
### Synthesis of V-65:



The requisite Horner-Wadsworth-Emmons reagent **V-65** was isolated as colorless oil in a quantitative yield by a microwave assisted Arbuzov reaction of benzyl bromide with triethyl phosphite using the procedure reported by Kiddle.

$^1\text{H}$  NMR (500 MHz,  $\text{CDCl}_3$ )  $\delta$  7.19-7.27 (m, 5 H), 3.91-3.97 (m, 4 H), 3.05 (d, 2 H,  $^2J_{\text{H-P}} = 21.5$  Hz), 1.15-1.18 (overlapping triplets, 6 H).  $^{13}\text{C}$  NMR (125 MHz,  $\text{CDCl}_3$ )  $\delta$  132.0, 129.75, 129.70, 128.48, 128.16, 126.81, 126.78, 62.08, 62.02, 34.30, 33.25 (d,  $J = 12.5$  Hz), 16.34, 16.29.

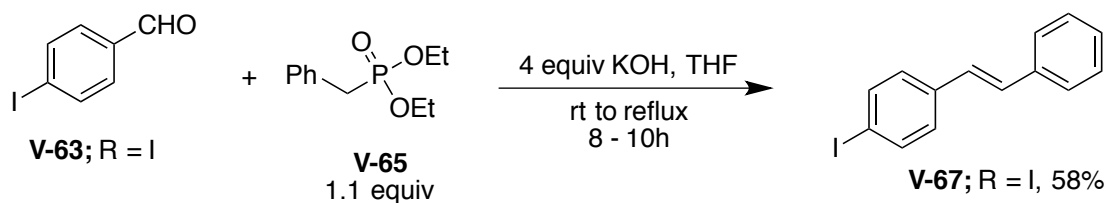
### Synthesis of V-66:



**V-66** was prepared using a modified protocol described by Lawrence and co-workers. While the original protocol uses 2 equiv of KOH in refluxing THF for 3 h, these conditions gave incomplete conversions. Using 4 equiv of KOH and refluxing for 8-10 h gave complete conversions. Products were purified by column chromatography using 5% EtOAc in Hexane as the eluent.

$^1\text{H}$  NMR (500 MHz,  $\text{CDCl}_3$ )  $\delta$  7.49 (d, 2 H, 8.3 Hz), 7.43 (d, 2 H, 8.3 Hz), 7.24-7.42 (m, 5 H), 7.04 (d, 2 H,  $J = 1.8$  Hz).  $^{13}\text{C}$  NMR (125 MHz,  $\text{CDCl}_3$ )  $\delta$  142.7, 135.8, 129.3, 128.8, 128.7, 127.9, 127.6, 127.4, 126.5

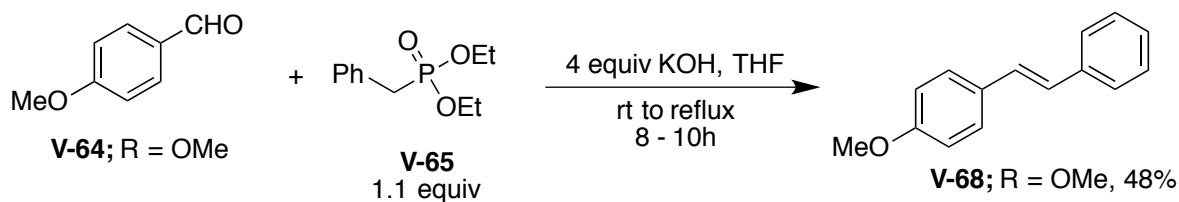
#### Synthesis of V-67:



**V-67** was synthesized using the same protocol used for the synthesis of **V-66**.

$^1\text{H}$  NMR (500 MHz,  $\text{CDCl}_3$ )  $\delta$  7.66 (d, 2 H,  $J = 8.5$  Hz), 7.49 (d, 2 H,  $J = 8.5$  Hz), 7.33-7.36 (m, 2 H), 7.24-7.28 (m, 3 H), 7.07 (d, 1H,  $J = 16.5$  Hz), 6.98 (d, 1H,  $J = 16.5$  Hz).  $^{13}\text{C}$  NMR (125 MHz,  $\text{CDCl}_3$ )  $\delta$  137.7, 129.5, 128.7, 128.2, 127.9, 127.5, 126.6

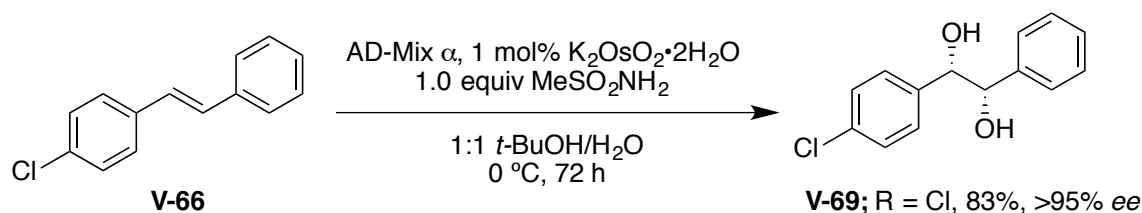
#### Synthesis of 17:



**V-68** was synthesized using the same protocol used for the synthesis of **V-66**.

M.P.: 126-129 °C.  $^1\text{H}$  NMR (500 MHz,  $\text{CDCl}_3$ )  $\delta$  7.4 -7.5 (m, 4 H), 7.33 (m, 2 H), 7.22 (m, 1H), 7.05 (d, 1H,  $J = 16.5$  Hz), 6.96 (d, 1H,  $J = 16.5$  Hz), 6.90 (d, 1H,  $J = 7.5$  Hz), 3.82 (s, 3 H).  $^{13}\text{C}$  NMR (125 MHz,  $\text{CDCl}_3$ )  $\delta$  159.3, 137.7, 130.2, 128.6, 128.2, 127.7, 127.2, 126.6, 126.2, 114.1, 55.3. Mass: 210.2 (Molecular ion), 195.1, 167.1, 152.1, 115.1, 102.1, 89.1, 77.1

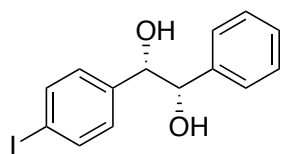
### Synthesis of V-69:



AD-Mix- $\alpha$  (440 mg) was stirred in 1.5 mL of a 1:1 *t*-BuOH-H<sub>2</sub>O solution at room temperature. MeSO<sub>2</sub>NH<sub>2</sub> (28mg, 0.28 mmol, 1.0 equiv) was then added and vigorous stirring was continued till the two phases were clear. 1 mg of K<sub>2</sub>OsO<sub>2</sub>·(2H<sub>2</sub>O) was then added and stirred for a further 10 min. Reaction was then cooled to 0 °C and **V-66** (60 mg, 0.28 mmol, 1.0 equiv) was added to it in a single portion. After stirring at 0 °C for 72 h, reaction was quenched by adding 440 mg of Na<sub>2</sub>SO<sub>3</sub>. After stirring vigorously at 0 °C for a further 10 min, reaction was allowed to warm to ambient temperature and then stirred for a further 30 min. Reaction mixture was extracted repeatedly with 5 mL portions of EtOAc. The combined organic fractions were washed with 3 M aq.KOH (1 x 10 mL), brine (1 x 5 mL), Na<sub>2</sub>SO<sub>4</sub> and concentrated to give the crude product. Purification by column chromatography using gradient elution (5% to 20% EtOAc in hexane) gave the desired product in 83% yield (based on 27% recovered starting material). <sup>1</sup>H NMR (500 MHz, CDCl<sub>3</sub>)  $\delta$  7.21-7.24 (m, 3 H), 7.16 (d, 2 H, *J* = 8.5 Hz), 7.06-7.08 (m, 2 H), 6.99 (d, 2 H, *J* = 8.5 Hz), 4.59 (d, 1H, *J* = 7.5 Hz), 4.53 (d, 1H, *J* = 7.5 Hz), 2.95 (br s, 2 H). <sup>13</sup>C NMR (125 MHz, CDCl<sub>3</sub>)  $\delta$  139.5, 138.3, 133.6, 128.31, 128.25, 128.2, 128.1, 126.9, 79.2, 78.5.

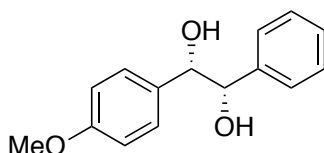
### Synthesis of V-70 and V-71:

Both these compounds were synthesized using the same protocol outlined above for the synthesis of **V-69**.



**V-70**

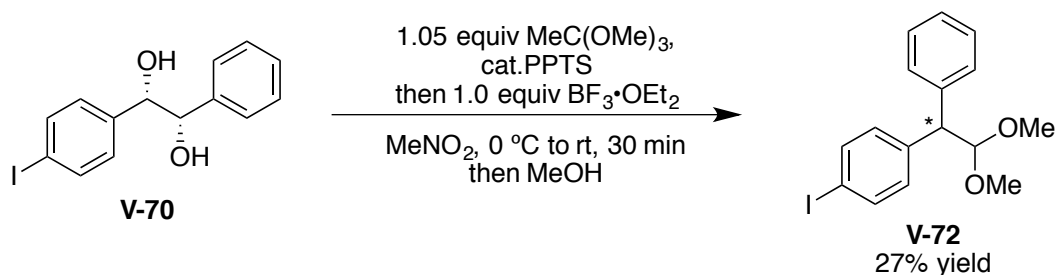
Desired product was isolated in 76% yield (based on 35% recovered starting material)  $^1\text{H}$  NMR (500 MHz,  $\text{CDCl}_3$ )  $\delta$  7.55 (d, 2 H,  $J = 8.5$  Hz), 7.25-7.28 (m, 3 H), 7.11-7.13 (m, 2 H), 6.84 (d, 2 H,  $J = 8.5$  Hz), 4.66 (d, 1 H,  $J = 7.5$  Hz), 4.62 (d, 1 H,  $J = 7.5$  Hz), 3.05 (br s, 1H), 2.89 (br s, 1H).  $^{13}\text{C}$  NMR (125 MHz,  $\text{CDCl}_3$ )  $\delta$  139.49, 139.46, 137.11, 128.87, 128.27, 128.15, 126.93, 93.45, 79.02, 78.52.



**V-71**

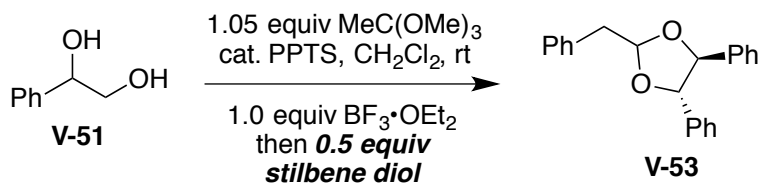
Desired product was isolated in 82% yield.  $^1\text{H}$  NMR (500 MHz,  $\text{CDCl}_3$ )  $\delta$  7.20-7.21 (m, 2 H), 7.08-7.12 (m, 2 H), 7.04 (d, 2 H,  $J = 8.7$  Hz), 6.76 (d, 2 H,  $J = 8.7$  Hz), 4.65 (dd, 2 H,  $J = 1.8$  Hz, 3.6 Hz), 3.74 (s, 3 H), 2.83 (d, 1H,  $J = 2.1$  Hz), 2.77 (d, 1H,  $J = 2.4$  Hz).  $^{13}\text{C}$  NMR (75MHz,  $\text{CDCl}_3$ )  $\delta$  146.9, 139.9, 131.9, 128.1, 127.9, 126.9, 113.5, 79.2, 78.7, 55.1.

**Rearrangement of the orthoester derived from V-70:**



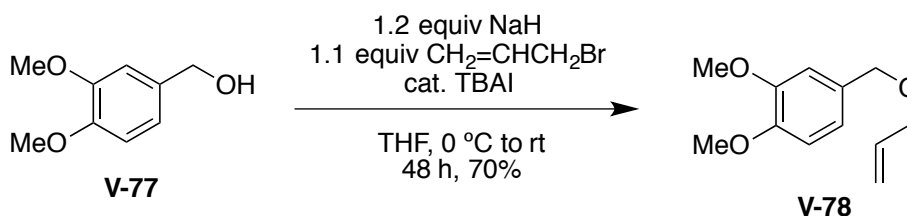
**V-70** (34 mg, 0.10 mmol, 1.0eq) and 2 mg of PPTS were dissolved in 1.4 mL MeNO<sub>2</sub>. MeC(OMe)<sub>3</sub> (15mL, 0.12 mmol, 1.2eq) was added at ambient temperature and the reaction was stirred till orthoester formation was complete (15 min). The reaction was then cooled in an ice bath and BF<sub>3</sub>·OEt<sub>2</sub> (13 μL, 0.10 mmol, 1.0 equiv) was added in a single portion. After stirring for a further 5 min at 0 °C, reaction was allowed to warm to ambient temperature. It was diluted with 1 mL MeOH and stirred for a further 30 min. After evaporating the volatiles, the crude residue was purified by column chromatography using 5% EtOAc in hexane as the eluent to give 27% yield of the desired product **V-72** as colorless oil. <sup>1</sup>H NMR (300 MHz, CDCl<sub>3</sub>) δ 7.56 (d, 2 H, *J* = 8.0 Hz), 7.22-7.29 (m, 7H), 7.17-7.20 (m, 1H), 7.02 (d, 2 H, *J* = 8.0 Hz), 4.88 (d, 1H, *J* = 7.5 Hz), 4.14 (d, 1H, 7.5 Hz), 3.29 (s, 3 H), 3.28 (s, 3 H). <sup>13</sup>C NMR (125 MHz, CDCl<sub>3</sub>) δ 140.8, 140.5, 137.4, 130.9, 128.7, 128.5, 126.7, 106.3, 54.3, 54.2, 54.1. Optical Rotation : [α]<sub>D</sub><sup>20</sup> = +10.6 ° (c 0.36, CHCl<sub>3</sub>)

#### Synthesis of V-53:



Styrene diol (60mg, 0.44 mmol, 1.0eq) and 2mg of PPTS were dissolved in 10mL DCM. MeC(OMe)<sub>3</sub> (58  $\mu$ L, 0.45 mmol, 1.05equiv) was added at ambient temperature and the reaction was stirred till orthoester formation was complete (30 min). BF<sub>3</sub>·OEt<sub>2</sub> (54  $\mu$ L, 0.43 mmol, 1.0eq) was then added in a single portion at ambient temperature. After stirring for a further 30 min stilbene diol (49 mg, 0.23 mmol, 0.50 equiv) was introduced into the reaction vessel. After stirring at ambient temperature for 1h, reaction was heated at reflux for a further 48 h. After quenching with aq. acetone, the volatiles were evaporated and the crude residue was purified by column chromatography using 5% EtOAc in hexane as the eluent to give 23 mg of the desired product as slightly colored oil. (Yield was 59% with respect to stilbene diol). <sup>1</sup>H NMR (300 MHz, CDCl<sub>3</sub>)  $\delta$  7.01-7.36 (m, 15 H), 5.67 (t, 1H, *J* = 4.2 Hz), 4.65 (d, 1H, *J* = 7.8 Hz), 4.52 (d, 1H, *J* = 7.8 Hz), 3.16 (dd, 2 H, *J* = 4.2 Hz, 1.5 Hz). <sup>13</sup>C NMR (125 MHz, CDCl<sub>3</sub>)  $\delta$  138.2, 136.8, 136.6, 135.8, 130.2, 128.47, 128.45, 128.4, 128.24, 128.23, 128.1, 126.8, 126.7, 126.5, 126.4, 109.7, 109.4, 105.4, 86.8, 85.4, 85.0, 41.3.

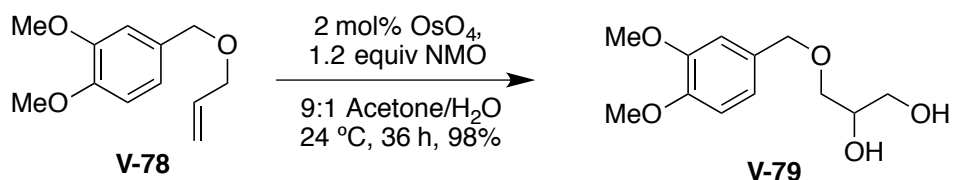
#### Synthesis of V-78:



To a stirred solution of 3,4-dimethoxy benzyl alcohol (**V-77**, 300 mg, 1.78 mmol, 1.0 equiv) in 10 mL THF was added NaH (78 mg of a 60% dispersion in mineral oil, 1.96 mmol, 1.1equiv) portion wise at 0 °C. After stirring for 30 min., allyl bromide (166  $\mu$ L, 1.96 mmol, 1.1 equiv) was added to the reaction mixture drop wise over a period of 5 min. followed by the addition of tetra-*n*-butyl ammonium iodide (74 mg, 0.36 mmol, 0.2 equiv) in a single portion. The reaction was allowed to

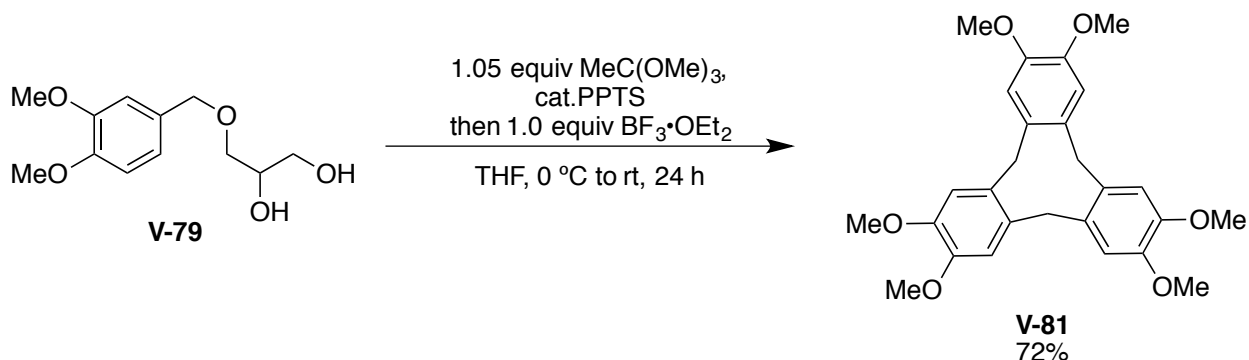
warm to ambient temperature and stirred for a further 48 h. It was quenched with saturated aq.  $\text{NH}_4\text{Cl}$  solution (10 mL). After separating the aqueous and organic phases, the aqueous fraction was extracted with EtOAc (3 x 10 mL). The combined organic fractions were washed with brine (1 x 5 mL), dried over anhydrous  $\text{Na}_2\text{SO}_4$  and concentrated to give the crude product. That was used in the next step without purification.  $^1\text{H}$  NMR (300 MHz,  $\text{CDCl}_3$ )  $\delta$  6.82-6.89 (overlapping multiplets, 3 H), 5.95 (m, 1H), 5.30(m, 2 H), 4.01 (m, 2 H), 3.87 (s, 3 H), 3.86 (s, 3 H).

### Synthesis of V-79:

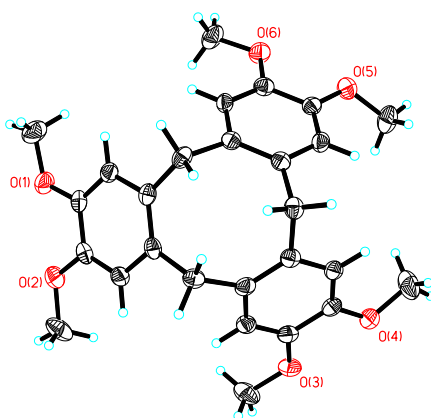


Olefin **V-78** (50 mg, 0.24 mmol, 1.0equiv) was dissolved in 5 mL of a 9:1 mixture of acetone- $\text{H}_2\text{O}$ . After stirring at ambient temperature for 5 min, NMO (34 mg, 0.29 mmol, 1.2 equiv) and  $\text{OsO}_4$  (15  $\mu\text{L}$  of 0.2 M solution in toluene, 0.003 mmol, 0.01 equiv) were sequentially added and the reaction was stirred for 36 h. It was quenched with saturated  $\text{Na}_2\text{SO}_3$  solution (5 mL) and extracted several times with portions of ethyl acetate. The combined organics were washed with brine, dried over anhydrous  $\text{Na}_2\text{SO}_4$  and concentrated *in vacuo* to give the crude product which was purified by column chromatography using gradient elution (1:1 EtOAc-Hexane to 100% EtOAc) to afford the desired product in quantitative yield as a light brown oil.  $^1\text{H}$  NMR (300 MHz,  $\text{CDCl}_3$ )  $\delta$  6.81-6.84 (m, 3H), 4.47 (s, 2H), 3.87 (s, 3 H), 3.86 (s, 3 H), 3.70 (dd, 1H,  $J$  = 4.0 Hz, 11.5 Hz), 3.62 (dd, 2 H,  $J$  = 5.5 Hz, 11.5 Hz), 3.52 (m, 3 H).  $^{13}\text{C}$  NMR (125 MHz,  $\text{CDCl}_3$ )  $\delta$  120.7, 111.4, 111.3, 73.80, 71.84, 70.78, 64.4, 55.2, 56.1

### Trimerization of V-79 to V-81:



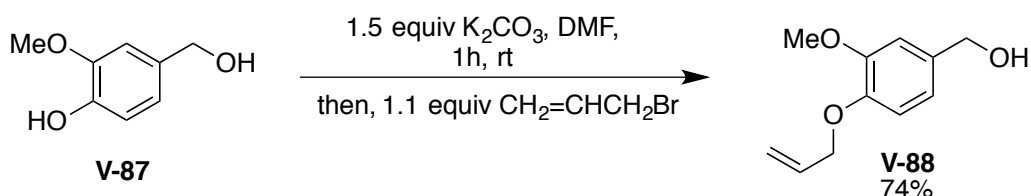
### Crystal structure of V-81



Diol **V-79** (20 mg, 0.08 mmol, 1.0 equiv) and a catalytic amount of PPTS were taken in a 3 mL capacity vial and stoppered with a rubber septum. After flushing with Ar, 1 mL THF was introduced and the resulting suspension was stirred for 5min at ambient temperature. MeC(OMe)<sub>3</sub> (10  $\mu$ L, 0.08 mmol, 1.05 equiv) was then added at ambient temperature and stirring continued for another 15 min by which time the diol was converted to the orthoester (TLC). After cooling in an ice bath, BF<sub>3</sub>·OEt<sub>2</sub> (10  $\mu$ L, 0.08 mmol, 1.0 equiv) was added to the reaction vessel in a single portion. Reaction was then allowed to warm to ambient temperature gradually. After stirring for 24 h, the reaction was concentrated *in vacuo* and the crude residue was adsorbed on

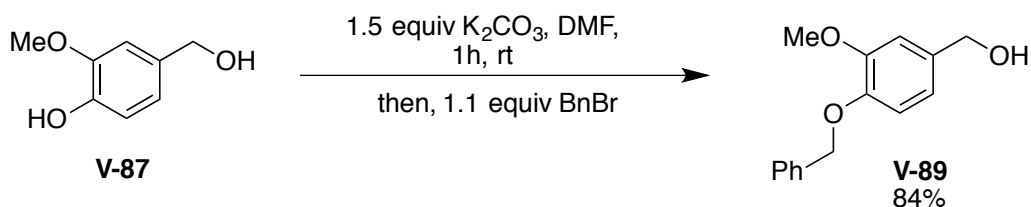
basified silica gel. It was purified by column chromatography using EtOAc-Hexane (15% to 50% EtOAc in hexane) as the eluent to afford 8 mg (72%) of the trimerized product as a white solid. M.P.: 225-227 °C (Lit. 232 °C)  $^1\text{H}$  NMR (300 MHz,  $\text{CDCl}_3$ )  $\delta$  6.81 (s, 6 H), 4.75 (d, 3 H,  $J = 13.8$  Hz), 3.82 (s, 18H), 3.54 (d, 3 H,  $J = 13.9$  Hz).  $^{13}\text{C}$  NMR (125 MHz,  $\text{CDCl}_3$ )  $\delta$  147.67, 131.73, 113.04, 55.99, 36.49. HRMS (ESI): Calcd for  $\text{C}_{27}\text{H}_{30}\text{O}_6\text{Na}$  : 473.1940; Found : 473.1945

### Synthesis of 88:



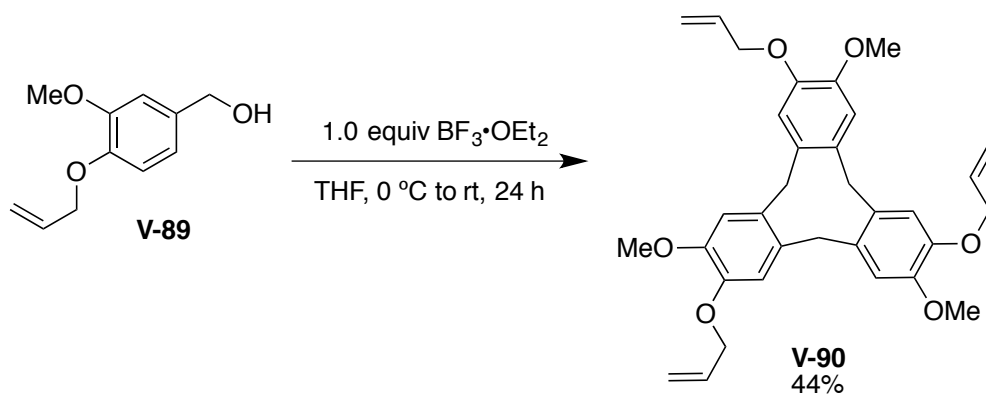
3-methoxy-4-hydroxybenzyl alcohol (154 mg, 1.0 mmol, 1.0 equiv.) was dissolved in 5 mL DMF and  $\text{K}_2\text{CO}_3$  (166 mg, 1.2 mmol, 1.2 equiv) was added in a single portion under  $\text{N}_2$ . After stirring for 1 h at ambient temperature, allyl bromide (101  $\mu\text{L}$ , 1.2 mmol, 1.2 equiv) was added drop wise. The reaction was stirred overnight and then diluted with water (10 mL). RM was extracted with EtOAc (3 x 10 mL). The combined organics were washed with brine (2 x 10 mL), dried ( $\text{Na}_2\text{SO}_4$ ) and concentrated *in vacuo* to give the crude product which was purified by column chromatography using 30% EtOAc in hexane as the eluent to give 74% of the pure product as thick viscous oil that solidified under high vacuum. M.P.: 67- 68 °C.  $^1\text{H}$  NMR (500 MHz,  $\text{CDCl}_3$ )  $\delta$  6.92 (d, 1H,  $J = 8.3$  Hz), 6.83 (m, 2 H), 6.05 (m, 1H), 5.39 (dd, 1H,  $J = 1.5$  Hz, 17.5 Hz), 5.36 (dd, 1H,  $J = 1.5$  Hz, 10.3 Hz), 4.59-4.61 (m, 4 H), 3.87 (s, 3 H), 1.57 (t, 1H,  $J = 5.5$  Hz).  $^{13}\text{C}$  NMR (125 MHz,  $\text{CDCl}_3$ )  $\delta$  133.94, 133.29, 119.29, 117.97, 113.35, 110.83, 69.94, 65.35, 55.89

### Synthesis of V-89:



Procedure for the synthesis was same as that for **V-88**. Desired product **V-89** was isolated as a white solid in 84% yield after column chromatography. MP: 68-70 °C. <sup>1</sup>H NMR (500 MHz, CDCl<sub>3</sub>) δ 7.42 (d, 2 H, *J* = 10.0 Hz), 7.35 (m, 2 H), 7.29 (d, 1H, *J* = 7.0 Hz), 6.93 (d, 1H, *J* = 2.0 Hz), 6.79-6.84 (m, 2 H), 5.14 (s, 2 H), 4.60 (d, 2 H, *J* = 6.0 Hz), 3.86 (s, 3 H), 1.58 (t, 1H, *J* = 5.5 Hz). <sup>13</sup>C NMR (125 MHz, CDCl<sub>3</sub>) δ 165.57, 137.14, 128.53, 127.8, 127.22, 119.33, 114.04, 110.99, 71.10, 65.33, 55.97.

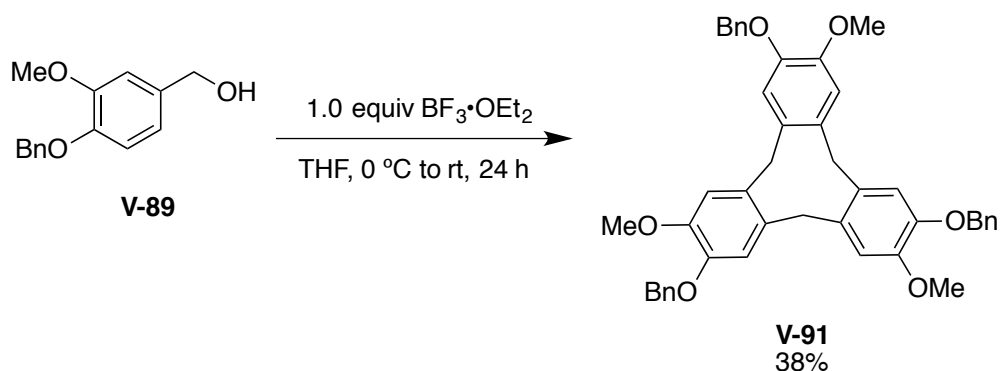
### Trimerization of V-88 to V-90:



**V-89** (58 mg, 0.30 mmol, 1.0 equiv) was dissolved in 3 mL THF and flushed with Ar. BF<sub>3</sub>·OEt<sub>2</sub> (38 mL, 0.30 mmol, 1.0 equiv) was added to it in a single portion. After allowing the reaction to stir at ambient temperature for 15 h, it was concentrated and the crude residue was purified by column chromatography (20% to 30% EtOAc in Hexane gradient) to give the desired product as

a white solid in 44% yield. M.P. 169-173 °C (Lit. 175 °C).  $^1\text{H}$  NMR (500 MHz,  $\text{CDCl}_3$ )  $\delta$  6.83 (s, 3 H), 6.77 (s, 3 H), 6.03 (m, 3 H), 5.37 (d, 3 H,  $J = 11.8$  Hz), 5.23 (d, 3 H, 12.0 Hz), 4.73 (d, 3 H,  $J = 14.0$  Hz), 4.57 (m, 6 H), 3.81 (s, 9H), 3.50 (d, 3 H,  $J = 14.0$  Hz).  $^{13}\text{C}$  NMR (125 MHz,  $\text{CDCl}_3$ )  $\delta$  148.24, 146.78, 133.76, 132.35, 131.76, 117.47, 115.64, 113.67, 70.22, 56.12, 36.52. HRMS (ESI): calculated for  $[\text{M}+\text{H}]$  529.2590, Found : 529.2588

#### Trimerization of V-89 to V-91:



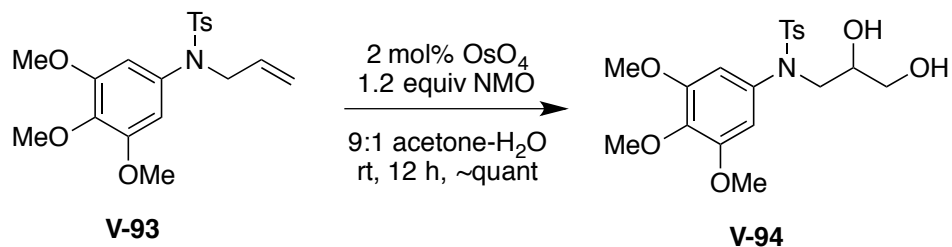
Procedure and scale of the reaction were identical to that of trimerization of **V-89**. Product was isolated as a slightly yellow solid in 39% yield. M.P.: 141-144 °C (Lit. 149 °C).  $^1\text{H}$  NMR (500 MHz,  $\text{CDCl}_3$ )  $\delta$  7.25-7.39 (m, 21 H), 6.81 (s, 3 H), 6.64 (s, 3 H), 5.09 (m, 6 H), 4.68 (d, 3 H,  $J = 14.0$  Hz), 3.68 (s, 9H), 3.42 (d, 3 H,  $J = 14.0$  Hz).  $^{13}\text{C}$  NMR (125 MHz,  $\text{CDCl}_3$ )  $\delta$  148.67, 147.41, 137.81, 132.78, 131.94, 128.80, 128.66, 128.02, 127.58, 127.18, 116.31, 71.81, 56.50, 36.74. HRMS (ESI): calculated for  $[\text{M}+\text{Na}]$  : 701.2879; Found : 701.2870

#### Synthesis of V-93:



3,4,5-trimethoxyaniline (200 mg, 1.09 mmol, 1.0 equiv), TsCl (208 mg, 1.09 mmol, 1.0 equiv) and DMAP (3 mg) were dissolved in 5 mL DCM. To it was added Et<sub>3</sub>N (450  $\mu$ L, 3.27 mmol, 3.0 equiv) drop wise at ambient temperature. After stirring overnight under Ar, the reaction was diluted with an equal amount of water and extracted with portions of EtOAc (3 x 10mL). The organic fractions were combined, washed with brine (1 x 10mL), dried over anhydrous Na<sub>2</sub>SO<sub>4</sub> and concentrated to afford the crude tosylated aniline that was subjected to the next step without purification. The crude product was dissolved in 5 mL dry DMF and K<sub>2</sub>CO<sub>3</sub> (151 mg, 1.09 mmol, 1.0 equiv) was added to it and stirred at ambient temperature for 1 h. Allyl bromide (92 mL, 1.09 mmol, 1.0 equiv) was introduced into the reaction vessel and the reaction was stirred overnight at ambient temperature. The reaction was then diluted with an equal amount of water and extracted with portions of ether (3 x 10mL). The organic fractions were combined, washed with brine (1 x 10 mL), dried over anhydrous Na<sub>2</sub>SO<sub>4</sub> and concentrated to afford the crude product which was purified by column chromatography using EtOAc-Hexane gradient to give the desired product (contaminated with a small quantity of TsCl) in ~ 90% yield over 2 steps. <sup>1</sup>H NMR (300 MHz, CDCl<sub>3</sub>)  $\delta$  7.50 (d, 2 H, *J* = 8.4 Hz), 7.21 (d, 2 H, *J* = 8.4 Hz), 6.17 (s, 2 H), 5.70 (m, 1H), 5.02 (m, 2 H), 4.07 (d, 2 H, *J* = 6.0 Hz), 3.78 (s, 3 H), 3.65 (s, 6 H), 2.37 (s, 3 H). <sup>13</sup>C NMR (125 MHz, CDCl<sub>3</sub>)  $\delta$  152.8, 143.5, 137.5, 135.2, 134.6, 132.7, 129.4, 129.2, 128.5, 127.8, 118.7, 106.3, 60.7, 55.9, 53.8, 21.4

### Synthesis of V-94:



**V-94** was synthesized by the Upjohn dihydroxylation of **V-93** using the same protocol as described for the synthesis of **V-79**. It was isolated by column chromatography of the crude product using 30% EtOAc-Hexane as the eluent as a white solid in >99% yield. M.P: 155-157 °C.  $^1\text{H NMR}$  (300 MHz,  $\text{CDCl}_3$ )  $\delta$  7.51 (d, 2 H,  $J = 8.4$  Hz), 7.26 (d, 2 H,  $J = 8.4$  Hz), 6.21 (s, 2 H), 3.82 (s, 3 H), 3.59-7.75 (m, 11 H), 2.6 (d, 1H, *exch.*,  $J = 4.5$  Hz), 2.42 (s, 3 H), 2.19 (t, 1H, *exch.*,  $J = 4.8$  Hz).

## REFERENCES

## REFERENCES

- (1) Pindur, U. In *Acid Derivatives (1992)*; John Wiley & Sons, Inc.: 2010, p 967.
- (2) Pindur, U.; Muller, J.; Flo, C.; Witzel, H. *Chem. Soc. Rev.* **1987**, *16*, 75.
- (3) Brånalt, J.; Kvarnström, I.; Classon, B. R.; Samuelsson, B. *J. Org. Chem.* **1996**, *61*, 3599.
- (4) Kolb, H. C.; Sharpless, K. B. *Tetrahedron* **1992**, *48*, 10515.
- (5) Kolb, H. C.; VanNieuwenhze, M. S.; Sharpless, K. B. *Chem. Rev.* **1994**, *94*, 2483.
- (6) Bozell, J. J.; Miller, D.; Hames, B. R.; Loveless, C. *J. Org. Chem.* **2001**, *66*, 3084.
- (7) Chatani, N.; Kajikawa, Y.; Nishimura, H.; Murai, S. *Organometallics* **1991**, *10*, 21.
- (8) Fujioka, H.; Kitagawa, H.; Kondo, M.; Kita, Y. *Heterocycles* **1994**, *37*, 743.
- (9) Zheng, T.; Narayan, R. S.; Schomaker, J. M.; Borhan, B. *J. Am. Chem. Soc.* **2005**, *127*, 6946.
- (10) Hayashi, Y.; Wariishi, K.; Mukaiyama, T. *Chem. Lett.* **1987**, 1243.
- (11) Methot, J.-L.; Morency, L.; Ramsden, P. D.; Wong, J.; Léger, S. *Tetrahedron Lett.* **2002**, *43*, 1147.
- (12) Schomaker, J. M.; Pulgam, V. R.; Borhan, B. *J. Am. Chem. Soc.* **2004**, *126*, 13600.
- (13) Schomaker, J. M.; Bhattacharjee, S.; Yan, J.; Borhan, B. *J. Am. Chem. Soc.* **2007**, *129*, 1996.
- (14) Clennan, E. L.; Pan, G.-l. *Org. Lett.* **2003**, *5*, 4979.
- (15) Harada, T.; Mukaiyama, T. *Bull. Chem. Soc. Jpn.* **1993**, *66*, 882.
- (16) Martín, R.; Buchwald, S. L. *Angew. Chem. Int. Ed.* **2007**, *46*, 7236.
- (17) García-Fortanet, J.; Buchwald, S. L. *Angew. Chem. Int. Ed.* **2008**, *47*, 8108.
- (18) Lawrence, N. J.; Muhammad, F. *Tetrahedron* **1998**, *54*, 15361.

- (19) Collet, A.; Jacques, J. *Tetrahedron Lett.* **1978**, *19*, 1265.
- (20) Cram, D. J.; Tanner, M. E.; Keipert, S. J.; Knobler, C. B. *J. Am. Chem. Soc.* **1991**, *113*, 8909.
- (21) Lindsey, A. S. *Journal of the Chemical Society (Resumed)* **1965**, 1685.
- (22) Brotin, T.; Roy, V.; Dutasta, J.-P. *J. Org. Chem.* **2005**, *70*, 6187.
- (23) Canceill, J.; Collet, A.; Gottarelli, G. *J. Am. Chem. Soc.* **1984**, *106*, 5997.